VOL. 541 NOS. 1 + 2 MARCH 22, 1991
COMPLETE IN ONE ISSUE

RNAL OF CHROMATOGRAPHY

LUDING ELECTROPHORESIS AND OTHER SEPARATION METHODS

ELSEVIER

JOURNAL OF CHROMATOGRAPHY

Scope. The *Journal of Chromatography* publishes papers on all aspects of chromatography, electrophoresis and related methods. Contributions consist mainly of research papers dealing with chromatographic theory, instrumental development and their applications. The section *Biomedical Applications*, which is under separate editorship, deals with the following aspects: developments in and applications of chromatographic and electrophoretic techniques related to clinical diagnosis or alterations during medical treatment; screening and profiling of body fluids or tissues with special reference to metabolic disorders; results from basic medical research with direct consequences in clinical practice; drug level monitoring and pharmacokinetic studies; clinical toxicology; analytical studies in occupational medicine.

Submission of Papers. Manuscripts (in English; *four* copies are required) should be submitted to: Editorial Office of *Journal of Chromatography*, P.O. Box 681, 1000 AR Amsterdam, The Netherlands, Telefax (+31-20) 5862 304, or to: The Editor of *Journal of Chromatography, Biomedical Applications*, P.O. Box 681, 1000 AR Amsterdam, The Netherlands. Review articles are invited or proposed by letter to the Editors. An outline of the proposed review should first be forwarded to the Editors for preliminary discussion prior to preparation. Submission of an article is understood to imply that the article is original and unpublished and is not being considered for publication elsewhere. For copyright regulations, see below.

Subscription Orders. Subscription orders should be sent to: Elsevier Science Publishers B.V., P.O. Box 211, 1000 AE Amsterdam, The Netherlands, Tel. (+31-20) 5803 911, Telex 18582 ESPA NL, Telefax (+31-20) 5803 598. The *Journal of Chromatography* and the *Biomedical Applications* section can be subscribed to separately.

Publication. The *Journal of Chromatography* (incl. *Biomedical Applications*) has 38 volumes in 1991. The subscription prices for 1991 are:

J. Chromatogr. (incl. *Cum. Indexes, Vols. 501–550*) + *Biomed. Appl.* (Vols. 535–572):
Dfl. 7220.00 plus Dfl. 1140.00 (p.p.h.) (total *ca.* US$ 4976.25)

J. Chromatogr. (incl. *Cum. Indexes, Vols. 501–550*) only (Vols. 535–561):
Dfl. 5859.00 plus Dfl. 810.00 (p.p.h.) (total *ca.* US$ 3969.75)

Biomed. Appl. only (Vols. 562–572):
Dfl. 2387.00 plus Dfl. 330.00 (p.p.h.) (total *ca.* US$ 1617.25).

Our p.p.h. (postage, package and handling) charge includes surface delivery of all issues, except to subscribers in Argentina, Australia, Brasil, Canada, China, Hong Kong, India, Israel, Malaysia, Mexico, New Zealand, Pakistan, Singapore, South Africa, South Korea, Taiwan, Thailand and the U.S.A. who receive all issues by air delivery (S.A.L. — Surface Air Lifted) at no extra cost. For Japan, air delivery requires 50% additional charge; for all other countries airmail and S.A.L. charges are available upon request. Back volumes of the *Journal of Chromatography* (Vols. 1–534) are available at Dfl. 208.00 (plus postage). Claims for missing issues will be honoured, free of charge, within three months after publication of the issue. Customers in the U.S.A. and Canada wishing information on this and other Elsevier journals, please contact Journal Information Center, Elsevier Science Publishing Co. Inc., 655 Avenue of the Americas, New York, NY 10010, U.S.A., Tel. (+1-212) 633 3750, Telefax (+1-212) 633 3990.

Abstracts/Contents Lists published in Analytical Abstracts, Biochemical Abstracts, Biological Abstracts, Chemical Abstracts, Chemical Titles, Chromatography Abstracts, Clinical Chemistry Lookout, Current Contents/Life Sciences, Current Contents/Physical, Chemical & Earth Sciences, Deep-Sea Research/Part B: Oceanographic Literature Review, Excerpta Medica, Index Medicus, Mass Spectrometry Bulletin, PASCAL-CNRS, Pharmaceutical Abstracts, Referativnyi Zhurnal, Research Alert, Science Citation Index and Trends in Biotechnology.

See inside back cover for Publication Schedule, Information for Authors and information on Advertisements.

0021-9673/91/$03.50

Printed in The Netherlands

VOL. 541, NO. 1+2 JOURNAL OF CHROMATOGRAPHY MARCH 22, 1991

CONTENTS

(Abstracts/Contents Lists published in Analytical Abstracts, Biochemical Abstracts, Biological Abstracts, Chemical Abstracts, Chemical Titles, Chromatography Abstracts, Current Contents/Life Sciences, Current Contents/Physical, Chemical & Earth Sciences, Deep-Sea Research/Part B: Oceanographic Literature Review, Excerpta Medica, Index Medicus, Mass Spectrometry Bulletin, PASCAL-CNRS, Referativnyi Zhurnal, Research Alert and Science Citation Index)

REGULAR PAPERS

Gas Chromatography

(Continued overleaf)

(Continued overleaf)

In articles with more than one author, the name of the author to whom correspondence should be addressed is indicated in the article heading by a 6-pointed asterisk (*)

Ion Chromatography

Principles and Applications

by **P.R. Haddad,** *University of New South Wales, Kensington, N.S.W., Australia and* **P.E. Jackson,** *Waters Chromatography Division, Milford, MA, USA*

(Journal of Chromatography Library, 46)

Ion chromatography (IC) was first introduced in 1975 for the determination of inorganic anions and cations and water soluble organic acids and bases. Since then, the technique has grown in usage at a phenomenal rate. The growth of IC has been accompanied by a blurring of the original definition of the technique, so that it now embraces a very wide range of separation and detection methods, many of which bear little resemblance to the initial concept of ion-exchange separation coupled with conductivity detection.

Ion Chromatography is the first book to provide a comprehensive treatise on all aspects of ion chromatography. Ion-exchange, ion-interaction, ion-exclusion and other pertinent separation modes are included, whilst the detection methods discussed include conductivity, amperometry, potentiometry, spectroscopic methods (both molecular and atomic) and post-column reactions. The theoretical background and operating principles of each separation and detection mode are discussed in detail. A unique extensive compilation of practical applications of IC (1250 literature citations) is presented in tabular form. All relevant details of each application are given to accommodate reproduction of the method in the laboratory without access to the original publication.

This truly comprehensive text on ion chromatography should prove to be the standard reference work for researchers and those involved in the use of the subject in practical situations.

1990 798 pages
Price: US$ 191.50 / Dfl. 335.00
ISBN 0-444-88232-4

Elsevier Science Publishers

P.O. Box 211, 1000 AE Amsterdam, The Netherlands
P.O. Box 882, Madison Square Station, New York, NY 10159, USA

Artificial Intelligence in Chemistry

Structure Elucidation and Simulation of Organic Reactions

by **Z. Hippe,** *Department of Physical and Computer Chemistry, I. Lukasiewicz Technical University, Rzeszów, Poland*

(Studies in Physical and Theoretical Chemistry, 73)

Coedition with and distributed in the East European Countries, China, Cuba, Mongolia and Vietnam by ARS POLONA Warsaw, Poland

This comprehensive overview of the application of artificial intelligence methods (AI) in chemistry contains an in-depth summary of the most interesting achievements of modern AI, namely, problem-solving in molecular structure elucidation and in syntheses design.

The book provides a brief history of AI as a branch of computer science. It also gives an overview of the basic methods employed for searching the solution space (thoroughly exemplified by chemical problems), together with a profound and expert discussion on many questions that may be raised by modern chemists wishing to apply computer-assisted methods in their own research. Moreover, it includes a survey of the most important literature references, covering all essential research in automated interpretation of molecular spectra to elucidate a structure and in syntheses design. A glossary of basic terms from computer technology for chemists is appended.

This book is intended to make the emerging field of artificial intelligence understandable and accessible for chemists, who are not trained in computer methods for solving chemical problems. The author discusses step-by-step basic algorithms for structure elucidation and many aspects of the automated design of organic syntheses in order to integrate this fascinating technology into current chemical knowledge.

1991 xiv + 272 pages
Price: Dfl. 240.00 / US$137.00
ISBN 0-444-98746-0

Elsevier Science Publishers

P.O. Box 211, 1000 AE Amsterdam, The Netherlands
P.O. Box 882, Madison Square Station, New York, NY 10159, USA

JOURNAL OF CHROMATOGRAPHY

VOL. 541 (1991)

JOURNAL of CHROMATOGRAPHY

INCLUDING ELECTROPHORESIS AND OTHER SEPARATION METHODS

ELSEVIER
AMSTERDAM — OXFORD — NEW YORK — TOKYO

J. Chromatogr., Vol. 541 (1991)

0021-9673/91/$03.50

Printed in The Netherlands

Journal of Chromatography, 541 (1991) 1–19
Elsevier Science Publishers B.V., Amsterdam

CHROM. 22 995

Computer simulation as an aid in method development for gas chromatography

I. The accurate prediction of separation as a function of experimental conditions

D. E. BAUTZ, J. W. DOLAN and L. R. SNYDER*
LC Resources Inc., 3182C Old Tunnel Road, Lafayette, CA 94549 (U.S.A.)
(First received August 13th, 1990; revised manuscript received November 13th, 1990)

ABSTRACT

Computer-simulation with commercially available software (DryLab GC) allows the prediction of isothermal or temperature-programmed gas chromatographic (GC) separation as a function of experimental conditions. In either case, two experimental runs are carried out initially, using a linear temperature program (heating rate different, all other conditions the same). Data from these two runs are entered into the computer, and separation can then be predicted for other conditions: different temperatures in the case of isothermal runs, or any kind of temperature program for programmed runs.

The reliability of resulting predictions was evaluated in the present study for several samples and a wide range in separation conditions. Retention time predictions were usually accurate within a few percent, and sample resolution was predicted within about ± 10%. The use of computer simulation should be a considerable help for the rapid development of superior GC methods.

INTRODUCTION

Computer simulation using DryLab software is proving to be a useful tool for method development in high-performance liquid chromatography (HPLC) [1–7]. Two experimental runs under standardized conditions are carried out initially, following which a personal computer can be used to optimize either mobile phase composition (%B) in isocratic separation or gradient steepness (b) in gradient elution. This approach can also be used to design complex, multisegment gradients, which are often of considerable value for improving resolution and/or shortening run time [1–10]. Much of the value of computer simulation in HPLC arises as a result of frequent changes in band spacing (values of α) when values of %B or b are changed [11].

In view of the value of computer simulation for HPLC method development, we have explored the similar application of this technique to gas chromatography (GC). GC separations in an isothermal or programmed-temperature mode are conceptually similar to corresponding separations by HPLC under isocratic or gradient conditions

0021-9673/91/$03.50

(*cf.* refs. 12 and 13). There are also several reports which show that band spacing[a] in GC can be varied by changes in either the temperature or programming rate [14–20] (although many chromatographers seem to be unaware of this possibility). These observations suggest that computer simulation similar to that now used for HPLC method development should also prove to be of value for GC.

Previously we have described software (DryLab GC) for the computer simulation of GC separations [21]. The present paper reports the application of this software to the separation of a number of different samples, in turn allowing an assessment of its accuracy for a wide range of conditions. A following paper [22] examines the general utility of controlling GC band spacing via selection of the best isothermal temperature or an optimized temperature program.

THEORY

Predictions of GC retention

Isothermal retention (values of the capacity factor k) in a defined GC system is related to temperature as

$$\log k = A + B/T \tag{1}$$

where A and B are constants for a given solute, and T is the column temperature (K); A and B depend on the entropy and enthalpy of vaporization, respectively [12,17]. Eqn. 1 assumes that A and B are independent of temperature, which is usually a reasonable approximation.

For the case of a linear temperature program (most often used in GC), the column temperature T is related to separation time t as

$$\begin{aligned} T &= T_0 + (T_f - T_0)(t/t_P) \\ &= T_0 + \Delta T(t/t_P) \end{aligned} \tag{2}$$

where T_0 and T_f refer to the initial and final temperatures, and t_P is the program time. Given values of A and B for the various solutes in a sample (for a defined GC system), it is possible to predict retention time t_R in separations based on linear (single-segment) temperature programs by means of the relationship [12,17]

$$1 = \int_0^{t_R} dt/[t_0(k + 1)] \tag{3}$$

Here t is the time after sample injection and the beginning of temperature programming, and t_0 is the column dead-time. Eqn. 3 assumes that band migration in temperature-programmed GC can be approximated as the sum of a series of (small) isothermal steps, each successive step being carried out at a slightly higher temperature.

---

[a] By a "change in band spacing" we mean changes in relative values of the separation factor α for different band pairs, and possibly (but not necessarily) changes in band retention order.

An explicit solution for eqn. 3 has not yet been derived [17]. However, use of the so-called linear-elution-strength (LES) approximation [21],

$$\log k \approx (\text{constant}) - ST \tag{4}$$

where S is a constant for a given solute and GC system, allows an approximate solution which is suitable for rapid computer simulation using a personal computer (PC). Bandwidths W can also be predicted by means of

$$W = 4t_0(1 + k_e)/N^{1/2} \tag{5}$$

Here k_e is the value of k for the solute at the time of elution, and N is the column plate number. A value of k_e can be obtained from eqn. 1, since t_R defines the column temperature at the time the band elutes from the column (eqn. 2 with $t = t_R$). A value of N can then be obtained from eqn. 6 by using experimental values of t_R and W from one of the two starting experimental runs.

Eqn. 5 assumes that N and t_0 do not vary with temperature (which is of course an approximation). In that case, the width of a band *on a given column* just prior to elution will be constant for every solute and every temperature. The derivation of eqn. 5 follows from the definition of N and the relation of t_R to k at the time of elution (k_e);

$$N = 16(t_R/W)^2 \tag{6}$$

$$t_R = t_0(1 + k_e) \tag{7}$$

See also the discussion of ref. 23. With the addition of a correction for the extra-column volume of the GC system [21], eqn. 5 has been shown to give reliable predictions of bandwidth as a function of isothermal temperature or programmed-temperature conditions.

We have used the foregoing approach to construct a program (DryLab GC) for the computer-simulation of GC runs [21]. DryLab GC uses two experimental programmed-temperature runs as input for computer simulation —in the same way that computer simulation has been carried out for method development in gradient elution [8–10]. Predictions of separation can then be made for (i) isothermal runs at any temperature, (ii) temperature-programming for any starting temperature and heating rate, and (iii) multi-ramp temperature programs (where the heating rate is varied stepwise during the separation). A more detailed description of the theoretical basis of DryLab GC is given in ref. 21.

EXPERIMENTAL

Equipment

The gas chromatograph was an HP5890A (Hewlett-Packard; Avondale, PA, U.S.A.) equipped with split/splitless injection port and flame ionization detector. The system makes use of Hewlett-Packard's INET system network for control of the HP3396A integrator and HP7672A autoinjector. ChromPerfect (Justice Innovations, Palo Alto, CA, U.S.A.) was used for data analysis. Most injections were performed manually.

Software

The computer program DryLab GC is available from LC Resources (Lafayette, CA, U.S.A.). It is designed to run on any IBM-compatible personal computer; the addition of a math coprocessor is recommended.

Columns

Three fused-silica capillary columns were used in the present study: a non-polar column (SPB-1, Supelco, Supelco Park, PA, U.S.A.), a slightly polar column (DB-5, J & W Scientific, Folsom, CA, U.S.A.) and a polar column (Nukol, Supelco). Each column had the same dimensions (30 m × 0.025 cm I.D.) and film thickness (0.25 μm). The column dead-time (air-peak measurement) varies with temperature [21]; an average value of $t_0 = 1.8$ min was assumed in the present study.

Samples

Several different test mixtures were used to evaluate the present DryLab GC software. A number of samples were purchased from Supelco: (a) "non-polar test mixture": 2-octanone, *n*-decane, 1-octanol, *n*-undecane, 2,6-dimethylphenol, 2,6-dimethylaniline, *n*-dodecane and *n*-tridecane; (b) "phenol test mixture": 2,4,6-trichlorophenol, 4-chloro-3-methylphenol, 2-chlorophenol, 2,4-dichlorophenol, 2,4-dimethylphenol, 2-nitrophenol, 4-nitrophenol, 2,4-dinitrophenol, 2-methyl-4,6-dinitrophenol, pentachlorophenol and phenol; (c) "herbicide test mixture": Eptam, Sutan, Tillam, Ordram, Ro-neet, Trifuluralin, Atrazine, Terbacil, Sencor, Bromacil, Paarlan, Goal and Hexazinone; (d) "rapeseed oil mixture": methyl myristate, palmitate, stearate, oleate, linoleate, linolenate, arachidate, eicosenoate, behenate, erucate and legnocerate; (e) "barbiturate test mixture": barbital, amobarbital, aprobarbital, pentobarbital, secobarbital, hexobarbital, mephobarbital, phenobarbital, cyclobarbital, butabarbital and butalbital; (f) "pesticide test mixture": 16 chlorinated hydrocarbons, mainly derivatives of BHC, aldrin, endrin and DDT.

Various oil samples (spearmint, peppermint, lime) were obtained from Lorann Oils, Lansing, MI, U.S.A.; lemon oil was purchased locally. Two narrow-boiling gasoline samples (A, 200–300°F; B, 300–350°F) were a gift from the Unocal Research Center. Several random mixtures were assembled from our chemical stockroom: samples (A) cyclohexane, ethyl acetate, methylene chloride, isopropyl alcohol, 3-pentanone and *tert.*-amyl alcohol; (B) chlorobenzene, cyclohexanone, *n*-hexanol, cyclohexanol and *p*-dichlorobenzene; (C) 1,2-propanediol, acetophenone, *p*-dibromobenzene, nitrobenzene, *p*-nitrotoluene and benzyl alcohol; (D) cyclohexane, ethyl acetate, methylene chloride, *tert.*-amyl alcohol, *n*-hexanol, cyclohexanol, acetophenone and benzyl alcohol.

RESULTS AND DISCUSSION

Simulation of linear temperature-programmed runs

The potential accuracy of computer simulation for either HPLC or GC predictions is limited by similar factors; these have been discussed for HPLC in refs. 24 and 25 and for GC in ref. 21. In the case of DryLab GC, the experimental input data for computer simulation are from two linear, temperature-programmed runs having different heating rates: *e.g.*, 4 and 8°C/min. We can expect [21] that predictions for runs

with intermediate heating rates (*e.g.*, 4–8°C/min) will be more accurate than for extrapolated conditions (*e.g.*, <4 or >8°C/min). Similarly, the accuracy of extrapolated simulations will decrease whan the initial (experimental) runs have heating rates that are similar (*e.g.*, 4 and 5°C/min). Heating-rate ratios >3 are usually recommended, but ratios <3 were explored in the present study in order to magnify possible errors for extrapolated conditions. A further discussion of possible errors in GC computer simulation is provided in this paper.

Retention time predictions. A number of experimental runs were carried out for different samples with variation of the heating rate. These data allow comparisons between predicted and experimental results for a wide range of conditions (only heating rate varying). Some typical results are summarized in Table I and Fig. 1.

Results for the 13-component herbicide sample summarized in Table I show excellent agreement between experimental and predicted retention times; average errors in computer-simulated values of t_R are only 0.3–1.2%. As expected, the average error in t_R is less for the interpolated run (0.3%, inputs of 4 and 8°C/min) *vs.* the extrapolated runs; *i.e.*, 0.8–1.2% errors for the last two runs of Table I. Fig. 1A and B compares experimental *vs.* predicted chromatograms for the 6°C/min herbicide run, and Fig. 1C and D shows a similar comparison (6°C/min) for the barbiturate sample (data of Table II).

TABLE I

COMPARISON OF EXPERIMENTAL *VS.* SIMULATED RETENTION TIMES FOR HERBICIDE MIXTURE

Conditions: DB-5 column, linear 100–300°C temperature program, 1.0 ml/min flow-rate; DryLab GC used for simulations. Avg. error refers to the average of absolute errors for individual solutes.

Heating rate r (°C/min)		Retention times t_R (min)			
Inputs	Simulation	Expt.	Calc.	Error	
				t_R	Δt_R
4/8	6	11.40	11.43	0.03	0.01
		12.01	12.05	0.04	0.02
		13.61	13.67	0.06	0.00
		15.58	15.64	0.06	−0.01
		16.37	16.42	0.05	0.01
		17.73	17.79	0.06	0.00
		18.95	19.01	0.06	0.00
		20.16	20.22	0.06	0.01
		21.42	21.49	0.07	0.00
		22.98	23.05	0.07	−0.01
		23.79	23.85	0.06	0.01
		25.59	25.66	0.07	0.00
		28.27	28.34	0.07	
		Avg. error		±0.06 (0.3%)	±0.007 (0.5%)

(Continued on p. 6)

TABLE I *(continued)*

Heating rate r (°C/min)		Retention times t_R (min)			
Inputs	Simulation	Expt.	Calc.	Error	
				t_R	Δt_R
4/6	8	9.84	9.77	−0.07	−0.01
		10.32	10.24	−0.08	−0.01
		11.61	11.52	−0.09	−0.01
		13.10	13.00	−0.10	0.01
		13.62	13.53	−0.09	−0.02
		14.71	14.60	−0.11	0.00
		15.65	15.54	−0.11	−0.01
		16.59	16.47	−0.12	0.00
		17.54	17.42	−0.12	−0.01
		18.71	18.58	−0.13	0.01
		19.29	19.17	−0.12	0.00
		20.68	20.54	−0.12	−0.03
		22.79	22.64	−0.15	
		Avg. error		±0.11 (0.8%)	±0.01 (0.9%)
6/8	4	13.95	13.79	−0.16	−0.02
		14.83	14.65	−0.18	−0.05
		17.03	16.81	−0.23	−0.03
		19.92	19.66	−0.26	0.02
		21.26	21.02	−0.24	−0.03
		23.13	22.86	−0.27	−0.02
		24.89	24.60	−0.29	−0.02
		26.62	26.31	−0.31	−0.01
		28.51	28.19	−0.32	−0.02
		30.86	30.52	−0.34	−0.01
		32.13	31.80	−0.33	−0.05
		34.74	34.36	−0.38	−0.01
		38.24	38.12	−0.39	
		Avg. error		±0.29 (1.2%)	±0.02 (1.2%)

Differences in predicted *vs.* experimental values of t_R should be small, although errors of 3–5% are generally acceptable. For the purposes of method development and optimizing the separation, however, errors in *retention time differences* are more important. Resolution R_s is proportional to the difference (Δt_R) in t_R values for an adjacent pair of bands: $\Delta t_R = t_2 - t_1$, where t_1 and t_2 refer to values of t_R for the first and second band in a given band-pair. It can be seen in Table I that errors in Δt_R (0.007–0.02 min) are very much smaller than are errors in t_R (0.06–0.29 min), and this was observed in every case. That is, errors in GC computer simulation are highly correlated with retention time t_R (see discussion of ref. 21). This is fortunate, because it

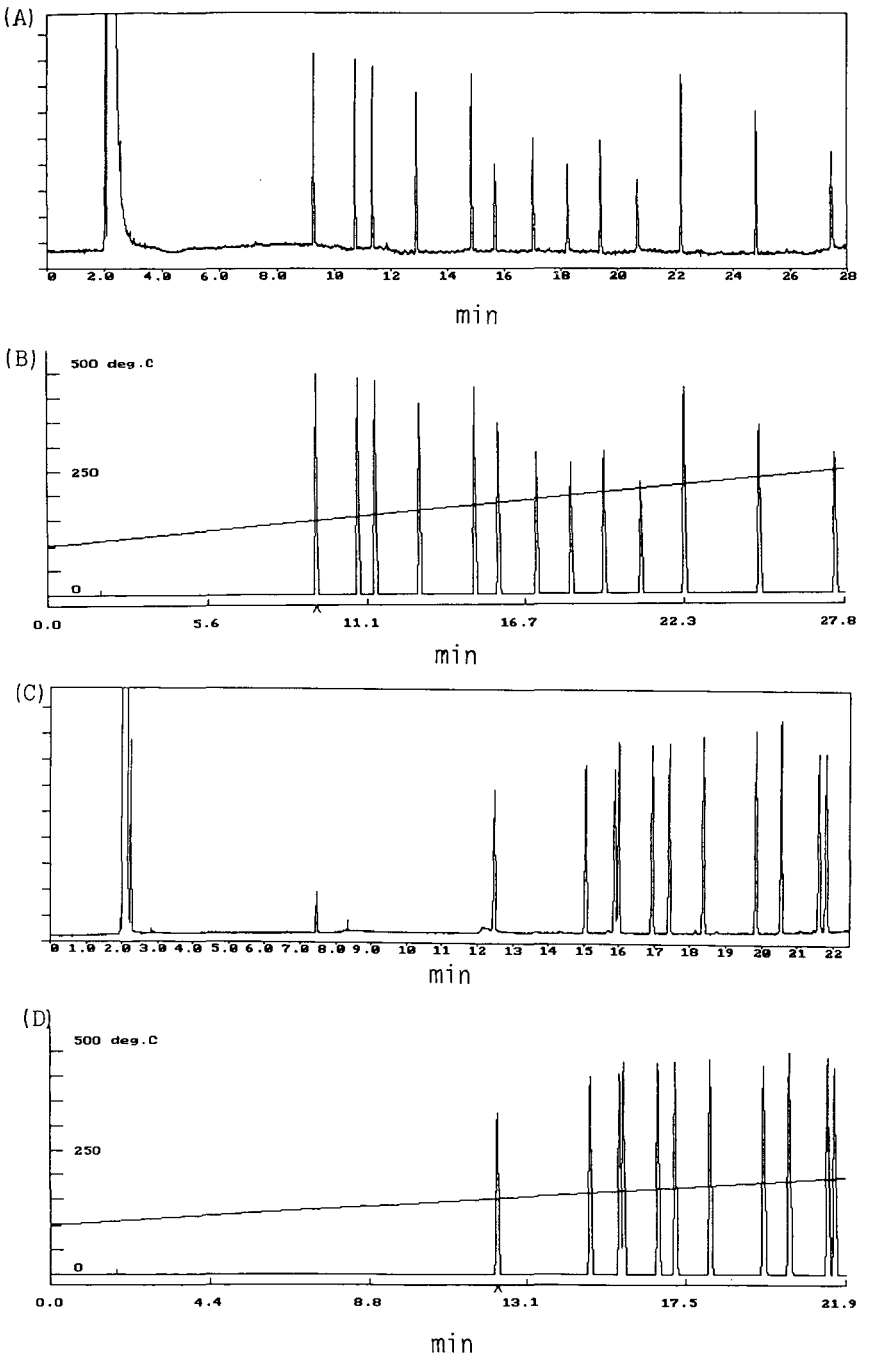

Fig. 1. Comparisons of experimental *vs.* computer-simulated (predicted) chromatograms for linear-program separations on DB-5 column. (A) Experimental chromatogram for herbicide sample of Table I (100–300°C, 6°C/min); (B) same, DryLab GC chromatogram (input data: 4 and 8°C/min); (C) experimental chromatogram for barbiturate sample of Table II (100–300°C, 6°C/min); (D) same, DryLab GC chromatogram (input data: 4 and 8°C/min).

TABLE II

SUMMARY OF COMPARISONS OF EXPERIMENTAL *VS.* PREDICTED RETENTION FOR LINEAR TEMPERATURE PROGRAMS AND DIFFERENT SAMPLES AND COLUMNS (AS IN TABLE I)

Sample (column/range)[a]	Heating rate r (°C/min)		Errors	
	Inputs	Simulation	t_R	Δt_R
Herbicides[b]	4/8	6	0.3%	0.5%
(DB-5/100–300°C)	4/6	8	0.8	0.9
	6/8	4	1.2	1.2
Non-polar[b]	4/8	6	0.2	0.9
(DB-5/100–300°C)	4/6	8	0.5	1.3
	6/8	4	0.6	1.6
Phenols[b]	4/8	6	0.4	0.8
(DB-5/100–300°C)	4/6	8	0.8	1.8
	6/8	4	1.0	2.1
Non-polar[b]	4/8	6	0.2	0.5
(Nukol/70–200°C)	4/6	8	0.4	1.2
	6/8	4	0.6	1.8
Phenols[b]	1/3	2	0.8	1.1
(Nukol/120–200°C)	1/2	3	1.6	1.7
	2/3	1	2.1	3.2
Rapeseed oil[b]	2/4	3	0.2	0.4
(DB-5/100–300°C)	2/3	4	0.4	0.9
	3/4	2	0.5	1.2
Barbiturates[b]	4/8	6	0.6	0.8
(DB-5/100–300°C)	4/6	8	1.5	0.6
	6/8	4	2.0	1.3
Sample A[c]	1/4	2	0.6	1.3
(Nukol/50–100°C)	1/2	4	1.7	0.4
	2/4	1	0.9	1.5
Sample B[c]	4/8	6	0.4	0.2
(Nukol/50–200°C)	4/6	8	1.3	0.7
	6/8	4	1.7	1.5
Sample C[c]	2/6	4	1.3	1.3
(Nukol/100–200°C)	2/4	6	3.0	2.0
	4/6	2	4.5	3.8
Sample D[c]	2/8	4	0.5	1.3
(Nukol/100–200°C)	2/4	8	1.2	2.4
	4/8	2	1.2	3.3
	Avg. errors[d]		±1.1	±1.4[a]

[a] Range refers to the change in temperature during the run.
[b] Supelco sample.
[c] Sample formulated by us.
[d] Average absolute errors.

means that predictions of resolution by computer simulation are more likely to be reliable —and therefore more useful for GC method development.

Similar comparisons as in Table I were carried out for several samples described in the Experimental section —using both the DB-5 and Nukol columns. These results are summarized in Table II. It is seen that predicted values of t_R and Δt_R are in every case in acceptable agreement with experimental values. Thus for interpolated heating rates, the average (absolute) errors in t_R and Δt_R were $\pm 0.4\%$ and 0.7%, respectively. Similarly, for extrapolated heating rates, the corresponding average errors were $\pm 1.2\%$ in t_R, and $\pm 1.4\%$ in Δt_R. These data suggest that computer simulation for GC may prove to be even more reliable than for HPLC (see HPLC comparisons of refs. 1–10, 24–26).

Bandwidth predictions. The prediction of bandwidth requires a value of the

TABLE III

SUMMARY OF COMPARISONS OF EXPERIMENTAL *VS.* PREDICTED BANDWIDTHS FOR VARIOUS SAMPLES AND COLUMNS (RUNS OF TABLE II); LINEAR TEMPERATURE PROGRAMS

See text for details.

Sample (column/range)[a]	Error (%)[b]
Herbicides (DB-5/100–300°C)	$+10 \pm 7$
Non-polar (DB-5/100–300°C)	$+17 \pm 5$
Phenols (DB-5/100–300°C)	$+6 \pm 4$
Rapeseed oil (DB-5/100–300°C)	-25 ± 12
Barbiturates (DB-5/100–300°C)	-3 ± 3
Non-polar (Nukol/70–200°C)	-8 ± 4
Phenols (Nukol/120–200°C)	-6 ± 4
Sample B (Nukol/50–200°C)	-6 ± 4
Sample C (Nukol/100–200°C)	-9 ± 3
Sample D (Nukol/50–200°C)	-9 ± 5
Sample A (Nukol/50–100°C)	-8 ± 10
Overall average	-4 ± 5

[a] Range refers to the change in temperature during the run.
[b] Values are average percentage error and range in error values (1 standard deviation).

column plate number N (eqn. 5). Average values of N were measured for each column from isothermal runs, using well retained bands to avoid extra-column errors[a]. For the DB-5 column at 160°C, the column plate number was $N = 100\,000$. For the Nukol column at 100°C, $N = 70\,000$.

Table III summarizes our comparison of experimental *vs.* predicted bandwidths (W) for the various runs of Table II. Errors were calculated as $100[(W_{calc}/W_{expt}) - 1]\%$; *i.e.*, positive errors indicate that experimental bandwidths are narrower than predicted. For a given separation (*e.g.*, a specified sample, column and experimental conditions) the errors in predicted bandwidths were first averaged and then the standard deviation of the errors was determined. The overall (average) error in these predicted bandwidths is -4%, with an average deviation in each separation of $\pm 5\%$ from the average for that run.

Simulation of isothermal runs

Some samples are better separated isothermally, rather than via temperature programming. The DryLab GC software alerts the user to this possibility, based on the arbitrary requirement of $0.5 < k < 50$ for all bands in an isothermal separation. We have carried out several isothermal separations for the samples of Table I, in order to determine the accuracy of isothermal predictions based on temperature-programmed input data.

Retention time predictions. Table IV compares experimental *vs.* predicted values of retention for four isothermal runs which involve two different samples and two different columns. Two temperature-programmed runs were used as input for computer simulation (as previously). The average (absolute) error in predicted retention times t_R ranges from 1.3–4.4%, with an average value of $\pm 1.8\%$. Similarly, retention time differences (and resolution) show an average (absolute) error of 2–11%, with an average value of $\pm 8\%$. While these predicted retention times are not as accurate as those of Table II for temperature-programmed runs, they are adequate for the purposes of GC method development. A similar situation has been observed in computer simulation for HPLC, where the use of gradient runs as input data yields more accurate predictions of gradient runs than for isocratic runs.

Fig. 2 compares experimental and simulated chromatograms for the separation of the barbiturate sample at 170°C. Reasonable agreement between the two chromatograms is observed.

Bandwidth predictions. The four isothermal separations of Table IV exhibited errors in predicted bandwidths of: $+7 \pm 4\%$, $+4 \pm 2$, $+5 \pm 1\%$ and $-4 \pm 2\%$, respectively, for an overall average of $+3\%$ and an average deviation in each run of $\pm 2\%$. This excellent agreement reflects the use of isothermal values of the plate number N; see the above discussion of Table III.

Simulation of temperature-programmed runs with multiple temperature ramps

A particularly useful application of computer simulation in HPLC is for the design of complex, multi-segment gradients [1–10]. Such gradients are advantageous

---

[a] $N = 5.54(t_R/W_{1/2})^2$, where t_R is the retention time and $W_{1/2}$ is the bandwidth at halfheight. Extra-column band broadening effects and the dependence of N on k were corrected for by assuming an extra-column bandwidth $W_{ec} = 0.025$ min; see the discussion of ref. 21.

TABLE IV

COMPARISON OF EXPERIMENTAL *VS.* SIMULATED RETENTION TIMES FOR ISOTHERMAL SEPARATION OF DIFFERENT SAMPLES

Conditions: 1.0 ml/min flow-rate. DryLab GC used for simulations with 4 and 8°C/min runs as input.

Sample (column/range)[a]	Temperature[b] (°C)	Retention times t_R (min)			
		Expt.	Calc.	Error	
				t_R	Δt_R
Non-polar (DB-5/100–300°C)	110	3.99	4.06	0.07	−0.01
		4.11	4.17	0.06	−0.02
		5.13	5.17	0.04	0.02
		5.76	5.82	0.06	−0.06
		6.05	6.05	0.00	−0.09
		7.89	7.80	−0.09	−0.07
		8.92	8.76	−0.16	0.63
		13.50	13.97	0.47	
		Avg. error[c]		±0.12 (1.3%)	±0.13 (9.5%)
Phenols (DB-5/100–300°C)	160	2.73	2.67	−0.06	0.05
		2.86	2.85	−0.01	0.04
		3.43	3.46	0.03	−0.02
		3.36	3.37	0.01	0.05
		3.61	3.67	0.06	0.07
		4.34	4.47	0.13	0.14
		5.34	5.61	0.27	0.36
		8.12	8.75	0.63	0.12
		8.41	9.16	0.75	0.29
		11.68	12.72	1.04	0.53
		19.57	21.14	1.57	
		Avg. error		±0.41 (2.5%)	0.16 (9.5%)
Non-polar (Nukol/70–200°C)		3.50	3.56	0.06	0.06
		4.45	4.57	0.12	0.03
		6.12	6.27	0.15	−0.01
		6.37	6.51	0.14	0.18
		20.44	20.12	−0.32	
		Avg. error		0.16 (0.9%)	0.07 (1.7%)
Phenols (Nukol/120–200°C)	180	6.52	6.67	0.15	−0.11
		6.34	6.38	0.04	0.26
		9.10	9.40	0.30	0.15
		10.89	11.34	0.45	0.36
		14.57	15.38	0.81	
		Avg. error		0.35 (4.4%)	0.22 (10.9%)

[a] Supelco samples; range refers to temperature program for two experimental input runs.
[b] Isothermal run.
[c] Average absolute error.

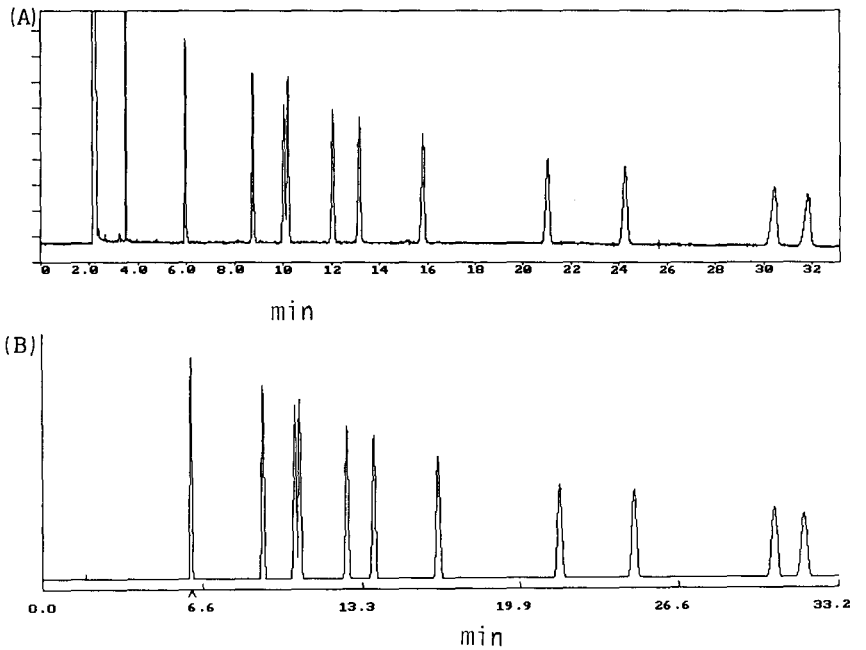

Fig. 2. Comparisons of experimental *vs.* computer-simulated (predicted) chromatograms for an isothermal separation. (A) Barbiturate sample at 170°C, DB-5 column, other conditions as in Table II; (B) same, DryLab GC chromatogram (input data: 4 and 8°C/min).

for a number of reasons. For example, steep gradients can be used to advantage for those parts of the chromatogram which have few, widely-separated peaks, in order to save run time. Likewise, flat gradients are able to increase the overall resolution of those parts of the chromatogram where the bands are more numerous and generally less well resolved. Perhaps the most rewarding application of segmented gradients, however, is the use of variations in gradient steepness at different parts of the chromatogram in order to optimize band spacing.

The similar application of segmented (multi-ramp) temperature programs in GC should prove equally useful. For this reason, several runs of this type were carried out for the samples of Table II, and the resulting chromatograms were compared with those obtained from computer simulation (starting with the usual two experimental runs as inputs to DryLab GC). In this way we were able to establish the relative accuracy of computer simulation for multi-ramp temperature programs.

Retention time predictions. Table V summarizes experimental *vs.* predicted retention times for a typical multi-ramp run: the barbiturate sample with a temperature program of 160/160/250/250°C in 0/14/18/22 min; *i.e.*, an initial isothermal hold followed by a 22.5°C/min temperature ramp followed by an isothermal hold. The retention times of the sample in this separation are distributed across the three segments of the temperature program, so that a good evaluation of the accuracy of multi-ramp predictions can be inferred from these data.

The data of Table V for this multi-ramp program exhibit larger errors in

TABLE V

COMPARISON OF EXPERIMENTAL *VS.* SIMULATED RETENTION TIMES FOR THE BARBITURATE SAMPLE AND A MULTI-RAMP TEMPERATURE PROGRAM

Conditions: DB-5 column, 1.0 ml/min flow-rate; 160/160/250/250°C in 0/14/18/22 min. DryLab GC used for simulations, with data for 100–300°C program in 25 and 50 min as input.

Retention times t_R (min)			
Expt.	Calc.	Error	
		t_R	Δt_R
7.68	8.33	0.65	0.51
11.93	13.09	1.16	−0.27
13.94	14.89	0.95	−0.11
14.21	15.05	0.84	−0.45
15.77	16.16	0.39	−0.12
16.30	16.57	0.27	−0.20
17.21	17.28	0.07	−0.23
18.32	18.16	−0.16	−0.12
18.84	18.56	−0.28	−0.12
19.60	19.20	−0.40	−0.01
19.75	19.34	−0.41	
Avg. error[a]		0.54 (4.5%)	0.22 (18%)

[a] Average absolute error.

predicted retention times (average of ±4.5%) than in the previous cases which involve either linear programs or isothermal separation (±0.2–3.5%). However, the corresponding errors in Δt_R are smaller (±0.22 min *vs.* ±0.54 min in Table V); the predicted error in resolution ±18% is marginally acceptable for method development (but note the following discussion in Table VI of very steep heating rates).

Table VI summarizes similar comparisons of experimental *vs.* predicted retention times for several multi-ramp separations. These data are arranged in order of increasing programming rate (°C/min, in parentheses, second column) for the steepest segment of the temperature program. It is seen that errors in Δt_R (and resolution) tend to increase for runs with steeper segments, as predicted for extrapolated heating rates. Thus, for segments with heating rates <20°C/min (first group of data in Table VI), the average error in Δt_R is ±5%. For segments with heating rates of 23–25°C/min (second group) or >33°C/min (third group), the average errors in Δt_R are ±9% and ±16%, respectively. These errors are still acceptable for method development purposes, but these examples do illustrate that larger errors are possible in the computer simulation of multi-ramp runs. It should also be noted that many workers avoid heating rates >20°C/min, because some GC systems are unreliable for very steep heating rates.

Fig. 3 compares experimental *vs.* predicted chromatograms for a multi-ramp separation of the herbicide sample (where the maximum programming rate is 33°C/min); reasonable agreement is observed for the two chromatograms.

Bandwidth predictions. For the runs of Table VI which do not involve

TABLE VI

SUMMARY OF COMPARISONS OF EXPERIMENTAL *VS.* PREDICTED RETENTION FOR MULTI-RAMP TEMPERATURE PROGRAMS AND DIFFERENT SAMPLES AND COLUMNS

Conditions: 1.0 ml/min; DryLab GC input runs as in Table II (4 and 8°C/min in most cases).

Sample (column)	Temperature program[a]	Errors	
		t_R	Δt_R
Non-polar (DB-5)	100/100/150/150°C (8) 0/5/11.25/16.25 min	±0.17 min (2.4%)	±0.02 min (1.9%)
Phenols (DB-5)	100/100/250/250°C (15) 0/8/18/23 min	±0.30 (2.2%)	±0.06 (4.2%)
Non-polar (Nukol)	70/110/110/200/200°C (20) 0/2/7/11.5/21.5 min	±0.11 (1.1%)	±0.09 (5.2%)
Phenols (Nukol)	120/160/160/200/200°C (20) 0/4/10/12/22 min	±0.29 (4.5%)	±0.09 (5.8%)
Sample C (Nukol)	100/180/180/200/200°C (20) 0/4/8/10/12 min	±0.34 (9.0%)	±0.07 (6.0%)
Sample D (Nukol)	50/60/60/200/200°C (23) 0/2.5/4.5/10.5/15 min	±0.29 (2.5%)	±0.14 (8.5%)
Barbiturates (DB-5)	160/160/250/250°C (23) 0/14/18/22 min	±0.54 (4.5%)	±0.22 (18%)
Rapeseed oil (DB-5)	200/200/300/300°C (25) 0/14/18/22 min	±0.42 (2.6%)	±0.11 (5.9%)
Herbicides (DB-5)	200/200/300/300°C (33) 0/5/8/12 min	±0.26 (3.6%)	±0.11 (18%)
Sample A (Nukol)	60/60/180/180°C (40) 0/2/4/5 min	±0.08 (6.0%)	±0.05 (18%)
Sample B (Nukol)	110/110/200/200°C (45) 0/4/6/8 min	±0.08 (3.8%)	±0.07 (13%)

[a] Numbers in parentheses are maximum heating rates (°C/min) for each separation.

programming rates >30°C/min, the overall (average) error in predicted bandwidths was 0 ± 15%. For temperature programs that involved steeper temperature ramps, the average error was −12 ± 21%. It appears that errors in bandwidth for multi-segment temperature programming are also somewhat greater (but acceptable) than for separations that involve linear programs.

Errors due to extrapolation and their empirical correction

The LES approximation used in DryLab GC does not seriously detract from the accuracy of predicted separations, as seen from the above discussion. However, the potential errors in computer simulation become larger, when the predicted separation is based on conditions that are far removed from those used for the initial two experimental runs used as input to DryLab GC. This is illustrated in Fig. 4 for the prediction of an isothermal GC separation. Here we assume isothermal input data, and

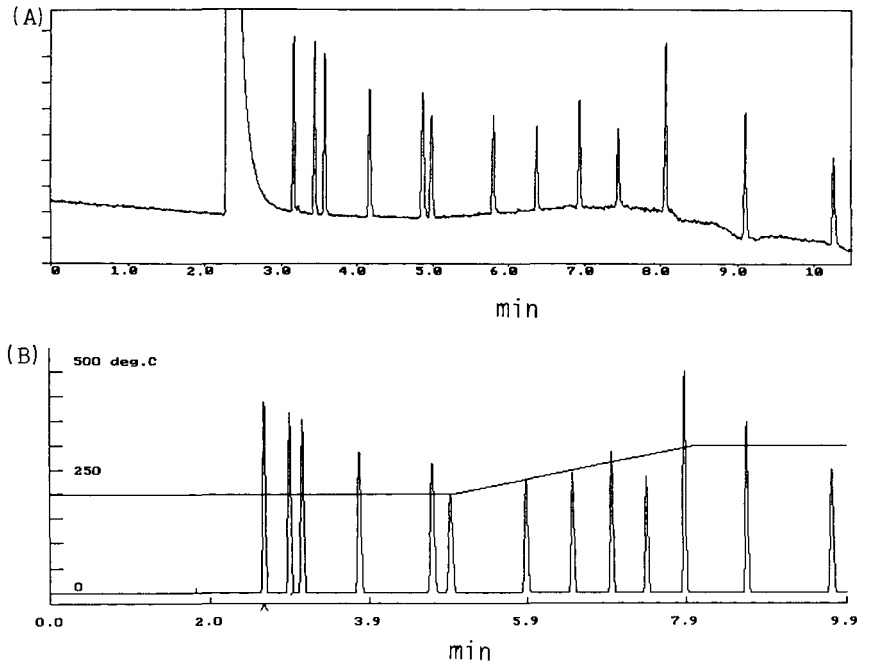

Fig. 3. Comparisons of experimental *vs.* computer-simulated (predicted) chromatograms for multi-segment temperature programming. (A) Herbicide sample, DB-5 column, 200/200/300/300°C in 0/5/8/12 min; other conditions as in Table VI; (B) same, DryLab GC chromatogram (input data: 4 and 8°C/min).

the curvature of the plots in Fig. 4 is exaggerated to better illustrate our point. A similar argument can be made for temperature-programmed runs (see discussion of Fig. 2 of following paper [23]).

Solute retention (log k) is plotted in Fig. 4A *vs.* temperature (solid curves), for two solutes that are to be separated. The input runs for computer simulation are carried out at 180 and 200°C (solid circles). The LES approximation is shown in Fig. 4A as dashed straight lines. It is assumed next that separation at 163°C is predicted by computer simulation (open circles), and the resulting chromatogram is shown in Fig. 4A. The experimental plots of log k *vs.* temperature indicate larger values of k at 163°C (solid squares) *vs.* those predicted by computer simulation (open circles). The experimental chromatogram therefore shows later elution of these two bands *vs.* the predicted (LES) separation, but little difference in resolution. This mirrors our previous comparisons of experimental *vs.* predicted separations (Tables I–VI).

Now consider a more complex case (Fig. 4B), where the two solutes to be separated show a change in band spacing as the temperature is varied. At 165°C the two bands have the same value of k, and the elution order of the two bands at lower temperatures (< 165°C) is reversed when the temperature is raised above 165°C. Again we assume that the initial experimental runs for input to computer simulation are 180 and 200°C (solid circles). Next assume that we predict the separation that will occur at 165°C (open circles of Fig. 4B); the predicted chromatogram shows baseline resolution of our two solutes. However, the experimental chromatogram exhibits complete

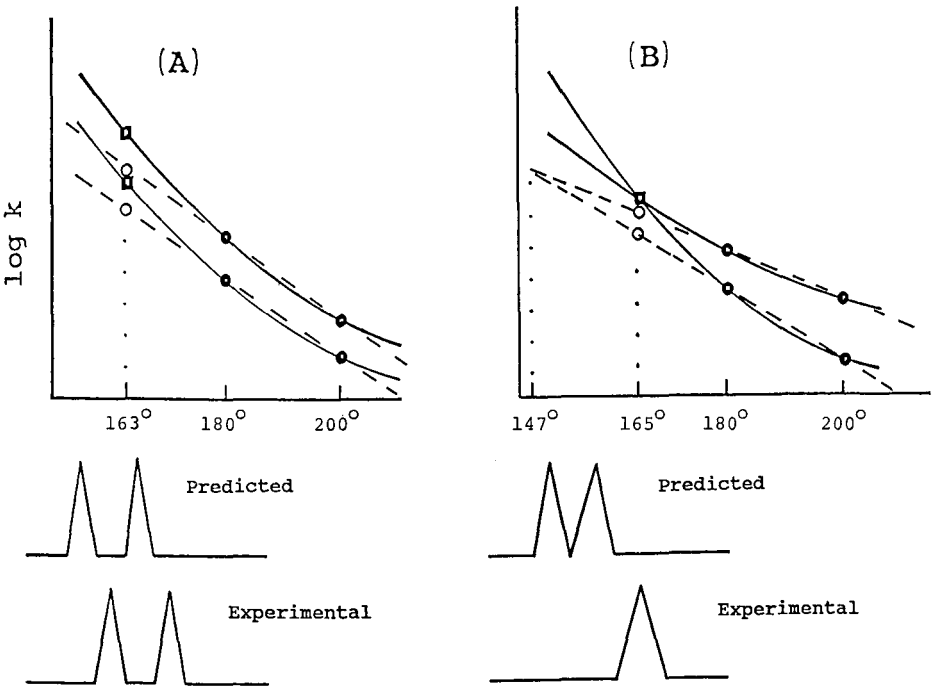

Fig. 4. Hypothetical (exaggerated) examples of errors in isothermal computer simulation due to use of the LES approximation. (A) Two solutes whose band spacing does not change with temperature; (B) two solutes whose band spacing changes with temperature. ● = Experimental input data for computer simulation; ○ = predictions of separation at a third temperature; ■ = experimental separation at a third temperature. See text for details.

overlap of the two bands, because of the error introduced by extrapolation beyond our starting data (closed circles).

The resulting error in computer simulation (Fig. 4B) is seen to be more serious than in the preceding example (Fig. 4A). To generalize, we can say that (i) extrapolation of experimental data as in Fig. 4 leads to greater possible errors, (ii) these errors can be magnified for the case where two bands exhibit large changes in band spacing as temperature is varied, and (iii) the practical effect of these errors is more serious for bands that are less well resolved. That is, if the average error in resolution is 10%, and if the average resolution (entire chromatogram) is $R_s = 5$, then the average error in R_s is ± 0.5 units, which does not appear very serious. If the predicted resolution for a critical (least resolved) band-pair is only 1.5, however, we might actually find R_s equal to 1.0 (or less) for the corresponding experimental run.

The errors illustrated in Fig. 4B can be corrected for (to a considerable extent) as follows. Note that the complete overlap of the two bands in Fig. 4B occurs at 165°C, whereas computer simulation (based on the LES approximation) predicts band overlap at 147°C. That is, the correct separation is predicted, but for the wrong temperature. The form of the LES approximation (see discussion of refs. 24, 25) is such as to make this generally true. That is, if an optimized separation is predicted for some

temperature T, and the experimental separation deviates significantly from that predicted, then a (usually) modest adjustment in the temperature should yield an experimental chromatogram that agrees with the separation predicted for temperature T. These small adjustments (in the right direction) are easily made, because of the predictable change in retention with temperature.

A similar situation exists for temperature-programmed runs. There small adjustments in heating rate may be required to obtain a good match between experimental and predicted chromatograms. With a little experience, most chromatographers should be able to carry out these "fine-tuning" adjustments with only one or two extra runs —in the occasional case where significant errors as in Fig. 4B are encountered.

CONCLUSIONS

A personal computer program (DryLab GC) is described for carrying out computer simulation as a means of facilitating method development for either isothermal or temperature-programmed GC. Based on two initial experimental runs as input to the computer, it is possible to predict separation as a function of experimental conditions: initial and final temperatures, temperature programming rate, multi-segment temperature programs, etc. Retention times, bandwidths and resolution can be displayed as tables, graphs or simulated chromatograms.

The accuracy of this program for predicting retention time and bandwidth (or resolution) was tested for several samples and two different columns, using variously (i) linear temperature programming, (ii) isothermal separation and (iii) multi-ramp (non-linear) temperature programming. On the basis of these comparisons of experiment and theory, it is concluded that the DryLab GC software is adequately reliable for method development. Retention times were predicted with an average accuracy of 1–2%, bandwidths are predicted with an average accuracy of about $\pm 5\%$, and resolution is predicted with an accuracy of about $\pm 10\%$.

SYMBOLS

All symbols for the present and following two papers [22,27].

a, b	constants in eqn. 2 of Part II
A, B	constants in eqn. 1 of Part I
b	temperature-program steepness parameter (eqn. 4, Part II); $b = t_0 r S$
GC	gas chromatography
i, j	solutes of Fig. 1, Part II
k	solute capacity factor (GC)
k'	solute capacity factor (HPLC)
$\bar{k}$	effective value of k during programmed-temperature separation; equal to value of k for band when it reaches the midpoint of the column (eqn. 4, Part II)
k_a, k_z	values of k for first and last bands in the chromatogram (eqn. 4, Part II)
k_e	value of k at elution
k_0	value of k for a solute at the beginning of a temperature programmed separation

LES	linear elution strength
LSS	linear solvent strength
N	column plate number
r	heating rate (°C/min)
RRM	relative resolution map
R_s	resolution of two adjacent bands
S	solute parameter of eqn. 5 (Part I)
S_i, S_j	values of S for solutes i and j (Fig. 1 of Part II)
t	time after sample injection and the beginning of the temperature program
t_0	column dead-time (min)
t_P	time of (linear) temperature program
t_R	retention time for temperature-programmed GC run
T	column temperature; usually in °C, except °K in eqn. 1
T_f	final temperature in temperature-programmed GC
T_0	initial temperature in temperature-programmed GC
W	baseline bandwidth (min)
W_{ec}	contribution to bandwidth from extra-column effect (min); see eqn. 14 of ref. 21
W_{expt}, W_{calc}	experimental and predicted values of W
α	separation factor
β	column phase ratio
$\Delta H_{v,i}$	enthalpy of retention (eqns. 1, 2 of Part II)
ΔR_s	a necessary change in R_s for a given band pair, in order to result in their adequate separation
ΔS	difference in S values for two adjacent bands (eqn. 4, Part II)
$\Delta S_{v,i}$	entropy of retention (eqns. 1, 2 of Part II)
Δt_R	difference in t_R values for two adjacent bands
φ	volume fraction of strong solvent B in binary mobile phase A/B (HPLC)
%B	% (v/v) of strong solvent B in binary mobile phase A/B (HPLC)

ACKNOWLEDGEMENT

The authors are grateful for a grant from the Small Business Innovation Research Program funded by the National Institutes of Health.

REFERENCES

1 J. W. Dolan, D. C. Lommen and L. R. Snyder, *J. Chromatogr.*, 485 (1989) 91.
2 J. Schmidt, *J. Chromatogr.*, 485 (1989) 421.
3 T. Sasagawa, Y. Sakamoto, T. Hirose, T. Yoshida, Y. Kobayashi, Y. Sato and K. Koizumi, *J. Chromatogr.*, 485 (1989) 533.
4 I. Molnar, R. Boysen and P. Jekow, *J. Chromatogr.*, 485 (1989) 569.
5 R. G. Lehmann and J. R. Miller, *J. Chromatogr.*, 485 (1989) 581.
6 D. J. Thompson and W. D. Ellenson, *J. Chromatogr.*, 485 (1989) 607.
7 J. D. Stuart, D. D. Lisi and L. R. Snyder, *J. Chromatogr.*, 485 (1989) 657.
8 B. F. D. Christ, B. S. Cooperman and L. R. Snyder, *J. Chromatogr.*, 459 (1989) 1.

9 B. F. D. Christ, B. S. Cooperman and L. R. Snyder, *J. Chromatogr.*, 459 (1989) 25.
10 B. F. D. Christ, B. S. Cooperman and L. R. Snyder, *J. Chromatogr.*, 459 (1989) 63.
11 L. R. Snyder, M. A. Quarry and J. L. Glajch, *Chromatographia*, 24 (1987) 33.
12 W. E. Harris and H. W. Habgood, *Programmed Temperature Gas Chromatography*, Wiley, New York, 1967.
13 L. R. Snyder, in Cs. Horváth (Editor), *High-Performance Liquid Chromatography —Advances and Perspectives*, Vol. 1, Academic Press, New York, 1980, p. 208.
14 R. A. Hively and R. E. Hinton, *J. Gas Chromatogr.*, 6 (1968) 903.
15 R. R. Freeman and W. Jennings, *J. High Resolut. Chromatogr. Chromatogr. Commun.*, 10 (1987) 231.
16 R. J. Pell and H. L. Gearhart, *J. High Resolut. Chromatogr. Chromatogr. Commun.*, 10 (1987) 388.
17 E. V. Dose, *Anal. Chem.*, 59 (1987) 2420.
18 G. Castello and T. C. Gerbino, *J. Chromatogr.*, 437 (1988) 33.
19 J. Krupcik, D. Repka, E. Benicka, T. Evesi, J. Nolte, B. Paschold and H. Mayer, *J. Chromatogr.*, 448 (1988) 203.
20 Y. Guan, J. Kiraly and J. Rijks, *J. Chromatogr.*, 472 (1989) 129.
21 D. E. Bautz, J. W. Dolan, W. J. Raddatz and L. R. Snyder, *Anal. Chem.*, 62 (1990) 1561.
22 J. W. Dolan, L. R. Snyder and D. E. Bautz, *J. Chromatogr.*, 541 (1991) 21.
23 L. R. Snyder, *Principles of Adsorption Chromatography*, Marcel Dekker, New York, 1968, pp. 16–17.
24 M. A. Quarry, R. L. Grob and L. R. Snyder, *Anal. Chem.*, 58 (1986) 907.
25 L. R. Snyder and M. A. Quarry, *J. Liq. Chromatogr.*, 10 (1987) 1789.
26 J. W. Dolan, L. R. Snyder and M. A. Quarry, *Chromatographia*, 24 (1987) 261.
27 L. R. Snyder, D. E. Bautz and J. W. Dolan, *J. Chromatogr.*, 541 (1991) 35.

Journal of Chromatography, 541 (1991) 21–34
Elsevier Science Publishers B.V., Amsterdam

CHROM. 22 996

Computer simulation as an aid in method development for gas chromatography

II. Changes in band spacing as a function of temperature

J. W. DOLAN, L. R. SNYDER* and D. E. BAUTZ
LC Resources Inc., 3182C Old Tunnel Road, Lafayette, CA 94549 (U.S.A.)
(First received August 13th, 1990; revised manuscript received November 13th, 1990)

ABSTRACT

Several different samples and three stationary phases of varying polarity have been examined for changes in band spacing as a function of temperature. The results of these studies have been expressed as a relative variability in the temperature coefficients of retention (S) for adjacent bands. A theoretical analysis suggests that useful changes in band spacing *vs.* temperature (or heating rate) can be expected when the difference in S values (ΔS) for two bands is larger than 1 to 2%. The samples studied exhibited variations in average values of ΔS of 0.6–6%. This suggests that optimizing the (isothermal) temperature or (programmed) heating rate of a gas chromatographic separation will often be advantageous.

INTRODUCTION

The preceding paper [1] describes software (DryLab GC) for the computer simulation of gas chromatographic (GC) separations as a function of isothermal temperature or temperature programming. Similar software exists (DryLab G) for the prediction of separations in high-performance liquid chromatography (HPLC) as a function of gradient conditions [2–8]. The fundamental theory of GC [9] and HPLC [10,11] suggests that temperature plays the same role in GC as mobile phase composition (%B) plays in HPLC. Therefore our detailed and comprehensive understanding of HPLC separation as a function of %B or gradient steepness [10-15] can be used to guide our development of GC separations as a function of temperature or programming rate. Many of the rules and generalizations that apply to gradient elution can be adapted directly to temperature-programmed GC.

Of major interest in this connection is the possible change in band spacing for a sample as the temperature is changed in a GC separation. Similar changes in band spacing as %B varies in HPLC are extensively documented [12–15], suggesting the usefulness of optimized multi-segment gradients [2–8, 13–15]. Several workers [16–18] have specifically noted changes in GC band spacing as temperature is varied, and similar results are reported elsewhere [19–22]. In this paper we will further explore

0021-9673/91/$03.50

these temperature-related changes in GC selectivity and relate them to the development of optimized temperature programs.

THEORY

Origins of temperature-related changes in GC band spacing

The capacity factor k_i of a solute i in GC is related to absolute temperature T as [23]

$$-T \ln k_i = -(\Delta H_{v,i}/R) + T[(\Delta S_{v,i}) + \ln \beta] \quad (1)$$

Here $\Delta H_{v,i}$ and $\Delta S_{v,i}$ refer to the partial molal enthalpy and entropy of vaporization from the stationary phase, respectively, R is the gas constant, and β is the phase ratio. Often the entropy of vaporization is roughly constant for different solutes and the same column (a variant of Trouton's rule [24]), or the enthalpy and entropy of retention for the components of a sample are related as

$$\Delta H_{v,i} \approx a\, \Delta S_{v,i} + b \quad (2)$$

where a and b are constants for the different solutes in a given sample. In either of these two cases, band spacing should not change with temperature, because it can then be shown that values of k are highly correlated with values of $\Delta H_{v,i}$ for a given separation temperature, and adjacent bands (with similar values of k) will then have similar values of $\Delta H_{v,i}$. Conditions that favor the applicability of Trouton's rule or eqn. 2 are (i) solute molecules that are similar to each in other in shape and size and (ii) non-polar solutes and/or stationary phases. Thus constancy in the entropy of retention requires solute molecules of similar shape, size and polarity; see also the discussion of ref. 25.

Similarly, eqn. 2 assumes either (i) solute–stationary phase interactions of the same "kind" for each solute in the sample, or no dependence of these interactions on temperature. Polar interactions (dipole–dipole or hydrogen bonding) decrease in strength with increasing temperature, while non-polar (dispersion) interactions do not. Thus if the overall polarity of the solute molecules in a given sample varies from one solute to the next, the dependence of k on temperature will also vary, and band spacing should change with temperature.

The basis of these changes in band spacing as a function of temperature (isothermal run) or heating rate (programmed run) is illustrated in Fig. 1 in terms of our linear-elution-strength (LES) model of GC retention. The LES approximation used in the present treatment (eqn. 4 of Part I) can be expressed as

$$\log k = \log k_o - S(T - T_o) \quad (3)$$

where S is a constant for a given solute, and k_o is the value of k at the starting temperature T_o. The slopes of the linear plots in Fig. 1 for solutes i and j are equal to the values of S (S_i and S_j) for each solute, and it is seen that $S_j > S_i$. As a result of this difference in S values, solute i elutes after j for temperatures $T < 180$°C, and before i for $T > 180$°C. At $T = 180$°C the two solutes have the same retention time and are unresolved.

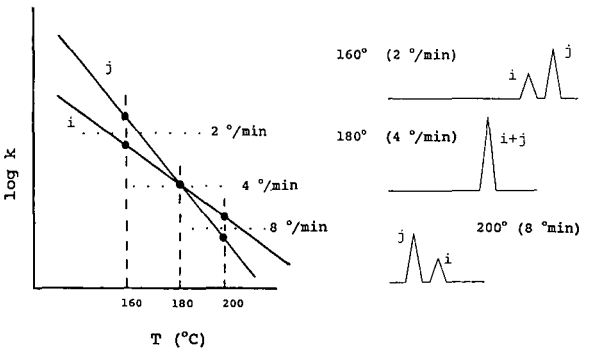

Fig. 1. Dependence of GC separation on isothermal plots of log k *vs.* temperature. See text for details.

The separation of the sample of Fig. 1 with a linear temperature program leads to similar results if the heating rate (instead of T) is varied. Thus in the analogous case of HPLC gradient elution, the linear-solvent-strength (LSS) approximation [10] predicts a value of k' that provides the same separation of a band pair in either isocratic or gradient elution. We will refer to this quantity as k' for isocratic separation and $\bar{k}$ for gradient elution. The value of $\bar{k}$ is determined by gradient steepness. A similar relationship for temperature-programmed GC can be assumed from the LES approximation of the present treatment (see later discussion of Figs. 4–6), with $\bar{k}$ given by[a]

$$\begin{aligned} \bar{k} &= 0.87\, t_P F/(V_m\, \Delta T\, S) \\ &= 0.87/(t_o\, r\, S) \\ &= 0.87/b \end{aligned} \tag{4}$$

Here t_P is the program time (run time for a linear program), F is the flow-rate, V_m is the column dead-volume, ΔT is the change in temperature during the program, S is defined by eqn. 3, t_o is the column dead-time, and r is the heating rate (°/min); $b = (t_o\, r\, S)$ is another measure of the steepness of a linear temperature program.

For a given program steepness b, the separation of any pair of adjacent bands will be the same as in an isothermal separation with some temperature T, when k (isothermal) = $\bar{k}$; here, k' and k refer to the average value for the band-pair. Values of S will be similar (but not exactly constant) for different solutes[b], so that values of $\bar{k}$ will also be approximately the same for different bands in a temperature programmed run (linear program). This contrasts with the variation of k for different bands in isothermal separation. Thus in plots as in Fig. 1, isothermal runs can be represented by vertical lines (for the same temperature), whereas programmed separations are given by horizontal lines (for a given value of $\bar{k}$ or programming rate).

---

[a] The quantity $\bar{k}$ in a temperature-programmed separation corresponds to the value of k for a band when it has migrated halfway through the column; see the related discussion of ref. 10 for gradient elution.

[b] The following discussion of Fig. 1 is deliberately simplified in order to give the reader a clearer picture of the interrelationship of isothermal and programmed-temperature separation. The approximations used here do not limit the accuracy of computer simulation as described in this and the preceding paper.

In the example of Fig. 1, it is assumed for purposes of discussion that k for an isothermal separation at 160°C is equal to $\bar{k}$ for a programmed run at 2°/min; similarly, isothermal separation at 180°C is equivalent to a programmed run at 4°/min, etc. In the GC system of Fig. 1, it is seen that i and j elute together for a 4°/min temperature program. For heating rates < 4°/min, j is retained more strongly, and *vice versa* for heating rates > 4°/min. This situation described in Fig. 1 is essentially similar to the liquid chromatographic separation of a sample, with %B varied rather than temperature (see the Discussion of refs. 12,14).

Correlation of values of S and k_o

During the application of DryLab GC to a given sample, values of $\log k_o$ and S are determined for each solute. If a plot of values of S *vs.* $\log k_o$ describes a single curve with little deviation of individual points from the curve (*e.g.*, Fig. 2A), there will be no changes in band spacing with change in temperature. Significant deviations of individual data points from such a curve (*e.g.*, Fig. 2B,C), on the other hand, will favor changes in band spacing as temperature is varied. It will prove useful to determine these average deviations in S for different samples —as an indication of the significance of band-spacing changes with temperature.

Dependence of separation on temperature (or heating rate) and values of S

A previous treatment for HPLC [12] has examined the necessary difference in solute S values that will allow the resolution of an initially unresolved band-pair by varying mobile phase composition (%B). Isocratic systems can be approximated by the LSS model, and the required fractional difference in S values for two adjacent bands ($\Delta S/S$) is (isocratic HPLC)

$$\Delta S/S = (8/2.3)\Delta R_s\, N^{-0.5}\, [(1+k')/k']/\log(20\, k_a/k_z) \qquad (5)$$

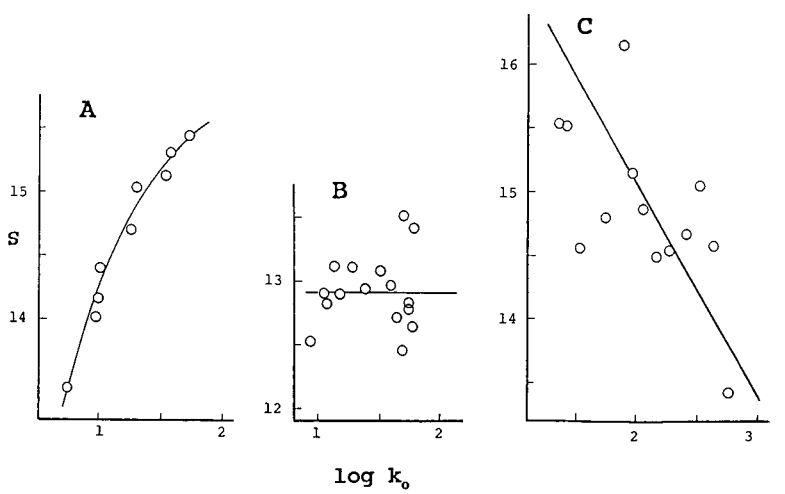

Fig. 2. Band-to-band variations in S for different samples. Conditions: DB-5 column; (A) rapeseed oil; (B) pesticides; (C) herbicides. See text for details.

Here S is the average of S values for the two bands, ΔR_s refers to the necessary increase in resolution (to be achieved by a change in %B), N is the column plate number, and k_a and k_z are the k' values of the first and last bands in the chromatogram. Because of the similarity of LC and GC separation in terms of the LSS and LEC approximations (see above discussion of eqn. 4), a relationship similar to eqn. 5 can be derived for GC separation as well. As a result of the wider range of k'–values (*ca.* 50-fold) that can be used in isothermal GC *vs.* isocratic LC, eqn. 5 must be modified to give (isothermal GC)

$$\Delta S/S = (8/2.3)\Delta R_s N^{-0.5}[(1+k)/k]/\log(50\ k_a/k_z) \quad (5a)$$

We can specify the necessary difference in S values for two unresolved bands such that a change in temperature will result in their separation with some required value of R_s. Assume (i) a required value of $\Delta R_s = 1.0$ (although smaller increases in resolution will often suffice), (ii) average value of $N = 100\,000$, (iii) the average value of k for a given band-pair = 5, and (iv) let the ratio $k_z/k_a = 10$. The necessary value of $\Delta S/S$ is then 0.019; *i.e.*, a 1.9% difference in the S values for the two solutes. If separation conditions can be selected that yield average differences in S of this magnitude, a change in temperature has a good chance of resolving an initially unseparated pair of bands.

The situation is somewhat more attractive for the case of a temperature-programmed GC run, as can be inferred from the similar discussion of ref. 12 for LC gradient elution. The corresponding equation for the required difference in solute S values is (temperature-programmed GC)

$$\Delta S/S = (8/2.3)\ \Delta R_s N^{-0.5}[(1+\bar{k})/\bar{k}]/\log(50) \quad (5b)$$

and the necessary value of $\Delta S/S$ is then only 0.008; *i.e.*, less than a 1% difference in S values.

A reviewer has asked whether the parameter S and related changes in band spacing with temperature are determined by the entropy or enthalpy of vaporization of the solute. S itself is more closely related to enthalpy than to entropy, but the related band spacing changes are determined by the *relationship* of entropy to enthalpy (deviations from eqn. 2).

EXPERIMENTAL

All experimental materials and procedures are discussed in the preceding paper [1].

RESULTS AND DISCUSSION

Part I [1] established that computer simulation (with DryLab GC) can be used in place of actual experimental runs to study GC separation as a function of conditions. A number of different samples were also described, any of which can be simulated in this fashion. In the following discussion we can therefore use simulated and experimental runs interchangeably, in order to gain increased insight into the effects of experimental conditions on band spacing and separation.

Similarity of separation by programmed-temperature and isothermal GC

In separations by HPLC, it has been shown [10] that the same separation of a group of adjacent bands can be achieved by either isocratic or gradient elution, provided that gradient conditions are adjusted so that the average k' value in the isocratic separation is equal to the average $\bar{k}$ value in gradient elution. Having specified the gradient conditions (%B/min, flow-rate, etc.), a corresponding value of gradient steepness b is defined[a], from which $\bar{k} = 1/1.15b$. A mobile phase composition (value of %B) can then be selected such that $k' = \bar{k}$.

We can proceed in the same way to show that a similar relationship exists for isothermal and temperature-programmed GC (as illustrated in Fig. 1). The value of this exercise will be more apparent in the following section, where we will examine changes in band spacing as a function of heating rate in temperature-programmed GC, *vs.* similar effects for isothermal separations. Fig. 3B shows a partial chromatogram of a spearmint oil, with one band-pair indicated by an asterisk. The values of S for these two bands are approximately equal (16.4 and 16.5, respectively), so that only

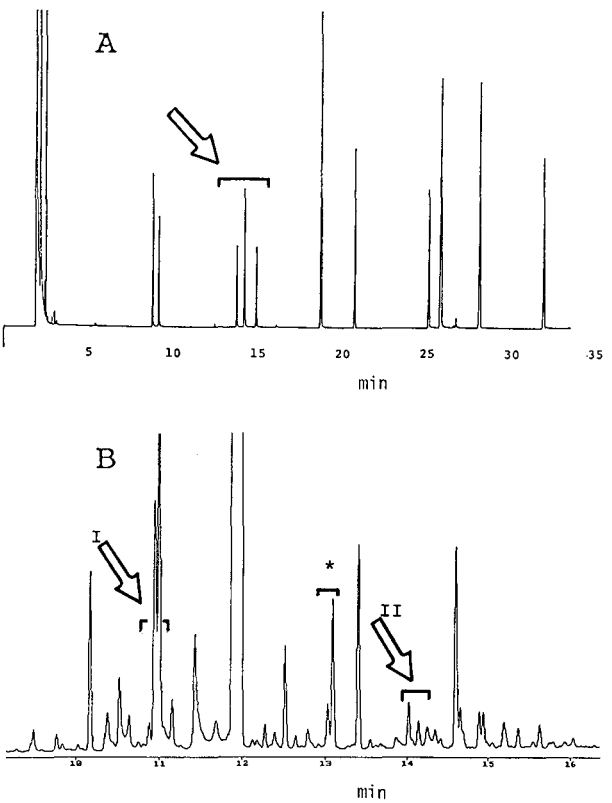

Fig. 3. Separation of phenol (A) and spearmint oil (B) samples by GC. Conditions: DB-5 column, 1 ml/min; (A) 50–200°C at 4.6 °C/min; (B) 50–300°C at 8 °C/min.

[a] For gradient elution, $b = V_m \Delta\varphi S/t_G F$, where $S = -\mathrm{d}(\log k')/\mathrm{d}\varphi$; see ref. 4; φ is the volume fraction of strong solvent B in a binary mobile phase A–B.

minor change in band spacing with change in temperature or heating rate is expected (for a moderate change in k or $\bar{k}$). This example will therefore serve as a reference case for comparison with the separation (as a function of temperature) of band pairs having different values of S.

Fig. 4 shows the change in separation (and resolution) of this band-pair (asterisk in Fig. 3B) as a function of heating rate (programmed separations, top; iso-

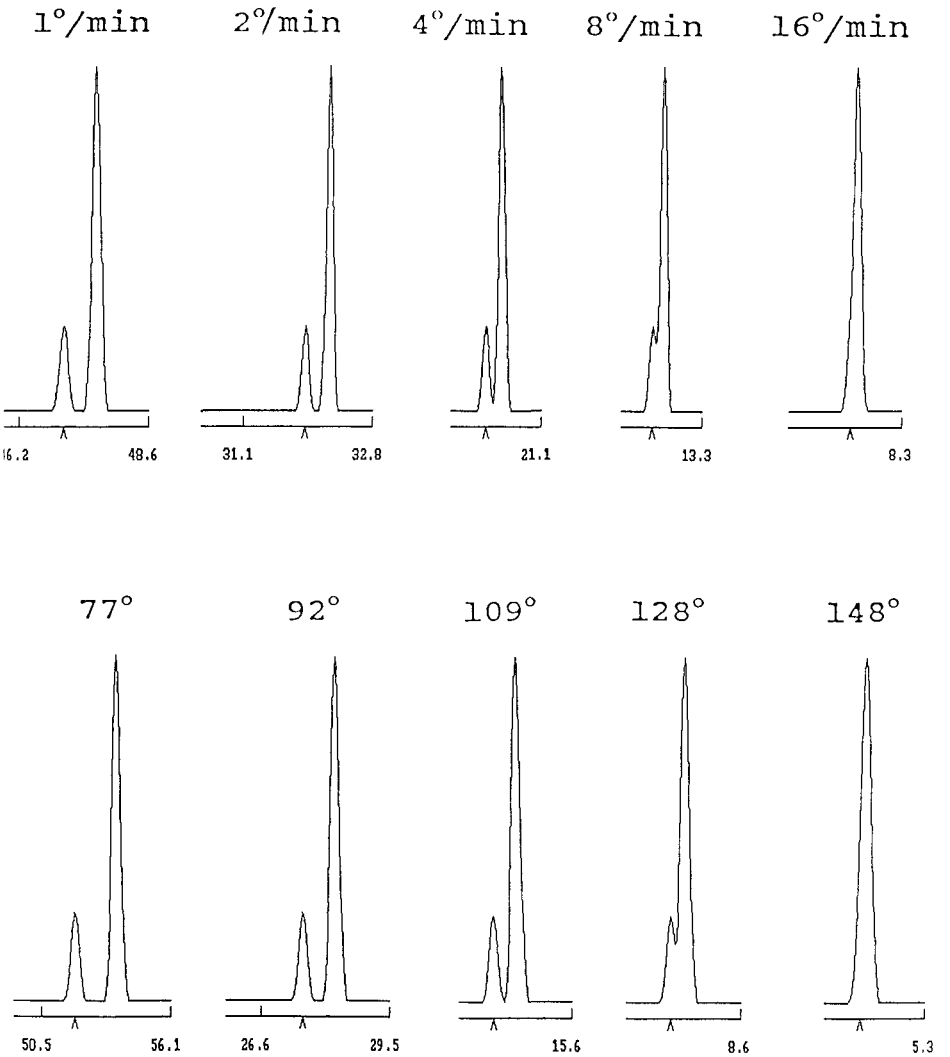

Fig. 4. Corresponding separations of band-pair marked by an asterisk in Fig. 3B (spearmint oil); temperature-programmed (top) *vs.* isothermal (bottom). Computer simulations based on experimental runs used as input for DryLab GC (2 and 8 °C/min, 50–300°C). Isothermal temperatures (bottom) chosen to give $k = \bar{k}$ for corresponding runs (*e.g.* 1°C/min and 77°C).

TABLE I

SUMMARY OF SEPARATIONS OF FIG. 4

Heating rate (°C/min)	b	$\bar{k}$	T^a (°C)	R_s	
				Prog[b]	Iso[b]
1	0.0295	29	77	2.1	2.7
2	0.059	14	92	1.8	2.1
4	0.110	7.2	109	1.4	1.5
8	0.236	3.6	128	1.0	0.9
16	0.472	1.8	148	0.5	0.4

[a] Temperature for isothermal separation where $k = \bar{k}$.
[b] Programmed-temperature ("Prog") and isothermal ("Iso") values.

thermal temperature bottom). The isothermal temperatures were selected[a] to give $k = \bar{k}$ for each set of corresponding runs (1°C/min, 77°C; 2°C/min, 92°C; etc.). It is readily seen that corresponding programmed and isothermal separations are generally similar, as predicted by analogy from the case of isocratic *vs.* gradient elution in HPLC. Table I provides a quantitative assessment of the comparisons of Fig. 4. Here it is seen that the resolution of corresponding runs (where $k = \bar{k}$) is about the same, as expected; the only exceptions are for large values of k, where the isothermal resolution tends to be a little higher (this minor discrepancy is a consequence of the LES approximation). The concept (embodied in Fig. 1) of corresponding temperature-programmed and isothermal separations is nevertheless confirmed.

Variability of values of S for different solutes

Values of S and k_0 were obtained for the components of several samples that were separated on the three columns described in ref. 1. Plots of S *vs.* $\log k_0$ were made for each sample/column combination, as illustrated in Fig. 2. The average deviation of values of S from the best-fit curve was determined and expressed as a "deviation in S" (%). Table II summarizes these results. Returning to Fig. 2A, we see that the relatively non-polar rapeseed-oil sample separated on the slightly polar DB-5 column shows only minor deviations of data points from the solid curve ($\pm 0.4\%$, see Table II). The more polar herbicide sample of Fig. 2C, however, exhibits a considerably greater scatter of data points, and the average deviation in S is correspondingly larger ($\pm 2.5\%$, Table II). The pesticide sample of Figure 2B exhibits an intermediate scatter of data points ($\pm 1.6\%$ in S, Table II).

As noted in the Theory section, deviations of S as in Fig. 2 (for a given GC system) should be smaller for non-polar samples separated on less polar stationary phases. Systems 1–3 of Table II are examples of "non-polar/non-polar" separations of this type, and moderate deviations in S are found[b] (1.6–2.3) as expected. The

[a] That is, given a heating rate r (*e.g.*, 2°C/min), eqn. 4 defines a value of $\bar{k}$, and eqn. 1 ($k = \bar{k}$) results in a corresponding value of the temperature T (*e.g.*, 92°C in the present example).

[b] The deviations in S for the gasoline samples (Nos. 1,2) of Table II are known to arise mainly from differences in molecular shape [25]; *e.g.*, *n*-alkanes *vs.* branched alkanes *vs.* cyclic hydrocarbons of various kinds. Similar differences in shape exist for the pesticide sample (No. 3) of Table II.

TABLE II

SUMMARY OF BAND-TO-BAND VARIATIONS IN S AS DETERMINED FROM PLOTS OF S *VS.* LOG k_0 FOR VARIOUS SAMPLES AND COLUMNS

See text and Fig. 2.

No.	Sample	Column	Deviations in S^a (%)	$\Delta S/S^b$
1	Gasoline A	SPB-1	1.8	0.025
2	Gasoline B	SPB-1	2.3	0.032
3	Pesticides	DB-5	1.6	0.022
4	Lime oil	DB-5	2.2	0.031
5	Lemon oil	DB-5	2.5	0.035
6	Rapeseed oil	DB-5	0.4	0.006
7	Barbiturates	DB-5	1.0	0.014
8	Herbicides	DB-5	2.5	0.035
9	Phenols	DB-5	4.8	0.067
10	Spearmint oil	Nukol	4.2	0.059
11	Peppermint oil	Nukol	4.4	0.062

[a] Average absolute deviation of values of S from best-fit curves as in Fig. 2.

[b] Average difference in S values (ΔS) for two adjacent bands, divided by S [ΔS is equal to $(2)^{0.5}$ times the "deviation in S"].

separation of moderately polar samples on less polar columns should also yield smaller deviations in S, when the solutes have a similar shape and functionality; examples of such separations are provided by systems 4–7 of Table II (deviations in S of ± 0.4–2.5%). Larger deviations of S from "best-fit" values are expected (and found) for (i) polar samples of varying functionality (systems 8 and 9 of Table II: ± 2.5–4.8%) and (ii) separations of moderately polar samples of similar functionality on polar columns (systems 10 and 11 of Table II: ± 4.2–5.9%).

The dependence of GC band-spacing on deviations in S and temperature

We have seen (Fig. 1) that differences in S for adjacent bands lead to changes in relative retention (band spacing) when the temperature is changed in isothermal separations, or when the heating rate is varied in temperature-programmed runs. Eqn. 5a and b of the Theory section describe the necessary difference in solute S values for a change in temperature or programming-rate to enable the resolution of a previously unresolved band pair. The values of $\Delta S/S$ are 0.008 (temperature programming) and 0.019 (isothermal), respectively. The average values of $\Delta S/S$ for the systems of Table II are in almost every case large enough to assure significant changes in band spacing as a result of varying the column temperature or heating rate. That is, the optimization of temperature or heating rate should be useful for the separation of most samples. A collaborative study of six randomly selected samples by five different laboratories has since found this to be true in every case [26].

The preceding discussion can be summarized as follows. A change in isothermal temperature or in the heating rate of a temperature-programmed GC separation will often lead to useful changes in band spacing and resolution. The likelihood of such changes in separation will increase for more polar stationary phases, for more polar

sample molecules, and for solutes of varying functionality or molecular shape. Some of these generalizations have been pointed out by other workers [17], and examples of these effects can be clearly seen in a number of published studies.

Examples of changes in band spacing with changes in heating rate or isothermal temperature

The various samples studied by us offer many examples of changes in band spacing with experimental conditions; *i.e.*, a change in the steepness of the temperature program or a change in isothermal temperature. Fig. 3 shows chromatograms of the phenol (A) and spearmint oil (B) samples, with specific band-triplets indicated (arrows) for further discussion.

Phenol sample. The band-triplet noted in Fig. 3A (arrow) consists of 2-nitrophenol, 2,4-dimethylphenol and 2,4-dichlorophenol. Fig. 5 shows the separation of this group of solutes as a function of heating rate in temperature-programmed separation (top) or isothermal temperature (bottom). The isothermal runs are selected to provide $k = \bar{k}$ (corresponding conditions) for the matched runs (1°C/min *vs.* 51°C, 4°C/min *vs.* 83°C, etc.). As in the examples of Fig. 4, corresponding separations are in each case quite similar in terms of resolution. However these separations show band spacing changing with heating rate or temperature, due to significant differences in S values for the compounds in question (Table III). In this case, the middle band (No. 2) has a larger value of S (15.6) *vs.* the values (14.6 and 14.7) of the first and last

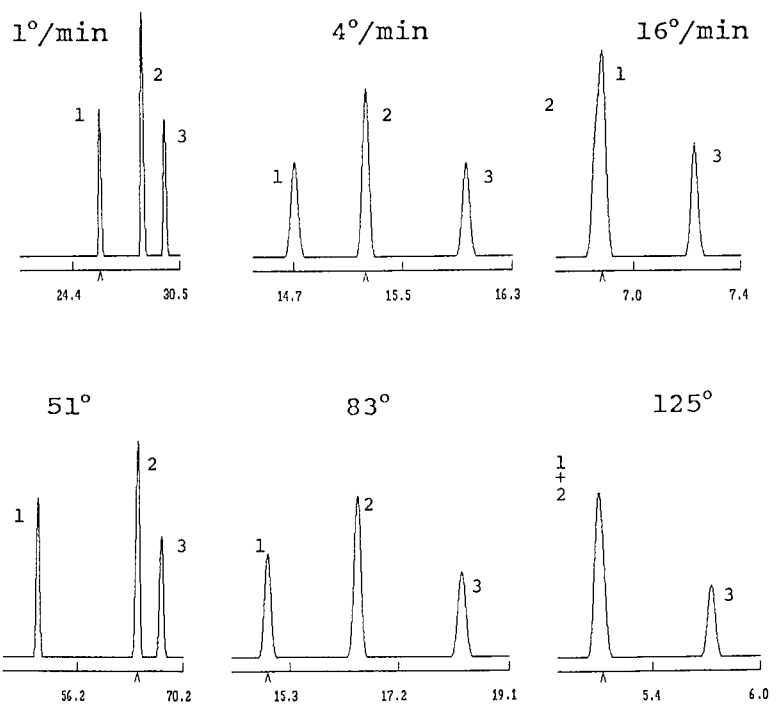

Fig. 5. Corresponding separations of phenol triplet from Fig. 3A (computer simulation). Conditions as in Fig. 3A, except as noted. Bands: 1 = 2-nitrophenol; 2 = 2,4-dimethylphenol; 3 = 2,4-dichlorophenol.

TABLE III

VALUES OF S FOR SELECTED COMPOUNDS IN THE SEPARATIONS OF FIG. 3

Solute group[a]	S[b]			$\Delta S/S$	
	1	2	3	2/1	3/2
Phenols	14.6	15.6	14.7	0.066	−0.060
Spearmint-I	16.4	16.3	16.6	−0.008	0.024
Spearmint-II	16.1	16.7	16.1	0.031	−0.031

[a] Indicated by arrows in Fig. 3; phenols (A) and spearmint oil (B).
[b] Values of S for indicated band (see Figs. 5 and 6).

bands. This means (see Fig. 1) that as k or $\bar{k}$ is increased, band 2 should move toward band 3. Examination of the examples of Fig. 5 shows this effect quite clearly. Thus for a slow heating rate (1°C/min) or a lower temperature (51°C), band 2 lies closer to band 3 than to band 1. As the heating rate or isothermal temperature is increased,

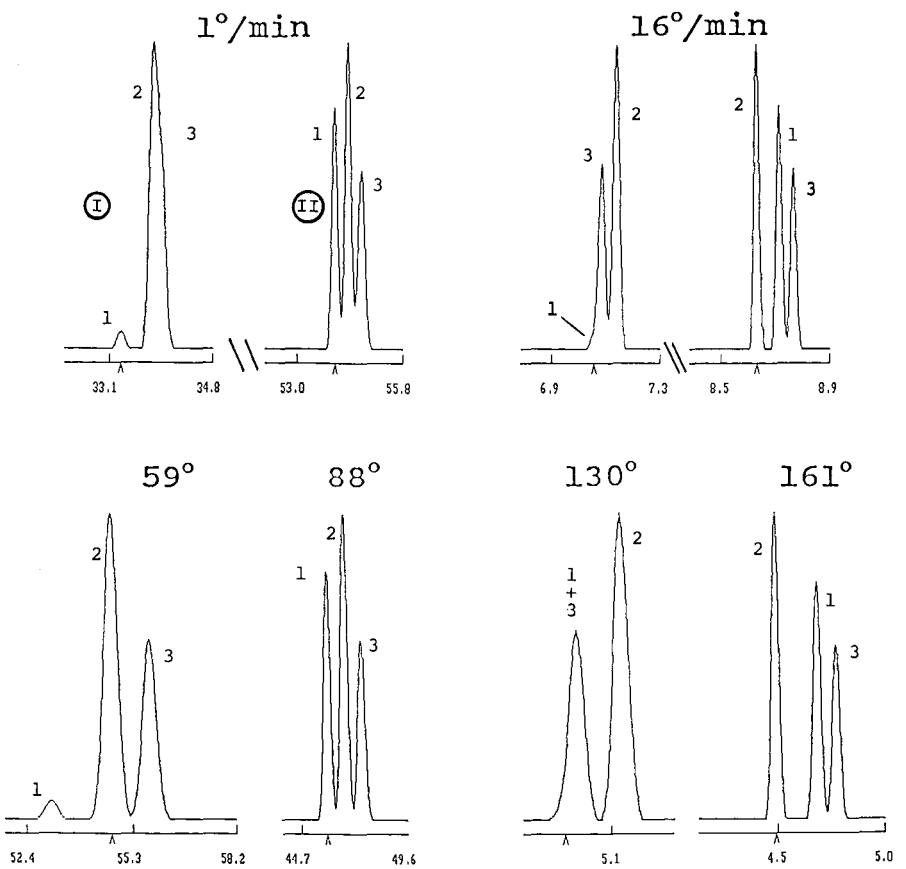

Fig. 6. Separation of band groups I and II of the spearmint oil sample (Fig. 3B, arrows) as a function of heating rate or isothermal temperature. Conditions as in Fig. 3B, except as noted.

band 2 moves toward band 1, and for the separations on the right of Fig. 5 (16°C/min or 125°C) bands 1 and 2 have merged together.

Conditions for the optimized separation of the sample of Fig. 5 would yield an equal spacing of the bands in temperature-programmed separation, corresponding to a heating rate $r = 3$°C/min. This example also emphasizes the importance of optimizing temperature-programmed or isothermal conditions for obtaining the best separation of a given sample.

Spearmint oil sample. Two groups of bands (I and II) are noted in the separation of Fig. 3B, each of which exhibits change in band spacing when heating rate or isothermal temperature is varied (Table III summarizes the relevant S values). For band-group I the last band (No. 3) has a higher value of S than the other two bands, therefore band 3 should migrate toward bands 1 and 2 as the heating rate or isothermal temperature is increased. For band-group II the second band (No. 2) has a higher value of S, so it should move toward band 1 as the heating rate or temperature is increased.

Fig. 6 shows the separation of these two band groups as a function of increase in heating rate or isothermal temperature. The vertically matched runs in Fig. 6 are for corresponding conditions ($k = \bar{k}$), and there is again a general similarity[a] in resolution for these matched runs. The general trends predicted by the S values of Table III are confirmed in these examples, and it is seen that these changes in band spacing even result in reversals of retention order: for band-group II, an increase in heating rate or temperature results in the inversion of the elution order of bands 1 and 2.

Fig. 7 shows the corresponding resolution maps for each band-group (I, 7A; II, 7B) of the spearmint sample, as well as the separation for an optimized heating rate (arrow). These examples again illustrate the potential dependence of separation on heating rate in temperature-programmed GC runs. Similar maps could be constructed for the isothermal separations, but these are not shown.

Change in column length or flow-rate

Once a temperature program has been designed for optimum band spacing (and resolution), it may be desirable to change the column length or flow-rate as a means of either increasing resolution or decreasing run time. It is important to recognize that a change in column length or flow-rate will generally change the band spacing, according to eqn. 4. That is, *if it is desired to maintain the same band spacing when varying column length or flow-rate, the value of b (or $\bar{k}$) in eqn. 4 must be maintained constant.* For example, if column length is increased by a factor x, or flow-rate is decreased by the same factor, then run time must be increased by x-fold. Otherwise b (and $\bar{k}$) changes, and band spacing can change as well; as seen in Fig. 1.

CONCLUSIONS

Previous workers have recognized that changes in band spacing (values of α) are possible when the column temperature is changed in GC, especially for mixtures of

[a] The similarity of corresponding separations in Figs. 5 and 6 is less pronounced than in Fig. 4, because eqn. 4 is strictly correct only for the case of band-groups that have equal S values.

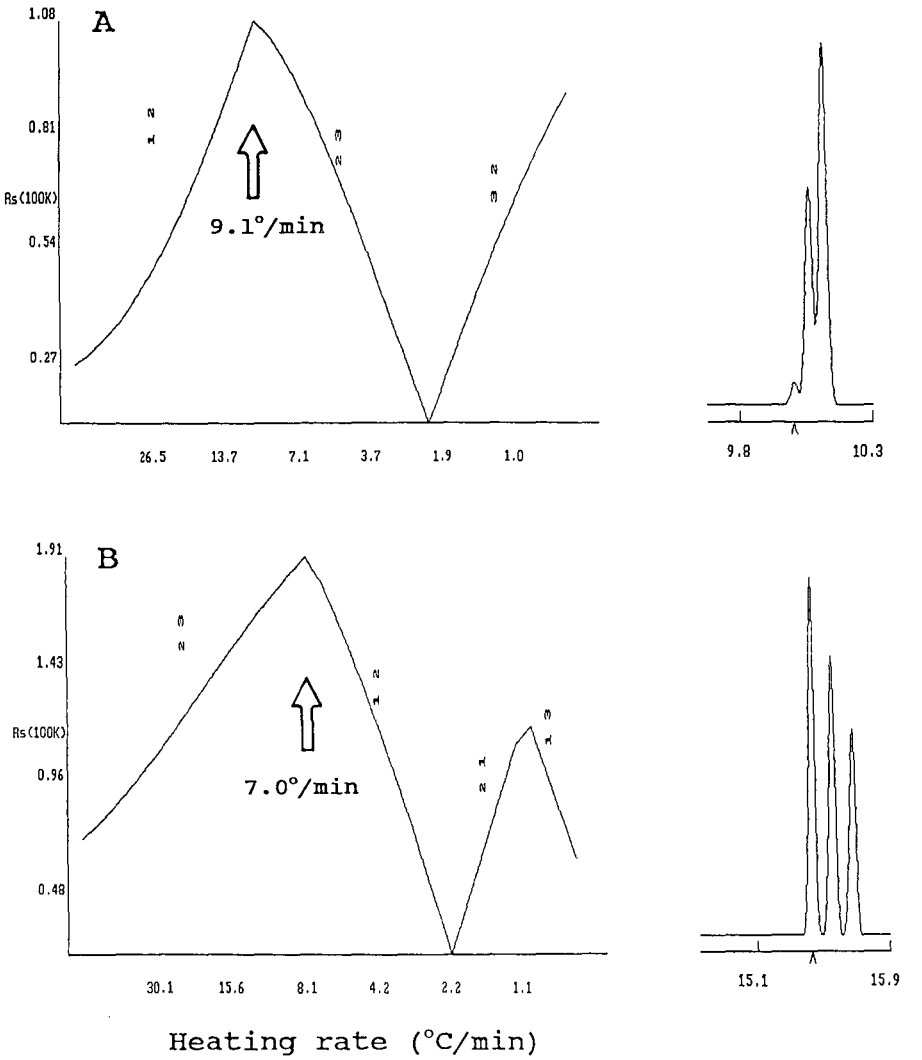

Fig. 7. Resolution maps and optimized separations (arrows) for the temperature programmed separations of band groups I (A) and II (B) of the spearmint oil sample; see Fig. 6.

polar and non-polar compounds separated on a polar column. This suggests that there is often an optimum (intermediate) isothermal temperature for such separations. In the present study, several sample/column combinations that involved hundreds of individual solutes of varying polarity were studied experimentally, in order to better understand this phenomenon. While the present study confirms the possible change of retention order for mixtures of polar plus non-polar compounds separated on polar columns, it appears that useful changes in separation with temperature are not limited to this case. Thus non-polar samples (*e.g.*, hydrocarbons) separated on

non-polar columns can also exhibit significant changes in band spacing (due primarily to differences in molecular shape).

A general treatment (based on a linear-elution-strength or LES model) is also presented for the dependence of band spacing on both heating rate or isothermal temperature in the GC separation of a sample. It is shown that similar separations of adjacent sample bands can be achieved by either temperature-programmed or isothermal elution, when "corresponding" conditions are used; *i.e.*, such that the average retention in isothermal (k) or programmed ($\bar{k}$) runs is made equal. This means that changes in heating rate will often result in changes in band spacing (and resolution) for the case of temperature-programmed GC separation.

On the basis of the present study, it appears that temperature-related changes in band spacing are generally large enough to be worth exploiting —in order to maximize sample resolution. Some examples of temperature-programmed GC method development based on this approach (including computer simulation) are described in ref. 26 and the following paper [27].

REFERENCES

1 D. E. Bautz, J. W. Dolan and L. R. Snyder, *J. Chromatogr.*, 541 (1991) 1.
2 J. W. Dolan, D. C. Lommen and L. R. Snyder, *J. Chromatogr.*, 485 (1989) 91.
3 J. Schmidt, *J. Chromatogr.*, 485 (1989) 421.
4 T. Sasagawa, Y. Sakamoto, T. Hirose, T. Yoshida, Y. Kobayashi, Y. Sato and K. Koizumi, *J. Chromatogr.*, 485 (1989) 533.
5 I. Molnar, R. Boysen and P. Jekow, *J. Chromatogr.*, 485 (1989) 569.
6 R. G. Lehmann and J. R. Miller, *J. Chromatogr.*, 485 (1989) 581.
7 D. J. Thompson and W. D. Ellenson, *J. Chromatogr.*, 459 (1989) 607.
8 J. D. Stuart, D. D. Lisi and L. R. Snyder, *J. Chromatogr.*, 459 (1989) 657.
9 W. E. Harris and H. W. Habgood, *Programmed Temperature Gas Chromatography*, Wiley, New York, 1967.
10 L. R. Snyder, in Cs. Horváth (Editor), *High-performance Liquid Chromatography —Advances and Perspectives*, Vol. 1, Academic Press, New York, 1980, p. 208.
11 P. Jandera and J. Churacek, *Gradient Elution in Column Liquid Chromatography*, Elsevier, Amsterdam, 1985.
12 L. R. Snyder, M. A. Quarry and J. L. Glajch, *Chromatographia*, 24 (1987) 33.
13 B. F. D. Ghrist, B. S. Cooperman and L. R. Snyder, *J. Chromatogr.*, 459 (1989) 1.
14 B. F. D. Ghrist and L. R. Snyder, *J. Chromatogr.*, 459 (1989) 25.
15 B. F. D. Ghrist and L. R.Snyder, *J. Chromatogr.*, 459 (1989) 43.
16 R. A. Hively and R. E. Hinton, *J. Gas Chromatogr.*, 6 (1968) 903.
17 R. R. Freeman and W. Jennings, *J. High Resolut. Chromatogr. Chromatogr. Commun.*, 10 (1987) 231.
18 R. J. Pell and H. L. Gearhart, *J. High Resolut. Chromatogr. Chromatogr. Commun.*, 10 (1987) 388.
19 G. Castello and T. C. Gerbino, *J. Chromatogr.*, 437 (1988) 33.
20 J. Krupcik, D. Repka, E. Benicka, T. Hevesi, J. Nolte, B. Paschold and H. Mayer, *J. Chromatogr.*, 448 (1988) 203.
21 Y. Guan, J. Kiraly and J. A. Rijks, *J. Chromatogr.*, 472 (1989) 129.
22 L. Bincheng, L. Bingchang and B. Koppenhoefer, *Anal. Chem.*, 60 (1988) 2135.
23 E. V. Dose, *Anal. Chem.*, 59 (1987) 2414.
24 J. H. Hildebrand and R. L. Scott, *The Solubility of Nonelectrolytes*, Dover, New York, 3rd edn., 1964, p. 77.
25 L. R. Snyder, *J. Chromatogr.*, 179 (1979) 167.
26 G. N. Abbay, E. F. Barry, S. Leepiopatpiboon, T. Ramstad, M. C. Roman, R. W. Siergiej, L. R. Snyder and W. Winniford, *LC · GC*, 9 (1991) 100.
27 L. R. Snyder, D. E. Bautz and J. W. Dolan, *J. Chromatogr.*, 541 (1991) 35.

Journal of Chromatography, 541 (1991) 35–58
Elsevier Science Publishers B.V., Amsterdam

CHROM. 22 997

Computer simulation as an aid in method development for gas chromatography

III. Examples of its application

L. R. SNYDER*, D. E. BAUTZ and J. W. DOLAN
LC Resources Inc., 3182C Old Tunnel Road, Lafayette, CA 94549 (U.S.A.)
(Received August 13th, 1990)

ABSTRACT

The use of computer simulation for developing optimized gas chromatographic (GC) separations is illustrated for several samples. Resolution maps (plots of R_s *vs.* heating rate r) for different starting temperatures provide a means for the rapid exploration of separation as a function of the temperature program in the case of programmed-temperature GC. Isothermal separations are easily developed by trial and error, because of the speed of computer simulation. More complex samples may require multi-ramp temperature programs; these require a greater method development effort, but partial resolution maps can help facilitate this process.

INTRODUCTION

The best approach to gas chromatographic (GC) method development depends on the sample and the goals of separation. If the quantitation of all sample components is required, the baseline resolution of every band pair ($R_s > 1.5$) will usually be the main objective. Even greater resolution may be desirable when the sample contains bands of quite different size, or when it is anticipated that future samples may contain additional components (*e.g.*, interferences) not present in the sample used during method development. Achieving an acceptable separation within a minimum run time is also a common goal. Finally, there may be other considerations; *e.g.*, a need to restrict the maximum column temperature within certain limits.

The choice of a method development procedure is also affected by the complexity of the sample. Many samples consist of literally hundreds of individual compounds, where it is usually impractical to attempt the resolution of all components. In many such cases, the separation and quantitation of a smaller number of "key" bands may be required. For samples that contain fewer components, isothermal separation will be preferred in some cases, because temperature-programmed runs (including the time for cooling the column oven after the separation) often require more time.

Method development can be somewhat tedious for the case of temperature-

0021-9673/91/$03.50

programmed separations (of primary interest in this study), because resolution and run time depend on several different variables: heating rate, starting temperature, and the shape of the temperature program (linear or multi-ramp). Thus a large number of experiments may be required to adequately explore the various separation options. Computer simulation can greatly reduce the time and effort required for GC method development, while achieving better final methods as measured by resolution, run time, etc. The preceding two papers [1,2] have described the basis of a computer-simulation approach to method development for GC. The accuracy of this software (DryLab GC) for the prediction of separation has been confirmed, and the value of optimizing the heating rate in temperature-programmed separations (or the temperature in isothermal runs) has been demonstrated.

In the present paper we will illustrate how computer simulation can be applied to GC method development for samples of different types and for different separation goals.

EXPERIMENTAL

Equipment, materials and procedures are described in Part I [1].

RESULTS AND DISCUSSION

The general similarity of temperature-programmed GC and gradient elution high-performance liquid chromatography (HPLC) has already been noted [1–3] and the development of optimized gradient elution procedures using computer simulation has been described in several previous papers [4–15]. These generalizations for gradient elution can be applied with little modification for the similar development of programmed-temperature GC separations. This will allow us to simplify and condense the following discussion. Three different samples will be used to illustrate how computer simulation can facilitate GC method development. Since it has been established in Part I [1] that DryLab GC can provide accurate predictions of separation, we will make use of both simulated and experimental runs in the following treatment.

Herbicide sample

The two initial chromatograms used for computer simulation of this 13-component sample are shown in Fig. 1A and B. Excellent resolution ($R_s > 7$) is noted for all bands in both runs, suggesting that the separation of this sample will not be difficult. Our major concern will therefore be with other aspects of separation: run time, isothermal *vs.* programmed separation, etc.

It is generally useful to examine a resolution map (Fig. 2) at the beginning of method development; *i.e.*, a plot of minimum resolution *vs.* heating rate r (for linear temperature programs). An arbitrary column plate number N can be assumed at this point, but it is recommended that bandwidths for two, well-resolved, early- and late-eluting peaks from the chromatogram of Fig. 1A (or B) be measured. This allows DryLab GC to predict plate numbers for each band in the chromatogram, as a function of experimental conditions (initial temperature, heating rate, shape of the temperature program, etc.) and the retention characteristics of the solute. All simulations described in this paper are based on the determination of column plate number in this way, as described in ref. 1.

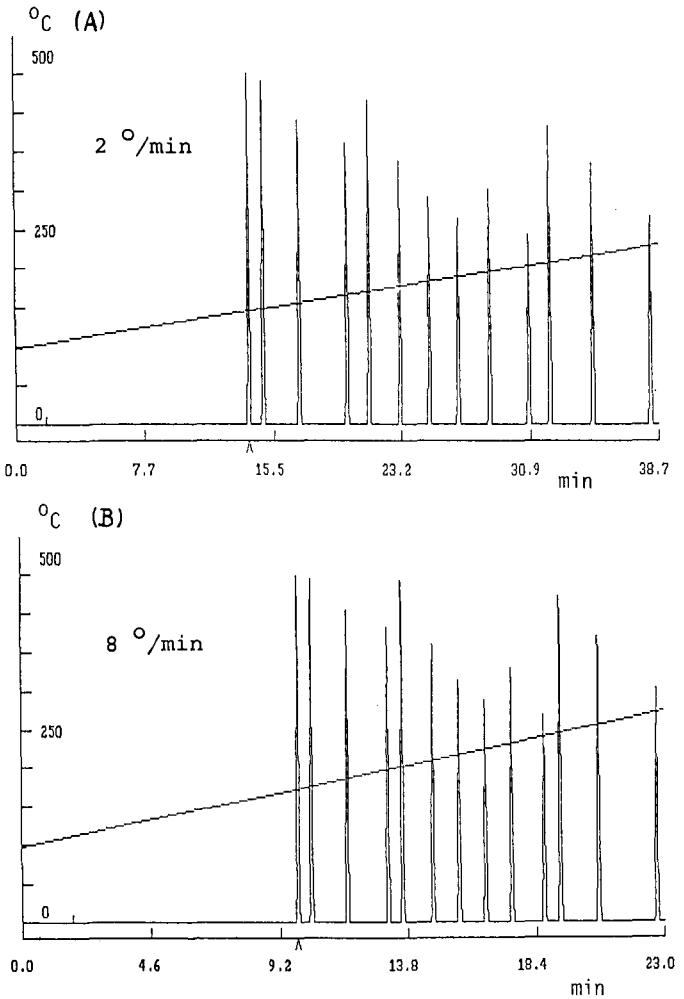

Fig. 1. Experimental chromatograms (recreated by computer simulation) for the herbicide sample; temperature programs shown as overlays. Conditions: DB-5 column, 1 ml/min, 100°C starting temperature; (A) 2°C/min; (B) 8°C/min.

Resolution maps as in Fig. 2 should be requested for different starting temperatures T_0. This allows a quick assessment of the trade-off between resolution and run time as a function of T_0. The map of Fig. 2A (T_0 = 50°C) indicates that bands 4 and 5 are the critical pair for heating rates r > 10°C/min, while bands 1 and 2 are the least resolved for lower values of r. Fig. 2A–C (for 50°C < T_0 < 150°C) show a continual increase in resolution as the heating rate is decreased (and run time increases). That is, there is no intermediate temperature which provides maximum resolution for the herbicide sample. There is also not much difference in the resolution maps of Fig. 2A–C, indicating that the starting temperature is not of critical importance, as long as T_0 < 150°C. The map for T_0 = 200°C (Fig. 2D), on the other hand, shows a marked

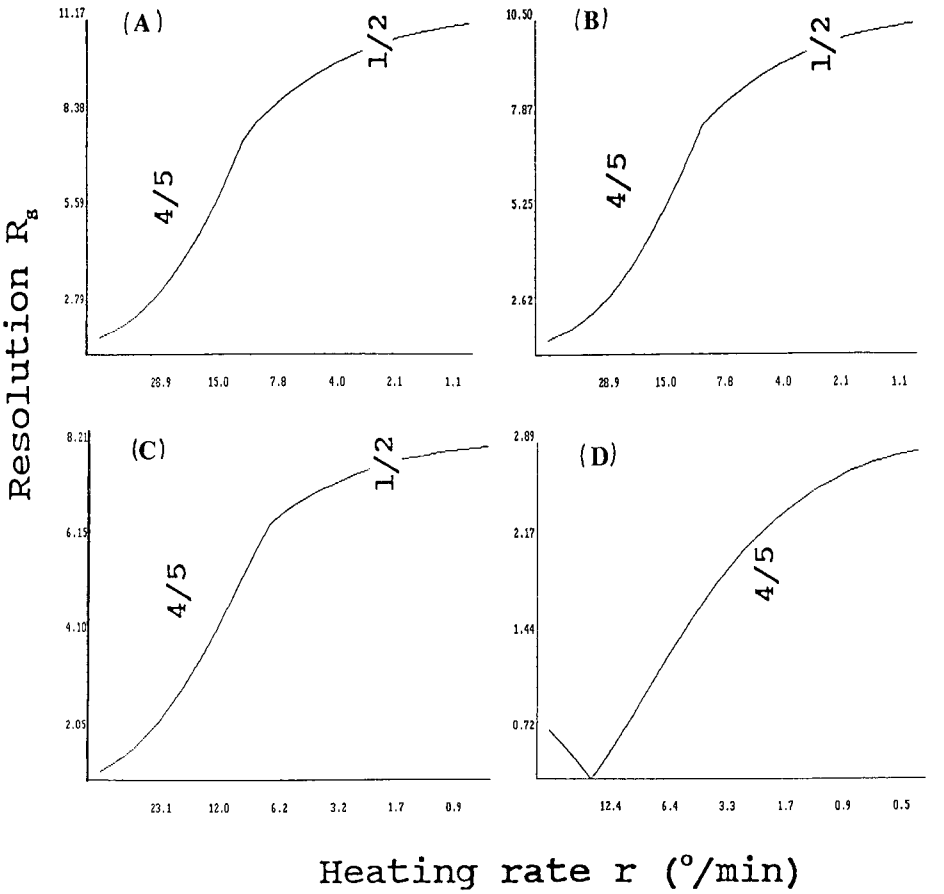

Fig. 2. Resolution maps for the herbicide sample as a function of starting temperature T_0 and heating rate r. Conditions as in Fig. 1 except where noted otherwise. (A) $T_0 = 50°C$; (B) $T_0 = 100°C$; (C) $T_0 = 150°C$; (D) $T_0 = 200°C$.

decrease in resolution for all values of r, suggesting that the optimum starting temperature is $T_0 < 200°C$.

If our goal is the separation of this sample in the shortest possible time, we can carry out computer simulations in order to predict run time and maximum column temperature (corresponding to elution of the last sample band) as a function of starting temperature, for some minimum resolution. Table I summarizes this information for the present sample, for a minimum value of $R_s = 2.0$. The shortest run time (10.0–10.2 min) is obtained with a starting temperature of 100–150°C and a heating rate of 17–23°C/min; the separation for $T_0 = 100°C$ and 23.5°C/min is shown in Fig. 3A. One consideration with these conditions, however, is the need to heat the column to 320–340°C in order to elute the last band. If the present column were not recommended for use above 250°C, the separation of Fig. 3A would then be impractical.

An alternative (assuming a maximum column temperature of 250°C) is to use a

TABLE I

CONDITIONS FOR THE SEPARATION OF THE HERBICIDE SAMPLE OF FIG. 1 IN MINIMUM TIME WITH A RESOLUTION R_s = 2.0

Linear temperature programs, computer simulations.

T_0 (°C)	r (°C/min)	Last band t_R[a] (min)	Maximum temperature[b] (°C)
50	25.5	11.6	346
100	23.5	10.2	340
150	17.0	10.0	320
200	2.5	18.9	247

[a] This is equal to the run time (excluding the time to cool down the column oven after each run).
[b] Temperature at which last band elutes.

linear program to 250°C and then maintain an isothermal hold for the balance of the separation. This option is demonstrated in Fig. 3B, for a starting temperature of 100°C and a heating rate of 23.5°C/min. Since the critical band pair is 4/5 for these

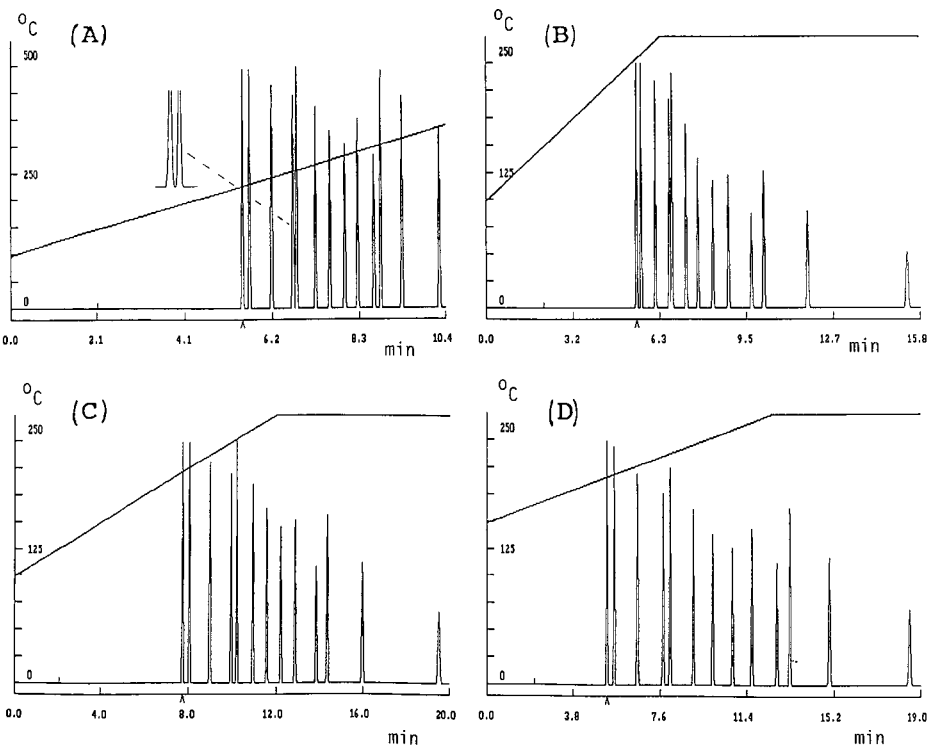

Fig. 3. Predicted separations of the herbicide sample for different conditions. (A) 100°C starting temperature, 23.5°C/min, R_s = 2.0; (B), same as (A) but with an isothermal hold after 250°C (R_s = 2.0); (C) 100°C starting temperature, 21°C/min, isothermal hold after 250°C, R_s = 5.0; (D) 150°C starting temperature, 8°C/min, isothermal hold after 250°C, R_s = 5.0.

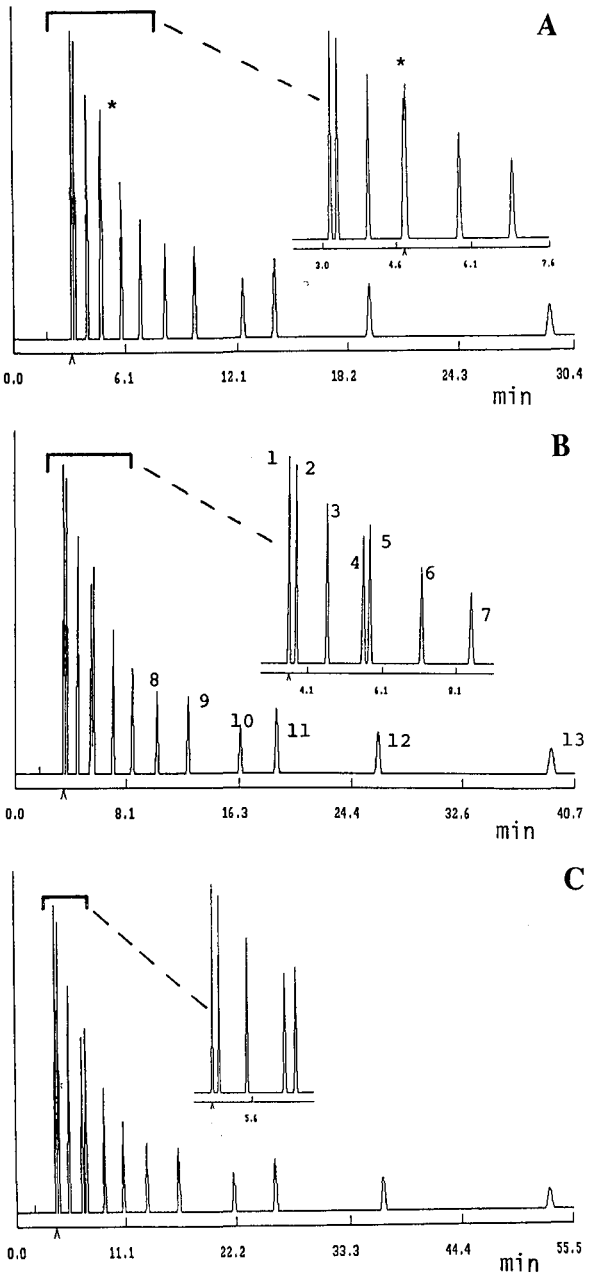

Fig. 4. Predicted isothermal separations of the herbicide sample for different temperatures: (A) 210°C; (B) 200°C; (C) 190°C. Other conditions as in Fig. 1. * = Overlapped bands.

conditions —which elutes well before 250°C— the resolution of the sample is not affected (*vs.* the separation of Fig. 3A) by the isothermal hold. The run time is increased from 10 min in Fig. 3A to 15 min in Fig. 3B, but any problem with excessive heating of the column has now been resolved.

For "easy" separations such as this, it is often attractive to aim for a sample resolution which is greater than "minimum", in order to build in a "safety factor". This allows a greater margin of error in the transfer of the method to other laboratories, and it ensures that the method will work for columns of lower plate number (*e.g.*, older columns). The resolution maps of Fig. 2 indicate that resolution increases quite rapidly with decrease in heating rate, suggesting that a major increase in R_s is possible for a modest increase in run time. This is indeed the case, as shown in Fig. 3C and D —for separation conditions that in each case yield a minimum resolution of $R_s = 5$[a]. The separation of Fig. 3D ($T_0 = 150$°C) is about a minute shorter than that of Fig. 3C, corresponding to a run time of 18.5 min. The column equilibration time will also be less for this run, because the final column temperature (250°C) needs to be lowered only to 150°C, rather than 100°C in the run of Fig. 3C.

A final consideration is the possibility of trading the extra resolution ($R_s = 5$) of the run in Fig. 3D for a much shorter run time, by shortening column length. Since resolution is approximately proportional[b] to (column length)$^{0.5}$, a reduction in column length by a factor of 4 (from 30 to 7.5 m for the present example) would still provide a resolution of bands 4/5 of $R_s = 0.5 \times 5 = 2.5$, but in a run time of only 5 min (run time is proportional to column length, other factors equal).

Isothermal separation. The possible isothermal separation of this sample is readily addressed by simulations at different temperatures. Fig. 4 summarizes predicted runs at 190, 200 and 210°C. The resolution of bands 4/5 is unacceptable at 210°C ($R_s = 0.7$ for bands 4 and 5; marked by the asterisk in Fig. 4), and the run time (55 min) is excessive for $T = 190$°C. An isothermal run at 200°C gives acceptable resolution for all bands ($R_s > 2.3$), but the 40-min run time is rather long, and the last bands are broadened to the point of diminished detectability. In short, it appears that the herbicide sample is not a good candidate for isothermal separation.

This application of computer simulation for the herbicide sample may appear trivial to practical workers, inasmuch as this sample is easily separated without much effort. However, the various computer simulations that are summarized above required less than an hour to carry out, and in the process a thorough understanding of the various separation options was achieved. Thus it is possible by using computer simulation to develop better methods in less time, even for the case of "easy" samples. As we will see, the potential advantages of computer simulation increase dramatically for more complex samples.

Phenol sample

This sample (initial experimental runs described in ref. 3) is also not difficult to separate. However, method development is somewhat more complicated, for reasons

---

[a] Here and in other figures, the temperature program for a given separation is shown as an overlay in computer-simulated chromatograms.

[b] This relationship is not exact, because of changes in the pressure drop across the column for the same flow-rate.

that will become apparent. Fig. 5A–D shows the resolution maps for this sample, based on starting temperatures of 25, 50, 75 and 100°C, respectively. As in the case of the herbicide sample (Fig. 2), starting temperatures of 25–75°C result in similar changes of resolution with heating rate (Fig. 5A–C). For a sufficiently high starting temperature (100°C, Fig. 5D), however, there is a significant drop in resolution. The resolution map for T_0 = 25°C can be used to discuss the features of the other maps (for T_0 < 100°C).

In Fig. 5A it is seen that there is an optimum intermediate temperature for this separation, corresponding to r = 7.0°C/min. For higher heating rates, the resolution of bands 3/4 decreases, while for lower values of r the resolution of bands 1/2 decreases. A heating rate of r = 7.0°C/min is therefore favored for this sample (if T_0 = 25°C). A similar situation is seen for starting temperatures of 50°C (Fig. 5B) and 75°C (Fig. 5C). For T_0 = 25°C (Fig. 5A) bands 1/2 change their separation order, band 2 being eluted first for r < 2 °C/min.

If we arbitrarily select a starting temperature of 50°C and the optimum value of r (4.5°C/min, Table II), the minimum sample resolution is predicted to be R_s = 4.8

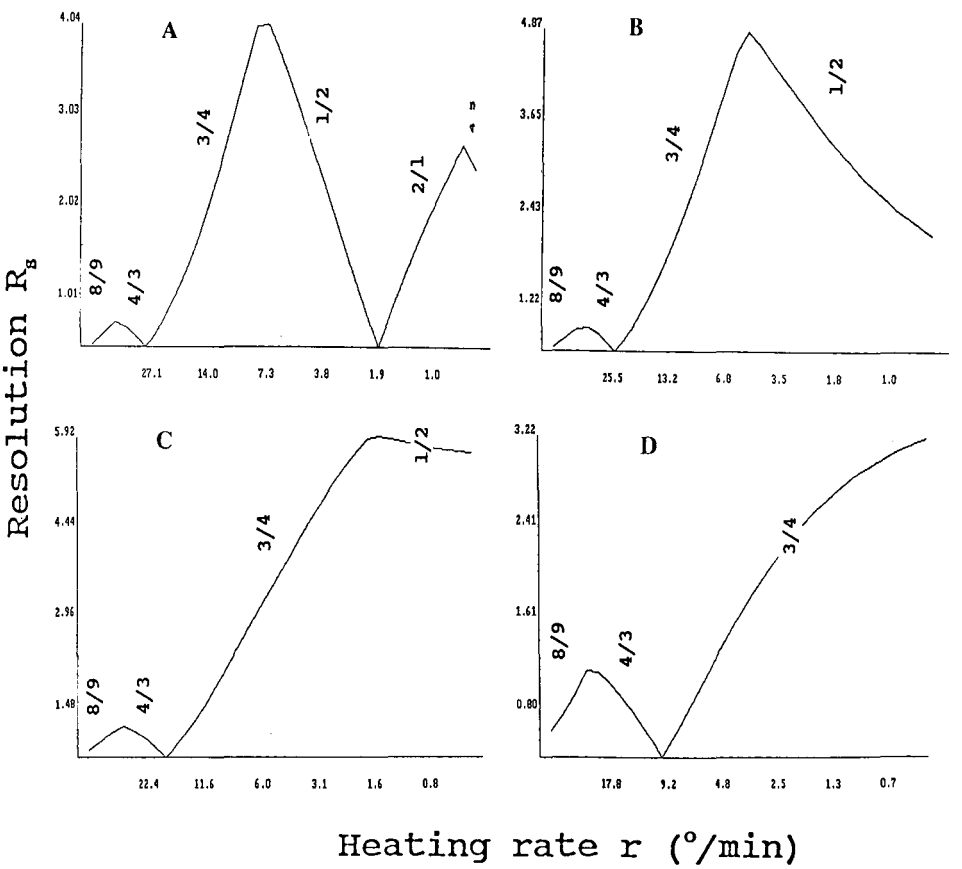

Fig. 5. Resolution maps for the phenol sample as a function of starting temperature T_0 and heating rate r. Conditions: DB-5 column, 1 ml/min. (A) T_0 = 25°C; (B) T_0 = 50°C; (C) T_0 = 75°C; (D) T_0 = 100°C.

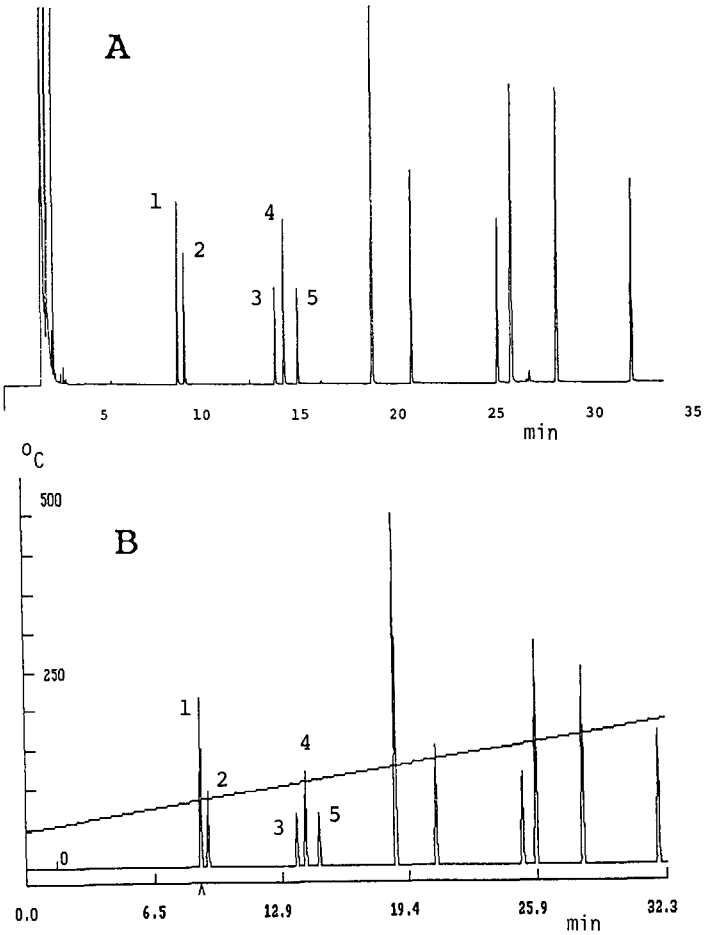

Fig. 6. Separation of the phenol sample with maximum resolution (as in Fig. 5B). Conditions: DB-5 column, 1 ml/min, 50–200°C, 4.6°C/min. (A) Experimental chromatogram; (B) predicted chromatogram.

with a run time of 32 min. This separation (experimental and predicted) is shown in Fig. 6. Note that the critical band pairs (1/2 and 4/5) occur near the beginning of the chromatogram. When this is the case, it is possible to shorten the run time significantly by increasing the heating rate after the elution of the last critical band pair (4/5). This is illustrated in Fig. 7, where run time (24 min) has been reduced by about 25%. The predicted separations of Figs. 6 and 7 agree with the experimental runs within $\pm 1.4\%$ for retention times and $\pm 5\%$ for resolution.

Table II summarizes some additional data from Fig. 5 which allow a further evaluation of the best starting temperature and heating rate for this sample. The maximum possible resolution is seen to increase with starting temperature, until $T_0 >$ 75°C. The run time increases at the same time, however, so it is not obvious which starting temperature should be preferred. If we normalize sample resolution to a value of $R_s = 2.0$, as in Table I for the herbicide sample, it is seen in Table II that any

TABLE II

SUMMARY OF RESULTS FOR PHENOL SAMPLE

Conditions: 30-m DB-5 column, 1 ml/min.

T_0 (°C)	Maximum R_s			R_s = 2.0	
	r (°C/min)	R_s	Last band t_R[a] (min)	r	t_R[a] (min)
25	7.0	4.2	27	11.5	18
50	4.6	4.8	32	10	18
75	1.5	5.9	55	7	20
100	0.5[b]	3.1	66	2.2	33

R_s = 2.0 using a shorter column (length = L)

T_0 (°C)	r[c] (°C/min)	L (m)	t_R (min)
25	7.0	11	9
50	4.5	8	9
75	1.5	5	10
100	0.5[b]	20	43

[a] Equal to run time.
[b] No maximum in R_s *vs.* heating rate map.
[c] Value for maximum resolution.

value of T_0 between 25 and 75°C will yield about the same run time (18–20 min). Since it is often undesirable to use starting temperatures near (or below) ambient, a starting temperature of 50°C with r = 10°C/min would probably be preferred for the phenol sample, if a minimum run time is important.

Run time (for R_s = 2.0) can also be reduced by reducing column length (< 30 m) rather than by increasing the heating rate. Using this approach, the run time can be shortened to about 9 min (Table II, T_0 = 25–50°C). In general, when run time is quite important, it will usually be advisable to optimize column length. The use of an increase in heating rate following elution of band 5 (as in Fig. 7) could reduce run time further from 9 to about 7 min.

Because the last band of the phenol sample elutes below 250°C, there is no need to consider limiting the temperature range of this separation, unlike the case of the herbicide sample.

Spearmint oil sample

Fig. 8 shows two experimental runs with this sample for use in computer simulation; these chromatograms are quite complex, with over 100 individual bands being recognizable. The best approach for optimizing separations such as this is determined by the separation goal, as discussed in the Introduction. In some cases, only the major bands will be of interest; *e.g.*, those comprising more than 1% of the total sample. In other instances certain trace components in the sample may require quantitation.

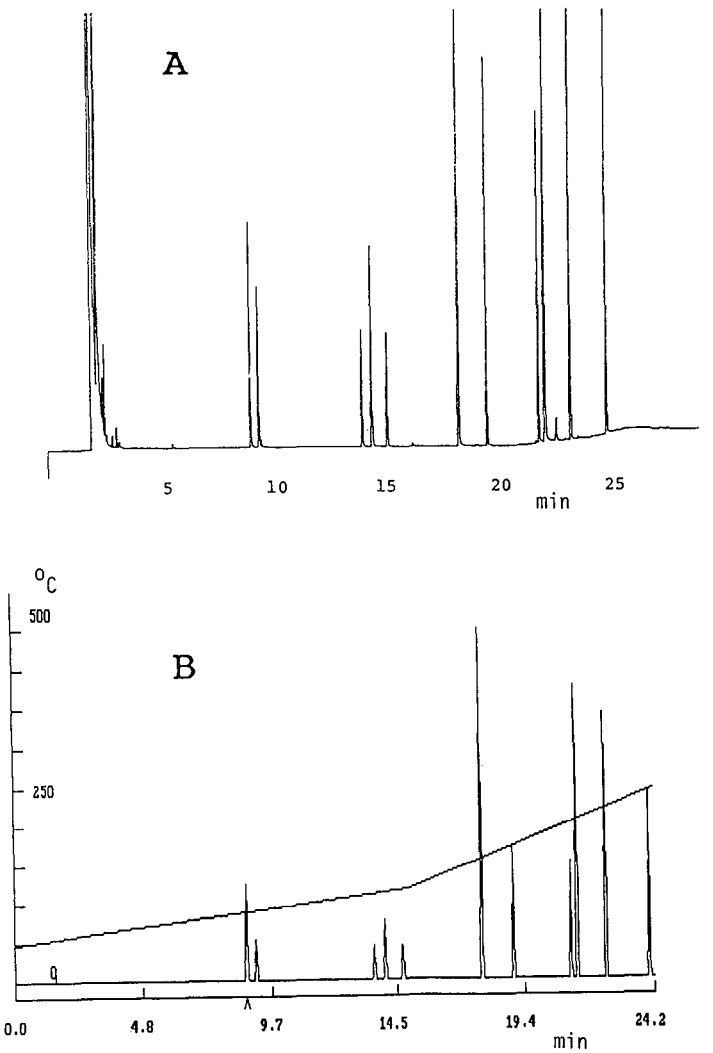

Fig. 7. Further shortening of run time in the separation of Fig. 6 by increasing the heating rate after elution of band 5. Temperature program of 50/120/250°C in 0/15/25 min; other conditions as in Fig. 6. (A) Experimental chromatogram; (B) predicted chromatogram.

Major components. Consider first the separation of the major bands in the spearmint oil sample; *i.e.*, the 19 bands with areas at least 5% as large as the largest sample band. Fig. 9 shows computer simulations that correspond to the experimental runs of Fig. 8 (same conditions), but with minor bands deleted from the chromatogram. Interestingly, all 19 bands are resolved with $R_s > 0.9$ in the run with the *higher* heating rate (8°C/min, Fig. 9B), whereas two band pairs (3/4 and 8/9) are poorly separated in the run at 2°C/min (Fig. 9A). Starting with the separation of Fig.

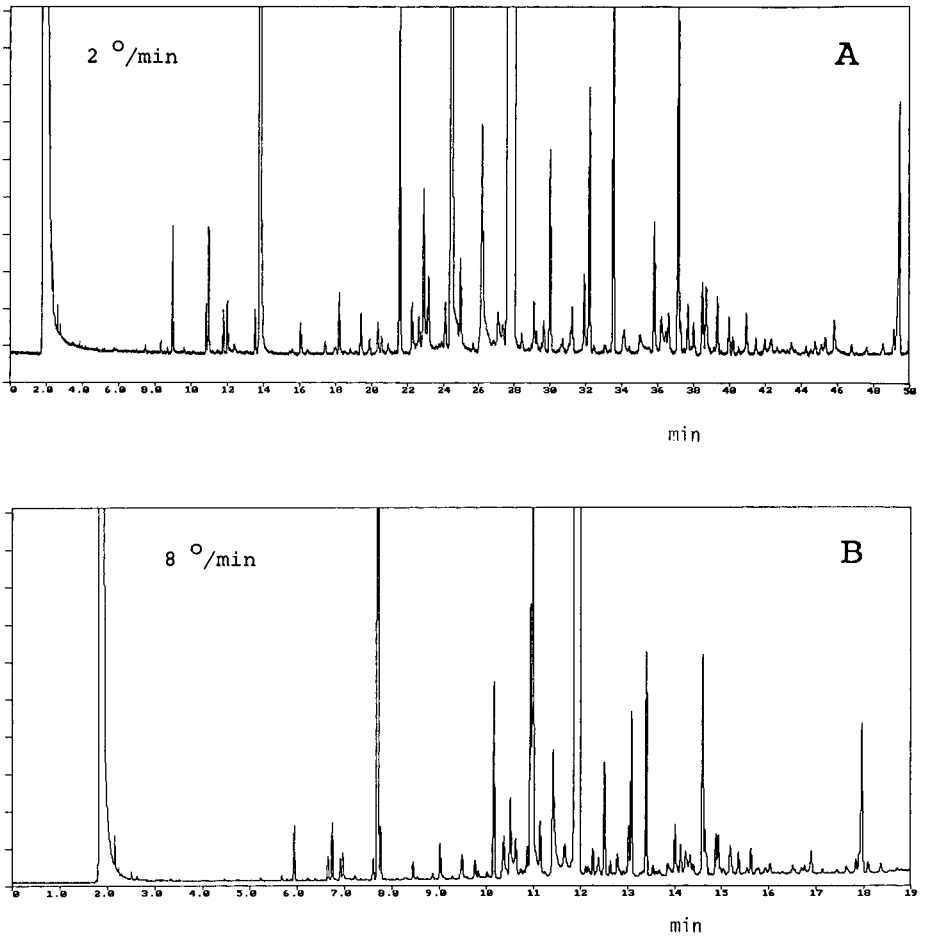

Fig. 8. Experimental runs for the spearmint oil sample. Conditions: 50–250°C, 1 ml/min, DB-5 column; (A) 2°C/min; (B) 8°C/min.

9A, conventional wisdom would suggest that a *decrease* in heating rate would be required to improve sample resolution, which in this case is not correct.

Resolution maps for the preceding 19-band sample are shown in Fig. 10A–D for T_0 = 50, 75, 100 and 125°C, respectively. It is seen that the maximum possible resolution increases with T_0 from 50 to 100°C, then decreases for T_0 = 125°C (similar to the case of the phenol sample in Fig. 5). This suggests that a starting temperature of 100°C is optimum for this sample, because of the need for maximum resolution ($R_s \geqslant 1.0$). The optimum heating rate is r = 2.8°C/min, and the predicted separation for these conditions (minimum R_s = 1.25) is shown in Fig. 11A. Because the last critical band-pair (14/15) elutes before 12 min, it is possible to shorten the run time by using a steeper temperature ramp (30 °C/min) after 12 min. The predicted separation for these conditions is shown in Fig. 11B, with a run time (16 min) that is 30% shorter than in Fig. 11A.

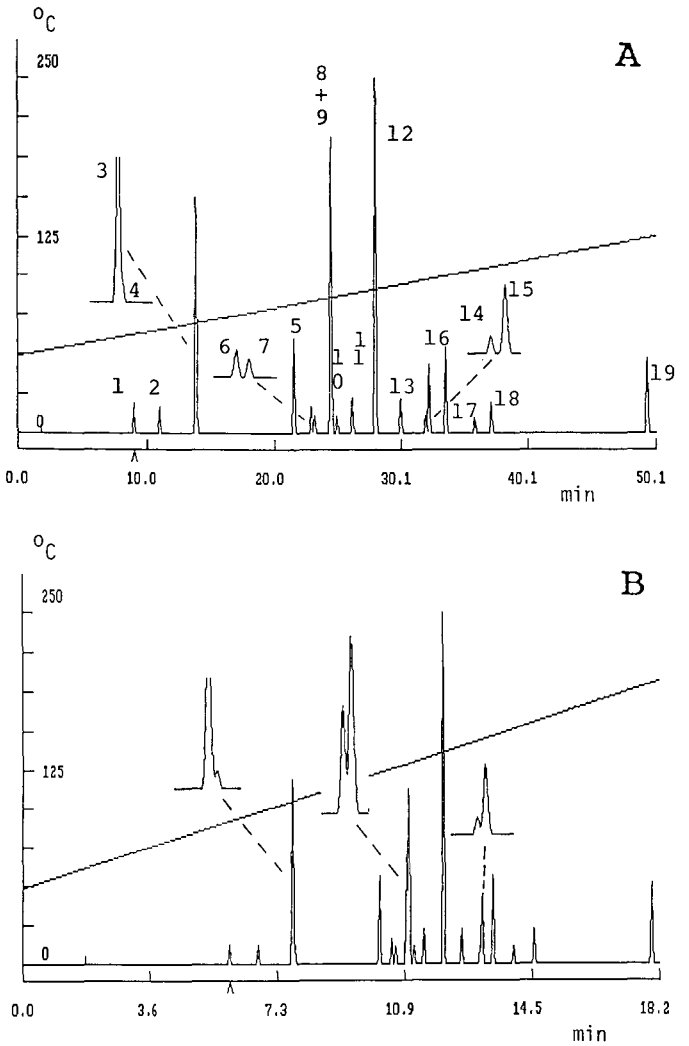

Fig. 9. Computer simulation of runs of Fig. 7 for the 19 largest bands in the chromatogram. Same conditions; (A) 2°C/min; (B) 8°C/min. Insets are magnifications of less-well-resolved band pairs.

Separations as in Fig. 11 that exhibit several critical band pairs (3/4, 8/9, 14/15; see also Fig. 10) can sometimes be improved by the use of multi-step temperature ramps. In these cases, the temperature ramp across each critical band pair is adjusted to maximize the resolution of that band pair (the similar applicability of multi-segment gradients in HPLC has been demonstrated for several samples [5,7–15]). Whether this is possible for a given sample can be quickly decided through the use of *partial resolution maps*, where the resolution of individual (critical) band pairs is studied as a function of heating rate (and starting temperature).

Fig. 12 shows such maps for T_0 = 100°C and band pairs 3/4, 8/9 and 14/15. Of

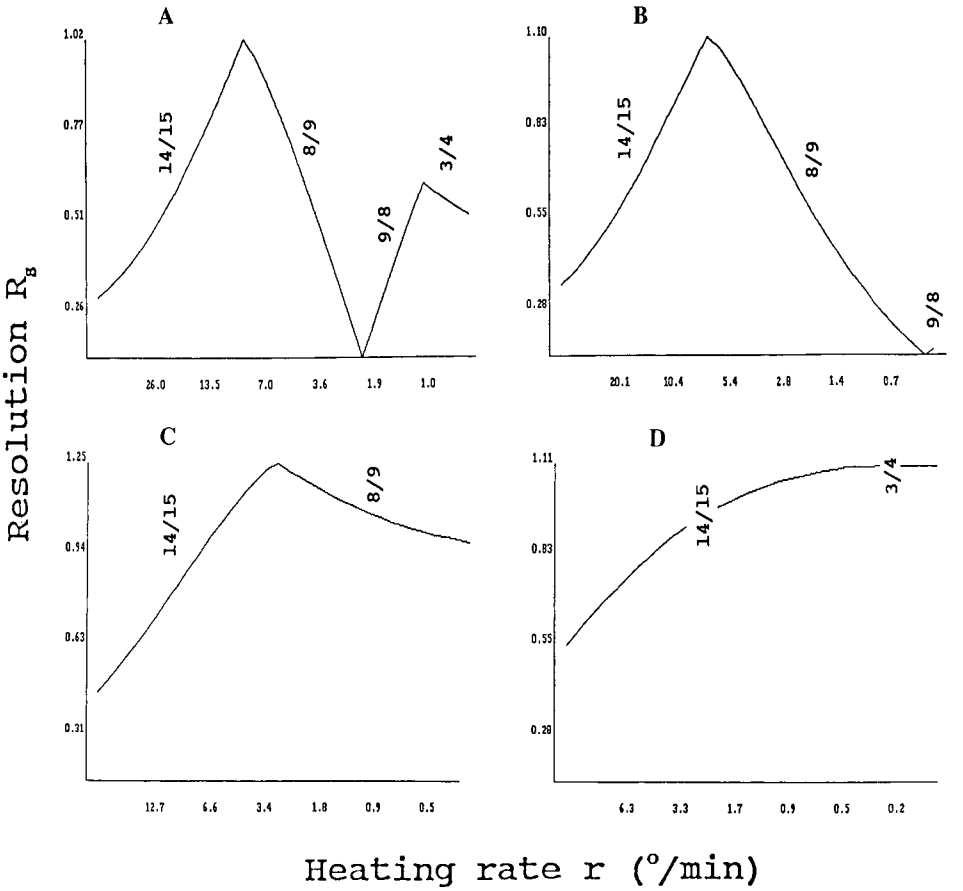

Fig. 10. Resolution maps for the 19 major bands in the spearmint oil sample, corresponding to experimental data of Fig. 8. (A) T_0 = 50°C; (B) T_0 = 75°C; (C) T_0 = 100°C; (D) T_0 = 125°C.

special interest is the map for bands 3/4, where the maximum resolution levels off at a value of R_s = 1.32. It was further established via other resolution maps that a change of T_0 does not improve this result; *i.e.*, the maximum possible resolution of bands 3/4 is R_s = 1.32 (assuming no change in stationary phase, column dimensions, flow-rate, etc). That is, no further change in the temperature program can significantly[a] increase the minimum resolution of the sample found in the linear temperature ramp of Fig. 11A (R_s = 1.25). Therefore it can be concluded that a multi-ramp temperature program will not be advantageous for the present sample.

Separation of additional bands. If bands having an area at least 2% of the largest band in the sample are included, there are a total of 47 bands to consider. We next examined optimum conditions for the separation of this 47-component sample. The

[a] A change in R_s by less than 0.1 unit is not considered significant, especially for the case of separations predicted by computer simulation.

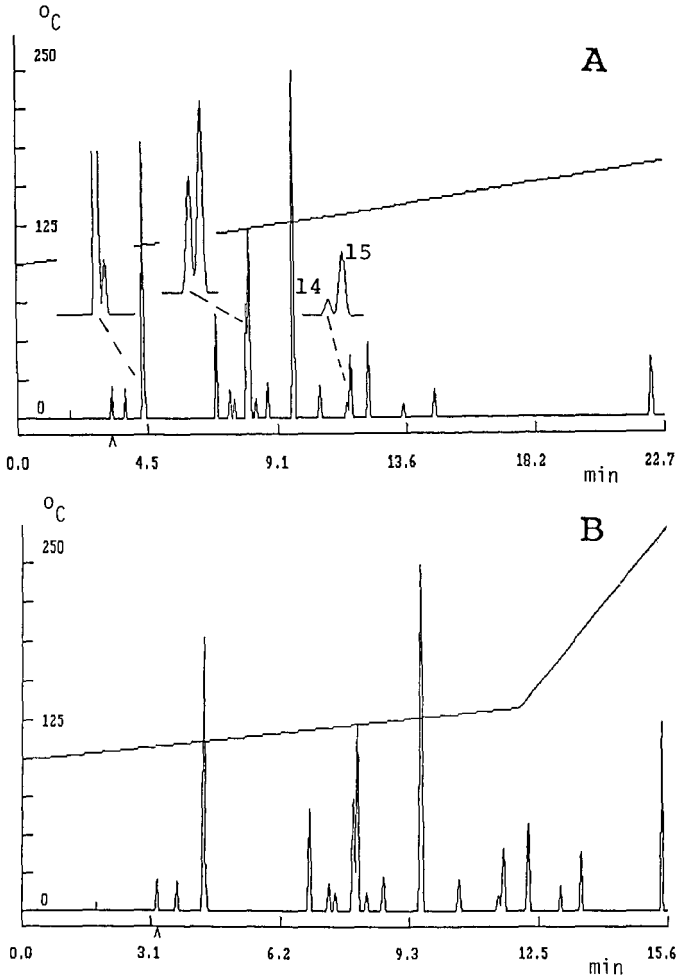

Fig. 11. Optimized separations of the 19 major bands in the spearmint oil sample. Conditions as in Fig. 7 except as otherwise noted. (A) T_0 = 100°C, 2.8°C/min; (B) same as (A), except 30°C/min after 12 min.

two experimental runs of Fig. 8 were again used as input data for computer simulation. However, for a sample this complex, it is imperative to verify that all bands have been properly matched between the two chromatograms. This is most easily accomplished by carrying out a run with an intermediate heating rate (4°C/min for the present case) and comparing the experimental and predicted retention times. If all bands have been properly assigned, there should be good agreement between these two sets of numbers. Such a comparison for a 4°C/min run with T_0 = 10°C is shown in Table III. Here it is seen that the two sets of retention times agree within ± 1.0% (average), and no individual retention-time pairs show unexpectedly large deviations.

Table IV summarizes the optimum conditions obtained from resolution maps for different values of T_0: heating rate r, value of R_s for this heating rate, and the run time. Maximum resolution can be obtained with starting temperatures of $50 < T_0 <$

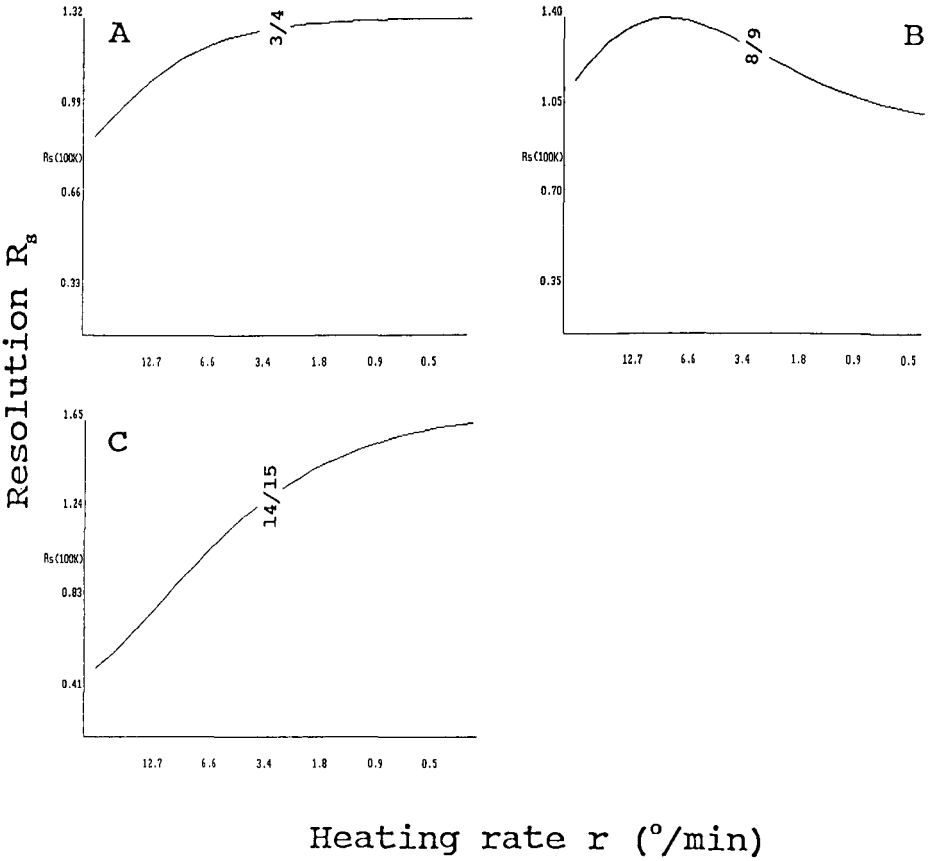

Fig. 12. Partial resolution maps for the 19 major bands of the spearmint oil sample. Conditions: T_0 = 100°C; otherwise as in Fig. 7. (A) map for bands 3/4; (B) map for bands 8/9; (C) map for bands 14/15. See text for details.

80°C, but 80°C is preferred because of the much shorter run time (21 min). Fig. 13 shows the resolution map for T_0 = 80°C.

Fig. 13 indicates that six band reversals occur (R_s = 0) for this sample, when the heating rate is increased from 1 to 20°C/min. In addition, the band spacing of several other band pairs changes significantly with variation in heating rate. Because of the complexity of Fig. 13, it is unlikely that trial-and-error changes in heating rate would lead the average chromatographer to an acceptable separation of this sample. Fig. 14 shows the predicted separation of this sample for the optimum conditions of Table IV: T_0 = 80°C and r = 4.4°C/min. The critical band pairs (4/5 and 14/15) are expanded and shown on the side of this Fig. 14 for a better picture of the resolution achieved.

Samples such as this which have a number of different critical band pairs are often better separated with a multi-ramp temperature program, because different parts of the chromatogram require different heating rates for optimum band spacing

TABLE III

COMPARISONS OF EXPERIMENTAL AND PREDICTED SEPARATIONS OF SPEARMINT OIL SAMPLE (47 bands)

Band	Retention times (min)				
	T_0 = 70°C/4°C/min[a]			Fig. 15	
	Expt.	Calc.	Error	Expt.	Calc.
1	5.23	5.21	−0.02	5.55	5.45
2	6.02	6.02	0.00	6.14	6.03
3	6.13	6.13	0.00	6.22	6.11
4	6.32	6.33	0.01	6.35	6.23
5	6.40	6.40	0.00	6.40	6.27
6	7.20	7.24	0.04	6.94	6.81
7	7.32	7.37	0.05	7.02	6.89
8	7.41	7.45	0.04	7.08	6.95
9	8.36	8.42	0.06	7.67	7.51
10	9.21	9.30	0.09	8.17	8.02
11	9.90	10.00	0.10	8.64	8.50
12	10.34	10.45	0.11	8.92	8.79
13	10.94	11.09	0.15	9.35	9.24
14	11.29	11.45	0.16	9.58	9.49
15	11.29	11.45	0.16	9.58	9.47
16	11.52	11.69	0.17	9.73	9.65
17	11.71	11.86	0.15	9.87	9.79
18	12.12	12.28	0.16	10.16	10.10
19	12.23	12.42	0.19	10.27	10.26
20	12.31	12.49	0.18	10.20	10.19
21	12.57	12.74	0.19	10.50	10.47
22	13.07	13.25	0.18	10.83	10.85
23	13.54	13.69	0.15	11.16	11.21
24	14.03	14.20	0.17	11.59	11.67
25	14.53	14.72	0.19	12.02	12.13
26	14.78	14.95	0.17	12.39	12.33
27	14.96	15.16	0.20	12.60	12.54
28	15.32	15.43	0.11	12.83	12.77
29	15.50	15.70	0.20	13.12	13.03
30	15.89	16.10	0.21	13.32	13.45
31	16.01	16.22	0.21	13.88	13.57
32	16.61	16.83	0.22	14.69	14.18
33	17.75	17.96	0.21	15.03	15.43
34	17.90	18.10	0.20	15.23	15.62
35	18.01	18.29	0.28	15.42	15.84
36	18.33	18.48	0.15	15.63	16.06
37	18.65	18.88	0.23	16.09	16.57
38	18.83	19.00	0.17	16.76	16.66
39	18.97	19.12	0.15	16.77	16.81
40	19.27	19.43	0.16	17.18	17.26
41	19.37	19.58	0.23	17.34	17.38
42	19.75	19.99	0.24	17.72	17.85
43	20.08	20.31	0.23	18.24	18.20
44	20.57	20.80	0.23	18.97	18.70
45	23.02	23.24	0.22	20.55	20.87
46	24.87	24.98	0.11	21.97	22.20
47	24.95	25.18	0.23	22.13	22.35

[a] Linear temperature program.

TABLE IV

SUMMARY OF RESOLUTION MAPS FOR 47 LARGEST BANDS OF SPEARMINT OIL SAMPLE

T_0 (°C)	Maximum resolution[a]			
	r (°C/min)	R_s	Run time (min)	Critical bands
40	5.0	0.59	28	14/15, 19/20
50	4.4	0.62	28	14/15, 19/20
60	3.7	0.63	29	14/15, 19/20
70	2.8	0.63	32	14/15, 19/20
80	4.4	0.66	21	4/5, 14/15
90	2.4	0.54	28	4/5, 14/15
100	0.5	0.37	48	3/4, 4/5

[a] For each value of T_0, a value of r giving maximum resolution was selected; the values of R_s and run time for this value of r are shown and the critical bands are identified.

and maximum resolution; *e.g.*, as in Fig. 12. The general approach for developing an optimized multi-ramp program for GC is similar to that used in the design of multi-segment gradients for HPLC, as discussed in detail in refs. 4 and 5. This involves optimizing the separation of early bands with a linear temperature program, followed by a change in heating rate for the next group of bands, and continuation of this process for the whole chromatogram. The ability (with computer simulation) to examine a large number of possible temperature programs greatly reduces the time required for this procedure (by a factor of a hundred or more).

A similar trial-and-error (plus logic) approach for the present sample (see ref. 16 for details) was successful in increasing the resolution of this 47-band sample to R_s = 1.2, corresponding to a doubling of the resolution found in the optimized

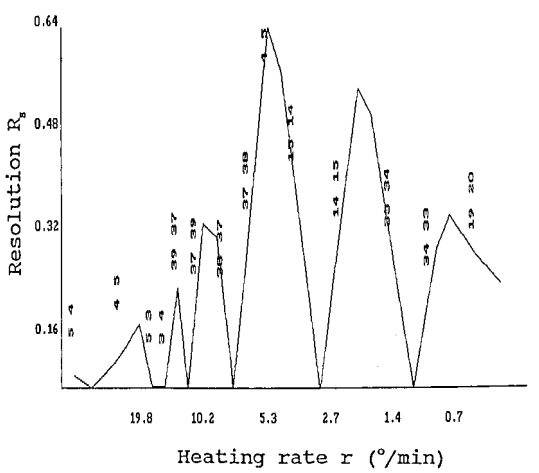

Fig. 13. Resolution map for the 47 largest bands of spearmint oil sample. Conditions: T_0 = 80°C, other conditions as in Fig. 8 unless noted otherwise.

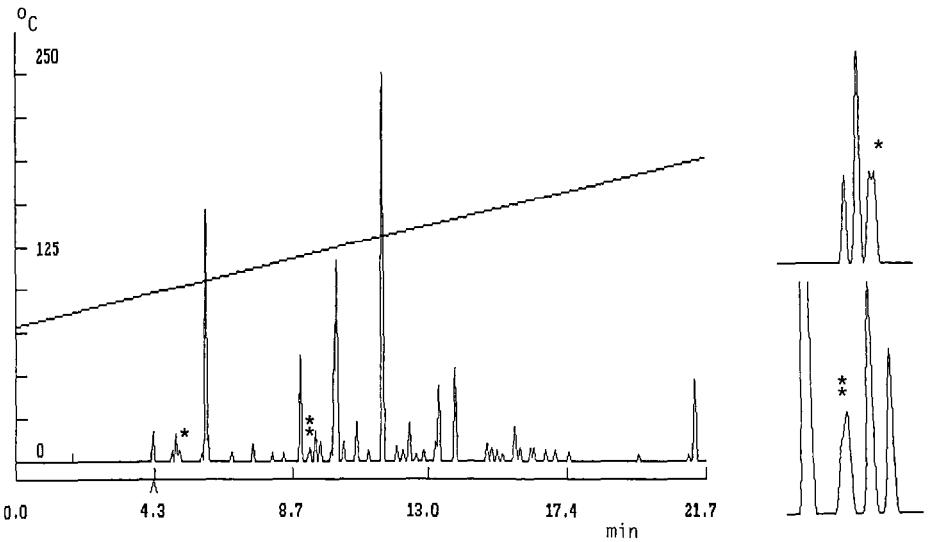

Fig. 14. Optimized separation of the spearmint oil (47 bands) based on a linear temperature program. Conditions: T_0 = 80°C, 4.4°C/min, other conditions as in Fig. 8. Critical band pairs [4/5 (*), 14/15 (**)] expanded on side.

linear-program separation of Fig. 14. The resulting separation is shown in Fig. 15, where predicted (A) and experimental (B) chromatograms are compared. The good agreement between these two separations is further documented in Table III, where retention times are compared. The average deviation between experimental and predicted retention times is only ±1.3%.

Optimizing the separation of individual compounds in complex chromatograms

For some GC assays, there may be more interest in particular compounds or in certain regions of the chromatogram, *vs.* the adequate resolution of the whole sample. In such cases we usually desire some minimum resolution of the compound(s) of interest in the shortest possible time. Computer simulation is particularly useful in optimizing a separation with respect to selected parts of the chromatogram. The general approach is similar to that pursued in Fig. 12, *i.e.*, using partial resolution maps. We will illustrate this for band 16 from the 47-band spearmint oil sample.

Partial resolution maps (as in Fig. 12) indicated that any starting temperature between 50 and 100°C would allow the adequate resolution (R_s = 2.0) of band 16. Systematic trial-and-error simulations were next used to map resolution and run time (retention time of band 16) *vs.* T_0 and r. These simulations are summarized in Fig. 16A, where resolution is plotted *vs.* the retention time of band 16 for different values of T_0 (r varying). It is apparent that a starting temperature of 100°C allows the quickest elution of band 16 with R_s = 2.

Once band 16 has left the column with adequate resolution and minimum run time, the heating rate can be increased sharply to elute the balance of the sample from the column in the shortest possible time. The resulting (optimized) separation of band 16 in the spearmint oil sample is illustrated in Fig. 16B (simulation) and compared

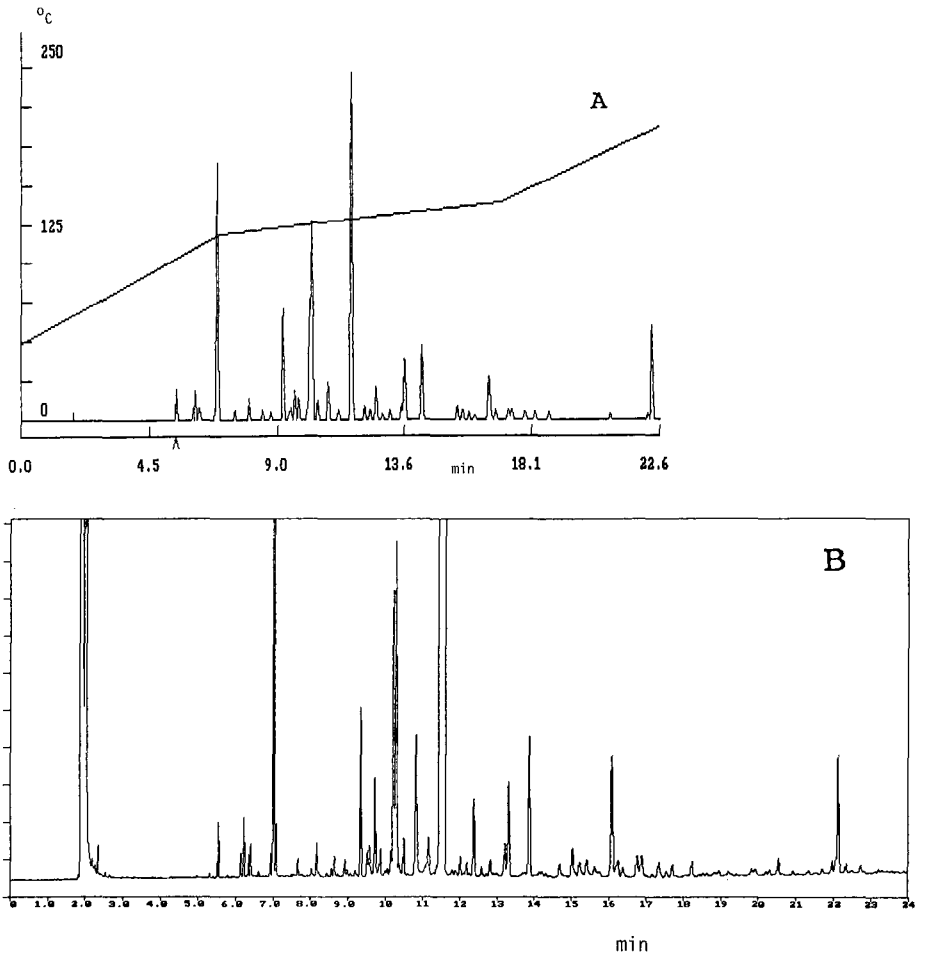

Fig. 15. Optimized multi-ramp separation of the spearmint oil (47 bands). Conditions: 50/120/140/188°C in 0/7/17/23 min, other conditions as in Fig. 8. (A), computer simulation; (B) experimental separation; (C) expansion of critical regions from (B).

with the experimental run in Fig. 16C. Again there is reasonable agreement between the predicted and experimental separations[a].

Change in column length or flow-rate

Once the temperature program has been optimized for band spacing and maximum resolution, it may be desirable to change column length or flow-rate for either

[a] The somewhat poorer resolution of bands 13–21 in the experimental chromatogram (Fig. 16C) is probably the result of several factors: (i) the presence of other (very) small bands, in addition to the 47 largest bands of this sample (see Fig. 17 in this connection), (ii) slight tailing of the various bands compared to a Gaussian peak, and (iii) a lower plate number in the separation of Fig. 16C *vs.* the input runs of Fig. 8 (the run of Fig. 16C was carried out several months later).

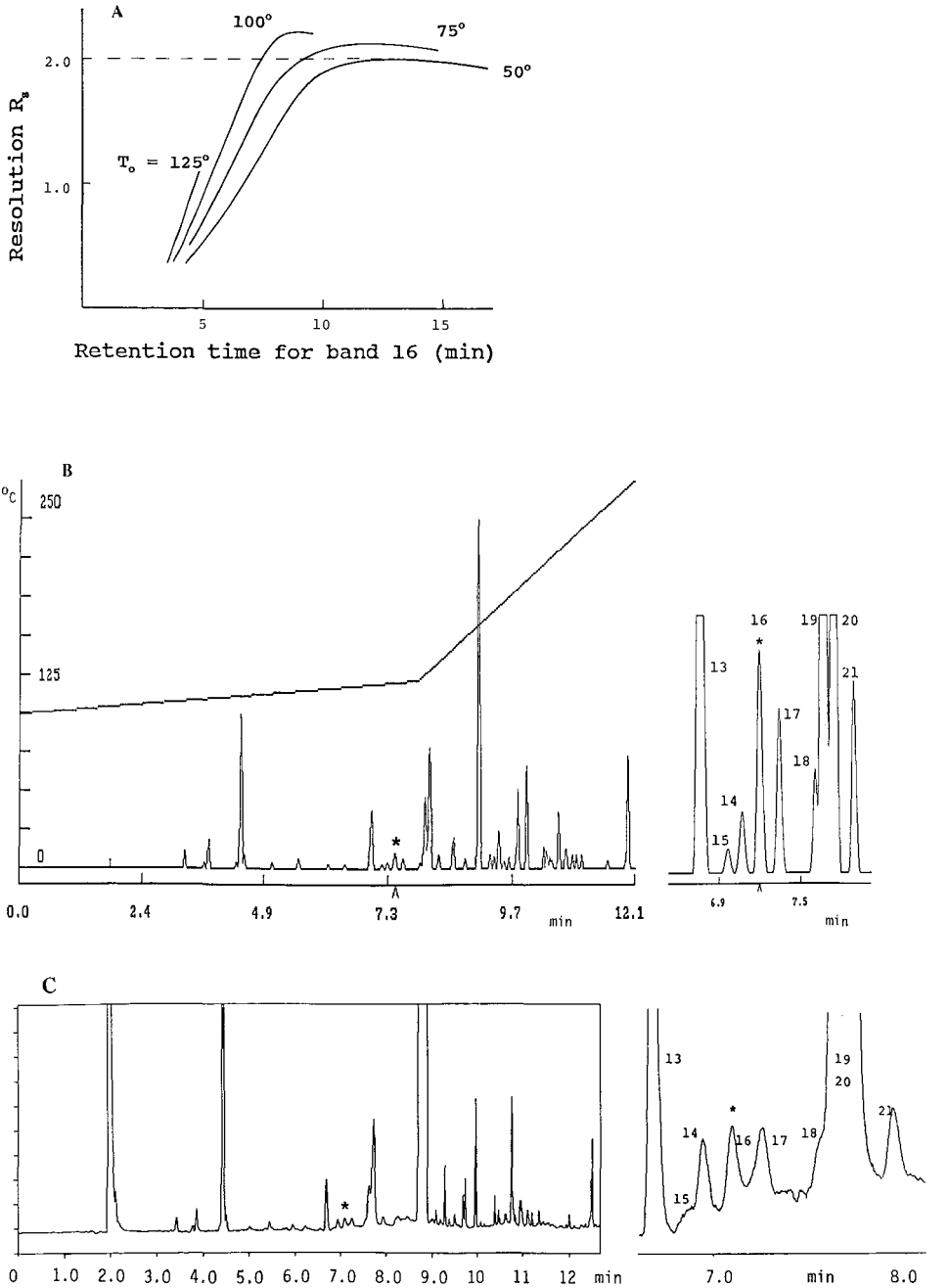

Fig. 16. Development of a GC assay for band 16 in the spearmint oil sample. Conditions as in Fig. 8 except where noted otherwise. (A) summary of computer simulations for resolution of band 16 as a function of the retention time for band 16 and the starting temperature T_0 (r varying); (B) predicted separation of band 16 (*) in minimum run time (12 min, R_s = 2.0); conditions: 100/122/250°C in 0/7.9/12 min; (C) experimental separation corresponding to (B).

an increase in resolution or a decrease in run time. This requires that the run-time be adjusted at the same time (as discussed in Part II [2]), in order to maintain b constant (eqn. 4, Part II) and preserve the optimized band spacing.

Minimizing errors in computer simulations of complex samples

Computer simulation requires accurate data, if the resulting predictions of separation are to be reliable. This means that the experimental runs used for this purpose must meet certain criteria that have been discussed in previous papers [1,3]. For complex samples such as the spearmint oil sample described in this paper, small errors in retention can result in large relative errors in predicted values of resolution. An analogous situation exists for the computer simulation of HPLC separations, as has been discussed in some detail [14]. One of the more common errors in the measurement of experimental retention times occurs for the case of severely overlapping bands, where only one retention time is reported by the data system. This is illustrated in Fig. 17A for overlapping bands 14 and 15 from the 8°C/min run used as input for the spearmint oil sample. If a single retention time (10.38 min) is used for both bands in computer simulation, significant errors (± 0.5 in R_s) can arise in the later prediction of resolution as a function of experimental conditions.

A comparison of band 14/15 in Fig. 17A (8°C/min run) with the same two bands in the 2°C/min run (Fig. 17B) shows that band 15 is eluted first in the run of Fig. 17A (note the bulge on the leading edge of this band). By making small adjustments in the estimated retention times of bands 14 and 15 in Fig. 17A, and using these estimates for the prediction of retention under other run conditions, a comparison of predicted and experimental retention can then be used to select the best retention times for bands 14 and 15 in Fig. 17A (10.39 and 10.35 min for bands 14 and 15, respectively). This procedure was used in the present study in order to refine the predictive accuracy of computer simulation for the spearmint oil sample. In this connection, note the good agreement for the predicted retention times of bands 14 and 15 in Table III (and especially the similar errors for each band).

In most cases, errors of this type (due to band overlap) will not be significant and can therefore be ignored. However, when important differences are found between subsequent predicted and experimental chromatograms, errors of this kind can be suspected and corrected as above.

CONCLUSIONS

The use of computer simulation for facilitating GC method development has been demonstrated for several different samples and applications. Method development begins by using resolution maps to define the dependence of programmed-temperature separations on the starting temperature and heating rate. For less complex samples, this usually leads directly to optimized separation conditions . Isothermal separations can also be evaluated as an alternative to temperature-programmed runs.

More complex samples can be approached in the same way, but often such samples cannot be separated by means of any linear temperature program (for any combination of starting temperature and heating rate). Using computer simulation, it is possible to identify samples of this type with minimum effort. It is also possible to

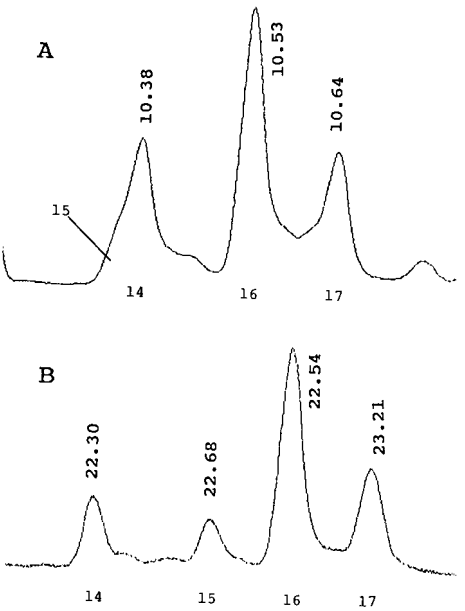

Fig. 17. Retention time errors in experimental runs due to overlapping bands (bands 14–17 shown). Bands 14 and 15 in 2 and 8°C/min runs used as input for the spearmint oil sample (47 bands). (A) 2°C/min; (B) 8°C/min. Numbers at peaks indicate retention times in min.

improve such separations significantly by means of multi-ramp temperature programs. The attempted development of optimized multi-ramp programs by the usual trial-and-error process (in the laboratory) will often prove impractical, because of the large number of experimental runs that would be required. Computer simulation can make use of partial resolution maps to reduce the number of required trial-and-error runs, while allowing such runs to be carried out (on the computer) in a small fraction of the time required in the laboratory.

Computer simulation is equally useful for the problem of optimizing the separation of one or a few bands in a complex sample, as opposed to resolving the entire sample. "Limited resolution maps" provide a systematic means of identifying optimum conditions for such cases, requiring only a few minutes of computer simulation.

REFERENCES

1 D. E. Bautz, J. W. Dolan and L. R. Snyder, *J. Chromatogr.*, 541 (1991) 1.
2 J. W. Dolan, L. R. Snyder and D. E. Bautz, *J. Chromatogr.*, 541 (1991) 21.
3 D. E. Bautz, J. W. Dolan, W. J. Raddatz and L. R. Snyder, *Anal. Chem.*, 62 (1990) 1561.
4 B. F. D. Ghrist and L. R. Snyder, *J. Chromatogr.*, 459 (1989) 25.
5 B. F. D. Ghrist and L. R. Snyder, *J. Chromatogr.*, 459 (1989) 43.
6 T. H. Jupille, J. W. Dolan and L. R. Snyder, *Am. Lab.*, December (1988) 20.
7 J. W. Dolan, D. C. Lommen and L. R. Snyder, *J. Chromatogr.*, 485 (1989) 91.
8 J. Schmidt, *J. Chromatogr.*, 485 (1989) 421.
9 T. Sasagawa, Y. Sakamoto, T. Hirose, T. Yoshida, Y. Kobayashi, Y. Sato and K. Koizumi, *J. Chromatogr.*, 485 (1989) 533.
10 I. Molnar, R. Boysen and P. Jekow, *J. Chromatogr.*, 485 (1989) 569.

11 R. G. Lehmann and J. R. Miller, *J. Chromatogr.*, 485 (1989) 581.
12 D. J. Thompson and W. D. Ellenson, *J. Chromatogr.*, 485 (1989) 607.
13 J. D. Stuart, D. D. Lisi and L. R. Snyder, *J. Chromatogr.*, 485 (1989) 657.
14 B. F. D. Ghrist, B. S. Cooperman and L. R. Snyder, *J. Chromatogr.*, 459 (1989) 1.
15 B. F. D. Ghrist, B. S. Cooperman and L. R. Snyder, *J. Chromatogr.*, 459 (1989) 25.
16 D. E. Bautz and J. W. Dolan, *Am. Lab.*, 22 (1990) 405.

Journal of Chromatography, 541 (1991) 59–74
Elsevier Science Publishers B.V., Amsterdam

CHROM. 23 020

Computer spreadsheet calculation of the optimum temperature and column lengths for serially coupled capillary gas chromatographic columns

R. G. WILLIAMS* and H. D. MITCHELL
The Upjohn Company, 1140-230-4, Kalamazoo, MI 49001 (U.S.A.)
(First received April 24th, 1990; revised manuscript received October 31st, 1990)

ABSTRACT

The application of computer spreadsheet calculations to the optimization of complex chromatographic separations on serially coupled capillary columns has been demonstrated. The equations used require a minimum of measured data for the prediction of retention times in the coupled systems. The calculations make no assumptions about equivalence of column diameters, and they can be easily extended to more than two columns, if desired. Temperature effects on flow-rate and on analyte capacity factors (k') are also taken into account. The spreadsheet allows convenient calculation of the minimum resolution at different combinations of column lengths and temperature. The method is shown to give reasonable agreement with measured retention times and excellent agreement with measured k' values.

INTRODUCTION

Much work has been published recently on the subject of optimizing capillary gas chromatographic (GC) separations through the use of serially coupled columns. A number of different variables have been manipulated to change the selectivity of the coupled system. Mathematical methods have been used to predict the temperature and pressure for an optimal separation for two columns connected directly [1–3] or with independent flow control [4–7]. Another potential mode of selectivity optimization is varying the lengths of the coupled columns. This method is practical only if calculations can give accurate predictions of retention times in the coupled system. Among the most active workers in this area are Buys and Smuts [8,9] and Purnell and co-workers [10–12], who emphasized the necessity of accounting for carrier-gas compressibility. These methods have been quite successful in predicting the retention times on coupled columns from the data on separate columns. Purnell determines the resistance to gas flow in a column by plotting the dead time at several different inlet pressures against a function of the pressure. This resistance factor is then used in calculation of the column dead-volume time at any specified inlet pressure. In the case of serially coupled columns, the resistance factors are used in calculation of the junction pressure for the two columns, from which further calculations give the ratio of dead-volume times on the front and back columns. The latter ratio is used in predicting

0021-9673/91/$03.50

the capacity factors (k') on the coupled system. The method may be applied to either packed or capillary columns, and it does not require that the columns to be connected have the same inside diameter.

A similar calculation has been employed successfully by Villalobos [13,14]. One difference in this method is that the retention time and resolution are calculated for the junction of the column as well as at the outlet. The method assumes that both columns involved have the same internal diameter, but this has been avoided by modifying the column lengths used in the calculation by a correction factor involving the fourth power of the ratio of column diameters.

We have been working independently on the problem of calculating the optimum lengths of dissimilar capillary columns which can be coupled to effect a desired separation. In the interest of simplicity of instrumentation, we have assumed a common mass flow-rate and a common temperature for the columns. While the calculations used are very similar to those of Purnell, they are limited to open-tubular columns, dealing primarily with the dimensions of the columns rather than with measured flow resistance. The algorithm begins with the specification of a desired volume flow-rate at the column outlet and predicts the head pressure and dead-volume time for each of the coupled columns. While in principle no chromatographic measurements are necessary to make these calculations, a single determination of flow-rate and dead-volume time for the separate columns at a known inlet pressure serves to determine the column I.D. more precisely and to increase the accuracy of the predictions. Once the dead-volume times are calculated, the retention times are calculated from known k' values on the individual columns as usual, except that the variation of k' with temperature is also taken into account. This paper shows how these equations can be used with a standard computer spreadsheet program to optimize separations in a coupled capillary system, with respect to both column length and temperature.

THEORY

The laminar flow occurring in a capillary GC column under typical operating conditions is described by Poiseuille's equation (see ref. 15)

$$-\frac{dP}{dx} = \frac{32\mu U}{D^2} \tag{1}$$

where P represents the pressure due to flow resistance, μ is the gas viscosity, U is the average velocity across the column diameter, x is the distance measured from the column head and D is the column inner diameter. Since the mass flow is constant and since for an ideal gas the volume is inversely proportional to the pressure, it follows that

$$U = \frac{P_o U_o}{P} \tag{2}$$

where P_o and U_o are the pressure and the flow velocity at the column outlet. Since it is

the volume flow-rate (f) which is usually measured at the column outlet, U_o is conveniently replaced by

$$U_o = \frac{4f}{\pi D^2} \tag{3}$$

Combining eqns. 2 and 3 with eqn. 1 gives

$$-\frac{dP}{dx} = \frac{128\mu f P_o}{\pi D^4 P} \tag{4}$$

Since the viscosity of an ideal gas is invariant with pressure, μ can be treated as a constant in eqn. 4 for any given temperature. Integration of eqn. 4 for a column of length L operating at inlet pressure P_i then gives Poiseuille's formula (see ref. 16) for the relationship between pressure and flow-rate

$$f = \frac{(P_i^2 - P_o^2)\pi D^4}{256\mu P_o L} \tag{5}$$

Since all of the parameters on the right-hand side of eqn. 5 can be measured, the flow-rate for a capillary column under any combination of temperature, inlet pressure and outlet pressure can in principle be predicted. In practice, the fourth-power dependence on column diameter means that the uncertainty in the diameter usually leads to significant errors in the predicted flow-rate. However, a single measurement of the flow-rate under known conditions of temperature and pressure gives in effect a calibration of the column diameter, so that the flow-rate may be accurately predicted for other conditions. Alternatively, solution of eqn. 5 for P_i allows prediction of the inlet pressure required for a desired flow-rate.

Integration of eqn. 4 for an arbitrary fraction of the column length leads to an expression for the pressure as a function of the distance from the column head

$$P = \sqrt{P_i^2 - \frac{x}{L}(P_i^2 - P_o^2)} \tag{6}$$

The dead-volume time for a column operating under steady-state conditions can be calculated from a consideration of the volume V which passes any point in the interior of the column in a unit of time. Keeping in mind the inverse relationship between volume and pressure, the following expression relates the volume flow at any point within the column to the flow-rate measured at the outlet and to the linear velocity of the gas

$$\frac{dV}{dt} = \frac{\pi D^2}{4}\frac{dx}{dt} = f\frac{P_o}{P} \tag{7}$$

where t is the time. Combining eqns. 6 and 7 then gives

$$\frac{dx}{dt} = \frac{4f}{\pi D^2} \frac{P_o}{\sqrt{P_i^2 - \frac{x}{L}(P_i^2 - P_o^2)}} \tag{8}$$

Solution of eqn. 8 for t gives the time required for the carrier gas to advance a distance x down the column

$$t = \frac{\pi D^2 L}{6fP_o(P_i^2 - P_o^2)} \left\{ P_i^3 - \left[P_i^2 - \frac{x}{L}(P_i^2 - P_o^2) \right]^{3/2} \right\} \tag{9}$$

When the variable x in eqn. 9 equals L, t equals the dead time t_o, and the expression reduces to the equivalent of Purnell's equation (see eqn. 5 in ref. 11) for column dead time

$$t_o = \frac{\pi D^2 L}{6f} \left[\frac{P_i^3 - P_o^3}{P_o(P_i^2 - P_o^2)} \right] \tag{10}$$

Eqn. 10 can be used to make a second determination of the column diameter if the outlet flow-rate and dead-volume time are measured at known inlet and outlet pressures. It is equivalent to the diameter determination given by eqn. 5, except that the viscocity of the carrier gas does not have to be known. We have found that the most consistent measurements of D are obtained from eqn. 10 after determination of the dead time according to the method of Ambrus [17]. The value of D thus obtained can be used to calculate t_o for any desired length of the column at any desired flow-rate.

The equations described provide the means to calculate retention times on any combination of serially coupled column portions. The details of the method are as follows:

(1) Measure the length of each column to be used.

(2) *With each column individually*, connect the head to an injector operating at a known pressure, and after equilibration measure the flow-rate at the outlet, the column temperature, the laboratory temperature, and the barometric pressure.

(3) Connect the column to the detector and inject a test mixture of hydrocarbons for determination of dead time by the method of Ambrus.

(4) After correcting the measured flow-rate to the column temperature, substitute the measured parameters into eqn. 10 to determine the diameter of each column.

(5) Choose a flow-rate for the coupled system and specify the length of the tail section. Use eqn. 5 to calculate P_i for that section.

(6) Using the pressure calculated in step 5 as P_o, use eqn. 5 to calculate P_i for the next column in the series. For this calculation, the volume flow-rate must be corrected to the new value of P_o, and the values of D and L which apply to this column segment must be used.

(7) Repeat step 6 for any more column segments to be connected to the head end of the series.

(8) Use eqn. 10 to calculate t_o for each column in the series.

(9) Calculate the retention time for each analyte on each segment from the corresponding k' value for that segment by the usual equation

$$t_n = t_o(k'_n + 1) \tag{11}$$

The total retention time for component n is then given by the sum of the retention times on the connected columns. It should be noted that the use of eqn. 11 assumes that each original column is uniform, so that the k' values for any segment will be the same as those measured on the entire column.

The calculation of retention times allows a simple form of chromatographic optimization by maximization of the spacing between adjacent peaks. A more systematic approach is the use of window diagrams [18] applied to the α values of adjacent peaks ($\alpha = k'_2/k'_1$). The window-diagram approach may be very conveniently applied with a spreadsheet. However, since it is really resolution which is being optimized, we chose to derive diagrams for the resolution of neighboring peak pairs. This requires a knowledge of the theoretical plate number for each component to be analyzed. While prediction of theoretical plate numbers has also been accomplished [19], it would make the spreadsheet much more complex. We chose the simplifying assumption that a given column would give the same inherent plate number for all analytes. The lower apparent plate number for peaks of lower retention time was assumed to be due to extra-column band broadening. It has been shown that the extra-column variance may be determined by a plot of the observed peak variance σ^2 *versus* t^2, where the slope of the plot is the inverse of the inherent column theoretical plate number N and the intercept is the extra-column variance σ_e^2 [20]. The apparent plate number N_a for a given peak is then given by

$$N_a = \frac{N}{N\sigma_e^2/t^2 + 1} \tag{12}$$

In our initial work, the assumption was also made that if a column of length L had N theoretical plates, a fragment of length l taken from this column would have N_l plates, according to the following formula:

$$N_l = \frac{l}{L} N \tag{13}$$

The inherent plate number for the combined column was then given by the sum of N_l for the individual columns. It has since been shown by Guiochon and Gutierrez [19] that the correct form is given by

$$H_c L_c = \sum_{i=1}^{n} H_i L_i \tag{14}$$

where H represents the height equivalent of a theoretical plate, L the column length,

subscript c the total coupled system, and subscript i the individual column segments which are connected. When, as is approximately true in the present work, the height equivalent of a theoretical plate for the column segments is the same, eqns. 13 and 14 lead to the same results. In the general case, the parameters H_c and L_c from eqn. 14 may be used to calculate the inherent plate number N_c for the coupled system, and the latter may be used in eqn. 12 to predict the apparent plate number as a function of retention time. Resolution is conveniently calculated by the usual expression

$$R_s = \frac{t_2 - t_1}{2(\sigma_2 + \sigma_1)} \tag{15}$$

While this treatment ignores the relationship between plate height and carrier velocity, this factor can be minimized by adjusting the inlet pressure to keep the calculated average linear velocity near the optimum value.

The other variable which may be conveniently controlled to optimize the coupled-column separation is temperature. It has already been shown (eqn. 5) that the only effect of temperature on the flow-rate for a capillary column lies in the temperature dependence of the carrier-gas viscosity. This is expressed in ref. 3 by the relationship

$$\mu = aT^{\alpha} \tag{16}$$

where a is a constant and T is the temperature. While the tabulated data for helium viscosity may be fitted to eqn. 16, a simple second-order regression gives a closer fit in the temperature range above 0°C. Expressing the viscosity as a function of temperature allows the relationship between pressure, flow-rate, and dead time to be calculated for any temperature. What remains for calculation of the selectivity is an expression for the relationship between k' and temperature. For the latter, we used the approach of measuring k' at three different temperatures and regressing log k' against the reciprocal of the absolute temperature. The regression parameters were used in the spreadsheet to express all of the k' values as a function of temperature. The chromatogram could thus be simulated for any combination of columns at any desired flow-rate and temperature.

EXPERIMENTAL

Chromatography was carried out on a Hewlett-Packard 5880 gas chromatograph with a split injector containing a packed insert. The insert contained about 1/4 in. of 2% SE-30 on 100–120-mesh Gas Chrom Q. The split flow was 50 ml/min, with column flow controlled by the constant head pressure. Helium was used as the carrier gas, and a flame-ionization detector was used.

Two fused-silica columns were used in this work, nominally 30 m × 0.32 mm I.D. The first contained a bonded methyl silicone phase (DB-1, J&W Scientific) of 1 μm thickness, while the second contained a bonded Carbowax phase (DBWax, J&W) of 0.5 μm thickness. The column length was determined by careful measurement of two unwrapped coils and by counting of the total number of coils.

The GC oven temperature was calibrated against a laboratory thermometer. The

column flow-rate was determined by attachment of the injector end as usual, while the detector end was extended through the detector jet to the top of the chromatograph. It was connected through a septum to a soap-film flow meter, which was previously filled with helium to prevent errors due to differential diffusion of helium across the soap film. After thermal equilibration of the column at a known temperature, the flow-rate was measured carefully, and the column head pressure, barometric pressure and laboratory temperature were recorded. The measured flow-rate was corrected for the vapor pressure of water and was then corrected to the column temperature.

After connection of the tail of the column to the detector, the dead time was determined by injection of a mixture of *n*-alkanes ranging from C_5 to C_{12}. A regression of the retention times according to the method of Ambrus was used for determination of t_o. The measured pressures, flow-rate, column length and dead time were used in eqn. 10 to determine the actual column diameter.

The retention times of the solvents to be separated were determined by injection of a few microliters into a septum vial. After the liquid had evaporated, 5 μl of vapor was injected onto the chromatograph. Vapor injection was used to avoid retention time shifts that might result from overloading of the column.

The resolution calculations were carried out with Lotus 1-2-3, version 2.01, running on an AT&T PC 6300. One spreadsheet was used to calculate the k' values and the resolution of neighboring peaks for varying lengths of connected columns. Another was used to generate a simulated chromatogram, assuming Gaussian peaks and using peak variances calculated as described in the Theory section.

RESULTS

The measurements used for initial characterization of the two columns are summarized in Table I. It may be seen that the column diameters calculated according to eqn. 10 are in good agreement with the nominal values. The measured k' values on both columns at three temperatures for the set of 34 solvents studied are given in Table II. With these constants, retention times were calculated for serially connected combinations at 50°C, starting with the full DBWax column at the head and increasing the DB-1 column length at the tail from zero to the full 30 meters. The DBWax column length was then reduced to zero. The results are shown in Fig. 1, with the same calculation assuming the DB-1 column at the head shown in Fig. 2. While dramatic differences in relative retention times are predicted, it is clear that there is no combination which gives good spacing for all 34 component peaks. Window diagrams

TABLE I

MEASUREMENTS USED TO CHARACTERIZE THE INDIVIDUAL COLUMNS

Column 1 = 30 m of bonded methylsilicone; column 2 = 30 m of bonded Carbowax.

Column	P_i (p.s.i.g.)[a]	P_o (p.s.i.g.)[a]	L (m)	T_{col} (°C)	T_{room} (°C)	F (ml/min)[b]	t_o (min)	D_{calc} (mm)
1	26.4	14.4	31.43	50	23	2.326	1.48	0.323
2	26.2	14.2	31.94	50	23	2.237	1.59	0.325

[a] Absolute pressures.

[b] Measured at P_o and room temperature.

TABLE II

EXPERIMENTAL k' VALUES FOR TEST SOLVENTS ON THE INDIVIDUAL COLUMNS

Measurements were made at P_i = 12 p.s.i.g.

Peak No.[a]	Name	T = 40°C		T = 50°C		T = 60°C	
		$k'_{col\ 1}$	$k'_{col\ 2}$	$k'_{col\ 1}$	$k'_{col\ 2}$	$k'_{col\ 1}$	$k'_{col\ 2}$
1	Methanol	0.364	1.718	0.274	1.156	0.196	0.811
2	Ethanol	0.460	2.372	0.362	1.560	0.275	1.066
3	Acetonitrile	0.508	3.835	0.423	2.565	0.301	1.754
4	Acetone	0.542	0.864	0.450	0.609	0.333	0.464
5	Isopropanol	0.623	2.262	0.483	1.473	0.373	1.010
	n-Pentane	0.726	0.068	0.571	0.054	0.438	0.048
6	*tert.*-Butanol	0.787	1.803	0.612	1.183	0.464	0.811
	Methyl acetate	0.869	0.968	0.652	0.672	0.497	0.501
7	Methylene chloride	0.842	2.197	0.659	1.461	0.503	1.016
8	*n*-Propanol	1.135	5.447	0.827	3.426	0.614	2.244
9	Methyl ethyl ketone	1.483	1.712	1.090	1.177	0.810	0.849
10	Ethyl acetate	1.831	1.550	1.320	1.050	0.954	0.756
11	*n*-Hexane	1.824	0.146	1.347	0.117	0.987	0.092
12	Chloroform	1.831	4.534	1.360	2.931	1.000	1.965
13	Tetrahydrofuran	2.076	1.265	1.535	0.899	1.124	0.675
14	Ethylene dichloride	2.316	6.443	1.697	4.085	1.235	2.710
	n-Butyl chloride	2.574	1.052	1.866	0.741	1.353	0.551
15	*n*-Butanol	2.888	12.735	2.021	7.675	1.425	4.819
	Benzene	2.888	2.359	2.095	1.632	1.516	1.159
16	Cyclohexane	3.141	0.417	2.277	0.306	1.647	0.253
	Dioxane	4.027	6.061	2.837	3.959	2.000	2.710
17	*n*-Heptane	4.593	0.320	3.194	0.243	2.222	0.191
18	Methyl isobutyl ketone	5.528	3.971	3.788	2.621	2.614	1.804
	Pyridine	5.528	15.414	3.788	9.680	2.614	6.239
19	Toluene	7.404	5.065	5.076	3.353	3.497	2.313
20	*n*-Butyl acetate	11.374	6.851	7.375	4.338	4.853	2.865
	n-Octane	11.558	0.722	7.577	0.514	5.020	0.253
21	Ethyl benzene	17.117	9.861	11.178	6.319	7.379	4.205
22	*m*-Xylene	18.502	10.922	12.021	6.968	7.895	4.627
23	*p*-Xylene	18.645	10.411	12.082	6.659	7.941	4.422
24	*o*-Xylene	22.397	15.039	14.408	9.473	9.405	6.196
	n-Nonane	29.082	1.615	17.955	1.107	11.320	0.787
	n-Decane	73.181	3.615	42.554	2.356	25.536	1.605
	n-Undecane	184.150	8.074	100.854	5.025	57.601	3.268

[a] Peak numbering for subset used in separation optimization.

confirmed this observation, with the minimum α value never exceeding 1.01. Variations in the temperature changed the selectivity somewhat, but no conditions could be found for simultaneous separation of all components with these columns.

Because of the complexity of the separation, we decided to limit the optimization to a subset of the solvents which were of most interest in our laboratoy. The components selected are those which are numbered in Table II. The plot of σ^2 *vs.* t^2 for these components on the DB-1 column gave a straight line, with the intercept corresponding to $\sigma_{external}$ = 0.018 min and the slope to a column plate number of

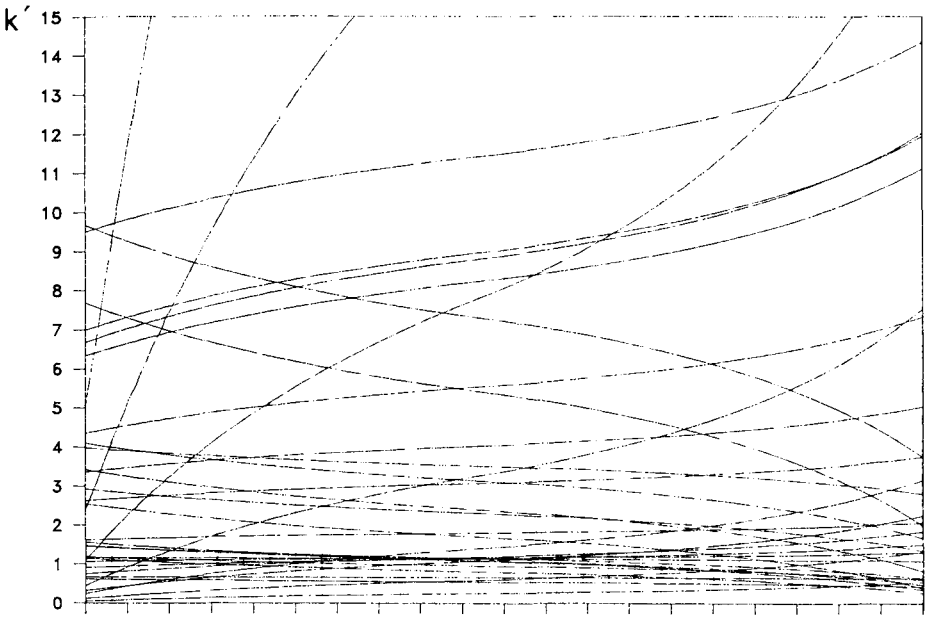

Fig. 1. Calculated k' values for 34 solvents on column 2 coupled ahead of column 1. The left side of the graph represents column 2 alone, with the length of column 1 increasing in the x-direction to its full length at the midpoint of the x-axis. Column 2 then decreases until the right side represents column 1 alone.

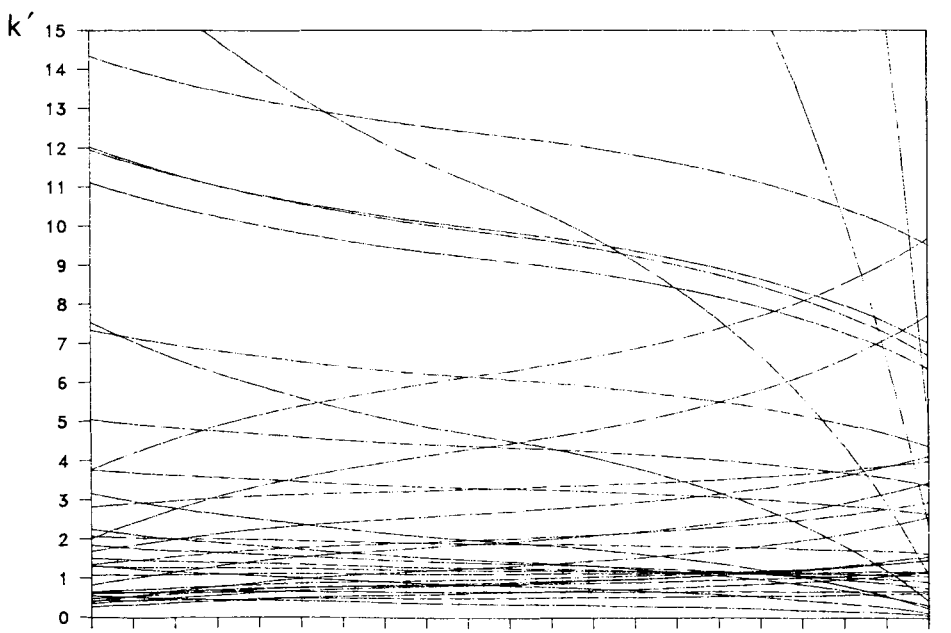

Fig. 2. Calculated k' values for 34 solvents on column 1 coupled ahead of column 2. The plot is the same as Fig. 1 except for the reversal of column order.

70 000. The corresponding plot for the DBWax column gave a poorer fit, primarily due to significant broadening of the peaks for some of the more-polar components. The broadening was accompanied by increased tailing, indicative of residual unblocked hydrogen-bonding sites on the DBWax column. The assumption of a common plate number for all components is thus not really true for this column, and the fit to a straight line was poorer. However, the linear regression gave the same $\sigma_{external}$ of 0.018 min, and the column plate number was 55 000. With these constants, the spreadsheet was programmed to calculate the retention times for each set of conditions, to sort the peaks in order of increasing retention time and to calculate the resolution of all adjacent peaks. The minimum resolution was tabulated for each case. A plot of this value *versus* column length gave a window diagram which suggested areas where calculations should be made at shorter intervals.

In order to test the validity of the theory, we first calculated the retention times expected for connection of the complete DBWax column ahead of the DB-1 column. For a temperature of 50°C and an outlet flow-rate of 3 ml/min, the method predicted a column head pressure of 24.2 p.s.i.g. The comparison of the retention times found under these conditions with those predicted is shown in Table III. While the peak order

TABLE III

COMPARISON OF CALCULATED AND EXPERIMENTAL RETENTION TIMES FOR SOLVENT SUBSET ON THE SERIALLY CONNECTED FULL COLUMNS

Values were measured at 50°C; P_i = 24.2 p.s.i.g.; retention times in min; number code for solvents as in Table II.

Solvent	t_{calc}	t_{exp}	k'_{calc}	k'_{exp}
1	5.70	5.22	0.81	0.79
2	6.58	6.09	1.09	1.08
3	8.54	7.96	1.71	1.72
4	4.87	4.53	0.55	0.55
5	6.58	6.09	1.09	1.08
6	6.17	5.74	0.96	0.96
7	6.77	6.26	1.15	1.14
8	10.75	9.94	2.41	2.40
9	6.76	6.26	1.15	1.14
10	6.81	6.26	1.16	1.14
11	5.02	4.66	0.59	0.59
12	10.44	9.67	2.31	2.31
13	6.77	6.26	1.15	1.14
14	13.09	12.13	3.16	3.15
15	20.36	18.89	5.46	5.46
16	6.56	6.09	1.08	1.08
17	7.55	7.01	1.40	1.40
18	12.85	11.94	3.08	3.08
19	15.84	14.72	4.03	4.03
20	20.57	19.14	5.53	5.54
21	29.05	27.05	8.22	8.25
22	31.34	29.18	8.95	8.98
23	30.83	28.75	8.79	8.83
24	39.09	36.37	11.41	11.43

agrees very well with that predicted, the observed times are all slightly shorter than expected. A possible explanation for the discrepancy is uncertainty of the column-head pressure, since the gauge was not calibrated against any outside standard. In addition, variations in the outlet (atmospheric) pressure on different days were not included in the calculations. Nevertheless, the last two columns of Table III show that the agreement between predicted and experimental k' values is very good, with an average deviation (root mean square, r.m.s.) of 0.8%.

With the success of the prediction for connection of the whole columns, we returned to the question of optimizing the separation. Calculations were made with variations in the column order, the lengths and the temperature. In the length calculations, the full length of one column was assumed while the other was varied. The temperature was varied over the range which gave a reasonable predicted total run time. Even with the analysis limited to the subset of solvents, complete resolution could not be obtained for all components simultaneously. The best conditions which could be found (17.8 m of DBWax column attached at the head of the 31.4-m DB-1 column, temperature 48°C) gave a predicted minimum resolution of 0.40. This occurred between the peaks for *tert.*-butyl alcohol and ethanol, with nearly the same resolution between ethanol and isopropyl alcohol.

To test the prediction, we cut a 17.8-m length from the DBWax column and attached it to the front of the DB-1 column. With a pressure of 17 p.s.i.g. and a column temperature of 48°C, the retention times found are given in Table IV, along with the predicted values. While again the observed times are systematically shorter than those predicted, the general agreement is good except in three areas. The ethanol–*tert.*-butanol (peaks 2 and 6), *m*-xylene–*p*-xylene (peaks 22 and 23) and acetonitrile–cyclohexane (peaks 3 and 16) pairs were found to be coincident. Since especially the latter peak pair seemed outside the expected range of variation, we looked for a cause. The compounds were chromatographed on the 17.8-m section of DBWax column alone, and the k' values were found to be larger than those measured on the original column by an average factor of 1.04. This is evidence that the initial assumption of invariant k' as a function of column length is not completely valid. Either a variation in stationary phase thickness along the length of the column or a variation in column diameter could give rise to this result. We have no evidence as to which factor is most significant, but if the variation is in column diameter, the derivation of eqns. 5 and 10 is not valid, and additional deviation between predicted and experimental chromatograms would be expected.

The revised k' values measured on the 17.8-m section of DBWax column were used in a repeat of the calculations. Essentially the same optimum separation was predicted, but with a DBWax section of 17.2 m. The DBWax section was therefore shortened to 17.2 m and re-attached to the DB-1 column. The retention times and k' values for a run with this combination at 48°C and 17.1 p.s.i.g. are given in Table V, compared with the predicted values. Once again, the measured retention times are systematically shorter than those predicted, but the k' values are in generally good agreement. The acetonitrile–cyclohexane pair now separate as predicted. The ethanol–*tert.*-butanol pair still elute as a single peak, although the k' values measured separately are slightly different. The lack of resolution may be partly due to the lower plate number mentioned earlier for these polar compounds on the DBWax column.

The spreadsheet was also used to generate a simulated chromatogram for the

TABLE IV

COMPARISON OF CALCULATED AND EXPERIMENTAL RETENTION TIMES FOR SOLVENT SUBSET AT THE PREDICTED OPTIMUM SERIAL COMBINATION

17.8 m of column 2 at head, 31.4 m of column 1 at tail; values were measured at 48°C; P_i = 17.2 p.s.i.g.; retention times in min; number code for solvents as in Table II.

Solvent	t_{calc}	t_{exp}	k'_{calc}	k'_{exp}
1	4.48	4.23	0.71	0.70
2	5.12	4.83	0.96	0.94
3	6.43	6.27	1.46	1.52
4	4.04	3.89	0.54	0.56
5	5.21	4.97	0.99	1.00
6	5.03	4.83	0.92	0.94
7	5.45	5.20	1.08	1.09
8	8.24	7.86	2.15	2.16
9	5.77	5.51	1.21	1.21
10	5.98	5.73	1.29	1.30
11	4.83	4.62	0.85	0.86
12	8.39	8.02	2.21	2.22
13	6.09	5.86	1.33	1.36
14	10.40	9.95	2.98	3.00
15	15.56	14.90	4.95	4.99
16	6.52	6.27	1.50	1.52
17	7.90	7.58	2.02	2.05
18	11.84	11.35	3.53	3.56
19	14.77	14.16	4.65	4.69
20	19.79	18.99	6.57	6.63
21	28.27	27.13	9.81	9.90
22	30.45	29.21	10.65	10.74
23	30.17	29.21	10.54	10.74
24	37.47	35.93	13.33	13.44

predicted separation, assuming Gaussian peaks and the plate numbers calculated above. The simulated and actual chromatograms are compared in Fig. 3. Except for the peak tailing for some components in the actual chromatogram, the two compare very well. The plot of σ^2 *vs.* t^2 for the coupled columns gave a scatter comparable to that for the DBWax column alone, with an intercept corresponding to $\sigma_{external}$ of 0.025 min and a slope corresponding to 102 000 theoretical plates. The slight increase of $\sigma_{external}$ (0.4 s) may not be significant, but it could be evidence for extra variance caused by coupling of the columns. The plate number agrees well with the 99 600 predicted by the calculation, with the major outliers being acetonitrile and the alcohols as for the DBWax column alone.

CONCLUSIONS

Standard spreadsheet programs running on a personal computer can be used to make very successful predictions of the chromatograms which will result from the serial coupling of capillary columns. A simple measurement of column dead time and of k' values for the analytes on each column is sufficient for the prediction of the separation for any desired combination of lengths. Determination of k' values at three

TABLE V

COMPARISON OF CALCULATED AND EXPERIMENTAL RETENTION TIMES FOR SOLVENT SUBSET AT THE REVISED PREDICTED OPTIMUM COMBINATION

17.2 m of column 2 at head, 31.4 m of column 1 at tail; values were measured at 48°C; P_i = 17.2 p.s.i.g.; retention times in min; number code for solvents as in Table II.

Solvent	t_{calc}	t_{exp}	k'_{calc}	k'_{exp}
1	4.44	4.11	0.72	0.68
2	5.08	4.76	0.97	0.95
3	6.39	6.03	1.48	1.47
4	4.00	3.82	0.55	0.56
5	5.17	4.86	1.01	0.99
6	4.99	4.73	0.94	0.93
7	5.41	5.10	1.10	1.09
8	8.20	7.64	2.19	2.12
9	5.73	5.41	1.23	1.21
10	5.94	5.63	1.31	1.30
11	4.79	4.57	0.86	0.87
12	8.36	7.84	2.25	2.21
13	6.06	5.77	1.35	1.36
14	10.37	9.70	3.03	2.97
15	15.53	14.47	5.04	4.92
16	6.48	6.20	1.52	1.53
17	7.86	7.51	2.06	2.07
18	11.81	11.16	3.59	3.56
19	14.74	13.94	4.73	4.70
20	19.76	18.70	6.68	6.65
21	28.25	26.73	9.98	9.93
22	30.43	28.77	10.83	10.76
23	30.15	28.42[a]	10.72	10.62[a]
24	37.46	35.35	13.57	13.45

[a] Retention time estimated from unresolved shoulder.

different temperatures further allows calculation of the chromatogram for any combination at any desired temperature. The columns need not be of the same diameter, and the method could easily be extended to the coupling of three or more columns, if desired. The primary limitation is the assumption of constant diameter and stationary phase thickness along each column, which has not proved quite true in practice.

The equations utilized in this study are also useful for work with a single capillary column. After measurement of the dead time at one column-head pressure and temperature, it is simple to calculate the head pressure required for a given dead time at any desired temperature. With gas chromatographs using pressure-controlled flows, this allows prediction of the pressure required to keep the average linear velocity within the optimum range for maximum plate number. It also allows a check on whether the column I.D. matches the nominal value. With the wide availability of personal computers, such methods can be a routine tool of the gas chromatographer.

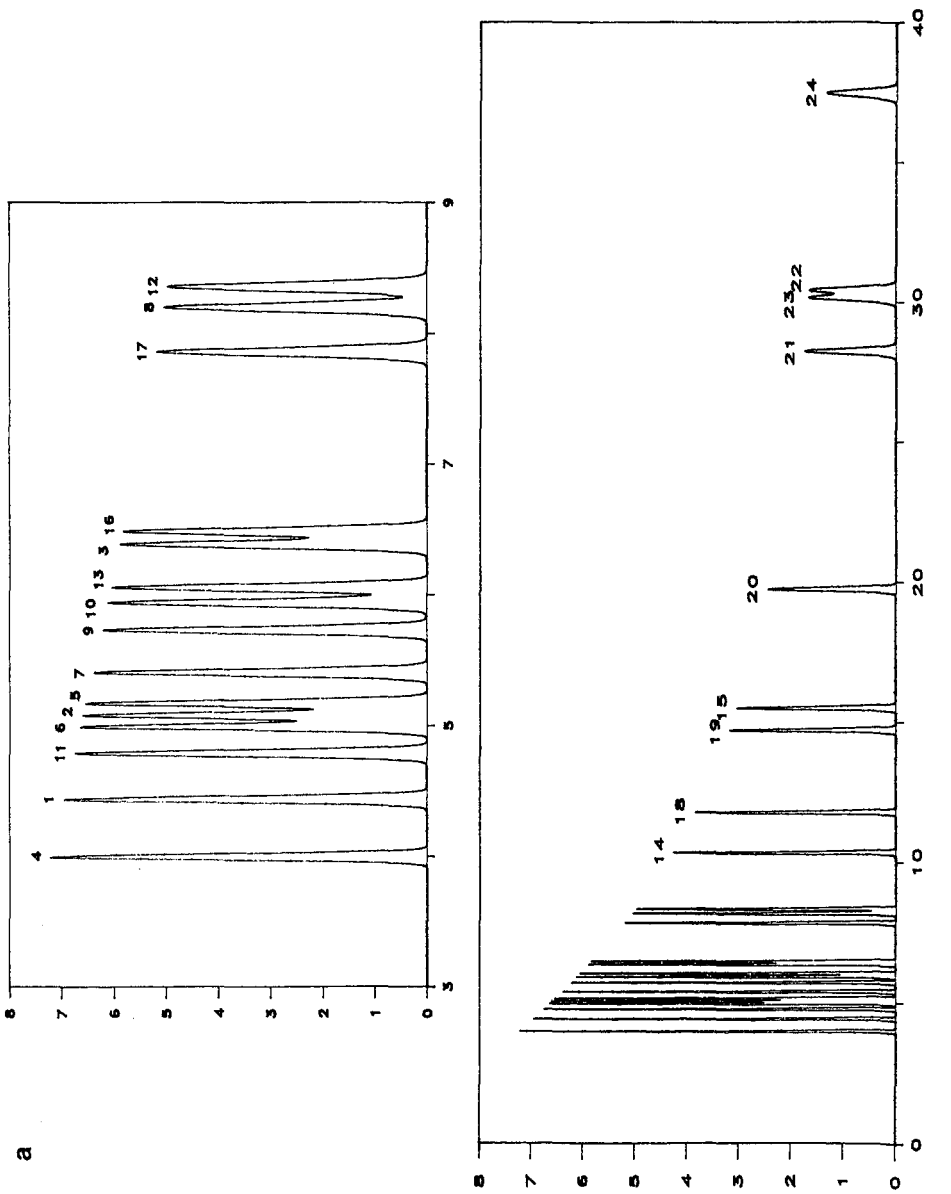
a
4
1
11
6
2
5
7
9
10
13
3
16
17
8
12
14
18
19
15
20
21
23
22
24
0
1
2
3
4
5
6
7
8
9
10
20
30
40

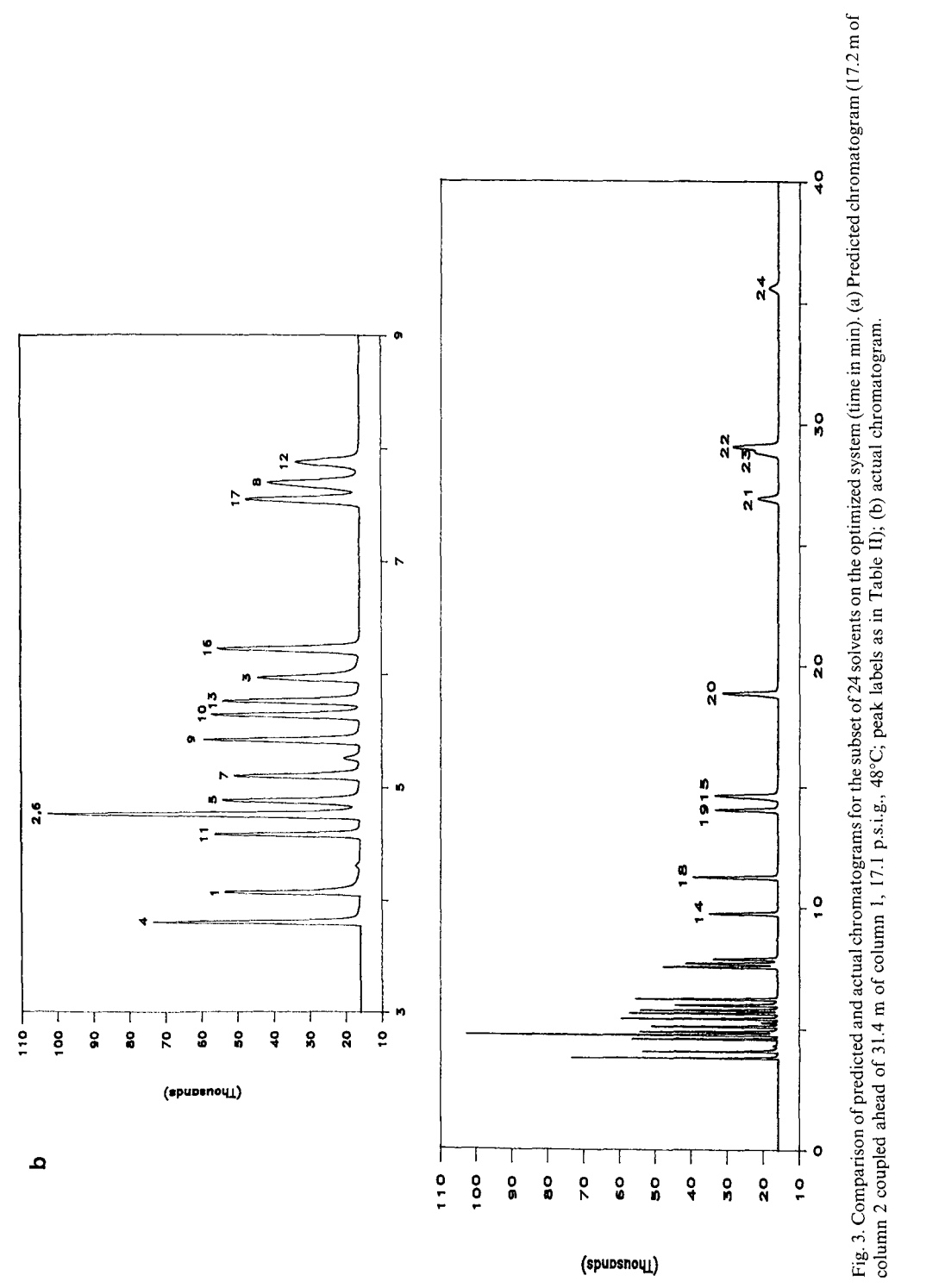

Fig. 3. Comparison of predicted and actual chromatograms for the subset of 24 solvents on the optimized system (time in min). (a) Predicted chromatogram (17.2 m of column 2 coupled ahead of 31.4 m of column 1, 17.1 p.s.i.g., 48°C; peak labels as in Table II); (b) actual chromatogram.

REFERENCES

1 G. P. Cartoni, G. Goretti, B. Monticelli and M. V. Russo, *J. Chromatogr.*, 370 (1986) 93.
2 D. Repka, J. Krupčík, E. Benická, P. A. Leclercq and J. A. Rijks, *J. Chromatogr.*, 463 (1989) 243.
3 T. Tóth and F. Garay, in P. Sandra (Editor), *Proc. VIIIth Int. Symp. on Capillary Chromatography*, Hüthig, Heidelberg, 1987, p. 585.
4 L. S. Ettre and J. V. Hinshaw, Jr., presented at the *37th Pittsburgh Conference, Atlantic City, NJ, March 10–14, 1986*, paper No. 1100.
5 J. V. Hinshaw, Jr. and L. S. Ettre, presented at the *37th Pittsburgh Conference, Atlantic City, NJ, March 10–14, 1986*, paper No. 1101.
6 J. V. Hinshaw, Jr. and L. S. Ettre, *Chromatographia*, 21 (1986) 669.
7 Z. Jianying, *J. High Resolut. Chromatogr. Chromatogr. Commun.*, 10 (1987) 418.
8 T. S. Buys and T. W. Smuts, *J. High Resolut. Chromatogr. Chromatogr. Commun.*, 3 (1980) 461.
9 T. S. Buys and T. W. Smuts, *J. High Resolut. Chromatogr. Chromatogr. Commun.*, 4 (1981) 102.
10 J. H. Purnell and P. S. Williams, *J. Chromatogr.*, 321 (1985) 249.
11 J. H. Purnell, M. Rodriguez and P. S. Williams, *J. Chromatogr.*, 358 (1986) 39.
12 J. H. Purnell, J. R. Jones and M. H. Wattan, *J. Chromatogr.*, 399 (1987) 99.
13 R. Villalobos, presented at the *40th Pittsburgh Conference, Atlanta, GA, March 6–9, 1989*, paper No. 1038.
14 R. Villalobos, *J. Chromatogr. Sci.*, 28 (1990) 341.
15 J. G. Knudsen and D. L. Katz, *Fluid Dynamics and Heat Transfer*, McGraw Hill, New York, 1958, p. 89.
16 P. W. Atkins, *Physical Chemistry*, W. H. Freeman, San Francisco, CA, 2nd ed., 1982, p. 883.
17 L. Ambrus, *J. Chromatogr.*, 294 (1984) 328.
18 R. J. Laub and J. H. Purnell, *J. Chromatogr.*, 112 (1975) 71.
19 G. Guiochon and J. E. N. Gutierrez, *J. Chromatogr.*, 406 (1987) 3.
20 H. H. Lauer and G. P. Rozing, *Chromatographia*, 14 (1981) 641.

Journal of Chromatography, 541 (1991) 75–81
Elsevier Science Publishers B.V., Amsterdam

CHROM. 22 965

Application of a hydrogen storage alloy to the determination of trace impurities in high-purity hydrogen by gas chromatography

Group analysis of C_1, C_2 and C_3 hydrocarbons

HIROSHI OGINO* AND YOKO AOMURA
Technical Research Laboratory, Toyo Sanso Co., Ltd., 3–3, Mizue-cho, Kawasaki-ku, Kawasaki-shi, Kanagawa 210 (Japan)
and
TOSHIYUKI HOBO
Department of Industrial Chemistry, Faculty of Technology, Tokyo Metropolitan University, Setagaya-ku, Tokyo 158 (Japan)
(First received August 7th, 1990; revised manuscript received October 31st, 1990)

ABSTRACT

A hydrogen storage alloy was applied as an absorbent for hydrogen and as a catalyst for the hydrogenation of unsaturated hydrocarbons such as ethylene, propylene and acetylene for the determination of trace hydrocarbons in hydrogen by gas chromatography with photoionization detection. The hydrogen storage alloy was used at ambient temperature and under the pressure of the carrier gas. The conversion yields were 103% for ethylene to ethane, 77% for acetylene to ethane and 102% for propylene to propane and the detection limits were 0.01 ppm for methane, 0.02 ppm for ethane and 0.01 ppm for propane.

INTRODUCTION

Gas chromatography (GC) has been widely used for the determination of hydrocarbons components, as inherent impurities, in process gases such as hydrogen, nitrogen, oxygen and argon [1]. Photoionization detection (PID), which is based on the emission from a direct current discharge in helium gas, is a universally sensitive detection method [1] and has especially high sensitivity for inert gases [2]. We have reported in previous papers [3,4] that PID is suitable for the determination of trace amounts of inert gases such as nitrogen, argon, krypton and xenon. PID has a higher sensitivity to hydrocarbons such as methane, ethane and propane, which have lower ionization potentials than that of helium, and has a sensitivity similar to or higher than that of flame ionization detection (FID) [5].

However, in the determination of hydrocarbons such as methane, ethane and propane in hydrogen, it has been difficult to separate and determine directly and

0021-9673/91/$03.50

accurately trace amounts of the hydrocarbons below the parts per million level without reducing the proportion of hydrogen, as a major component, prior to introduction into the detector.

From the viewpoint of quality control of cylinder and/or bulk hydrogen gas, it is more practical to determine the total hydrocarbons in hydrogen in order to evaluate its purity; the carbon content in gases is a major concern in semiconductor manufacturing processes because the carbon may be deposited on the surface of water and influence the product yields of the device.

It is not necessary to determine individual hydrocarbon impurities, such as ethane, ethylene and acetylene, in hydrogen. If unsaturated hydrocarbons can be converted quantitatively into the corresponding saturated hydrocarbons, the gas chromatograms obtained will be simpler and the analysis time can be reduced. We found that unsaturated hydrocarbons could be converted quickly and very efficiently into saturated hydrocarbons by the use of a precolumn packed with a suitable hydrogen storage alloy (HSA), which was operated at room temperature and at the pressure of the carrier gas.

An HSA was used for the absorption of hydrogen, which is a major component of the sample gas, and also for the catalytic conversion of unsaturated hydrocarbons (*e.g.*, ethylene, acetylene and propylene) to the corresponding saturated hydrocarbons.

This paper describes a method for the group determination of C_1–C_3 hydrocarbons in hydrogen with the use of PID and the hydrogenation ability of an HSA at room temperature.

EXPERIMENTAL

Apparatus

A schematic diagram of the experimental apparatus is shown in Fig. 1. It consists of a gas sampler, a precolumn (hydrogen absorber) and a gas chromatograph (GC-263-30; Hitachi, Tokyo, Japan) with a photoionization detector. A precolumn was installed between the gas sampler (1.5 ml) and the stainless-steel analytical column (3 m × 3 mm I.D.), which was packed with active alumina (60–80 mesh). The precolumn (30 cm × 9.5 mm O.D. U-shaped stainless-steel tube) was filled with

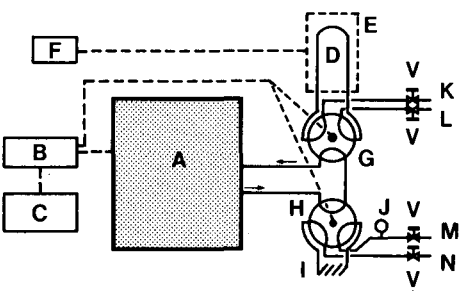

Fig. 1. Schematic diagram of the experimental apparatus. A = Gas chromatograph; B = interface; C = integrator; D = precolumn (HSA); E = heating block; F = thermo-controller; G, H = air-actuated six-port valves; I = sample loop; J = pressure transducer; K = hydrogen and helium gas inlet for HSA activation and purge; L = hydrogen and helium gas outlets; M = sample gas inlet; N = sample gas outlet; V = diaphragm stop valves (the arrow shows the direction of carrier gas flow).

a hydrogen storage alloy (HSA, 16–60 mesh) as described previously [4]. All fittings, such as the reducer and union tee (Nupro, Willoughby, OH, U.S.A.) were made of stainless-steel. This system can be programmed with a computerized integrator (C-R4A; Shimadzu, Kyoto, Japan) through an interface and is able to analyse and automatically report the results. Analytical results are computed by an absolute calibration method from the peak area. The operating conditions for the GC–PID system and the precolumn were as follows: oven temperature, 80°C; detector temperature, 100°C; carrier gas, helium at a flow-rate of 50 ml/min; discharge gas, helium at a flow-rate of 40 ml/min; discharge potential, 750 V; and precolumn temperature, room temperature (*ca.* 25°C).

Materials

The HSAs used, obtained from Japan Metals and Chemicals (Tokyo, Japan) are listed in Table I. The particle size of the pulverized HSA was initially in the range 16–60 mesh.

TABLE I

HYDROGEN STORAGE ALLOYS

HSA	Composition
HSA-1	$LaNi_{4.9}\ Al_{0.1}$
HSA-2	$MnNi_{4.5}\ Al_{0.5}$ [4]
HSA-3	$CaNi_5$

Reference gases were prepared by the gravimetric method and were supplied by Toyo Sanso (Tokyo, Japan). Most of the experiments to evaluate the applicability of the HSA as a hydrogenation catalyst were conducted with reference gases having the following compositions: (1) 10.0 ppm CH_4, 9.7 ppm C_2H_6, 9.6 ppm C_3H_8 in H_2; (2) 9.1 ppm C_2H_4, 9.5 ppm C_3H_6 in H_2; (3) 10.2 ppm C_2H_2 in H_2; and (4) 8.0 ppm C_2H_4, 9.3 ppm C_2H_6, 8.5 ppm C_2H_2, 8.9 ppm C_3H_6, 8.5 ppm C_3H_8 in He. High-purity helium (Toyo Sanso, [A] grade, 99.9999%) was employed as the carrier gas and discharge gas without further purification. The activation and regeneration of HSA were carried out with the procedure used previously [4], as shown in Table II.

RESULTS AND DISCUSSION

Selection of HSA

Several HSAs were examined to see if unsaturated hydrocarbons (*e.g.*, ethylene) can be converted completely into saturated hydrocarbons (*e.g.*, ethane). The chromatographic profiles obtained after passing through the precolumn, which were packed with different HSAs, are shown in Figs. 2–4. HSA-1 led to unasymmetrical and strongly tailing peaks for C_3 hydrocarbons, as shown in Fig. 2. HSA-2 and HSA-3 provided better peak shapes for C_2 and C_3 hydrocarbons. The quantitative results showed that the HSA-3 had an improved performance, *i.e.*, it could absorb much more hydrogen than HSA-2 without any loss of saturated hydrocarbons such as methane,

TABLE II

ACTIVATION AND REGENERATION PROCEDURES FOR PRECOLUMN FILLED WITH HSA-1–3

Activation steps	Regeneration steps
Precolumn turned to the activation position	Precolumn turned to the activation position
Evacuation (under vacuum for 30 min)	Evacuation (under vacuum at 140°C for 30 min)
Hydrogen absorption (at *ca.* 25°C, 6 atm for 30 min)	Precolumn turned back to the analytical position (heat at 180°C for 30 min)
Evacuation (under vacuum at 140°C for 30 min)	Precolumn cooled to *ca.* 25°C
Precolumn turned back to the analytical position (heat at 180°C for 30 min)	GC analysis
Precolumn cooled to *ca.* 25°C	
GC analysis	

ethane and propane and also could be successfully activated and regenerated by the procedures described previously [4]; HSA-3 provided better peak shapes, especially for propylene, than the other HSAs. The HSA-3 was therefore chosen for subsequent use.

Efficiency of hydrogenation

A series of experiments were conducted to evaluate the hydrogenation efficiency for converting C_1–C_3 unsaturated hydrocarbons at sub-parts per million levels in hydrogen into saturated hydrocarbons using activated HSA-3. The peak area for each

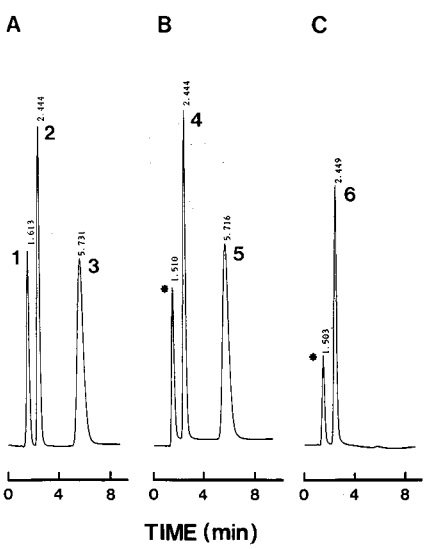

Fig. 2. Chromatograms obtained with HSA-1. (A) 1 = CH_4 (1.0 ppm); 2 = C_2H_6 (1.0 ppm); 3 = C_3H_8 (1.0 ppm). (B) 4 = C_2H_6 from C_2H_4 (1.0 ppm); 5 = C_3H_8 from C_3H_6 (1.0 ppm). (C) 6 = C_2H_6 from C_2H_2 (1.0 ppm). Asterisks show air peak.

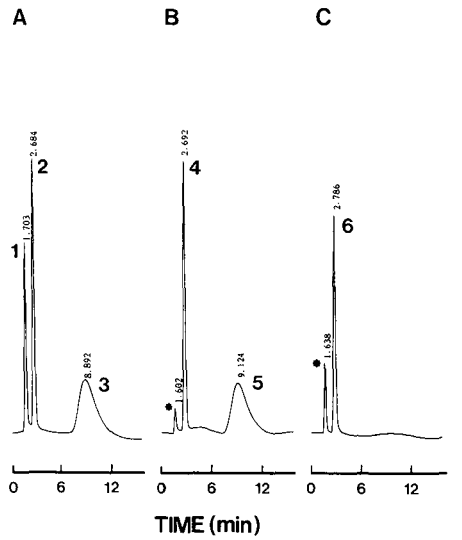

Fig. 3. Chromatograms obtained with HSA-2. A, B and C as in Fig. 2.

of the gases that passed through the precolumn was compared with that obtained without the precolumn; the sample gases used in both experiments were prepared by diluting the standard gas with high-purity hydrogen by the use of mass flow controllers.

The results showed that ethylene and propylene were completely converted into ethane and propane, respectively, within experimental error and acetylene was partially absorbed and converted into ethane with a constant hydrogenation ratio of

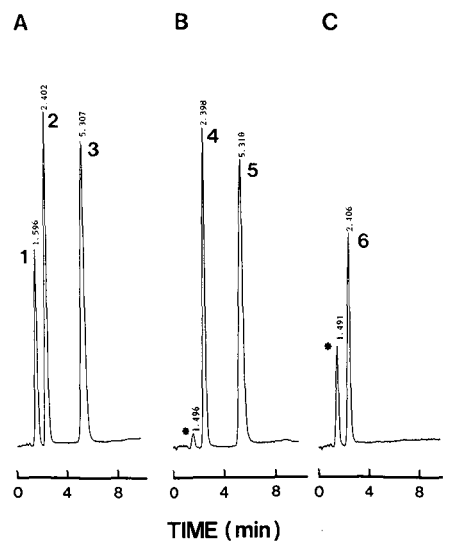

Fig. 4. Chromatograms obtained with HSA-3. A, B and C as in Fig. 2.

103 ± 2%, 77 ± 3% and 102 ± 3% for C_2H_4, C_2H_2 and C_3H_6, respectively. Only acetylene, which has a carbon–carbon triple bond, showed a lower efficiency of hydrogenation than the other unsaturated hydrocarbons. Hence if a sample contains acetylene and other C_2 hydrocarbons, the analytical result obtained will be slightly lower than the real value. Fortunately, this will only slightly affect the determination of the purity of hydrogen as the impurity is present in mere trace amounts. In the 30 cm × 9.5 mm O.D. precolumn, over 120 ml of hydrogen could be absorbed; with a sample size of 1.5 ml, more than 80 samples can be analyzed.

Typical gas chromatogram

Typical gas chromatograms of gas mixtures in hydrogen obtained by a direct method (without the precolumn) and the present method (with the precolumn) are shown in Fig. 5. In the former chromatogram, a large hydrogen peak overlapped the peaks of later eluted components. Consequently, it was difficult and/or impossible to measure th peak areas of trace amounts of impurities accurately owing to the tailing of the large hydrogen peak. It takes more than 30 min untill the complete elution of hydrogen is achieved and the next analysis is possible. On the other hand, such a large hydrogen peak did not appear on the chromatogram obtained by the present method and also only saturated hydrocarbon peaks were eluted and an analysis could be finished within 10 min.

Reproducibility and detection limits

In order to evaluate the quantitative performance of the system, standard gas mixtures were repeatedly injected into the system. The results showed that the reproducibilities (relative standard deviation, n = 5–6) were 1.49, 0.76, 0.81, 0.34, 2.73 and 0.51% for CH_4 (1.04 ppm), C_2H_6 (1.01 ppm), C_3H_8 (1.04 ppm), C_2H_4 (0.98 ppm), C_2H_2 (1.08 ppm) and C_3H_6 (1.03 ppm), respectively. The detection limits, which were

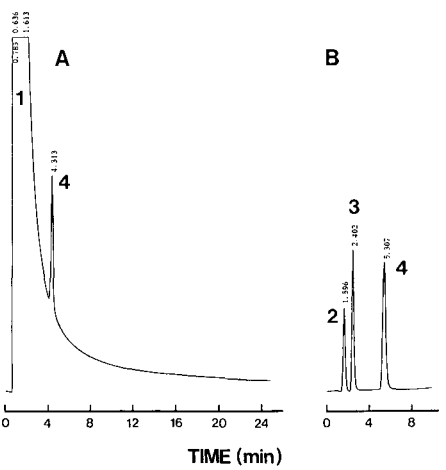

Fig. 5. Comparison between chromatograms obtained for C_1–C_3 hydrocarbons with and without the precolumn (HSA-3). Sample gas contains CH_4 (1.0 ppm), C_2H_6 (1.0 ppm) and C_3H_8 (1.0 ppm) in hydrogen. 1 = H_2; 2 = CH_4; 3 = C_2H_6; 4 = C_3H_8.

calculated from the minimum peak areas given by the integrator detection, were *ca.* 0.02, 0.01 and 0.01 ppm for CH_4, C_2H_6 and C_3H_8, respectively.

The calibration graphs were linear up to *ca.* 5 ppm in the concentration range examined. The relative sensitivities (methane = 100) were 174 ± 3 for ethane and ethylene, 127 ± 5 for acetylene and 247 ± 3 for propane and propylene, respectively.

In conclusion, the proposed procedure could be used to determine C_1–C_3 hydrocarbons down to the parts per billion level if the gas chromatograph is equipped with a highly sensitive detector such as a photoionization detector or a helium ionization detector [5].

ACKNOWLEDGEMENT

The authors express their thanks to Dr. M. Uchiyama (General Manager of Technical Division of Toyo Sanso) for reviewing the manuscript.

REFERENCES

1 C. J. Cowper and A. J. DeRose, *The Analysis of Gases by Chromatography* (*Pergamon Series in Analytical Chemistry*, Vol. 7), Pergamon Press, Oxford, 1985.
2 G. R. Verga, *J. High Resolut. Chromatogr. Chromatogr. Commun.*, 8 (1985) 456.
3 H. Ogino, Y. Aomura, M. Komuro and T. Kobayashi, *Anal. Chem.*, 61 (1989) 2237.
4 H. Ogino, Y. Aomura and M. Mizuno, *Anal. Chem.*, 62 (1990) 994.
5 G. D. Sandrock and E. L. Huston, *CHEMTECH*, (1981) 754.

Journal of Chromatography, 541 (1991) 83–88
Elsevier Science Publishers B.V., Amsterdam

CHROM. 22 964

Determination of monocyclic aromatic hydrocarbons in plant cuticles by gas chromatography–mass spectrometry

R. KEYMEULEN[a,*], H. VAN LANGENHOVE and N. SCHAMP
Laboratory of Organic Chemistry, Faculty of Agricultural Sciences, State University of Ghent, Coupure Links 653, B-9000 Ghent (Belgium)
(First received June 14th, 1990; revised manuscript received October 30th, 1990)

ABSTRACT

A method for the determination of benzene, toluene, ethylbenzene and xylenes in plant foliage was developed. Using a gas chromatography–quadrupole mass spectrometer in the selected-ion monitoring mode, calibration graphs and detection limits for these hydrocarbons were determined. *Pseudotsuga menziesii* (Mirb.) Franco needles and *Cotoneaster dammeri* Schn. "Skogholm" leaves were extracted with dichloromethane; the optimum extraction time was determined to be 6 h. Differences in the amounts of the hydrocarbons absorbed could be measured.

INTRODUCTION

Monocyclic aromatic hydrocarbons (MAHs) constitute an important fraction of the volatile organic compounds (VOCs) in ambient air. They are emitted by industrial processes and automobile exhausts. Average concentrations of benzene, toluene, ethylbenzene and xylenes in urban air vary from 1 to 70 $\mu g\ m^{-3}$, with peaks for benzene and toluene above 100 $\mu g\ m^{-3}$ [1–3]. As an increase in the content of benzene and other aromatics compensates for the decrease in octane number in unleaded fuel, increases in emission may be expected.

Exposure to aromatic hydrocarbons can cause serious health problems. Benzene is known to be a leukaemic agent in humans. The toxic properties of toluene, ethylbenzene and xylenes have also been frequently studied [4,5]. In addition, these hydrocarbons are photochemically reactive and contribute to smog.

An important feature of MAHs is their high lipophilicity [6]. They may be enriched in plant cuticles by their partitioning between the vapour state and the lipophilic cuticle. Recently, there has been some interest in the absorption of organic compounds by plant foliage. Frank and Frank [7] measured the uptake of tetrachloroethene by spruce needles and determined the partition ratios between air and

[a] R.K. is "aspirant" (research assistant) at the "Nationaal Fonds voor Wetenschappelijk Onderzoek" (Natural Fund for Scientific Research, Belgium).

0021-9673/91/$03.50

needles. In several studies, the accumulation of mainly persistent semi-volatile chlorinated hydrocarbons in coniferous needles was investigated [8–11].

The aim of this study was to develop a simple but sensitive method for measuring amounts of benzene, toluene, ethylbenzene and xylenes absorbed in plant cuticles, in order to evaluate whether this is an important mechanism for the elimination of these pollutants from air.

EXPERIMENTAL

Sample preparation

Samples of *Pseudotsuga menziesii* (Mirb.) Franco needles were collected along a highway in the north of Belgium, running from the southeast to the northwest, which is approximately perpendicular to the direction of the prevailing winds in this area. Needles were sampled at 1.5 m above the ground on the side exposed to the highway by cutting them from the twigs with a pair of scissors. They were dropped into glass tubes provided with screw-caps without touching with the fingers. Approximately 1 g of needles (fresh weight), corresponding to 90–110 needles, were sampled per tube.

Leaves of *Cotoneaster dammeri* Schn. "Skogholm", a 0.5-m high shrub, were collected on the side of a road with dense traffic in the city of Ghent, Belgium, in the same way as the *Pseudotsuga* needles.

Dichloromethane, containing an internal standard (5 ng μl^{-1}), was added to the tubes to extract MAHs from the cuticle [1.2 ml of dichloromethane per gram of needles (fresh weight)]. The tubes were tightly closed with screw-caps and Teflon tape and placed in a slowly rotating drum (to improve contact between the solvent and the needles) for a certain period of time (see Results). The extracts were then filtered (Millex-HV 0.45 μm) and aliquots of 1 μl of filtrate were injected into the gas chromatograph

Analysis

A Hewlett-Packard Model 5890 gas chromatograph equipped with a Model 5970A quadrupole mass spectrometer and a Model 200 computer system was used to analyse the leaf extracts. A 30 m × 0.258 mm I.D. fused-silica capillary column coated with a 0.25-μm thick layer of DB-5 stationary phase was used with splitless injection. The carrier gas was helium at a linear velocity of 0.48 m s^{-1}. The injector temperature was 250°C and the gas chromatograph–mass spectrometer interface temperature 260°C. The initial oven temperature was 20°C, increased at 2°C min^{-1} for 14 min to 48°C, then at 15°C min^{-1} to 230°C. The sampling rate was five selected ion monitoring cycles per second.

RESULTS AND DISCUSSION

Instrumental parameters

The HP quadrupole mass spectrometer was used in the selected-ion monitoring mode. In Table I, the selected masses used for data acquisition and the time interval for each group of ions sampled are given.

As the leaf extracts also contained large amounts of terpenes, exhibiting retention times of 15 min and more, data acquisition had to be terminated at 14 min,

TABLE I

PARAMETERS FOR DATA ACQUISITION IN SELECTED-ION MONITORING

Group	Time interval for sampling (min)	*m/z*	Compound
1	2.50–4.00	77, 78	Benzene
2	4.00–6.60	91, 92	Toluene
3	6.60–9.00	66, 98	Perdeuterooctane
4	9.00–14.00	91, 106	Ethylbenzene, *m-/p*-xylene, *o*-xylene

immediately after elution of the *o*-xylene peak. At this moment, the rate of column temperature increase was changed in order to elute the terpenes quickly from the column.

To avoid peak tailing, which easily occurs at the low concentrations used, the internal standard in the extracts should be an apolar compound. As it should also be completely absent from ambient air, perdeuterooctane was chosen.

Calibration graphs

To obtain calibration graphs, eight standard solutions of mixture of 0.25, 0.5, 0.75, 1, 2.5, 5, 7.5 and 10 ng μl^{-1} benzene, toluene, ethylbenzene, *m-/p*-xylene and *o*-xylene and a constant concentration of 5 ng μl^{-1} internal standard (perdeuterooctane) were injected. Then the ratios of the peak area of the MAH to that of the internal standard were plotted against corresponding concentrations for each aromatic compound. In this way, five linear eight-point calibration graphs with

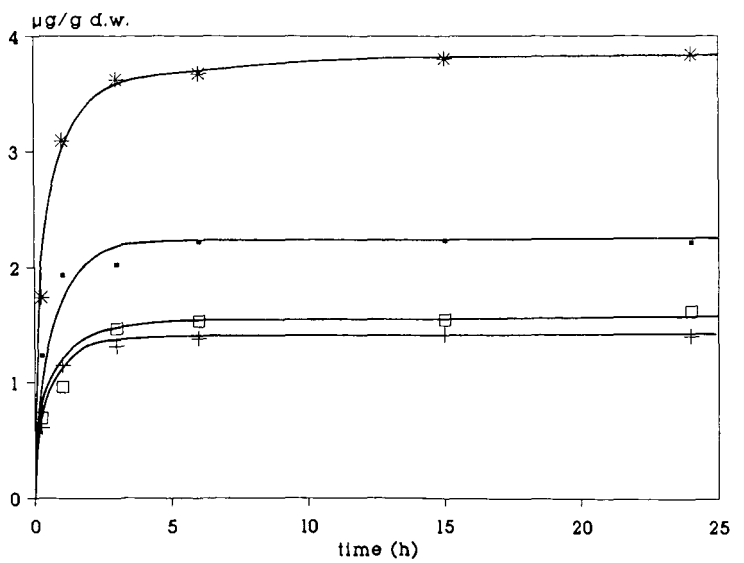

Fig. 1. Concentrations of (■) toluene, (+) ethylbenzene, (*) *m-/p*-xylene and (□) *o*-xylene in *Pseudotsuga menziesii* (Mirb.) Franco needles ($\mu g\ g^{-1}$ dry weight) as a function of the extraction time.

TABLE II

CONCENTRATIONS OF MAH IN LEAVES OF SIX *PSEUDOTSUGA MENZIESII* (MIRB.) FRANCO TREES AND SIX *COTONEASTER DAMMERI* SCHN. "SKOGHOLM" SHRUBS ($\mu g\ g^{-1}$ DRY WEIGHT)

Compound	*Pseudotsuga menziesii* (Mirb.) Franco												*Cotoneaster dammeri* Schn. "Skogholm"					
	1-year-old needles						2-year-old needles						1	2	3	4	5	6
	1	2	3	4	5	6	1	2	3	4	5	6						
Benzene	–	–	–	–	–	–	–	–	–	–	–	–	0.30	0.44	0.48	0.60	0.38	0.74
Toluene	3.26	3.24	4.46	3.27	3.56	3.58	3.48	2.05	4.48	2.51	3.06	2.92	0.03	0.04	0.03	0.06	0.05	0.08
Ethylbenzene	2.15	1.75	2.45	1.80	1.78	1.86	4.67	2.37	4.95	2.47	4.22	2.39	–	–	–	–	–	–
m-p-Xylene	4.69	3.73	5.25	4.35	3.89	4.06	10.15	5.46	10.95	5.31	9.06	5.64	–	–	–	–	–	–
o-Xylene	2.36	1.86	2.77	2.19	1.69	1.78	5.38	2.92	5.96	2.75	4.14	2.47	–	–	–	–	–	–

correlation coefficients of 0.999 were obtained. The relative standard deviations of the ratios for 1 ng μl^{-1} were determined to vary from 1.6 to 3% for five injections.

Detection limits

Detection limits of the MAHs were determined by diluting the standard solution until signal-to-noise ratio of 3 was reached. In this way, detection limits of 50 pg μl^{-1} for ethylbenzene, *m*-/*p*-xylene and *o*-xylene and 10 pg μl^{-1} for benzene and toluene were obtained (the relative standard deviations varied from 10.2 to 13.9% for five injections).

Analysis of plant extracts

Extraction efficiency. The amount of aromatic compounds that is extracted from the leaves is dependent on the extraction time. The most efficient extraction time was determined by analysing samples of dichloromethane that had been in contact with *Pseudotsuga menziesii* (Mirb.) Franco needles for 0.25, 1, 3, 6, 15 and 24 h. Fig. 1 shows that the extraction is completed after 6 h.

To understand why this long extraction time is necessary, the morphological structure of the plant cuticle should be considered. The plant cuticle is composed of different layers: an outermost epicuticular wax layer, soluble in organic solvents, and the cuticle proper and cuticular layers, which are insoluble in organic solvents [12]. As 10–30 s are sufficient to extract the epicuticular wax layer from leaves [12], and as in these experiments 6 h are necessary to extract MAHs, it seems that only a very small fraction of the MAHs can be absorbed in the epicuticular wax layer. The largest fraction of the MAHs can be assumed to be absorbed in the cuticle proper and the cuticular layers. The cuticle proper consists of insoluble polymeric cutin, whereas the cuticular layers are composed of a polymeric structure of cutin and cellulose, in which wax and pectin are embedded [12,13]. The extraction time of 6 h can thus be rationalized as the time necessary for the MAHs to migrate out of this polymeric structure into the dichloromethane solution.

Concentrations. With the method described, concentrations of MAHs in 1- and 2-year-old needles of six different *Pseudotsuga menziesii* (Mirb.) Franco trees and in the leaves of six different *Cotoneaster dammeri* Schn. "Skogholm" shrubs were determined (Table II).

In needle extracts of *Pseudotsuga menziesii* (Mirb.) Franco, benzene could not be detected. The xylenes were found in the highest concentrations (up to 10 μg/g of needle dry weight). Differences in concentrations between the needles of six *Pseudotsuga menziesii* (Mirb.) Franco trees and between 1- and 2-year-old needles are observed. Especially the concentrations of ethylbenzene, *m*-/*p*-xylene and *o*-xylene are higher in 2- than in 1-year-old needles from the same tree. In leaves of *Cotoneaster dammeri* Schn. "Skogholm", only benzene (0.3–0.7 $\mu g\ g^{-1}$ dry weight) and toluene (0.03–0.08 $\mu g\ g^{-1}$ dry weight) could be detected. Differences in MAH content between the leaves from six *Cotoneaster* shrubs can also be noticed.

CONCLUSION

Using the proposed method, differences in the concentrations of benzene, toluene, ethylbenzene, *m*-/*p*-xylene and *o*-xylene, absorbed in 1- and 2-year-old needles

of different *Pseudotsuga menziesii* (Mirb.) Franco trees and in leaves of different *Cotoneaster dammeri* Schn. "Skogholm" shrubs could be determined.

Apparently, the absorption of monocyclic aromatic compounds is dependent on the plant species, the individual plant and the age of the leaves. Further investigations are necessary to find the causes of these differences. Also, experiments on any possible degradation of MAHs in plants are necessary in order to determine elimination rates of MAHs from air by plants.

REFERENCES

1 H. B. Singh, L. J. Salas, B. K. Cantrell and R. Redmond, *Atmos. Environ.*, 19 (1985) 1911–1919.
2 B. M. Wathne, *Atmos. Environ.*, 17 (1983) 1713–1722.
3 A. Person, A. M. Laurent, Y. Le Moullec, F. Coviaux and B. Festy, *Pollut. Atmos.*, 120 (1988) 401–410.
4 M. Sittig, *Toxic Priority Pollutants, Health Impacts and Allowable Limits,* Noyes Data, Park Ridge, NJ, 1980, pp. 87–90, 344–347, 217–220.
5 B. J. Dean, *Mutat. Res.*, 47 (1978) 75–97.
6 A. Sato and T. Nakajima, *Br. J. Ind. Med.*, 36 (1979) 231–234.
7 H. Frank and W. Frank, *Environ. Sci. Technol.*, 23 (1989) 365–367.
8 A. Reischl, M. Reissinger, H. Thoma and O. Hutzinger, *Chemosphere*, 18 (1989) 561–568.
9 G. Eriksson, S. Jensen, H. Kylin and W. Strachan, *Nature (London)*, 341 (1989) 42–44.
10 C. Gaggi and E. Bacci, *Chemosphere*, 14 (1985) 451–456.
11 E. H. Buckley, *Science*, 216 (1982) 520–522.
12 J. T. Martin and B. E. Juniper, *The Cuticles of Plants*, Arnold, London, 1970, pp. 74–75.
13 P. J. Holloway, in D. F. Cutler, K. L. Alvin and C. E. Price (Editors), *The Plant Cuticle*, Academic Press, New York, 1982, pp. 1–4.

Journal of Chromatography, 541 (1991) 89–98
Elsevier Science Publishers B.V., Amsterdam

CHROM. 22 979

Location of double bonds in polyunsaturated fatty acids by gas chromatography–mass spectrometry after 4,4-dimethyloxazoline derivatization

LAURENT FAY* and URS RICHLI
Nestec Ltd. Research Centre, Vers-chez-les-Blanc, P.O. Box 44, CH-1000 Lausanne 26 (Switzerland)
(First received August 17th, 1990; revised manuscript received November 13th, 1990)

ABSTRACT

The location of double bonds in polyunsaturated fatty acids is determined by gas chromatography–mass spectrometry after 4,4-dimethyloxazoline (DMOX) derivatization. A procedure for DMOX preparation, starting from fatty acid methyl esters (FAMEs) is proposed. The most interesting properties of these derivatives are presented especially for the analysis of long-chain polyenoic fatty acids. The use of DMOX derivatives in combination with FAMEs can be very useful for the identification of fatty acids in unknown samples.

INTRODUCTION

A major problem in the analysis of unsaturated fatty acids is the determination of the position of the double bond in the alkyl chain. In the past, a number of different mass spectrometric methods for the structure elucidation of fatty acids have been proposed and excellent reviews [1,2] summarize all the different aspects.

In contrast to the methods of analysing underivatised fatty acids by tandem mass spectrometry [3,4], derivatization methods which introduce a group of low ionization potential (fragmentation-directing functionality) are attractive because they can be performed on a simple gas chromatographic-mass spectrometric (GC–MS) system working in the electron impact (EI) ionization mode. Following the latter approach, many different derivatives of the carboxylic group have been investigated: pyrrolidides [5,6], picolinyl [7–12], piperidyl and morpholinyl [13] esters, triazolopyridines [14] and 2-alkenylbenzoxazoles [15]. Using these derivatives, the determination of the position of functionalities such as double and triple bonds, branches or cyclopropane rings has been described.

However, these derivatives have low volatility, especially with long-chain polyunsaturated fatty acids, and their chromatographic behaviour is not good enough to permit the separation of all the acid derivatives which are often present in complex mixtures. In addition, their mass spectra sometimes leave doubt about the sites of unsaturation.

0021-9673/91/$03.50

Recently, Zhang *et al.* [16] described the use of 2-alkenyl-4,4-dimethyloxazolines (DMOX) for the location of double bonds in long-chain olefinic acids. These derivatives have a high volatility for chromatographic analysis and their mass spectra show easily recognizable diagnostic peaks for the determination of the position of unsaturation. The same derivatives have also been used for the determination of methyl branching [17] and cyclopentenyl and triple bond location [18,19]. However, the described reaction between free fatty acids and 2-amino-2-methylpropanol was not quantitative and residual material could not be removed.

This paper describes another way of obtaining DMOX derivatives, starting from FAMEs routinely used for the analysis of lipids by GC. The methyl esters, obtained by transesterification of the triglycerides, form the corresponding DMOX derivatives by reaction with 2-amino-2-methylpropanol (Scheme 1). The products can easily be extracted from the reaction mixture.

EXPERIMENTAL

Materials

All fatty acid standards were purchased from Supelco (Gland, Switzerland). Acetyl chloride and 2-amino-2-methylpropanol were obtained from Fluka (Buchs, Switzerland) and were used without further purification. All solvents were of analytical-reagent grade.

Derivatization

The direct transesterification method of Lepage and Roy [20] was slightly modified (hexane replacing benzene [21]). In a Reacti-vial (Pierce, Socochim, Pully, Switzerland), 10 μl of fat sample were dissolved in 1 ml of methanol–hexane (4:1) and 100 μl of acetyl chloride were slowly added. The vials were tightly closed and heated at 100°C for 1 h. After cooling, 1 ml of 6% K_2CO_3 and 1 ml of hexane were added and the mixture was gently shaken. The hexane phase was dried (Na_2SO_4) and evaporated under a stream of nitrogen at room temperature. The DMOX derivatization was carried out by adding 500 μl of 2-amino-2-methylpropanol, heated overnight at 180°C. After cooling, the reaction mixture was dissolved in 5 ml of dichloromethane and washed twice with 2 ml of distilled water. The dichloromethane solution was dried (Na_2SO_4) and evaporated under a stream of nitrogen at room temperature. The residue was dissolved in hexane and was ready for injection.

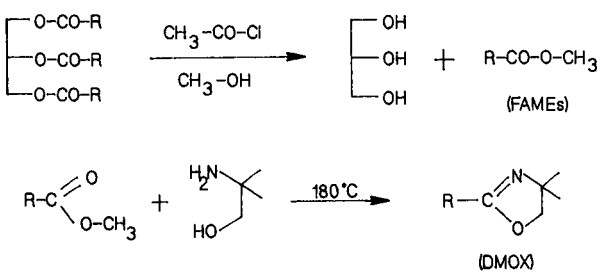

Scheme 1.

Gas chromatography–mass spectrometry

The equipment used was a Hewlett-Packard 5880 gas chromatograph, a Kratos MS-30 mass spectrometer and a DS55 data system (Kratos, Manchester, U.K.). The GC–MS conditions were as follows: fused-silica column (30 m × 0.32 mm I.D.) DB-WAX; carrier gas (helium) pressure, 10 p.s.i.; on-column injection at 60°C; oven temperature programme, 60°C (1 min), increased at 30°C/min to 200°C and then at 3°C/min to 240°C (5 min); ion source temperature, 240°C; EI ionization at 70 eV.

An HP-5971A GC–MS system with an HP-G1030A MS Chemstation (Hewlett-Packard, Geneva, Switzerland) was also used. The oven temperature programme was 50°C (1 min), increased at 30°C/min to 150°C and then at 4°C/min to 250°C (10 min).

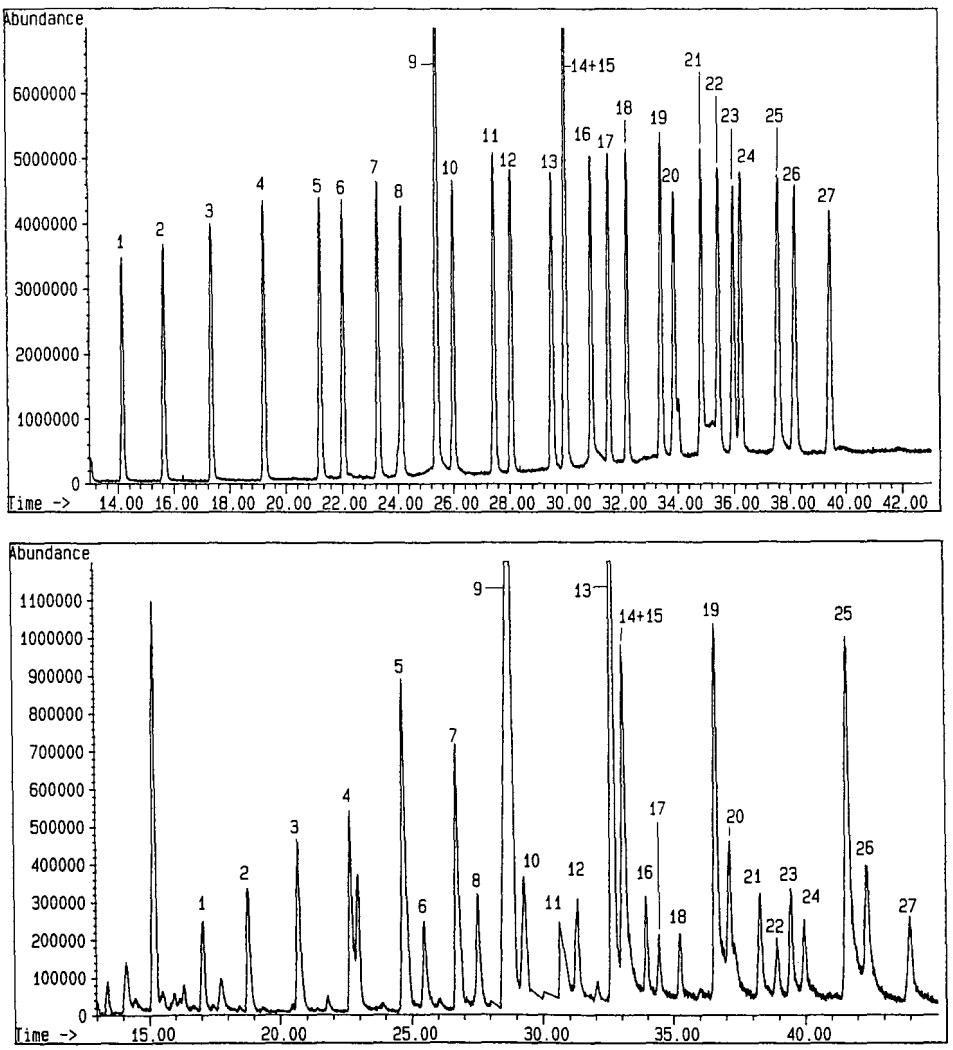

Fig. 1. Separation of a FAME standard mixture (top) and the corresponding DMOX derivatives (bottom) on a DB-WAX capillary column. See Experimental for the chromatographic conditions.

RESULTS AND DISCUSSION

In our first experiments, the DMOX derivatization reaction of free fatty acids according to Zhang *et al.* [16] was not complete and the gas chromatograms showed residual materials interfering with DMOX derivatives. Therefore, we developed a new DMOX derivatization procedure starting from FAMEs. This method allows the qualitative and quantitative analysis of fatty acids in an unknown sample in two steps. First, all the common fatty acids are easily determined by analysis of the FAME derivatives obtained after the direct transesterification of triglycerides. In a second step, if there is doubt about the structure of unsaturated acids, the FAMEs can be derivatized directly to the corresponding DMOX derivatives, which are then analysed by GC–MS.

Fig. 1 shows the chromatograms of a standard mixture of 27 FAMEs and of the DMOX derivatives obtained with the same column under the same conditions. The elution orders of DMOX and FAME derivatives are identical. The chromatographic properties of DMOX derivatives allow their resolution on a polar column without applying high temperature or long isothermal periods. Typical elution temperatures of DMOX are about 10–15°C higher than those required by the corresponding FAMEs.

The proposed reaction of FAMEs with 2-amino-2-methylpropanol is carried out overnight at 180°C. The procedure yields a quantitative derivatization and after extraction with dichloromethane no residual FAMEs interfere with the DMOX derivatives (Fig. 2).

These drastic conditions are required in order to obtain a complete reaction between FAMEs and 2-amino-2-methylpropanol and quantitative formation of oxazoline derivatives. If the reaction is performed at lower temperatures residual FAMEs are still present and produce interferences with DMOX derivatives. Under the chosen conditions, no discrimination effect and no decomposition products of fatty

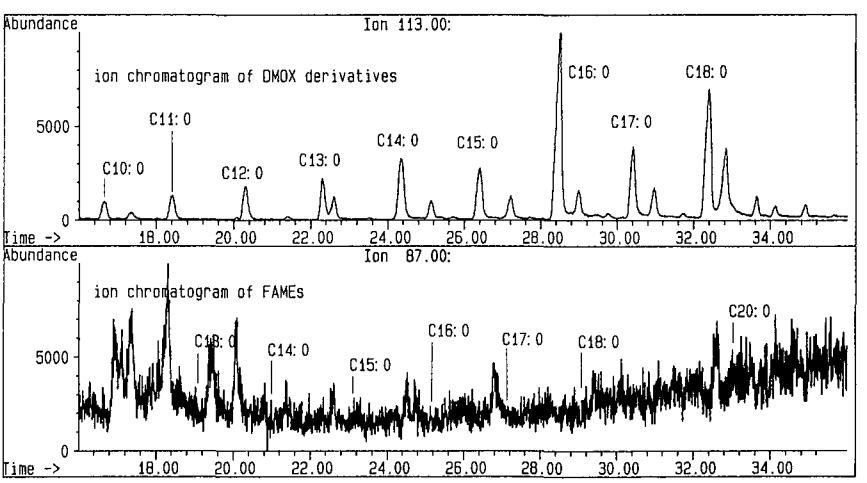

Fig. 2. Mass chromatograms of DMOX derivatives (*m/z* 113) and FAMEs (*m/z* 87) in a standard mixture after DMOX derivatization carried out overnight at 180°C. No residual FAMEs can be detected in the sample.

acids have been detected. The derivatives obtained are stable for at least 1 week at room temperature.

The mass spectra of DMOX derivatives clearly show the positions of the double bonds in mono- or polyunsaturated fatty acids. An unsaturation is located by an interruption of the regular pattern produced by successive chain cleavages of methylene units. The double bond position can be determined using the rule formulated by Andersson and co-workers [22,23] for pyrrolidide derivatives: if an interval of 12 atomic mass units (a.m.u.), instead of the regular 14 a.m.u., is observed between the most intense peaks clusters of fragments containing n and $n - 1$ carbon atoms in the acid moiety, a double bond occurs between carbons n and $n + 1$ in the molecule.

Fig. 3 shows the mass spectrum of C22:1 (13), which contains two peaks at m/z 252 and 264 locating a C-13 double bond. The base peak at m/z 113 and the intense ion at m/z 126 are produced by McLafferty rearrangement and a cyclization reaction, respectively [16].

For all monoenoic acids studied, the double bond located between carbons n and $n + 1$ also gives abundant ions with $n + 2$, $n - 2$ [16] and $n + 3$ carbon atoms. In this case, the small ions locating the double bond are always surrounded by three ions with more abundant intensities. For example, the spectrum in Fig. 3 presents such a pattern with prominent peaks at m/z 238, 292 and 306.

DMOX derivatives are very attractive for the analysis of long-chain polyenoic fatty acids. Unlike pyrrolidide, picolinyl or triazolopyridine derivatives, DMOX of polyunsaturated fatty acids are well eluted on polar GC columns and easily transferred into the MS source. After EI ionization, they produce mass spectra which clearly show the molecular ion and the positions of unsaturation.

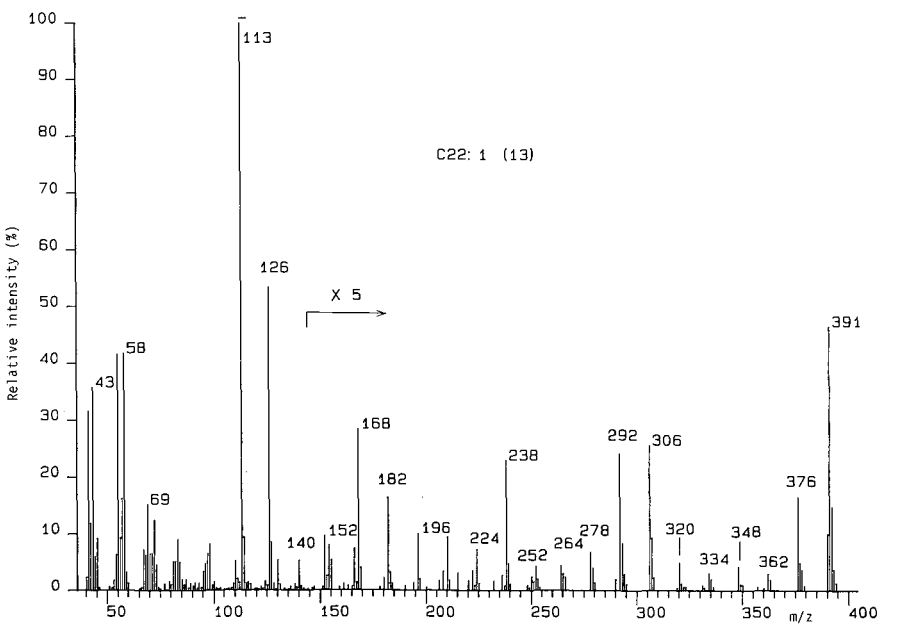

Fig. 3. Mass spectrum of the DMOX derivative of C22:1 (13).

Table I summarizes the results obtained for 22 unsaturated fatty acids after DMOX derivatization. Only the diagnostic fragments, locating the double bond positions, are presented.

Fig. 4 shows the spectrum of C22:6 (4,7,10,13,16,19). The rule of the 12 a.m.u. intervals can easily be applied and indicates double bonds at the C-7, -10, -13, -16 and -19 positions. However, the location of the C-4 unsaturation cannot be identified by the 12 mass units rule. This unsaturation is located by an intense odd-mass ion at *m/z* 139. The formation of this ion could be explained by ionization of the nitrogen atom followed by cyclization and cleavage of the rest of the aliphatic chain (Scheme 2). For C-5 and C-6 unsaturations, corresponding ions were observed at *m/z* 153 and 167.

The use of ions at *m/z* 139, 153 and 167 allows the unambiguous location of C-4, -5 and -6 double bonds even for fatty acids with a non-regular distribution of the unsaturations. As an illustration, Fig. 5 presents the mass spectrum of the C18:3 (5,9,12) acid. The C-9 and -12 double bonds are located by the 12 a.m.u. interval and the C-5 unsaturation by the intense peak at *m/z* 153.

The method described here has also been used successfully for fatty acids with conjugated double bonds. An example is the analysis of seed oil from *Calendula*

TABLE I

CHARACTERISTIC IONS IN EI MASS SPECTRA OF DMOX DERIVATIVES OF 22 UNSATURATED FATTY ACIDS

Fatty acid DMOX	$M^{+\cdot}$ *m/z* (intensity, %)	Diagnostic fragments *m/z* (intensity, %)
C22:6 (4,7,10,13,16,19)	381(5)	166(4), 178(3), 206(3), 218(2), 246(3), 258(2), 286(1), 298(1), 326(0.5), 338(0.1), 139(9)
C20:4 (5,8,11,14)	357(9)	180(3), 192(2), 220(3), 232(2), 260(1), 272(1), 153(19)
C20:5 (5,8,11,14,17)	355(5)	180(3), 192(2), 220(3), 232(2), 260(2), 272(1), 300(1), 312(1), 153(17)
C18:1 (6)	335(4)	166(13), 167(24)
C18:3 (6,9,12)	331(18)	194(13), 206(8), 234(7), 246(4), 220(27), 274(19), 166(21), 167(33)
C18:4 (6,9,12,15)	329(8)	194(6), 206(3), 234(4), 246(2), 274(2), 286(1), 220(7), 260(6), 166(9), 167(12)
C22:4 (7,10,13,16)	385(14)	168(7), 180(13), 208(7), 220(4), 248(9), 260(4), 288(3), 300(2)
C22:5 (7,10,13,16,19)	383(7)	168(6), 180(9), 208(6), 220(4), 248(6), 260(2), 288(3), 300(2), 328(2), 340(1)
C20:3 (8,11,14)	359(4)	182(2), 194(1), 222(2), 234(1), 262(1), 274(1)
C14:1 (9)	279(7)	196(2), 208(3), 182(16), 236(13), 250(9)
C16:1 (9)	307(7)	196(2), 208(2), 182(15), 236(11), 250(12)
C18:1 (9)	335(13)	196(3), 208(3), 182(16), 236(13), 250(11)
C18:2 (9,12)	333(10)	196(3), 208(2), 236(5), 248(2), 222(15), 276(11)
C18:3 (9,12,15)	331(20)	196(3), 208(2), 236(6), 248(3), 276(8), 288(2)
C15:1 (10)	293(8)	210(1), 222(2), 196(10), 250(11), 264(9)
C17:1 (10)	321(7)	210(2), 222(2), 196(9), 250(9), 264(9)
C18:1 (11)	335(10)	224(1), 236(3), 210(7), 264(9), 278(9)
C20:1 (11)	363(10)	224(1), 236(2), 210(6), 264(8), 278(8)
C20:2 (11,14)	361(15)	224(1), 236(3), 264(5), 276(2)
C20:3 (11,14,17)	359(16)	224(2), 236(1), 264(5), 276(2), 304(5), 316(2)
C22:1 (13)	391(9)	252(1), 264(1), 238(5), 292(5), 306(5)
C22:2 (13,16)	389(19)	252(1), 264(1), 292(3), 304(2)

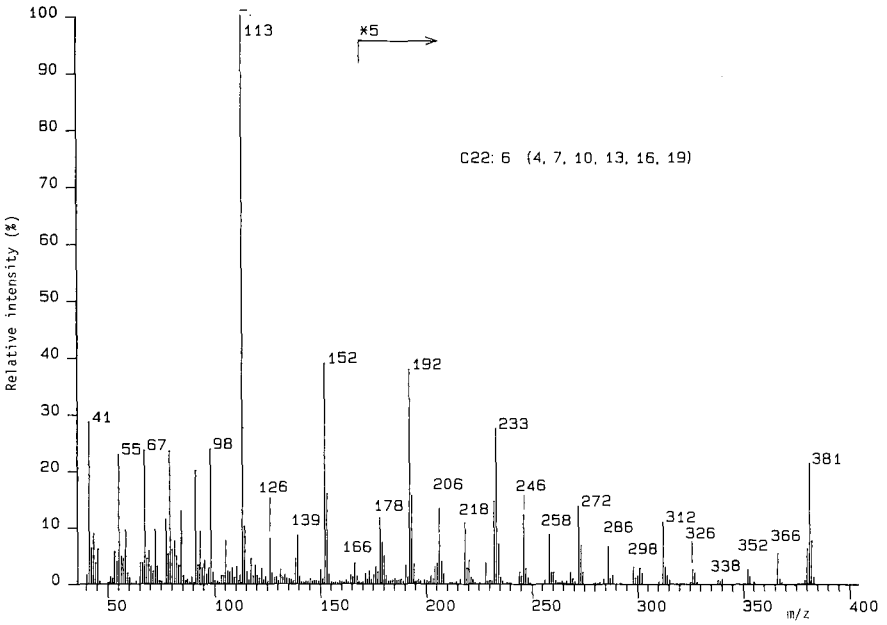

Fig. 4. Mass spectrum of the DMOX derivative of C22:6 (4,7,10,13,16,19).

officinalis. After transesterification, the GC–MS analysis of the FAMEs obtained shows two unknown peaks. The chromatogram of the corresponding DMOX derivatives is presented in Fig. 6 and the mass spectrum of the first unknown peak in Fig. 7. This peak 1 was identified as C18:3 (8,10,12). Its spectrum shows characteristic ions between *m/z* 182 and 260. Peak 2 has the same mass spectrum and is identified as

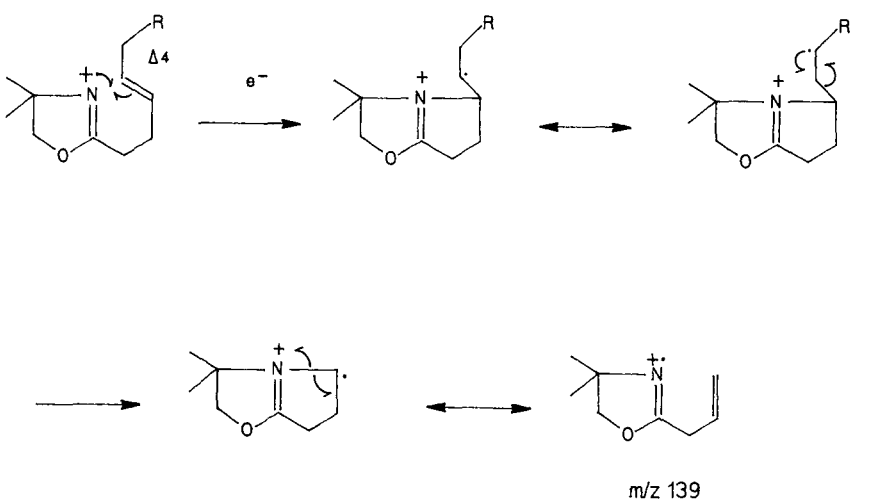

Scheme 2.

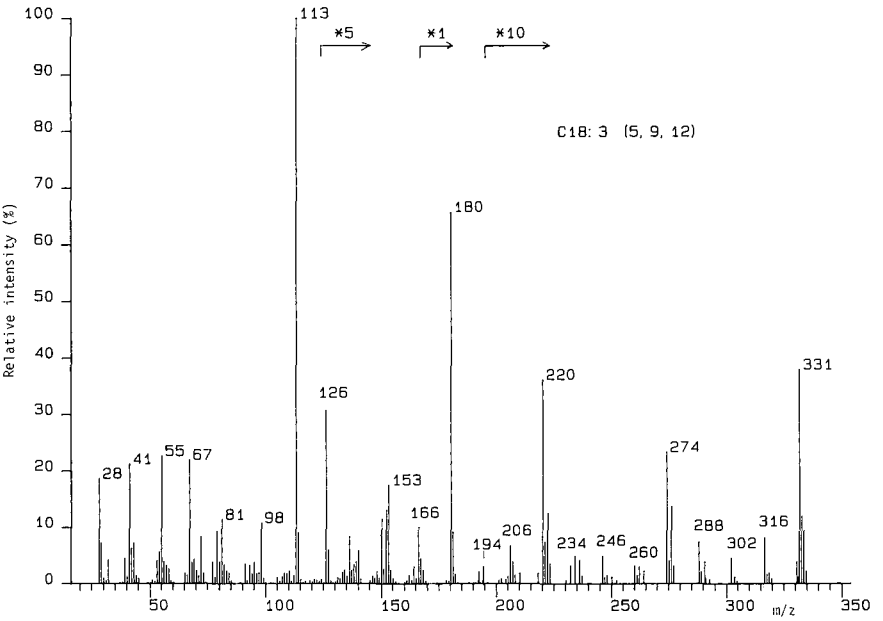

Fig. 5. Mass spectrum of the DMOX derivative of C18:3 (5,9,12).

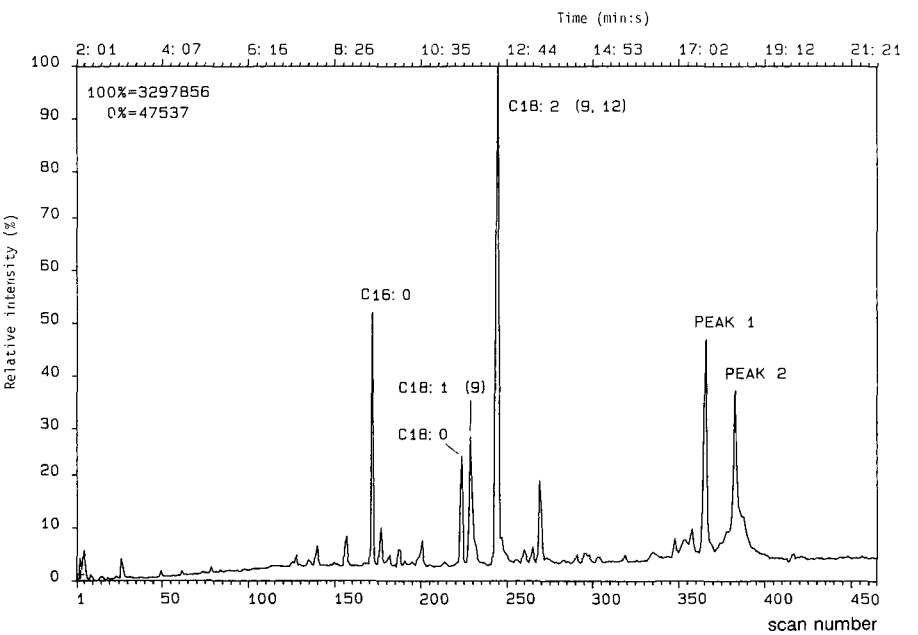

Fig. 6. Separation of the DMOX derivatives of the seed oil of *Calendula officinalis*.

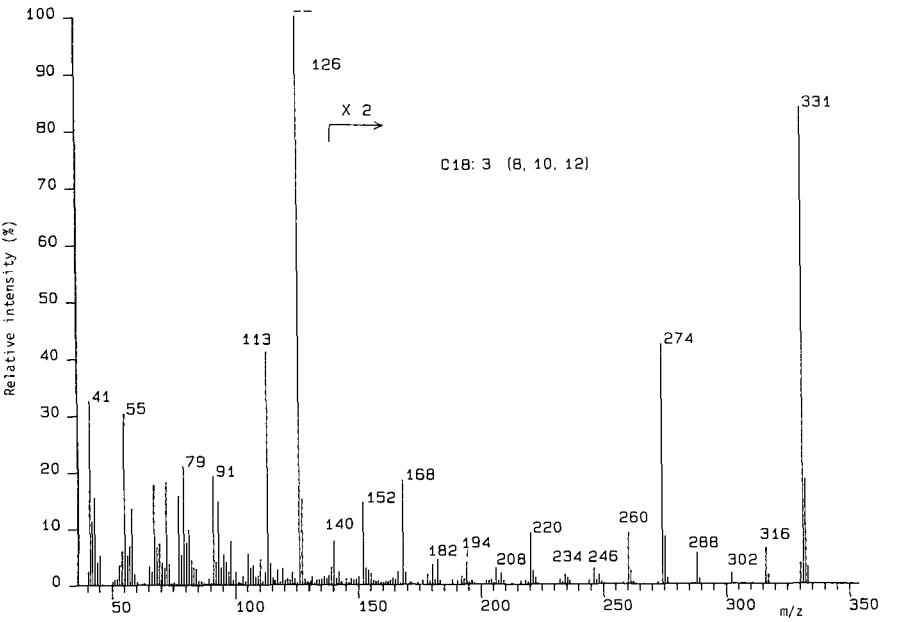

Fig. 7. Mass spectrum of the DMOX derivative of C18:3 (8,10,12) identified in the seed oil of *Calendula officinalis*.

an isomer. The difference between these two acids is probably the *cis/trans* configuration of the double bonds. For this oil various isomers of octadecatrienoic acids, including calendic acid (*trans*-8,*trans*-10,*cis*-12-octadecatrienoic acid), have been proposed [24].

In conclusion, DMOX derivatives of fatty acids can be obtained easily and quantitatively from the corresponding methyl esters. Mass spectra of DMOX derivatives are very useful for double bond location, especially in polyunsaturated and conjugated systems. The good chromatographic properties of DMOX derivatives allow the effective resolution of complex mixtures. The combined use of FAMEs and DMOX derivatives can be a very attractive method for fatty acid analysis.

ACKNOWLEDGEMENTS

The authors thank Drs. R. Liardon and T. Huynh-Ba for helpful discussions, Dr. H. J. Wille for the seed oil of *Calendula officinalis* and Dr. G. Crozier Willi for revising the manuscript.

REFERENCES

1 N. J. Jensen and M. L. Gross, *Mass Spectrom. Rev.*, 6 (1987) 497.
2 R. J. Anderegg, *Mass Spectrom. Rev.*, 7 (1988) 395.
3 K. B. Tomer, F. W. Crow and M. L. Gross, *J. Am. Chem. Soc.*, 105 (1983) 5487.
4 N. J. Jensen and M. L. Gross, *Lipids*, 21 (1986) 362.
5 W. W. Christie, E. Y. Brechany, S. B. Johnson and R. T. Holman, *Lipids*, 21 (1986) 657.
6 A. J. Valicenti, W. H. Heimermann and R. T. Holman, *J. Org. Chem.*, 44 (1979) 1068.

7 D. J. Harvey, *Biomed. Mass Spectrom.*, 9 (1982) 33.
8 D. J. Harvey, *Biomed. Mass Spectrom.*, 11 (1984) 187.
9 D. J. Harvey, *Biomed. Mass Spectrom.*, 11 (1984) 340.
10 D. J. Harvey, *Biomed. Mass Spectrom.*, 18 (1989) 719.
11 W. W. Christie, E. Y. Brechany, F. D. Gunstone, M. S. F. Lie Ken Jie and R. T. Holman, *Lipids*, 22 (1987) 664.
12 W. W. Christie, E. Y. Brechany and M. S. F. Lie Ken Jie, *Chem. Phys. Lipids*, 46 (1988) 225.
13 M. Jutila and J. Jalonen, *Biomed. Mass Spectrom.*, 17 (1988) 433.
14 W. Vetter, W. Meister and G. Oesterhelt, *Biomed. Mass Spectrom.*, 23 (1988) 566.
15 Q. T. Yu, J. Y. Zhang and Z. H. Huang, *Biomed. Mass Spectrom.*, 13 (1986) 211.
16 J. T. Zhang, Q. T. Yu, B. N. Liu and Z. H. Huang, *Biomed. Mass Spectrom.*, 15 (1988) 33.
17 Q. T. Yu, B. N. Liu, J. Y. Zhang and Z. H. Huang, *Lipids*, 23 (1988) 804.
18 J. Y. Zhang, H. Y. Wang, Q. T. Yu, X. J. Yu, B. N. Liu and Z. H. Huang, *J. Am. Oil Chem. Soc.*, 66 (1989) 242.
19 J. Y. Zhang, X. J. Yu, H. Y. Wang, B. N. Liu, Q. T. Yu and Z. H. Huang, *J. Am. Oil Chem. Soc.*, 66 (1989) 256.
20 G. Lepage and C. C. Roy, *J. Lipid Res.*, 27 (1986) 114.
21 H. Traitler, personal communication.
22 B. A. Andersson and R. T. Holman, *Lipids*, 9 (1974) 185.
23 B. A. Andersson, W. W. Christie and R. T. Holman, *Lipids*, 10 (1975) 215.
24 T. Takagi and Y. Itabashi, *Lipids*, 16 (1981) 546.

Journal of Chromatography, 541 (1991) 99–108
Elsevier Science Publishers B.V., Amsterdam

CHROM. 22 958

Determination of peroxyacetyl nitrate, peroxypropionyl nitrate and alkyl nitrates of atmospheric importance using capillary columns

GERASSIMOS MINESHOS, NIKOLAOS ROUMELIS and SOTIRIOS GLAVAS*
Department of Chemistry, University of Patras, GR-261 10 Patras (Greece)
(First received August 3rd, 1990; revised manuscript received October 29th, 1990)

ABSTRACT

Three capillary columns were studied for the determination of peroxyacetyl nitrate, peroxypropionyl nitrate and some alkyl nitrates of atmospheric importance. Two non-polar HP-1 100% dimethyl polysiloxane columns, of 0.53 and 0.32 mm I.D., yielded the best resolution of all compounds studied. The intermediate polarity HP-17 50% methyl–50% phenyl polysiloxane wide-bore column could not resolve peroxypropionyl nitrate from 2-butyl nitrate. Compared with capillary columns with polar Carbowax stationary phases, the columns studied gave a better resolution of peroxyacetyl nitrate and peroxypropionyl nitrate, and there was no interfering water peak. Alkyl nitrates could be determined simultaneously. Detection limits were in the low ppb range.

INTRODUCTION

Peroxyacetyl nitrate (PAN) is a significant component of photochemical smog in urban centres [1,2]. In addition, PAN is ubiquitous in clean atmospheres, where it constitutes a major part of odd nitrogen [3]. Peroxypropionyl nitrate (PPN), the next higher PAN homologue, occurs in the atmosphere at concentrations that are a small fraction of those of PAN. Because of these extremely low concentrations of PPN, few ambient measurements of this compound have been reported [4]. Similarly, very few recent studies of atmospheric determinations of organic nitrates have been published [5,6].

The determination of PAN, PPN and organic nitrates is usually carried out by gas chromatography with electron-capture detection (GC–ECD). The columns used for the separation of PAN and PPN are usually packed columns with the stationary phases Carbowax 400 or Carbowax 600 and 4.8% QF-1 + 0.18% diglycerol on deactivated Chromosorb [4,7,8]. Recently capillarly columns have been employed for the determination of PAN and PPN [9–11]. ECD of PAN, PPN and organic nitrates is the preferred method of detection because of its high sensitivity. Calibrating the detector for PAN remains a very different task, however despite the numerous calibration procedures reported in the literature [12,13]. For the calibration of the detector for organic nitrates and PPN there are virtually no data. It is usually assumed

0021-9673/91/$03.50

that PPN and alkyl nitrates have the same response factors as PAN [1].

As we have recently shown, destruction of PAN and PPN on the column owing to their residence in the chromatographic column during analysis is much more extensive on a packed column than on a wide-bore capillary column [11], probably owing to the greater inertness of the capillary columns. In addition, capillary columns give better resolution and shorter analysis times. In this work we evaluated three capillary columns, differing in inside diameter, length and polarity of stationary phase, for the determination of PAN and PPN and examined their use for the simultaneous determination of some alkyl nitrates of atmospheric importance.

EXPERIMENTAL

All mixtures were prepared at room temperature in a 4.5-l glass flask, equipped with two ports with septa and a Teflon stopcock and connected to a vacuum line provided with Teflon stopcocks. Pure PAN and PPN solutions in tridecane were synthesized by nitration of the corresponding peroxy acids following the procedure of Gaffney *et al.* [14]. The peroxyacids were prepared from the anhydrides of acetic and propionic acids as specified by Nielsen *et al.* [15]. Methyl and ethyl nitrate were prepared by nitration of methanol and ethanol according to standard methods [16]. 2-Butyl nitrate was prepared by stirring 2-bromobutane dissolved in tetrahydrofuran (THF) with silver nitrate dissolved in water at room temperature for 4 h in the dark. After filtration of silver bromide, the THF layer containing 2-butyl nitrate was separated in a separating funnel. A pale yellow product remained after vacuum vaporization of THF at room temperature.

GC–ECD of the vapour of this reaction product diluted in air yielded only one peak. All the compounds studied were identified by their retention times. In addition, PAN and PPN were identified by observing that their chromatographic peaks disappeared when an air stream containing separately pure PAN and pure PPN was passed through an alkaline solution. Similarly, methyl and ethyl nitrate, which are major thermal decomposition products of PAN and PPN, respectively, were identified by observing that their peak areas increased when pure PAN or pure PPN was left to decompose in a glass flask at 50°C.

Gas chromatography

Three capillary columns were evaluated for the determination of PAN, PPN and methyl, ethyl and 2-butyl nitrate: two wide-bore columns of different polarity, *viz.*, a non-polar HP-1 5-m fused-silica cross-linked 100% dimethyl polysiloxane (gum) of 0.53 mm I.D. and 2.65 μm film thickness, and an intermediate polarity HP-17 10-m fused-silica cross-linked 50% phenyl–50% methyl polysiloxane of 0.53 mm I.D. and 2.0 μm film thickness, and a non-polar HP-1 cross-linked methylsilicone gum 15-m column of 0.32 mm I.D. and 1.05 μm film thickness.

A Hewlett-Packard 5890A gas chromatograph equipped with a ^{63}Ni electron-capture detector, operated in the constant-current, variable-frequency mode, was employed in all analyses. The injector and oven temperatures in all instances were maintained at 30°C and the detector at 45°C. These temperatures were found in a recent study to be optimum for the determination of PAN and PPN [11]. Helium was the carrier gas at a flow-rate of 5 ml/min for the HP-1, 7 ml/min for the HP-17

wide-bore columns and 3 ml/min for the HP-1 0.32 mm I.D. column. The make-up gas was 10% CH_4/Ar with flow-rates 30 ml/min for all columns used.

Two factors were taken into consideration when selecting the flow-rates of the carrier and make-up gases: first that an optimum separation of all five compounds in the shortest possible time, principally in order to limit the destruction of PAN and PPN on the column, should be attained and second that the response of the detector should be as high as possible. Direct injections of 0.5 ml of sample mixtures were made manually into the injection port using gas-tight syringes provided with Teflon plungers for the wide-bore columns. The variation in the manual injections was $\pm 5\%$, as established from five replicate injections. For the column of 0.32 mm I.D., 0.1 ml of sample was introduced in the splitless mode of a split/splitless injection port. The integrator used was an HP Model 3396A.

Calibration

As mentioned earlier, calibration of the detector for the tested compounds is a major task. With PAN and PPN, the difficulty lies primarily in obtaining pure PAN and PPN standards and in their thermal instability. The methods of preparing PAN and PPN solutions in hexane or tridecane have solved the problem of preparation of the standards [15,16]. However, as these standards are not 100% pure and because of the thermal destruction of PAN and PPN, a primary calibration procedure is still necessary.

The first method of calibration that we employed involved alkaline hydrolysis of PAN or PPN and determination of the resulting nitrite anion by ion chromatography. PAN or PPN gaseous mixtures in synthetic air were prepared by injecting appropriate amounts of liquid PAN–tridecane into a FEP Teflon bag of *ca.* 100-l volume to make a PAN or PPN air mixture of approximate concentration 200 ppb. The PAN or PPN air mixture was pumped for 120 min through an impinger containing 10 ml of 25 m*M* sodium hydroxide solution at a flow-rate of 100 ml/min, such that gaseous samples taken after the impinger gave no ECD signal for PAN or PPN. Aliquots of the hydrolysis mixture were diluted 1:5 with eluent in order to reduce the system peak and injected into the ion chromatograph employing a 100-μl sample loop. From the total concentration of NO_2^- to which nitrate anion was added, as NO_3^- is probably an oxidation product of NO_2^-, and the volume of air passed through the impinger, we calculated the PAN concentration in the FEP bag. Simultaneous injection of a PAN or PPN air mixture into the gas chromatograph allowed the calibration of the detector for the given compound.

Attempts to employ the same calibration procedure for the alkyl nitrates failed because the alkyl nitrates were less than 10% retained in the hydrolysis solution and in an irregular manner. We also attempted to use the determination of acetate anions as the basis of calibration. This yielded 3 mol of acetate ions per mole of nitrite ions, however. This great deviation from the expected 1:1 mole ratio could be attributed to the presence of peracetic acid, which GC–ECD showed to be present, left over from the PAN synthesis.

A Dionex 4500i ion chromatograph with a conductivity detector was used for the determination of nitrite and nitrate anions. The columns used were Dionex AS4A with a Dionex AG4A precolumn and a micro-membrane suppressor column. With 1.8 m*M* $NaHCO_3$–1.7 m*M* Na_2CO_3 as the eluent at a flow-rate of 2 ml/min, the nitrite anions

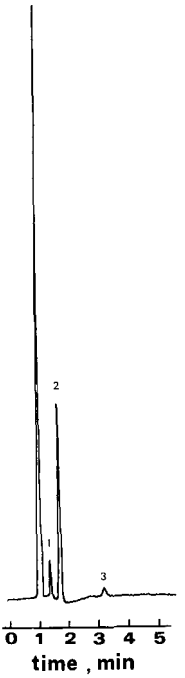

Fig. 1. Typical ion chromatogram from calibration procedure for PAN. Peaks: 1 = Cl^-; 2 = NO_2^-; 3 = NO_3^-.

eluted in 1.8 min, well resolved from the previous Cl^- peak, as shown in Fig. 1.

Before ion chromatography became available in our laboratory, we carried out calibration of the electron-capture detector for PAN, PPN and organic nitrates by first converting them to NO followed by chemiluminescence detection of NO. The main components of this system are a Pye Unicam Model 104 gas chromatograph, a molybdenum converter (a 20-cm long quartz tube of O.D. 1/4 in., packed with molybdenum cut wire heated to the desired temperature) and a chemiluminescence reaction cell situated in front of an EMI 9658R cooled photomultiplier.

In contrast to the commercially available NO_x instruments, our laboratory-made NO_x detector is operated at flow-rates typical of GC, *ca.* 30 ml/min, and has a detection limit of 10 ppb of NO. In the past this system was operated with a chromatographic column packed with the same material as the analytical packed column employed in GC–ECD. The idea was to separate the nitrogen-containing compounds on the column, convert them to NO as they elute from the column and detect them with the NO_x detector. As the NO_x detector can easily be calibrated with a primary NO standard, simultaneous injection of the nitrogen-containing compounds into the GC–ECD system would allow its calibration as well. Now, however, we operate our GC–NO_x system without this column because of destruction of PAN and PPN on the column and also because the NO primary standard does not yield reproducible results when passed through a column. Care must be exercised to introduce nitrogen-containing compounds that are as pure as possible, or at least without nitrogeneous impurities.

The first step in using the GC–NO_x system is to make an NO_x signal *vs.* molybdenum converter temperature plot, such as shown in Fig. 2, in order to find the converter temperature necessary for the complete conversion of nitrogen-containing compounds to NO. At the plateau of the diagram for each compound we assume a 100% conversion to NO.

Intercomparison of our two ECD calibration methods for PAN and PPN showed that the NO_x method yields only 77 ± 5% of the concentration obtained by ion chromatography for both PAN and PPN. This difference could presumably be attributed to a less than 100% efficiency of their conversion to NO.

RESULTS AND DISCUSSION

Response factors

Using the GC–NO_x chemiluminescence detection system we were able to determine the ECD response factors of all the compounds studied. The response factors of PAN and PPN obtained by GC–NO_x detection were corrected by 23% according to the calibration results based on the ion chromatographic method. As shown in Table I, contrary to the assumptions reported in the literature [1], the alkyl nitrates have different response factors to PAN. PAN and PPN have the highest response factors equal within experimental uncertainty. Although there was a slight column to column variation, the ECD response of methyl nitrate is on average 50 ± 5%, of ethyl nitrate 68 ± 2% and of 2-butyl nitrate 46 ± 2% of that of PAN. The PPN response, within the experimental uncertainty, is identical with that of PAN.

Chromatographic analyses

The primary aim of this work was to find a chromatographic column for the better determination of PAN and PPN, *i.e.*, with better resolution, shorter retention times and hence minimal on-column destruction. Recent interest in alkyl nitrates in the atmosphere, however, prompted us to examine whether the same column could also be used for the simultaneous determination of peroxyacyl nitrates and alkyl nitrates. For

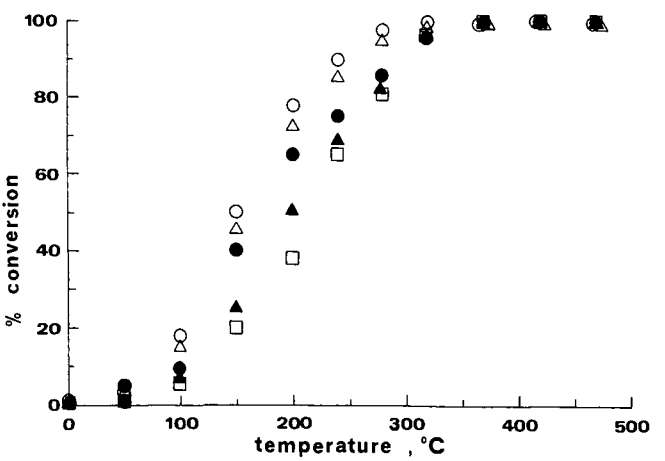

Fig. 2. Effect of temperature on conversion of nitrogen-containing compounds to NO on the molybdenum converter. ○, PAN; △, PPN; ●, methyl nitrate; ▲, ethyl nitrate; □, 2-butyl nitrate.

TABLE I

RESPONSE FACTORS (%) COMPARED WITH PAN BASED ON THE GC–NO_x DETECTION SYSTEM

Column	Methyl nitrate	Ethyl nitrate	2-Butyl nitrate	PAN	PPN
HP-1 wide-bore	45	70	48	100	93
HP-1 0.32 mm I.D.	59	69	44	100	89
HP-17 wide-bore	45	66	–	100	105

the alkyl nitrates we selected methyl and ethyl nitrate, which are the major organo-nitrogen thermal decomposition products of PAN and PPN, respectively, and 2-butyl nitrate, which was recently shown to occur in the atmosphere in the highest concentration of all $>C_3$ alkyl nitrates [5]. In addition to the resolution and retention times achieved, the three columns were also evaluated for the detection limits attained.

Figs. 3, 4 and 5 show typical chromatograms of a mixture of the above compounds with the 5-m wide-bore HP-1, the 15 m × 0.32 mm I.D. HP-1 and the 10-m wide-bore HP-17 columns, respectively. With all the columns the carrier gas flow-rate was adjusted so that the retention times of PAN and PPN would be ca. 2–3 and 4.5–6.5 min, respectively, in order to minimize as much as possible their destruction on the column, provided of course that the resolution was satisfactory. The make-up gas was adjusted so as to obtain the maximum ECD response without impairing the resolution of the least resolved peaks, air–methyl nitrate and PPN–2-butyl nitrate.

PAN and PPN on the non-polar HP-1 wide-bore column are eluted in 2.00 and 4.60 min, respectively. A typical chromatogram is shown in Fig. 3. PAN and ethyl nitrate are baseline resolved from the other peaks. The resolution between PPN and 2-butyl nitrate is 0.6, as shown in Table II. This column gives a poorer separation of methyl nitrate from the air peak. One can, however, still use this column to determine methyl nitrate down to the low ppb range for direct injection. Although the resolutions achieved with this short column are inferior to those with the HP-1 0.32 mm I.D. column, consistent with its small number of theoretical plates, as shown in Table II, its great advantage is its large sample capacity. Sample volumes up to 1 ml could be used with this column, thus improving the detection limits for the determination of PAN, at the expense of the resolution of methyl nitrate from the air peak and thus its poor detection. With this column the detection limit of PAN could be lowered to 50 ppt for direct injection of a 1-ml sample. PPN, which has the same ECD response factor as PAN, would have the same detection limit as PAN when measured alone. When PPN

TABLE II

CHROMATOGRAPHIC CHARACTERISTICS OF THE THREE COLUMNS

Column	I.D. (mm)	Length (m)	N_{sys} (maximum)	Resolution, PPN–2-butyl nitrate
HP-1	0.53	5	1200	0.6
HP-1	0.32	15	7600	1.4
HP-17	0.53	10	520	–

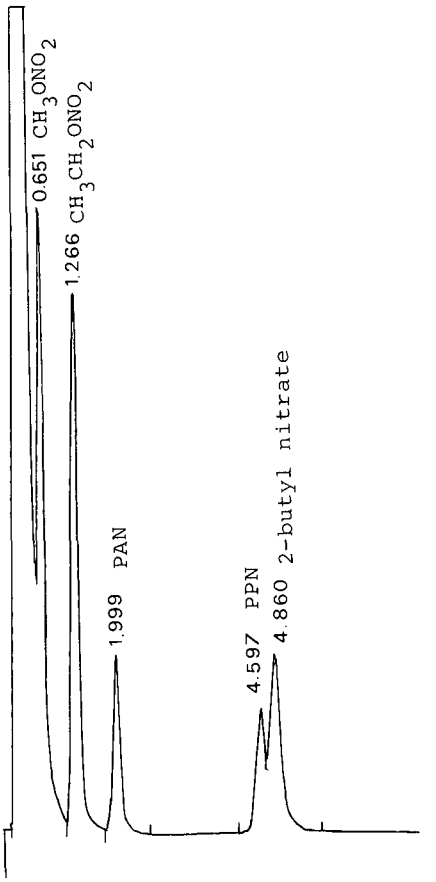

Fig. 3. Typical chromatogram of studied mixture with HP-1 wide-bore column. Numbers at peaks indicate retention times in min.

is present in the mixture studied, however, it has a higher detection limit because of its slight overlapping with 2-butyl nitrate and therefore increased uncertainty in the integration. It is estimated that in samples with approximately equal area counts of PPN and 2-butyl nitrate, the PPN detection limit for direct injection of a 0.5-ml sample would be 0.2 ppb.

The detection limits of methyl, ethyl and 2-butyl nitrate are 7, 1 and 5 ppbv, respectively. As with PPN, the detection limits, in addition to the varied response factors, depended on the resolution achieved. This explains the lower detection limit for ethyl nitrate compared with the other alkyl nitrates.

The HP-1 0.32 mm I.D. capillary column yielded a much better resolution of methyl nitrate from the air peak and of PPN from 2-butyl nitrate, as shown in Fig. 4. The optimum retention times of PAN and PPN with this column increased by almost 25% compared with the HP-1 wide-bore column. These increased retention times would result in increased destruction of PAN and PPN during their passage through the column [11]. For this reason, and as the resolution achieved was satisfactory, it was

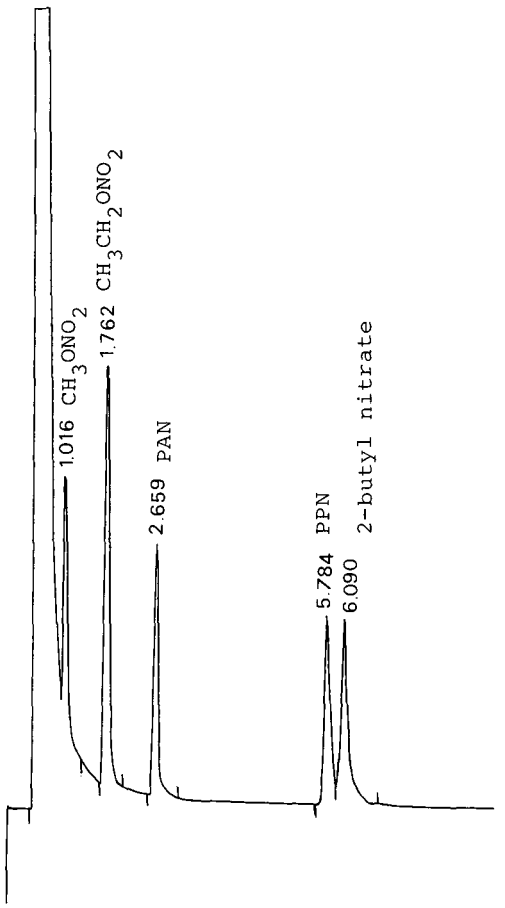

Fig. 4. Typical chromatogram of studied mixture with HP-1 0.32 mm I.D. column.

not necessary to employ a full 25- or 30-m capillary column. The resolution of 1.4 between PPN and 2-butyl nitrate achieved with this column was the best of all columns when the sample injected was 0.1 ml. The low sample capacity of this column, however, did not allow injection volumes larger than 0.2 ml without significant deterioration of the resolution of methyl nitrate from the air peak, at a methyl nitrate concentration of 8 ppb. This sample limitation was only applicable to methyl nitrate. Sample volumes of 0.5 ml can easily be injected in the splitless mode and thus lower the detection limits mainly of PAN and ethyl nitrate, but also of PPN and 2-butyl nitrate. The detection limits obtained were 0.3, 0.6, 7 and 3 ppbv for PAN, ethyl nitrate, 2-butyl nitrate and PPN, respectively.

The intermediate polarity HP-17 column also gives very good separations of PAN. As shown in Fig. 5 however, PPN is not resolved from 2-butyl nitrate. On the other hand, it is obvious that on this column methyl nitrate is better resolved from the air peak than with the HP-1 columns. The number of theoretical plates of this column calculated from the PAN peak, which is eluted in 3.07 min when the carrier gas

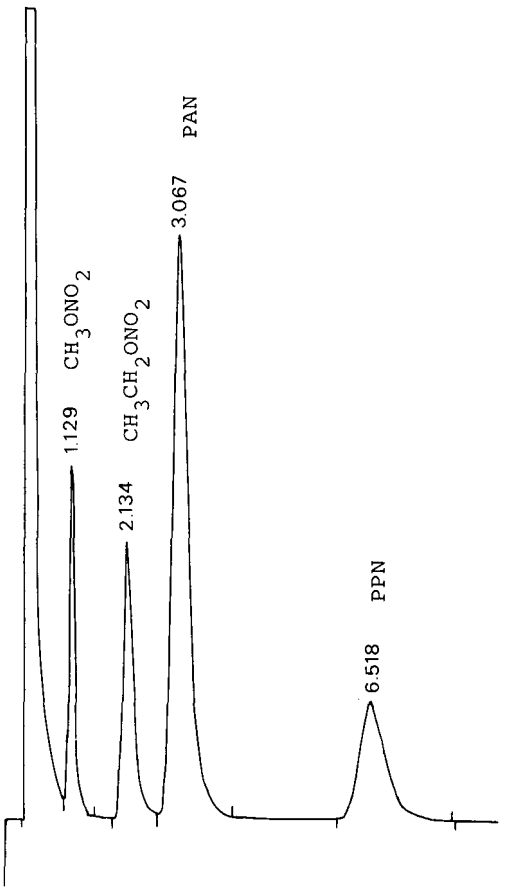

Fig. 5. Typical chromatogram of studied mixture with HP-17 wide-bore column.

flow-rate is 7 ml/min, is significantly less than those for the other two columns, as shown in Table II. The numbers of theoretical plates were calculated taking into account the slight peak asymmetry using the equation

$$N_{sys} = 41.7(t_R/W_{0.1})^2/(B/A + 1.25)$$

where t_R is the retention time, $W_{0.1}$ is the peak width at 0.1 of the peak height and B/A accounts for the peak asymmetry [17]. The detection limits for PAN and methyl and ethyl nitrate, which are almost baseline resolved, were 0.1, 1 and 0.7 ppbv, respectively, for a direct 0.5-ml sample injection.

CONCLUSIONS

The non-polar 100% dimethyl polysiloxane gum column is superior to the more polar 50% dimethyl–50% phenyl polysiloxane column for the separation of PAN,

PPN and alkyl nitrates. When these columns are compared with a capillary column with a polar Carbowax stationary phase, as recently reported by Helmig *et al.* [10], they present clear advantages. First, PAN and PPN are better resolved with all the columns examined in this work and second, and very important, there is no water peak, so that no precolumn and backflushing are required. An additional advantage, of course, is that our tested columns can be used for the simultaneous determination of alkyl nitrates. The elution of chlorofluorocarbons with these columns does not seem to be a disadvantage because preliminary tests with some chlorofluorocarbons have shown them to elute in the "windows" of the chromatogram of PAN, PPN and alkyl nitrates. Finally, the columns used in this work have been in continuous operation for almost 2 years with an average number of 30 injections per day, which could explain their small number of theoretical plates. Comparison with the capillary Carbowax column, which has a short lifetime, again favours the less polar stationary phases presented here. As the HP-1 wide bore column seems to be comparable to, if not better than, the HP-1 0.32 mm I.D. column, and given the facility with which wide-bore columns can be installed in a gas chromatograph equipped with packed-type injection ports, we propose this type of column for the determination of nitrogen compounds of atmospheric importance.

ACKNOWLEDGEMENTS

This work was financially supported by the Commission of the European Communities under Contract EV4V-0070-D(B). N.R. thanks the Hellenic Refineries of Aspropyrgos for a fellowship.

REFERENCES

1 J. M. Roberts, *Atmos. Environ.*, 24A (1990) 243.
2 P. J. Temple and O. C. Taylor, *Atmos. Environ.*, 17 (1983) 1583.
3 H. B. Singh, *Environ. Sci. Technol.*, 21 (1987) 320.
4 H. B. Singh and L. J. Salas, *Atmos. Environ.*, 23 (1989) 231.
5 E. Atlas, *Nature (London)*, 331 (1988) 426.
6 F. Juttner, *J. Chromatogr.*, 442 (1988) 157.
7 J. Rudolph, B. Vierkorn-Rudolph and F. Z. Meixner, *J. Geophys. Res.*, 92 (1987) 6653.
8 E. Tsani-Bazaca, S. Glavas and H. Gusten, *Atmos. Environ.*, 22 (1988) 2283.
9 J. M. Roberts, R. W. Fajer and S. R. Springston, *Anal. Chem.*, 61 (1989) 771.
10 D. Helmig, J. Muller and W. Klein, *Atmos. Environ.*, 23 (1989) 2187.
11 N. Roumelis and S. Glavas, *Anal. Chem.*, 61 (1989) 2731.
12 H. Meyrahn, G. Helas and P. Warneck, *J. Atmos. Chem.*, 5 (1987) 405.
13 D. Grosjean and J. Harrison, *Environ. Sci. Technol.*, 19 (1985) 749.
14 J. S. Gaffney, R. Fajer and G. I. Senum, *Atmos. Environ.*, 18 (1984) 215.
15 T. Nielsen, A. M. Hansen and E. L. Thomsen, *Atmos. Environ.*, 16 (1984) 2447.
16 A. P. Black and F. H. Babers, in A. H. Blatt (Editor), *Organic Syntheses*, Collective Vol. 2, Wiley, New York, 1967, p. 412.
17 J. P. Foley and J. G. Dorsey, *Anal. Chem.*, 55 (1983) 730.

Journal of Chromatography, 541 (1991) 109–120
Elsevier Science Publishers B.V., Amsterdam

CHROM. 23 006

Détection spécifique par chromatographie gazeuse–spectrométrie de masse des amines sympathomimétiques urinaires dans le cadre des contrôles antidopage

A. FRANCESCHINI, J. M. DUTHEL et J. J. VALLON*
Laboratoire de Biochimie, Toxicologie et Analyse des Traces, Hôpital Edouard Herriot, Place d'Arsonval, 69437 Lyon Cédex 03 (France)
(Reçu le 20 juin 1990; manuscrit modifié reçu le 23 novembre 1990)

ABSTRACT

Use of gas chromatography–mass spectrometry for urinary sympathomimetic amine detection in anti-doping control

A specific, sensitive and reliable gas chromatography–mass spectrometry (GC–MS) technique for detection of sympathomimetic amines following urinary extraction is proposed.

Amphetamine, phentermine, ephedrine, mephenorex, methylphenidate, benzphetamine, clobenzorex and internal standard (fenfluramine) are extracted from urines at pH 7.0 using elution by chloroform–isopropanol on C_{18} cartridges. Derivatization followed by GC–MS analysis allows identification of these drugs founded on relative retention times and mass spectra.

The quantitation limit for derivatizable drugs was found to be 200 ng/ml and 500 ng/ml for underivatizable drugs.

INTRODUCTION

Les amines sympathomimétiques non phénoliques: amphétamine (AM), phentermine (PT), éphédrine (EPH), méfénorex (MF), clobenzorex (CB), benzphétamine (BM), methylphénidate (MPD) sont largement utilisées chez les sportifs [1] et chez les drogués [2,3]; de ce fait, il est nécessaire de développer des techniques de détection sensibles et fiables. Les techniques de dosage radioimmunologique (RIA) [4] ou fluoroimmunologique [5] ne sont pas spécifiques d'une molécule donnée et présentent des réactions croisées avec des substances de structure voisine. La détection des amphétamines par chromatographie sur couche mince [6] offre des limites de détection plus élevées que par chromatographie gazeuse–spectrométrie de masse (CG–SM). D'autre part, les screenings réalisés en chromatographie gazeuse couplée, soit à un détecteur NPD [7], soit à un détecteur à ionisation de flamme [8], ne permettent d'identifier la drogue recherchée que par son temps de rétention relatif à un étalon interne.

La CG–SM permet une détection de faibles quantités de drogues dans l'urine et

0021-9673/91/$03.50

leur identification absolue directement, de façon précise et exacte, par leur temps de rétention relatif et leur spectre de masse. La technique que nous avons développée utilise une extraction des drogues sur cartouche C_{18} suivie d'une dérivation par l'anhydride trifluoro acétique (TFA). Les amines sympathomimétiques sont ensuite analysées par CG–SM.

MATÉRIELS ET MÉTHODES

Appareillage

Ensemble chromatographe en phase gazeuse–spectromètre de masse, CG–SM, QP 1000, Shimadzu; passeur automatique d'échantillon AOC-9, Shimadzu; système informatique pour le stockage et le traitement des données, ordinateur V 286 Victor relié à une imprimante KX-P 1083 Panasonic.

Matériels et réactifs

Bac d'extraction Vac-Elut; cartouches C_{18}, 500 mg de phase, 3 ml, Bond-Elut; thermobloc Gebr-Liebisch, Brackwede (R.F.A.); vortex Janke et Kunfel, IKA-Werk (R.F.A.); pH-mètre, PHN 75, Tacussel; méthanol, Uvasol, Merck; éthanol absolu, pro analysis, Merck; 2-propanol, pro analysis, Merck; eau pour préparations injectables, Aguettant; chloroforme, Spectrosol, SDS; acétate d'éthyle, Codex, Carlo Erba; TFA anhydride, Pierce; soude, R. P. Normapur, Prolabo; acide chlorhydrique, Rectapur, Prolabo; amphétamine sulfate, Rhone Poulenc; méthyl amphétamine hydrochloride, Delagrange; phentermine base, Roussel Uclaf; clobenzorex hydrochloride, Roussel Uclaf; (±) éphédrine hydrochloride, Aldrich; fenfluramine hydrochloride, Servier; benfluorex hydrochloride, Servier; méfénorex hydrochloride, Roche; méthylphénidate hydrochloride, Ciba-Geigy; benzphétamine hydrochloride, Upjohn.

Les solutions mères sont préparées par dissolution du produit pur dans l'éthanol, sauf pour l'amphétamine qui est dissoute dans l'eau. Elles ont une concentration de 1000 mg de produit pur sous forme base par litre de solvant.

Conditions opératoires de la séparation par CG–SM

Chromatographie. Colonne "wide-bore" en verre, SPB-1, 30 m × 0,75 mm I.D., 1,0 µm d'épaisseur de film, Supelco; gaz vecteur hélium N 60, Air liquide; pression en tête de colonne: 0,25 bar; injecteur: mode splitless, 300°C; programmation des températures du four: 120°C pendant 4 min puis programmation de 20°C/min jusqu'à 260°C puis stable pendant 1 min; durée du cycle chromatographique: 20 min.

Injecteur automatique. Volume d'injection, 1 µl.

Spectromètre de masse. Mode d'ionisation, impact électronique à 70 eV; filament, 60 µA; température du séparateur, 280°C; température de la source, 250°C; gaz d'appoint, 20 ml/min; gain, 1750 V; gamme de balayage de 49 à 549 u.m.a. (vitesse de balayage de 1,1 s.).

MISE AU POINT DE LA DÉRIVATION

Certaines amines sympathomimétiques possédant un groupement amine I ou amine II sont polaires (Tableau I). Cette polarité provoque un effet de traînée sur les tracés chromatographiques d'où un manque de résolution des pics. En transformant

TABLEAU I

STRUCTURE CHIMIQUE DES AMINES SYMPATHOMIMÉTIQUES

EPHEDRINE

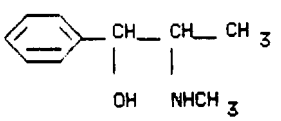

PHENTERMINE

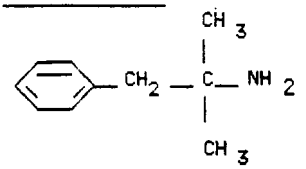

METHYLPHENIDATE

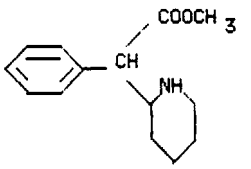

AMPHETAMINE ET DERIVES AMPHETAMINIQUES

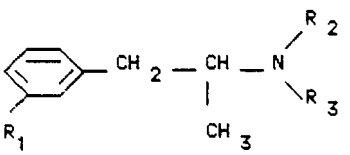

Dénomination Commune Internationale	R_1	R_2	R_3
Amphétamine	H	H	H
Fenfluramine	CF_3	H	C_2H_5
Benzphétamine	H	CH_3	$CH_2C_6H_5$
Méfénorex	H	H	$(CH_2)_3Cl$
Clobenzorex	H	H	$CH_2C_6H_4Cl$
Benfluorex	CF_3	H	$(CH_2)_2OCOC_6H_5$

ces amines I et II en amines III trifluorées, ce problème disparait. L'agent de dérivation utilisé est le TFA [9].

Nous avons choisi le benfluorex (BFR) comme étalon pour la mise au point de la dérivation car il présente une structure chimique et un comportement chromatographique proche des amines sympathomimétiques, et il n'est pas dérivable.

Les différents essais de dérivation ont été réalisés avec des solutions de travail à 100 mg/l pour AM, PT, EPH, FFR, MF, CB et MPD, et à 250 mg/l pour BFR. Les solutions de travail sont préparées par dilution des solutions mères dans un volume approprié d'éthanol.

Quantité de réactif

Sur deux résidus secs A et B (A = AM, PT, EPH, FFR et BFR; B = MF, MPD, CB et BFR) ont été testées différentes quantités de TFA: 50, 100, 200 et 500 μl. Pour chaque quantité, deux essais ont été réalisés. Les variations des intensités relatives des pics chromatographiques sont sensiblement identiques ($\pm$ 5% d'écart) quelque soit la quantité de TFA. Nous avons opté pour une quantité de TFA de 200 μl.

Température de dérivation

Les résidus secs A et B, aprés ajout du réactif de dérivation, ont été soumis à différentes températures: 55, 65, 75, 85, et 95°C. Deux essais ont été réalisés pour chaque température. Les réponses relatives sont plus importantes de 18 à 20% pour AM et PT, pour une température comprise entre 75 et 95°C. Pour les autres substances, les variations des intensités relatives des pics chromatographiques restent identiques: une variation de $\pm 3\%$ a été observée.

Temps de réaction

Nous avons testé les temps de contact: 5, 10, 15, 30 et 60 min sur les résidus A et B. Deux essais ont été faits pour chaque temps. Pour le temps 5 min, nous obtenons la meilleure réponse. La répétabilité de la dérivation dans les conditions suivantes —volume de réactif de 200 μl, température de 85°C et temps de contact de 5 min— donne des coefficients de variation allant de 5,4 à 9,2% sauf pour EPH pour laquelle il est de 11% (nombre d'essais égal à 6). Alors que pour un temps de 15 min [9], les coefficients de variation varient entre 2,5 et 5,6% (sauf pour EPH pour laquelle il est de 9,2%, pour un même nombre d'essais). Malgré une réponse inférieure de 13 à 28% à 15 min par rapport à 5 min, nous avons choisi le temps de contact de 15 min car nous avons une meilleure répétabilité de dérivation.

Donc, les conditions de dérivations sont: quantité de TFA, 200 μl; température, 85°C; temps de réaction, 15 min.

MISE AU POINT DE L'EXTRACTION URINAIRE

Le screening est pratiqué en CG–SM, mode courant ionique total (TIC). Un logiciel de fragmentométrie a été utilisé pour l'intégration des pics. Nous avons utilisé le mode TIC et non le fragmentométrie de masse (SIM) car l'un des intérêt de ce screening est, d'une part, la détection rapide des amines sympathomimétiques, et d'autre part la future adaptation de cette méthode à beaucoup d'autres composés.

Un essai préliminaire, par injection des amines sympathomimétiques, a permis d'obtenir leurs spectres de masse (Figures 1 et 2). Le Tableau II regroupe les ions utilisés en fragmentométrie. La Figure 3 représente le fragmentogramme d'un extrait urinaire avec les ions principaux de chaque substance.

Choix de la technique d'extraction

Les techniques d'extraction liquide–liquide fréquemment employées [8,10,11] décrivent une méthodologie consommatrice de temps, de solvants et nécessitant des extractions multiples pour obtenir un rendement correct et des extraits débarrassés des impuretés.

Pour remédier à ces inconvénients, nous avons choisi l'extraction solide–liquide sur cartouche C_{18}. En effet, cette méthodologie présente les avantages suivants [12,13]: économie de solvants, rapidité de la manipulation, faibles volumes d'échantillons traités, taux de récupération élevés, et elle permet d'obtenir des extraits propres.

Description de notre technique

Nous avons utilisé des cartouches C_{18} à 500 mg de phase greffée. Un échantillon de 10 ml d'urine amené au pH désiré et contenant l'étalon interne fenfluramine (FFR)

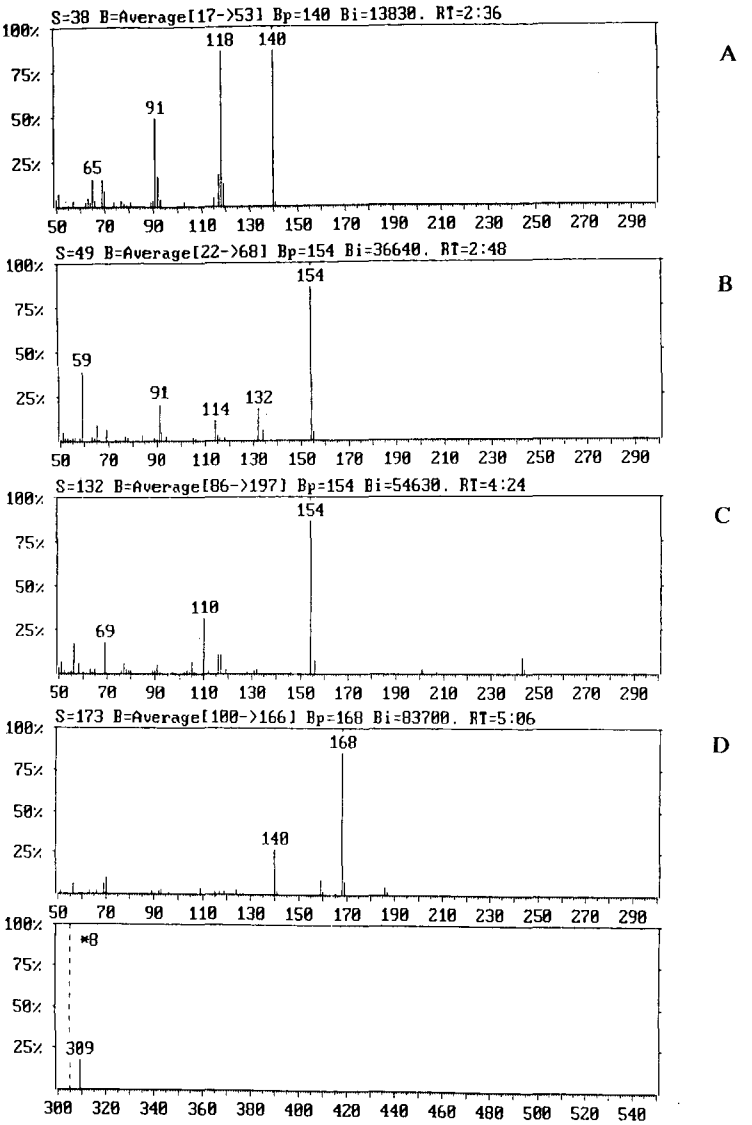

Fig. 1. Spectres de masse des amines sympathomimétiques (impact électronique:70 eV). (A) Amphétamine-TFA; (B) phentermine-TFA; (C) éphédrine; (D) fenfluramine-TFA.

a été passé goutte à goutte sur la colonne. Aprés rinçage de la colonne par 1 ml d'eau, l'élution a été faite par divers mélanges chloroforme–isopropanol. Après évaporation de l'éluant sous courant d'azote à une température inférieure à 70°C, le résidu sec est dérivé par le TFA. Après évaporation du TFA sous courant d'azote à température ambiante, le résidu sec est repris par 300 μl d'acétate d'éthyle. L'injection de 1 μl dans le chromatographe a été faite par l'injecteur automatique.

Les différents paramètres de l'extraction sont testés dans les paragraphes

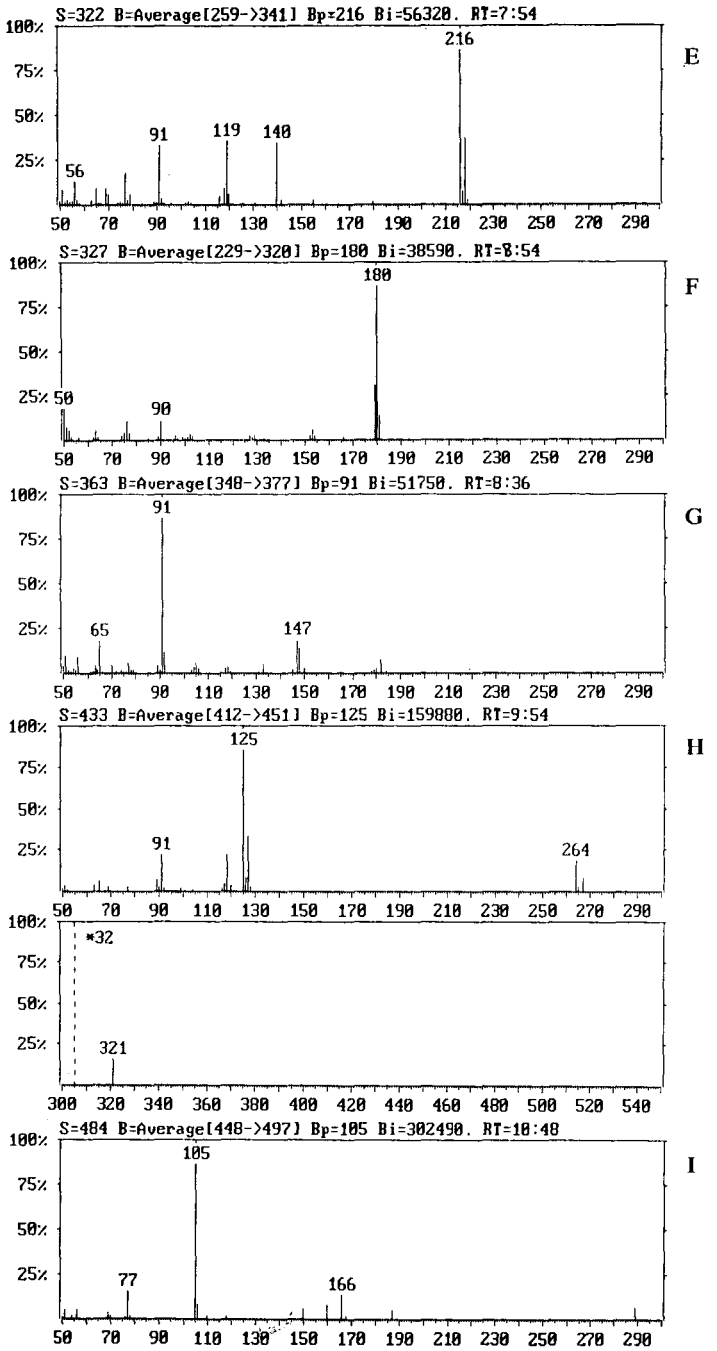

Fig. 2. Spectres de masse des amines sympathomimétiques (impact électronique: 70 eV). (E) Méfénorex-TFA; (F) méthylphénidate-TFA; (G) benzphétamine; (H) clobenzorex-TFA; (I) benfluorex.

TABLEAU II

IONS UTILISÉS POUR LA FRAGMENTOMÉTRIE

Substances	Ions (m/z)
AM-TFA	140
PT-TFA	140
EPH-TFA	154
FFR-TFA	168
MF-TFA	216
MPD-TFA	180
CB-TFA	125
BM	91

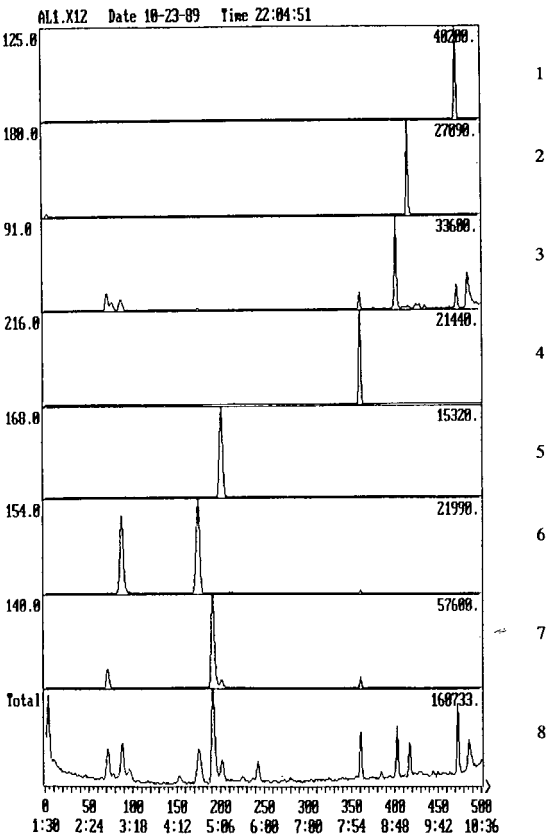

Fig. 3. Fragmentogramme d'un extrait urinaire, chargé en amines sympathomimétiques (1 μg/ml). 1 = Clobenzorex; 2 = méthylphénidate; 3 = benzphétamine; 4 = méfénorex; 5 = fenfluramine; 6 = phentermine et éphédrine; 7 = amphétamine; 8 = courant ionique total du chromatogramme correspondant. Temps de retention en min:s.

suivants. Pour évaluer leur variabilité, la FFR est alors utilisée comme étalon externe; elle est introduite avant l'étape de dérivation.

Choix du solvant à pH fixe

Par transposition de l'extraction liquide–liquide [10] à l'extraction solide–liquide, nous avons testé différents mélanges de chloroforme–isopropanol.

Pour un volume de chloroforme 1,5 à 3,5 fois supérieur au volume d'isopropanol, la quantité de substance éluée reste constante.

Nous avons choisi le mélange de solvant chloroforme–isopropanol (3:2, v/v).

Volume de solvant nécessaire

Le volume de solvant, à pH 7, nécessaire pour une élution supérieure à 95% des amines sympathomimétiques, est de 3 ml.

Par mesure de sécurité, nous avons choisi un volume de 4 ml.

Influence du pH urinaire

Dans la gamme de pH testé, la Figure 4 montre que l'élution est la plus importante à pH 7 pour la majorité des substances.

Limite de quantification

La concentration minimale urinaire d'amines sympathomimétiques détectables en utilisant le TIC est de 200 ng/ml pour les substances dérivables et de 500 ng/ml pour les substances non dérivables.

Validation de la technique d'extraction

Pour la validation, nous avons effectué des essais de stabilité des amines sympathomimétiques dans l'urine, de reproductibilité et de rendement d'extraction.

Essai de stabilité des produits dans l'urine. Deux pools d'urines chargées P_1 (contenant AM, PT et BM) et P_2 (contenant EPH, MF, MPD et CB) ont été stockés à jour 0 (J_0) à + 4°C pendant 21 jours.

À J_0, J + 1, J + 7, J + 14 et J + 21, deux aliquots de chaque pool sont prélevés et analysés.

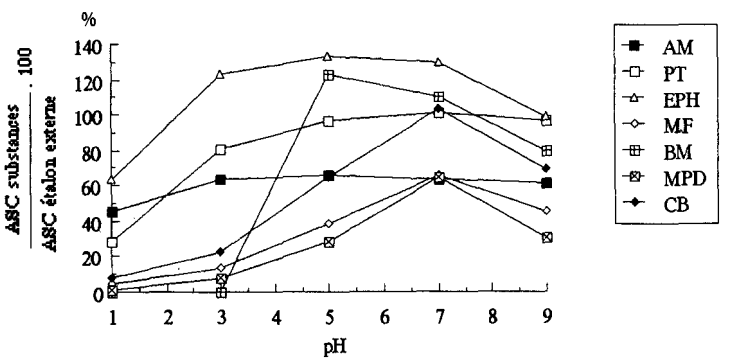

Fig. 4. Influence du pH sur l'extraction des amines sympathomimétiques.

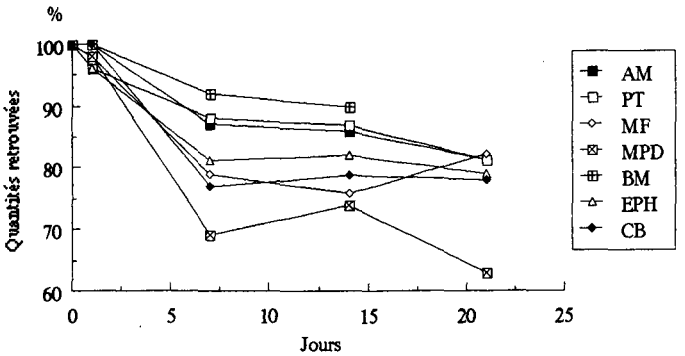

Fig. 5. Étude de la stabilité dans les urines des amines sympathomimétiques en fontion du temps à +4°C.

La Figure 5 montre la stabilité des produits sur 21 jours. Entre J + 1 et J + 7, nous constatons une diminution de la quantité de substance extraite puis une stabilisation des pourcentages extraits (pour BM, nous n'avons obtenu des résultats que sur 14 jours). Au vu de ces résultats, un stokage des échantillons urinaires à −20°C est préférable.

Essai de stabilité des extraits urinaires. Des extraits ont été conservés à température ambiante pendant trois jours. Pour les substances dérivées, nous obtenons le troisième jour une variation de ±2% de la réponse par rapport au premier jour. Pour la benzphétamine (non dérivable), nous obtenons une variation supérieure à ±10%.

Reproductibilité de l'extraction. Elle a été testée sur trois jours à trois niveaux de concentration différents: le niveau bas qui correspond à la limite de quantification (Lq), le niveau moyen qui est égal à cinq fois Lq et le niveau haut qui vaut 50 fois Lq.

Sur ces trois jours, pour chacun des trois niveaux de concentration, nous avons extrait cinq aliquots. L'étalon interne (FFR) est ajouté à l'urine au moment de l'extraction. Le Tableau III donne les coefficients de variation obtenus sur l'ensemble

TABLEAU III

REPRODUCTIBILITÉ DE L'EXTRACTION

Les moyennes sont celles des rapports de surface des pics par rapport à l'étalon externe (FFR). C.V. = Coefficient de variation.

Drogue	Niveau					
	Bas		Moyen		Haut	
	$\bar{x}$	C.V. (%)	$\bar{x}$	C.V. (%)	$\bar{x}$	C.V. (%)
AM	66,25	9,7	62,55	3,9	56,82	4,0
PT	129,85	4,5	159,9	3,7	176,0	3,9
BM	92,45	10,6	109,3	9,2	172,9	7,7
EPH	136,1	6,7	127,0	4,8	160,4	5,6
MPD	111,1	4,7	88,6	8,9	125,2	5,5
MF	95,3	4,8	87,0	6,9	87,8	4,1
CB	140,2	4,6	142,8	4,7	151,0	4,8

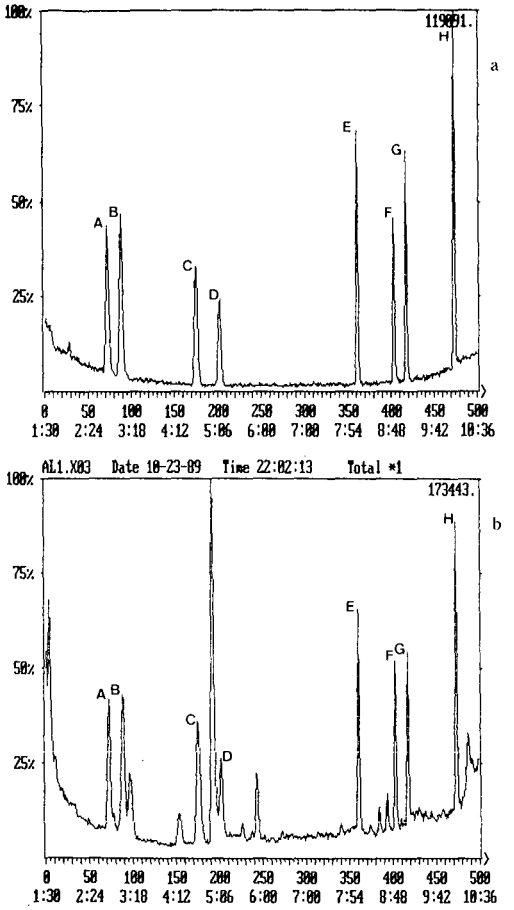

Fig. 6. Courants ioniques totaux d'amines sympathomimétiques (1 μg/ml). (a) Mélanges de solutions pures; (b) extrait urinaire. A = Amphétamine; B = phentermine; C = éphédrine; D = fenfluramine; E = méfénorex; F = benzphétamine; G = méthylphénidate; H = clobenzorex. Temps de rétention en min:s.

TABLEAU IV

RENDEMENT D'EXTRACTION

Drogue	Rendement (%; $n = 5$)
AM	101 ± 4,1
PT	99 ± 3,9
EPH[a]	97 ± 3,0
MF	101 ± 7,2
BM	108 ± 10,0
MPD	95 ± 8,9
CB	102 ± 5,2

[a] Nombre d'essais = 2.

des trois jours et pour chaque niveau. La Figure 6a montre le courant ionique total obtenu à partir d'un mélange de solutions pures, alors que la Figure 6b montre celui d'un extrait urinaire pour une quantité injectée équivalente.

Rendement ou taux de récupération. Les essais de rendement ont été faits sur l'ensemble des substances pour une concentration urinaire de 1 μg/ml. Les résultats sont consignés dans le Tableau IV.

CONCLUSION

L'extraction des urines sur cartouche C_{18} suivie d'une acétylation et d'une analyse par CG–SM permet un screening rapide et fiable des amines sympathomimétiques.

Après administration orale, 30 à 80% de la dose sont éliminés dans les urines de 24 h sous forme inchangée [14–16]. Les limites de quantification obtenues par notre méthode correspondent à une prise orale minimale par jour de 10 mg pour les substances dérivables et de 25 mg pour les drogues non dérivables, ce qui correspond aux limites basses des posologies thérapeutiques [17].

Par conséquent, la technique peut servir au dosage des amines sympathomimétiques dans les liquides biologiques.

Nous proposons de l'utiliser comme technique de contrôle antidopage chez les sportifs et pour la surveillance des drogués.

REMERCIEMENTS

Nous remercions tout particulièrement les laboratoires Rhône-Poulenc, Delagrange, Roussel Uclaf, Aldrich, Servier, Roche, Ciba-Geigy et Upjohn pour la fourniture des amines sympathomimétiques étalon.

RÉSUMÉ

Une technique rapide, sensible, spécifique et fiable d'extraction et de détection des amines sympathomimétiques dans les urines, utilisant la CG–SM, est décrite.

Après ajustement du pH urinaire à 7 et addition de l'étalon interne (fenfluramine), l'amphétamine, la phentermine, l'éphédrine, le méfénorex, le méthylphénidate, la benzphétamine et le clobenzorex sont extraits sur cartouche C_{18} par un mélange chloroforme–isopropanol. Le solvant organique est évaporé. Les drogues sont dérivées par l'anhydride trifluoro acétique (TFA), qui est ensuite évaporé. L'extrait final est repris dans l'acétate d'éthyle et injecté en CG–SM.

Les drogues sont identifiées par leur temps de rétention relatif et leur spectre de masse. La limite de quantification est de 200 ng/ml pour les substances dérivables et de 500 ng/ml pour celles qui ne le sont pas.

BIBLIOGRAPHIE

1 J. P. Rapp, *Le Doping des Sportifs*, Éditions Médicales et Universitaires, Paris, 1977, pp. 24–42.
2 E. C. Klatt, S. Montgomery, T. Namiki et T. T. Noguchi, *Clin. Toxicol.*, 24 (1986) 441.
3 D. N. Bailey, *Clin. Toxicol.*, 25 (1987) 399.
4 P. A. Mason, T. S. Bal, B. Law et A. C. Moffat, *Analyst*, 108 (1983) 603.

5 Y. H. Caplan, B. Levine et B. Golberger, *Clin. Chem.*, 33 (1987) 1200.
6 B. A. O'Brien, J. M. Bonicamp et D. W. Jones, *J. Anal. Toxicol.*, 6 (1982) 143.
7 D. Fretthold, P. Jones, G. Sebrosky et I. Sunshine, *J. Anal. Toxicol.*, 10 (1986) 10.
8 B. Kinberger, A. Holmen et P. Wahrgren, *J. Chromatogr.*, 207 (1981) 148.
9 D. H. Catlin, R. C. Kammerer, C. K. Hatton, M. H. Sekera et J. L. Merdink, *Clin. Chem.*, 33 (1987) 319.
10 V. Aggarwal, R. Bath et I. Sunshine, *Clin. Chem.*, 20 (1974) 307.
11 S. J. Mule et G. A. Casella, *J. Anal. Toxicol.*, 12 (1988) 102.
12 H. Sekine et Y. Nakahara, *Bunseki Kagaku*, 32 (1983) 453.
13 R. W. Taylor, S. D. Le, S. Philip et N. C. Jain, *J. Anal. Toxicol.*, 13 (1989) 293.
14 L. G. Dring, R. L. Smith et R. T. Williams, *J. Pharm. Pharmac.*, 18 (1966) 402.
15 A. H. Beckett et G. R. Wilkinson, *J. Pharm. Pharmacol.*, 17 Suppl. (1965) 1075.
16 A. H. Beckett et M. Rowland, *J. Pharm. Pharmacol.*, 17 Suppl. (1965) 1095.
17 *AHFS Drug Information*, American Society of Hospital Pharmacists, Bethesda, MD, 1989.

Journal of Chromatography, 541 (1991) 121–130
Elsevier Science Publishers B.V., Amsterdam

CHROM. 23 027

Detection of sarin and soman in a complex airborne matrix by capillary column ammonia chemical ionization gas chromatography–mass spectrometry and gas chromatography–tandem mass spectrometry

P. A. D'AGOSTINO* and L. R. PROVOST
Defence Research Establishment Suffield, P.O. Box 4000, Medicine Hat, Alberta T1A 8K6 (Canada)
and
P. W. BROOKS
Institute of Sedimentary and Petroleum Geology, 3303-33rd. Street N.W., Calgary, Alberta T2L 2A7 (Canada)

(First received September 27th, 1990; revised manuscript received December 12th, 1990)

ABSTRACT

The chemical warfare agents, sarin and soman, were detected and confirmed during full scanning capillary column ammonia chemical ionization mass spectrometry at nanogram levels in spiked extracts of a diesel exhaust environment sampled onto the charcoal of a Canadian C2 respirator canister. The selectivity of ammonia chemical ionization enabled the use of selected ion monitoring and resulted in detection limits of 40 pg and just above 500 pg for sarin and soman respectively in this extract. This diesel exhaust environment, typical of what might be encountered under battlefield conditions, was used to evaluate capillary column ammonia chemical ionization tandem mass spectrometry as a possible verification technology. Chemical interferences were reduced and significantly better detection limits, 15 pg and 80 pg for sarin and soman respectively, were obtained during gas chromatographic–tandem mass spectrometric analysis of these agents in the presence of numerous interfering diesel exhaust and charcoal bed components.

INTRODUCTION

Chemical weapon use, although prohibited by the 1925 Geneva Protocol, has been documented in several armed conflicts, including the Iran/Iraq war [1]. Verification of chemical agent use has often been difficult, due in part to inadequate battlefield sampling and identification procedures. Capillary column gas chromatography (GC)–flame ionization detection may be used for the routine screening of samples for the presence of chemical warfare agents [2,3]. However, it is generally agreed that confirmation of the chemical warfare agents or their degradation products requires identification by mass spectrometry (MS). Electron impact (EI), the traditional MS method of ionization, has gained wide acceptance for the verification of organophosphorus chemical warfare agents, as the EI mass spectra of numerous

chemical warfare agents, their decomposition products and related compounds have been published [4–9].

EI mass spectra generally provide excellent structural information [10], but the presence of little or no molecular ion information often hinders the identification of organophosphorus compounds. Chemical ionization (CI) MS [11], a milder ionization technique, has been used with increasing frequency to provide molecular ion information for these compounds [12]. CI-MS using methane, isobutane, ethylene or methanol has been applied to the analysis of organophosphorus chemical warfare agents [5,13] and pesticides [14–19]. More recently, the efficacy of ammonia CI-MS [20] has been demonstrated for phosphorus oxyacids [21], several organophosphorus pesticides [14,18,22] and organophosphorus chemical warfare agents, their decomposition products and related impurities [6,8,9,23,24].

During a recent study designed to evaluate MS methods for the verification of chemical warfare agents in airborne samples similar to those collected during battlefield airborne sampling, it was apparent that the major limitation during capillary column GC–EI-MS analysis was the chemical noise associated with the hydrocarbon content [25]. Ionization under ammonia CI-MS conditions should result in better detection limits than under EI conditions, with the benefit of molecular ion information, as hydrocarbons are not sufficiently basic to ionize under ammonia CI conditions. This mode of operation should reduce the chemical noise associated with the airborne extract and enable the trace detection of the organophosphorus chemical warfare agents, sarin and soman. As in the previous study [25], tandem mass spectrometry (MS–MS) was evaluated as a potential technology for the confirmation of trace levels of organophosphorus chemical warfare agents in the presence of this complex airborne matrix.

Tandem mass spectrometers offer a number of highly specific scan functions including; parent ion, daughter ion, constant neutral loss and reaction ion monitoring. During reaction ion monitoring, the method of choice for many trace "target' compound applications, the first mass analyser is tuned to allow a desired mass (*e.g.*, $(M + NH_4)^+$) into the collisional activated dissociation (CAD) cell while the second mass analyser allows only characteristic ion(s) derived from fragmentation(s) of the ion selected by the first analyser to be detected. The two degrees of selectivity offered by the MS–MS instrument are further enhanced by the use of gas chromatographic sample introduction.

MS–MS has been reviewed recently [26–29], and methods have been reported for selected organophosphorus pesticides [19,30,31], organophosphorus chemical warfare agents [24,25] and mustard [25]. Although capillary column ammonia chemical ionization GC–MS–MS has been suggested as a possible means of chemical warfare agent confirmation in complex environmental samples [24], there have been no reported applications of this methodology.

A capillary column GC study using ammonia CI-MS and ammonia CI-MS–MS detection was initiated with the principal objective being the development and evaluation of these methods for the detection and confirmation of sarin (isopropyl methylphosphonofluoridate or GB) and soman (pinacolyl methylphosphonofluoridate or GD) in a complex airborne matrix. The air samples during this study contained the volatile components of diesel exhaust and was very similar in composition to battlefield air sampled onto charcoal during a recent interlaboraroty analytical

exercise [32]. Charcoal from exposed C2 Canadian respirator canisters was solvent extracted and spiked at several levels to allow evaluation of ammonia CI-MS and ammonia CI-MS–MS for the trace detection of the chemical warfare agents, sarin and soman.

EXPERIMENTAL

Standards and sample handling

Sarin and soman were provided by the Defence Research Establishment Suffield Organic Chemistry Laboratory. Distilled-in-glass dichloromethane was purchased from BDH (Edmonton, Canada). All samples and standards were stored in PTFE-lined screw-capped vials at 4°C prior to GC analysis. Anhydrous-grade ammonia (99.99%) was used during CI-MS analyses (Liquid Carbonic).

Air from a diesel exhaust environment was sampled through a Canadian C2 charcoal canister for 4 h at the typical working respiratory rate of 20 l/min. The canister charcoal (108 g) was Soxhlet extracted for 6 h with 250 ml of dichloromethane and concentrated to 10 ml under a gentle stream of nitrogen.

Instrumental

Capillary column ammonia chemical ionization GC–MS full scanning and selected ion monitoring analyses were performed with a VG 70/70E double focusing mass spectrometer (VG Analytical, Wythenshawe, U.K.) interfaced to a Varian 3700 gas chromatograph under the following chromatographic conditions. All injections were on-column [2] at 40°C onto a 15 m × 0.32 mm I.D. J & W DB-5 (0.25 μm) capillary column with a 40°C (2 min) → 10°C/min → 280 °C temperature program. CI-MS operating conditions were as follows: accelerating voltage, 6 kV; emission, 500 μA; electron energy, 50 eV; source temperature, 120°C and source pressure, $9 \cdot 10^{-5}$ Torr. Full scanning CI data were collected over the 400 to 35 u mass range at 1 s/decade. Both the $(M + NH_4)^+$ and $(M + H)^+$ ions for sarin (m/z 158 and m/z 141) and soman (m/z 200 and m/z 183) were acquired with a 80 ms dwell time and 20 ms delay per ion during selected ion monitoring CI-MS analysis.

Capillary column ammonia chemical ionization GC–MS–MS analyses were performed with a VG 70SQ hybrid tandem mass spectrometer equipped with a Hewlett-Packard 5890 gas chromatograph. All injections were on-column at 40°C using a Hewlett-Packard on-column injector. The 15 m × 0.32 mm I.D. J&W DB-5 (0.25 μm) capillary column was held at this temperature for 2 min and then programmed at either 8°C or 20°C/min to a maximum of 280°C. Ammonia CI source conditions were identical to those employed during GC–MS analysis with the following exceptions: accelerating voltage, 8 kV and emission, 1000 μA. The daughter mass spectra of m/z 158 for sarin and m/z 200 for soman were obtained under the following conditions: CAD cell, 20 eV (laboratory scale)/air ($6 \cdot 10^{-7}$ Torr) and a quadrupole scan function of 300 to 20 u at 0.5 s/decade. Reaction ion monitoring for sarin was carried out using the CAD conditions listed above on the m/z 158 to m/z 141 and m/z 158 to m/z 99 transitions with a 80 ms dwell time and 20 ms delay. Soman reaction ion monitoring was carried out in an identical manner on the m/z 200 to m/z 183 and m/z 200 to m/z 99 transitions.

RESULTS AND DISCUSSION

The diesel exhaust environment sampled onto the charcoal of Canadian C2 canisters contained primarily hydrocarbon compounds [25] and was similar in composition to the volatile battlefield components extracted from a respirator canister circulated as part of a recent interlaboratory analytical exercise [32]. Charcoal extracts used in this study were further complicated by the presence of silicon-containing compounds adsorbed onto the charcoal bed of the Canadian C2 canisters. The development of suitable mass spectrometric confirmation methods for chemical warfare agents adsorbed onto charcoal under realistic conditions would be valuable in a Chemical Weapons Convention verification role as charcoal mask canisters represent a possible retrospective sampling device.

Capillary column ammonia chemical ionization GC–MS

An interpretable full scanning ammonia CI mass spectrum was obtained for sarin during capillary column GC–MS analysis of the charcoal extract spiked at the 5 ng level. The acquired ammonia CI mass spectrum contained both $(M + NH_4)^+$ and $(M + H)^+$ ions with relative intensities of 100 and 20 respectively. Soman, which elutes in a more complex region of the extract chromatogram, could only be tentatively identified at the retention time of the first chromatographic peak (two chromatographic peaks due to diastereoisomeric pairs), due to the co-elution of an interference(s). Characteristic ions due to $(M + NH_4)^+$ and $(M + NH_4\text{-}C_6H_{12})^+$ at m/z 200 and 116 respectively were observed with relative intensities of 100 and 80 respectively. The $(M + H)^+$ ion (typically about 5% of the base ion) was not detectable. The second chromatographic peak for soman was effectively masked by the matrix with only the m/z 200 ion being discernable above the chemical background.

A reduction in chemical background during ammonia CI-MS, as compared to previous EI-MS analysis [25], enabled the use of selected ion monitoring for the trace detection of sarin and soman. Both the $(M + H)^+$ and $(M + NH_4)^+$ pseudo-molecular ions of sarin and soman were monitored during analysis of the unspiked extract and the same extract spiked with sarin and soman at the 500 pg and 50 pg levels. The pseudo-molecular ions for sarin at m/z 158 and m/z 141 were observed without interference at both spiked levels in the same area ratio as observed for a sarin standard. A detection limit of about 40 pg (signal-to-noise, S/N ratio of 5:1) in the presence of this complex matrix was estimated, based on the detection of both sarin pseudo-molecular ions. Fig. 1 illustrates the m/z 158 selected ion monitoring chromatograms obtained for the unspiked extract and the same extract spiked with sarin at the 500 pg and 50 pg levels.

In the case of soman, only the m/z 200 ion was detected above the background chemical noise during capillary column ammonia CI-MS selected ion monitoring analysis of the charcoal extracts spiked at the 500 and 50 pg levels (Fig. 2). This ion, due to $(M + NH_4)^+$, was detected with a S/N ratio of about 8:1 during analysis of the 50 pg spiked extract. The $(M + H)^+$ ion for soman, at m/z 183, was detected with a S/N ratio of approximately 4:1, which suggested a method detection limit of just over 500 pg, based on the detection of both pseudo-molecular ions. Monitoring of the two most intense soman ions, at m/z 200 and m/z 116 (instead of m/z 200 and m/z 183), was not considered viable under voltage scanning selected ion monitoring due to the

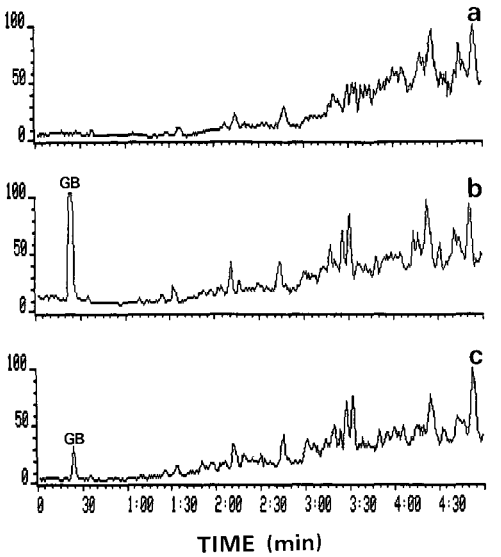

Fig. 1. Capillary column ammonia chemical ionization GC–MS selected ion monitoring chromatograms obtained for m/z 158 [$(M + NH_4)^+$ ion for sarin] during analysis of (a) dichloromethane extract of the equivalent of $4.8 \cdot 10^{-4}$ m^3 of air sampled onto the charcoal of a C2 canister and the previous sample spiked with sarin (GB) at the (b) 500 pg and (c) 50 pg levels. Column 15 m × 0.32 mm I.D. J&W DB-5; temperature, 40°C (2 min) → 10°C/min → 280°C.

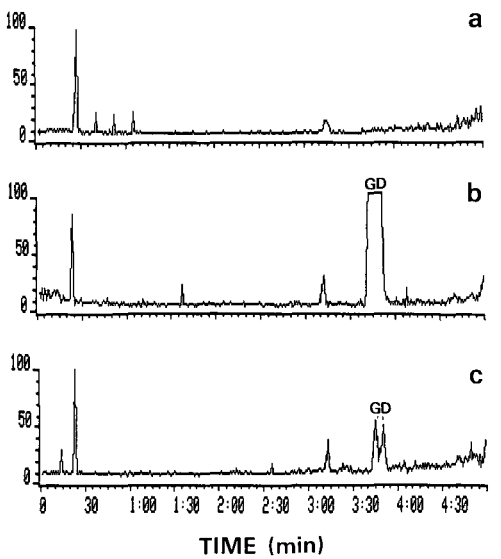

Fig. 2. Capillary column ammonia chemical ionization GC–MS selected ion monitoring chromatograms obtained for m/z 200 [$(M + NH_4)^+$ ion for soman] during analysis of (a) dichloromethane extract of the equivalent of $4.8 \cdot 10^{-4}$ m^3 of air sampled onto the charcoal of a C2 canister and the previous sample spiked with soman (GD) at the (b) 500 pg and (c) 50 pg levels. Conditions as in Fig. 1.

large mass range, but should be considered for quadrupole or magnetic scanning selected ion monitoring.

Capillary column ammonia chemical ionization GC–MS–MS

Hesso and Kostiainen [24] reported the first daughter spectra for the pseudo-molecular ions formed during ammonia chemical ionization of sarin, soman, tabun and VX. The utility of reaction ion monitoring (RIM) for the detection of chemical warfare agents in a complex or environmental matrix, while mentioned, was not demonstrated. Use of GC–MS–MS under ammonia CI conditions, for the trace detection of these chemical warfare agents was investigated in this study, as this technique could prove to be a more sensitive and specific approach for the trace confirmation of sarin and soman in a complex matrix.

The daugher spectra of the $(M + NH_4)^+$ pseudo-molecular ions of sarin and soman were acquired under CAD conditions, which, while perhaps not optimal, provided lower mass ions suitable for use in a RIM experiment. Fig. 3 illustrates the daughter spectra acquired during analysis of a standard. Daughter ions at *m/z* 99 and *m/z* 141 and, at *m/z* 85, *m/z* 99 and *m/z* 183 were observed for sarin and soman respectively. Relative daughter ion intensities were different than those observed by Hesso and Kostiainen [24], which may be due to the use of different CAD gases, pressures and instruments. The data from these experiments suggested the use of the $(M + NH_4)^+$ to $(M + H)^+$ and $(M + NH_4)^+$ to $[(CH_3)(F)P(OH)_2]^+$ RIM transitions for the confirmation of sarin and soman in the airborne sample extracts.

Figs. 4 and 5 illustrate the RIM chromatograms for the unspiked extract and, 500 pg and 50 pg spiked extracts obtained during monitoring of the $(M + NH_4)^+$ to $(M + H)^+$ (*m/z* 158 to *m/z* 141) and $(M + NH_4)^+$ to $[(CH_3)(F)P(OH)_2]^+$ (*m/z* 158 to *m/z* 99) transitions respectively. Sarin was readily detected, with no interferences, at both levels during capillary column ammonia chemical ionization GC–MS–MS analysis of the spiked extracts under these conditions. Chemical noise due to the extract components was particularly low for the *m/z* 158 to *m/z* 99 transition, as this loss is more diagnostic than simply loss of NH_3 from the $(M + NH_4)^+$ ion. Conservative

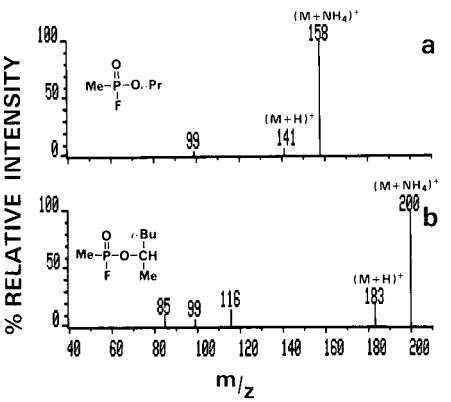

Fig. 3. Daughter spectra obtained for $(M + NH_4)^+$ ions of (a) sarin and (b) soman during capillary column ammonia chemical ionization GC–MS analysis of a standard.

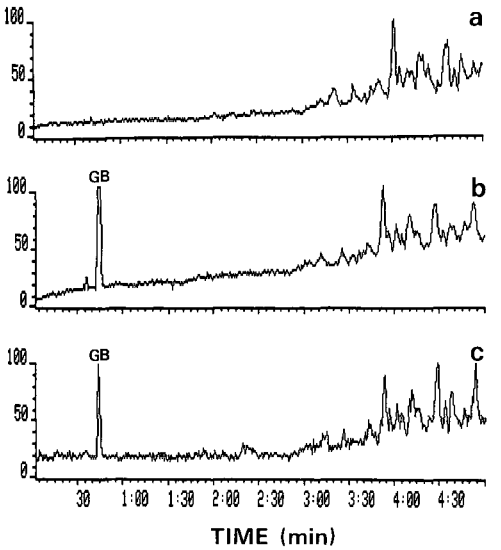

Fig. 4. Reaction ion monitoring chromatogram for m/z 158 to m/z 141 obtained during capillary column ammonia chemical ionization GC–MS–MS analysis of (a) dichloromethane extract of the equivalent of 4.8 $\cdot 10^{-4}$ m^3 of air sampled onto the charcoal of a C2 canister and the previous sample spiked with (b) 500 pg and (c) 50 pg of sarin (GB). Column, 15 m × 0.32 mm I.D. J&W DB-5; temperature, 40°C (2 min) → 20°C/min → 280°C.

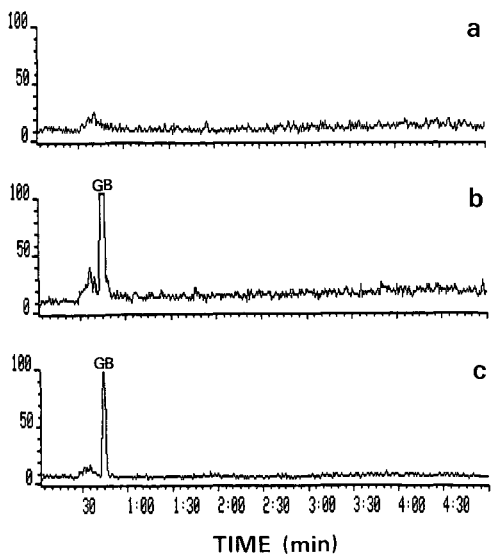

Fig. 5. Reaction ion monitoring chromatogram for m/z 158 to m/z 99 obtained during capillary column ammonia chemical ionization GC–MS–MS analysis of (a) dichloromethane extract of the equivalent of 4.8 $\cdot 10^{-4}$ m^3 of air sampled onto the charcoal of a C2 canister and the previous sample spiked with (b) 500 pg and (c) 50 pg of sarin (GB). Conditions as in Fig. 4.

CI-MS–MS sample detection limits for sarin, based on a S/N ratio of 5:1, were better than under CI-MS conditions and were estimated to be 20 pg for the $(M + NH_4)^+$ to $(M + H)^+$ (m/z 158 to m/z 141) transition and 15 pg for the $(M + NH_4)^+$ to $[(CH_3)(F)P(OH)_2]^+$ (m/z 158 to m/z 99) transition.

Soman, as was the case during capillary column ammonia CI-MS analysis, was not as readily confirmed in the presence of this complex matrix. It was confirmed at both the 500 pg and 50 pg (S/N = 3:1) level during RIM of the $(M + NH_4)^+$ to $(M + H)^+$ (m/z 200 to m/z 183) transition, but was only confirmed at the 500 pg level during monitoring of the $(M + NH_4)^+$ to $[(CH_3)(F)P(OH)_2]^+$ (m/z 200 to m/z 99) transition. The inability to detect soman for the latter transition at the 50 pg level was likely due to the reduced relative ion intensity of the m/z 99 ion in the daughter spectrum of soman. Conservative CI-MS–MS sample detection limits for soman, based on a S/N ratio of 5:1, were much better than obtained under CI-MS conditions and were estimated to be 80 pg for the $(M + NH_4)^+$ to $(M + H)^+$ (m/z 200 to m/z 183) transition and 350 pg for the $(M + NH_4)^+$ to $[(CH_3)(F)P(OH)_2]^+$ (m/z 200 to m/z 99) transition.

Detection limit comparison

The charcoal extract spiked during this study was used in a prior capillary column GC–MS and GC–MS–MS study under EI ionization conditions [25]. Table I compares the ammonia CI-MS detection limits with those obtained under EI-MS conditions for three chemical warfare agents spiked into the same airborne sample extract. Ammonia CI-MS holds a decided advantage over EI-MS during full scanning and selected ion monitoring. This was due to a reduction of chemical noise, as hydrocarbons are not sufficiently basic to form pseudo-molecular ions under ammo-

TABLE I

COMPARISON OF MASS SPECTROMETRIC METHODS FOR THE ANALYSIS OF CHEMICAL WARFARE AGENTS IN A COMPLEX AIRBORNE MATRIX

N/A = Not applicable for this compound; SIM = selected ion monitoring; RIM = reaction ion monitoring.

Method	Detection limit[a]		
	Sarin	Soman	Mustard
GC–MS (EI)[b] (Full scanning)	20 ng	20 ng	20 ng
GC–MS–MS(EI)[b] (RIM on 1 transition)	70 pg	60 pg	30 pg
GC–MS (NH_3-CI) (Full scanning)	5 ng	> 5 ng	N/A
GC–MS (NH_3-CI) [SIM of $(M + H)^+$ and $(M + NH_4)^+$]	40 pg	> 500 pg	N/A
GC–MS–MS (NH_3CI) (RIM on 1 transition)	15 pg	80 pg	N/A

[a] Interpretable mass spectrum for full scanning methods and S/N ratio of 5:1 for SIM and RIM methods.

[b] Data from ref. 25.

nia CI conditions. The major disadvantage of this selectivity was the inability of this method to detect other compounds of chemical defense interest such as the sulfur vesicant, mustard. Mustard, like the hydrocarbons, was not sufficiently basic to form significant pseudo-molecular ions during ammonia CI-MS. Mustard and related compounds do however form abundant $(M + H)^+$ pseudo-molecular ions under isobutane CI conditions [33–35]. However, use of this reagent gas would also lead to hydrocarbon ionization and likely lead to little, if any, gain in sensitivity. GC–MS–MS, under EI conditions, remains the most practical approach for the verification of mustard in this complex matrix.

CONCLUSIONS

The chemical warfare agents, sarin and soman, were detected and confirmed during full scanning capillary column ammonia CI-MS at nanogram levels in spiked dichloromethane extracts of a diesel exhaust environment sampled onto the charcoal of a Canadian C2 gas mask canister. The selectivity of this ionization method enabled the use of selected ion monitoring and resulted in detection limits of 40 pg and just above 500 pg for sarin and soman respectively in the presence of this airborne extract.

This matrix, typical of what might be encountered under battlefield conditions, was used to evaluate capillary column ammonia chemical ionization GC–MS–MS as a possible verification technology. Daughter spectra, obtained during capillary column ammonia chemical ionization GC–MS–MS analysis of sarin and soman, suggested use of both the $(M + NH_4)^+$ to $(M + H)^+$ and $(M + NH_4)^+$ to $[(CH_3)(F)P(OH_2]^+$ transitions for reaction ion monitoring. Reaction ion monitoring of these collisional activated processes proved to be the most sensitive of the methods evaluated for the verification of sarin and soman. Chemical interferences were significantly reduced and detection limits of 15 pg and 80 pg for sarin and soman respectively were obtained during capillary column ammonia CI-MS–MS analysis of these agents in the presence of matrix component concentrations two to three orders of magnitude greater than the spiked agents.

Application of tandem mass spectrometry, under ammonia CI conditions, for the detection of organophosphorus chemical warfare agents appears to be an attractive approach for the verification of "target" compounds in complex environmental matrices such as those that may be encountered during airborne sampling of battlefield emissions.

REFERENCES

1 *Report of the Mission Dispatched by the Secretary-General to Investigate Allegations of the Use of Chemical Weapons in the Conflict between the Islamic Republic of Iran and Iraq, United Nations Security Council S/20060,* United Nations, New York, July 20, 1988.
2 P. A. D'Agostino and L. R. Provost, *J. Chromatogr.*, 331 (1985) 47–54.
3 P. A. D'Agostino and L. R. Provost, *J. Chromatogr.*, 436 (1988) 399–411.
4 *Chemical and Instrumental Verification of Organophosphorus Warfare Agents,* The Ministry of Foreign Affairs of Finland, Helsinki, 1977.
5 S. Sass and T. L. Fisher, *Org. Mass Spectrom.*, 14 (1979) 257–264.
6 P. A. D'Agostino, A. S. Hansen, P. A. Lockwood and L. R. Provost, *J. Chromatogr.*, 347 (1985) 257–266.
7 E. R. J. Wils and A. G. Hulst, *Org. Mass Spectrom.*, 21 (1986) 763–765.

8 P. A. D'Agostino, L. R. Provost and J. Visentini, *J. Chromatogr.*, 402 (1987) 221–232.
9 P. A. D'Agostino, L. R. Provost and K. M. Looye, *J. Chromatogr.*, 465 (1989) 271–283.
10 R. G. Gillis and J. L. Occolowitz, In M. Halman (Editor), *The Mass Spectrometry of Phosphorus Compounds*, Interscience, New York, 1972, pp. 295–331.
11 M. S. B. Munson and F. H. Field, *J. Am. Chem Soc.*, 88 (1966) 2621–2630.
12 J. R. Chapman, *Organophosphorus Chem.*, 14 (1983) 278–304.
13 *Identification of Potential Organophosphorus Warfare Agents*, Ministry of Foreign Affairs of Finland, Helsinki, 1979.
14 R. L. Holmstead and J. E. Casida, *J. Assoc. Off. Anal Chem.*, 57 (1974) 1050–1055.
15 H. J. Stan, *Fresenius Z. Anal. Chem.*, 287 (1977) 104–111.
16 H. J. Stan, *Z. Lebensm.-Unters.-Forsch.*, 164 (1977) 153–159.
17 K. L. Busch, M. M. Bursey, J. R. Hass and G. W. Sovocool, *Appl. Spectrosc.*, 32 (1978) 388–399.
18 T. Cairns, E. G. Siegmund and R. L. Bong, *Anal. Chem.*, 56 (1984) 2547–2552.
19 T. Cairns and E. G. Siegmund, *J. Assoc. Off. Anal. Chem.*, 70 (1987) 858–862.
20 J. B. Westmore and M. M. Alauddin, *Mass Spectrom. Rev.*, 5 (1986) 381–465.
21 P. A. Cload and D. W. Hutchinson, *Org. Mass Spectrom.*, 18 (1983) 57–59.
22 T. Cairns, E. G. Siegmund, G. M. Doose and A. C. Oken, *Anal. Chem.*, 57 (1985) 572A–576A.
23 P. A. D'Agostino, L. R. Provost, *Biomed. Environ. Mass Spectrom.*, 13 (1986) 231–236.
24 A. Hesso and R. Kostiainen, *Proc. 2nd. Int. Symp. Protection Against Chemical Warfare Agents, Stockholm, June 15–19, 1986*, National Defence Research Institute, Umeå, 1986, pp. 257–260.
25 P. A. D'Agostino, L. R. Provost, J. F. Anacleto and P. W. Brooks, *J. Chromatogr.*, 504 (1990) 259–268.
26 R. G. Cooks and G. L. Glish, *Chem. Eng. News*, Nov. (1981) 40–52.
27 R. W. McLafferty, *Tandem Mass Spectrometry*, Wiley, New York, 1983.
28 J. V. Johnson and R. A. Yost, *Anal. Chem.*, 57 (1985) 758A–768A.
29 G. L. Glish and S. A. McLuckey, *Anal. Instrum.*, 15 (1986) 1–36.
30 S. V. Hummel and R. A. Yost, *Org. Mass Spectrom.*, 21 (1986) 785–791.
31 J. A. Roach and L. J. Carson, *J. Assoc. Off. Anal. Chem.*, 70 (1987) 439–442.
32 J. R. Hancock, P. A. D'Agostino and L. R. Provost, *The Analysis of a Respirator Canister: Fourth International Training Exercise*, Defence Research Establishment Suffield, Medicine Hat, Canada, June 1986, internal document (available on request).
33 E. Ali-Mattila, K. Siivinen, J. Kentamaa and P. Savolahti, *Int. J. Mass Spectrom. Ion. Phys.*, 47 (1983) 371–374.
34 P. A. D'Agostino and L. R. Provost, *Biomed. Environ. Mass Spectrom.*, 15 (1988) 553–564.
35 P. A. D'Agostino, L. R. Provost, A. S. Hansen and G. A. Luoma, *Biomed. Environ. Mass Spectrom.*, 18 (1989) 484–491.

Journal of Chromatography, 541 (1991) 131–183
Elsevier Science Publishers B.V., Amsterdam

CHROM. 23 013

Gas chromatographic separations of all 136 tetra- to octa-polychlorinated dibenzo-*p*-dioxins and polychlorinated dibenzofurans on nine different stationary phases[a]

JOHN J. RYAN*, HENRY B. S. CONACHER, LUZ G. PANOPIO, BENJAMIN P.-Y. LAU and JACQUES A. HARDY

Food Research Division, Bureau of Chemical Safety, Food Directorate, Health Protection Branch, Health and Welfare Canada, Ottawa K1A 0L2 (Canada)

and

YOSHITO MASUDA

Daiichi College of Pharmaceutical Sciences, Fukuoka 815 (Japan)

(First received July 31st, 1990; revised manuscript received November 27th, 1990)

ABSTRACT

All 49 polychlorinated dibenzo-*p*-dioxins and 87 polychlorinated dibenzofurans containing 4 to 8 chlorines have been synthesized and purified as individual compounds in quantitative amounts. These standards have been chromatographed on a series of nine fused-silica capillary gas chromatography (GC) columns containing silicone stationary phases of diverse polarity (100% methyl, 5% phenyl methyl, 50% phenyl methyl, 50% methyl trifluoropropyl, 50%, 75%, 90% and 100% cyanopropyl and liquid crystalline smectic). The data, expressed in a series of GC chromatograms and in tables of relative retention times, are the most comprehensive to date with regard to individual congeners and variety of stationary phases and provide a confirmation of much earlier work. The information shows that all 136 compounds, including the biologically important 2,3,7,8-substituted congeners, can be separated from each other mostly with two stationary phases. However, possible variation in GC conditions and stationary phases necessitates assessment of the resolution of near eluting isomers. Comparisons and contrasts to previously published reports have also been noted.

INTRODUCTION

Polychlorinated dibenzo-*p*-dioxins (PCDDs) and polychlorinated dibenzofurans (PCDFs) are two classes of environmental contaminants which are present as impurities in a variety of industrial chemicals such as chlorophenols and polychlorinated biphenyls (PCBs). They are also formed in heat processes particularly in the incineration of municipal waste [1], and recently have been found in the bleaching of pulp and paper [2,3]. The PCDDs (49 congeners) and PCDFs (87 congeners) of

[a] This study was conducted as project 32/85 of the Working Group on Halogenated Hydrocarbon Environmental Contaminants, Food Chemistry Commission, International Union of Pure and Applied Chemistry (IUPAC).

0021-9673/91/$03.50

TABLE I

NUMBER OF ISOMERS AND CONGENERS OF THE PCDDs AND PCDFs

Chlorine number homologue	Acronyms[a]	Number of isomers		Total
		PCDD	PCDF	
1	MCDD/MCDF	2	4	6
2	DiCDD/DiCDF	10	16	26
3	TrCDD/TrCDF	14	28	42
4	TCDD/TCDF	22	38	60
5	PnCDD/PnCDF	14	28	42
6	HxCDD/HxCDF	10	16	26
7	HpCDD/HpCDF	2	4	6
8	OCDD/OCDF	1	1	2
Total		Number of congeners		
1–8		75	135	210
1–3		26	48	74
4–6		46	82	128
4–8		49	87	136

[a] CDD = chlorinated dibenzo-*p*-dioxin; CDF = chlorinated dibenzofuran; M = mono; Di = di; Tr = tri; T = tetra; Pn = penta; Hx = hexa; Hp = hepta; O = octa.

biological interest contain 4 to 8 chlorines and these along with their acronyms are shown in detail in Table I. For brevity and simplicity when describing and comparing different congeners, the chlorine substitution is usually designated without using commas to separate the arabic numbers. PCDDs and PCDFs with the 2,3,7,8-configuration (17 congeners) are the most toxic in experimental animals. These congeners have been found in wildlife [4], human tissues [5], and food samples [6], and are the most important for purposes of identification and quantification. Mass spectrometry (MS) provides unequivocal identification of the elemental composition (molecular formula) of a substance, but gas chromatographic (GC) techniques are required to separate and identify those compounds having the same elemental composition but different structure or constitution (isomers). For example, MS can detect all 22 TCDD isomers but GC is needed to specify which of these has the 2,3,7,8-substitution.

A plethora of data has been published [7–44] in the last 10 years on the separation of the isomers and congeners of PCDDs/PCDFs using gas chromatography. In the late 1970s and early 1980s most of this work was performed using stationary phases coated on inert supports (packed GC columns). In the last 5 years or so virtually all separations have been carried out on the better resolving capillary columns where the stationary phase is coated on or chemically bonded to the glass surface of the wall. In particular, studies on the separation of all 38 TCDFs and 22 TCDDs on both non-polar (methyl silicone) [15,16,35] and polar (cyanopropyl silicone) [14–16, 18,23,35,40] columns are available and the GC properties of all 128 PCDDs/PCDFs containing 4 to 6 chlorines are known for both non-polar and polar phases [9,11,13,19–22, 25–29,30, 32–34,39,42]. However, information on GC separa-

tions is often lacking or incomplete for: (a) the homologues higher than tetrachloro for medium polar (methyl–phenyl silicones) phases and (b) for all homologues on certain uncommon phases (*e.g.* methyl–trifluoropropyl silicones and liquid crystalline). In addition much of the data are scattered throughout the literature, and are incomplete for the congeners of biological interest. Some discrepancies also exist between separations and relative peak assignments reported by various research groups. As a result, we obtained authentic standards of all 136 PCDDs/PCDFs of biological interest in pure separate quantitative amounts (not mixtures) by synthesis and exchange. Their elution order and separations were then examined on a wide variety of stationary phases on either bonded or wall-coated fused-silica capillary columns using the liquid phases most commonly in the field as well as these advocated by Yancey [45–47] in his review of liquid phases. However, this report does not attempt to predict or provide a theoretical model for separation based on molecular structure.

EXPERIMENTAL

Definition and nomenclature

The terms, congener, isomer, and homologue are often used to describe the different kinds of PCDDs and PCDFs but unfortunately the usage of these terms has been inconsistent and confusing. In this paper we use congener to refer to any member of the class of PCDDs or PCDFs regardless of the degree of chlorination. In this respect there are 75 possible congeners of PCDDs and 135 congeners of the PCDFs (Table I). Isomers are compounds with the same elemental compositon or molecular formula (number and kinds of atoms) but with different structural or configurational arrangement. It is well known that there are 22 structural isomers of the TCDDs. Homologues usually refer to groups of compounds with a common structure (*e.g.* CDD or CDF) but differing by a constant increment of common atoms (*e.g.* number of chlorines). Mass spectrometry (MS) can readily distinguish one homologue group of PCDDs/PCDFs from another simply by their mass to charge ratio. However, MS is generally unable to specify which isomer of any homologue is present. Such an assignment requires the technique of gas chromatography. A combination of both GC and MS techniques permits, in theory, the identification of all congeners of the PCDDs/PCDFs.

The nomenclature for the numbering of the chlorine positions in the CDD and CDF ring system is that given in Fig. 1 subscribing to the usage of Chemical Abstracts

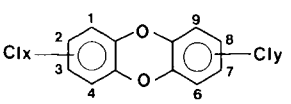

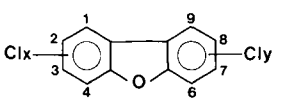

x + y = 1 to 8

Fig. 1. Chemical structures of the congeners of PCDDs/PCDFs.

TABLE II

SOURCES AND PURITY OF THE 49 PCDDs WITH 4 TO 8 CHLORINES

No.	Isomer	CA registry number	Systematic number	Base hex number	Source and purity[a]
TCDDs					
1	1234	30746-58-8	162	f0D	Analabs, U.S.A.; 98%
2	1236	71669-25-5	163	78D	D. Firestone, U.S.A.; S1 with 1239-D (3:2 mixture); RP-HPLC, 97%
3	1237	67028-18-6	164	74D	(a) KOR Isotope, U.S.A.; S1, mixture with 1238-D (b) Pyrolysis (3); RP-HPLC (3), 98% (c) Photolysis of 12367-D
4	1238	53555-02-5	165	72D	(a) KOR Isotope; S1, mixture with 1237-D (b) Pyrolysis (3); RP-HPLC (3), 97% (c) Photolysis of 12389-D
5	1239	71669-26-6	166	71D	D. Firestone; S1, mixture with 1236-D (2:3); RP-HPLC (2), 97%
6	1246	71669-27-7	167	b8D	Pyrolysis; RP-HPLC, 97%
7	1247	71669-28-8	168	b4D	Pyrolysis (2); RP-HPLC; NP-HPLC (2), 95%
8	1248	71669-29-9	169	b2D	Pyrolysis (2); RP-HPLC; NP-HPLC (2), 90%
9	1249	71665-99-1	170	b1D	Pyrolysis; RP-HPLC (2), 97%
10	1267	40581-90-6	171	3CD	Pyrolysis (2); RP-HPLC, 95%
11	1268	67323-56-2	172	3aD	Pyrolysis (2); RP-HPLC (3), 95%
12	1269	40581-91-7	173	39D	Pyrolysis; RP-HPLC, 95%
13	1278	34816-53-0	174	36D	(a) KOR Isotope; S1, 98% (b) Pyrolysis; RP-HPLC, 97%
14	1279	71669-23-3	175	35D	Pyrolysis (2); RP-HPLC (3), 95%
15	1289	62470-54-6	176	33D	Pyrolysis (2); RP-HPLC (2), 95%
16	1368	33423-92-6	177	5aD	(a) Ultra Scientific, U.S.A.; 98% (b) Pyrolysis (2); RP-HPLC, 97% (c) D. Firestone; 3:1 mixture with 1379-D
17	1369	71669-24-4	178	59D	Pyrolysis; RP-HPLC (2), 95%
18	1378	50586-46-1	179	56D	KOR Isotope; S1; 98%
19	1379	62470-53-5	180	55D	(a) Pyrolysis; RP-HPLC, 95% (b) D. Firestone; 1:3 mixture with 1368-D
20	1469	40581-93-9	181	99D	Pyrolysis; RP-HPLC, 95%
21	1478	40581-94-0	182	96D	Pyrolysis; RP-HPLC (2), 95%
22	2378	1746-01-6	183	66D	(a) Dow Chemical, U.S.A.; 95% (b) P. Kearney, U.S.A.; 95% (c) D. Firestone; 98% (d) National Bureau Standards, Washington, U.S.A., 98%
PnCDDs					
1	12346	67028-19-7	184	f8D	Pyrolysis (2); RP-HPLC, 98%
2	12347	39227-61-7	185	f4D	W. Miles, Canada; S1; 97%
3	12367	71925-15-0	186	7CD	Pyrolysis (2); RP-HPLC (3); 81% pure; 12467-D, 8%; 12489-D, 11%
4	12368	71925-16-1	187	7aD	Pyrolysis; RP-HPLC, 90%, some 12479-D
5	12369	82291-34-7	188	79D	Pyrolysis; RP-HPLC (3), 90%, some 12479-D
6	12378	40321-76-4	189	76D	(a) Pyrolysis (2); RP-HPLC (b) W. Miles; S1; 97% (c) D. Firestone; S1; 97%,

TABLE II *(continued)*

No.	Isomer	CA registry number	Systematic number	Base hex number	Source and purity[a]
7	12379	71925-17-2	190	75D	Pyrolysis; RP-HPLC, 98%
8	12389	71925-18-3	191	73D	Pyrolysis (2); RP-HPLC, 98%
9	12467	82291-35-8	192	bcD	Pyrolysis (2); RP-HPLC (2), 97%
10	12468	71998-76-0	193	baD	Pyrolysis (3); RP-HPLC (3), 90% pure, rest 12479-D
11	12469	82291-36-9	194	b9D	Pyrolysis (2); RP-HPLC (2) 98%
12	12478	58802-08-7	195	b6D	D. Firestone; S1; 98%
13	12479	82291-37-0	196	b5D	Pyrolysis (3); RP-HPLC (3), 90%, rest 12468-D
14	12489	82291-38-1	197	b3D	Pyrolysis (2); RP-HPLC (3), 96%
HxCDDs					
1	123467	58200-66-1	198	fcD	Pyrolysis (2); RP-HPLC (3), 97%
2	123468	58200-67-2	199	faD	Pyrolysis (2); RP-HPLC, 97%
3	123469	58200-68-3	200	f9D	Pyrolysis (90%); RP-HPLC (4), contains 10% 124679/124689-D
4	123478	39227-28-6	201	f6D	KOR Isotopes; S1; 98%
5	123678	57653-85-7	202	7eD	(a) Pyrolysis (b) J. Moore, U.S.A.; S2; 98%
6	123679	64461-98-9	203	7dD	(a) D. Firestone; S1, 1:1 mixture with 123689-D, m.p. 202–205°C; RP-HPLC (2), 96%, rest 123689-D (b) J. Moore; S1, 1:1 mixture with 123689-D (c) Pyrolysis (2), mixtures with 123689-D; RP-HPLC (2)
7	123689	58200-69-4	204	7bD	(a) D. Firestone; S1, 80% mixture with 123679-D, m.p. 233–242°C; RP-HPLC (2), 95% pure, rest 123679-D (b) J. Moore; S1, 1:1 mixture with 123679-D (c) Pyrolysis (2), mixtures with 123679-D; RP-HPLC (2)
8	123789	19408-74-3	205	77D	(a) Pyrolysis mixture (b) D. Firestone; S2, 98%
9	124679	39227-62-8	206	bdD	(a) Pyrolysis (2); RP-HPLC (3), 80% pure, 3% 123679-D, 17% 124689-D (b) A. Dobbs, U.K.; 1:2 mixture with 124689-D (c) D. Firestone; pyrolysis mixture
10	124689	58802-09-8	207	bbD	(a) Pyrolysis (2); RP-HPLC (3), 96% pure (b) A. Dobbs; 2:1 mixture with 124679-D (c) D. Firestone; pyrolysis mixture
HpCDD					
1	1234678	35822-46-9	208	feD	(a) KOR Isotope; S1; 98% (b) Pyrolysis
2	1234679	58200-70-7	209	fdD	(a) D. Firestone; S1; 98% (b) Pyrolysis (c) A. Dobbs; 98%
OCDD					
1	12346789	3268-87-9	210	ffD	(a) Analabs; 99% (b) Pyrolysis

[a] Pyrolysis: chlorophenol(s) in equal molar amounts with copper filings and potassium carbonate dissolved in freshly prepared excess methanolic KOH, evaporated to dryness, and heated at 280–300°C for 1 h as in refs. 11 and 17; number in parenthesis after pyrolysis refers to different reaction mixtures of chlorophenols or routes used to obtain the same product. S1: synthesis by alkali condensation of chlorocatechol or chloroguiacol with chloronitrobenzene. S2: synthesis by alkali condensation of 2-bromo-3,4,5-trichlorophenol followed by selective crystallization of mixture. RP-HPLC: reversed-phase high-performance liquid chromatography (number in parenthesis refers to number of cycles needed to obtain stated purity). NP-HPLC: normal-phase HPLC.

(CA). In addition, CA nomenclature states that the lowest number possible must be used when alternatives exist. In particular, in the TCDF series (*cf.* Table I for acronyms), 1678 is used and not 2349; in the PnCDF series, 12678, 12679, 13678, and 14678 are the correct numbering and not the alternatives 23489, 13489, 23479 and 23469, respectively, and; in the HxCDF series, the isomeric designations are 124679 and 134678 and not 134689 and 234679, respectively. All of the above alternatives have been used in some instances in the literature.

Standards

PCDDs. All 49 congeners of the PCDDs of homologue from tetrachloro- to octachloro- were obtained as authentic individual standards in low milligram amounts either by synthesis [pyrolysis of 10–25 mg quantities of the appropriate chlorophenols or by two other routes (S1 and S2) as noted in Table II and refs. 11 and 17], or by exchange with or donation from other research groups. Table II gives the CA registry number, the systematic number [28] and the hex base number [48] along with the source, method of synthesis, and purity for each congener. The pyrolysis reaction products and other mixtures were purified to single compounds by repeated separation on preparative scale reversed-phase (RP) high-performance liquid chromatography (HPLC) columns containing octyldecylsilane (ODS) as stationary phase. The eluents were various combinations of methanol, ethanol, isopropanol and acetonitrile, some with the addition of small amounts (1 to 10%) of water similar to previous reports [10,14,15,22,23]. Several passes by HPLC were needed in some cases in order to obtain the purity stated in Table II. Particularly difficult congeners to separate and purify were the combinations of 1247/1248, 12468/12479, 124679/124689 and 123679/123689 and the congeners 12367, 12368 and 123469 all of which contained small amounts (3 to 10%) of other congeners. The isomer pair 1247/1248 was the only PCDD which could not be resolved by RP-HPLC but did separate nicely on normal-phase HPLC.

The assignment of the configuration of each PCDD was unequivocal in most cases. Some PCDDs/PCDFs have been authenticated by X-ray diffraction [49,50] and these primary standards have been compared in the literature to other congeners with regard to their physical and chemical properties. For instance, it has been established [11,17] by photolysis of congeners of known constitution that those congeners containing adjacent chlorines on both sides of the planar ring next to the oxygen (*e.g.* 123789-HxCDD, 12389-PnCDD and 1289-TCDD) are sterically strained and are the isomers that elute last on most GC columns. Because of the Smiles rearrangement [51,52], pyrolysis of many chlorinated phenols generated two isomers which differed only in the relative orientation of the two lateral aromatic rings. By judicious choice of the starting material, other mixtures can be synthesized containing one of a pair from a previous pyrolysis. This allowed an assignment to be made in most cases as detailed earlier [17]. In addition, in many cases certain standards were available from other research groups or commercial sources. These were sometimes synthesized by other routes (*e.g.* condensation of a chlorocatechol with a nitrobenzene) and could be directly compared to one synthesized by the chlorophenol route. In one case of Smiles-rearranged products, the 1237/1238-TCDD pair, specific assignment could be made. Photolysis of individual aliquots of 12367 and 12389-PnCDD caused loss of chlorine giving TCDD mixtures. Comparison of these TCDD mixtures on GC to the two isomers comprising the 1237/1238-TCDD pair from the Smiles rearrangement

(themselves separable by RP-HPLC) showed that 1237-TCDD eluted first on polar GC columns but second on RP-HPLC. Conversely, the peak from the 1237/1238-TCDD pair eluting second on polar GC columns but first on RP-HPLC was in fact the 1238-TCDD isomer. Six congener pairs synthesized as mixtures, 1246/1249-TCDD, 1247/1248-TCDD, 12468/12479-PnCDD, 12467/12489-PnCDD, 124679/124689-HxCDD, and 123679/123689-HxCDD could not be unequivocably assigned. In these cases, the isomer with the lowest numerical nomenclature designation has been assigned as the earliest eluting compound on RP-HPLC (NP-HPLC for the 1247/1248-TCDD pair). For example with the pair 1246/1249-TCDD, the first eluting isomer on RP-HPLC has been assigned arbitrarily as 1246-TCDD and this designation is used in the GC chromatograms. All standards were checked for purity using GC with electron capture (EC) detection supplemented in some cases with flame detection. Identity was confirmed by using GC with MS detection.

Purified amounts (50 to 500 μg) of standards were weighed on a Cahn 26 electrobalance which has been calibrated for accuracy against a known mass. Precision of weighing of 200 μg quantities was less than 2%. Usually a stock solution of the weighed material was made up in 10 ml of toluene in a volumetric flask and serial dilutions of this concentration were caried out to produce 1.0 ng/μl and 0.1 ng/μl solutions in 5 ml volumes.

PCDFs. Most of the 87 PCDFs of homologue tetrachloro- to octachloro- were synthesized either by dehydrogenation of the corresponding chlorinated diphenyl ether [53] (synthesized from the chlorinated phenol and chlorinated diphenyl iodonium salt; route S2 in Table III) or by condensation of the corresponding chlorophenol and chloronitrobenzene followed by reductive cyclization [20] (route S1 in Table III). In the few cases where a PCDF could not be synthesized from these two routes, they were prepared by two other methods (S3 or S4 in Table III) or obtained from other research groups or commercial sources. The reaction mixtures were separated by RP-HPLC in a similar fashion as for the PCDDs except that fewer passes were needed to obtain the stated purity since PCDF mixtures show greater resolution on RP-HPLC than do the PCDDs. Impurities in the PCDFs mixtures were often one homologue lower than the desired product *i.e.* dechlorination rather than dehydrochlorination. Assignment of isomeric structure of the PCDFs is given in more detail in refs. 15, 16 and 22 with the additional support in this work that many of the PCDFs were supported by NMR data [20].

Instrumentation

The gas chromatographs used were Varian models 3500 and 6000 equipped with capillary columns and on-column injectors. The ovens and injectors could be programmed independently of each other. The method of injection was by the solute focusing on-column technique whereby the injector was kept at 80°C [below the boiling point of the solvent (usually toluene)], and then the injector heat ramped quickly (1 to 3 min) to 230–260°C – the final column temperature. The oven and the column itself were initially held at 120°C, just above the boiling temperature of the solvent, then heated rapidly to 160–180°C and then slowly (2 to 3°C per min) to the final temperature. Carrier gas for the capillary columns was helium at a linear velocity of 30 cm/s corresponding to a volume flow of about 2.0 ml/min. Chart speed for the chromatograms varied between 2.0 and 4.0 cm/s and volume of injection between 0.6

TABLE III

SOURCES AND PURITY OF THE 87 PCDFs WITH 4 TO 8 CHLORINES

No.	Isomer	CA registry number	Systematic number	Base hex number	Source and purity[a]
TCDFs					
1	1234	24478-72-6	49	f0F	H. Markens, The Netherlands; 98%
2	1236	83704-21-6	50	78F	S1; 97%
3	1237	83704-22-7	51	74F	S1; 97%
4	1238	62615-08-1	52	72F	S1; 97%
5	1239	83704-23-8	53	71F	(a) Wellington, Ontario, Canada; 98% (b) C. Rappe, Sweden; S3 with 1237-F; 98%
6	1246	71998-73-7	54	b8F	S1; 95%
7	1247	83719-40-8	55	b4F	S1; 98%
8	1248	64126-87-0	56	b2F	(a) S2; 97% (b) D. Firestone, U.S.A.
9	1249	83704-24-9	57	b1F	S1; 98%
10	1267	83704-25-0	58	3CF	S1; 97%
11	1268	83710-07-0	59	3aF	S2 with 2368-F; RP-HPLC, 97%
12	1269	70648-18-9	60	39F	(a) C. Rappe; S2 with 1469-F, 98% (b) Wellington; mixture with 1469-F
13	1278	58802-20-3	61	3bF	(a) S1; 98% (b) S2; with 2378-F; RP-HPLC, 98% (c) D. Firestone
14	1279	83704-26-1	62	35F	S1; 98%
15	1289	70648-22-5	63	33F	(a) S2; mixture with 2378-F, 1278-F, <1% yield; RP-HPLC (3) (b) C. Rappe; S2; 95%
16	1346	83704-27-2	64	d8F	S1; 95%
17	1347	70648-16-7	65	d4F	S1; 97%
18	1348	92341-04-3	66	d2F	S1; 98%
19	1349	83704-28-3	67	d1F	(a) Wellington; 95% (b) C. Rappe; S3; with 1347-F, 95%
20	1367	57117-36-9	68	5cF	(a) S1; 98% (b) Canadian Wildlife, Ottawa, Canada; qual., 95%
21	1368	71998-72-6	69	5aF	S1; 98%
22	1369	83690-98-6	70	59F	S1; 98%
23	1378	57117-35-8	71	56F	(a) S1; 98% (b) Canadian Wildlife; qual., 95%
24	1379	64560-17-4	72	55F	S1; 98%
25	1467	66794-59-0	73	9cF	S1; 98%
26	1468	82911-58-8	74	9aF	D. Firestone; 98%
27	1469	70648-19-0	75	99F	(a) C. Rappe; S2; 95% (b) Wellington; 80% with 1269-F
28	1478	83704-29-4	76	96F	S1; 98%
29	1678	83704-33-0	77	1dF	S1; 93%
30	2346	83704-30-7	78	d8F	S1; 98%
31	2347	83704-31-8	79	d4F	S1; 98%
32	2348	83704-32-9	80	d2F	S1; 98%
33	2367	57117-39-2	81	6cF	(a) S1; 98% (b) Canadian Wildlife; qual., 95%
34	2368	57117-37-0	82	6aF	(a) S2 with 1268-F; 98%; RP-HPLC (b) J. McKinney, U.S.A.; 98%

TABLE III *(continued)*

No.	Isomer	CA registry number	Systematic number	Base hex number	Source and purity[a]
35	2378	51207-31-9	83	66F	(a) J. McKinney; 94% (b) KOR Isotope, U.S.A.; 98% (c) D. Firestone; 95%
36	2467	57117-38-1	84	acF	(a) S1; 98% (b) Canadian Wildlife; qual., 95%
37	2468	58802-19-0	85	aaF	(a) S1; 98% (b) D. Firestone; 98%
38	3467	57117-40-5	86	ccF	(a) S1; 98% (b) Canadian Wildlife; qual., mixture
PnCDFs					
1	12346	83704-47-6	87	f8F	S1; 97%
2	12347	83704-48-7	88	f4F	S1; 99%
3	12348	67517-48-0	89	f2F	(a) S2; 98% (b) C. Rappe; S2; 98%
4	12349	83704-49-8	90	f1F	S1; 98%
5	12367	57117-42-7	91	7cF	(a) S1; 98% (b) Canadian Wildlife; 98%
6	12368	83704-51-2	92	7aF	(a) S2; 92% (b) C. Rappe; S2; 98%
7	12369	83704-52-3	93	79F	C. Rappe; S2; 98%
8	12378	57117-41-6	94	76F	(a) S2; with 12389-F; RP-HPLC, 98% (b) H. Poiger, Switzerland; qual., 98% (c) Canadian Wildlife; 98%
9	12379	83704-53-4	95	75F	(a) Wellington; 98% (b) C. Rappe; S3; 98%
10	12389	83704-54-5	96	73F	S2 with 12378-F; RP-HPLC, 98%
11	12467	58802-15-6	97	bcF	S1; 97%
12	12468	69698-57-3	98	baF	S2; 96%
13	12469	70648-24-7	99	b9F	S1; 99%
14	12478	58802-15-6	100	b6F	(a) D. Firestone; 98% (b) S2; with 12489-F; RP-HPLC (2), 98%
15	12479	71998-74-8	101	b5F	S1; 98%
16	12489	70648-23-6	102	b3F	S2; with 12478-F; RP-HPLC (2), 98%
17	12678	69433-00-7	103	3eF	S2; with 23478-F; RP-HPLC, 98%
18	12679	70872-82-1	104	3dF	C. Rappe; S2, 98%
19	13467	83704-36-3	105	dcF	S1; 98%
20	13468	83704-55-6	106	daF	(a) S1; 98% (b) C. Rappe; S2; 98%
21	13469	70648-15-6	107	d9F	C. Rappe; S2; 98%
22	13478	58802-16-7	108	d6F	S1; 98%
23	13479	70648-15-6	109	d5F	(a) S1; 98% (b) C. Rappe; S3; 96%
24	13678	70648-21-4	110	5eF	Wellington; 98%
25	14678	83704-35-2	111	9eF	Wellington; 98%
26	23467	57117-43-8	112	ecF	(a) S1; 98% (b) Canadian Wildlife; 97%
27	23468	67481-22-5	113	eaF	S2; 98%
28	23478	57117-31-4	114	e6F	(a) S2; with 12678-F; RP-HPLC, 98% (b) S1; 98% (c) H. Poiger; qual. (d) Canadian Wildlife; 98%

(Continued on p. 140)

TABLE III *(continued)*

No.	Isomer	CA registry number	Systematic number	Base hex number	Source and purity[a]
HxCDFs					
1	123467	79060-60-9	115	fcF	S1; 98%
2	123468	69698-60-8	116	faF	S2; 98%
3	123469	91538-83-9	117	f9F	S1; 98%
4	123478	70648-26-9	118	f6F	(a) S2; with 123489-F; RP-HPLC, 95% (b) Cambridge Isotope, U.S.A.; 98%
5	123479	91538-84-0	119	f5F	S1; 98%
6	123489	92341-07-6	120	f3F	S2 with 123478-F; RP-HPLC (2), 98%
7	123678	57117-44-9	121	7eF	(a) Canadian Wildlife; 98% (b) S2; 98%
8	123679	92341-06-5	122	7dF	C. Rappe; S3; 98%
9	123689	75198-38-8	123	7bF	S2; RP-HPLC; 98%
10	123789	72918-21-9	124	77F	(a) Cambridge Isotope; 98% (b) C. Rappe, S3; 98%
11	124678	67562-40-7	125	bcF	S2; 98%
12	124679	75627-02-0	126	bdF	S2; RP-HPLC, 98%
13	124689	69698-59-5	127	bbF	S2; RP-HPLC, 98%
14	134678	71998-75-9	128	deF	S2; 98%
15	134679	92341-05-4	129	ddF	(a) Wellington; 70% (b) C. Rappe; S3; 98%
16	234678	60851-34-5	130	eeF	(a) S2; 98% (b) Canadian Wildlife; mixture
HpCDFs					
1	1234678	67562-39-4	131	feF	S2; 98%
2	1234679	70648-25-8	132	fdF	S2; RP-HPLC, 98%
3	1234689	69698-58-4	133	fbF	D. Firestone; 98%
4	1234789	55673-89-7	134	f7F	S2; RP-HPLC; 98%
OCDF					
1	12346789	1010-77-1	135	ffF	(1) Analabs, U.S.A.; 98% (2) S2; 98%

[a] S1 Synthesis from corresponding chlorophenol and chloronitrobenzene followed by reductive cyclization [20].

S2 Synthesis from corresponding chlorophenol and chlorodiphenyl iodonium salt to chlorodiphenyl ether followed by palladium acetate cyclization [53].

S3 Synthesis from corresponding chlorophenol and iodobenzene followed by palladium acetate cyclization [53].

S4 Synthesis by nucleophilic displacement of corresponding chlorophenol on chlorobenzene followed by palladium acetate cyclization.

RP-HPLC Reversed phase high-performance liquid chromatography (number in parenthesis is number of collection cycles needed to obtain stated purity).

and 2.0 μl. Detection was usually carried out with a nickel-63 (8 mCi) electron-capture detector kept at 300°C with a nitrogen make-up gas flow of 20 ml/min. A flame ionization detector with air and hydrogen gases was used to monitor impurities in certain cases.

GC capillary columns

Table IV lists, for each GC stationary phase, the manufacturer, coating,

dimensions and temperature programming. These polysiloxane columns are grouped as follows: (i) non-polar (DB-1; 100% methyl and DB-5; 5% phenyl); (ii) medium polar (DB-17, OV-17; 50% phenyl-methyl and DB-210; trifluoropropyl); (iii) polar (DB-225, CPS-1, SP-2331, CP-Sil 88; all cyanopropyl) and (iv) other (SB-smectic).

The chromatograms shown in the figures for the homologues of the PCDDs/PCDFs have been derived from injection of six composite standards of about 0.2 ng/μl each of all isomers of a specific homologue (Table I). Since the analytes have been detected using electron-capture detection (ECD), the absolute response for a given isomer varied by as much as an order of magnitude even though equal amounts were injected. Assignment of a given GC peak to a specific isomer within a group was made by the separate injection of solutions containing one or two isomers along with a retention time (RT) standard, the earliest eluting isomer of that homologue group. These RT reference standards were: (1) for the PCDDs; 1368-TCDD, 12468-PnCDD and 124679-HxCDD and (2) for the PCDFs; 1368-TCDF, 13468-PnCDF and 123468-HxCDF. A combination of results from these injections allowed an unequivocable assignment of the elution order of a specific isomer within a composite mixture. As the retention time windows of most homologue groups of the PCDDs/PCDFs overlap to some extent on capillary columns, particularly polar phases, the injections were carried out by individual homologues. Isomers which co-eluted or eluted near each other were co-injected to define further their degree of resolution.

RESULTS

Three mixtures of the PCDDs (22 tetra, 14 penta and 10 hexa) and three mixtures of the PCDFs (38 tetra, 28 penta and 16 hexa) were prepared at a concentration of 0.2 ng/μl for each congener. The GC elution pattern of these six solutions for nine different GC stationary phases on capillary columns are presented in Figs. 2–10 and their relative retention times (RRT) are listed in Tables V–XIII. The elution order, and degree of separation are best seen from the figures which represent possible separations when all isomers are present in a mixture. For those isomers which did not produce two peaks by co-injection even though they had slightly different relative retention time (RRT), the one first reported on the figure has the shorter RRT. The RRT in the nine tables are based on the earliest eluting isomer of that particular group being arbitrarily assigned a value of 1.000. The RRT of the six RT reference standards are also listed in each table enabling an estimate to be made of the degree of overlap between homologues as a function of stationary phase. The absolute retention time of a selected isomer can be approximated from the tables but should be used only for guidance since this parameter will change from column to column, with usage, and GC conditions. The higher chlorinated hepta- and octa-congeners are not shown in these figures and tables since they are readily resolved from each other on all columns investigated. For all columns, the elution order of the PCDDs is 1234679 and 1234678 for the two hepta isomers followed by octa-dioxin. For the PCDFs, the corresponding elution order for the four hepta isomers is 1234678, 1234679, 1234689 and 1234789, and then octa-furan.

As mentioned in he experimental part, six pairs of PCDDs (12 congeners), separable by HPLC, could only be effectively separated on GC with the liquid crystalline smectic phase. However their exact structure and hence elution order on

TABLE IV

GC SILICONE FUSED-SILICA CAPILLARY COLUMNS USED FOR SEPARATION OF PCDDs AND PCDFs AND THEIR TEMPERATURE PROGRAMS

No.	Name	Manufacturer	Coating and type	Length (m)	Inner diameter (mm)	Film thickness (μm)	Program
1	DB-1	J&W Scientific, CA, U.S.A.	dimethyl (100%), bonded	60	0.32	0.25	120 (1 min) to 180°C (50°C/min) to 280°C (3°C/min)
2	DB-5	J&W Scientific,	methyl (95%) phenyl (5%), bonded	30	0.32	0.25	120 (1 min) to 180°C (50°C/min) to 280°C (3°C/min)
3a	DB-17	J&W Scientific,	methyl (50%) phenyl (50%), bonded	30	0.32	0.25	120 (1 min) to 160°C (20°C/min) to 280°C (3°C/min)
3b	OV-17	Quadrex, New Haven, CT, U.S.A.	methyl (50%) phenyl (50%), bonded	50	0.32	0.25	120 (1 min) to 160°C (20°C/min) to 280°C (3°C/min)
4	DB-210	J&W Scientific,	methyl trifluoropropyl (100%), bonded	30	0.32	0.25	120 (0 min) to 160°C (20°C/min) to 240°C (2°C/min)
5	DB-225	J&W Scientific,	methylcyanopropyl (50%) methyl-phenyl (50%), bonded	30	0.32	0.25	120 (0 min) to 160°C (20°C/min) to 240°C (2°C/min)
6	CPS-1	Quadrex	methylcyanopropyl (75%) phenyl-methyl propyl (25%), bonded	50	0.25	0.25	120 (1 min) to 180°C (30°C/min) to 230°C (2°C/min)
7	SP-2331	Supelco, PA, U.S.A.	biscyanopropyl (90%) phenylcyanopropyl 1:1 (10%), wall coated	60	0.25	0.20	120 (1 min) to 200°C (50°C/min) to 260°C (2°C/min)
8	CP-Sil 88	Chrompack, Middelburg, The Netherlands	biscyanopropyl (100%), wall coated	50	0.22	0.20	150 (0 min) to 180°C (30°C/min) to 230°C (2°C/min)
9	SB-Smectic	Lee Scientific Salt Lake City, UT, U.S.A.	liquid crystalline methyl (80%) diphenyl carboxylic ester (20%), wall coated	25	0.32	0.15	100 (1 min) to 180°C (30°C/min) to 230°C (3°C/min)

GC (either a then b or b then a) could not be definitely assigned. Since these congeners have arbitrarily been assigned with the lowest number in nomenclature eluting first on RP-HPLC, this uncertainly is noted by an asterisk for the data from the smectic column in Fig. 10b and Table XIII. The actual structure of these pairs and hence their GC and HPLC elution order could be determined either by chemical means (dechlorination or chlorination to known congeners) or by physical means (X-ray diffraction crystallography or GC–matrix isolation Fourier-transform infrared spectroscopy).

DISCUSSION

The separations shown in the figures and the RRT in the tables are those that can be obtained using the standards, GC columns, and conditions as described in the experimental section. No particular effort was made to optimize GC conditions such as injector temperature, type of injection, gas flow, temperature programming or other variables to maximize resolution of certain congeners paricularly those which are 2,3,7,8-substituted. Thus it may be possible to obtain slightly different separations than those listed by using other conditions. In this regard we have compared separations on columns purchased at different times from the same manufacturer and with different lot numbers. With both DB-5 and DB-210, identical separations and patterns were obtained from both columns. In the case of the cyanopropyl phases, CP-Sil 88 and SP-2331, columns purchased at different times showed slight differences in resolution in isolated cases *e.g.* isomers co-eluting on one column were found to have some degree of separation on a second different column.

One phenomenon we did notice with the SP-2331 column was the change in elution order and even improved separation as the column deteriorated. After several months of use, the chromatographic peak shape degraded as evidenced by tailing peaks —a phenomenon often attributed to oxygen attack on the stationary phase. Nevertheless, a few separations now occurred which previously with a new column and better peak shape were not possible. For example, 12378-PnCDF was completely separated from the previous co-eluter 12348-PnCDF (now earlier) but co-eluted with the previously separated 12346-PnCDF. 1678-TCDF and 1234-TCDF were now separate peaks on the deteriorated column but co-eluted on the new chromatographic column. On the other hand, 12378-PnCDD and 12369-PnCDD now co-eluted on the degraded column where previously they were well separated. A similar loss in resolution with the TCDF isomers has been noted by Swerev and Ballschmiter [54] for the SP-2331 phase although no new separations were reported.

Most of the 136 PCDDs and PCDFs can be readily separated from each other using a combination of conventional GC phases. Exceptions to this are certain pairs of PCDDs containing mostly 124-substitution. These are 1247/1248, 1246/1249, 12468/12479, 12467/12489, 124679/124689 and 123679/123689 for which there is little or no resolution on the common GC phases. However, the newly developed smectic liquid crystalline phase [36,37,41] is unique in its resolving powers and is readily capable of resolving to base line the above six PCDD pairs. In fact it has not been possible until the advent of this stationary phase to specify the relative proportions of these isomer pairs. The smectic crystalline phase appears to have other unusual properties. Our separations for the TCDDs differ from those of Mahle *et al.* [41] in

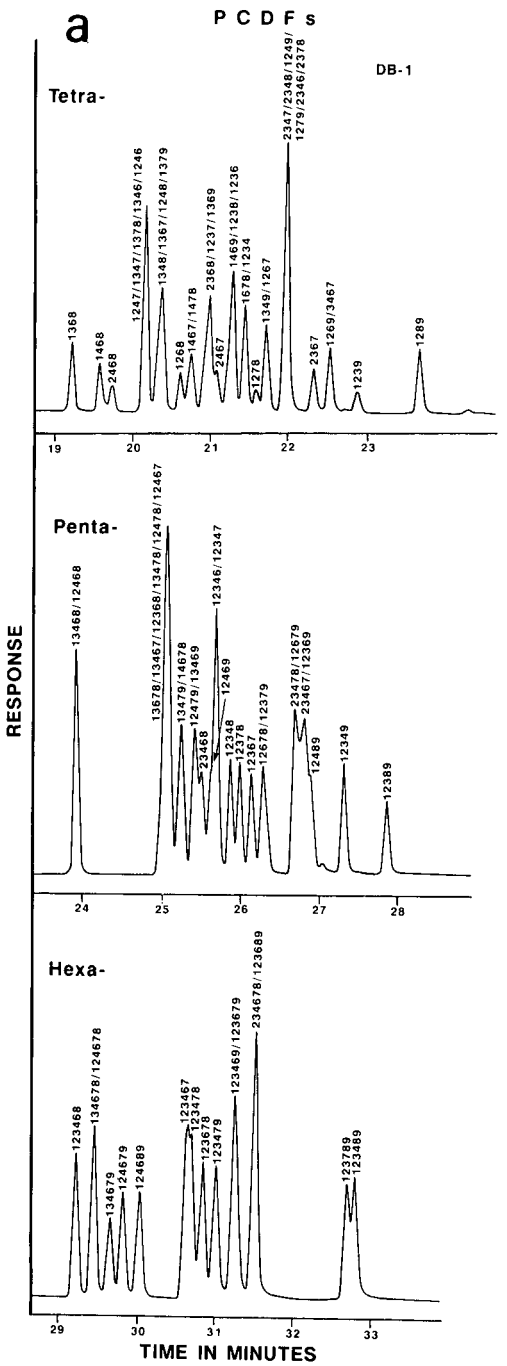
a
PCDFs
DB-1
Tetra-
1368
1468
2468
1247/1347/1378/1346/1246
1348/1367/1248/1379
1268
1467/1478
2368/1237/1369
2467
1469/1238/1236
1678/1234
1278
1349/1267
2347/2348/1249/
1279/2346/2378
2367
1269/3467
1239
1289
19
20
21
22
23
Penta-
13468/12468
13678/13467/12368/13478/12478/12467
13479/14678
12479/13469
23468
12346/12347
12469
12348
12378
12367
12678/12379
23478/12679
23467/12369
12489
12349
12389
24
25
26
27
28
Hexa-
123468
134678/124678
134679
124679
124689
123467
123478
123678
123479
123469/123679
234678/123689
123789
123489
29
30
31
32
33
RESPONSE
TIME IN MINUTES

Fig. 2.

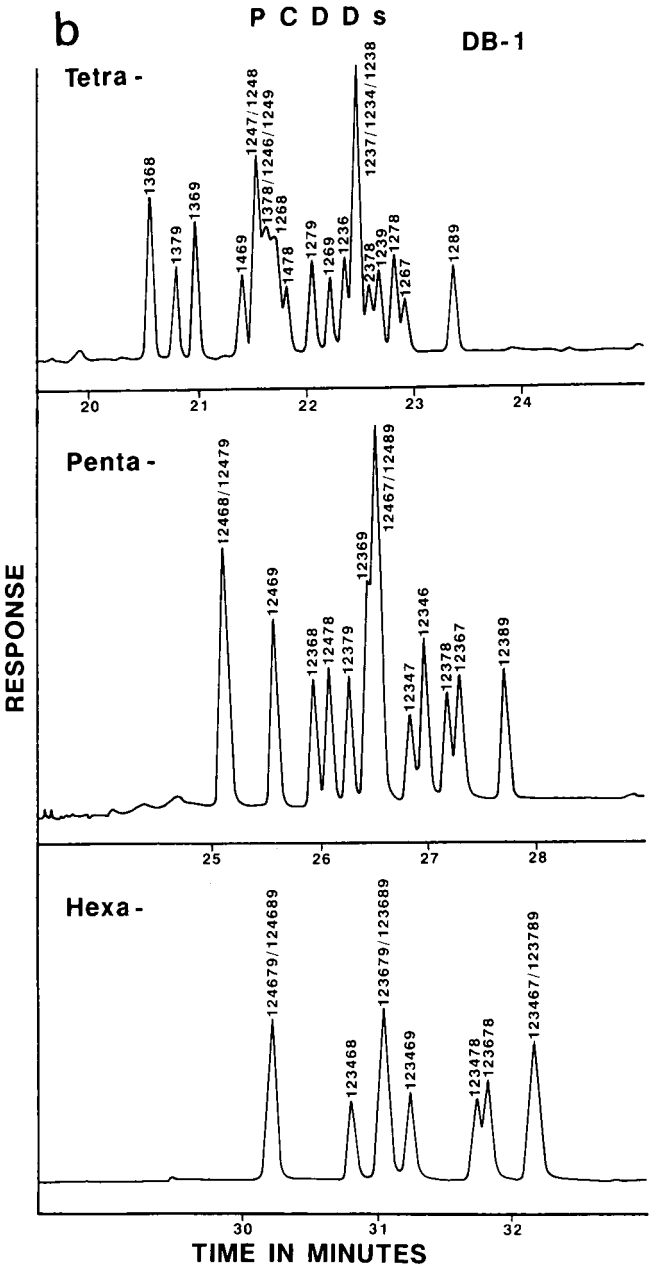

Fig. 2. (a) GC–ECD tracing of the separation of 38 TCDFs, 28 PnCDFs, and 16 HxCDFs on a DB-1 fused-silica bonded phase capillary column. (b) GC–ECD tracing of the separation of 22 TCDDs, 14 PnCDDs, and 10 HxCDDs on a DB-1 fused-silica bonded phase capillary column.

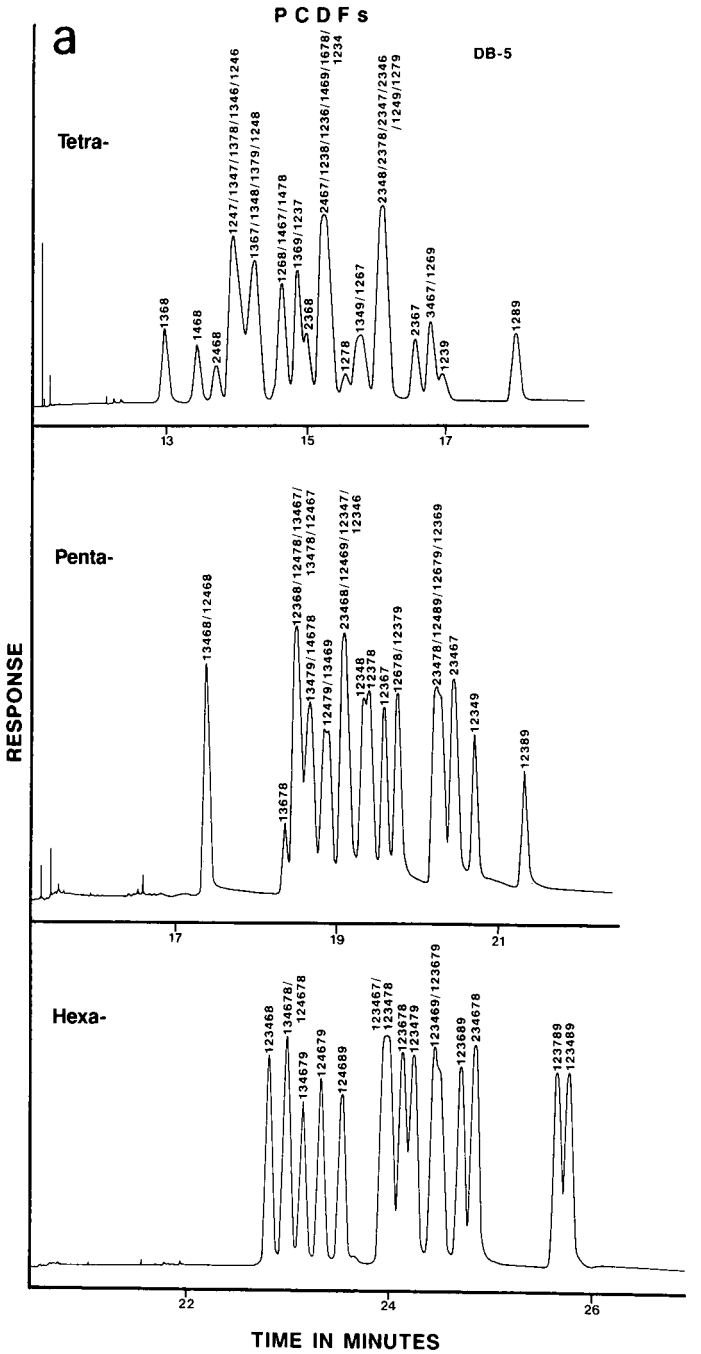
a
PCDFs
DB-5
Tetra-
1368
1468
2468
1247/1347/1378/1346/1246
1367/1348/1379/1248
1268/1467/1478
1369/1237
2368
2467/1238/1236/1469/1678/1234
1278
1349/1267
2348/2378/2347/2346/1249/1279
2367
3467/1269
1239
1289
13
15
17
Penta-
13468/12468
13678
12368/12478/13467/13478/12467
13479/14678
12479/13469
23468/12469/12347/12346
12348
12378
12367
12678/12379
23478/12489/12679/12369
23467
12349
12389
17
19
21
Hexa-
123468
134678/124678
134679
124679
124689
123467/123478
123678
123479
123469/123679
123689
234678
123789
123489
22
24
26
RESPONSE
TIME IN MINUTES

Fig. 3.

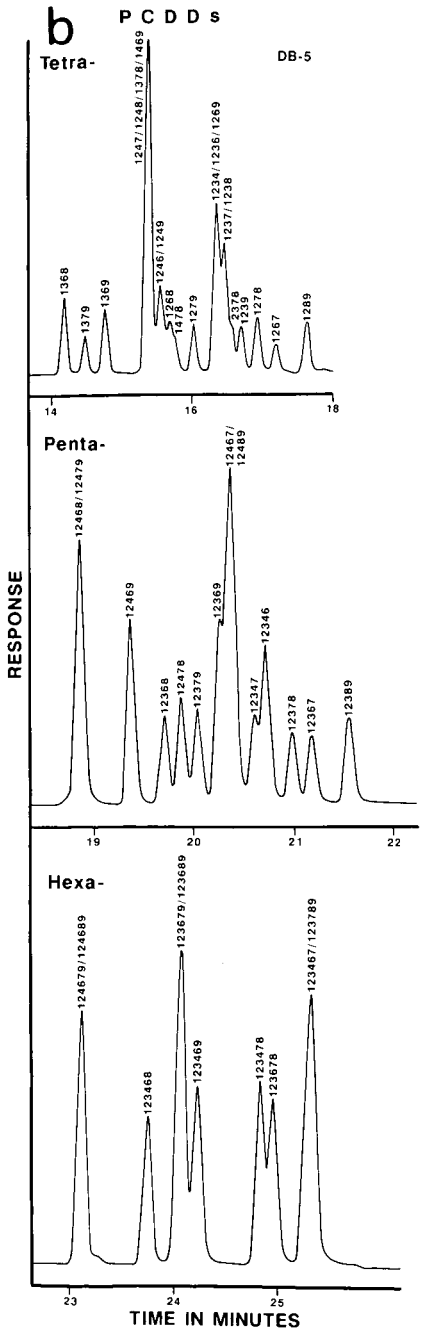

Fig. 3 (a) GC–ECD tracing of the separation of 38 TCDFs, 28 PnCDFs, and 16 HxCDFs on a DB-5 fused-silica bonded phase capillary column. (b) GC–ECD tracing of the separation of 22 TCDDs, 14 PnCDDs, and 10 HxCDDs on a DB-5 fused-silica bonded phase capillary column.

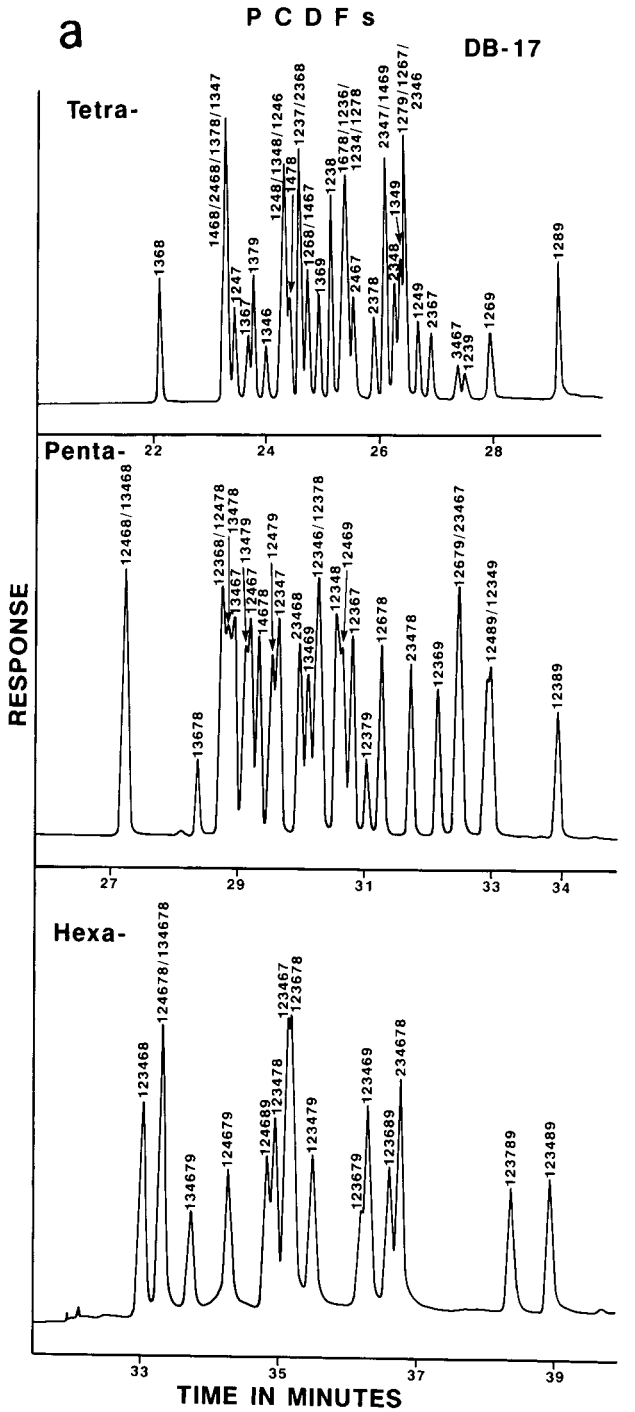
a
P C D F s
DB-17
Tetra-
1368
1468/2468/1378/1347
1247
1379
1367
1346
1248/1348/1246
1478
1237/2368
1268/1467
1369
1238
1678/1236/
1234/1278
2467
2378
2347/1469
1279/1267/
2346
2348
1349
1249
2367
3467
1239
1269
1289
Penta-
22
24
26
28
12468/13468
13678
12368/12478
13478
13467
13479
12467
14678
12479
12347
23468
13469
12346/12378
12348
12469
12367
12379
12678
23478
12369
12679/23467
12489/12349
12389
27
29
31
33
34
Hexa-
123468
124678/134678
134679
124679
124689
123478
123467
123678
123479
123679
123469
123689
234678
123789
123489
33
35
37
39
RESPONSE
TIME IN MINUTES

Fig. 4.

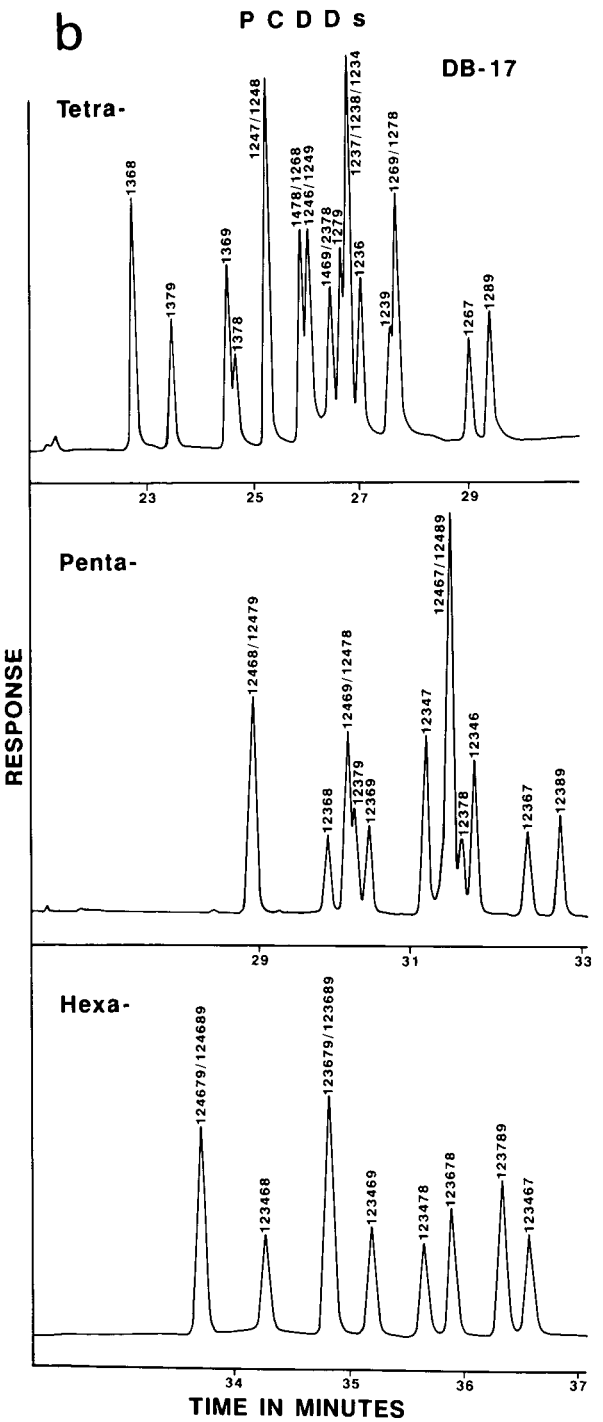

Fig. 4. (a) GC–ECD tracing of the separation of 38 TCDFs, 28 PnCDFs, and 16 HxCDFs on a DB-17 fused-silica bonded phase capillary column. (b) GC–ECD tracing of the separation of 22 TCDDs, 14 PnCDDs, and 10 HxCDDs on a DB-17 fused-silica bonded phase capillary column.

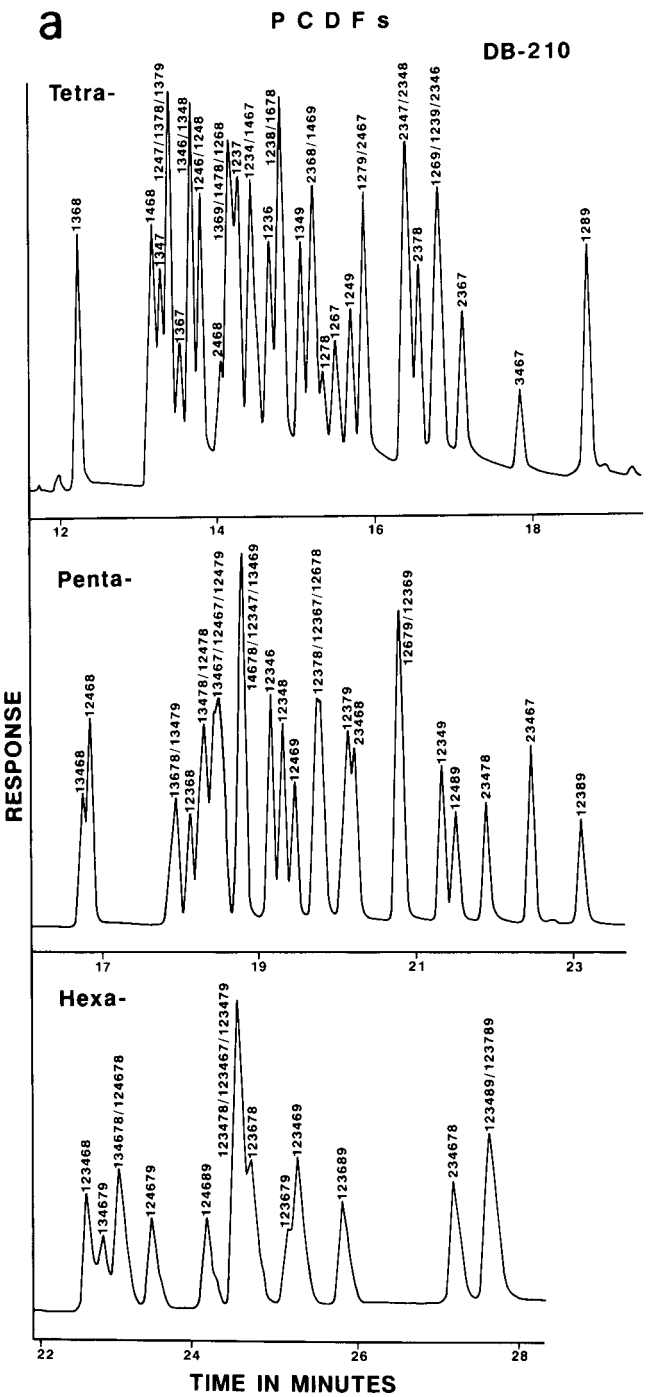
a
PCDFs
DB-210
Tetra-
1368
1468
1247/1378/1379
1347
1346/1348
1367
1246/1248
1369/1478/1268
2468
1237
1234/1467
1238/1678
1236
1349
2368/1469
1278
1267
1249
1279/2467
2347/2348
2378
1269/1239/2346
2367
3467
1289
12
14
16
18
Penta-
13468
12468
13678/13479
12368
13478/12478
13467/12467/12479
14678/12347/13469
12346
12348
12469
12378/12367/12678
12379
23468
12679/12369
12349
12489
23478
23467
12389
17
19
21
23
Hexa-
123468
134679
134678/124678
124679
124689
123478/123467/123479
123678
123679
123469
123689
234678
123489/123789
22
24
26
28
RESPONSE
TIME IN MINUTES

Fig. 5.

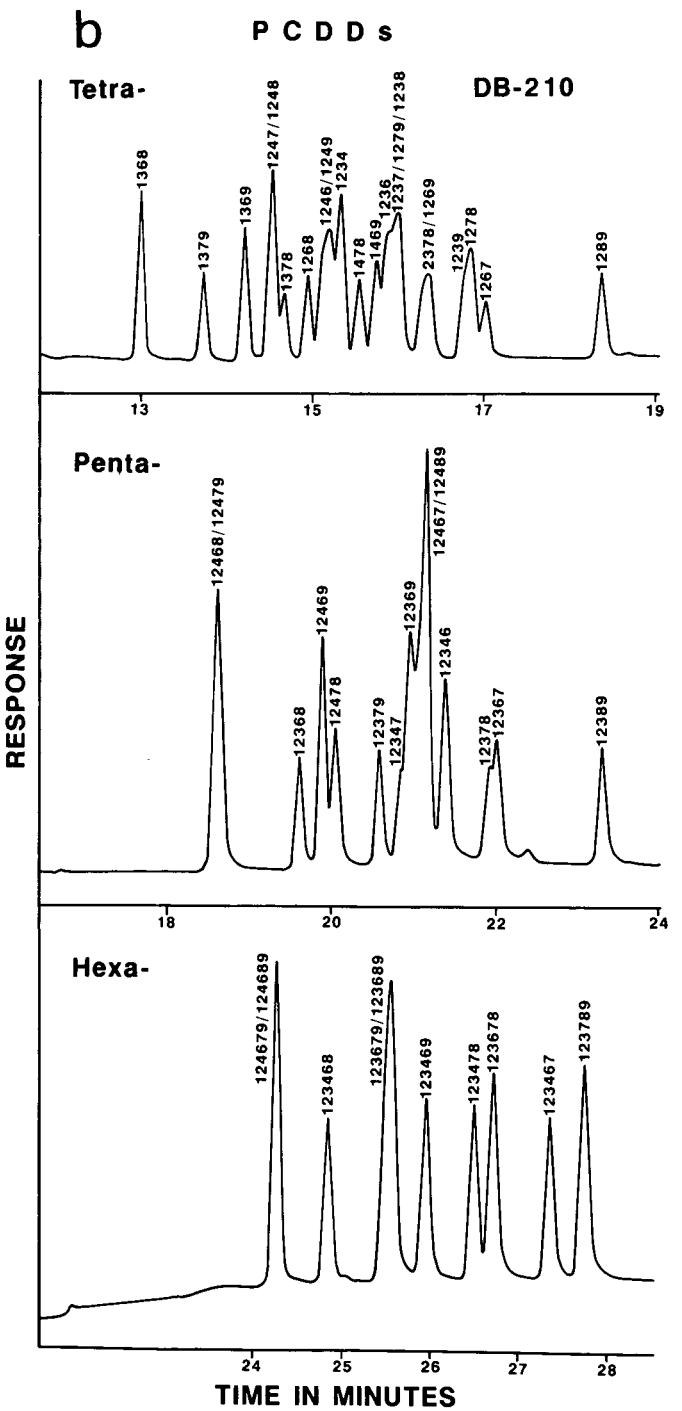

Fig. 5. (a) GC–ECD tracing of the separation of 38 TCDFs, 28 PnCDFs, and 16 HxCDFs on a DB-210 fused-silica bonded phase capillary column. (b) GC–ECD tracing of the separation of 22 TCDDs, 14 PnCDDs, and 10 HxCDDs on a DB-210 fused-silica bonded phase capillary column.

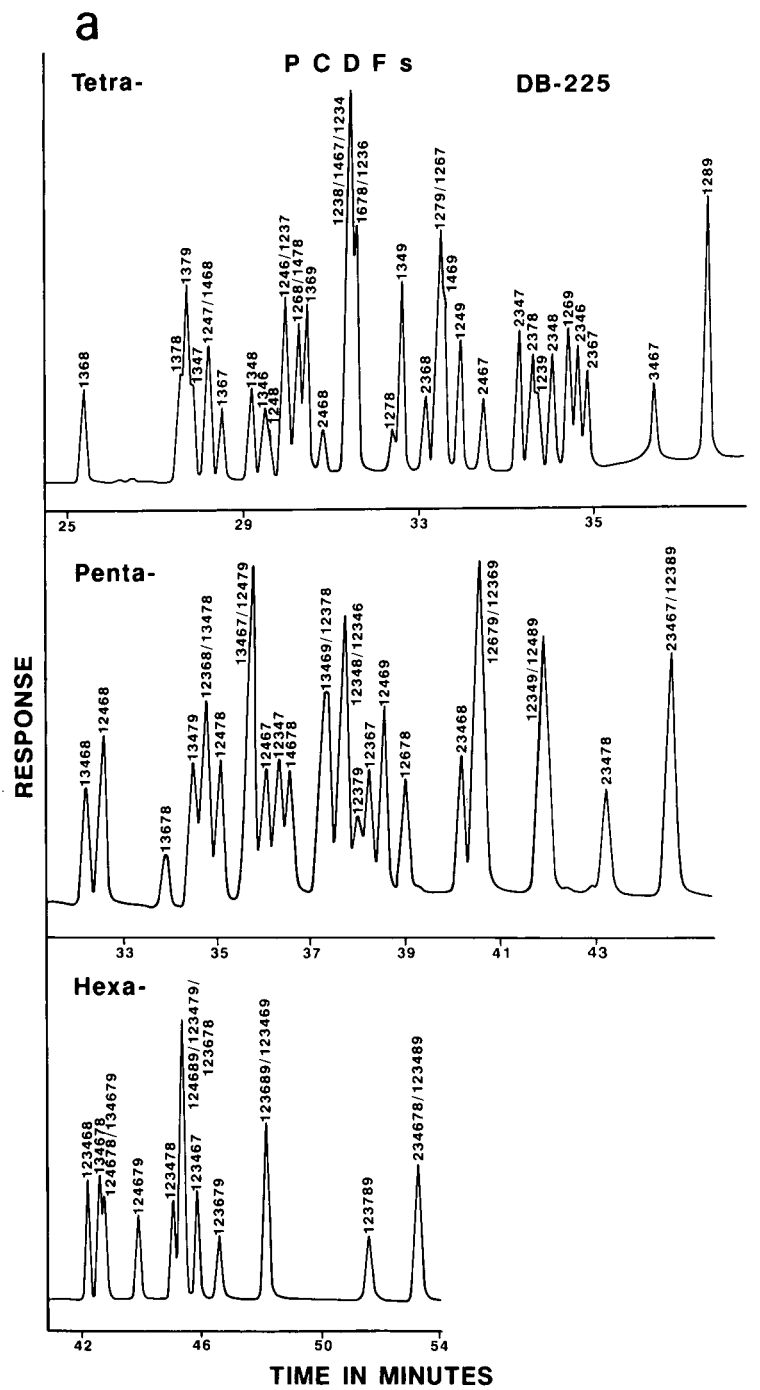
a
P C D F s
Tetra-
DB-225
1368
1378
1379
1347
1247/1468
1367
1348
1346
1248
1246/1237
1268/1478
1369
2468
1238/1467/1234
1678/1236
1278
1349
2368
1279/1267
1469
1249
2467
2347
2378
1239
2348
1269
2346
2367
3467
1289
25
29
33
35
Penta-
13468
12468
13678
13479
12368/13478
12478
13467/12479
12467
12347
14678
13469/12378
12379
12348/12346
12367
12469
12678
23468
12679/12369
12349/12489
23478
23467/12389
33
35
37
39
41
43
Hexa-
123468
134678
124678/134679
124679
123478
124689/123479/
123678
123467
123679
123689/123469
123789
234678/123489
42
46
50
54
RESPONSE
TIME IN MINUTES

Fig. 6.

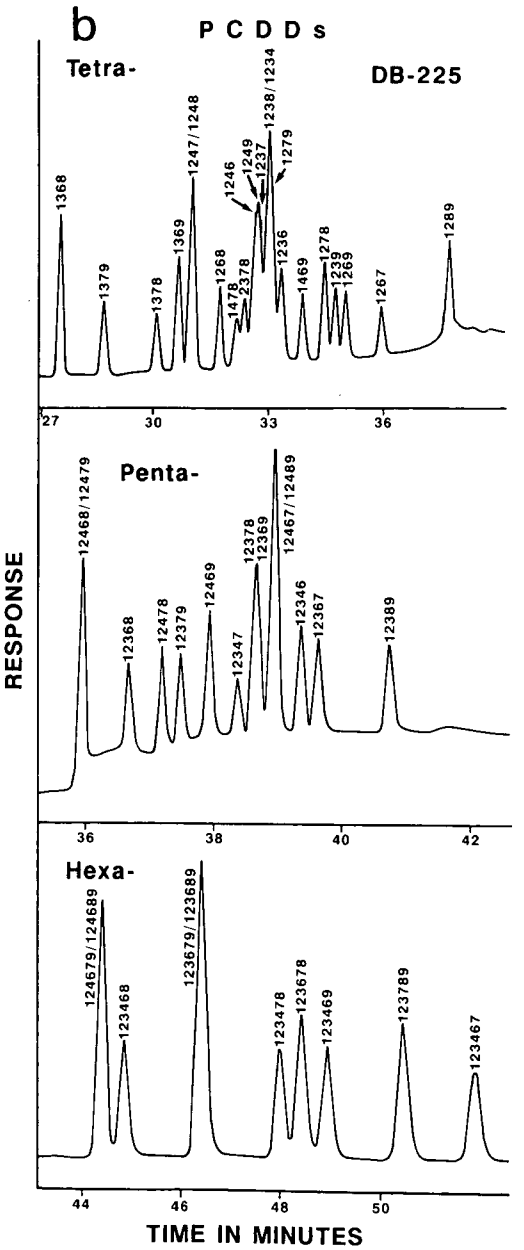

Fig. 6. (a) GC–ECD tracing of the separation of 38 TCDFs, 28 PnCDFs, and 16 HxCDFs on a DB-225 fused-silica bonded phase capillary column. (b) GC–ECD tracing of the separation of 22 TCDDs, 14 PnCDDs, and 10 HxCDDs on a DB-225 fused-silica bonded phase capillary column.

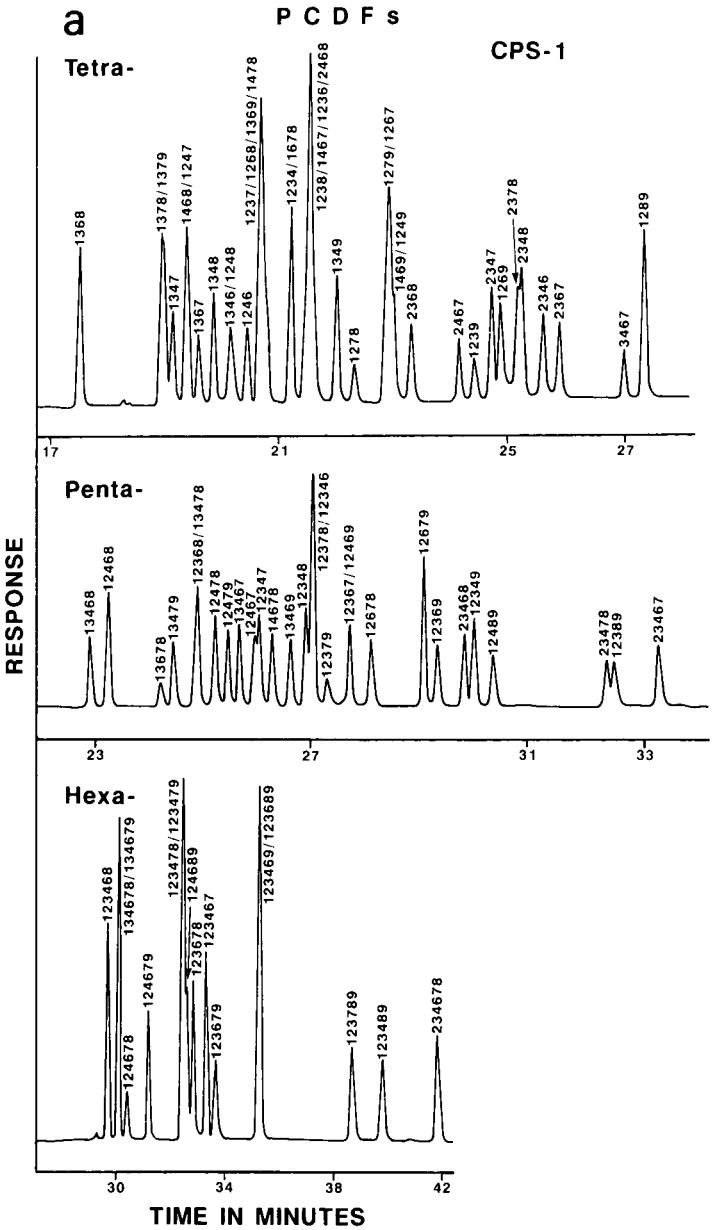
a
P C D F s
CPS-1
Tetra-
1368
1378/1379
1347
1468/1247
1367
1348
1346/1248
1246
1237/1268/1369/1478
1234/1678
1238/1467/1236/2468
1349
1278
1279/1267
1469/1249
2368
2467
1239
2347
1269
2378
2348
2346
2367
3467
1289
17
21
25
27
Penta-
13468
12468
13678
13479
12368/13478
12478
12479
13467
12467
12347
14678
13469
12348
12378/12346
12379
12367/12469
12678
12679
12369
23468
12349
12489
23478
12389
23467
23
27
31
33
Hexa-
123468
134678/134679
124678
124679
123478/123479
124689
123678
123467
123679
123469/123689
123789
123489
234678
30
34
38
42
RESPONSE
TIME IN MINUTES

Fig. 7.

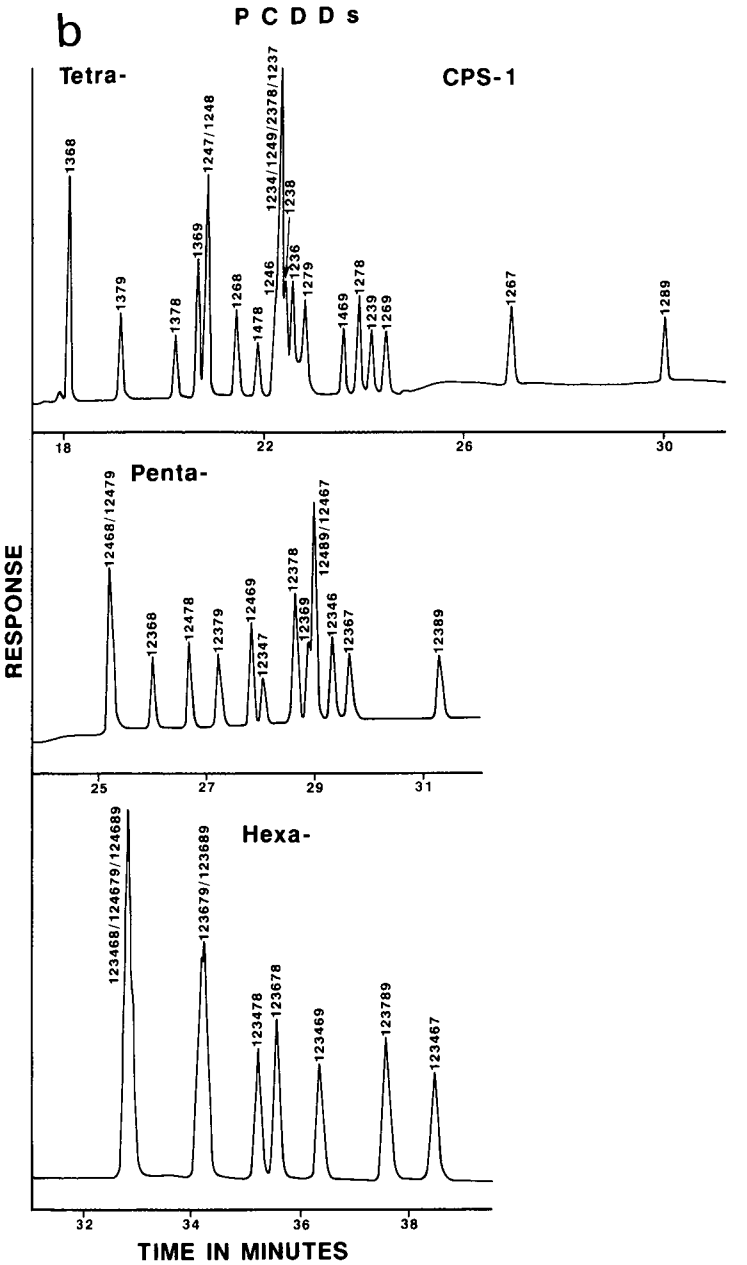

Fig. 7. (a) GC–ECD tracing of the separation of 38 TCDFs, 28 PnCDFs, and 16 HxCDFs on a CPS-1 fused-silica capillary column. (b) GC–ECD tracing of the separation of 22 TCDDs, 14 PnCDDs, and 10 HxCDDs on a CPS-1 fused-silica capillary column.

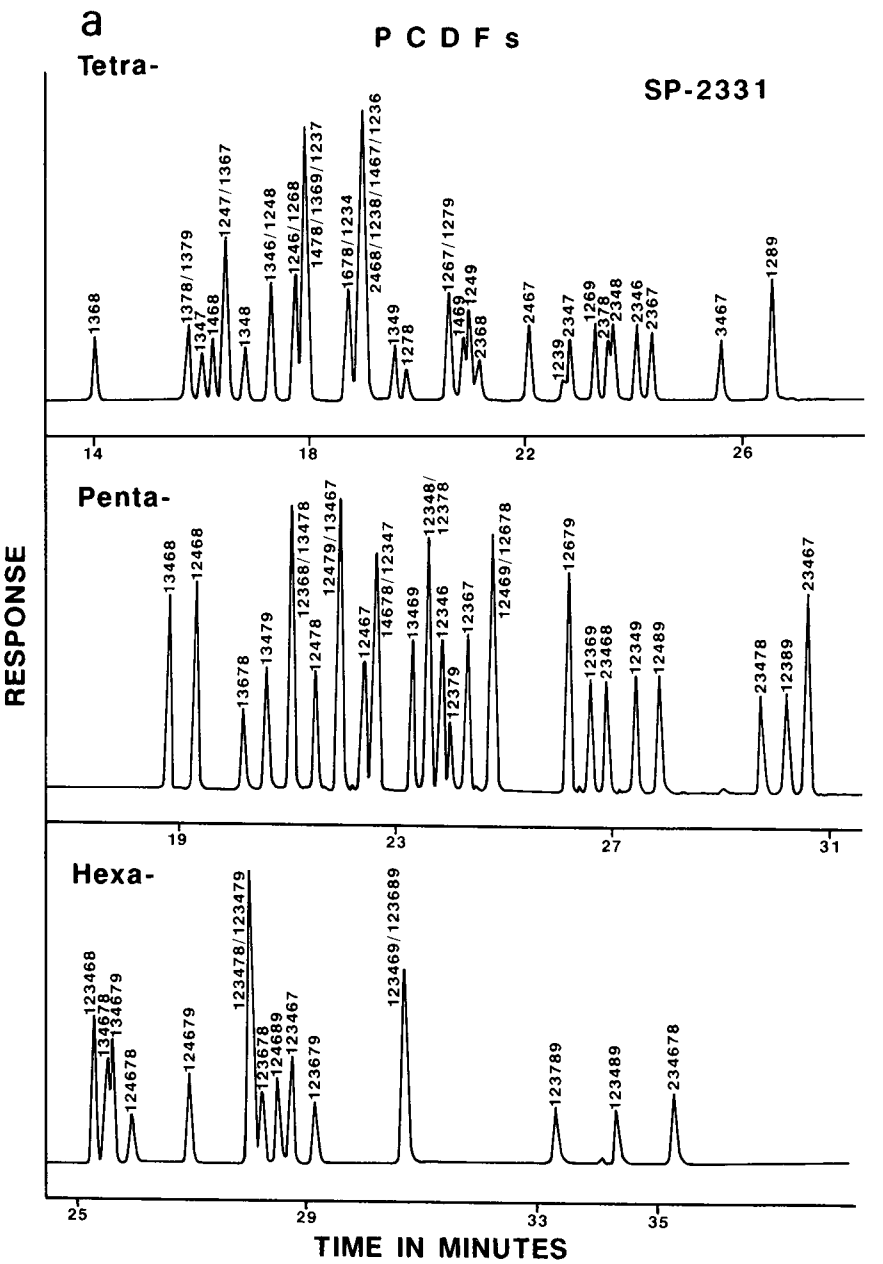
a
PCDFs
SP-2331
Tetra-
1368
1378/1379
1347
1468
1247/1367
1348
1346/1248
1246/1268
1478/1369/1237
1678/1234
2468/1238/1467/1236
1349
1278
1267/1279
1469
1249
2368
2467
1239
2347
1269
2378
2348
2346
2367
3467
1289
14
18
22
26
Penta-
13468
12468
13678
13479
12368/13478
12478
12479/13467
12467
14678/12347
13469
12348/
12378
12346
12379
12367
12469/12678
12679
12369
23468
12349
12489
23478
12389
23467
19
23
27
31
Hexa-
123468
134678
134679
124678
124679
123478/123479
123678
124689
123467
123679
123469/123689
123789
123489
234678
25
29
33
35
RESPONSE
TIME IN MINUTES

Fig. 8.

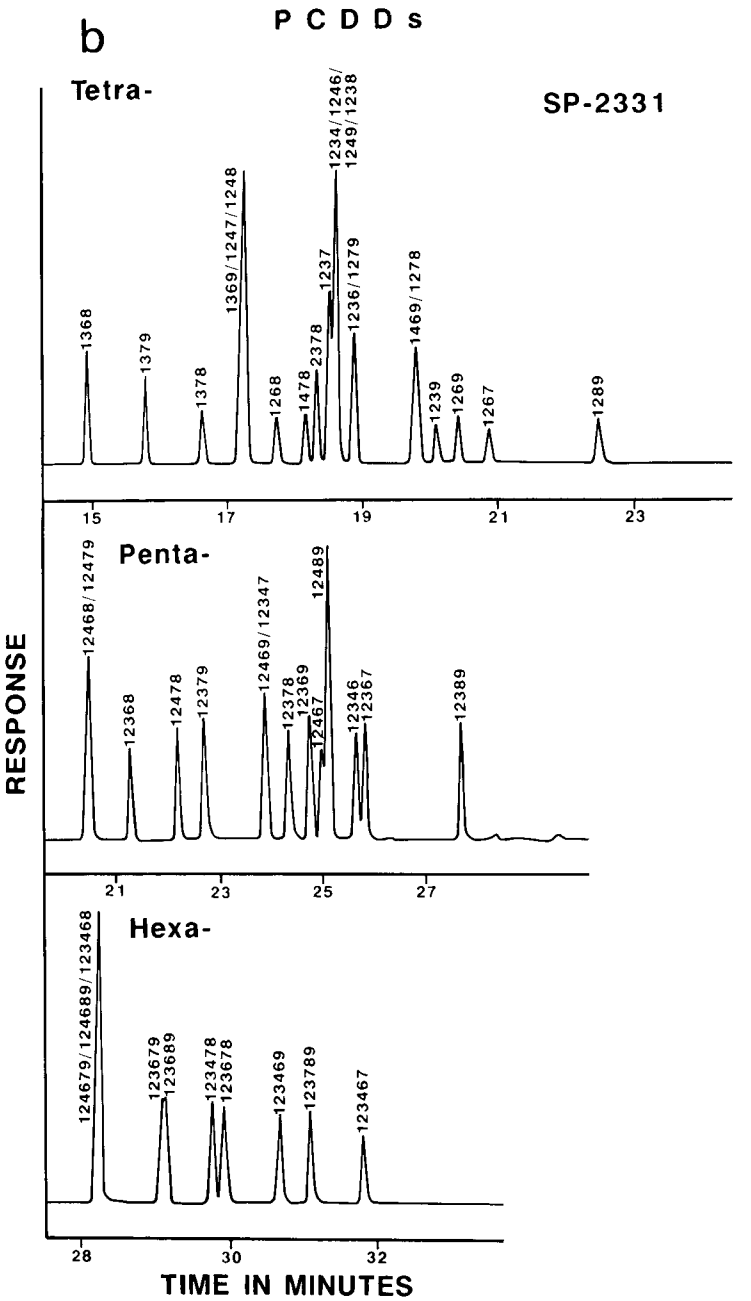

Fig. 8. (a) GC–ECD tracing of the separation of 38 TCDFs, 28 PnCDFs, and 16 HxCDFs on a SP-2331 fused-silica capillary column. (b) GC–ECD tracing of the separation of 22 TCDDs, 14 PnCDDs, and 10 HxCDDs on a SP-2331 fused-silica capillary column.

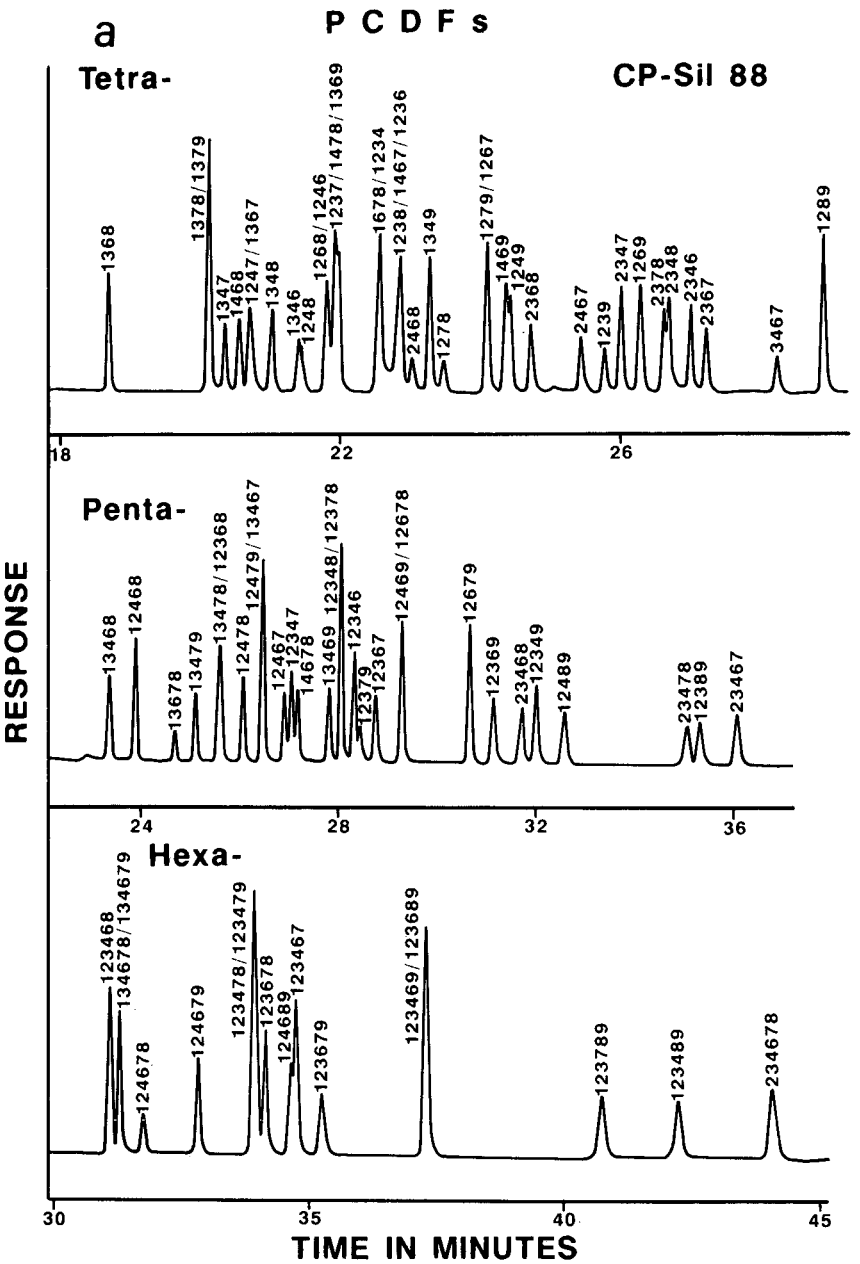
a
P C D F s
Tetra-
CP-Sil 88
1368
1378/1379
1347
1468
1247/1367
1348
1346
1248
1268/1246
1237/1478/1369
1678/1234
1238/1467/1236
1349
2468
1278
1279/1267
1469
1249
2368
2467
1239
2347
1269
2378
2348
2346
2367
3467
1289
18
22
26
Penta-
13468
12468
13678
13479
13478/12368
12478
12479/13467
12467
12347
14678
13469
12348/12378
12346
12379
12367
12469/12678
12679
12369
23468
12349
12489
23478
12389
23467
24
28
32
36
Hexa-
123468
134678/134679
124678
124679
123478/123479
123678
124689
123467
123679
123469/123689
123789
123489
234678
30
35
40
45
RESPONSE
TIME IN MINUTES

Fig. 9.

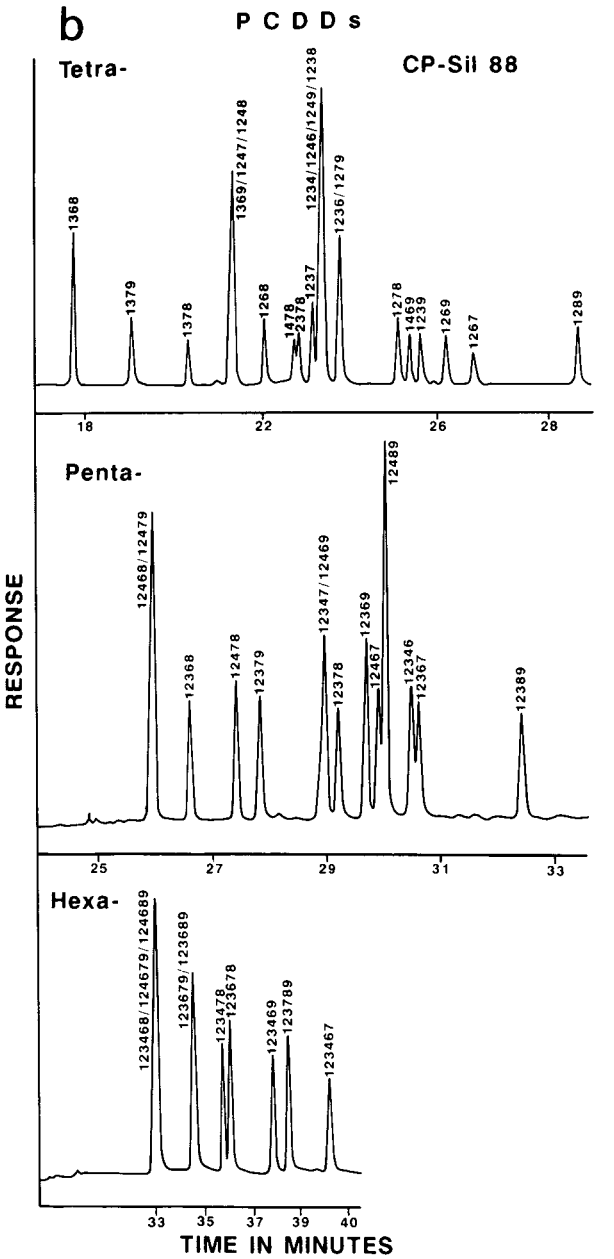

Fig. 9. (a) GC–ECD tracing of the separation of 38 TCDFs, 28 PnCDFs, and 16 HxCDFs on a CP-Sil 88 fused-silica capillary column. (b) GC–ECD tracing of the separation of 22 TCDDs, 14 PnCDDs, and 10 HxCDDs on a CP-Sil 88 fused-silica capillary column.

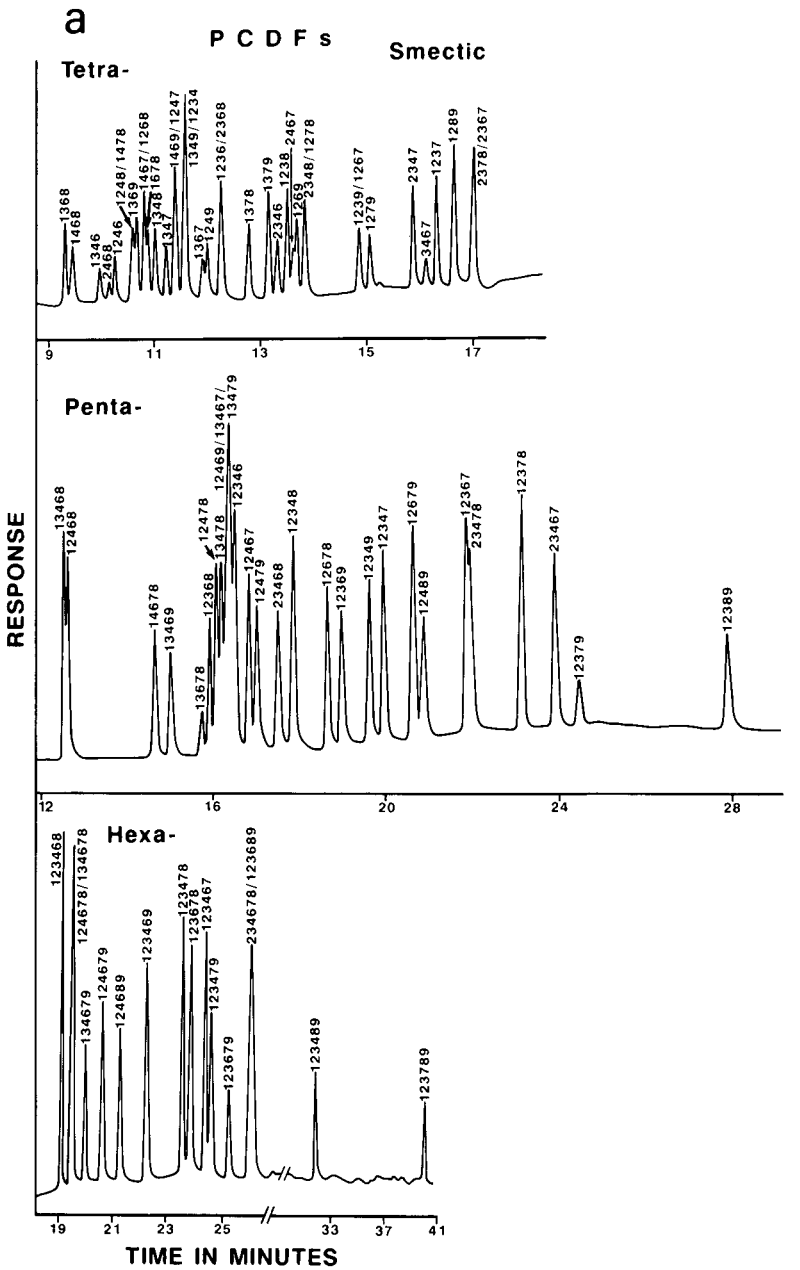
a
PCDFs
Smectic
Tetra-
1368
1468
1346
2468
1248/1478
1246
1369
1467/1268
1348
1678
1469/1247
1349/1234
1367
1249
1236/2368
1378
1379
2346
1238
2467
1269
2348/1278
1239/1267
1279
2347
3467
1237
1289
2378/2367
9
11
13
15
17
Penta-
RESPONSE
13468
12468
14678
13469
13678
12368
12478
13478
12469/13467/
13479
12346
12467
12479
23468
12348
12678
12369
12349
12347
12679
12489
12367
23478
12378
23467
12379
12389
12
16
20
24
28
Hexa-
123468
124678/134678
134679
124679
124689
123469
123478
123678
123467
123479
123679
234678/123689
123489
123789
19
21
23
25
33
37
41
TIME IN MINUTES

Fig. 10.

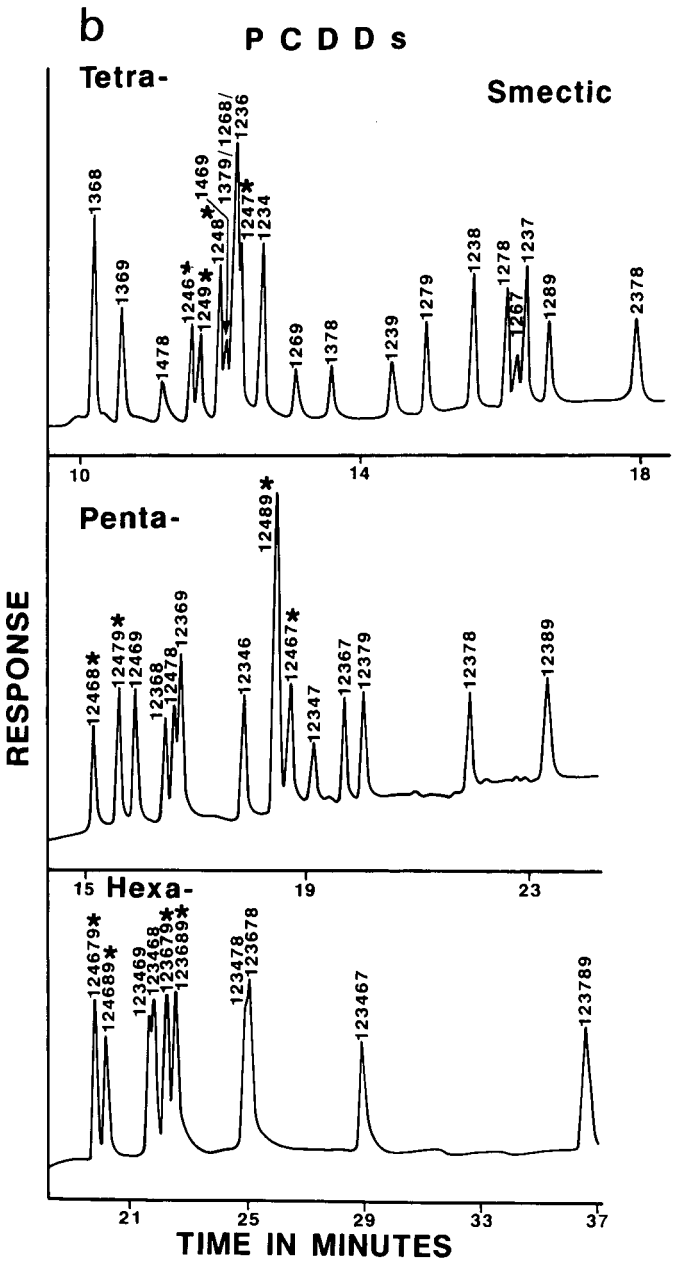

Fig. 10. (a) GC–ECD tracing of the separation of 38 TCDFs, 28 PnCDFs, and 16 HxCDFs on a liquid crystalline smectic fused-silica capillary column. (b) GC–ECD tracing of the separation of 22 TCDDs, 14 PnCDDs, and 10 HxCDDs on a liquid crystalline smectic fused-silica capillary column; congeners marked with an asterisk are pairs which cannot be unequivocably assigned (*cf.* text.).

TABLE V

GC RETENTION TIMES OF PCDF/PCDD ISOMERS RELATIVE TO RT REFERENCE STANDARDS ON A DB-1 FUSED-SILICA BONDED PHASE CAPILLARY COLUMN

Elution order	Isomer	RRT	Elution order	Isomer	RRT
TCDF[a]					
1	1368	1.000	20	1469	1.091
2	1468	1.016	21	1238	1.091
3	2468	1.023	22	1236	1.091
4	1247	1.041	23	1678	1.099
5	1347	1.041	24	1234	1.099
6	1378	1.041	25	1278	1.105
7	1346	1.041	26	1349	1.111
8	1246	1.041	27	1267	1.111
9	1348	1.051	28	2347	1.122
10	1367	1.051	29	2348	1.122
11	1248	1.051	30	1249	1.122
12	1379	1.051	31	1279	1.122
13	1268	1.062	32	2346	1.122
14	1467	1.068	33	2378	1.122
15	1478	1.068	34	2367	1.138
16	2368	1.078	35	1269	1.147
17	1237	1.078	36	3467	1.147
18	1369	1.078	37	1239	1.162
19	2467	1.082	38	1289	1.198
–	13468-PnCDF	1.232	–	123468-HxCDF	1.513
–	1368-TCDD	1.056			
PnCDF[b]					
1	13468	1.000	15	12346	1.074
2	12468	1.000	16	12347	1.074
3	13678	1.048	17	12348	1.082
4	13467	1.048	18	12378	1.087
5	12368	1.048	19	12367	1.093
6	13478	1.048	20	12678	1.099
7	12478	1.048	21	12379	1.099
8	12467	1.048	22	23478	1.116
9	13479	1.056	23	12679	1.116
10	14678	1.056	24	23467	1.121
11	12479	1.063	25	12369	1.121
12	13469	1.063	26	12489	1.125
13	23468	1.067	27	12349	1.142
14	12469	1.071	28	12389	1.164
HxCDF[c]					
1	123468	1.000	9	123678	1.048
2	134678	1.007	10	123479	1.053
3	124678	1.007	11	123469	1.060
4	134679	1.013	12	123679	1.060
5	124679	1.018	13	234678	1.067
6	124689	1.024	14	123689	1.067
7	123467	1.042	15	123789	1.102
8	123478	1.043	16	123489	1.105

TABLE V *(continued)*

Elution order	Isomer	RRT	Elution order	Isomer	RRT
TCDD[d]					
1	1368	1.000	12	1279	1.075
2	1379	1.012	13	1269	1.084
3	1369	1.021	14	1236	1.091
4	1469	1.043	15	1237	1.096
5	1247	1.050	16	1234	1.096
6	1248	1.050	17	1238	1.096
7	1378	1.054	18	2378	1.103
8	1246	1.054	19	1239	1.107
9	1249	1.054	20	1278	1.114
10	1268	1.058	21	1267	1.118
11	1478	1.064	22	1289	1.142
–	12468-PnCDD	1.233	–	124679-HxCDD	1.469
–	1368-TCDF	0.947			
PnCDD[e]					
1	12468	1.000	8	12467	1.054
2	12479	1.000	9	12489	1.054
3	12469	1.018	10	12347	1.067
4	12368	1.032	11	12346	1.072
5	12478	1.038	12	12378	1.080
6	12379	1.045	13	12367	1.084
7	12369	1.052	14	12389	1.100
HxCDD[f]					
1	124679	1.000	6	123469	1.037
2	124689	1.000	7	123478	1.054
3	123468	1.021	8	123678	1.057
4	123679	1.030	9	123467	1.069
5	123689	1.030	10	123789	1.069

[a] RT reference standard is 1368-TCDF.
[b] RT reference standard is 13468-PnCDF.
[c] RT reference standard is 123468-HxCDF.
[d] RT reference standard is 1368-TCDD.
[e] RT reference standard is 12468-PnCDD.
[f] RT reference standard is 124679-HxCDD.

some of the elution orders. In this respect Riehle *et al.* [37] have noticed that the retention times and even relative elution orders of the PCDDs/PCDFs on various smectic columns changed according to the thermal history of the column. This enigmatic property of the smectic phase may explain the different reported elution orders.

Thus for any sample containing mixtures of PCDDs and PCDFs, it is possible to assign the exact isomeric configuration of any peak except the six pairs noted provided two or more GC columns are used. For samples such as fly ash, waste material or PCB extracts, many congeners will be present and probably more than two GC columns would be necessary for detailed specific identification. This data would also be useful in the selection of stationary phases for use in dual or multi-dimensional GC [21,55].

TABLE VI

GC RETENTION TIMES OF PCDF/PCDD ISOMERS RELATIVE TO RT REFERENCE STANDARDS ON A DB-5 FUSED-SILICA BONDED PHASE CAPILLARY COLUMN

Reference standards as in Table V.

Elution order	Isomer	RRT	Elution order	Isomer	RRT
TCDF					
1	1368	1.000	20	1238	1.122
2	1468	1.025	21	1236	1.122
3	2468	1.040	22	1469	1.122
4	1247	1.053	23	1678	1.122
5	1347	1.053	24	1234	1.122
6	1378	1.053	25	1278	1.139
7	1346	1.053	26	1349	1.151
8	1246	1.053	27	1267	1.151
9	1367	1.069	28	2348	1.168
10	1348	1.069	29	2378	1.168
11	1379	1.069	30	2347	1.168
12	1248	1.069	31	2346	1.168
13	1268	1.090	32	1249	1.168
14	1467	1.090	33	1279	1.168
15	1478	1.090	34	2367	1.193
16	1369	1.102	35	3467	1.205
17	1237	1.102	36	1269	1.205
18	2368	1.109	37	1239	1.214
19	2467	1.122	38	1289	1.271
–	13468-PnCDF	1.298	–	123468-HxCDF	1.667
–	1368-TCDD	1.073			
PnCDF					
1	13468	1.000	15	12347	1.093
2	12468	1.000	16	12346	1.093
3	13678	1.053	17	12348	1.107
4	12368	1.061	18	12378	1.110
5	12478	1.061	19	12367	1.120
6	13467	1.061	20	12678	1.129
7	13478	1.061	21	12379	1.129
8	12467	1.061	22	23478	1.156
9	13479	1.070	23	12489	1.156
10	14678	1.070	24	12679	1.156
11	12479	1.080	25	12369	1.156
12	13469	1.082	26	23467	1.167
13	23468	1.093	27	12349	1.182
14	12469	1.093	28	12389	1.216
HxCDF					
1	123468	1.000	9	123678	1.061
2	134678	1.008	10	123479	1.066
3	124678	1.008	11	123469	1.078
4	134679	1.016	12	123679	1.078
5	124679	1.024	13	123689	1.088
6	124689	1.034	14	234678	1.095
7	123467	1.052	15	123789	1.133
8	123478	1.056	16	123489	1.138

TABLE VI *(continued)*

Elution order	Isomer	RRT	Elution order	Isomer	RRT
TCDD					
1	1368	1.000	12	1279	1.102
2	1379	1.016	13	1234	1.120
3	1369	1.032	14	1236	1.120
4	1247	1.066	15	1269	1.120
5	1248	1.066	16	1237	1.126
6	1378	1.066	17	1238	1.126
7	1469	1.066	18	2378	1.131
8	1246	1.075	19	1239	1.139
9	1249	1.075	20	1278	1.152
10	1268	1.083	21	1267	1.166
11	1478	1.088	22	1289	1.191
–	12468-PnCDD	1.298	–	124679-HxCDD	1.603
–	1368-TCDF	0.932			
PnCDD					
1	12468	1.000	8	12467	1.073
2	12479	1.000	9	12489	1.073
3	12469	1.025	10	12347	1.085
4	12368	1.041	11	12346	1.090
5	12478	1.049	12	12378	1.103
6	12379	1.057	13	12367	1.112
7	12369	1.068	14	12389	1.130
HxCDD					
1	124679	1.000	6	123469	1.045
2	124689	1.000	7	123478	1.070
3	123468	1.026	8	123678	1.075
4	123679	1.039	9	123467	1.090
5	123689	1.039	10	123789	1.090

Comparison to published reports

The data generated in this report is a confirmation of much previous work and agrees in all respects with that reported in the literature except for the following.

TCDDs. Taylor *et al.* [23] of Wright State University noted a difference between their work and two earlier reports [10,11] in the elution order of three TCDDs, 1268-, 1278- and 1279-TCDD, on both a DB-5 and SP-2331 columns and were unable to distinguish the correct elution order. Subsequently Gurka *et al.* [56], Gelbaum *et al.* [30] and Donnelly *et al.* [34] all investigated these elution orders and agreed with the elution order of Buser and Rappe [11]. We also find the same elution order as did Buser and Rappe [11]. Harden *et al.* [40] reported further separations of all 22 TCDDs and all 38 TCDFs on 4 additional GC phases including 3 in this report (DB-225, SP-2401 equivalent to DB-210, and SP-2250 equivalent to DB-17). While we are in complete agreement with their TCDF assignments, we differ markedly for those on the 1268-, 1278-, and 1279-TCDD isomers and suspect they may have used the earlier Dow assignment [10] rather than that of Buser and Rappe [11] which we and others believe to be correct.

TABLE VII

GC RETENTION TIMES OF PCDF/PCDD ISOMERS RELATIVE TO RT REFERENCE STANDARDS ON A DB-17 FUSED-SILICA BONDED PHASE CAPILLARY COLUMN

Reference standards as in Table V.

Elution order	Isomer	RRT	Elution order	Isomer	RRT
TCDF					
1	1368	1.000	20	1678	1.156
2	1468	1.056	21	1236	1.156
3	2468	1.056	22	1234	1.156
4	1378	1.056	23	1278	1.156
5	1347	1.056	24	2467	1.163
6	1247	1.063	25	2378	1.180
7	1367	1.074	26	2347	1.189
8	1379	1.078	27	1469	1.189
9	1346	1.089	28	2348	1.196
10	1248	1.103	29	1349	1.202
11	1348	1.105	30	1279	1.205
12	1246	1.105	31	1267	1.205
13	1478	1.109	32	2346	1.205
14	1237	1.118	33	1249	1.217
15	2368	1.118	34	2367	1.228
16	1268	1.124	35	3467	1.250
17	1467	1.124	36	1239	1.256
18	1369	1.134	37	1269	1.278
19	1238	1.114	38	1289	1.336
–	13468-PnCDF	1.235	–	123468-HxCDF	1.493
–	1368-TCDD	1.053			
PnCDF					
1	12468	1.000	15	12346	1.101
2	13468	1.000	16	12378	1.103
3	13678	1.039	17	12348	1.114
4	12368	1.052	18	12469	1.117
5	12478	1.052	19	12367	1.122
6	13478	1.055	20	12379	1.130
7	13467	1.058	21	12678	1.138
8	13479	1.063	22	23478	1.155
9	12467	1.067	23	12369	1.169
10	14678	1.072	24	12679	1.180
11	12479	1.079	25	23467	1.180
12	12347	1.082	26	12489	1.197
13	23468	1.095	27	12349	1.197
14	13469	1.098	28	12389	1.233
HxCDF					
1	123468	1.000	9	123678	1.055
2	124678	1.007	10	123479	1.064
3	134678	1.007	11	123679	1.082
4	134679	1.018	12	123469	1.085
5	124679	1.033	13	123689	1.093
6	124689	1.047	14	234678	1.097
7	123478	1.050	15	123789	1.139
8	123467	1.052	16	123489	1.154

TABLE VII *(continued)*

Elution order	Isomer	RRT	Elution order	Isomer	RRT
TCDD					
1	1368	1.00	12	2378	1.123
2	1379	1.024	13	1279	1.129
3	1369	1.059	14	1237	1.134
4	1378	1.064	15	1238	1.134
5	1247	1.084	16	1234	1.136
6	1248	1.084	17	1236	1.142
7	1478	1.104	18	1239	1.161
8	1268	1.104	19	1269	1.164
9	1246	1.109	20	1278	1.164
10	1249	1.109	21	1267	1.210
11	1469	1.123	22	1289	1.223
–	12468-PnCDD	1.235	–	124679-HxCDD	1.450
–	1368-TCDF	0.950			
PnCDD					
1	12468	1.000	8	12347	1.079
2	12479	1.000	9	12467	1.089
3	12368	1.034	10	12489	1.089
4	12469	1.042	11	12378	1.095
5	12478	1.042	12	12346	1.100
6	12379	1.045	13	12367	1.124
7	12369	1.052	14	12389	1.139
HxCDD					
1	124679	1.000	6	123469	1.049
2	124689	1.000	7	123478	1.064
3	123468	1.018	8	123678	1.072
4	123679	1.037	9	123789	1.086
5	123689	1.037	10	123467	1.094

With regard to the isomer pair, 1246/1249-TCDD, we readily separate them on HPLC using an ODS packing and a 5% water in methanol eluent, but O'Keefe *et al.* [14], Taylor *et al.* [23] and Wagel *et al.* [57] all reported no such separation. Moreover, we are unable to separate these two isomers on the polar CP-Sil 88 phase even though both Zoller and Ballschmiter [32] and Gelbaum *et al.* [30] achieved a small separation on that column. There is some degree of separation (20–30%) for this pair of TCDD isomers on the CPS-1 and DB-210 columns and a clear resolution on the liquid crystalline smectic.

The isomer pairs, 1237/1238-TCDD, from the Smiles rearrangement are not easy to separate and even more difficult to assign their structures using conventional means. We are unable to obtain significant GC separations of this pair on the first four GC phases listed in Table IV but do obtain almost 100% resolution on the other five phases (four of them being cyanopropyl and one the smectic). Because of our photolytic experiments with 12389-PnCDD and 12367-PnCDD, we assign 1237-TCDD and 1238-TCDD as the earlier and later eluters, respectively, on the cyanopropyl GC phases. On the other hand, the elution order on the smectic phase and

TABLE VIII

GC RETENTION TIMES OF PCDF/PCCD ISOMERS RELATIVE TO RT REFERENCE STANDARDS ON A DB-210 FUSED-SILICA BONDED PHASE CAPILLARY COLUMN

Reference standards as in Table V.

Elution order	Isomer	RRT	Elution order	Isomer	RRT
TCDF					
1	1368	1.000	20	1238	1.212
2	1468	1.077	21	1678	1.212
3	1347	1.086	22	1349	1.233
4	1247	1.095	23	2368	1.245
5	1378	1.095	24	1469	1.245
6	1379	1.095	25	1278	1.256
7	1367	1.106	26	1267	1.269
8	1346	1.118	27	1249	1.285
9	1348	1.118	28	1279	1.299
10	1246	1.128	29	2467	1.299
11	1248	1.128	30	2347	1.342
12	2468	1.149	31	2348	1.342
13	1369	1.158	32	2378	1.355
14	1478	1.158	33	1269	1.375
15	1268	1.158	34	1239	1.375
16	1237	1.167	35	2346	1.375
17	1234	1.180	36	2367	1.401
18	1467	1.180	37	3467	1.461
19	1236	1.199	38	1289	1.530
–	13468-PnCDF	1.381	–	123468-HxCDF	1.858
–	1368-TCDD	1.084			
PnCDF					
1	13468	1.000	15	12348	1.151
2	12468	1.005	16	12469	1.160
3	13678	1.070	17	12378	1.178
4	13479	1.070	18	12367	1.178
5	12368	1.081	19	12678	1.180
6	13478	1.092	20	12379	1.202
7	12478	1.092	21	23468	1.205
8	13467	1.100	22	12679	1.239
9	12467	1.103	23	12369	1.239
10	12479	1.103	24	12349	1.271
11	14678	1.121	25	12489	1.281
12	12347	1.121	26	23478	1.304
13	13469	1.121	27	23467	1.338
14	12346	1.142	28	12389	1.376
HxCDF					
1	123468	1.000	9	123479	1.085
2	134679	1.009	10	123678	1.092
3	134678	1.018	11	123679	1.113
4	124678	1.018	12	123469	1.118
5	124679	1.036	13	123689	1.143
6	124689	1.067	14	234678	1.206
7	123478	1.085	15	123489	1.226
8	123467	1.085	16	123789	1.226

TABLE VIII *(continued)*

Elution order	Isomer	RRT	Elution order	Isomer	RRT
TCDD					
1	1368	1.000	12	1469	1.196
2	1379	1.053	13	1236	1.205
3	1369	1.087	14	1237	1.209
4	1247	1.109	15	1279	1.211
5	1248	1.109	16	1238	1.211
6	1378	1.120	17	2378	1.237
7	1268	1.139	18	1269	1.241
8	1246	1.154	19	1239	1.266
9	1249	1.158	20	1278	1.273
10	1234	1.166	21	1267	1.287
11	1478	1.182	22	1289	1.383
–	12468-PnCDD	1.415	–	124679-HxCDD	1.840
–	1368-TCDF	0.923			
PnCDD					
1	12468	1.000	8	12369	1.113
2	12479	1.000	9	12467	1.122
3	12368	1.048	10	12489	1.122
4	12469	1.061	11	12346	1.133
5	12478	1.069	12	12378	1.156
6	12379	1.095	13	12367	1.164
7	12347	1.102	14	12389	1.225
HxCDD					
1	124679	1.000	6	123469	1.068
2	124689	1.000	7	123478	1.089
3	123468	1.024	8	123678	1.098
4	123679	1.052	9	123467	1.123
5	123689	1.052	10	123789	1.139

on RP-HPLC is reversed *i.e.* 1238-TCDD first followed by 1237-TCDD. In this regard we do not agree with the separations of Brown *et al.* [44] on DB-225 for 1234-, 1237- and 1238-TCDD. However column differences may account for some of this incompatability. Lastly, in this report and that of Buser and Rappe [17], the elution of 1239-TCDD on OV-1 is subsequent to that of 2378-TCDD whereas it was given by Oehme and Kirschmer [18] as preceding 2378-TCDD.

PnCDDs and HxCDDs. We can find no significant differences that have not already been noticed between our results and those reported previously for the above two homologues.

TCDFs. The early pioneering work by Mazer and co-workers [15,16] on this homologue and by Bell and Gara [22] on all PCDFs resulted in a comprehensive data base on their GC properties on methyl silicone (SE-54 equivalent to DB-5) and the SP-2330 phase (cyanopropyl). Mazer *et al.* [15] made two corrections to their list (ref. 15, p. 1648), one for 1236-TCDF on SE-54 and one for 2368-TCDF on SP-2330, both of which we are in agreement. Bell and Gara [22] also reported for the 1246-TCDF

TABLE IX

GC RETENTION TIMES OF PCDF/PCDD ISOMERS RELATIVE TO RT REFERENCE STANDARDS ON A DB-225 FUSED SILICA BONDED PHASE CAPILLARY COLUMN

Reference standards as in Table V.

Elution order	Isomer	RRT	Elution order	Isomer	RRT
TCDF					
1	1368	1.000	20	1678	1.207
2	1378	1.073	21	1236	1.207
3	1379	1.078	22	1278	1.235
4	1347	1.084	23	1349	1.242
5	1247	1.095	24	2368	1.261
6	1468	1.095	25	1279	1.271
7	1367	1.106	26	1267	1.271
8	1348	1.128	27	1469	1.275
9	1346	1.139	28	1249	1.287
10	1248	1.142	29	2467	1.305
11	1246	1.154	30	2347	1.331
12	1237	1.154	31	2378	1.342
13	1268	1.164	32	1239	1.347
14	1478	1.164	33	2348	1.357
15	1369	1.170	34	1269	1.369
16	2468	1.183	35	2346	1.377
17	1238	1.202	36	2367	1.384
18	1467	1.202	37	3467	1.435
19	1234	1.202	38	1289	1.475
–	13468-PnCDF	1.298	–	123468-HxCDF	1.642
–	1368-TCDD	1.065			
PnCDF					
1	13468	1.000	15	12348	1.139
2	12468	1.009	16	12346	1.139
3	13678	1.044	17	12379	1.148
4	13479	1.058	18	12367	1.153
5	12368	1.065	19	12469	1.161
6	13478	1.065	20	12678	1.173
7	12478	1.073	21	23468	1.203
8	13467	1.089	22	12679	1.212
9	12479	1.089	23	12369	1.212
10	12467	1.097	24	12349	1.248
11	12347	1.105	25	12489	1.248
12	14678	1.110	26	23478	1.282
13	13469	1.128	27	23467	1.317
14	12378	1.131	28	12389	1.317
HxCDF					
1	123468	1.000	9	123678	1.081
2	134678	1.010	10	123467	1.093
3	124678	1.015	11	123679	1.112
4	134679	1.015	12	123689	1.152
5	124679	1.043	13	123469	1.152
6	123478	1.073	14	123789	1.240
7	124689	1.081	15	234678	1.282
8	123479	1.081	16	123489	1.282

TABLE IX *(continued)*

Elution order	Isomer	RRT	Elution order	Isomer	RRT
TCDD					
1	1368	1.000	12	1237	1.178
2	1379	1.039	13	1238	1.184
3	1378	1.086	14	1234	1.184
4	1369	1.105	15	1279	1.189
5	1247	1.117	16	1236	1.196
6	1248	1.117	17	1469	1.215
7	1268	1.142	18	1278	1.234
8	1478	1.157	19	1239	1.244
9	2378	1.164	20	1269	1.254
10	1246	1.171	21	1267	1.286
11	1249	1.175	22	1289	1.346
–	12468-PnCDD	1.314	–	124679-HxCDD	1.639
–	1368-TCDF	0.939			
PnCDD					
1	12468	1.000	8	12369	1.104
2	12479	1.000	9	12378	1.105
3	12368	1.028	10	12467	1.115
4	12478	1.048	11	12489	1.115
5	12379	1.059	12	12346	1.130
6	12469	1.077	13	12367	1.141
7	12347	1.093	14	12389	1.184
HxCDD					
1	124679	1.000	6	123478	1.072
2	124689	1.000	7	123678	1.081
3	123468	1.009	8	123469	1.091
4	123679	1.040	9	123789	1.122
5	123689	1.040	10	123467	1.151

isomer an RRT on DB-5 greater than that of 2378-TCDF which is different from this report and ref. 15 and probably incorrect.

For the close eluting isomer pair 1349/1267-TCDF, Waddell *et al.* [35] reported an RRT on DB-5 slightly later than 2378-TCDF whereas all other work including this one find an RRT slightly earlier than 2378-TCDF on this non-polar phase. Whether this difference is due to variation in phase type, GC conditions or other factors is not certain. All of the above groups report the same RRT for these isomers on SP-2330.

Ligon and May [21] gave separations on Silar 10C, a 100% cyanopropyl phase similar to CP-Sil 88. Those shown for 1249- and 2468-TCDF, for 1269-TCDF (after 2378-TCDF), and 2346/2367-TCDF (reversed in ref. 21) all differ significantly from other work including the present one on the equivalent phase, CP-Sil 88. Separations reported by all groups for the other homologues of the PCDFs are the same for the two types of cyanopropyl columns. Whether the differences for the TCDFs are due to manufacturing processes or misidentification is not clear.

Recently, the US EPA [58] reported an isomer specific separation on a DB-225 phase of 2378-TCDF from all other TCDFs including the near elutors, 2347-TCDF

TABLE X

GC RETENTION TIMES OF PCDF/PCCD ISOMERS RELATIVE TO RT REFERENCE STANDARDS ON A CPS-1 FUSED-SILICA CAPILLARY COLUMN

Reference standards as in Table V.

Elution order	Isomer	RRT	Elution order	Isomer	RRT
TCDF					
1	1368	1.000			
2	1378	1.086	20	1236	1.239
3	1379	1.086	21	2468	1.239
4	1347	1.097	22	1349	1.267
5	1468	1.111	23	1278	1.286
6	1247	1.111	24	1279	1.321
7	1367	1.124	25	1267	1.321
8	1348	1.139	26	1469	1.322
9	1346	1.157	27	1249	1.325
10	1248	1.157	28	2368	1.345
11	1246	1.174	29	2467	1.394
12	1237	1.188	30	1239	1.410
13	1268	1.188	31	2347	1.428
14	1369	1.188	32	1269	1.437
15	1478	1.188	33	2378	1.456
16	1234	1.220	34	2348	1.459
17	1678	1.220	35	2346	1.482
18	1238	1.239	36	2367	1.499
19	1467	1.239	37	3467	1.566
–	13468-PnCDF	1.316	38	1289	1.586
–	1368-TCDD	1.047	–	123468-HxCDF	1.719
PnCDF					
1	13468	1.000	15	12378	1.176
2	12468	1.014	16	12346	1.176
3	13678	1.055	17	12379	1.188
4	13479	1.065	18	12367	1.205
5	12368	1.085	19	12469	1.205
6	13478	1.085	20	12678	1.222
7	12478	1.099	21	12679	1.263
8	12479	1.109	22	12369	1.275
9	13467	1.118	23	23468	1.296
10	12467	1.130	24	12349	1.304
11	12347	1.134	25	12489	1.319
12	14678	1.144	26	23478	1.408
13	13469	1.159	27	12389	1.415
14	12348	1.171	28	23467	1.450
HxCDF					
1	123468	1.000	9	123678	1.103
2	134678	1.013	10	123467	1.119
3	134679	1.013	11	123679	1.131
4	124678	1.024	12	123469	1.183
5	124679	1.050	13	123689	1.183
6	123478	1.091	14	123789	1.295
7	123479	1.091	15	123489	1.332
8	124689	1.096	16	234678	1.399

TABLE X *(continued)*

Elution order	Isomer	RRT	Elution order	Isomer	RRT
TCDD					
1	1368	1.000	12	2378	1.215
2	1379	1.054	13	1237	1.215
3	1378	1.109	14	1238	1.220
4	1369	1.132	15	1236	1.228
5	1247	1.140	16	1279	1.241
6	1248	1.140	17	1469	1.279
7	1268	1.171	18	1278	1.295
8	1478	1.192	19	1239	1.308
9	1246	1.204	20	1269	1.323
10	1234	1.211	21	1267	1.456
11	1249	1.215	22	1289	1.605
–	12468-PnCDD	1.379	–	124679-HxCDD	1.791
–	1368-TCDF	0.955			
PnCDD					
1	12468	1.000	8	12378	1.136
2	12479	1.000	9	12369	1.146
3	12368	1.031	10	12489	1.150
4	12478	1.058	11	12467	1.150
5	12379	1.080	12	12346	1.163
6	12469	1.104	13	12367	1.176
7	12347	1.113	14	12389	1.242
HxCDD					
1	123468	1.000	6	123478	1.075
2	124679	1.000	7	123678	1.085
3	124689	1.000	8	123469	1.110
4	123679	1.044	9	123789	1.148
5	123689	1.044	10	123467	1.175

(earlier) and 1239-TCDF (later). Both this work and that of Harden *et al.* [40] find the same elution order as above but the resolution between 2378-TCDF and 1239-TCDF is small. Again this difference may be affected by injection techniques, temperature programming or even slight variation in the phases themselves.

PnCDFs. The earliest complete collection of data for this homologue is that of Rappe [19] followed by Bell and Gara [22] both on the polar phase SP-2330. For the isomers, 13479- and 13478-PnCDF, the elution order given by Bell and Gara [22] is as written above while that of Rappe [19] is reversed. We agree with Bell and Gara [22] for both the SP-2330 and CP-Sil 88 phases *i.e.* 13479-PnCDF elutes before 13478-PnCDF and the latter co-elutes with 12368-PnCDF. Similarly, Bell and Gara [22] found that the isomer 12678-PnCDF (equivalent to 23489-) co-eluted with 12469-PnCDF followed much later by 23468-PnCDF. Rappe [19] has the elution order 23468- and 12678-PnCDF —we concur with the 1985 data [22]. The elution order given by Rappe [19] for the above pentafuran isomers has been used for structure assignment by Zoller and Ballschmiter [32] in chlorophenol pyrolysates, by Abraham *et al.* [59] in a rat study, by Wakimoto *et al.* [60] in determination of PCDFs in PCBs, and by Oehme *et*

TABLE XI

GC RETENTION TIMES OF PCDF/PCCD ISOMERS RELATIVE TO RT REPRENCE STANDARDS ON A SP-2331 FUSED-SILICA CAPILLARY COLUMN

Reference standards as in Table V.

Elution order	Isomer	RRT	Elution order	Isomer	RRT
TCDF					
1	1368	1.000	20	1467	1.330
2	1378	1.115	21	1236	1.330
3	1379	1.115	22	1349	1.371
4	1347	1.133	23	1278	1.383
5	1468	1.149	24	1267	1.435
6	1247	1.163	25	1279	1.435
7	1367	1.163	26	1469	1.457
8	1348	1.187	27	1249	1.461
9	1346	1.218	28	2368	1.473
10	1248	1.218	29	2467	1.533
11	1246	1.250	30	1239	1.576
12	1268	1.250	31	2347	1.582
13	1478	1.256	32	1269	1.616
14	1369	1.256	33	2378	1.633
15	1237	1.256	34	2348	1.639
16	1678	1.312	35	2346	1.667
17	1234	1.312	36	2367	1.685
18	2468	1.330	37	3467	1.770
19	1238	1.330	38	1289	1.835
–	13468-PnCDF	1.356	–	123468-HxCDF	1.845
–	1368-TCDF	1.062			
PnCDF					
1	13468	1.000	15	12378	1.240
2	12468	1.026	16	12346	1.249
3	13678	1.070	17	12379	1.262
4	13479	1.091	18	12367	1.277
5	12368	1.114	19	12469	1.300
6	13478	1.114	20	12678	1.300
7	12478	1.137	21	12679	1.368
8	12479	1.158	22	12369	1.389
9	13467	1.158	23	23468	1.405
10	12467	1.181	24	12349	1.432
11	14678	1.192	25	12489	1.453
12	12347	1.192	26	23478	1.546
13	13469	1.225	27	12389	1.569
14	12348	1.240	28	23467	1.593
HxCDF					
1	123468	1.000	9	124689	1.123
2	134678	1.009	10	123467	1.131
3	134679	1.012	11	123679	1.148
4	124678	1.026	12	123469	1.206
5	124679	1.064	13	123689	1.206
6	123478	1.105	14	123789	1.308
7	123479	1.105	15	123489	1.347
8	123678	1.114	16	234678	1.385

TABLE XI *(continued)*

Elution order	Isomer	RRT	Elution order	Isomer	RRT
TCDD					
1	1368	1.000	12	1246	1.288
2	1379	1.068	13	1249	1.288
3	1378	1.137	14	1238	1.288
4	1369	1.180	15	1236	1.311
5	1247	1.182	16	1279	1.311
6	1248	1.182	17	1469	1.380
7	1268	1.220	18	1278	1.384
8	1478	1.252	19	1239	1.406
9	2378	1.266	20	1269	1.431
10	1237	1.281	21	1267	1.467
11	1234	1.288	22	1289	1.592
–	12468-PnCDD	1.430	–	124679-HxCDD	1.894
–	1368-TCDF	0.941			
PnCDD					
1	12468	1.000	8	12378	1.167
2	12479	1.000	9	12369	1.184
3	12368	1.037	10	12467	1.195
4	12478	1.076	11	12489	1.198
5	12379	1.098	12	12346	1.222
6	12469	1.146	13	12367	1.229
7	12347	1.146	14	12389	1.390
HxCDD					
1	123468	1.000	6	123478	1.069
2	124679	1.000	7	123678	1.077
3	124689	1.000	8	123469	1.111
4	123679	1.038	9	123789	1.130
5	123689	1.040	10	123467	1.162

al. [61] in PCDFs from magnesium smelting. Interestingly, Rappe *et al.* [62] correctly report the elution order of 12678-/23468-PnCDF in their more recent study on urban air.

HxCDFs. The only discrepancy we noted for the HxCDF homologues is for the 134678/124678-HxCDF pair which we and Bell and Gara [22] report as resolved peaks in the above order on the polar SP-2330 and CP-Sil 88 columns and not as first reported [19] in reverse order, and subsequently used to assign isomers in fly ash [60] and urban air [62].

2378-substituted PCDD/PCDF. Since the 2378-substituted PCDD/PCDF congeners are so important in both environmental and biological samples, their separation for the tetra-, penta- and hexa-homologues is shown in more detail in Tables XIV and XV for all nine GC phases. From Table XIV for the PCDDs, it is seen that the polar cyanopropyl columns such as SP-2331 and CP-Sil 88, and the smectic liquid crystalline phase can separate both 2378-TCDD from the other 21 isomers and the other four higher chlorinated 2378-substituted PCDDs from their respective isomers. The medium polar DB-17 is next best in the separation of these compounds with only

TABLE XII

GC RETENTION TIMES OF PCDF/PCCD ISOMERS RELATIVE TO RT REFERENCE STANDARDS ON A CP-Sil 88 FUSED-SILICA CAPILLARY COLUMN

Reference standards as in Table V.

Elution order	Isomer	RRT	Elution order	Isomer	RRT
TCDF					
1	1368	1.000	20	1236	1.277
2	1378	1.095	21	2468	1.289
3	1379	1.095	22	1349	1.306
4	1347	1.111	23	1278	1.318
5	1468	1.125	24	1279	1.361
6	1247	1.135	25	1267	1.361
7	1367	1.135	26	1469	1.378
8	1348	1.156	27	1249	1.382
9	1346	1.182	28	2368	1.403
10	1248	1.183	29	2467	1.450
11	1268	1.208	30	1239	1.473
12	1246	1.208	31	2347	1.489
13	1237	1.216	32	1269	1.507
14	1478	1.216	33	2378	1.529
15	1369	1.218	34	2348	1.534
16	1678	1.258	35	2346	1.555
17	1234	1.258	36	2367	1.569
18	1238	1.277	37	3467	1.636
19	1467	1.277	38	1289	1.681
–	13468-PnCDF	1.291	–	123468-HxCDF	1.670
–	1368-TCDD	1.013			
PnCDF					
1	13468	1.000	15	12378	1.194
2	12468	1.022	16	12346	1.206
3	13678	1.055	17	12379	1.211
4	13479	1.073	18	12367	1.224
5	13478	1.093	19	12469	1.246
6	12368	1.093	20	12678	1.246
7	12478	1.112	21	12679	1.304
8	12479	1.129	22	12369	1.324
9	13467	1.129	23	23468	1.347
10	12467	1.147	24	12349	1.359
11	12347	1.153	25	12489	1.383
12	14678	1.158	26	23478	1.487
13	13469	1.185	27	12389	1.498
14	12348	1.194	28	23467	1.529
HxCDF					
1	123468	1.000	9	124689	1.128
2	134678	1.007	10	123467	1.132
3	134679	1.009	11	123679	1.150
4	124678	1.024	12	123469	1.224
5	124679	1.063	13	123689	1.224
6	123478	1.102	14	123789	1.349
7	123479	1.102	15	123489	1.403
8	123678	1.116	16	234678	1.471

TABLE XII *(continued)*

Elution order	Isomer	RRT	Elution order	Isomer	RRT
TCDD					
1	1368	1.000	12	1246	1.249
2	1379	1.059	13	1249	1.249
3	1378	1.116	14	1238	1.249
4	1369	1.160	15	1236	1.269
5	1247	1.160	16	1279	1.269
6	1248	1.160	17	1278	1.327
7	1268	1.193	18	1469	1.339
8	1478	1.222	19	1239	1.350
9	2378	1.227	20	1269	1.376
10	1237	1.241	21	1267	1.403
11	1234	1.249	22	1289	1.509
–	12468-PnCDD	1.405	–	124679-HxCDD	1.818
–	1368-TCDF	0.987			
PnCDD					
1	12468	1.000	8	12378	1.133
2	12479	1.000	9	12369	1.153
3	12368	1.027	10	12467	1.162
4	12478	1.060	11	12489	1.167
5	12379	1.077	12	12346	1.185
6	12347	1.123	13	12367	1.191
7	12469	1.123	14	12389	1.265
HxCDD					
1	123468	1.000	6	123478	1.073
2	124679	1.000	7	123678	1.082
3	124689	1.000	8	123469	1.129
4	123679	1.042	9	123789	1.145
5	123689	1.042	10	123467	1.191

1469-TCDD interfering. The non-polar DB-1 and DB-5 columns have many congeners which co-elute with the 2378-substituted PCDDs.

In the case of the 2378-substiuted PCDFs (Table XV), the situation is more complicated. Only the DB-17 column was successful in our hands in separating 2378-TCDF from the other 37 TCDFs. The more polar DB-210, SP-2331 and CP-Sil 88 all had difficulty separating 2348-TCDF from 2378-TCDF. Interestingly, the other bonded phase methyl-phenyl (50%) (OV-17) column did not separate 1469- from 2378-TCDF. There may be major differences in the resolving power of this and other phases depending on batch number and manufacturer in addition to GC conditions such as temperature and injection mode. However the OV-17 column did allow complete isomeric identification of 12378-PnCDF which DB-17 did not (interference from 12346-PnCDF on the latter column). DB-210 was also successful in the separation of 12378- from 12348-PnCDF which the cyanopropyl and methyl silicone columns could not accomplish. The non-polar DB-1 and DB-5 have many isomers in the tetra- and penta-series which potentially overlap with the 2378-substituted PCDFs. As mentioned previously, the DB-225 column we used could not separate 1239-TCDF

TABLE XIII

GC RETENTION TIMES OF PCDF/PCDD ISOMERS RELATIVE TO RT REFERENCE STANDARDS ON A LIQUID CRYSTALLINE SMECTIC FUSED-SILICA CAPILLARY COLUMN

Reference standards as in Table V.

Elution order	Isomer	RRT	Elution order	Isomer	RRT
TCDF					
1	1368	1.000	20	1236	1.331
2	1468	1.016	21	2368	1.331
3	1346	1.074	22	1378	1.389
4	2468	1.095	23	1379	1.430
5	1246	1.107	24	2346	1.450
6	1248	1.144	25	1238	1.470
7	1478	1.144	26	2467	1.483
8	1369	1.151	27	1269	1.490
9	1467	1.168	28	2348	1.508
10	1268	1.168	29	1278	1.508
11	1678	1.175	30	1239	1.624
12	1348	1.191	31	1267	1.624
13	1347	1.215	32	1279	1.646
14	1469	1.233	33	2347	1.737
15	1247	1.233	34	3467	1.764
16	1349	1.253	35	1237	1.786
17	1234	1.253	36	1289	1.822
18	1367	1.292	37	2378	1.865
19	1249	1.302	38	2367	1.865
–	13468-PnCDF	1.386	–	123468-HxCDF	2.077
–	1368-TCDD	1.095			
PnCDF					
1	13468	1.000	15	23468	1.311
2	12468	1.006	16	12348	1.333
3	14678	1.133	17	12678	1.384
4	13469	1.156	18	12369	1.404
5	13678	1.201	19	12349	1.444
6	12368	1.212	20	12347	1.464
7	12478	1.221	21	12679	1.507
8	13478	1.228	22	12489	1.522
9	12469	1.238	23	12367	1.583
10	13467	1.242	24	23478	1.589
11	13479	1.242	25	12378	1.664
12	12346	1.248	26	23467	1.712
13	12467	1.269	27	12379	1.742
14	12479	1.280	28	12389	1.962
HxCDF					
1	123468	1.000	9	123678	1.249
2	124678	1.020	10	123467	1.278
3	134678	1.020	11	123479	1.289
4	134679	1.046	12	123679	1.323
5	124679	1.079	13	234678	1.365
6	124689	1.113	14	123689	1.369
7	123469	1.163	15	123489	1.581
8	123478	1.233	16	123789	2.228

TABLE XIII *(continued)*

Elution order	Isomer	RRT	Elution order	Isomer	RRT
TCDD					
1	1368	1.000	12	1234	1.239
2	1369	1.042	13	1269	1.288
3	1478	1.100	14	1378	1.338
4	1246*[a]	1.140	15	1239	1.425
5	1249*	1.153	16	1279	1.472
6	1248*	1.179	17	1238	1.539
7	1469	1.188	18	1278	1.586
8	1379	1.199	19	1267	1.601
9	1268	1.199	20	1237	1.613
10	1236	1.199	21	1289	1.646
11	1247*	1.205	22	2378	1.915
–	12468-PnCDD	1.482	–	124679-HxCDD	2.098
–	1368-TCDF	0.913			
PnCDD					
1	12468*	1.000	8	12489*	1.231
2	12479*	1.032	9	12467*	1.250
3	12469	1.053	10	12347	1.279
4	12368	1.092	11	12367	1.318
5	12478	1.103	12	12379	1.343
6	12369	1.111	13	12378	1.478
7	12346	1.191	14	12389	1.577
HxCDD					
1	124679*	1.000	6	123689*	1.108
2	124689*	1.015	7	123478	1.202
3	123469	1.072	8	123678	1.207
4	123468	1.079	9	123467	1.360
5	123679*	1.096	10	123789	1.661

[a] Congeners marked with an asterisk are pairs which cannot be unequivocably assigned (*cf.* text).

from 2378-TCDF although this has been reported by others [58]. With regard to the HxCDFs, Table XV shows that a combination of using both a non-polar and medium or high polar column will allow unequivocal identification of all 2378-substituted HxCDFs and indeed of all 16 isomers.

The data show that all the isomers and congeners can be separated from each other by a combination of a minimum of two columns. In particular, all of the biologically important 2378-substituted PCDDs/PCDFs commonly found in animal species are readily differentiated on two GC columns. It is emphasized that, due to factors such as variation in columns and GC conditions, each laboratory must test the resolving power of their GC columns by demonstrating that those isomers eluting in the immediate vicinity of the congener in question as judged from this report are in fact suitably resolved. This information is the most comprehensive to date with regard to the number of single congeners reported and with respect to the number and range of polarity of the capillary columns. It also provides a confirmation of much earlier work. Except for six closely related PCDD pairs, the isomeric PCDD–PCDF content can be

TABLE XIV

ISOMERS WHICH COULD POTENTIALLY INTERFERE WITH THE 2378-SUBSTITUTED PCDDs ON FUSED-SILICA SILICONE CAPILLARY GC COLUMNS

Percent resolution between isomers in brackets; GC conditions as in Table IV.

2378-isomer	GC phase									
	DB-1	DB-5	DB-17	OV-17	DB-210	DB-225	CPS-1	SP-2331[a]	CP-Sil 88	Smectic
2378	1239 (50%)	1237 (50%) 1238 (30%)	1469 (0%)	1279 (0%)	1269 (0%)	1246 (0%) 1249 (30%)	1234 (0%) 1249 (0%) 1237 (0%) 1238 (40%)	1237 (100%; 0%)	1478 (50%)	None
12378	12367 (60%)	None	None	12346 (10%)	12367 (10%)	12369 (0%)	None	12369 (100%; 0%)	None	None
123478	123678 (60%)	123678 (50%)	None	None	None	None	None	None	None	123678 (20%)
123678	123478 (60%)	123478 (50%)	None	None	None	None	None	None	None	123478 (20%)
123789	123467 (0%)	123467 (0%)	None	None	None	None	None	None	None	None

[a] Resolution for SP-2331 in brackets shown first for a new column and then for one which has deteriorated with use.

TABLE XV

ISOMERS WHICH COULD POTENTIALLY INTERFERE WITH THE 2378-SUBSTITUTED PCDFs ON FUSED-SILICA SILICONE CAPILLARY GC COLUMNS

Percent resolution between isomers in brackets; GC conditions as in Table IV.

2378-isomer	GC phase									
	DB-1	DB-5	DB-17	OV-17	DB-210	DB-225	CPS-1	SP-2331[a]	CP-Sil 88	Smectic
2378	2347, 2348 1249, 1279, 2346 (all 0%)	2348, 2347, 2346, 1249, 1279 (all 0%)	None	1469 (0%)	2348 (70%)	1239 (10%)	2348 (10%)	2348 (30; 0%)	2348 (30%)	2367 (0%)
12378	12348 (90%)	12348 (10%)	12346 (0%)	None	12367 (0%) 12678 (0%)	13469 (10%)	12346 (0%)	12346 (100; 0%) 12348 (0; 100%)	12348 (0%)	None
23478	12679 (0%) 23467 (50%) 12369 (50%)	12489, 12679, 12369 (all 0%)	None	None	None	None	12389 (70%)	None	None	12367 (20%)
123478	123467 (10%)	123467 (0%)	124689 (50%)	None	123467 (0%) 123479 (10%) 123678 (70%)	None	123479 (0%) 124689 (10%)	123479 (0%; 0%)	123479 (0%)	None
123678	None	123479 (60%)	123467 (10%)	123467 (30%)	123467 (70%) 123479 (70%) 123478 (70%)	124689 (0%) 123479 (0%)	None	124689 (0;100%)	None	None
234678	123689 (0%)	123689 (90%)	123689 (70%)	123689 (50%)	None	123489 (0%)	None	None	None	123689 (0%)
123789	123489 (40%)	123489 (70%)	None	None	123489 (0%)	None	None	None	None	None

[a] Resolution for SP-2331 in brackets shown first for a new column and then for one which has deteriorated with use.

unambiguously specified for complex environmental samples containing many peaks or for the simpler biologically incurred samples containing mostly 2378-PCDD/PCDFs.

ACKNOWLEDGEMENTS

The authors are grateful to all those scientists and institutions listed in Table II and III who generously donated and/or exchanged their purified standards for this study. Harvey Newsome, Health Welfare Canada, is also thanked for providing many of the chlorinated diphenyl ethers as precursors to the PCDFs. Gordon Dean, Health Protection Branch, drew the many detailed figures from the raw GC data. Nisu Sen and Dorcas F. Weber kindly provided critical review of the manuscript.

REFERENCES

1 *Polychlorinated Dibenzo-p-dioxins (PCDDs) and Polychlorinated Dibenzofurans (PCDFs), Scientific Criteria Document for Standard Development No. 4-84*, Ontario Ministry of the Environment, Intergovernmental Relations and Hazardous Contaminants Coordination Branch, Toronto, Sept. 1985.
2 G. Amendola, D. Barna, R. Blosser, L. LaFleur, A. McBride, F. Thomas, T. Tiernan and R. Whittemore, *Chemosphere*, 18 (1989) 1181.
3 R. E. Clement, C. Tashiro, S. Suter, E. Reiner and D. Hollinger, *Chemosphere*, 18 (1989) 1189.
4 J. J. Ryan, B. P.-Y. Lau, J. A. Hardy, W. B. Stone, P. O'Keefe and J. F. Gierthy, *Chemosphere*, 15 (1986) 537.
5 J. J. Ryan, R. Lizotte and B. P.-Y. Lau, *Chemosphere*, 14 (1985) 697.
6 J. J. Ryan, R. Lizotte, T. Sakuma and B. Mori, *J. Agri. Food Chem.*, 33 (1985) 1021.
7 H. R. Buser, H.-P. Bosshardt and C. Rappe, *Chemosphere*, 7 (1978) 165.
8 H. R. Buser, H.-P. Bosshardt, C. Rappe and R. Lindahl, *Chemosphere*, 7 (1978) 419.
9 H. R. Buser, *Chemosphere*, 8 (1979) 415.
10 T. J. Nestrick, L. L. Lamparski and R. H. Stehl, *Anal. Chem.*, 51 (1979) 2273.
11 H. R. Buser and C. Rappe, *Anal. Chem.*, 52 (1980) 2257.
12 L. L. Lamparski and T. J. Nestrick, *Chemosphere*, 10 (1981) 3.
13 W. A. Korfmacher and R. K. Mitchum, *J. High Resol. Chromatogr. Chem. Comm.*, 5 (1982) 681.
14 P. W. O'Keefe, R. Smith, C. Meyer, D. Hilker, K. Aldous and B. Jelus-Tyror, *J. Chromatogr.*, 242 (1982) 305.
15 T. Mazer, F. D. Hileman, R. W. Noble and J. J. Brooks, *Anal. Chem.*, 55 (1983) 104; 1648 (correction).
16 T. Mazer, F. D. Hileman, R. W. Noble, M. D. Hale and J J. Brooks, in G. Choudhary, L. H. Keith and C. Rappe (Editors), *Chlorinated Dioxins and Dibenzofurans in the Total Environment*, Butterworth, Boston, 1983, Ch. 3, p. 23.
17 H. R. Buser and C. Rappe, *Anal. Chem.*, 56 (1984) 442.
18 M. Oehme and P. Kirschmer, *Anal. Chem.*, 56 (1984) 2754.
19 C. Rappe, *Environ. Sci. Technol.*, 18 (1984) 78A.
20 H. Kuroki, K. Haraguchi and Y. Masuda, *Chemosphere*, 13 (1984) 561.
21 W. V. Ligon, Jr. and R. J. May, *J. Chromatogr.*, 294 (1984) 87.
22 R. A. Bell and A. Gara, in L. H. Keith, C. Rappe and G. Choudhary (Editors), *Chlorinated Dioxins and Dibenzofurans in the Total Environment II*, Butterworth, Boston, 1985, Ch. 1, p. 3.
23 M. L. Taylor, T. O. Tiernan, B. Ramalingam, D. J. Wagel, J. H. Garrett, J. G. Solch and G. L. Ferguson, in L. H. Keith, C. Rappe and G. Choudhary (Editors), *Chlorinated Dioxins and Dibenzofurans in the Total Environment II*, Ch. 2, p. 17.
24 C. Rappe, S. Marklund, L.-O. Kjeller, P.-A. Bergqvist and M. Hansson, in L. H. Keith, C. Rappe and G. Choudhary (Editors), *Chlorinated Dioxins and Dibenzofurans in the Total Environment II*, Ch. 29, p. 401.
25 D. Fung, R. K. Boyd, S. Safe and B. S. Chittim, *Biomed. Mass Spectrom.*, 12 (1985) 247.
26 T. Humppi and K. Heinola, *J. Chromatogr.*, 331 (1985) 410.
27 K. Ballschmiter, H. Buchert, Th. Class, W. Krämer, H. Magg, A. Munder, U. Reuter, W. Schäfer, M. Swerev, R. Wittlinger and W. Zoller, *Fres. Z. Anal. Chem.*, 320 (1985) 711.

28 K. Ballschmiter, W. Zoller, H. Buchert and Th. Class, *Fres. Z. Anal. Chem.*, 322 (1985) 587.
29 J. Meyer, F. Umland, W. Funcke, E. Balfanz and J. König, *Chemosphere*, 15 (1986) 2035.
30 L. T. Gelbaum, D. S. Patterson and D. F. Groce, in C. Rappe, G. Choudhary and L. H. Keith (Editors), *Chlorinated Dioxins and Dibenzofurans in Perspective*, Lewis, Michigan, 1986, Ch. 31, p. 479.
31 B. S. Chittim, J. A. Madge and S. H. Safe, *Chemosphere*, 15 (1986) 1931.
32 W. Zoller and K. Ballschmiter, *Chemosphere*, 15 (1986) 2129.
33 F. Kuhlman, *Frez. Z. Anal. Chem.*, 323 (1986) 11.
34 J. R. Donnelly, W. D. Munslow, R. K. Mitchum and G. W. Sovocool, *J. Chromatogr.*, 393 (1987) 51.
35 D. S. Waddell, H. S. McKinnon, B. S. Chittim, S. Safe and R. K. Boyd, *Biomed. Environ. Mass Spectrom.*, 14 (1987) 457.
36 M. Swerev and K. Ballschmiter, *J. High Resol. Chromatogr. Chem. Commun.*, 10 (1987) 544.
37 U. Riehle, J. Ehmann, M. Swerev and K. Ballschmiter, *Fres. Z. Anal. Chem.*, 331 (1988) 821.
38 P. Schmid, *J. High Resol. Chromatogr.*, 12 (1989) 665.
39 I. O. O. Korhonen and K. M. Mäntykoski, *J. Chromatogr.*, 473 (1989) 153; 477 (1989) 327.
40 L. A. Harden, J. H. Garett, J. G. Solch, T. O. Tiernan, D. J. Wagel and M. L. Taylor, *Chemosphere*, 18 (1989) 85.
41 N. H. Mahle, L. L. Lamparski and T. J. Nestrick, *Chemosphere*, 18 (1989) 2257.
42 D. F. Groce, C. C. Alley and D. G. Patterson, Jr., *Chemosphere*, 19 (1989) 225.
43 D. G. Patterson, Jr., V. V. Reddy, E. R. Barnhart, D. L. Ashley, C. R. Lapeza, Jr., L. R. Alexander and L. T. Gelbaum, *Chemosphere*, 19 (1989) 223.
44 R. S. Brown, K. Pettit and P. W. Jones, *Chemosphere*, 19 (1989) 171.
45 Y. A. Yancey, *J. Chromatogr. Sci.*, 23 (1985) 161.
46 Y. A. Yancey, *J. Chromatogr. Sci.*, 23 (1985) 370.
47 Y. A. Yancey, *J. Chromatogr. Sci.*, 24 (1986) 117.
48 V. Zitko, *Chemosphere*, 14 (1985) 165.
49 P. J. Slonecker, J. L. Pyle and J. S. Cantrell, *Anal. Chem.*, 54 (1983) 1543.
50 J. S. Cantrell, P. J. Slonecker and T. A. Beiter, in C. Rappe, G. Choudhary and L. H. Keith (Editors), *Chlorinated Dioxins and Dibenzofurans in Perspective*, Lewis, Michigan, 1986, Ch. 29, p. 453.
51 A. S. Kende and M. R. DeCamp, *Tetrahedron Let.*, (1975) 2877.
52 A. P. Gray, V. M. Dipinto and I. J. Solomon, *J. Org. Chem.*, 41 (1976) 2428.
53 A. Gara, K. Andersson, C.-A. Nilsson and A. Norström, *Chemosphere*, 10 (1981) 365.
54 M. Swerev and K. Ballschmiter, *Anal. Chem.*, 59 (1987) 2536.
55 M. Swerev and K. Ballschmiter, *Fres. Z. Anal. Chem*, 327 (1987) 50.
56 D. F. Gurka, S. Billets, J. W. Brasch and C. J. Riggle, *Anal. Chem.*, 57 (1985) 1975.
57 D. Wagel, T. O. Tiernan, M. L. Taylor, B. Ramalingam, J. H. Garrett and J. B. Solch, in C. Rappe, G. Choudhary and L. H. Keith (Editors), *Chlorinated Dioxins and Dibenzofurans in Perspective*, Lewis, Michigan, 1986, Ch. 21, p. 305.
58 United States Environmental Protection Agency, Method 1613: *Tetra- through Octa-Chlorinated Dioxins and Furans by Isotope Dilution*, Office of Water Regulations and Standards, Washington, DC, July 1989.
59 K. Abraham, T. Weismüller, H. Brunner, R. Krowke, H. Hagenmaier and D. Neubert, *Arch. Toxicol.*, 63 (1989) 193.
60 T. Wakimoto, N. Kannan, M. Ovo, R. Tatsukawa and Y. Masuda, *Chemosphere*, 17 (1988) 743.
61 M. Oehme, S. Mano, E. M. Brevik and J. Knutzen, *Frez. Z. Anal. Chem.*, 335 (1989) 987.
62 C. Rappe, L.-O. Kjeller, P. Bruckman and K.-H. Hackhe, *Chemosphere*, 17 (1988) 3.

Journal of Chromatography, 541 (1991) 185–194
Elsevier Science Publishers B.V., Amsterdam

CHROM. 23 021

Quantitative extraction of linear alkylbenzenesulfonates using supercritical carbon dioxide and a simple device for adding modifiers

STEVEN B. HAWTHORNE* and DAVID J. MILLER
Energy and Environmental Research Center, University of North Dakota, Grand Forks, ND 58202 (U.S.A.)
and
DAVID D. WALKER, DAVID E. WHITTINGTON and BILLY L. MOORE
Procter and Gamble Company, Human and Environmental Safety Division, Ivorydale Technical Center, Cincinnati, OH 45217 (U.S.A.)

(First received September 19th, 1990; revised manuscript received December 4th, 1990)

ABSTRACT

Quantitative extraction of anionic surfactants, linear alkylbenzenesulfonates (LAS), from soil, sediment, and municipal wastewater treatment sludge was achieved using a simple apparatus for the preparation of high concentrations of organic modifiers in supercritical CO_2. The method allows several different modifiers to be tested without the necessity of mixing modifiers in the pump or purchasing pre-mixed fluids. Of the several modifiers tested, methanol yielded the best extraction efficiencies, and >90% recoveries of LAS were achieved using a 30-min extraction at 380 atm with *ca.* 40 mol % methanol in CO_2. Extraction efficiency *versus* time plots for ^{14}C-labeled and native LAS showed good agreement, indicating that the spiked LAS was representative of the native LAS.

INTRODUCTION

The use of supercritical fluids for analytical-scale extraction of organic chemicals from environmental samples has received increasing attention because of several potential advantages over conventional liquid solvent extractions including speed, superior recoveries, reduction in liquid solvent usage and solvent waste, and the ability to directly couple the extraction step with capillary gas chromatography (GC) and supercritical fluid chromatography (SFC) [1]. The majority of investigations involving environmental samples have used pure supercritical fluids (primarily CO_2 and, to a lesser extent, N_2O) to extract relatively non-polar analytes, *e.g.*, those that are amenable to GC analysis including fuel hydrocarbons, polycyclic aromatic hydrocarbons (PAHs), polychlorinated biphenyls (PCBs), and non-polar pesticides [2–7]. When more polar and higher molecular weight analytes need to be extracted, conventional supercritical fluids such as CO_2 generally do not have sufficient polarity for efficient extractions. In such cases, the addition of organic modifiers is used to increase the polarity of the fluid, and thus increase the extraction efficiency [1,8–10].

0021-9673/91/$03.50

Modified supercritical fluids are generally introduced as mixtures of the modifier and CO_2 in the pump, or supplied by dual pumping systems. Both of these approaches involve exposing the pump to the organic modifier, which may cause contamination of the pump by the modifier, and makes the rapid evaluation of several different modifiers experimentally difficult. Small volumes of modifiers can also be added directly to the sample before performing supercritical fluid extraction (SFE) under static conditions [9], but this approach can not supply a continuous supply of modified CO_2 extraction fluid. A simple device to provide a constant high concentration of modified CO_2 for dynamic SFE that does not require exposing the pumping system to the organic modifier, and simplifies the testing of several different modifiers for optimizing extractions is described here. This device has been used to develop quantitative extraction conditions for widely-used anionic surfactants, linear alkylbenzenesulfonates (LAS) from environmental solids.

Commercial LAS is a mixture of homologues and isomers with the predominant formulation having *n*-alkyl chain lengths from C_{11} to C_{14} [11]. LAS is extensively used in domestic detergent formulations, and as an ionic compound, approximately 75% of LAS is disposed as part of domestic wastes in municipal wastewater treatment facilities [12], where it is largely removed from the water by biological degradation and adsorption to solids [13]. The sludges from the treatment facility are often disposed of by mixing into agricultural soils [11], providing a route for LAS to enter the environment. Because of the potential for finding LAS in environmental solids, the SFE methods were evaluated for the extraction of LAS from soil, river sediment, and sludge from a municipal wastewater treatment facility.

EXPERIMENTAL

Samples

Anaerobic digester sludge was collected from a municipal wastewater treatment facility in a non-industrialized rural town. Soil and river sediment samples (alluvial silty clays) were collected in the Ohio River valley. The soil was from an agricultural field which had been used for the disposal of wastewater treatment sludge approximately one year before sample collection, and is henceforth referred to as "sludge amended soil". Small rocks and sticks were removed from the soil and sediment samples, and all samples were air dried and crushed to <600 μm prior to use.

Portions of the three samples were spiked by suspending 7 g in 20 ml ethanol containing ^{14}C-labeled dodecylbenzenesulfonate (^{14}C-LAS), stirring for 3 h, then air drying for several days. Resulting concentrations of the ^{14}C-LAS were *ca.* 2 μg/g with an activity of *ca.* 100 000 dpm/g. All spiked samples were aged for a minimum of 3 months prior to use.

Supercritical fluid extractions

All extractions were performed at 380 atm using a syringe pump (ISCO Model 260D, Lincoln, NE, U.S.A.) filled with SFC-grade CO_2 or N_2O (Scott Specialty Gases, U.S.A.) and a 1-ml extraction cell (JASCO, Japan) for 1-g samples, or cells constructed as previously described from 1/16-in. "Parker" fittings for 50-mg samples [14]. A schematic of the device used for generating the modified CO_2 is shown in Fig. 1. The CO_2 is pumped to a 4-port valve which can be switched so that the flow goes

either directly to the extraction cell, or through the 9.5-ml stainless-steel modifier vessel. (*Caution*: Care must be taken to ensure that the modifier chamber and all related fittings have appropriate pressure ratings. Materials must also be chemically resistant to any modifiers used.) The modifier vessel's temperature was controlled at 60°C by placing it in a GC oven. The temperature of the extraction cell was controlled by a thermostatted tube heater which contained a 1/2 m coil of the stainless-steel transfer line to equilibrate the fluid's temperature before reaching the extraction cell. The loaded sample cells were placed in the tube heater for 5 min before extracting to ensure that the sample was preheated to the extraction temperature.

Extractions were performed by first pressurizing the sample cell with pure CO_2 for *ca.* 3 s, then rotating the valve so that the CO_2 flowed through the modifier vessel as shown by the arrows in Fig. 1. The CO_2 became saturated with the modifier (at the 60°C oven temperature) then flowed through the 4-port valve to the sample cell.

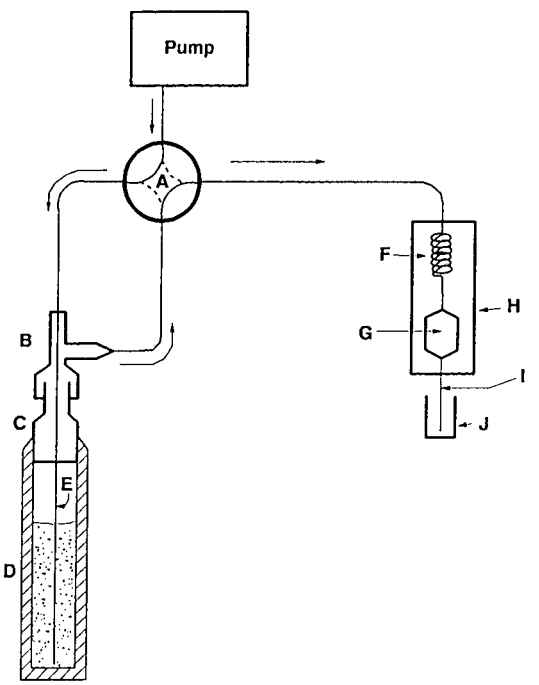

Fig. 1. Schematic diagram of the device used for the preparation of modified supercritical CO_2. Arrows show the flow directions during extraction with the modified supercritical fluid. Components: A = four-port valve; B = "Parker" or "Swagelok" brand 1/16 × 1/16 × 1/4 in. stainless-steel "tee" tubing fitting; C = 1/4-in. normal pipe thread × 1/4 in. tubing stub fitting which is threaded and welded into D; D = modifier chamber which was constructed by drilling a 1.1-cm diameter hole 10 cm long into an 11 cm long × 1.9 cm (3/4 in. diameter) stainless-steel rod. The modifier chamber (D) is placed into a GC oven for temperature control. The 1/16 in. O.D. stainless-steel tubing (E) is inserted through the tee fitting (B) and the tubing stub (C) so that the end of the tubing is at the bottom of the modifier reservoir (D). The CO_2 exits the tubing (E) and percolates through the modifier before exiting from the side arm of the tee fitting (B). The modified supercritical fluid is then preheated to the extraction temperature in the 1/2 m coil of 1/16-in. O.D. tubing (F), and finally enters the extraction cell (G) which is inside of the tube heater (H). The extracted analytes are then swept through the restrictor (I) and collected in the solvent vial (J). All pressurized components were chosen to have ratings of at least 600 atm.

Extracted analytes were then swept through the sample extraction cell outlet restrictor and collected in a scintillation vial which contained 5 ml of ethanol. Flow through the extraction cell (as liquid CO_2 measured at the pump) was maintained at 1.2 ± 0.1 ml/min or at 0.45 ± 0.1 ml/min, respectively, using 10-cm lengths of either 30 or 25 μm I.D,. fused-silica tubing as outlet restrictors. After the extraction was complete, the modifier chamber was refilled by detaching the tee at the tubing fitting at the top of the chamber, and pipetting in additional modifier. The chamber can easily be rinsed and/or baked out between modifiers without any detectable evidence of carryover.

Analysis of extracts

Extraction efficiencies of the ^{14}C-LAS were determined with standard scintillation counting techniques. The activities of both the extract and the extracted solid (CabO-Sil suspension) were determined for each extraction. Analysis of the native LAS extracted from the unspiked samples was performed using high-performance liquid chromatography (HPLC) with fluorescence detection as previously described [11].

RESULTS AND DISCUSSION

The modifier chamber allowed extractions of LAS using several different organic modifiers to be evaluated in a a relatively short time, since the apparatus was simple to clean, and reloading the chamber required only *ca.* 1 min. During the initial development of the SFE method for LAS, several different modifiers were tested using 50-mg samples, a relatively short extraction time (15 min) and a CO_2 flow-rate of *ca.* 1.2 ml/min. A 5-ml volume of the test modifier was added to the saturation chamber before each extraction. Approximate concentrations of the modifiers in the CO_2 saturated at 60°C (estimated by the volume of CO_2 required to empty the saturation vessel) were propylene carbonate (15 mol%), 2-methoxyethanol (20%), acetic acid (25%), 1-butanol (20%), and methanol (40%). The digester sludge was chosen for the modifier survey since it was expected to have the highest concentration of LAS, and therefore would be the most rigorous test of the ability of the modified supercritical fluids to dissolve the LAS.

Table I shows the effect of several different modifiers in CO_2 on the recovery of ^{14}C-LAS from the digester sludge at extraction temperatures of 65 and 125°C. While neither pure CO_2 nor N_2O yielded any detectable recovery of the LAS, the modifiers yielded recoveries ranging from *ca.* 50% for propylene carbonate to near quantitative recovery with the methanol modifier. In most cases the extraction at 125°C was more efficient than extraction at 65°C. The increased efficiency at 125°C may (or may not) be because extractions with some of the modifiers could possibly not have been supercritical at the lower temperatures. Unfortunately, phase diagrams are not available in the literature to allow determination of the critical parameters for most of the modifier mixtures tested. However, published results do show that the extractions with methanol modified CO_2 were supercritical at both temperatures [15].

The increased recoveries using methanol modifier for the LAS extraction was fortuitous since methanol is much more convenient to use than, for example, acetic acid. However, it is clear that different modifiers could be superior depending on the

TABLE I

RECOVERIES OF ^{14}C-LAS FROM DIGESTER SLUDGE USING 15-min EXTRACTIONS WITH DIFFERENT POLARITY MODIFIERS

Modifier	Recovery (%)[a]	
	65°C	125°C
Carbon dioxide (pure)	<1	<1
Nitrous oxide (pure)	<1	<1
Modifiers in carbon dioxide		
Propylene carbonate	47	54
2-Methoxyethanol	67	55
Acetic acid	55	64
1-Butanol	64	70
Methanol	85	98

[a] A 5-ml volume of each modifier was used for each 15-min extraction at 380 atm. Recoveries were based on the average of two extractions at each extraction temperature.

polarity of target analytes and, perhaps, the sample matrix. For example, the same extracts generated for Table I were also analyzed for the cation of the fabric softener DTDMAC, $(C_nH_{2n+1})_2N(CH_3)_2Cl$ where n = 16 or 18, using fast atom bombardment mass spectrometry [16]. The relative amounts of DTDMAC extracted from the digester sludge were estimated based on the ratio of characteristic ions (m/z = 550, 522, and 494 for the di-C_{18}–, mixed C_{18}–/C_{16}–, and di-C_{16}–DTDMAC, respectively) to those of the fast atom bombardment reagent (dithioerythritol/dithiothreitol "magic bullet" at m/z = 222). Based on these ratios, the relative extraction efficiencies achieved using the various modifiers was nearly opposite those for LAS. For DTDMAC, propylene carbonate was the most effective modifier followed, in order of decreasing efficiency, by methoxyethanol, butanol, acetic acid, and methanol.

Since the device used in this study provides CO_2 that is saturated with the test modifier (at the 60°C oven temperature), there was initially some concern that the fluid could separate into two phases sometime during the extraction process. Preliminary experiments with CO_2–methanol demonstrated that phase separation did indeed occur if the extraction cell was not properly heated. Fortunately, phase separation was simple to determine by observing the pump flow-rate display. With a single phase system, the flow-rate of CO_2 was essentially unchanged whether the extraction was being performed with pure or modified CO_2, as would be expected since the viscosity of the modified CO_2 should not be greatly different from that of the pure CO_2 as long as the modified CO_2 remained a single-phase system. However, if phase separation occurred, the flow-rate of CO_2 dropped dramatically because the relatively high viscosity of the liquid phase greatly reduced the flow through the outlet restrictor. Since the solubilities of modifiers in CO_2 generally increase with temperature, extraction temperatures used in this study were higher than the modifier chamber temperature to ensure that a single phase system existed during the extractions. For example, the CO_2 flow (at the pump) with CO_2–methanol saturated at 60°C remained constant at 1.2 ml/min when the extraction temperature was held above 60°C, but dropped to <0.1 ml/min when the temperature of the extraction cell was lowered. However, the

flow returned to normal when the sample cell and the inlet end of the restrictor were heated to above the modifier chamber temperature. In all of the extractions reported here, the flow of CO_2 was monitored and care was taken that the extraction cell was completely heated to the desired temperature before beginning the extraction. With this precaution, no phase separation occurred as evidenced by a consistent flow-rate at the pump.

Based on the results of the modifier and temperature studies summarized in Table I, each subsequent extraction was performed at 125°C and the modifier chamber was completely filled with methanol (9.5 ml). Since, during an extraction, the CO_2 becomes saturated with the modifier, the flow-rate used for the extraction determines how long the modified supercritical fluid is supplied before the chamber is empty. With an extraction flow-rate of *ca.* 1.2 ml/min (as CO_2 at the pump), the 9.5 ml of methanol lasted *ca.* 10 min before it was exhausted. However, when the extraction flow was lowered to *ca.* 0.45 ml/min, the 9.5 ml of methanol lasted *ca.* 28 min. Both flow-rates resulted in a concentration of the methanol modifier of *ca.* 40 mol% (estimated based on the volume of CO_2 used to dissolve the 9.5 ml of methanol) but, since the lower flow-rate resulted in longer contact time between the modified supercritical fluid and the sample, it was suspected that the lower flow-rate might yield improved extraction efficiencies. The sludge amended soil was chosen for this comparison since initial extractions demonstrated that recoveries of LAS were poorer from the sludge amended soil than either the river sediment or digester sludge. Each extraction was carried our for 30 min, with the only difference being in the flow-rate of the supercritical fluid. As shown in Table II, the longer contact time with the methanol modifier afforded by the lower extraction flow-rate yielded significantly higher recoveries of the ^{14}C-LAS from the sludge amended soil. Table II also shows that the recoveries of the ^{14}C-LAS from the river sediment and the digester sludge were essentially quantitative using a 30-min extraction at the lower flow-rate.

TABLE II

RECOVERIES OF ^{14}C-LAS USING 30-min EXTRACTIONS AT 380 atm WITH METHANOL-MODIFIED CO_2

Trial	Recovery (%)			
	Sludge amended soil		Digester sludge, 0.45 ml/min	Sediment, 0.45 ml/min
	1.2 ml/min[a]	0.45 ml/min		
1	74.2	91.4	97.3	99.1
2	76.3	89.0	98.7	99.6
3	74.8	90.1	96.7	98.2
4	75.7	91.7	–	98.1
5	76.9	91.8	–	98.0
Mean ± S.D.	75.6 ± 1.1	90.8 ± 1.3	97.6 ± 1.0	98.6 ± 0.7

[a] Extraction flow-rates (measured as liquid CO_2 at the pump) were controlled at *ca.* 1.2 ml/min or 0.45 ml/min as described in the text. Each extraction was performed at 125°C with 9.5 ml methanol modifier.

Since the extractions shown in Table II were all performed on 50- to 60-mg samples (to conserve the limited supply of ^{14}C-LAS), there was some concern that the recovery of LAS from larger samples would be lower, particularly for the highly concentrated digester sludge sample which was shown by HPLC analysis to contain 3.5 mg of native LAS/g. The extraction of samples larger than 50 mg would also be useful to ensure more representative sampling. Sufficient quantities of the spiked digester sludge and the sludge amended soil were available to allow single extraction of 1-g samples in order to determine whether the 30-min extraction was sufficient to yield good recoveries of the ^{14}C-LAS. A comparison of the extraction rates for a 57-mg and a 1-g sample of the spiked digester sludge is shown in Fig. 2. While the extraction of the 1-g sample did proceed at a slightly lower rate, recoveries were still essentially quantitative with 95% of the ^{14}C-LAS being recovered in 30 min (compared to 98% for the 57-mg sample), and 99% being recovered in 60 min. (For extractions longer than 30 min, the modifier chamber was refilled at 20-min intervals to ensure a constant supply of methanol.)

In contrast to the digester sludge extractions, the recoveries of the LAS from 1.1-g and 50-mg samples of the sludge amended soil proceeded at essentially identical rates, with 93% of the LAS recovered from the 1.1-g sample in 30 min (compared to 92% for the 50-mg sample), and 97% recovery after 60 min. It is also interesting to

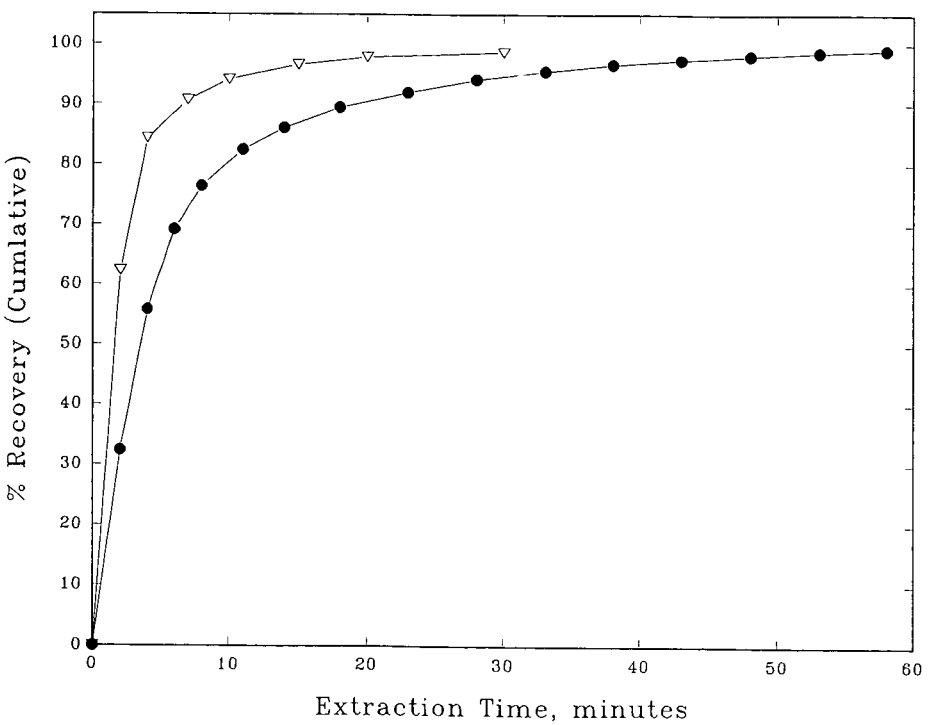

Fig. 2. Relative extraction rates of ^{14}C-LAS from 57-mg (▽) and 1-g (●) samples of digester sludge from a municipal wastewater treatment facility. Extractions were performed with 380 atm CO_2 at 125°C with methanol modifier as described in the text.

note that the 1-g samples of digester sludge and sludge amended soil showed nearly identical extraction efficiency curves despite having greatly different concentrations of native LAS (3.5 mg/g for the digester sludge versus 0.12 mg/g for the sludge amended soil). This similarity indicates that saturation of the supercritical fluid with LAS, which could reduce the extraction rate for the digester sludge, did not occur.

The extraction of the 1-g sample of digester sludge also provided enough LAS for HPLC analysis to allow the individual extraction curves for the major LAS species, C_{12}-, C_{13}- and C_{14}-LAS to be plotted (Fig. 3). While each of the species was >50% recovered after only two minutes of extraction, the extraction rates were slightly slower for the higher molecular weight LAS homologues, as might be expected since both the solubility and diffusivity of the C_{14}LAS should be lower in the supercritical extraction fluid than those of the lower molecular weight homologues.

Even though the spiked samples were all aged for several months prior to extraction, there was some concern that the ^{14}C-LAS spike was not truly representative of the native LAS found on the samples, and thus the ^{14}C-LAS may be more easily extracted than the native LAS. In order to investigate the extraction characteristics of the spiked and native LAS, unspiked samples of digester sludge and sludge amended soil were extracted under identical conditions to those used for the spiked 1g samples just discussed, except that the extraction of each sample was continued for

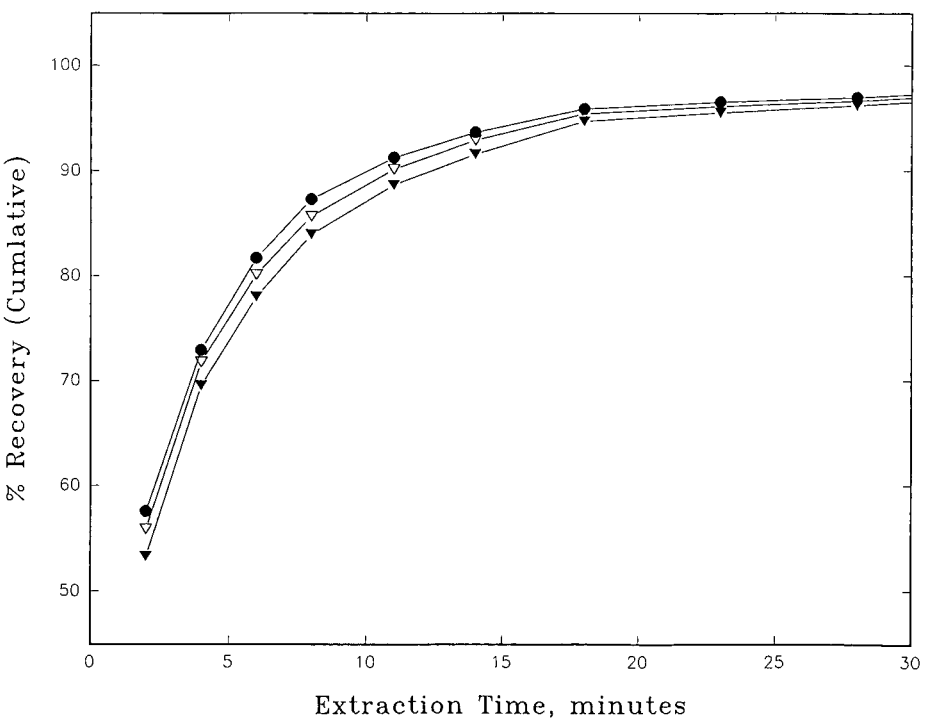

Fig. 3. Relative extraction rates of dodecyl (●), tridecyl (▽) and tetradecyl (▼) homologues of LAS from a 1-g sample of municipal wastewater treatment digester sludge. Extraction conditions are the same as for Fig. 2.

100 min, *i.e.*, until no more detectable LAS was recovered. Each fraction was then analyzed by HPLC for LAS as described above, and the extraction efficiency curves were compared with those of the spiked ^{14}C-LAS extractions. Fig. 4 shows a comparison of the extraction curves for the spiked and native LAS from the sludge amended soil samples. The good agreement between the extraction curves shows that the extraction behavior of the spiked ^{14}C-LAS and the native LAS was essentially identical, indicating that the use of the spiked ^{14}C-LAS was valid for these studies. The extraction rates for the spiked LAS (Fig. 2) and native LAS (Fig. 3) from the digester sludge sample were also very similar, further indicating that the spiked LAS was representative of the native LAS.

CONCLUSIONS

A simple and inexpensive saturation chamber can be used to provide organically modified supercritical CO_2 for supercritical fluid extractions of polar analytes from solid samples. Using this device, reproducible and quantitative recoveries (>90%) of anionic linear alkylbenzenesulfonates can be achieved from soil, sediment, and municipal wastewater sludge in 30 min with methanol modified CO_2.

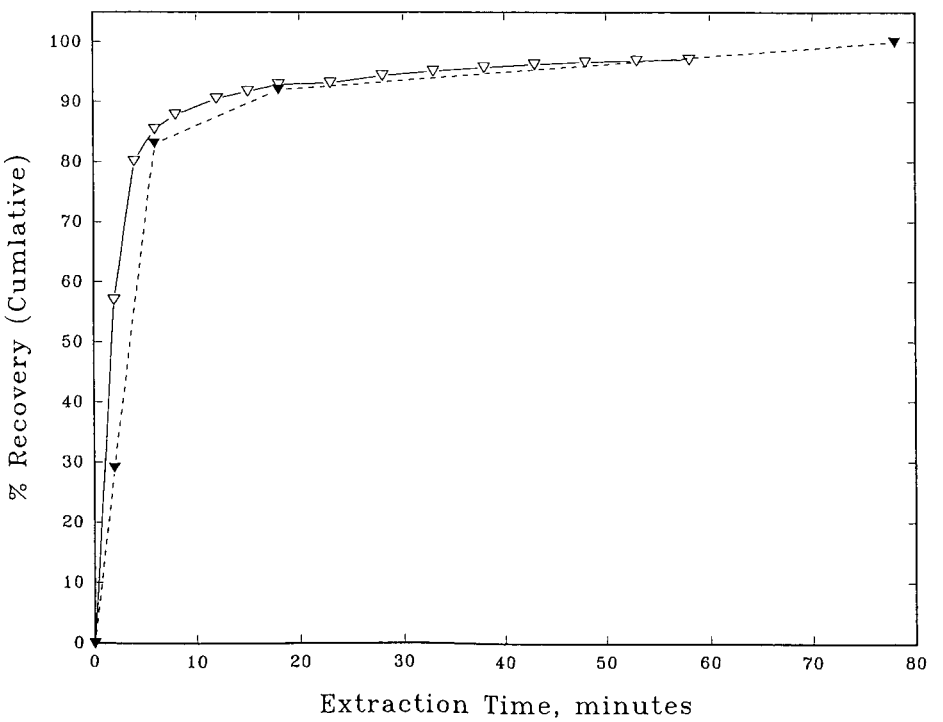

Fig. 4. Relative extraction rates of spiked ^{14}C-LAS (▽) and native LAS (▼) from agricultural soil which had been used for the disposal of digester sludge one year before sample collection.

ACKNOWLEDGEMENTS

The authors would like to thank David Lawrence (Procter and Gamble Company, Cincinnati, OH, U.S.A.) for performing the DTDMAC analysis, ISCO for provinding the pump used in this study, and JASCO for providing the 1-ml extraction cell.

REFERENCES

1 S. B. Hawthorne, *Anal. Chem.*, 62 (1990), 633A.
2 B. W. Wright, C. W. Wright and J. S. Fruchter, *Energy Fuels*, 3 (1989) 474.
3 V. Janda, G. Steenbeke and P. Sandra, *J. Chromatogr.*, 479 (1989) 200.
4 J. M. Levy, R. A. Cavalier, T. N. Bosch, A. M. Rynaski and W. E. Huhak, *J. Chromatogr. Sci.*, 27 (1989) 341.
5 S. B. Hawthorne, D. J. Miller and J. J. Langenfeld, *J. Chromatogr. Sci.*, 28 (1990) 2.
6 M. W. Raynor, I. L. Davies, K. D. Bartle, A. A. Clifford, A. Williams, J. M. Chalmers and B. W. Cook, *J. High Resolut. Chromatogr. Chromatogr. Commun.*, 11 (1988) 766.
7 S. B. Hawthorne and D. J. Miller, *Anal. Chem.*, 59 (1987) 1705.
8 N. Alexandrou and J. Pawliszyn, *Anal. Chem.*, 61 (1989) 2770.
9 J. R. Wheeler and M. E. McNally, *J. Chromatogr. Sci.*, 27 (1989) 534.
10 F. I. Onuska and K. A. Terry, *J. High Resolut. Chromatogr.*, 12 (1989) 357.
11 M. A. Castles, B. L. Moore and S. R. Ward, *Anal. Chem.*, 61 (1989) 2534.
12 R. A. Rapaport and W. S. Eckhoff, *Environ. Toxicol. and Chem.*, 9 (1990) 1245.
13 R. A. Rapaport, *Environ. Toxicol Chem.*, 7 (1988) 107.
14 S. B. Hawthorne and D. J. Miller, *J. Chromatogr.*, 403 (1987) 63.
15 E. Brunner, W. Hultenschmidt and G. Schlichtharle, *J. Chem. Thermodynamics*, 19 (1987) 273.
16 J. R. Simms, T. Keough, S. R. Ward, B. L. Moore and M. M. Bandurraga, *Anal. Chem.*, 60 (1988) 2613.

Journal of Chromatography, 541 (1991) 195–206
Elsevier Science Publishers B.V., Amsterdam

CHROM. 22 937

Effect of the intersection of the individual isotherms in displacement chromatography

SADRODDIN GOLSHAN-SHIRAZI, M. ZOUBAIR EL FALLAH and GEORGES GUIOCHON*
* *Department of Chemistry, University of Tennessee, Knoxville, TN 37996-1600 and Division of Analytical Chemistry, Oak Ridge National Laboratory, Oak Ridge, TN 37831-6120 (U.S.A.)*
(First received March 20th, 1990; revised manuscript received October 18th, 1990)

ABSTRACT

Neither the existence of an intersection between the two single-component isotherms drawn on the same graph, nor the fact that the column saturation capacity for the more retained component is lower than that of the lesser retained component, have any major consequence on the chromatographic behavior of elution bands or on the formation of the isotachic train, as long as the equilibrium isotherms of the two components are properly described by the competitive Langmuir model. Significant deviation from this model could make impossible the formation of an isotachic train in displacement chromatography, but definitive experimental proof of the existence of this effect is lacking.

INTRODUCTION

The calculation of elution band profiles in preparative chromatography requires the knowledge of the equilibrium isotherms of the components involved [1–3]. It has been shown that the competitive Langmuir isotherm [4] is sometimes an excellent model [5] but that more often it is barely acceptable [6,7]. However, the use of the Langmuir model permits the achievement of realistic results in simulation studies. These results can be used for investigations of the mechanism of band separation and band interactions in overloaded columns. Experimental results agree qualitatively very well with the predictions obtained in these calculations [5,7].

In practice, it is generally observed that the best set of competitive Langmuir isotherms which fit experimental results corresponds to different column saturation capacities for the various components of the mixture. Analysis of experimental data shows that in a number of instances the more retained component is also the one for which the column saturation capacity is the smaller. This situation should be expected especially in reversed-phase chromatography, as the bulkiest component, which has the smallest column saturation capacity, is often also the one which is adsorbed the most strongly. The phenomenon, however, is not peculiar to adsorption chromatography.

When two compounds exhibit this type of behavior, their single-component isotherms plotted on the same graph intersect and, for this reason, the effect has often been referred to as *isotherm intersection*. The isotherm intersection effect has been

0021-9673/91/$03.50

reported recently in overloaded elution [1] and displacement [2,3] chromatography. Cox and Snyder [1] suggested that the consequence of a lower saturation capacity of the more retained compound is that the displacement effect of the first-eluted compound by the second in overloaded elution is minimal. Subramanian and Cramer [3] showed that when the isotherms intersect, an isotachic displacement train cannot be achieved experimentally. They had to change the mobile phase composition to eliminate the isotherm intersection in order to perform displacement separations. They stated that their experimental results cannot be explained by a Langmuir-based model, as such a model predicts that the order of the bands in the isotachic displacement train depends only on the initial slopes of the isotherms and is independent of the displacer concentration, whether the isotherms of the feed components intersect or not.

In a recent paper, we reported a study of the influence of the column saturation capacity on the intensity of the displacement and tag-along effects [8]. We showed that the major contributions to the intensity of these effects are the ratio of the column saturation capacities for the two components and the feed composition which determines the ratio of the loading factors and the sample size. *If we assume that the competitive Langmuir isotherm model remains valid in this case*, the main consequence of a lower column saturation capacity for the more retained compound is that the displacement effect is enhanced and at the same time the separation deteriorates [8]. This is because, for a given sample size, the loading factor increases with decreasing column saturation capacity whereas the degree of column overload increases with increasing loading factor. On the other hand, at constant loading factor (*i.e.*, if the sample size is decreased in proportion to the column saturation capacity), the separation is improved because of the enhanced displacement effect. These results of the ideal model of chromatography are confirmed by those of numerical solutions of the semi-ideal model [9].

The aim of this paper is a detailed discussion of the interactive behavior of the bands of two components in the case of intersecting single-component isotherms, when the competitive isotherms of the two components are assumed to follow the competitive Langmuir isotherm model. This study applies to both overloaded elution and displacement.

THEORY

Properties of the isotherm intersection

The competitive Langmuir isotherm for a component i is given by:

$$Q_i = \frac{a_i C_i}{1 + b_1 C_1 + b_2 C_2} \tag{1}$$

where C_i and Q_i are the equilibrium concentrations of the component i in the mobile and stationary phases, respectively, and a_i and b_i are numerical coefficients. The column saturation capacity, $q_{s,i}$, is the product of the specific saturation capacity, $Q_{s,i} = a_i/b_i$, and the volume of stationary phase contained in the column. The column saturation capacity is the natural unit of the sample size used in preparative chromatography. The loading factor for one component is the ratio of the actual amount of this compound in the sample and the column saturation capacity.

As discussed previously [9], the competitive isotherms of the components of a binary mixture are two surfaces which must intersect. This is easily demonstrated. When the relative concentration, C_1/C_2, of the two components in the mobile phase varies from 0 to infinity at constant total concentration ($C_1 + C_2 = C$), the amount, $Q_1(C_1,C_2)$, of the first component adsorbed at equilibrium increases from 0 to $Q_1(C,0)$, whereas the amount of the second component adsorbed, $Q_2(C_1,C_2)$, decreases from $Q_2(0,C)$ to 0. Thus, the intersection of the isotherm surfaces by a vertical cylinder, which are two curves drawn on that cylinder, must intersect somewhere. Hence, the two surfaces intersect along a certain curve.

To help in understanding the situation, a concrete representation of the isotherms is useful. This can be achieved with either false three-dimensional (3-D) plots or contour maps. Fig. 1a shows a view of the 3-D plot of the Langmuir isotherms in a case where the single-component isotherm intersection effect takes place ($RQ_s = Q_{s,2}/Q_{s,1} = 0.5$). This figure does not exhibit any unusual feature resulting from the fact that the two single-component isotherms would intersect if they were drawn in the same plane.

Fig. 1b and c shows contour maps of the two sets of Langmuir isotherms used in the present work [$RQ_s = 1.0$ (Fig. 1b) and $RQ_s = 0.25$ (Fig. 1c)]. It is seen that these contour maps, showing the intersection of the surfaces $Q_i = f(C_1,C_2)$ by horizontal planes of increasing height, are fans of straight lines. For the isotherm of the first component, the general equation of these lines is

$$C_2 = -\frac{1}{b_2} + \frac{1}{b_2}\left(\frac{a_1}{k} - b_1\right)C_1 \tag{2}$$

where k is the height of the horizontal plane. C_2 must be positive; this is possible only if k is smaller than the saturation capacity for the first compound, $Q_{s,1}$ and for values of C_1 larger than $k/(a_1 - b_1k)$. Eqn. 2 defines a family of straight lines which all pass through the point of coordinates $C_1 = 0$, $C_2 = -1/b_2$ (note that only positive concentrations have a physical meaning). The contours of the second-component isotherm are also straight lines whose equation can be obtained by exchanging the indices 1 and 2 in eqn. 2. Their general equation can be rearranged into

$$C_2 = \frac{k}{a_2 - kb_2} + \frac{kb_1}{a_2 - kb_2}C_1 \tag{3}$$

All the straight lines defined by eqn. 3 pass through the point of coordinates $C_1 = -1/b_1$, $C_2 = 0$. Thus, we obtain two fan-like families of straight lines as contour maps for a binary mixture. This result is seen in Fig. 1b and c. It comes from the properties of eqn. 1, which defines a conoid surface.

The two straight lines of the two families which correspond to the same value of k, *i.e.*, the intersections of the two isotherm surfaces by the same horizontal plane, intersect in a point whose coordinates are such that $C_1 = \alpha C_2$. As a consequence, the intersection of the two isotherm surfaces, $Q_1(C_1,C_2)$ and $Q_2(C_1,C_2)$ is a curve in the vertical plane of trace $C_1 = \alpha C_2$. This result has already been demonstrated otherwise [6,9].

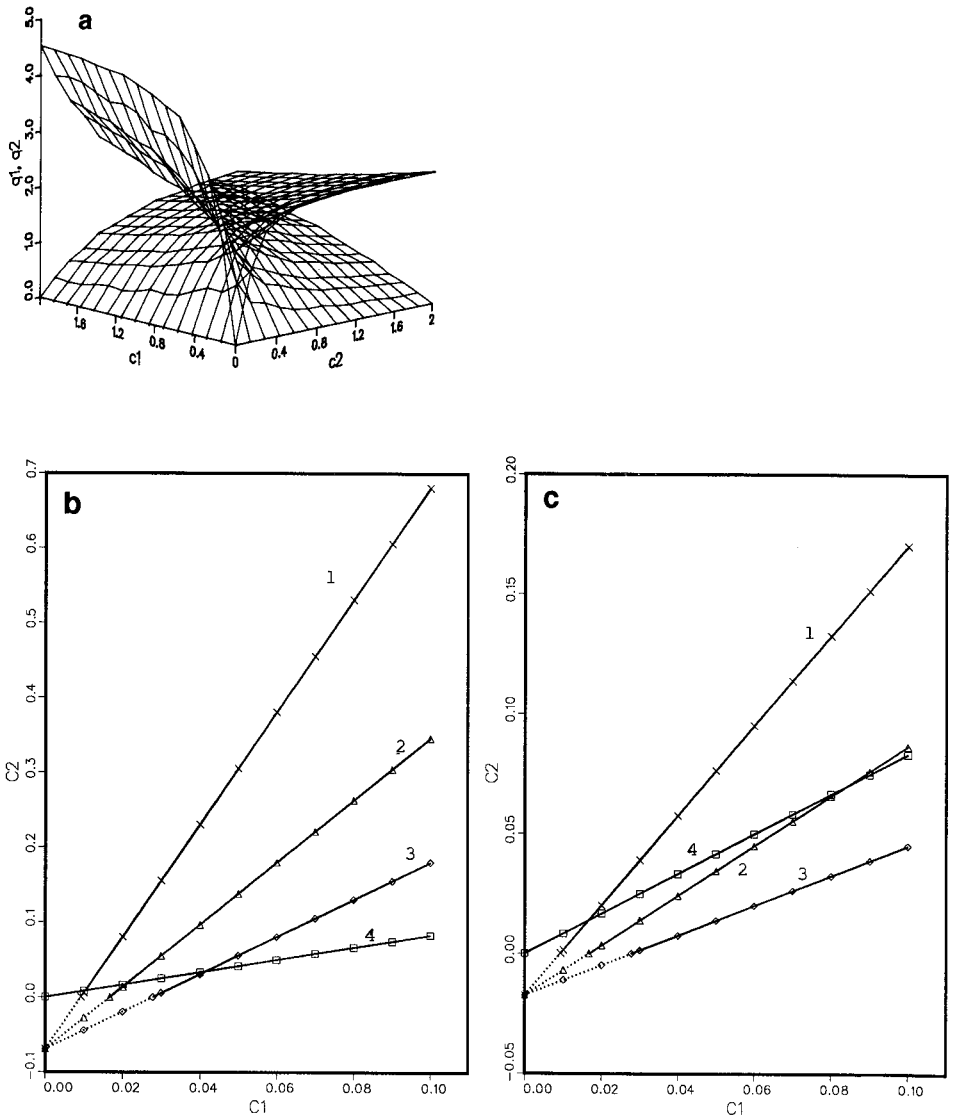

Fig. 1. Three-dimensional representation of the Langmuir competitive isotherm surface for the two components of a binary mixture. (a) False 3-D plot of the isotherm surfaces for the two components. $RQ_s = 0.5$. The specific column saturation capacity is larger for the first component ($Q_{s,1} = 5$) than for the second ($Q_{s,2} = 2.5$). Apparent isotherm intersection takes place ($a_1 = 24$; $a_2 = 28.8$). (b) Contour map of the isotherm surface for the first compound. $RQ_s = 1.0$. Isotherm coefficients: $a_1 = 24$; $a_2 = 28.8$; $b_1 = 12$; $b_2 = 14.4$. The specific saturation capacity is the same for the two components $Q_{s,1} = Q_{s,2} = 2.0$. The pure component isotherms do not intersect. The straight lines are intersections of the isotherm surface with the following planes: 1, $Q_1 = 0.10\, Q_{s,1}$ (×); 2, $Q_1 = 0.167\, Q_{s,1}$ (△); 3, $Q_1 = 0.25\, Q_{s,1}$ (◇); 4, line $C_2 = 1/\alpha C_1$ (□). (c) Same as (b), except $RQ_s = 0.25$ ($Q_{s,1} = 2.0$, $Q_{s,2} = 0.5$, $b_2 = 57.6$). The single-component isotherms intersect (see Fig. 2).

Fig. 1b and c has the same features. For both components, the isotherm surfaces obtained in either instance look similar. The isotherms corresponding to the case when the column saturation capacity is four times larger for the lesser than for the more retained component do not have any special property. In cases where the competitive Langmuir model is valid, isotherm intersection cannot have any direct consequence in chromatography, as the coordinates of the intersection point have no physical significance and the separation factor of the system for the two components $[(Q_2/C_2)/(Q_1/C_1) = a_2/a_1 = \alpha]$ is independent of the concentrations. It is also independent of the column saturation capacities of the two components but depends only on the ratio of the origin slopes of the isotherms.

Fig. 2 shows the overlaid plots of the single-component isotherms of both components of the mixture in the case when the column saturation capacity of the second-eluted component is four times smaller than that of the first. The single-component isotherms which intersect on a $Q_i(C_i)$ *versus* C_i plot are in fact the curves $Q_1(C_1)$ and $Q_2(C_2)$, which have nothing in common, not even the abscissa! The first curve is a plot of Q_1 *versus* C_1, at equilibrium of the first component between the two phases of the system, and the second curve is a plot of Q_2 *versus* C_2 under the same conditions. The intersection point has two different sets of coordinates depending on whether it is

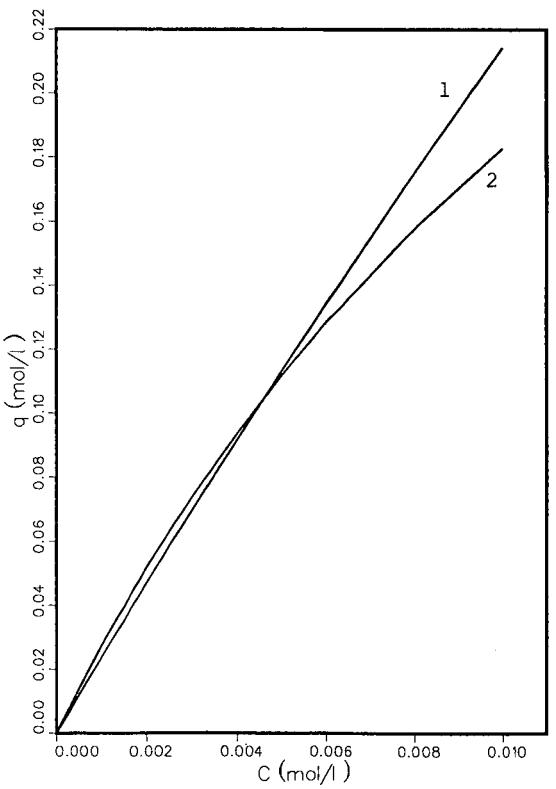

Fig. 2. Single-component isotherm of two solutes. $Q_1 = a_1C_1/(1+b_1C_1)$, $Q_2 = a_2C_2/(1+b_2C_2)$, $a_i = k'_{0,i}/F$, $k'_{0,1} = 6$, $Q_{s,1} = 2$, $Q_{s,2} = 0.5$, $b_i = a_i/Q_{s,i}$. The two isotherms intersect at $C = 0.00463$ M.

considered as a point on the first curve or a point on the second curve. It has no physical meaning. It does not exist on Fig. 1c.

The situaton may be different in displacement chromatography; it has been claimed that displacement is impossible in the case when single-component isotherms intersect because the elution order of the plateau concentration of the isocratic train would be different from the elution order at very low concentrations [3]. This requires further investigation.

Effect of single-component isotherm intersection in displacement chromatography

Rhee and Amundson [10] reported a detailed theoretical study of displacement chromatography within the framework of the ideal model, using the competitive Langmuir isotherm. They showed that in this case it is always possible to achieve an isotachic train provided that a sufficiently long column is used and that the displacer concentration exceeds a threshold concentration given by

$$C_d > \frac{1}{b_d}\left(\frac{a_d}{a_f} - 1\right) \tag{4}$$

where C_d is the displacer concentration, $a_d/a_f = k'_{0,d}/k'_{0,f}$ is the ratio of the slopes of the displacer isotherm and of the less retained component isotherm at infinite dilution and $b_d = a_d/q_{s,d}$ is the second parameter of the competitive Langmuir isotherm of the displacer.

We have recently shown that in the case of an actual column with a finite efficiency, the critical parameters in displacement chromatography are the displacer concentration, the loading factor and the column efficiency. This efficiency is the limiting efficiency obtained with very small size samples and results from the effects of axial dispersion and the resistances to mass transfers [11]. The same condition as stated by eqn. 4 applies in non-ideal and ideal chromatography. However, when the displacer concentration increases, the plateau becomes narrower and narrower. In non-ideal chromatography the plateau is eroded because of the finite rate of the mass-transfer kinetics. It may disappear if the displacer concentration is too large [11].

Thus, the theory of non-linear chromatography predicts that, as long as the competitive Langmuir isotherm model is valid, we must be able to generate isotachic trains in displacement chromatography, even if the single-component isotherm intersect. In this last case, the column saturation capacity for the second component is smaller than that of the first. To illustrate this point, which is important, let us compare the separation of two binary mixtures, A + B and A + B′, and assume that the only difference between these problems is in the column saturation capacity for the second component, which is larger for B than for B′. The isotherm surface for the first component, A, and the coefficient a_2 for the second component, B or B′, is the same in both instances. If we inject the same amount of a feed having the same relative concentration ([A]/[B] = [A]/[B′]) of the two components, the loading factor of the second component is larger in the second case (B′) than in the first (B). The successful formation of an isotachic displacement train in the second case (lower column saturation capacity for B′) requires that we reduce the loading factor for B′ by using either a smaller sample size or a longer column. The proper set of experimental conditions may be more difficult to achieve for B′ than for B.

The calculation of the chromatograms obtained in displacement chromatography under a variety of experimental conditions illustrates these theoretical considerations.

RESULTS AND DISCUSSION

Fig. 2 shows the single-component isotherms corresponding to the competitive isotherms in Fig. 1c. These two isotherms intersect at $C_1 = C_2 = 0.00463$ M. Figs. 3 and 4 compare the profiles of the zones of two compounds in displacement chromatography, for the same sample size. In Fig. 3, the column saturation capacities of the two components are identical ($Q_{s,1} = Q_{s,2} = 2.0$; the isotherms are not shown, since they are classical). In this figure, a successful isotachic displacement train has been formed. In Fig. 4 ($Q_{s,1} = 2$, $Q_{s,2} = 0.5$), in contrast, the isotachic displacement train is not formed although the amounts of the two components injected are the same for both Figs. 3 and 4. The zone profiles observed are typical of those taking place during this isotachic train formation [11,12]. The reason is that, as the sample size is the

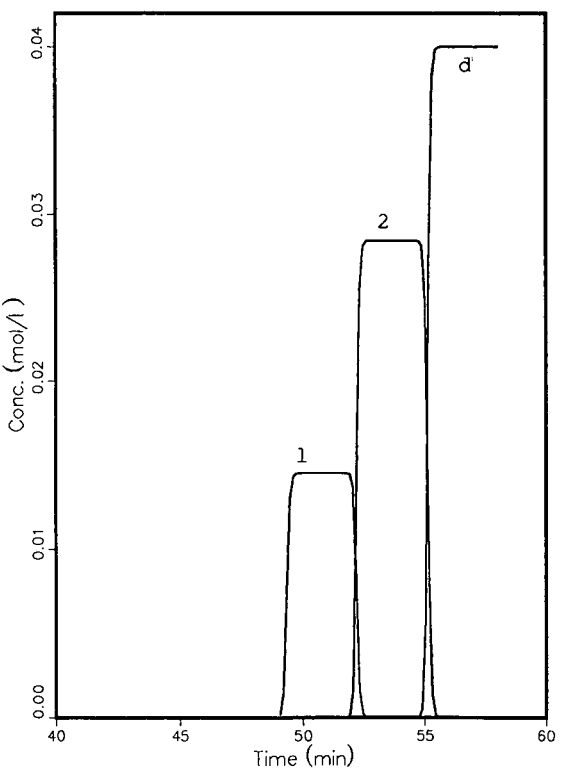

Fig. 3. Calculated zone profiles in displacement chromatography. Experimental conditions: phase ratio, $F = 0.25$; flow velocity, 0.05 cm/s; column length, 25 cm; efficiency, $N = 5000$ theoretical plates. Langmuir competitive isotherm: $Q_i = a_i C_i/(1 + b_1 C_1 + b_2 C_2 + b_d C_d)$, $a_i = k'_{0,i}/F$, $k'_{0,1} = 6$, $\alpha_{1,2} = k'_{0,2}/k'_{0,1} = 1.2$, $\alpha_{2,d} = k'_{0,d}/k'_{0,2} = 1.2$, $Q_{s,1} = Q_{s,2} = Q_{s,d} = 2$, $b_i = a_i/Q_{s,i}$. Sample size: injection time, $t_p = 250$ s; feed concentration, $C_1^0 = 0.01$ M, $C_2^0 = 0.02$ M, $C_d^0 = 0.04$ M; $L_{f,1} = 0.01$, $L_{f,2} = 0.02$.

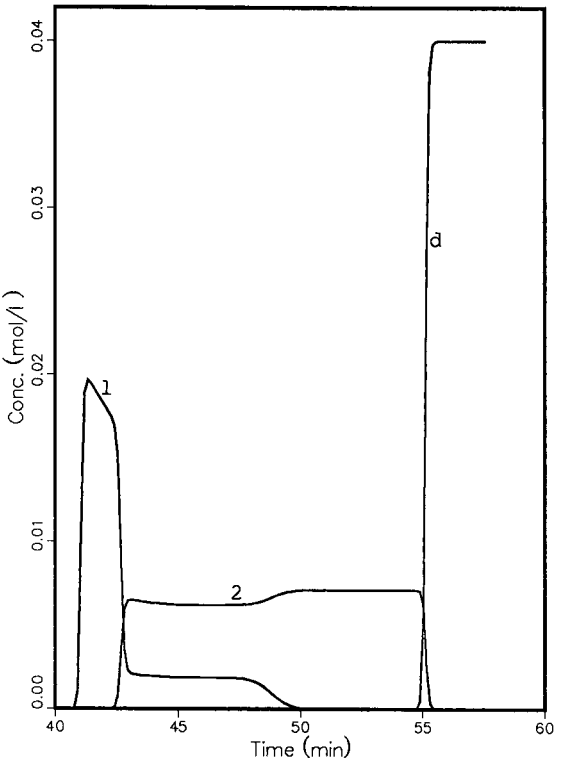

Fig. 4. Calculated zone profiles in displacement chromatography. Experimental conditions as for Fig. 3, except $Q_{s,1} = Q_{s,d} = 2$, $Q_{s,2} = 0.5$, $L_{f,1} = 0.01$, $L_{f,2} = 0.08$.

same for both figures and the column saturation capacity of the second component is four times smaller for Fig. 4 than for Fig. 3, the loading factor for the second component is four times larger in Fig. 4 than in Fig. 3, 8% instead of 2%. The loading factor is inversely proportional to the volume of stationary phase, and hence decreases with increasing column length, in proportion to the reverse of this length.

The zone profiles of the same binary mixture used for Fig. 4 is shown in Figs. 5 and 6, with longer columns, 35 and 50 cm, respectively. Thus, for the same sample size, the loading factors for the second component are 5.7% and 4%, respectively. The formation of the isotachic train is more advanced in Fig. 5 than in Fig. 4 and it is successful in Fig. 6. *We note, however, a remarkable difference between Figs. 3 and 6.* In Fig. 3, the heights of the plateaux of each successive zone increase from the first to the second component and to the displacer. This is the normal behavior, when single-component isotherms do not intersect: the operating lines intersect successively the isotherms of these compounds in this order, corresponding to increasing mobile phase concentrations [10–12]. However, *when the single-component isotherms intersect and if the displacer concentration is high enough, the operating line encounters the second component isotherm before, and at a lower concentration than, the first component isotherm.* Thus, the plateau of the second zone is lower than the plateau of the first.

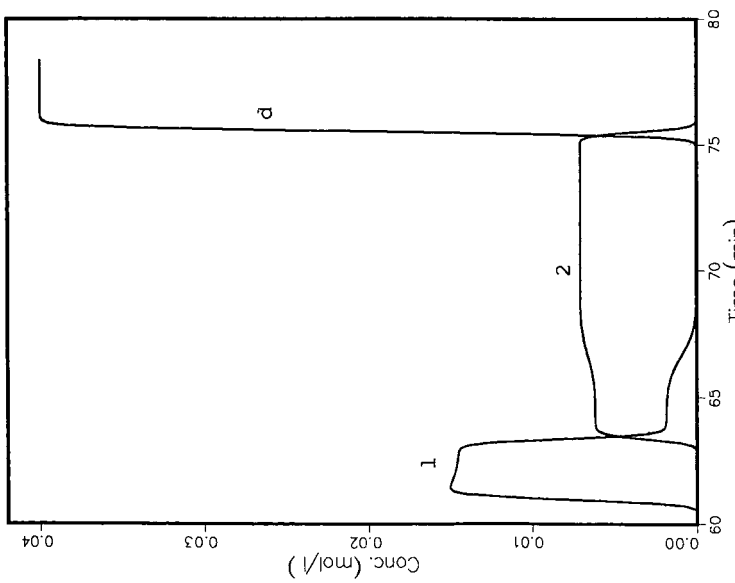

Fig. 5. Calculated zone profiles in displacement chromatography. Experimental conditions as for Fig. 4 (including sample size), except column length, $L = 35$ cm; hence $L_{f,1} = 0.007$, $L_{f,2} = 0.057$.

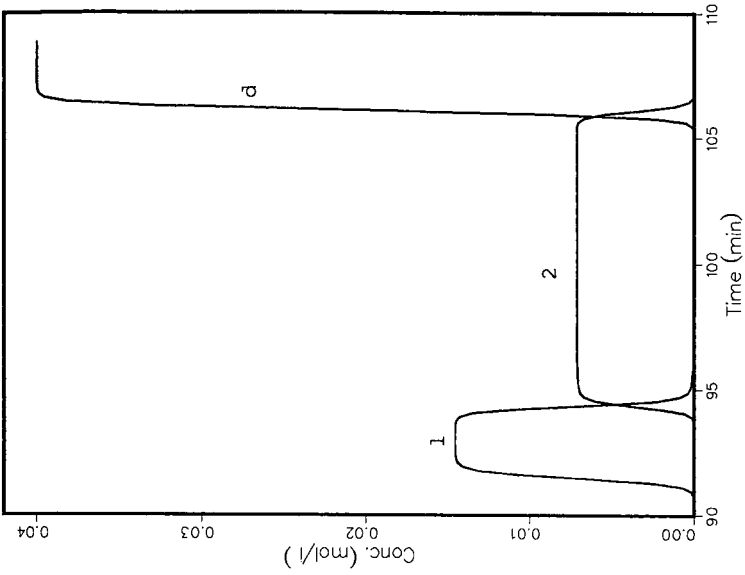

Fig. 6. Calculated zone profiles in displacement chromatography. Experimental conditions as for Fig. 4, except column length, $L = 50$ cm; hence $L_{f,1} = 0.005$, $L_{f,2} = 0.04$.

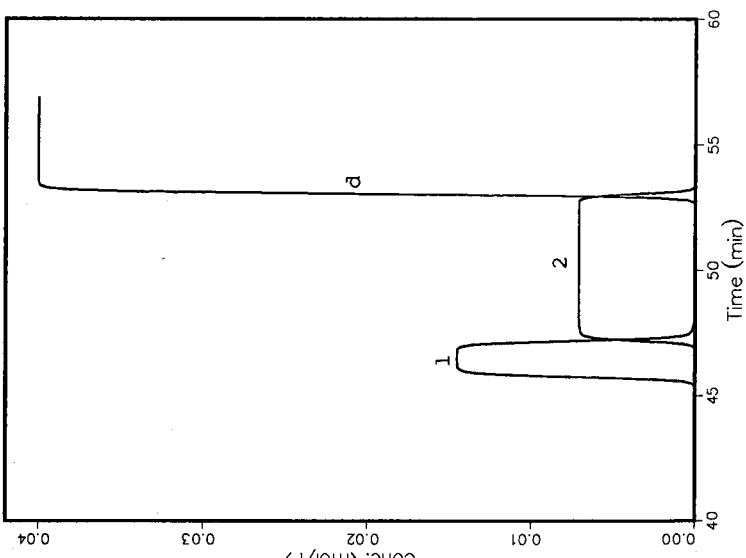

Fig. 7. Calculated zone profiles in displacement chromatography. Experimental conditions as for Fig. 4 (including column length and feed composition), except sample size, $t_p = 125$ s; hence $L_{f,1} = 0.005$, $L_{f,2} = 0.04$.

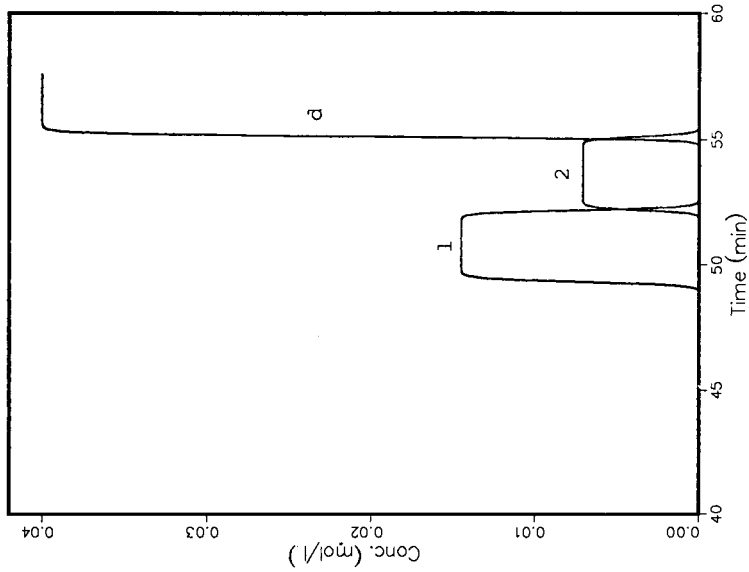

Fig. 8. Calculated zone profiles in displacement chromatography. Experimental conditions as for Fig. 4 (including injection time), except $C_{0,2} = 0.005$ M; hence $L_{f,1} = 0.01$, $L_{f,2} = 0.02$.

This result is also in agreement with the prediction of the equations giving the heights of the zones in displacement chromatography [10,11].

Instead of decreasing the loading factor by using a longer column, we can decrease it by using a smaller sample size. We show in Fig. 7 the chromatogram obtained with a sample size half that in Fig. 4 and a column length of 25 cm; the loading factors for the two components are the same as in Fig. 6. In Fig. 8, the composition of the feed has been changed so that the amount of first component injected is the same as in Fig. 3 or 4, but the amount of second component injected is four times smaller. The corresponding loading factors for the second component are 4% for Fig. 7 and 2% for Fig. 8. The loading factors for the two components are now the same in Figs. 3 and 8. In both instances, the successful formation of an isotachic displacement train is observed, although in Fig. 3 the single-component isotherms do not intersect ($Q_{s,2}/Q_{s,1} = 1$) whereas in Fig. 8 they do ($Q_{s,2}/Q_{s,1} = 0.25$). As expected, the heights of the plateaux of the two components are the same in Figs. 6–8, as the displacer concentration is the same in all instances, but the lengths of the plateaux are two and four times shorter in Figs. 7 and 8 than in Fig. 6, respectively.

These theoretical results and also those derived in overloaded elution chromatography [8,9] are in contradiction with most experimental observations [1–3] whereas they agree well when the column saturation capacities are equal [5]. This suggests that the Langmuir competitive isotherm fails to predict correctly the equilibrium behavior of a binary mixture when the column saturation capacities of the two components are different. A more sophisticated model, such as that provided by the ideal adsorbed solution theory (IAS) [13], must be used. The IAS model predicts that the separation factor of the mixture (Q_2C_1/C_2Q_1) depends on the concentrations of the two components. As a consequence, very different results are obtained with this model which are in qualitative agreement with experimental observations [14,15].

CONCLUSION

The formation of an isotachic displacement train is possible, whether the single-component isotherms intersect or not, under the condition that the equilibrium behavior of the binary mixture studied is correctly accounted for by the competitive Langmuir model. This result completes the demonstration that in this instance single-component isotherm intersection is not a physical phenomenon but an illusion (similarly to optical illusions). The formation of an isotachic displacement train simply requires that the loading factor be lower than a critical threshold. This result can be achieved by adjusting properly either the column length or the sample size.

It should be emphasized that thermodynamic consistency requires that the column saturation capacities for two compounds whose binary competitive adsorption is accounted for by the Langmuir model should be the same. Otherwise, the Gibbs–Duhem equation is not satisfied [16]. Frey [17] has given an interesting demonstration of the thermodynamic impossibility of an isotachic displacement train when the two isotherms intersect and the concentrations exceed those corresponding to the intersection point. He showed that the free energy consumed at the hypothetical front between the two components (with the component more retained at low concentrations placed upstream, as predicted by the Langmuir model) would be negative. Finally, and importantly, the competitive Langmuir isotherm model does

not give a very good representation of equilibrium data in most instances and this is especially true when the ratio of the column saturation capacities of the two compounds is significantly different from unity [7]. We consider this to be the main block at present to further progress in the understanding of the separation process in chromatography and in the derivation of accurate predictions of production rates and recovery yields.

Finally, all the conclusions of this work are valid only as long as the competitive Langmuir isotherm model represents correctly the phase equilibria involved. Serious deviations from this model resulting in single-component isotherms which intersect may also lead to situations where displacement would be impossible, even though the isotherms are still convex upwards. If we assume that the single-component isotherms follow the Langmuir behavior, the IAS theory predicts that the separation factor depends on the concentrations of both components when the column saturation capacities of the two components are different. It predicts a reversal of the elution order when the single-component isotherms intersect. Then the formation of an isotachic train may become impossible, at least in some range of experimental conditions.

ACKNOWLEDGEMENTS

This work was supported in part by Grant CHE-8901382 of the National Science Foundation and by the cooperative agreement between the University of Tennessee and the Oak Ridge National Laboratory. We acknowledge support of our computational effort by the University of Tennessee Computing Center.

REFERENCES

1 G. B. Cox and L. R. Snyder, *J. Chromatogr.*, 483 (1989) 95.
2 G. Viscomi, S. Lande and Cs. Horváth, *J. Chromatogr.*, 440 (1989) 157.
3 G. Subramanian and S. Cramer, *Biotechnol. Prog.*, 5, No. 3 (1989) 92.
4 G. M Schwab, in *Ergebnisse der Exacten Naturwissenschaften*, Vol. 7, Springer, Berlin, 1928, p. 276.
5 S. Jacobson, S. Golshan-Shirazi and G. Guiochon, *J. Am. Chem. Soc.*, 112 (1990) 6492.
6 J.-X. Huang and G. Guiochon, *J. Interface Colloid Sci.*, 128 (1989) 577.
7 A. M. Katti and G. Guiochon, *J. Chromatogr.*, 499 (1990) 21.
8 S. Golshan-Shirazi and G. Guiochon, *Anal. Chem.*, 62 (1990) 217.
9 M. Z. El Fallah, S. Golshan-Shirazi and G. Guiochon, *J. Chromatogr.*, 511 (1990) 1.
10 H. K. Rhee and N. R. Amundson, *AIChE J.*, 28 (1982) 423.
11 S. Golshan-Shirazi and G. Guiochon, *Anal. Chem.*, 61 (1989) 1960.
12 A. M. Katti and G. Guiochon, *J. Chromatogr.*, 449 (1988) 25.
13 M. D. Le Van and T. Vermeulen, *J. Phys. Chem.*, 85 (1981) 3247.
14 S. Golshan-Shirazi and G. Guiochon, *J. Chromatogr.*, submitted for publication.
15 Cs. Horváth, presented at the *7th International Symposium on Preparative Chromatography*, Ghent, April 1990.
16 C. Kemball, E. K. Rideal and E. A. Guggenheim, *Trans. Faraday Soc.*, 44 (1948) 948.
17 D. Frey, *J. Chromatogr.*, 409 (1987) 1.

Journal of Chromatography, 541 (1991) 207–220
Elsevier Science Publishers B.V., Amsterdam

CHROM. 22 911

Sample displacement mode chromatography: purification of proteins by use of a high-performance anion-exchange column[a]

K. VEERARAGAVAN, A. BERNIER and E. BRAENDLI*

BioSeparation Group, Biochemical Engineering Section, Biotechnology Research Institute, National Research Council of Canada, Montreal, Quebec, H4P 2R2 (Canada)

(First received June 18th, 1990; revised manuscript received October 4th, 1990)

ABSTRACT

In sample displacement mode (SDM) chromatography, the column is overloaded with sample until it is saturated with the product of interest, while weakly binding impurities are displaced. Because the method makes use of the full capacity of a column, it is interesting for large-scale fine purfication of proteins. By using two columns in series, the product can be separated from both strongly and weakly binding impurities. The working principle of SDM was proved by using Mono Q ion-exchange columns. Crude samples of ovalbumin and soybean trypsin inhibitor were applied to one- and two-column systems and the sequence and purity of both the displaced and the eluted components were determined by off-line analyses. Conditions such as column dimensions, load flow-rate, buffer type and temperature have to be optimized for each target protein and associated impurities in order to maximize the yield and purity by minimizing overlapping.

INTRODUCTION

Displacement mode chromatography has been used to efficiently purify antibiotics [1–3], steroids [3–5], amino acids [6], peptides [3,7,8] and proteins [3,9] at semi-preparative and preparative scales on reversed stationary phases. In this method, the sample mixture in a carrier solvent that has a low affinity for the stationary phase is loaded and the bound components are displaced by a solution of displacer which has a greater affinity for the stationary phase than any of the sample components [10].

This concept has recently been extended to sample displacement mode (SDM) chromatography by Hodges *et al.* [11], who used it to purify peptides with reversed-phase columns. During loading, there is competition among the sample components for the hydrophobic adsorption sites of the stationary phase. The more hydrophobic components compete more successfully for these sites than the more hydrophilic components, which are displaced and eluted from the column. Finally, the adsorbed components are eluted with an aqueous organic eluent. Whereas in ordinary

[a] NRCC No. 32 402.

0021-9673/91/$03.50

displacement chromatography the displacement train fully develops during the elution of the non-saturated column, in the sample displacement mode the bands form only during the load procedure and the columns are fully saturated. Hodges *et al.* [11] used a two-column SDM strategy to purify the peptide of interest from a synthetic mixture of prepurified hydrophobic and hydrophilic impurities. The hydrophobic impurities were adsorbed on the precolumn whereas the hydrophilic impurities were displaced from the main column, leaving the main column filled with the peptide of interest. The adsorbed components from the columns were eluted separately by a solvent gradient. The size of the precolumn was optimized based on the known concentration of the impurities present in the sample.

The purification of peptides by reversed-phase SDM chromatography by Hodges *et al.* [11] is the only report to date. As organic solvents are involved, reversed-phase high-performance liquid chromatographic (HPLC) columns generally cannot be used to separate native proteins. Therefore, in this paper we tried to purify two proteins, ovalbumin and soybean trypsin inhibitor (STI), by SDM chromatography using high-resolution anion-exchange (Mono Q) columns. The matrix of Mono Q columns consists of monodisperse hydrophilic material. The working principle of SDM chromatography and its potential to generate highly purified proteins had to be proved with this column type.

EXPERIMENTAL

Chemicals

Bovine serum albumin (BSA), soybean trypsin inhibitor (STI), trypsin (L-1-tosylamide-2-phenylethyl chloromethyl ketone treated), Nα-benzoyl-L-arginine-*p*-nitroanilide (BAPNA) hydrochloride and Tris were obtained from Sigma (St. Louis, MO, U.S.A.). Chemicals used for electrophoresis were obtained from Bio-Rad Labs. (Mississauga, Canada). HPLC-grade acetonitrile was obtained from Fisher Scientific (Montreal, Canada). HPLC-grade trifluoroacetic acid (TFA) was obtained from Pierce (Rockford, IL, U.S.A.). All other chemicals were of analytical-reagent grade.

Apparatus

The fast protein liquid chromatographic (FPLC) system consisted of an LCC-500 controller, two P-500 pumps, an MV-7 injection valve, a solvent mixer, a sample loop (50 ml), a UV-1 monitor, a dual-pen recorder and a Frac-100 fraction collector from Pharmacia (Baie D'Urfé, Canada). High-resolution anion-exchange columns, Mono Q 5/5 (Pharmacia), were used in the FPLC unit. In the SDM experiments, the protein samples (200–500 mg dry weight) dissolved in 25 m*M* piperazine–HCl buffer (pH 6.0) (buffer A) were loaded on one Mono Q column or two Mono Q columns connected in series. After loading the samples, the columns were washed individually with buffer A and the adsorbed proteins were eluted with a gradient of sodium chloride in buffer A. The fractions collected were desalted on a PD-10 column (Pharmacia) and used for further analyses. An aliquot (200 μl) of each fraction containing about 0.5 mg of protein was analysed by FPLC on a Mono Q column under the conditions described in Fig. 2, to evaluate its composition.

Another aliquot of each fraction was analysed by HPLC to monitor the composition of the sample. The HPLC analyses were performed with a Waters Assoc.

(Mississauga, Canada) HPLC system consisting of two Model 590 pumps, a Model 490 programmable multi-wavelength detector, a Model 712 WISP autoinjector, a Model 840 data collection system and an LA50 recorder. A Vydac C_{18} reversed-phase column (CSC, Montreal, Canada) was used for this purpose. The proteins adsorbed on the reversed-phase column were eluted by a gradient of 0.1% TFA–acetonitrile in 0.1% TFA–water.

Gel electrophoresis

Electrophoretic analyses were performed in the Bio-Rad system. Selected eluted fractions were analysed for purity by native and sodium dodecyl sulphate polyacrylamide gel electrophoresis (SDS-PAGE). Electrophoresis was performed with a 4% stacking and 10% running gels as described in detail elsewhere [12]. The gels were stained with Coomassie Brilliant Blue R-250 (0.025%) and destained in 10% (v/v) isopropanol containing 10% (v/v) acetic acid as described by Krueger *et al.* [13].

STI assay

STI activity was measured by the method of Fritz *et al.* [14] using BAPNA as substrate. The specific activity of STI was expressed as international inhibitor milli unit (ImU)/mg protein. One ImU is defined as a decrease of $\Delta E = 0.00332$ per min per 3 ml (or 0.01 per 3 min per 3 ml) in the extinction change at 405 nm resulting from the formation of *p*-nitroaniline from BAPNA.

Protein concentration

The protein concentration was determined by the method of Bradford [15] using BSA as standard. STI concentration was determined using a specific absorbance, $A_1^{1\%}{}_{cm}$ (280 nm), of 8.9.

RESULTS

Ovalbumin

A typical elution chromatogram of 0.7 mg of ovalbumin sample applied at 1.0 ml/min to a Mono Q column with a capacity of 30–50 mg of protein is shown in Fig. 1. There is one main peak (peak 5) and five minor peaks (peaks 1–4 and 6). When the peak 5 was analysed by SDS-PAGE, it showed a molecular mass of 43 000, indicating that it

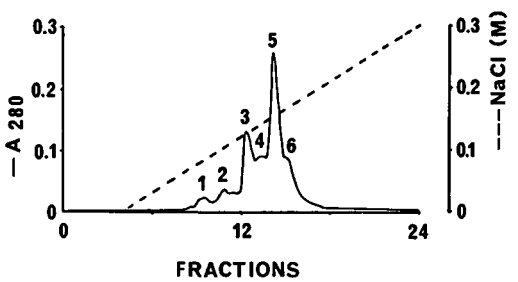

Fig. 1. Typical elution chromatogram of 0.7 mg of crude ovalbumin. Ovalbumin (0.7 mg in 0.5 ml) was loaded on a 5/5 Mono Q column at 1.0 ml/min, washed with 4 ml of 20 m*M* piperazine–HCl buffer (pH 6.0) and eluted with a 0–0.3 *M* linear gradient of NaCl in 20 m*M* piperazine–HCl buffer (pH 6.0) over 20 min.

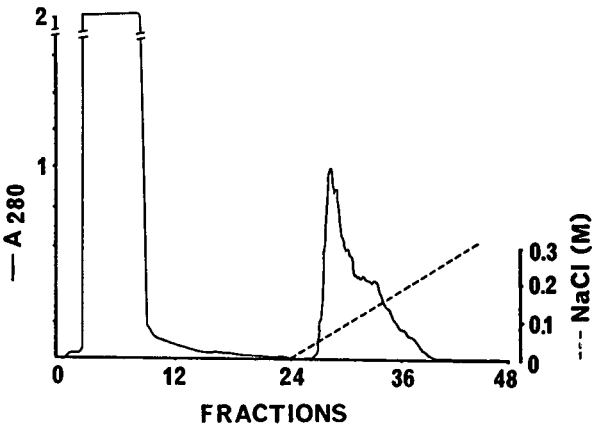

Fig. 2. SDM chromatogram of 200 mg of crude ovalbumin on a 5/5 Mono Q column. The sample (10 mg/ml) was loaded at a flow-rate of 0.2 ml/min, washed with 20 m*M* piperazine–HCl buffer (pH 6.0) at a flow-rate of 1.0 ml/min and eluted at a flow-rate of 1.0 ml/min with a 0–0.3 *M* linear gradient of NaCl in the same buffer for 20 min. Fractions of 2 ml while loading and 1 ml while washing and eluting were collected.

is an ovalbumin peak (data not shown). There is just one major compound (peak 6) in the mixture that binds more strongly than ovalbumin.

To isolate peak 5 from peak 6, which is more anionic, and peaks 1–4, which are less anionic proteins, 200 mg of crude ovalbumin (10 mg/ml) were loaded on one Mono Q column at a flow-rate of 0.2 ml/min (Fig. 2). The column flow-through, wash and eluted fractions were analysed by FPLC with a Mono Q column under standard conditions (Fig. 3).

The analysis of the flow-through fractions showed that after four fractions or 8 ml of sample had been loaded on the column, only proteins of peaks 1–3 were detected in the column effluent. In other words, the column was already saturated with these compounds and they were being displaced by the more strongly binding protein components. Fraction 6 of the flow-through indicated that the product, peak 5, was starting to be displaced and fraction 8 was similar to the load sample; only peak 6 was still fully retained in the column. According to this displacement pattern, we expect the whole amount of peak 6 and part of peak 5 to be bound in the column. The elution profile of the saturated Mono Q column did not allow any interpretation, as distinct protein peaks were not visible. An analysis of the early fraction 28 of the eluted material showed that even after extensive washing of the column with buffer until the absorbance at 280 nm was zero, small amounts of peaks 3 and 4 could still be found in the eluate with the main peak 5 of the product. This finding was unexpected, as peak 5 was already found in the effluent and peaks 3 and 4 should have been displaced. Peak overlapping can obviously be a problem.

To study further the efficiency of displacing the less anionic by the more anionic species in a sample, 500 mg of ovalbumin were passed through two Mono Q columns connected in series. After loading the sample, the columns were separated, washed and eluted individually (Fig. 4). All the flow-through, washing and eluted fractions were analysed not only by FPLC but also by HPLC and native gel electrophoresis.

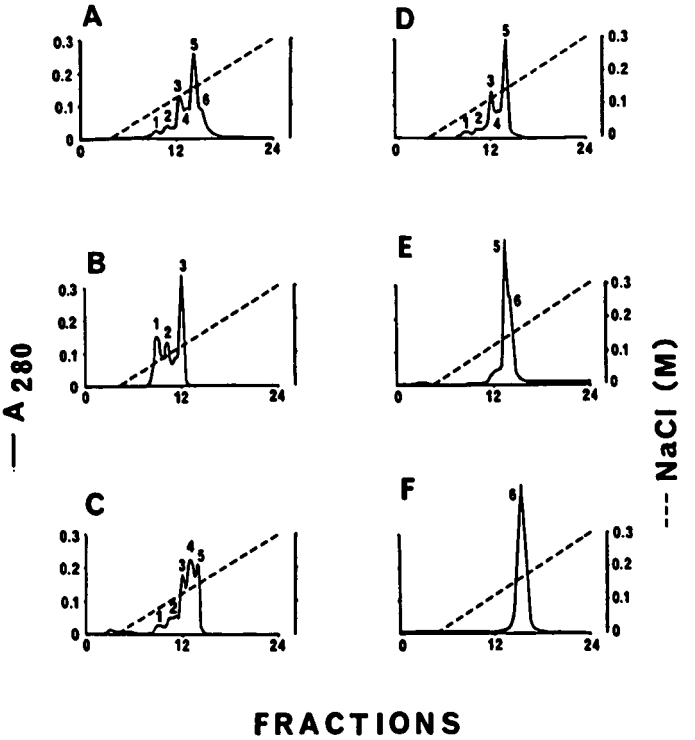

Fig. 3. FPLC analyses of the fractions from Fig. 2. The loading, washing and elution conditions were as in Fig. 1. (A) Crude ovalbumin; (B) fraction 4; (C) fraction 6; (D) fraction 8; (E) fraction 29; (F) fraction 36. Samples of about 0.7 mg of protein were analysed.

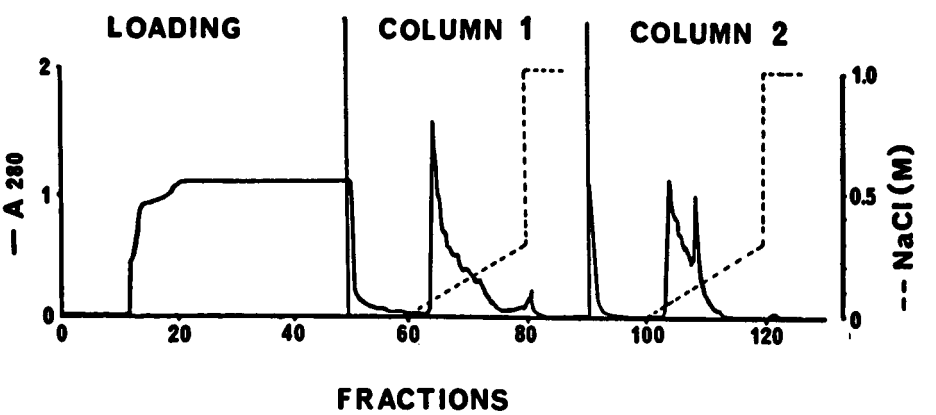

Fig. 4. SDM chromatogram of 500 mg of crude ovalbumin on two 5/5 Mono Q columns connected in series. The sample (10 mg/ml) was loaded at a flow-rate of 0.2 ml/min. After loading, the columns were disconnected and each column was individually washed with 20 m*M* piperazine–HCl buffer (pH 6.0) at a flow-rate of 1.0 ml/min and eluted at a flow-rate of 1.0 ml/min with a 0–0.3 *M* linear gradient of NaCl in the same buffer over 20 min. Fractions of 1 ml were collected.

After the application of about 10–12 ml of protein solution (100–120 mg of total protein) to the column, the absorbance at 280 nm in the effluent started to increase. Different compounds emerged sequentially and could be identified in the collected fractions (Figs. 4 and 5). The ovalbumin could be detected first in fraction 25. At that moment only material of peaks 5 and 6 should theoretically be bound in the two columns. Another 250-mg sample was loaded. The elution of columns 1 and 2 showed that only one wide peak could be detected by FPLC of these fractions (Fig. 5).

The HPLC analyses showed the presence of less anionic proteins which were displaced from both columns in early flow-through fractions (Fig. 6). Similarly, more anionic proteins (peaks 6 and 5) were accumulating in columns 1 and 2, respectively (Fig. 6C and D). However, two peaks were not resolved by the reversed-phase column.

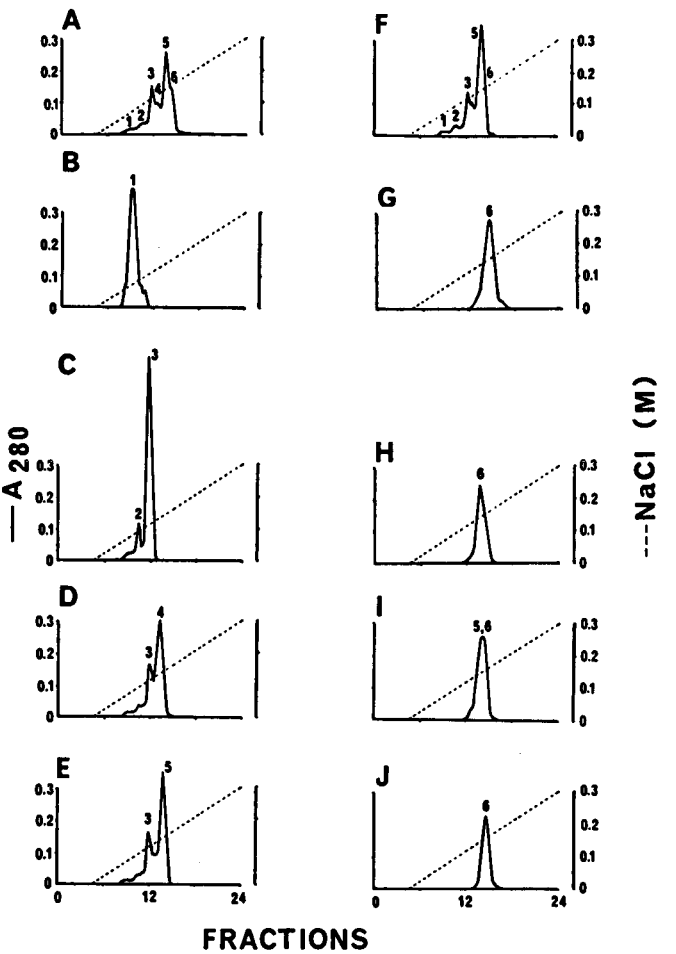

Fig. 5. Analyses of the fractions from Fig. 4. The loading, washing and elution conditions are explained in Fig. 1. (A) Crude ovalbumin; (B) fraction 13; (C) fraction 15; (D) fraction 21; (E) fraction 30; (F) fraction 49 (column I); (G) fraction 66; (H) fraction 70; (I) fraction 105 (column II); (J) fraction 109. Samples of 0.7 mg of protein were analysed.

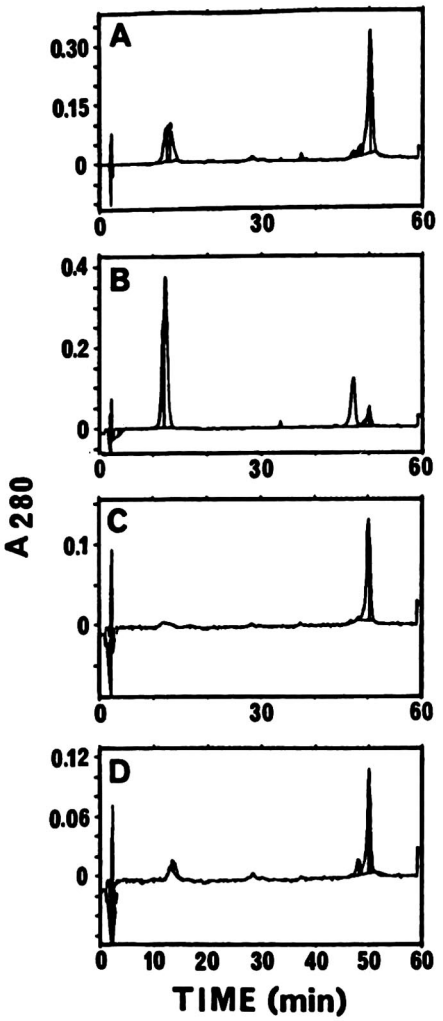

Fig. 6. HPLC analyses of fractions from loading and elution. (A) 250 μg of ovalbumin; (B) fraction 13; (C) fraction 66; (D) fraction 105. Fractions containing about 300 μg of protein were analysed.

Selected fractions were therefore analysed by native gel electrophoresis (Fig. 7), which confirmed the displacement process during the sample loading (Fig. 7C–F). The electrophoretic pattern of the eluate of column 1 (fractions 66 and 70) showed that at least three bands could be distinguished with this method. We expected only two bands, the ovalbumin and the strong binding material of the FPLC peak 6. Only in the elution fractions 109 and 110 of column 2 could highly purified ovalbumin be found.

The working principle having been proved by this first model system, we studied a second sample, which was a crude mixture of a trypsin inhibitor. In addition to analysis by FPLC, HPLC and electrophoresis, the purity and yield of this inhibitor compound could be calculated from activity determination.

Fig. 7. Native polyacrylamide (10%) gel electrophoresis of loading and elution fractions. (a) Low-molecular-mass standards (Bio-Rad Labs); (b) crude ovalbumin (40 μg); (c) fraction 13 (32 μg); (d) fraction 15 (45 μg); (e) fraction 21 (42 μg); (f) fraction 30 (31 μg); (g) fraction 66 (21 μg); (h) fraction 70 (38 μg); (i) fraction 109 (45 μg); (j) fraction 110 (36 μg). kD = kilodaltons.

Soybean trypsin inhibitor

Fig. 8 is a typical chromatogram of 2 mg of crude STI, showing at least eight distinguishable protein peaks. When these peaks were analysed for trypsin-inhibiting activity, all except peak 6 did not inhibit the enzyme. Therefore, we attempted to isolate the STI peak (peak 6) from the more anionic (peaks 8 and 7) and less anionic (peaks 1–5) proteins. Peak 6 showed a molecular mass of 21 500 by SDS-PAGE (data not shown). Peak 1 consists of material that is not or only slightly retained under the running conditions. Peak 8 only appears at very high salt concentrations compared with the salt gradients used for elution of the compounds.

To purify STI from the crude sample, 500 mg of protein solution (10 mg/ml) was passed at a flow-rate of 0.2 ml/min through two Mono Q columns connected in series. After loading the sample, the columns were washed and eluted individually (Fig. 9). All the flow-through, washing and eluted fractions were analysed by FPLC, HPLC and native gel electrophoresis.

The absorbance at 280 nm of the effluent started to rise after 22 fractions or 27 ml had been collected. The beginning (Fig. 10B), middle (Fig. 10C) and end (Fig. 10D) of the flow-through fractions analysed by FPLC are shown. The less anionic proteins were displaced one by one from both columns. The product peak 6 started to be displaced and could be detected by FPLC in fraction 30. The more strongly binding component of peak 8 could not be found in the column effluent during loading and was not found in the elution fractions of column 2. Even after extensive washing, the

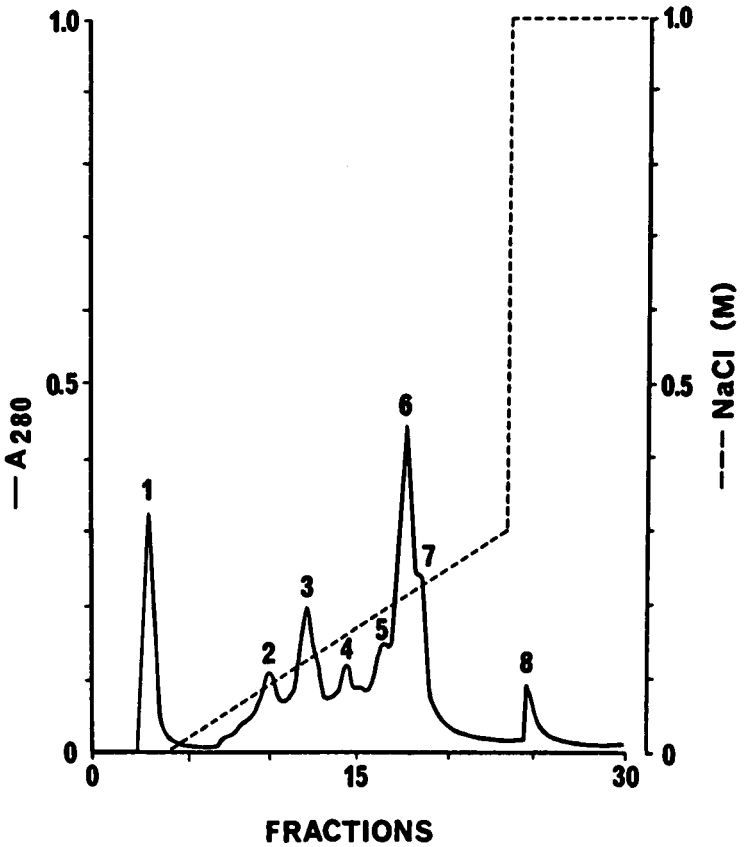

Fig. 8. Typical elution chromatogram for 2 mg of crude STI. STI (2 mg in 0.5 ml) was loaded on a 5/5 Mono Q column at a flow-rate of 1.0 ml/min, washed until 4.0 min with 20 m*M* piperazine–HCl buffer (pH 6.0) and eluted with a 0–0.3 *M* linear gradient of NaCl in the same buffer for 20 min and then with 1.0 *M* NaCl for 10 min.

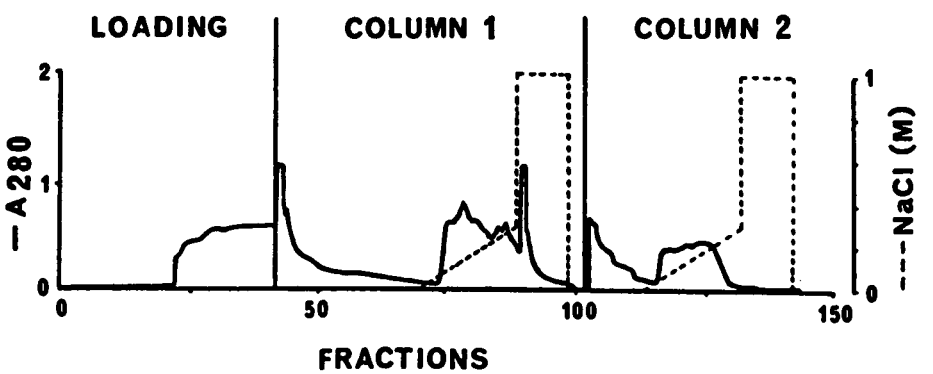

Fig. 9. Chromatogram of 500 mg of crude STI on two 5/5 Mono Q columns connected in series. The sample (10 mg/ml) was loaded at a flow-rate of 0.2 ml/min. After loading, the columns were disconnected and each column was washed individually with 20 m*M* piperazine–HCl buffer (pH 6.0) at a flow-rate of 1.0 ml/min and eluted at a flow-rate of 1.0 ml/min with a 0–0.3 *M* linear gradient of NaCl in the same buffer for 20 min and then with 1.0 *M* NaCl for 10 min. Fractions of 1.2 ml while loading and 1.0 ml while washing and eluting were collected.

TABLE I

PURIFICATION OF SOYBEAN TRYPSIN INHIBITOR BY SAMPLE DISPLACEMENT MODE CHROMATOGRAPHY

Fraction	Total protein (mg)	Specific activity (ImU/mg protein)	Purification (fold)	Recovery (%)
Crude	500	1940	1.0	100
Column 1	26	3233	1.7	8.7
Column 2	22	3798	2.0	8.8

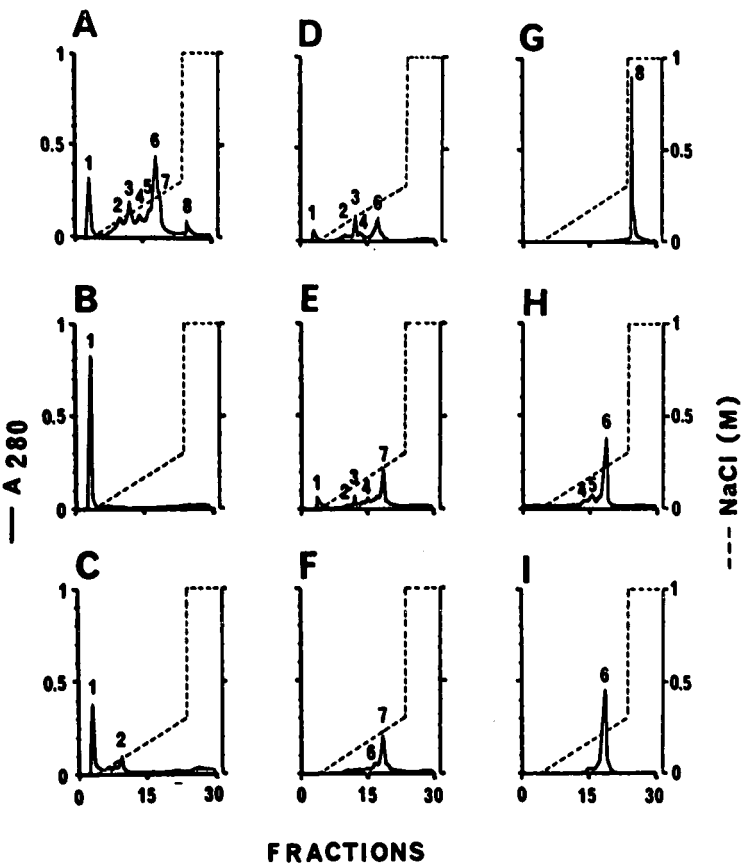

Fig. 10. Analyses of fractions (Fig. 9) by elution chromatography. The loading, washing and elution conditions were as in Fig. 8. (A) Elution chromatogram of 2 mg of crude STI; (B) fraction 5; (C) fraction 25; (D) fraction 30; (E) fraction 40; (F) fraction 77; (G) fraction 90; (H) fraction 122; (I) fraction 125. About 0.5 mg of protein was analysed for each fraction.

absorbance at 280 nm indicated that proteins were leaching from the column. The analysis of the wash fractions of columns 1 and 2 showed that material of peaks 2–6 was flushed from the columns. The wash buffer obviously not only removed the protein material in the void volume of the columns, but also displaced the less tightly binding components.

The first fractions eluted from column 1 contained product peak 6 and minor peaks 3–5. Already fraction 77 showed detectable amounts of impurity peak 7. Peak

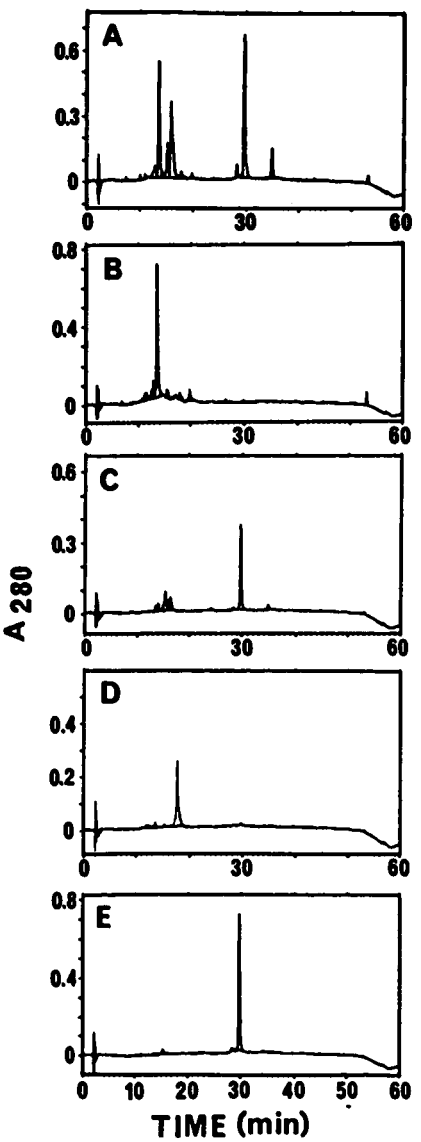

Fig. 11. HPLC analyses of the loading and eluted fractions. (A) 100 μg of crude STI; (B) fraction 5; (C) fraction 78; (D) fraction 90; (E) fraction 127. Fractions containing about 70 μg of protein were analysed.

7 is found mainly in fractions 78–87, simultaneously with peak 6. Only after increasing the salt concentration could the accumulated peak 8 be eluted as a highly purified fraction from column 1.

Column 2 was expected to be saturated by less strongly binding compounds, and this was confirmed by the FPLC analysis of the fractions. The main peak was STI, accompanied by peaks 3–5 in the early fractions. Peaks 7 and 8 could not be detected in these highly pure samples. Active fractions (123–126) were pooled and were found to be more than 95% pure by FPLC; they had a specific activity of 3798 ImU/mg protein (Table I). A two-fold purification of STI was achieved by this method. Nearly homogeneous protein was recovered from the second column. However, the STI recovered from the pooled fractions (77–80) from the first column had a specific activity of 3233 ImU/mg protein (Table I). The STI obtained from the selected fractions of columns I and II amounted to 26.19 and 22.41 mg of STI activity, accounting for 8.7 and 8.8% recoveries, respectively.

HPLC of the fractions revealed that the STI obtained from the later fractions in the second column (Fig. 11E) was homogeneous. However, STI recovered in the earlier eluting fractions from the first column contained a few less anionic impurities (Fig. 11C). These findings demonstrate that peaks 7 and 8 are efficiently adsorbed by the first column, but it is difficult to displace totally the less strongly binding compounds.

The fractions were analysed by native gel electrophoresis (Fig. 12). The results (Fig. 12c–e) confirmed that the different components in the mixture (Fig. 12b) were well displaced during sample loading starting with peak 1. The product peak 6 showed up in the latest load fractions. The two columns were therefore saturated with the components of peaks 6, 7 and 8. Fig. 12f and g show that highly pure material of peak 8 is eluted from column 1 under isocratic conditions with 1 *M* sodium chloride in the elution buffer. Electrophoretically pure STI could be eluted from column 2, as shown in Fig. 12h–j. As the concentration of STI in the eluate was very high, a large amount of material could be loaded directly on the gel.

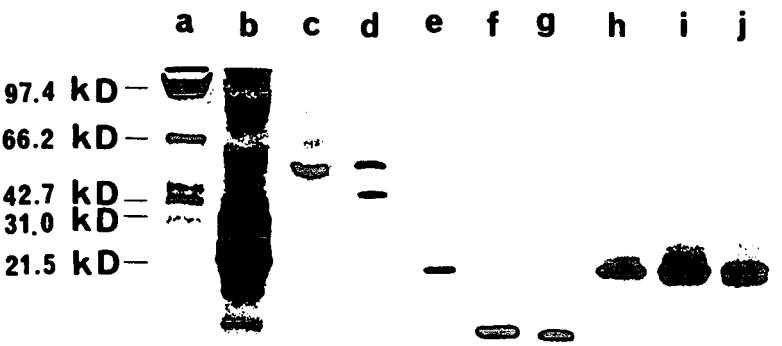

Fig. 12. Native polyacrylamide (12%) gel electrophoresis of the loading and eluted fractions. (a) Low-molecular-mass standards (Bio-Rad Labs.); (b) crude STI (40 μg); (c) fraction 5 (28 μg); (d) fraction 15 (24 μg); (e) fraction 40 (24 μg); (f) fraction 89 (23 μg); (g) fraction 90 (26 μg); (h) fraction 122 (29 μg); (i) fraction 125 (32 μg); (j) fraction 127 (26 μg). kD = kilodaltons.

DISCUSSION

By ordinary linear gradient elution chromatography on Mono Q, the number of components in the two samples ovalbumin and STI, and their relative binding strengths could be determined according to their elution sequence. Even by loading less than 3% of the column capacity in both examples, no baseline resolution was possible. In the overload run, the load flow-rate was reduced to 20%. By analyses of the effluent fractions in one-column experiments, we observed the expected competition between the various proteins present in the mixtures for the limited number of binding sites available in the column, which resulted in a sample displacement process. The elution pattern based on absorbance at 280 nm did not allow any interpretation concerning fraction composition. The analyses had to be done by high-resolution methods.

The results of the trials with ovalbumin gave valuable hints concerning the strategy of purification by sample displacement chromatography. Two situations are very favourable: (a) the product peak is the first peak in the elution chromatogram; in this instance, pure product can be collected in the column effluent until the column becomes saturated with the next most strongly binding compound. This application is only of interest when the product is a major component of the mixture, *i.e.*, the column has a reasonable capacity for the impurities. (b) The product is the most strongly binding compound in the mixture; in this instance, it can displace major amounts of impurities and then be eluted from a one-column system. However, these two favourable situations will rarely be met.

The next step towards a multi-column system, in which theoretically every component of the protein sample could be fixed to a column of the proper dimensions, was a two-column arrangement. The results indicated that the impurities that bind more strongly than the products could be caught in the first column. We expected the second column to be saturated with pure product only. The early eluted fractions in both examples, however, contained traces of weaker binding impurities, indicating that band overlapping due to semi-quantitative displacement will be a challenge in process development. We had not optimized the size of the columns to capture impurities and products and therefore were only able to collect a small percentage of the applied amount as pure products. To evaluate the required dimensions of a two-column system the breakthrough curves of the product and the next more strongly binding impurity will have to be determined. As the two-column approach in SDM leads to columns fully saturated with only the product of interest, the method enables the user to make maximum use of the binding capacity of the column.

These trials were planned to test the feasibility of SDM ion-exchange chromatography. The results show the need for systematic parameter variation in order to optimize throughput, yields and purity. Process optimization and the necessary automation require on-line analysis of the column effluent fractions.

ACKNOWLEDGEMENTS

The authors thank Dr. Yasuo Konishi for helpful discussions and Dr. Ian Reid for support during the preparation of the manuscript.

REFERENCES

1 H. Kalasz and Cs. Horváth, *J. Chromatogr.*, 215 (1981) 295.
2 K. Valko, P. Slégel and J. Bati, *J. Chromatogr.*, 386 (1987) 345.
3 G. Subramanian, M. W. Phillips and S. M. Cramer, *J. Chromatogr.*, 439 (1988) 341.
4 H. Kalasz and Cs. Horváth, *J. Chromatogr.*, 239 (1982) 423.
5 M. Verzele, C. Dewaele, J. Van Dijck and D. Van Hauer, *J. Chromatogr.*, 249 (1982) 231.
6 Cs. Horváth, J. Frenz and Z. El Rassi, *J. Chromatogr.*, 255 (1983) 273.
7 Gy. Vigh, Z. Varga-Puchany, G. Szepesi and M. Gazdog, *J. Chromatogr.*, 386 (1987) 353.
8 S. M. Cramer, Z. El-Rassi and Cs. Horváth, *J. Chromatogr.*, 394 (1987) 305.
9 G. Subramanian and S. M. Cramer, *Biotechnol. Prog.*, 5 (1989) 92.
10 Cs. Horvath, A. Nahum and J. H. Frenz, *J. Chromatogr.*, 218 (1981) 365.
11 R. S. Hodges, T. W. L. Burke and C. T. Mant, *J. Chromatogr.*, 444 (1988) 349.
12 U. K. Laemmli, *Nature (London)*, 227 (1970) 680.
13 B. K. Krueger, J. Forn and P. Greengard, *J. Biol. Chem.*, 252 (1977) 2764.
14 H. Fritz, I. Trautschold and E. Werle, in H. U. Bergmeyer (Editor), *Methods of Enzymatic Analysis*, Academic Press, New York, 2nd ed., 1974, p. 1064.
15 M. M. Bradford, *Anal. Biochem.*, 72 (1976) 248.

Journal of Chromatography, 541 (1991) 221–229
Elsevier Science Publishers B.V., Amsterdam

CHROM. 22 993

Measurement of lipophilicity indices by reversed-phase high-performance liquid chromatography: comparison of two stationary phases and various eluents

ANTOINE BECHALANY, ANNA TSANTILI-KAKOULIDOU[a], NABIL EL TAYAR and BERNARD TESTA*

Institut de Chimie Thérapeutique, Ecole de Pharmacie, Université de Lausanne, B.E.P., CH-1015 Lausanne (Switzerland)

(First received June 8th, 1990; revised manuscript received November 15th, 1990)

ABSTRACT

Twenty-eight benzene derivatives spanning a broad range of lipophilicities were used as model compounds to examine the optimum stationary phase and eluent conditions for the determination of lipophilic indices by reversed-phase high-performance liquid chromatography. This was assessed by linear regressions comparing published octanol–water partition coefficients with isocratic capacity factors and capacity factors extrapolated to 100% water in the eluent. Methanol–water eluents are always to be preferred to acetonitrile–water and tetrahydrofuran–water eluents. The octadecylsilane (ODS) phase yielded good correlations especially when a masking agent was added to the eluent, but this introduced an additional experimental variable. The octadecyl–polyvinyl copolymer (ODP) phase was just as satisfactory as the ODS phase without the need for a masking agent, and thus appears to be a valuable alternative.

INTRODUCTION

Lipophilicity, a medicinally relevant physico-chemical property, plays an influential role in many biological processes and therefore finds numerous applications in quantitative structure–activity relationship (QSAR) studies [1–4].

Partition coefficients have been measured in nearly 100 solvent–water systems, mainly by means of the traditional shake-flask method [2]. *n*-Octanol–water is widely accepted as the reference system because of its analogy with biomembranes [3]. However, practical disadvantages and the limitation to log P values between -2 and $+4$ have led researchers to investigate other methods for measuring lipophilicity [4,5]. In recent years, reversed-phase high-performance liquid chromatography (RP-HPLC) has become a popular alternative, capacity factors frequently being used as substitutes for octanol–water partition coefficients in QSAR studies.

The measurement of lipophilicity by RP-HPLC is based on the principle of the partition of a solute between a polar eluent and a stationary phase of low polarity.

[a] Permanent address: Faculty of Pharmacy, University of Athens, Athens, Greece.

0021-9673/91/$03.50

Under most conditions pure water cannot be used as the eluent and an organic modifier must be added to shorten the retention of solutes.

In order to suppress the effect of the organic modifier and to establish lipophilicity indices independent of eluent conditions the isocratic capacity factors determined at different organic modifier to water ratios are extrapolated to 100% water, yielding $\log k_w$ values [6,7]. Generally, the extrapolation is based on a quadratic relationship between isocratic capacity factors and the volume fraction x of the organic modifier [8,9]. When methanol is used as the organic modifier, a linear relationship is obtained for many solutes over a wide range of volume fractions; exceptions include very polar compounds such as caffeine or protonated bases [10]. Deviations from linearity have been attributed to silanophilic interactions, conformational changes of the solute, organic modifier absorbed on the stationary phase or changes in ionization in the case of ionizable solutes [11]. Further, methanol is unique among organic modifiers as it provides a strong hydrogen bond donor and acceptor capability and thus does not markedly alter the hydrogen-bonded network of water or affect polar interactions of solutes [12]. However, as methanol leads to inconveniently long retention times for the more lipophilic solutes, acetonitrile and tetrahydrofuran have also been used as organic modifiers in order to reduce retention times and to broaden the lipophilicity range measurable by RP-HPLC [13].

Octadecylsilane (ODS) is the most frequently used lipophilic stationary phase. This type of column, however, possesses a high proportion of free silanol groups which induce silanophilic interactions with basic and other polar compounds. This adsorption mechanism severely affects the partition behaviour of solutes between the eluent and the stationary phase; the addition of a masking agent such as *n*-decylamine or N,N-dimethyloctylamine to the mobile phase may decrease [14,15] but not necessarily suppress [16] such interactions. Unfortunately, a masking agent introduces an additional variable into the conditions owing to its own selective effect on retention [17]. In addition, its applicability is limited, as it cannot be used with acidic compounds owing to ion pair formation.

Recently, an octadecyl–polyvinyl copolymer [ODP, a poly(vinyl alcohol) gel esterified with octadecanoyl groups] has become available; being devoid of silanophilic interactions, it was shown to provide a valuable alternative as a stationary phase in lipophilicity measurements [18–20].

To assess better the relative merits of the ODS and ODP phases, we compared their performance under a variety of eluent conditions. Specifically, three organic modifiers were used, namely methanol as a hydrogen bond donor and acceptor, acetonitrile as a hydrogen bond acceptor of high polarity and tetrahydrofuran (THF) as a less polar hydrogen bond acceptor. The effects of *n*-decylamine as a masking agent of silanol groups were also investigated with each organic modifier in conjunction with the ODS stationary phase. Extrapolated lipophilicity indices ($\log k_w$) using methanol as the organic modifier were taken from a previously published study [19]. In the latter, lipophilicity indices were used to compare different stationary phases only.

EXPERIMENTAL

Materials

Monosubstituted benzenes purchased from Fluka (Buchs, Switzerland) and

Merck (Darmstadt, Germany) were of analytical-ragent grade and used without further purification. Methanol, acetonitrile and THF were purchased from Merck and were of adequate purity for HPLC.

Chromatography

A Siemens S 101 chromatograph equipped with an Orlita type DMP-AE 10.4 pump was used. The detector was a Uvikon 760 LC from Kontron operating at 254 nm. A Spectra-Physics SP 4100 computing integrator was used for peak registration and calculation of retention times.

Columns

The ODS column (25 cm × 4 mm I.D.) was prepacked with LiChrosorb RP-18, particle size 10 μm (Knauer, Berlin, Germany). The ODP column (15 cm × 6 mm I.D.) was prepacked with the copolymer gel, particle size 5 μm (Asahi Chemicals, Kawasaki, Japan).

Mobile phase preparation

Mobile phases were made up volumetrically from various combinations of methanol, acetonitrile and THF with a 0.02 *M* 3-morpholinopropanesulphonate buffer (pH 7.4), once with *n*-decylamine (0.2%, v/v) and once without. All solutions were purified by filtration using a Millipore Q system. Retention times, t_r, were obtained at ambient temperature (21 ± 1°C). The flow-rate was adjusted to 1.5 ml/min and the column dead time, t_0, was determined using the organic modifier as the non-retained compound. Capacity factors, log k_i, defined as $\log[(t_r - t_0)/t_0]$, were determined at 4 to 8 different fractions of organic modifier (range 90–10%) and extrapolated to 100% water as the mobile phase to yield log k_w values.

RESULTS AND DISCUSSION

The log k_w values were derived by extrapolation of the isocratic capacity factors, log k_i, and are presented in Tables I–III. Extrapolation was performed linearily when methanol was used as the organic modifier. Quadratic extrapolation was necessary when acetonitrile and THF were the organic modifiers. It should be noted that quadratic extrapolation has drawbacks, particularly when insufficient data are available in water-rich volume fractions. In such instances a possible error in isocratic capacity factors may be amplified, leading to unreliable log k_w values. Such extrapolation errors are apparent for log k_w values of some lipophilic compounds in our series, *e.g.*, the "unreasonably" high log k_w value of benzene obtained using acetonitrile on ODS. Indeed benzene, under these conditions, appears to be more lipophilic than toluene and benzophenone and almost as lipophilic as naphthalene.

To assess the validity of the different sets of log k_w values as lipophilicity indices, it was useful to establish their relationships with the corresponding octanol–water log *P* values obtained from the Hansch and Leo database [21] (Tabel IV). The isocratic capacity factors with organic solvent–water (50:50, v/v) eluents (data not given) were also included in such regression analyses in order to illustrate some limitations of extrapolating to 100% water.

TABLE I

EXTRAPOLATED CAPACITY FACTORS OF 28 MONOSUBSTITUTED BENZENES DETERMINED WITH VARIOUS ORGANIC SOLVENTS USING AN ODS STATIONARY PHASE AND A MASKING AGENT

No.	Compound	Log k_w		
		CH_3OH–D[a]	ACN–D[b]	THF–D[c]
1	Benzenesulphonamide	0.77 ± 0.21	1.43 ± 0.09	0.97 ± 0.06
2	Methyl phenyl sulphone	0.93 ± 0.01	1.13 ± 0.02	0.76 ± 0.03
3	Methyl phenyl sulphoxide	0.77 ± 0.02	1.02 ± 0.05	0.44 ± 0.03
4	Benzamide	0.81 ± 0.04	0.91 ± 0.06	0.73 ± 0.02
5	Aniline	0.95 ± 0.02	1.11 ± 0.03	1.56 ± 0.07
6	Benzyl alcohol	1.05 ± 0.02	1.17 ± 0.03	1.03 ± 0.02
7	Acetanilide	1.17 ± 0.01	1.31 ± 0.04	1.20 ± 0.01
8	2-Phenylethanol	1.42 ± 0.03	1.50 ± 0.07	1.38 ± 0.02
9	Phenol	1.28 ± 0.01	1.45 ± 0.04	1.55 ± 0.05
10	Benzaldehyde	1.54 ± 0.06	1.42 ± 0.08	1.31 ± 0.05
11	Benzonitrile	1.51 ± 0.02	1.76 ± 0.05	1.56 ± 0.05
12	Nitrobenzene	1.70 ± 0.04	2.01 ± 0.06	2.30 ± 0.02
13	N-Methylaniline	1.51 ± 0.02	1.74 ± 0.03	1.93 ± 0.03
14	N,N-Dimethylaniline	2.28 ± 0.01	2.32 ± 0.12	2.50 ± 0.02
15	Phenyl acetate	1.57 ± 0.04	1.87 ± 0.04	1.52 ± 0.04
16	Methyl benzoate	2.15 ± 0.02	2.09 ± 0.09	2.17 ± 0.02
17	Thioanisole	2.72 ± 0.04	2.26 ± 0.09	2.89 ± 0.04
18	Anisole	2.01 ± 0.03	2.22 ± 0.06	2.33 ± 0.27
19	Benzene	1.91 ± 0.04	2.06 ± 0.09	2.31 ± 0.15
20	Fluorobenzene	2.07 ± 0.04	2.28 ± 0.08	2.57 ± 0.02
21	Chlorobenzene	2.72 ± 0.03	2.30 ± 0.08	3.11 ± 0.08
22	Bromobenzene	2.88 ± 0.03	2.78 ± 0.14	3.10 ± 0.07
23	Iodobenzene	3.14 ± 0.04	2.81 ± 0.17	2.69 ± 0.14
24	Toluene	2.62 ± 0.02	2.11 ± 0.13	2.70 ± 0.05
25	Trifluoromethylbenzene	3.11 ± 0.03	2.69 ± 0.10	3.37 ± 0.08
26	Biphenyl	3.92 ± 0.08	3.46 ± 0.57	3.40 ± 0.11
27	Benzophenone	3.45 ± 0.16	2.75 ± 0.19	2.97 ± 0.12
28	Naphthalene	3.29 ± 0.05	2.90 ± 0.21	2.70 ± 0.09

[a] Log k_w (CH_3OH–D) is the lipophilic index extrapolated linearly to 100% water using the ODS column, methanol as the organic solvent and *n*-decylamine as a masking agent. Data from ref. 19.

[b] Log k_w (ACN–D) is the lipophilic index extrapolated quadratically to 100% water using the ODS column, acetonitrile as the organic solvent and *n*-decylamine as a masking agent.

[c] Log k_w (THF–D) is the lipophilic index extrapolated quadratically to 100% water using the ODS column, THF as the organic solvent and *n*-decylamine as a masking agent.

Methanol as organic modifier

Using methanol as the organic modifier and ODS as the stationary phase, eqns. 1 and 2 (Table IV) were established between octanol–water partition coefficients (log *P*) and both extrapolated and isocratic capacity factors (50% methanol).

In these equations the slope is larger than 1 and the intercept is significantly different from 0. The isocratic capacity factors result in a slightly better relationship with log *P* values. Adding *n*-decylamine to the mobile phase as a masking agent led to eqns. 3 and 4. The slope and intercept in eqn. 3 are close to 1 and 0, respectively,

TABLE II

EXTRAPOLATED CAPACITY FACTORS OF 28 MONOSUBSTITUTED BENZENES DETERMINED WITH VARIOUS ORGANIC SOLVENTS USING AN ODS STATIONARY PHASE WITHOUT A MASKING AGENT

Compound No.	Log k_w			Log P^d
	CH_3OH^a	ACN^b	THF^c	
1	0.90 ± 0.06	0.89 ± 0.05	0.78 ± 0.02	0.31
2	1.29 ± 0.07	1.34 ± 0.08	0.79 ± 0.02	0.49
3	1.33 ± 0.06	1.28 ± 0.07	0.49 ± 0.07	0.55
4	1.04 ± 0.07	1.00 ± 0.06	0.74 ± 0.02	0.64
5	1.13 ± 0.04	1.12 ± 0.06	1.03 ± 0.02	0.90
6	1.32 ± 0.04	1.27 ± 0.06	1.10 ± 0.02	1.10
7	1.45 ± 0.03	1.44 ± 0.06	1.25 ± 0.02	1.16
8	1.73 ± 0.04	1.66 ± 0.06	1.47 ± 0.01	1.36
9	1.30 ± 0.03	1.27 ± 0.04	1.58 ± 0.05	1.46
10	1.67 ± 0.04	1.71 ± 0.04	1.46 ± 0.02	1.45
11	1.85 ± 0.09	1.74 ± 0.15	1.67 ± 0.04	1.56
12	2.00 ± 0.06	2.07 ± 0.06	2.40 ± 0.04	1.85
13	1.74 ± 0.06	1.79 ± 0.04	2.02 ± 0.08	1.66
14	2.36 ± 0.04	2.33 ± 0.09	2.60 ± 0.07	2.31
15	2.04 ± 0.09	1.89 ± 0.03	1.64 ± 0.04	1.49
16	2.26 ± 0.04	2.34 ± 0.06	2.25 ± 0.10	2.12
17	2.71 ± 0.11	2.87 ± 0.09	3.25 ± 0.10	2.74
18	2.20 ± 0.05	2.11 ± 0.06	2.43 ± 0.02	2.11
19	2.08 ± 0.04	3.05 ± 0.13	2.25 ± 0.14	2.13
20	2.18 ± 0.05	2.16 ± 0.08	2.75 ± 0.06	2.27
21	2.75 ± 0.08	2.86 ± 0.10	3.26 ± 0.09	2.84
22	2.89 ± 0.09	2.59 ± 0.11	2.87 ± 0.23	2.99
23	3.16 ± 0.09	3.09 ± 0.11	3.33 ± 0.12	3.25
24	2.62 ± 0.06	2.79 ± 0.08	2.95 ± 0.08	2.73
25	3.11 ± 0.09	2.58 ± 0.07	3.40 ± 0.10	2.79
26	3.88 ± 0.10	3.52 ± 0.30	3.75 ± 0.13	4.09
27	3.11 ± 0.16	2.64 ± 0.14	2.91 ± 0.07	3.18
28	3.22 ± 0.10	3.11 ± 0.07	2.85 ± 0.39	3.30

[a] Log k_w (CH_3OH) is the lipophilicity index extrapolated linearly to 100% water using an ODS column and methanol as the organic solvent without any masking agent. Data taken from ref. 19.

[b] Log k_w (ACN) is the lipophilicity index extrapolated quadratically to 100% water using an ODS column and acetonitrile as the organic solvent without any masking agent.

[c] Log k_w (THF) is the lipophilicity index extrapolated quadratically to 100% water using an ODS column and tetrahydrofuran as the organic solvent without any masking agent.

[d] Log P is the logarithm of *n*-octanol–water partition coefficient (data from ref. 21).

indicating a slightly hyperdiscriminative capacity of this partition system compared with the octanol–water system. The addition of *n*-decylamine increases the discriminative capability of the HPLC system. This is reflected in the higher extrapolated capacity factors found for some lipophilic compounds. Thus log k_w values determined in this system offer the advantage of being very similar to log P values over a wide range of lipophilicity and may be used directly as substitutes for log P. In this case also isocratic capacity factors lead to a slightly better relationship with log P values (eqn. 4).

TABLE III

EXTRAPOLATED CAPACITY FACTORS OF 28 MONOSUBSTITUTED BENZENES DETERMINED WITH VARIOUS ORGANIC MODIFIERS USING AN ODP STATIONARY PHASE

Compound No.	Log k_w		
	ODP–CH_3OH[a]	ODP–ACN[b]	OD–THF[c]
1	1.12 ± 0.03	1.24 ± 0.12	1.11 ± 0.04
2	1.18 ± 0.05	1.59 ± 0.15	1.20 ± 0.04
3	0.68 ± 0.05	1.09 ± 0.15	0.67 ± 0.14
4	1.24 ± 0.17	1.24 ± 0.09	0.87 ± 0.04
5	1.46 ± 0.07	1.29 ± 0.06	1.47 ± 0.02
6	1.33 ± 0.03	1.29 ± 0.07	1.21 ± 0.01
7	1.52 ± 0.06	1.77 ± 0.14	1.32 ± 0.03
8	1.93 ± 0.14	1.45 ± 0.09	1.44 ± 0.05
9	1.81 ± 0.08	1.33 ± 0.04	1.91 ± 0.06
10	1.74 ± 0.03	2.00 ± 0.17	1.82 ± 0.02
11	2.35 ± 0.15	1.78 ± 0.04	2.05 ± 0.03
12	2.62 ± 0.04	2.01 ± 0.05	2.56 ± 0.09
13	2.26 ± 0.07	1.59 ± 0.07	2.21 ± 0.05
14	2.87 ± 0.07	1.75 ± 0.09	2.62 ± 0.05
15	2.21 ± 0.19	1.80 ± 0.14	1.82 ± 0.04
16	2.48 ± 0.04	1.72 ± 0.14	2.21 ± 0.05
17	3.23 ± 0.07	2.16 ± 0.21	2.87 ± 0.05
18	2.46 ± 0.03	1.83 ± 0.10	2.26 ± 0.07
19	2.40 ± 0.05	1.75 ± 0.16	2.44 ± 0.11
20	2.93 ± 0.13	1.56 ± 0.09	2.50 ± 0.11
21	3.25 ± 0.14	1.85 ± 0.14	2.77 ± 0.10
22	3.64 ± 0.15	1.90 ± 0.15	3.00 ± 0.13
23	3.89 ± 0.22	2.06 ± 0.10	3.22 ± 0.14
24	3.25 ± 0.14	2.13 ± 0.19	2.85 ± 0.09
25	3.68 ± 0.25	1.83 ± 0.16	2.88 ± 0.09
26	4.63 ± 0.14	2.28 ± 0.13	3.43 ± 0.12
27	3.71 ± 0.17	1.94 ± 0.09	2.78 ± 0.11
28	3.94 ± 0.21	2.03 ± 0.15	3.09 ± 0.09

[a] Log k_w (ODP–CH_3OH) is the lipophilicity index extrapolated linearly to 100% water using an ODP stationary phase and methanol as the organic solvent. Data from ref. 19.

[b] Log k_w (ODP–ACN) is the lipophilicity index extrapolated quadratically to 100% water using an ODP column and acetonitrile as the organic modifier.

[c] Log k_w (ODP–THF) is the lipophilicity index extrapolated quadratically to 100% water using an ODP column and tetrahydrofuran as the organic solvent.

Using ODP as the stationary phase, similar equations were obtained; the slope and intercept in eqns. 5 and 6 indicate that the log k values obtained in this system are larger than the corresponding log P values. Unlike eqns. 2 and 4, the isocratic capacity factors do not lead to an improved correlation with log P values, presumably because measurements at low methanol fractions are not possible owing to the high hydrophobicity of the ODP phase.

TABLE IV

RELATIONSHIP BETWEEN LIPOPHILICITY INDICES DETERMINED BY RP-HPLC AND THE SHAKE-FLASK METHOD

n is the number of compounds in the analysis, r is the correlation coefficient, s is the standard deviation of the equation and F is the Fischer test.

(A) Methanol as the organic modifier				
(A1) ODS as the stationary phase, no masking agent				
$\log P = 1.23(\pm 0.05)\log k_w - 0.65(\pm 0.12)$ $n = 28, r = 0.976, s = 0.216, F = 532$	(1)	$\log P = 1.71(\pm 0.05)\log k_{50} + 0.95(\pm 0.04)$ $n = 28, r = 0.988, s = 0.156, F = 1060$	(2)	
(A2) ODS stationary phase using n-decylamine as a masking agent				
$\log P = 0.91(\pm 0.03)\log k_w + 0.18(\pm 0.12)$ $n = 28, r = 0.983, s = 0.181, F = 763$	(3)	$\log P = 1.67(\pm 0.04)\log k_{50} + 1.05(\pm 0.03)$ $n = 28, r = 0.993, s = 0.118, F = 1830$	(4)	
(A3) ODP stationary phase				
$\log P = 0.94(\pm 0.04)\log k_w - 0.35(\pm 0.22)$ $n = 28, r = 0.978, s = 0.206, F = 573$	(5)	$\log P = 1.57(\pm 0.07)\log k_{50} + 0.39(\pm 0.09)$ $n = 28, r = 0.980, s = 0.209, F = 736$	(6)	
(B) Acetonitrile as the organic modifier				
(B1) ODS stationary phase, no masking agent				
$\log P = 1.33(\pm 0.07)\log k_w + 0.78(\pm 0.14)$ $n = 27^a, r = 0.971, s = 0.245, F = 408$	(7)	$\log P = 2.43(\pm 0.13)\log k_{50} + 0.73(\pm 0.08)$ $n = 28, r = 0.963, s = 0.268, F = 337$	(8)	
(B2) ODS stationary phase using n-decylamine as a masking agent				
$\log P = 1.41(\pm 0.08)\log k_w - 0.80(\pm 0.17)$ $n = 28, r = 0.957, s = 0.288, F = 286$	(9)	$\log P = 2.38(\pm 0.12)\log k_{50} + 0.88(\pm 0.07)$ $n = 28, r = 0.969, s = 0.247, F = 401$	(10)	
(B3) ODP stationary phase				
$\log P = 2.53(\pm 0.35)\log k_w - 2.40(\pm 0.06)$ $n = 28, r = 0.815, s = 0.580, F = 51.3$	(11)	$\log P = 2.24(\pm 0.17)\log k_{50} + 1.05(\pm 0.10)$ $n = 28, r = 0.932, s = 0.363, F = 171$	(12)	
(C) Tetrahydrofuran as the mobile phase				
(C1) ODS as the stationary phase, no masking agent				
$\log P = 1.00(\pm 0.05)\log k_w - 0.15(\pm 0.13)$ $n = 28, r = 0.964, s = 0.267, F = 338$	(13)	$\log P = 2.95(\pm 0.25)\log k_{50} + 1.11(\pm 0.10)$ $n = 28, r = 0.918, s = 0.397, F = 408$	(14)	
(C2) ODS as the stationary phase using n-decylamine as a masking agent				
$\log P = 1.07(\pm 0.07)\log k_w - 0.22(\pm 0.16)$ $n = 28, r = 0.943, s = 0.331, F = 211$	(15)	$\log P = 2.75(\pm 0.24)\log k_{50} + 1.34(\pm 0.09)$ $n = 28, r = 0.916, s = 0.402, F = 135$	(16)	
(C3) ODP stationary phase				
$\log P = 1.23(\pm 0.07)\log k_w - 0.69(\pm 0.16)$ $n = 28, r = 0.960, s = 0.281, F = 303$	(17)	$\log P = 2.26(\pm 0.23)\log k_{50} + 1.59(\pm 0.10)$ $n = 28, r = 0.886, s = 0.464, F = 94.7$	(18)	

[a] Benzene excluded.

Acetonitrile as organic modifier

As with methanol, several equations were established (Table IV). Eqn. 7 (benzene excluded) does not actually differ from eqn. 1 when the ODS stationary phase is used with methanol. We thus observe that the selective effect of the solvent is not reflected in log k_w values and no difference should be expected when either methanol or acetonitrile is used. However, it is interesting that when the data for the

same compound are compared using either methanol or acetonitrile, the log k_w values are different. The addition of *n*-decylamine (eqns. 9 and 10) does not improve the correlation compared with eqns. 7 and 8. As acetonitrile has a weak hydrogen bonding ability, it does not attract sufficient water to the stationary phase [22], thus presumably preventing *n*-decylamine (which exists in the protonated form) from reaching the stationary phase.

Eqns. 11 and 12 demonstrate that acetonitrile is not suitable as an organic modifier when the ODP stationary phase is used. Indeed, a very long equilibration time between the mobile and stationary phase is needed, particularly at volume fractions rich in water. Large errors are expected for the measurements performed in this region and consequently will be reflected in the extrapolation values. Indeed, isocratic capacity factors (eqn. 12) lead to better correlations with log *P* than the extrapolated values (eqn. 11). In addition, the experimental conditions could not be kept sufficiently stable.

Tetrahydrofuran as organic modifier

Under comparable conditions, eqns. 13–18 (Table IV) were obtained using THF as the mobile phase. Eqn. 13, which correlates the extrapolated values obtained by using THF and the ODS column with log *P*, is still acceptable. Interestingly, the coefficients of the equation denote a remarkable similarity with the octanol–water system, with a slope close to 1 and an intercept not significantly different from 0. This similarity may be due to an attenuation of silanophilic interactions caused by the large amount of water brought into contact with the stationary phase by THF [22].

The addition of *n*-decylamine (eqns. 15 and 16) does not improve the correlation compared with eqns. 13 and 14, as the effects of silanol groups have already been attenuated by the associated THF–water.

Using THF with an ODP stationary phase (eqn. 17), a reasonable correlation between log k_w and log *P* values is obtained compared with eqn. 5. However, the selective effect of THF is clear in eqn. 18. Generally, all relationships between log *P* and isocratic capacity factors have deteriorated (eqns. 14, 16 and 18) compared with eqns. 13, 14 and 17.

CONCLUSIONS

As far as the organic modifier is concerned, methanol clearly appears to be the solvent of choice for the determination of lipophilicity by RP-HPLC. *n*-Decylamine, although effective as a masking agent, should not be used unless essential, as it introduces an additional variable and exerts its own effects on retention. The ODP stationary phase is a promising alternative to ODS for the assessment of lipophilicity as it leads to good lipophilicity indices without the necessity for a masking agent. However, the ODP stationary phase cannot be used with acetonitrile as the organic modifier.

From the present and previous studies, we conclude that the best system currently available for the determination of lipophilicity indices by RP-HPLC consists of ODP as the stationary phase and water–methanol as the eluent.

ACKNOWLEDGEMENTS

B.T. is indebted to the Swiss National Foundation for research grant 31-8859.86. A.T.-K. thanks the Fondation Herbette (Université de Lausanne) for a travel grant.

REFERENCES

1 H. van de Waterbeemd and B. Testa, *Adv. Drug. Res.*, 16 (1987) 85.
2 H. Walter, D. E. Brooks and D. Fisher, *Partitioning in Aqueous Two Phase Systems,* Academic Press, London, 1985.
3 H. Kubinyi, *Prog. Drug. Res.*, 23 (1979) 97.
4 S. Yamana, A. Tsuji, E. Miyamoto and S. Kubo, *J. Pharm. Sci.*, 66 (1977) 747.
5 D. J. Minnick, D. A. Brent and J. Frenz, *J. Chromatogr.*, 461 (1989) 177.
6 D. J. Minnick, J. H. Frenz, M. A. Patrick and D. A. Brent, *J. Med. Chem.*, 31 (1988) 1923.
7 T. Braumann, *J. Chromatogr.*, 373 (1986) 191.
8 P. J. Schoenmaker, H. A. Billiet and L. de Galan, *J. Chromatogr.*, 185 (1979) 179.
9 D. Reymond, G. N. Chung, J. M. Mayer and B. Testa, *J. Chromatogr.*, 391 (1987) 97.
10 A. Opperhuizen, T. L. Sinnige and J. van der Steen and O. Hutzinger, *J. Chromatogr.*, 388 (1987) 51.
11 N. El Tayar, H. van der Waterbeemd and B. Testa, *J. Chromatogr.*, 320 (1985) 305.
12 B. L. Karger, J. Gant, A. Hartkopf and P. H. Weiner, *J. Chromatogr.*, 127 (1976) 65.
13 C. Horváth and W. Melander, *J. Chromatogr. Sci.*, 15 (1977) 393.
14 E. Bayer and A. Paulus, *J. Chromatogr.*, 400 (1987) 1.
15 D. C. Leach, M. A. Stadalius, J. S. Berus and L. R. Snyder, *LC·GC Int.*, 1 (1988) 22.
16 N. El Tayar, A. Tsantili-Kakoulidou, T. Röthlisberger, B. Testa and J. Gal, *J. Chromatogr.*, 439 (1988) 237.
17 R. N. Nikolov, *J. Chromatogr.*, 286 (1984) 147.
18 K. Yasukawa, Y. Tamura, T. Uchida, Y. Yanagihara and K. Noguchi, *J. Chromatogr.*, 410 (1987) 129.
19 A. Bechalany, T. Röthlisberger, N. El Tayar and B. Testa, *J. Chromatogr.*, 473 (1989) 115.
20 Y. Arai, M. Hirukawa and T. Hanai, *J. Liq. Chromatogr.*, 10 (1987) 635.
21 C. Hansch and A. Leo, *Pomona College Medicinal Chemistry Project Log P and Parameter Database*, Issue 23, Comtex Scientific, New York 1983.
22 E. D. Katz, K. Ogan and R. P. W. Scott, *J. Chromatogr.*, 352 (1986) 67.

Journal of Chromatography, 541 (1991) 231–241
Elsevier Science Publishers B.V., Amsterdam

CHROM. 22 960

Liquid chromatography–mass spectrometry system using column-switching techniques

NAOKI ASAKAWA*, HIROSHI OHE, MASANORI TSUNO, YUKUO NEZU, YUTAKA YOSHIDA and TADASHI SATO

Department of Physical and Analytical Chemistry, Tsukuba Research Laboratories, Eisai Co., Ltd., 1–3 Tokodai 5-chome, Tsukuba-shi, Ibaraki 300-26 (Japan)

(First received May 29th, 1990; revised manuscript received October 29th, 1990)

ABSTRACT

A liquid chromatography–mass spectrometry (LC–MS) system, was developed to overcome the problems imposed by the use of non-volatile mobile phases, such as buffers. The peak of interest was heart-cut from the effluent from the analytical column, passed into sampling loops and adsorbed on a trapping column after dilution with the analytical mobile phase. The buffer constituents were washed out and the compounds of interest were eluted from the trapping column and re-chromatographed with a suitable mobile phase for LC–MS. The potential of this system was explored in the LC–frit-fast atom bombardment-MS determination of tocopherol and riboflavin. The system can provide high sensitivity.

INTRODUCTION

Combined liquid chromatography–mass spectrometry (LC–MS) has become one of the most useful and powerful techniques for the analysis of non-volatile and thermolabile organic compounds, which cannot be analysed by gas chromatography–mass spectrometry. Although LC–MS has been applied to the characterization of molecular species, the identification of metabolites and the determination of drugs, the interface remains a major problem. Most LC–MS interfaces which have been developed do not allow the use of a mobile phase containing the non-volatile buffers which are usually used in routine LC, because in LC–MS the use of these buffers causes serious problems such as inhibition of ionization or precipitation at a heated nebulizer in the thermospray method and at atmospheric pressure ionization interfaces. Therefore, the optimum mobile phase for separation of compounds of interest often cannot be utilized.

In recent papers [1–4], an approach based on the use of valve-switching techniques has been discussed as a means of overcoming some of these problems. In particular, Verheij *et al.* [5] have described the use of coupled column chromatography, called phase-system switching (PSS), which has been developed to solve problems of mobile phase incompatibility in LC–MS target compound analysis.

We have developed a new column-switching LC system, consisting of the

0021-9673/91/$03.50

analytical LC column (LC-1), the introduction LC column (LC-3) for passing materials to the mass spectrometer and the trapping LC column (LC-2) which is installed between LC-1 and LC-3. Each LC column is run independently. The mobile phase in LC-1 moves through LC-2 and the components of the mobile phase are exchanged for the most favourable mobile phase for MS analysis.

In order to explore the potential of this LC system combined with frit fast atom bombardment MS (LC–frit-FAB-MS), which was developed by Ishii and co-workers [6,7], we have attempted to optimize the LC system (reversed-phase mode) to be combined with MS by using tocopherol as a test sample, and applied it to the determination of riboflavin with phosphoric acid as a non-volatile buffer.

EXPERIMENTAL

Materials and reagents

Methanol of HPLC grade and phosphoric acid, ammonium acetate, trifluoroacetic acid and glycerol of analytical-reagent grade were purchased from Wako (Osaka, Japan). α-, β- and δ-tocopherol were synthesized in our laboratories. Riboflavin was obtained from Sigma (St. Louis, MO, U.S.A.).

Samples

Stock solutions of α-, β- and δ-tocopherol (100 ng/ml) were each prepared in volumetric flasks by dissolution in and dilution to volume with methanol. A stock solution of riboflavin (100 μg/ml) was prepared in a volumetric flask by dissolution in and dilution to volume with methanol–water (1:1, v/v).

Chromatographic system

A schematic diagram of the system consisting of three HPLC instruments is illustrated in Fig. 1. All the LC equipment was obtained from Shimadzu (Kyoto, Japan).

In LC-1, a pump (P1) (Model LC-6AD), which was controlled by a gradient controller (Model SCL-6B), delivered the mobile phase (M1). The effluent was monitored with monitored with a variable-wavelength UV detector (D1) (Model SPD-6A). Injection was performed using a manual injector (I) [Rheodyne (Berkeley, CA, U.S.A.) Model 7125] with a 500-μl loop.

In LC-2, a pump (P2) (Model LC-9A) delivered the mobile phase (M2) for adsorption of the compounds of interest on the trapping column (TC).

In LC-3, a pump (P3) (Model LC-9A) delivered the mobile phase (M3) at a flow-rate of 20 μl/min for elution of the compounds of interest from the trapping column. Before being passed to the LC–MS interface, the compounds of interest were re-chromatographed on the microcolumn (C2), monitoring with a UV detector (D2) (Model SPD-6A) equipped with a micro-cell (cell volume 0.6 μl).

Switching was done with Rheodyne 7000 (V1, V4) and Rheodyne 7060 (V2, V3, R) switching valves.

The introduction to the frit-FAB-MS system was performed by using a pneumatic splitter [8] (S) (Model MS-PNS; JEOL, Tokyo, Japan) in order to reduce the flow-rate from 20 to 1 μl/min.

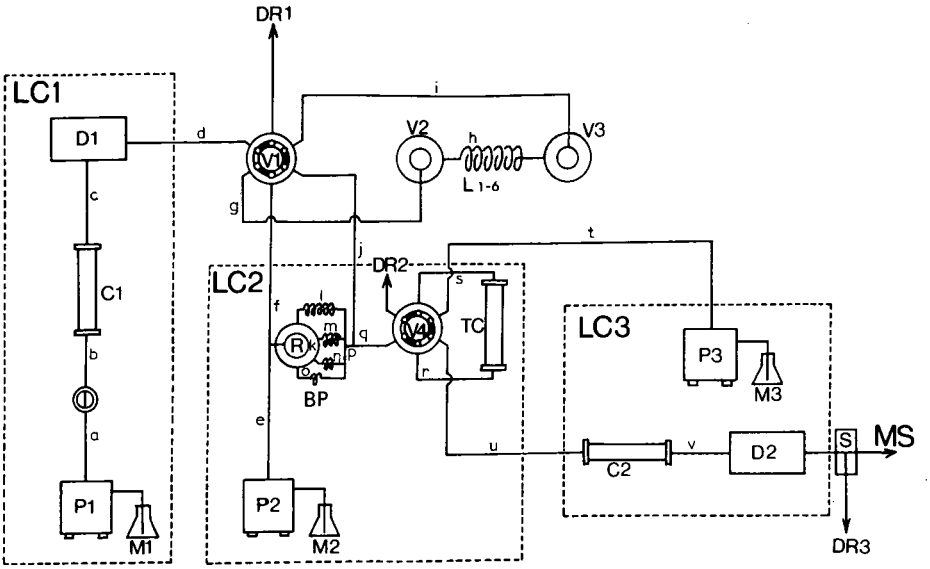

Fig. 1. Schematic diagram of the column switching system for LC–MS. P1 = solvent pump; M1 = mobile phase for separation; C1 = analytical column; D1 = UV detector for monitoring separation with the analytical column; P2 = solvent pump for trapping; M2 = mobile phase for trapping on the trapping column (TC); BP = by-pass line; L = sampling loops; P3 = solvent pump for flow to mass spectrometer; C2 = micro-column for re-chromatography; D2 = UV detector with micro-cell for monitoring the flow to the mass spectrometer; S = splitter; V1, V4 = six-port switching valves for changing the flow direction; V2, V3 = six-port switching valves for selection of sampling loops; R = six-port switching valve for changing the dilution ratio; DR1, DR2 and DR3 = drain. Sizes of connecting tubes: (a) 400 mm × 0.25 mm; (b) 930 mm × 0.25 mm I.D.; (c) 200 mm × 0.20 mm I.D.; (d) 310 mm × 0.25 mm I.D.; (e) 480 mm × 0.25 mm I.D.; (f) 60 mm × 0.25 mm I.D.; (g) 100 mm × 0.50 mm I.D.; (h) 500 mm × 0.80 mm I.D.; (i) 200 mm × 0.25 mm I.D.; (j) 430 mm × 0.50 mm I.D.; (k) 360 mm × 0.50 mm I.D.; (l) 280 mm × 0.25 mm I.D.; (m) 140 mm × 0.25 mm I.D.; (n) 90 mm × 0.25 mm I.D.; (o) 70 mm × 0.25 mm I.D.; (p) 720 mm × 0.50 mm I.D.; (q) 320 mm × 0.25 mm I.D.; (r) 100 mm × 0.10 mm; (s) 200 mm × 0.10 mm I.D.; (t) 350 mm × 0.25 mm I.D.; (u) 200 mm × 0.10 mm I.D.; (v) 100 mm × 0.20 mm.

Column

C1 (the analytical column) was Inertsil ODS-2 (150 mm × 4.6 mm I.D., particle size 5 μm; Gaskuro Kogyo). TC (the trapping column) was a reversed-phase Inertsil ODS-2 cartridge precolumn (10 mm × 4 mm I.D., particle size 5 μm). The separation using C2 (microcolumn) was performed on Inertsil ODS-2 (150 mm × 0.7 mm I.D., particle size 5 μm).

Mass spectrometry (MS)

The combined LC–MS system with a frit-FAB interface was performed on a JEOL JMS-HX100 apparatus. MS conditions in the FAB mode included a xenon atom beam from a saddle field gun operated at 8 kV and 1.0 mA; the scan range was 100–1100 dalton at a scan speed of 3.1 per decade. The FAB mass spectra were recorded with a normal resolving power of 1000. The source operating pressure was typically 10^{-5} Torr.

Column-switching procedure

As shown in Fig. 1, this system consisted of three HPLC instruments. LC-1 was a conventional HPLC set-up with C1 and M1 (the optimum mobile phase) to separate the compounds of interest. LC-2 served to trap the compounds on the trapping column (TC) and LC-3 to pass the compounds to the frit-FAB-MS system after re-chromatography. The three instruments were connected with V1, V2, V3, V4 and R.

The valve-switching procedure is illustrated in Fig. 2. In the first stage, the three columns were run independently so the flow pattern through the apparatus (Fig. 1) is as shown in Fig. 2a. The sample solution was injected at I and eluted from C1, peaks being detected at D1. In the second stage, when a peak was detected at D1 the valve V1 was switched so the flow pattern changed to that shown in Fig. 2b. The valves V2 and V3 were adjusted so that the sample-containing eluate flowed into one of six 1-ml loops connecting the two, where it was stored. When the detector D1 showed that the sample was no longer leaving the column, valve V1 was returned to its original position (*i.e.*, the flow pattern returned to that in Fig. 2a) until the next peak was detected. Thus, by repeating the process of switching V1 and adjusting V2 and V3, samples of up to six different peaks could be stored in the 1-ml loops. In the third stage, the compounds in the loops (L) were pushed out with M2 by P2 and sent to TC while simultaneously being diluted with M2 via the by-pass (BP) in order to improve the adsorption of the compounds of interest on TC. A valve (R) was fitted to BP so that the dilution ratio could be adjusted by varying the resistance to the flow of M2 in the apparatus. This was

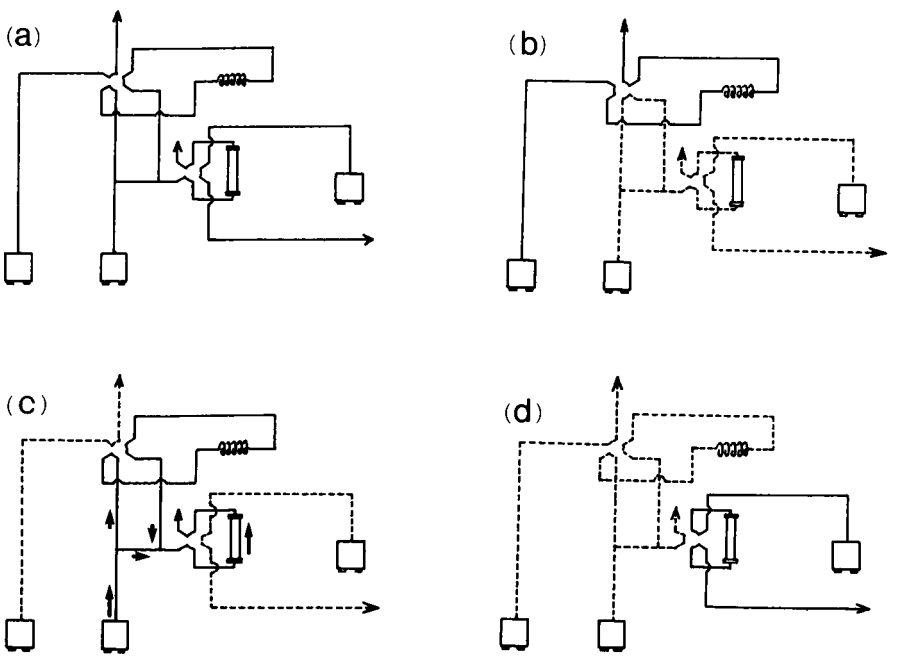

Fig. 2. Column-switching procedure showing (a) separation configuration, (b) sampling configuration, (c) sample washing configuration (the arrows show the relative flow-rates using one tube at BP in Fig. 1 when the dilution ratio was 2) and (d) flow to mass spectrometer and re-chromatography configuration.

done by using different lengths of stainless-steel tubing connecting R and V4 (see Fig. 1, l–o). When the flow-rate of M2 (using water) was 1 ml/min, the flow-rate at BP for dilution ratios of 2, 3, 4 and 5 were 0.48, 0.68, 0.73 and 0.81 ml/min, respectively. M1 in L was drained through TC together with M2. The compounds were adsorbed on TC and M1 was exchanged with M2 (see Fig. 2c). In the fourth stage, the adsorbed compounds were eluted from TC with M3 by P3, sent to C2 for re-chromatography and introduced into the Frit FAB MS system (see Fig. 2d). After the completion of these four stages, the procedure could be repeated for another sample.

RESULTS AND DISCUSSION

We attempted to optimize the LC system to be combined with MS by using tocopherols as test samples. It has been shown that the frit-FAB interface can be used effectively in an on-line LC–MS system.

Liquid chromatography of tocopherols

HPLC was performed according to the procedure described under Experimental. α-Tocopherol was dissolved in methanol and adjusted to 1 mg/ml.

In LC-1, 1 μl of α-tocopherol solution (1 μg as α-tocopherol) was injected into C1. M1 was methanol at a flow-rate of 1 ml/min. The peak of tocopherol was monitored by D1 and D2 at 282 nm.

In LC-2, M2 for adsorption on TC was glycerol–methanol–water (0.8:30:70, v/v/v) at a flow-rate of 1 ml/min.

In LC-3, α-tocopherol was passed to C2 and was eluted with glycerol–methanol (0.8:100, v/v) at a flow-rate of 20 μl/min.

α-Tocopherol could not be adsorbed on TC without BP in Fig. 1, because M1 in the 1-ml L made α-tocopherol elute from TC. In order to adsorb α-tocopherol on TC, M1 in L had to be sufficiently diluted with M2 before reaching TC. Therefore, BP was attached between L and the TC. This is a critical feature of the system.

If more hydrophilic compounds are applied, it is necessary to increase the dilution ratio or to change M2 to a more aqueous mobile phase in order to allow the compounds to be adsorbed on TC. α-Tocopherol could be adsorbed on TC by setting the dilution ratio at 2.

The diffusion of α-tocopherol in this LC system was investigated with C2 connected (Fig. 3b) and without C2 (Fig. 3c), monitoring with D2. The results are shown in Fig. 3. The chromatographic efficiency of α-tocopherol was very high in Fig. 3b but low in Figs. 3c. Hence, it was possible to decrease the diffusion by connecting C2[a]. This is very important in order to increase the sensitivity in MS analysis. In addition, the separation of tocopherol analogues was investigated by using only C2. In LC-1 α-, β- and δ-tocopherol were simultaneously injected into C1 and sampled in L with monitoring by D1. After adsorption of the tocopherol analogues on TC, the chromatogram obtained with D2 is shown in Fig. 4. C2 clearly has the ability to separate α-, β- and δ-tocopherol. Hence, if the separation in C1 is poor, it can be improved by using C2 to obtain a sufficient separation for the MS analysis. When

[a] A reference pointed out that this implies that the connecting tubing had too large an I.D. We used the narrowest gauge of tubing available, which was 200 mm × 0.1 mm I.D. stainless steel.

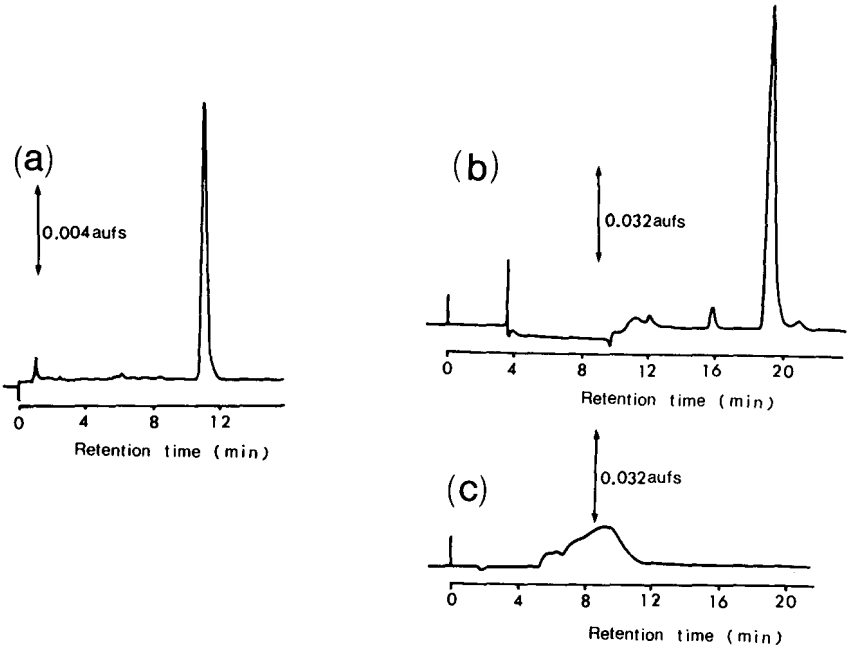

Fig. 3. Liquid chromatograms for a 1-μg injection of α-tocopherol: (a) detection at D1 (282 nm); (b) detection at D2 (282 nm) with C2; (c) detection at D2 (282 nm) without C2.

LC–frit-FAB-MS is used, not more than a few microlitres per minute can be passed to the FAB-MS system [6,7]. Therefore, if an LC microcolumn is directly coupled to a FAB-MS or frit-FAB-MS system, the injection volume into the microcolumn must usually be less than 1 μl. This is unsuitable for microanalysis. In our LC system using the microcolumn, the same volume could be injected as in the usual LC.

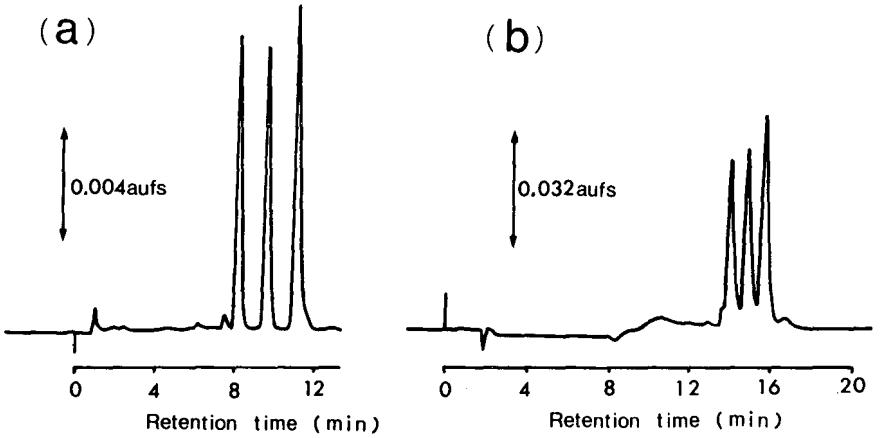

Fig. 4. Liquid chromatograms for a 1-μg injection of tocopherol analogues: (a) detection at D1 (282 nm); (b) detection at D2 (282 nm) with C2.

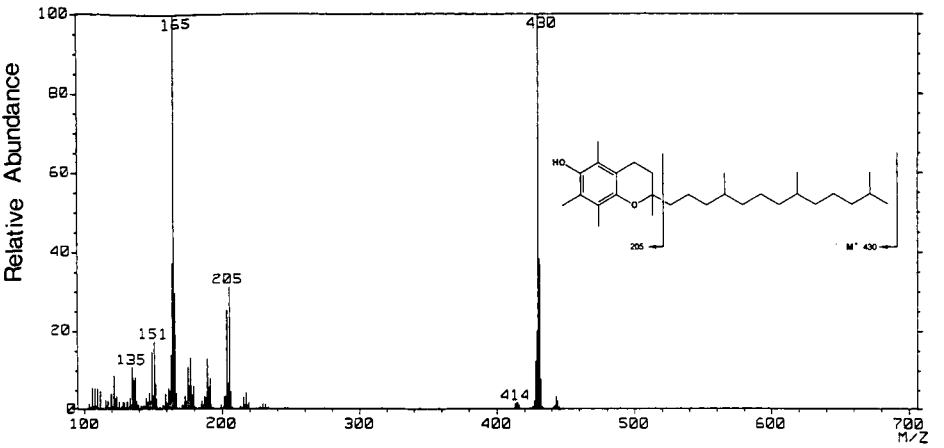

Fig. 5. FAB glycerol mass spectrum of about 1 μg of α-tocopherol using the direct insertion probe.

FAB-MS of α-tocopherol from a glycerol matrix

Initially, about 1 μg of α-tocopherol was analysed by FAB-MS using a direct insertion probe and a glycerol matrix. The spectrum and fragmentation pattern of α-tocopherol are shown in Fig. 5. The FAB-MS of α-tocopherol showed the molecular ion ($M^{+\cdot}$) at *m/z* 430.

FAB-MS of α-tacopherol obtained with the LC–frit-FAB-MS system

The flow-rate of the mobile phase passed to the FAB-MS system (JEOL JMS-HX 100) was restricted to 1 μl/min. In LC-1, 100 ng of α-tocopherol were injected into C1. The mass spectrum of α-tocopherol is shown in Fig. 6a and the mass chromatogram of the molecular ion ($M^{+\cdot}$) at *m/z* 430 in Fig. 6b. The molecular ion at *m/z* 430 was clearly observed and the spectrum was the same as that shown in Fig. 5. The protonated molecular ion was still observable when 500 pg were injected.

FAB-MS of riboflavin from a glycerol matrix

Initially, about 1 μg of riboflavin was analysed by FAB-MS using a direct insertion probe and a glycerol matrix. The spectrum and fragmentation pattern of riboflavin are shown in Fig. 7. The FAB mass spectrum of riboflavin showed a protonated molecule [$(M + 2H)^{+\cdot}$] at *m/z* 378.

When a mixture of riboflavin, glycerol and phosphoric acid was used, it was impossible to obtain the spectrum owing to the inhibition of ionization by the phosphoric acid, a so-called non-volatile buffer.

Liquid chromatography of riboflavin

HPLC was performed according to the procedure described under Experimental. In LC-1 1 μl of riboflavin solution (1 μg as riboflavin) was injected into C1. M1 was phosphoric acid–methanol–water (0.5:30:70, v/v/v) at a flow-rate of 1 ml/min. The peak of riboflavin was monitored by D1 and D2 at 254 nm. In LC-2, M2 for adsorption on TC was glycerol–0.5% aqueous ammonium acetate (0.8:100, v/v) at a flow-rate of

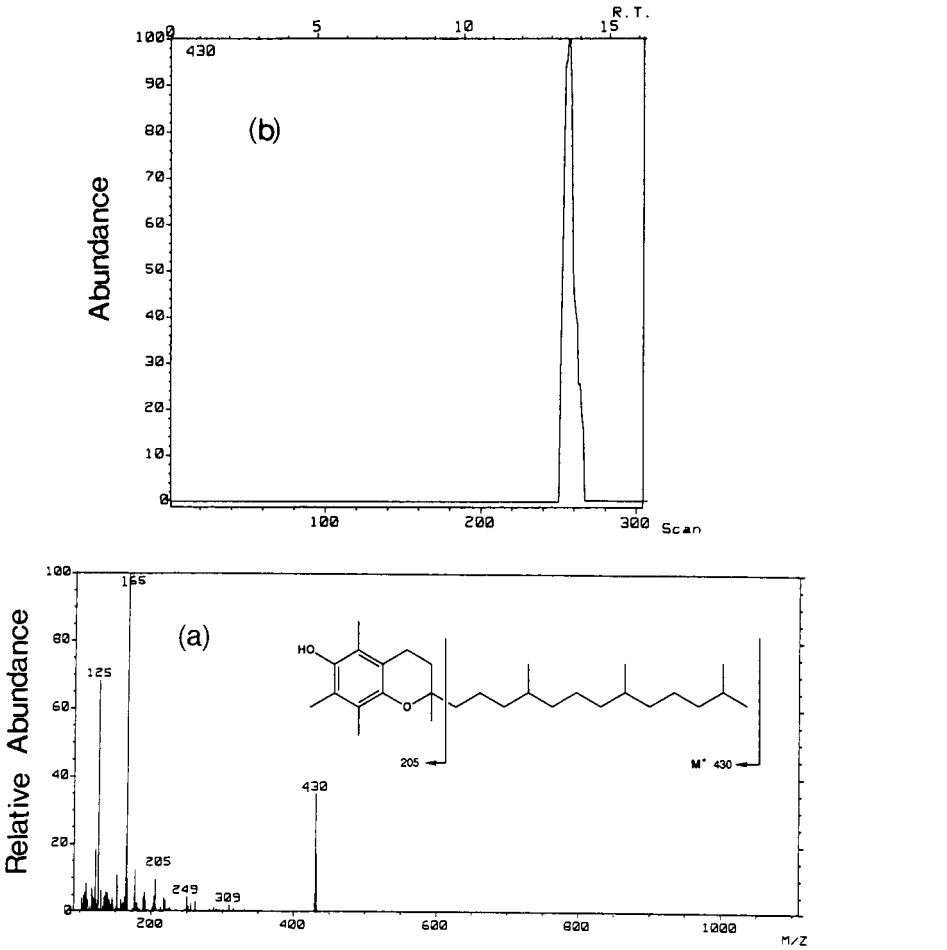

Fig. 6. (a) FAB mass spectrum of 100 ng of α-tocopherol obtained with LC–frit-FAB-MS; (b) mass chromatogram at *m/z* 430. R.T. is scanning time in min.

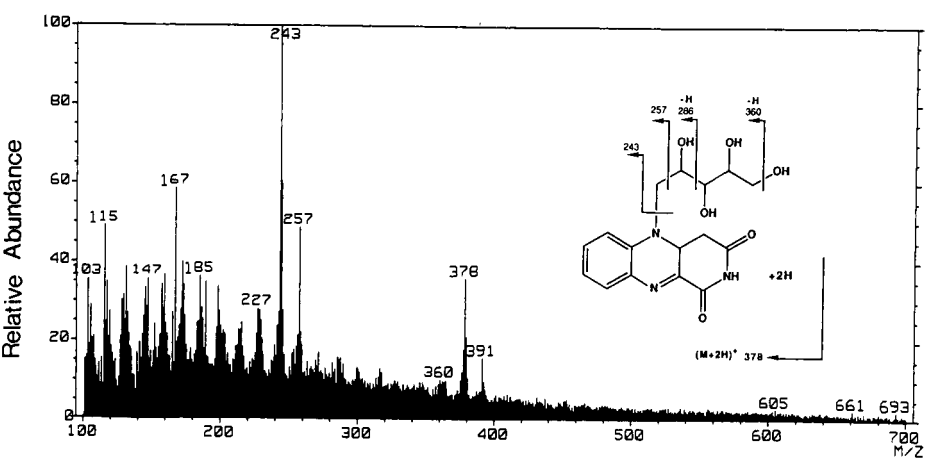

Fig. 7. FAB glycerol mass spectrum of about 1 μg of riboflavin using the direct insertion probe.

1 ml/min. In LC-3, riboflavin was passed into C2 and M3 was glycerol–trifluoroacetic acid–methanol–water (0.8:0.2:30:70, v/v) at a flow-rate of 20 μl/min.

The adsorption of riboflavin on TC was investigated, and chromatograms showing the effect of dilution ratio at D2 are presented in Fig. 8. The efficiency of the chromatography of riboflavin increased with increasing dilution ratio. These phenomena may be due to the diffusion of riboflavin in TC. In order to minimize the diffusion in TC and to obtain a high sensitivity, a high dilution ratio had to be used. Hence, the attachment of the sampling loop L to this system could change the dilution ratio.

FAB-MS of riboflavin obtained with the LC–frit-FAB-MS system

The mass chromatogram and the mass spectrum of riboflavin after injection of 1 μg into C1 are shown in Fig. 9. The spectrum showed a protonated molecule

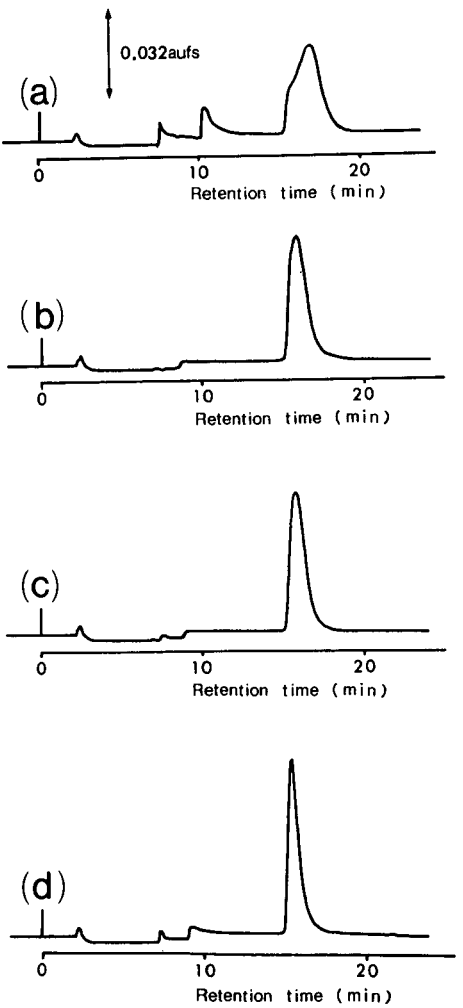

Fig. 8. Effect of dilution ratio on LC for a 1-μg injection of riboflavin with D2 at 254 nm. Dilution ratio: (a) 2; (b) 3; (c) 4; (d) 5.

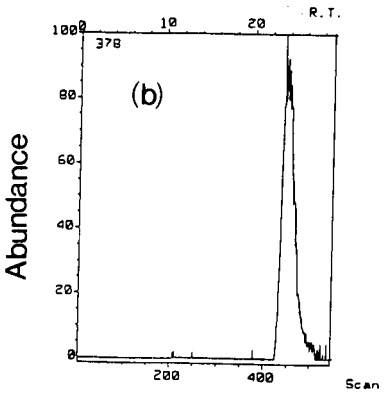

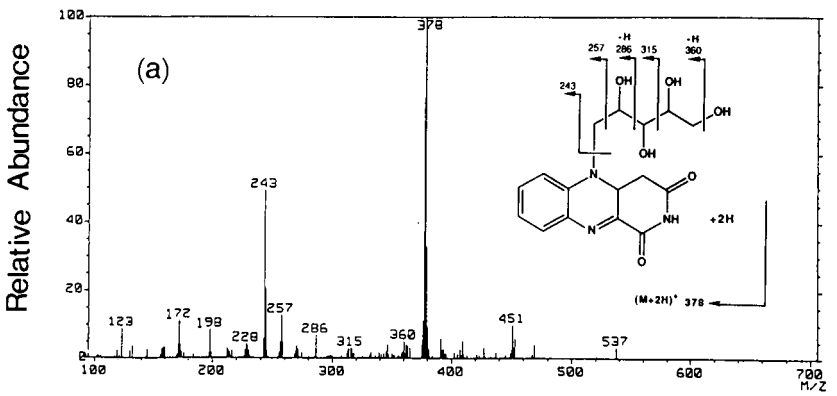

Fig. 9. (a) FAB mass spectrum of 1 μg of riboflavin obtained with LC–frit–FAB-MS; (b) mass chromatogram at m/z 378. R.T. is scanning time in min.

$[(M + 2H)^{+\cdot}]$ at m/z 378. It was still observable when 300 ng were injected. The spectrum was the same as that obtained with the direct insertion probe in the absence of phosphoric acid (see in Fig. 7). When phosphoric acid was added to M3, the mass spectrum of riboflavin could not be obtained. Hence, a non-volatile buffer could be used as the mobile phase for optimum separation in this LC–frit-FAB-MS system without incurring the problem of inhibition of ionization. This system is very powerful and offers high sensitivity.

CONCLUSIONS

It has been shown that a LC–frit-FAB-MS interface can be used effectively for on-line LC–MS. The application of a valve-switching technique in a new LC system allowed us to overcome previous limitations of LC–MS interfaces so that optimum mobile phases (containing non-volatile buffers) could be used to separate the

compounds of interest. The method offers high sensitivity. Investigations aimed at improving the sensitivity further are in progress.

ACKNOWLEDGEMENT

The authors are grateful to Mr. S. Ryo of Gasukuro Kogyo.

REFERENCES

1 J. van der Greef, W. M. A. Niessen and U. R. Tjaden, *J. Chromatogr.*, 474 (1989) 5.
2 P. Kokkonen, W. M. A. Niessen, U. R. Tjaden and J. van der Greef, *J. Chromatogr.*, 474 (1989) 59.
3 A. Walhagen, L. E. Edholm, C. E. M. Heeremans, R. A. M. van der Hoeven, W. M. A. Niessen, U. R. Tjaden and J. van der Greef, *J. Chromatogr.*, 474 (1989) 257.
4 W. Luiten, G. Damien and J. Capart, *J. Chromatogr.*, 474 (1989) 265.
5 E. R. Verheij, H. J. E. M. Reeuwijk, W. M. A. Niessen, U. R. Tjaden, J. van der Greef and G. F. LaVos, *Biomed. Environ. Mass Spectrom.*, 16 (1989) 393.
6 Y. Ito, D. Ishii, T. Takeuchi and M. Goto, *J. Chromatogr.*, 346 (1985) 161.
7 Y. Ito, T. Takeuchi, D. Ishii and M. Goto, *J. Chromatogr.*, 358 (1986) 201.
8 T. Kobayashi, K. Matsuura, K. Otsuka, E. Kubota, Y. Itagaki, B. D. Musselman and T. Higuchi, presented at the *36th ASMS Conference on Mass Spectrometry and Allied Topics, June 5–10, 1988, San Francisco, CA.*

Journal of Chromatography, 541 (1991) 243–255
Elsevier Science Publishers B.V., Amsterdam

CHROM. 22 959

Ultrasonic nebulizer interface system for coupling liquid chromatography and electrothermal atomic absorption spectrometry

J. STUPAR*
Institut "Jozef Stefan", Jamova 39, 61000 Ljubljana (Yugoslavia)
and
W. FRECH
Department of Analytical Chemistry, University of Umeå, S-901 87 Umeå (Sweden)
(First received June 6th, 1990; revised manuscript received October 30th, 1990)

ABSTRACT

An ultrasonic nebulizer interface for direct "on-line" coupling of high-performance liquid chromatography (HPLC) with atomic absorption spectrometry with electrothermal atomization is described. Two modes of operation were evaluated for measurement of metal-containing chromatographic peaks. In the continuous mode the atomizer was kept at a preselected constant temperature during the chromatographic run while the analyte species were monitored. This mode of operation is suitable only for elements of high and medium volatility and provides poor detection limits. In the collection mode, the effluent from the HPLC column was thermally decomposed so that sample species, adsorbed on the cool parts of the atomizer, were available for subsequent pulse atomization. Only chromatographic peaks of reasonably different retention times can be measured separately in this mode.

The effects of parameters such as effluent flow-rate and composition, aerosol carrier gas flow-rate and collection temperature of the atomizer were investigated. The effects of different matrices on lead and chromium signals were studied. In the collection mode the detection limit of the system was below 1 ng for both chromium and lead.

INTRODUCTION

Determination of species rather than total metal concentrations at trace levels has been recognized to be vital in biochemical, agricultural and environmental studies. This has stimulated the development of so-called "hybrid techniques", which combine the abilities to separate effectively particular species and provide a sensitive element-specific detection. One of the most popular approaches in speciation is to couple liquid or gas chromatography (GC) and one of the spectroscopic techniques. In this instance, flame and electrothermal atomic absorption spectrometry (ETAAS), inductively coupled plasma (ICP) [1] and laser-stimulated ionization (LEI) [2] have been employed. In most instances, coupling of the two techniques is relatively simple, for example, high-performance liquid chromatography (HPLC)–flame AAS or ICP, but the direct "on-line" measurement of HPLC effluents by ETAAS, which is one of

0021-9673/91/$03.50

the most sensitive techniques, is difficult. To circumvent problems with interfacing, the HPLC effluent has been collected in fractions ranging from 60 μl up to a few millilitres, and subsequently analysed by ETAAS. Most of the papers employing this technique are related to the determination of different copper and zinc blood proteins [3–6] and amino acids [7], but other applications [8–11] have also been published. The major drawback of the technique is that only well separated species can be distinguished.

Brinckman's group at the former National Bureau of Standards developed "well sampler" indirect coupling [12], involving a 50-μl PTFE flow-through cell. The effluent from the HPLC column, continuously passing the cell, is sampled (10–50 μl) at constant time intervals of 40–60 s and atomized in the electrothermal atomizer. This sampling mode has been successfully employed for determination of various organometallic (As, Sn, Hg, Si) compounds [13–15]. The same interface system was used by Fish and co-workers [16–18] in the determination of vanadyl and nickel porphyrin and non-porphyrin compounds in crude oil.

Other similar systems employing a sampling valve, an injector and associated electronics to control the analysis sequence have been developed independently by Vickrey *et al.* [19] and Stockton and Irgolic [20]. These systems delivered 40 μl of column effluent every 30–45 s into an ETAAS system equipped with Zeeman-effect background correction. Organocopper complexes in soil pore water [11] and selenite–selenate in river water [21] were measured by this technique. Both types of interface systems were employed by Brinkman *et al.* [22] for the determination of various arsenic species in soil extracts and drinking water. These two interfaces operate in the so-called "pulsed" mode of sampling, as the atomic absorption data are not continuous in terms of the effluent flow. The frequency of sampling depends merely on the duration of the atomization cycle (30–45 s), and therefore the best results are obtained at low effluent flow-rates and for broad chromatographic peaks. Narrow peaks at high effluent flow-rates can be missed completely by the AA detection system. As an improvement, a "peak storage" interface has been proposed by Vickrey *et al.* [23]. The effluent containing the peak is stored in a capillary tube during the chromatographic run and analysed off-line sequentially by ETAAS. In this way, more measurements can be made per chromatographic peak, which significantly improves the accuracy of the technique. The chromatographic peaks were reported to be broadened, but the resolution can be maintained if the storage tube volume is approximately equal to the peak volume. The concept of Vickrey *et al.* [23] was further modified by Bäckström and Danielsson [24], who connected an extraction system to the interface.

The first real "on-line" coupling of HPLC to a continuously heated graphite atomizer was described by Nygren *et al.* [25], who employed a thermospray interface. The performance of this was evaluated for speciation of tri- and dibutyltin using ion-exchange chromatography. The only limitation of the system was the relatively low effluent flow-rate (up to 0.2 ml/min) which could be tolerated. However, recent developments in designing "thermospray" devices for aerosol production in flame AAS [26] and ICP [27,28] indicate wider possibilities for this type of interface.

The aim of this work was to design and evaluate an interface which would tolerate the higher effluent flow-rates normally used in HPLC and yet provide continuous detection of metal-containing chromatographic peaks by ETAAS. An ultrasonic nebulizer spray chamber–aerosol desolvation system was constructed for this purpose and connected to a graphite atomizer. A similar system has been described recently [29] for interfacing HPLC to a flame photometric detector.

EXPERIMENTAL

Description of the interface

The main components of the ultrasonic nebulizer interface are shown in Fig. 1. The ceramic piezoelectric transducer (Channel Products, Chesterland, OH, U.S.A.) was clamped into the PTFE body by means of a PTFE nut. To prevent nebulizing solution entering the rear of the transducer, a sealing ring was placed in front of it. A brass ring and the centrally positioned brass container provide electrical contacts to the transducer. In order to ensure efficient heat exchange and good electrical contact, the surface of the brass container touching the transducer was polished and the container was spring loaded. The latter permitted relatively free vibration of the transducer.

The transducer temperature was maintained between 50 and 60°C by circulating tap water through the brass container. The transducer was powered by a commercial ultrasonic humidifier (Burg, SIBE International, Spånga, Sweden), which was modified to operate at a resonant frequency of 1.35 MHz. A maximum of 45 V was applied to the transducer. The effluent from the chromatographic column flowed continuously onto the working side of the transducer via a stainless-steel needle (1.1 mm O.D.). A small (17-ml) conical spray chamber, 140 mm long, was held in the PTFE nut, a tight connection being provided by a rubber sealing ring. Constant aerosol transport was maintained by directing a fixed argon flow through the chamber. The effluent condensing in the chamber was removed continuously through the drain tube. The conical part of the spray chamber, which ended in a 105 mm × 6 mm I.D.

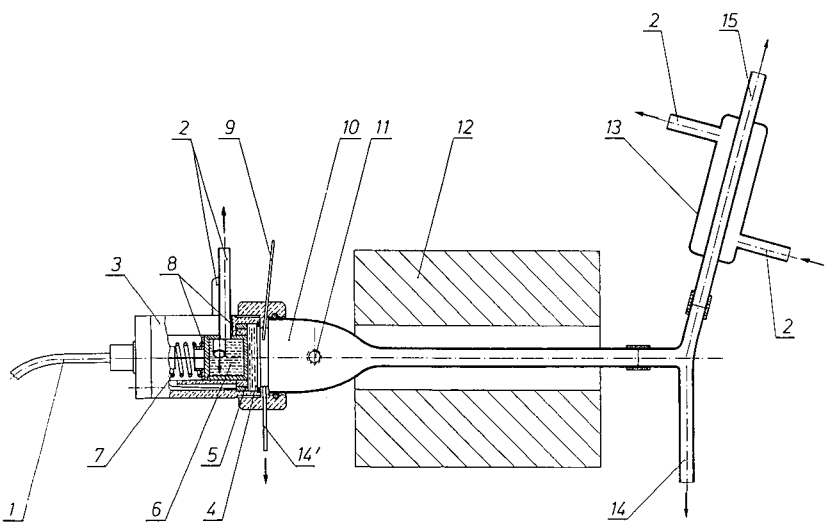

Fig. 1. Ultrasonic nebulizer interface. 1 = Electrical connection (50 V maximum, 1.35 MHz); 2 = cooling water circulating systems; 3 = PTFE body; 4 = piezoelectric transducer; 5 = brass ring providing electrical contact to the front side of the transducer; 6 = brass container for cooling water providing electrical contact to the rear of the transducer; 7 = spring; 8 = PTFE insulation; 9 = inlet tube for HPLC effluent; 10 = glass chamber; 11 = inlet for aerosol carrier gas; 12 = furnace; 13 = glass cooler; 14 = drain; 14′ = drain connected to peristaltic pump; 15 = aerosol supply to the graphite atomizer.

tube, was inserted into an electrically heated oven. The end of the spray chamber was connected to the cooler via a T-piece which provides an outlet for drainage of the condensed solvent. The dry aerosol was injected into the furnace through a 26 mm × 2.0 mm I.D. glassy carbon tube (Ringsdorff-Werke, Bonn, Germany). The latter was inserted into the enlarged sampling hole (3.2 mm diameter) of the atomizer tube so that it did not obstruct the light beams from the hollow-cathode lamps.

Description of the graphite atomizer

The two-step atomizer used in this work has been described in detail previously [30] and incorporates integrated contact (IC) tubes [31] and IC cups. The tube and cup can be heated independently of each other by two separate power supplies. A laboratory-constructed power supply equipped with an optical feed-back system [32] to provide temperature control was used to heat the IC tube. The cup was heated using a Perkin-Elmer HGA-500 power supply. Some measurements were carried out using IC tubes without the cup.

The atomizer was installed in a research spectrometer system [30,31] incorporating a Varian Techtron AA-6 monochromator complete with a hydrogen lamp for background correction. A Tecmar Labmaster with 12-bit ADC was used to interface the spectrometer with an Ericsson PC with a Facit 4513 A4 matrix printer.

Temperature measurements of the inner tube surface and of the inner cup bottom were made using a disappearing filament pyrometer (Keller Spezialtechnik Pyrowerk, Model PBO 6A F3) above 1300 K and otherwise with a NiCr–Ni thermocouple. Hamamatsu hollow-cathode lamps were used as light sources.

Instrumental parameters are listed in Table I.

TABLE I

INSTRUMENTAL PARAMETERS

Parameter	Pb	Cr
Wavelength (nm)	283.3	357.9
Spectral band width (nm)	0.7	0.2
Lamp current (mA)	4	8
Continuous mode of operation		
Atomization temperature (°C)		
Cup	1300[a]	–
Tube	1300[a]	–
Collection mode of operation		
Collection temperature (°C)		
Cup	2200[a]	2500
Tube	Not heated[a]	Not heated[a]
Atomization temperature (°C)		
Cup[b]	1800	2500
Tube[c]	1300	2050

[a] If not stated otherwise.
[b] Heating commenced 2 s after the start of the tube heating.
[c] Atomization time varied between 8 and 15 s.

Reagents and materials

$Pb(NO_3)_2$ and K_2CrO_4 aqueous solutions containing 1 mg/ml of metal were used for measurements of lead and chromium, respectively. Lower standards were prepared freshly in different water–methanol mixtures. Chromium standard solutions contained in addition $5 \cdot 10^{-4}$ *M* tetrabutylammonium phosphate (Supelco, Bellefonte, PA, U.S.A.).

In the interference study, 0.1 *M* NaCl (Merck, Darmstadt, Germany) and 1 *M* NH_4NO_3 (Merck) were used. All solutions were prepared from reagents of the highest available purity. The gas employed for the furnace and as an aerosol carrier was spectroscopic-grade argon. IC tubes and IC cups were manufactured from single pieces of RW0-quality graphite and coated with pyrolytic graphite (Ringsdorff-Werke). The IC tubes had a wall thickness of 0.6 mm and were of 5.7 mm I.D. and 19 mm long (round tubes) or of 5 mm square internal section and 24 mm long. Cups were 8 mm long, 7 mm in depth, of 5.2 mm O.D. and 2.8 mm I.D.

Operating procedure

The interface and electrothermal atomizer could be operated in two different modes:

(1) The "continuous mode", in which the ETA was held at a constant temperature during the whole period of the chromatographic separation. While the effluent was nebulized and transferred to the ETA, the absorbance was monitored continuously. In this mode, a two-step atomizer is not essential and a simpler commercially available system can be employed.

(2) The "collection mode". When the effluent containing the chromatographic peak of interest enters the interface, the atomizer tube or cup was heated to a preselected temperature, characteristic of the element of interest, and maintained constant for a period of time equivalent to the width of the chromatographic peak. Subsequently, the condensed species were atomized by the "pulse technique". The integrated absorbance can be used as a measure of the total metal content in a particular chromatographic peak.

To facilitate the optimization of the interface and ETA performance, the HPLC effluent flow was simulated by a peristaltic pump and a range of flow-rates (0.5–2.0 ml/min) normally encountered in HPLC were investigated. The chromatographic peak width and the total mass of element in a particular peak were varied by introducing samples into the stream of eluent over different time periods (5–20 s) and changing the concentration of the element in the solution.

RESULTS AND DISCUSSION

Continuous mode of operation

For this mode of operation the flow-rate of the carrier gas affects both aerosol transport efficiency and residence time of atoms in the detector. At very small flow-rates the residence time of droplets in the aerosol chamber becomes relatively long and, owing to the high rate of coalescence, considerable deposition losses of the effluent occur. This reduction in sample transport efficiency is, however, outweighed by an increase in detector sensitivity at lower flow-rates. The dependence of the detector sensitivity on aerosol carrier gas flow-rate is shown in Fig. 2. To achieve

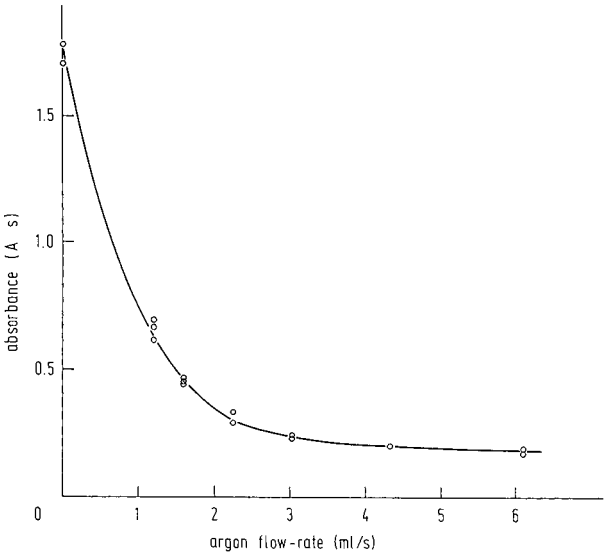

Fig. 2. Sensitivity of the detector varied by the aerosol carrier gas flow-rate (10 ng Pb).

reasonable precision, flow-rates below 1.0 ml/s should be avoided. For further experiments we used a flow-rate of 2.3 ml/s, thus lowering the sensitivity to *ca.* 20% of its maximum value.

The influence of effluent flow-rate on the sensitivity (sample throughput) was investigated in separate experiments, and very little variation in the signal magnitude was found in the range of flow-rates from 0.8 to 1.8 ml/min; 1 ml/min was chosen for further experiments.

The sensitivity of measurements employing the continuous mode was found to be relatively poor owing to the low sample transport efficiency of the interface and the detrimental effect of argon flow-rate on atom residence time in the graphite tube. In addition, the variations of the blank values were large because of long integration times and resulted in poor detection limits compared with previously described interface techniques [12–23].

Further, the 13-ml dead volume of the interface caused postcolumn chromatographic peak broadening of less than 20%. Another difficulty associated with the continuous mode of operation arises when elements requiring high atomization temperatures are monitored. In this instance the atomizer has to be kept at temperatures exceeding 2000°C for extended periods of time, which means that special furnaces have to be designed. To obviate these problems, an alternative method of chromatographic peak measurement was sought. In a recent paper, Demarin *et al.* [33], while determining various organogermanium and organosilicon species by GC–ETAAS, proposed a technique by which these compounds were decomposed and collected on the wall of the furnace and subsequently atomized in the "pulse mode". Detection limits 7–8 times lower than those in the continuous mode of operation were reported.

A similar approach was therefore investigated for the HPLC–ETAAS combination.

Collection mode of operation

The necessary requirement to employ this mode of operation is that the retention times (t_r) and approximate widths of the chromatographic peaks are known. The difference in the t_r values of two subsequent species of interest should be large enough to permit atomization of the first species collected before the collection parameters are re-established.

In order to collect analyte species efficiently, it is important that aerosol particles are vaporized before they are carried out of the atomizer by the convective gas stream. In contrast to aerosol particles, vapours will be trapped more readily, in particular if large temperature gradients exist in the graphite atomizer. Therefore, the use of the two-step atomizer was regarded as advantageous, as either the cup or the tube can be heated to vaporize the aerosol. Collection of the vapour species can then take place at the graphite parts which are not heated. It should be emphasized that the temperature required to vaporize the aerosol depends on its thermochemical properties, hence optimum temperatures have to be selected for a particular analyte and the matrix.

Collection of lead

In the first approach the tube was heated to various temperatures to vaporize the aerosol, which in this instance can be assumed to be present as lead nitrate particles. The analyte species were subsequently collected on the cool cup wall, which was not directly heated. As can be seen from Fig. 3, optimum collection efficiencies were obtained for tube temperatures between 650 and 750°C. Lead nitrate decomposes at 470°C, however, and the higher temperatures needed for best collection should be ascribed to effects caused by the convective argon flow, which will cool the gas phase of the tube and shorten the residence time of particles therein. Therefore, at insufficiently high temperatures particles might leave the tube only being partly vaporized. On the

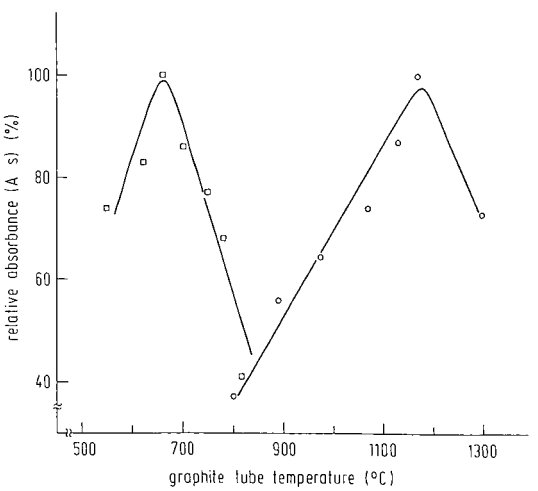

Fig. 3. Collection efficiency for 68.7 ng of lead (□), and 11 ng chromium (○) as a function of the graphite tube temperature. A two-step atomizer and a 19 mm long IC tube was used for lead and chromium, respectively. Solutions contained methanol–water (1:1, v/v). The effluent flow-rate was 1 ml/min. Aerosol carrier gas flow-rates of 2.6 ml/s (Pb) and 9.7 ml/s (Cr) were employed.

other hand, at too high temperatures a fraction of the analyte will be lost by re-evaporation.

In the second approach, the possibility of trapping the analyte species resulting from lead nitrate on the atomizer tube surface was investigated. In this instance, the cup was heated and the optimum temperature was found to be between 2200 and 2400°C. In this range the sensitivity and hence transport and/or collection efficiencies were 2–3 times higher than in the first approach and variations of the cup temperature in this temperature interval only slightly changed the sensitivity. Therefore, in subsequent experiments only the mode with the cup heated was investigated.

Collection of chromium

The temperature dependence of the collection of chromium species was investigated using IC tubes only or the two-step atomizer with the cup heated and the tube kept cool. The results are shown in Fig. 3 and it can be seen that collection efficiencies are strongly temperature dependent.

Effect of carrier gas flow-rate on sensitivity

An increase in the carrier gas flow-rate is expected to improve the transport efficiency of the aerosol from the spray chamber to the graphite atomizer and will, at the same time, reduce the residence time of the analyte species in the atomizer. The velocity of the gas through the graphite tube is in addition dependent on the applied collection temperature. This effect will be more pronounced if the tube is heated during aerosol collection. In this instance, it can be generally expected that lower flow-rates of carrier gas will be required for optimum collection, in contrast to the situation where the cup is heated. In the latter arrangement the aerosol particles are ejected from the entrance port at high speeds directly to the hot cup bottom where vaporization takes place. The convective flow of argon is maintained predominantly through the atomizer tube arms and thus an increase in the flow-rate does not influence to the same extent the removal of analyte species from the cup.

The effect of the argon flow-rate on the sensitivity of lead when the cup was heated for collection is shown in Table II. The optimum argon flow-rate extends over a fairly wide range, between 14 and 18 ml/s.

Effect of effluent flow-rate and matrix composition on transport efficiency and analytical signal

In HPLC, effluents containing various concentrations of organic solvents are usually obtained at flow-rates of 0.1–2 ml/min. Methanol, as one of the most frequently used mobile phases, was employed in this work. The effects of varying the composition of the methanol–water mixture and of the effluent flow-rate on the absorption signal were studied. In addition, the influence of some salt matrices was also examined.

Table III shows that a fairly low flow-rate of solution in the range 0.5–0.7 ml/min results in the most efficient sample transport. Towards lower or higher flow-rates the nebulization efficiency decreased for the vertically positioned transducer which was used here. The reason is that at very low flow-rates the sample makes contact with only a relatively small area of the vibrating surface, resulting in poor and irregular nebulization. At higher flow-rates the crystal surface is entirely covered by a regular

TABLE II

PEAK-AREA ABSORBANCES FOR 34 ng OF LEAD IN METHANOL–WATER (1:1) AS A FUNCTION OF AEROSOL CARRIER GAS FLOW-RATE

Cup temperature during collection, 2400°C.

Argon flow-rate (ml/s)	Peak area (A s)	Argon flow-rate (ml/s)	Peak area (A s)
5.0	0.185	14.5	0.588
6.8	0.235	16.8	0.586
10.7	0.435	18.3	0.620
12.5	0.539	20	0.518

liquid film, which will increase [34] in thickness so that the proportion of larger droplets formed will increase [35], reducing the transport efficiency.

It is well known that the diameter and the number of droplets formed during the nebulization process are merely dependent on the viscosity and surface tension of the nebulized solution [35]. This means that a change in the concentration of methanol is likely to affect the transport efficiency in the interface used in this work. However, measurements of lead using methanol–water solutions showed no systematic variation of peak-area absorbance on changing the methanol content from 50% to 90%. In a similar experiment, an increase in absorbance equal to twice the standard deviation of measurements was observed for chromium. This indicates that the interface can be used successfully for chromatographic separations using gradient elution. In order to check the extent to which the analytical results are affected by salt matrices, lead in the presence of 0.1 *M* NaCl and 1 *M* NH_4NO_3 was investigated. As can be seen from Table IV, 80 mg/ml of NH_4NO_3 did not alter the sensitivity of lead, whereas a ten times lower concentration of NaCl increased the signal significantly. It has been shown in previous studies [36] that ultrasonic nebulizers can tolerate fairly high salt concentrations in the solution without affecting the nebulization rate. The reason for the observed effect of 0.1 *M* NaCl present in methanol–water (1:1) effluent on the lead absorbance signal should therefore be sought in some other phenomena. It should be noted that a background signal, caused by NaCl, was observed during the atomization

TABLE III

NORMALIZED PEAK AREA FOR LEAD IN METHANOL–WATER (1:1) AS A FUNCTION OF EFFLUENT FLOW-RATE

Aerosol carrier gas flow-rate, 14.5 ml/s; collection temperature, 2200°C.

Effluent flow-rate (ml/min)	Peak area per ng Pb (A s)	Effluent flow-rate (ml/min)	Peak area per ng Pb (A s)
0.28	0.0147	1.00	0.0164
0.55	0.0225	1.43	0.0117
0.77	0.0191	1.96	0.0089

TABLE IV

MATRIX INTERFERENCE EFFECTS ON 30 ng OF LEAD

Effluent flow-rate, 1 ml/min; collection time, 10 s; carrier gas flow-rate, 14 ml/s; cup temperature, 2200°C.

Matrix	Peak area (A s)	Matrix	Peak area (A s)
H_2O	0.690 ± 0.020	H_2O	0.808 ± 0.064
1 *M* NH_4NO_3	0.726 ± 0.079	0.1 *M* NaCl	1.077 ± 0.085

of lead (see Fig. 4). If it is assumed that the atomization efficiency of lead is decreased in the presence of sodium chloride, the positive effect of this matrix on aerosol transport and/or collection would be even more pronounced. It is also evident from the signals shown in Fig. 4 that the major part of the analyte is not collected on the tube surface but on the cup surface which was heated during the collection. In the mode in which the graphite atomizer was operated, the upper part of the cup which is in direct contact with the cool tube will attain relatively low temperatures in comparison with the remainder of the cup. Sample vapours may therefore predominantly condense at the vicinity of the top, *i.e.*, on the rim of the cup. It is also reasonable to assume that convective gas flows are lower in the cup than in the tube, which favours condensation in the cup.

During atomization, the tube is heated first and then, after a selected delay time, the cup. In this mode of operation the upper part of the cup will be heated to some extent by the tube and when cup heating commences the entire cup will approach spatial isothermality.

In separate experiments, the effect of the power setting on the transducer performance was investigated. An increase in power resulted in a higher aerosol output. However, for long-term operation it is not recommended to use the highest settings because of the risk for overheating the transducer.

Dependence of peak width on sensitivity

In order to ensure an accurate determination of the analyte present as various species, separated by HPLC procedures, employing the interface in the collection mode, the influence of the chromatographic peak width on the sensitivity was examined. In this experiment the mass of lead was varied between 20 and 340 ng while the peak half-width, equivalent to the time of sample introduction, was varied between 5 and 20 s. The results showed a linear relationship between integrated absorbance and mass of lead, regardless of peak half-width.

Detection limits and reproducibility

Detection limits for chromium were measured on several occasions using both the two-step atomizer and the IC tube without a cup. The values obtained, based on three times the standard deviation for samples containing 7–14 ng of chromium corrected for blank values, were in the range 0.4–1.2 ng. In each series, blanks and samples were run alternately and each value reported is based on 10–15 measurements.

The detection limit for lead was determined using only the two-step atomizer with the cup heated for collection. The value obtained for samples containing 1.1 ng of

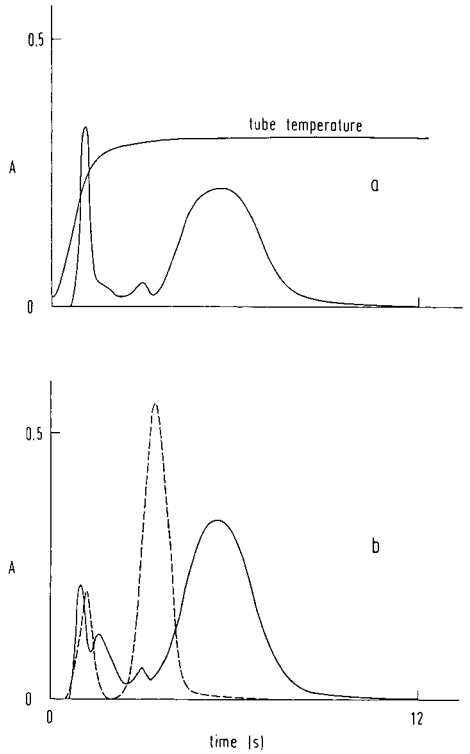

Fig. 4. Signal traces for 30 ng of lead trapped with the two-step atomizer (the cup was heated for collection). (a) Aqueous solution; (b) lead in 0.1 *M* NaCl. The dashed line denotes the background absorption.

lead was 0.3 ng using the above criteria for calculation. In both instances methanol–water (1:1) was employed.

The relative standard deviations of measurements were typically between 3 and 10%. If larger masses of chromium (above 100 ng) were determined, the signals started to tail resulting in poor reproducibility and memory effects. This problem is caused by the glassy carbon capillary inserted in the tube (even during atomization). The capillary does not reach a sufficiently high temperature for complete removal of large masses of chromium during the atomization step. This memory effect is eliminated by introducing an additional atomization sequence without sample.

CONCLUSIONS

The interface system described here facilitates "on-line" coupling of an HPLC column to an ETAAS system. Various effluents at flow-rates commonly encountered in HPLC can be employed without problems. Two modes of operation are proposed, a continuous and a collection mode, both yielding approximately the same sensitivity. The convective flow of argon through the atomizer in the continuous mode and incomplete trapping of the analyte in the graphite atomizer during collection are the limiting factors.

However, in the collection mode the detection limits are substantially improved (typically by one order of magnitude), and in addition the measured signals are not affected by the dispersion of the chromatographic system and/or postcolumn peak broadening. The system should be applicable to a large number of elements and the detection of less than 1 ng of analyte present in one chromatographic peak is possible.

Many inter-element variables critically affect the performance of the interface–graphite atomizer and hence optimization of the system for a particular chromatographic separation is necessary. In this respect it is desirable to investigate separately effects of effluent composition on processes such as nebulization, aerosol transport, trapping and atomization of the analyte.

ACKNOWLEDGEMENTS

The authors thank Svante Jonsson and Lars Lundmark for technical assistance and Douglas Baxter for linguistic revision. This work was supported by the Swedish Centre for Environmental Research and the Natural Science Research Council.

REFERENCES

1 L. Ebdon, S. Hill and R. W. Ward, *Analyst (London)*, 112 (1987) 1.
2 K. S. Epler, T. C. O'Haver, G. C. Turk and W. A. MacCrehan, *Anal. Chem.*, 60 (1988) 2062.
3 P. E. Gardiner, J. M. Ottaway, G. S. Fell and R. R. Burns, *Anal. Chim. Acta*, 124 (1981) 281.
4 J. W. Foote and H. T. Delves, *Analyst (London)*, 108 (1983) 492.
5 J. W. Foote and H. T. Delves, *Analyst (London)*, 109 (1984) 709.
6 D. C. Chilvers, J. B. Dawson, M. H. Bahreyni-Toosi and A. Hodgkinson, *Analyst (London)*, 109 (1984) 871.
7 N. Kahn and J. C. Van Loon, *J. Liq. Chromatogr.*, 2 (1979) 23.
8 P. Tittarelli and A. Mascherpa, *Anal. Chem.*, 53 (1981) 1466.
9 A. A. Grabinski, *Anal. Chem.*, 53 (1981) 966.
10 G. Drasch, L. V. Meyer and G. Kauert, *Fresenius' Z. Anal. Chem.*, 311 (1982) 695.
11 L. Brown, S. J. Haswell, M. M. Rhead, P. O'Neil and K. C. C. Bancroft, *Analyst (London)*, 108 (1983) 1511.
12 F. E. Brinckman, W. R. Blair, K. L. Jewett and P. V. Iverson, *J. Chromatogr. Sci.*, 15 (1977) 493.
13 E. J. Parks, F. E. Brinckman and W. R. Blair *J. Chromatogr.*, 185 (1979) 563.
14 K. L. Jewett and F. E. Brinckman, *J. Chromatogr. Sci.*, 19 (1981) 583.
15 E. J. Parks, R. B. Johannesen and F. E. Brinckman, *J. Chromatogr.*, 255 (1983) 439.
16 R. H. Fish, F. E. Brinckman and K. L. Jewett, *Environ. Sci. Technol.*, 16 (1982) 174.
17 R. H. Fish and J. J. Komlenic, *Anal. Chem.*, 56 (1984) 510.
18 R. H. Fish, J. J. Komlenic and B. K. Wines, *Anal. Chem.*, 56 (1984) 2452.
19 T. M. Vickrey, M. S. Buren and H. E. Howell, *Anal. Lett.*, A11 (1978) 1075.
20 R. A. Stockton and K. J. Irgolic, *Int. J. Environ. Anal. Chem.*, 6 (1979) 313.
21 D. Chakraborti, D. C. J. Hillman, K. J. Irgolic and R. A. Zingaro, *J. Chromatogr.*, 249 (1982) 81.
22 F. E. Brinckman, K. J. Jewett, W. P. Iverson, K. J. Irgolic, K. C. Ehrhardt and R. A. Stockton, *J. Chromatogr.*, 191 (1980) 31.
23 T. M. Vickrey, H. E. Howell and M. T. Paradise, *Anal. Chem.*, 51 (1979) 1880.
24 K. Bäckström and L. G. Danielsson, *Anal. Chem.*, 60 (1988) 1354.
25 O. Nygren, C. Nilsson and W. Frech, *Anal. Chem.*, 60 (1988) 2204.
26 J. W. Robinson and D. S. Choi, *Spectrosc. Lett.*, 20 (1987) 375.
27 J. A. Koropchak and D. H. Winn, *Appl. Spectrosc.*, 41 (1987) 1311.
28 J. A. Koropchak and H. Aryamanya-Mugisha, *Anal. Chem.*, 60 (1988) 1838.
29 J. F. Karnicky, L. T. Zitelli and Sj. Van der Wal, *Anal. Chem.*, 59 (1987) 327.
30 W. Frech, D. C. Baxter and E. Lundberg, *J. Anal. At. Spectrosc.*, 3 (1988) 21.
31 W. Frech, D. C. Baxter and B. Hütsch, *Anal. Chem.*, 58 (1986) 1973.

32 G. Lundgren, L. Lundmark and G. Johansson, *Anal. Chem.*, 46 (1974) 1028.
33 V. T. Demarin, N. K. Rudnevski, L. V. Sklemina, V. A. Krylov and A. E. Nikolaev, *Zh. Anal. Khim.*, 42 (1987) 296.
34 R. J. Lang, *J. Acoust. Soc. Am.*, 34 (1962) 6.
35 J. Stupar and J. B. Dawson, *Appl. Opt.*, 7 (1968) 1351.
36 J. Stupar, *PhD. Thesis*, University of Ljubljana, Ljubljana, 1974.

Journal of Chromatography, 541 (1991) 257–264
Elsevier Science Publishers B.V., Amsterdam

CHROM. 22 914

Sensitivity of electrokinetic detection of acidic aromatic nitro derivatives using column as a detector

RADIM VESPALEC* and JIŘÍ NEČA[a]
Institute of Analytical Chemistry of the Czechoslovak Academy of Sciences, 611 42 Brno (Czechoslovakia)
(First received January 25th, 1990; revised manuscript received October 8th, 1990)

ABSTRACT

A stainless-steel analytical column of 2 mm I.D. served as an electrokinetic detector. The minimum detectable amounts of nitrophenols eluted from both unmodified and chemically modified silica gel with *n*-heptane–acetone (90:10) acidified with 10 ppm of nitric acid were of the order of 10^{-9}–10^{-11} mol. The minimum detectable quantity of dipicrylamine, $1.8 \cdot 10^{-13}$ mol, represents a detection sensitivity one order of magnitude higher than the highest possible using photometric detection.

INTRODUCTION

Electrokinetic detection is considerably selective towards ionizing solutes [1,2] and suitable even for columns of small dimensions [3]. The technique is based on the measurement of the charge acquired by the liquid flowing along the solid surface.

Charging of the liquid results from the tendency for any phase (in a physico-chemical sense) to accept the charge. This tendency depends only on the composition [4]. If two phases of different chemical composition come into contact, their charges and also those originating from the contact between the two phases will redistribute. As a result, the positive charge is in excess in one phase and the negative charge is in excess in the other. Redistributed charges of opposite polarities attract one another. They are therefore localized at the plane of contact of the phases and form an electric double layer.

The model of the electric double layer at the solid–liquid boundary (Fig. 1) assumes that the charge acquired by the liquid occurs within a certain distance from the solid surface [4]. The thickness of the electric double layer is usually 5–200 nm in aqueous solutions of electrolytes [4]. In low-polarity mixtures of organic solvents it can even be more than 10 μm [5]. If the liquid is made to move by the pressure gradient, it carries part of the charge scattered in the liquid [4]. The charge carried can be trapped on the electrode and then measured as the streaming current, I_s, and sometimes also as

[a] Present address: Institute of Forest Ecology, Agricultural University, 644 00 Brno-Soběšice, Czechoslovakia.

0021-9673/91/$03.50

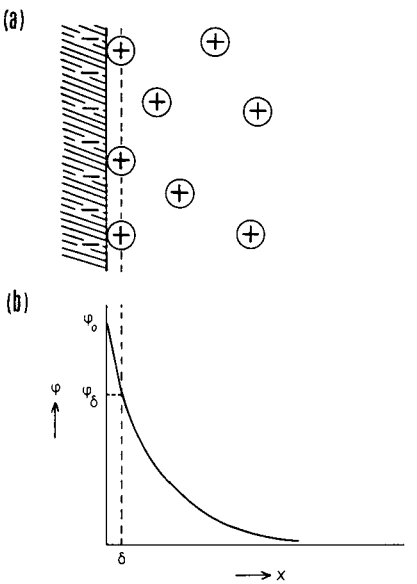

Fig. 1. Stern's model of electric double layer at a solid–liquid interface. (a) Distribution of charges on the solid surface and in the liquid. (b) Course of the potential created by the solid-phase charge in the liquid. δ = Thickness of the compact layer of electric double layer; ϕ_0 = surface potential of the solid-phase; ϕ_δ = potential at the boundary between the compact and the diffuse layers of the electric double layer.

the streaming potential [4,6]. Generation of responses by solute zones results from the dependence of the redistributed charge on the flowing liquid composition.

Minimum detectable quantities (MDQ) of ionizable solutes of the order of 10^{-9}–10^{-11} are typical of reversed-phase columns of I.D. 4–4.6 mm [1,2]. An MDQ one order of magnitude lower was reported in a single instance [7]. Post-column electrokinetic detectors were used. The measured signal was generate either in an empty or a filled capillary. The disadvantage of these detectors, *viz.*, a high pressure drop, can be eliminated if the chromatographic column is used as a source of the measured signal [3]. If the column was operated as a detector, carboxylic acids were detected in a reversed-phase system with a sensitivity [8] comparable to that obtained with detectors behind the column [1,2]. The possibility to reaching sufficiently high sensitivities in normal-phase systems with the column as a detector was therefore tested in this work.

EXPERIMENTAL

The design used for the sensing of the streaming current from the metallic column jacket, the measurement procedure and the apparatus used were described previously [8]. The streaming current was measured with a Model 427 current amplifier (Keithley Instruments, Cleveland, OH, U.S.A.). If not stated otherwise, 150 × 2 mm I.D. columns were used. Silasorb 300 (mean particle diameter d_p = 12.4 μm, specific surface area S = 350 m^2/g, specific pore volume v_p = 0.79 ml/g) supplied by Lachema (Brno, Czechoslovakia) served as a stationary phase. Methyl (Silasorb C_2), octyl

TABLE I

INJECTED SOLUTES

Solute	pK_a[a]	Abbreviation
3-Nitrophenol	8.29	3-NP
4-Nitrophenol	7.15	4-NP
2,4-Dinitrophenol	4.08	2,4-DNP
2,5-Dinitrophenol	5.15	2,5-DNP
Picric acid	0.80	HPi
Dipicrylamine	5.42[b]	DPA

[a] Ref. 9.
[b] Ref. 10.

(Silasorb C_8) and cyanopropyl (Silasorb Nitrile) derivatives were prepared from Silasorb 300 by common derivatization procedures. A methyl derivative (Silasorb 600 C_2) was also prepared from Silasorb 600 (Lachema) (d_p = 12.4 μm, S = 460 m^2/g, v_p = 0.80 ml/g).

The filled columns were flushed with 200 ml of ethanol (flow-rate 2 ml/min), 40 ml of distilled water (1 ml/min), 100 ml of 20 m*M* nitric acid (0.2 ml/min), 25 ml of distilled water (1 ml/min) and 40 ml of ethanol (1 ml/min). Prior to the measurement each column had been being flushed with the mobile phase (0.5 ml/min) until the streaming current generated by the mobile phase (background current), I_s, was constant for at least 1 h.

n-Heptane, acetone and nitric acid used for the preparation of the mobile phases were of analytical-reagent grade. Solutes of analytical-reagent grade (Table I) were injected by a microsyringe as solutions in acetone. pK_a values are valid for aqueous solutions at 25°C.

RESULTS AND DISCUSSION

The solute response is expressed as the change of the background current, ΔI_s, at the zone maximum. In reversed-phase systems the detection sensitivity increases with the background current, I_s, [1] and solute pK_a [1,7]. Chemical derivatization of silica gel increases the acidity of residual silanols [11] and hence also I_s. The influence of the derivatization appeared very marked with the *n*-heptane–acetone (90:10) mobile phase [5] and this mobile phase was therefore chosen for the present study. The acidity of nitrophenol depends on the number and position of nitro groups in the molecule (Table I). Dipicrylamine was used as a nitro compound of another type.

With *n*-heptane–acetone (90:10) mobile phase all nitrophenols were eluted from the column filled with Silasorb 300. However, the zones of more acidic solutes, especially picric acid, were asymmetric. The addition of 10 ppm of nitric acid suppressed zone asymmetry (Fig. 2). The elution time of dipicrylamine was longer than 2 h.

The electrokinetic detection has character of mass detection in the experimental arrangement used [12]. The charge generated by unit mass of the solute (the charge yield) is therefore an exact theoretical measure of the detection sensitivity. Charge

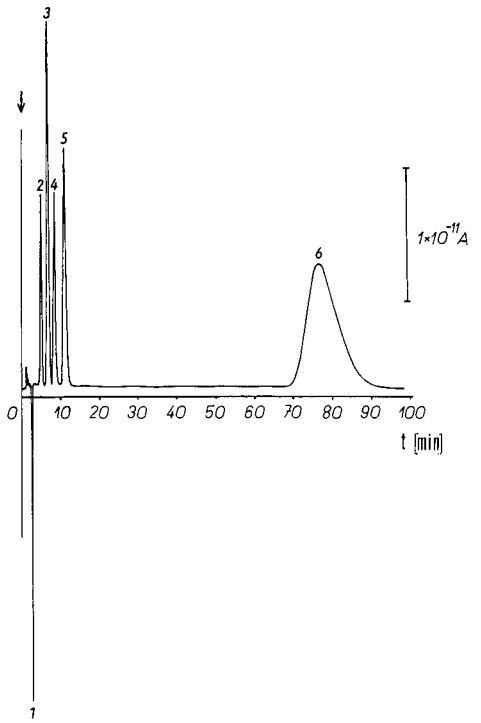

Fig. 2. Chromatogram of a mixture of phenol nitro derivatives. Column, 150 × 2 mm I.D.; stationary phase, Silasorb 300; mobile phase, *n*-heptane–acetone with 10 ppm of HNO_3; flow-rate, 0.2 ml/min; noise, $1 \cdot 10^{-13}$ A. Peaks: 1 = acetone (1 μl); 2 = 2,5-DNP ($4.0 \cdot 10^{-7}$ mol); 3 = 2,4-DNP ($3.0 \cdot 10^{-7}$ mol); 4 = 3-NP ($4.0 \cdot 10^{-7}$ mol); 5 = 4-NP ($2.0 \cdot 10^{-7}$ mol); 6 = HPi ($3.0 \cdot 10^{-7}$ mol).

yields obtained from the chromatogram in Fig. 2 and re-calculated for 1 mol (molar charge yields, Q) are summarized in Table II. With a common assumption that only univalent ions exist in low-polarity liquids [13], Q can theoretically reach 96 500 C/mol. The calculated Q values are 4–7 orders of magnitude lower.

TABLE II

MOLAR CHARGE YIELDS (Q) AND MINIMUM DETECTABLE QUANTITIES (MDQ) OF AROMATIC NITRO DERIVATIVES IN A SEPARATION SYSTEM OF SILASORB 300 WITH *n*-HEPTANE–ACETONE (90:10) ACIDIFIED WITH 10 ppm OF NITRIC ACID

The values were calculated from the chromatogram in Fig. 2.

Solute	Q (C/mol)	MDQ (mol)
3-Nitrophenol	$1.8 \cdot 10^{-3}$	$5.8 \cdot 10^{-9}$
4-Nitrophenol	$5.4 \cdot 10^{-3}$	$2.5 \cdot 10^{-9}$
2,4-Dinitrophenol	$3.9 \cdot 10^{-3}$	$2.2 \cdot 10^{-9}$
2,5-Dinitrophenol	$1.5 \cdot 10^{-3}$	$5.3 \cdot 10^{-9}$
Picric acid	1.6	$6.5 \cdot 10^{-11}$

TABLE III

INFLUENCE OF DIFFERENT ORGANIC GROUPS MODIFYING SILICA GEL SURFACE ON BACKGROUND CURRENT (I_s), CAPACITY FACTORS (k'), MOLAR CHARGE YIELDS (Q) AND MINIMUM DETECTABLE QUANTITIES (MDQ) OF SELECTED SOLUTES IN *n*-HEPTANE–ACETONE (90:10) MOBILE PHASE ACIDIFIED WITH 10 ppm OF NITRIC ACID

For other conditions of measurements, see Fig. 2.

Stationary phase	I_s (pA)	4-NP			HPi		
		k'	$Q \cdot 10^3$ (C/mol)	MDQ $\cdot 10^{10}$ (mol)	k'	Q (C/mol)	MDQ $\cdot 10^{10}$ (mol)
Silasorb 300	15	2.9	5.4	25	27.6	1.6	0.7
Silasorb C_2	15	–	–	–	5.1	2.0	1.1
Silasorb C_8	300	–	–	–	1.7	3.3	3.2
Silasorb Nitrile	90	0.9	3.2	200	7.3	0.9	1.9
Silasorb 600 C_2	25	1.3	2.3	64	8.8	1.9	0.5

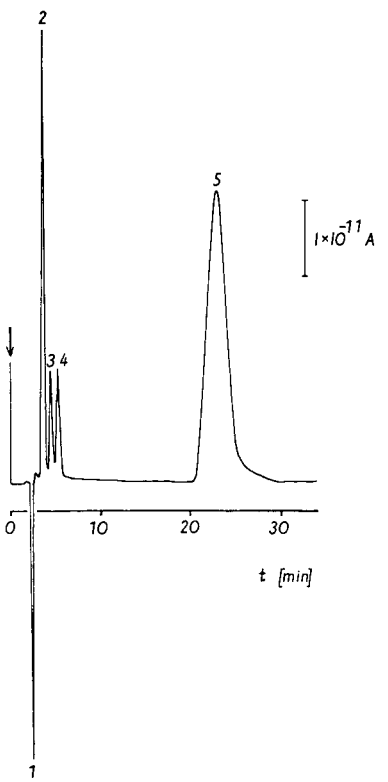

Fig. 3. Chromatogram of a mixture of phenol nitro derivatives. Stationary phase, Silasorb 600 C_2. For other conditions, see Fig. 1. Noise, $3 \cdot 10^{-13}$ A. Peaks: 1 = acetone (1 μl); 2 = 2,4-DNP ($3.0 \cdot 10^{-7}$ mol); 3 = 3-NP ($2.0 \cdot 10^{-7}$ mol); 4 = 4-NP ($1.5 \cdot 10^{-7}$ mol); 5 = HPi ($3.0 \cdot 10^{-9}$ mol).

The practical measure of detection sensitivity is the MDQ. The MDQs in Table II were calculated as the minimum quantities of solute causing a response equal to twice the background current noise (peak-to-peak).

The background current is strongly dependent on the groups bonded to silica gel [5]. The influence of bonded groups on both Q and MDQ was therefore investigated. However, neither the expected growth of the molar charge yield nor an increase in MDQ with increasing I_s was found (Table III). Zones of more acidic solutes and picric acid in particular were highly asymmetric on Silasorb C_2 and Silasorb Nitrile. A reference experiment with Silasorb 600 C_2 showed (Fig. 3) that bad peak shapes on both Silasorb C_2 and probably Silasorb Nitrile cannot be ascribed to bonding of organic groups unambiguously. Dipicrylamine was detected with a higher sensitivity than nitrophenols with elution from any modified silica gel. The highest detection sensitivity for dipicrylamine was observed with Silasorb C_2 (Fig. 4).

The MDQ of dipicrylamine ($k' = 8.8$) calculated from Fig. 4, $1.8 \cdot 10^{-13}$ mol, is one order of magnitude lower than the lowest value reported for a post-column electrokinetic detector (Table IV). In this experiment [7], sulphuric acid was eluted in the column exclusion volume with water as the mobile phase. The best results for nitrophenols are comparable to the highest sensitivities measured using reversed-phase systems with post-column electrokinetic detectors (Table IV).

The composition of the mobile phase was not optimized from the viewpoint of the detection of individual compounds. The nitric acid concentration was chosen tentatively to ensure the symmetry of the zone of the most acidic solute, picric acid, on elution from Silasorb 300. The responses of all the solutes decreased about five-fold with increase in nitric acid concentration to 20 ppm. During the elution from the column filled with Silasorb 300 modified by octadecyl groups, the solute responses increased more than ten-fold after the replacement of acetone mobile phase with acetonitrile [8]. It can therefore be expected that the sensitivity of the electrokinetic detection can be increased further by optimizing the chromatographic system composition from the viewpoints of both separation and electrokinetic detection. Comparison of Q values summarized in Tables II and III with the theoretical value $Q = 96\,500$ C/mol supports such an expectation.

To compare the sensitivity of the electrokinetic detection that has so far been achieved with that of photometric detection let us consider a good UV spectrophoto-

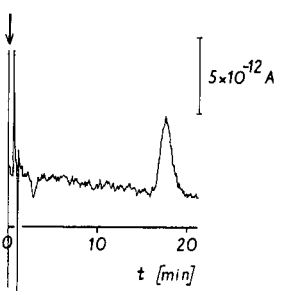

Fig. 4. Chromatogram of DPA. Stationary phase, Silasorb 600 C_2; mobile phase flow-rate, 0.5 ml/min; amount of solute injected, $6.9 \cdot 10^{-13}$ mol in 1 μl of acetone. For other conditions, see Fig. 1. Noise, $8 \cdot 10^{-13}$ A.

TABLE IV

COMPARISON OF THE BEST MDQ VALUES IN THE PRESENT WORK WITH THE BEST FROM REF. 1

Solute	MDQ (mol)	
	Measured	Reported [1]
3-Nitrophenol	$5.8 \cdot 10^{-9}$	$5.7 \cdot 10^{-8}$
4-Nitrophenol	$2.5 \cdot 10^{-9}$	$4.0 \cdot 10^{-9}$
2,4-Dinitrophenol	$2.2 \cdot 10^{-9}$	$3.7 \cdot 10^{-11}$
2,5-Dinitrophenol	$5.3 \cdot 10^{-9}$	–
Picric acid	$5.0 \cdot 10^{-11}$	$2.5 \cdot 10^{-11}$
Dipicrylamine	$1.9 \cdot 10^{-13}$	–
Sulphuric acid	–	$3.5 \cdot 10^{-12}$[a]

[a] From ref. 7.

meter with a noise level of $2 \cdot 10^{-5}$ absorbance and a cell path length of 10 mm. A typical column ($N = 3 \cdot 10^4$–$5 \cdot 10^4$ plates/m) will dilute a sample ($k' = 1$–10) by at least a factor of 10. If the solute has a very high molar absorptivity of about $4 \cdot 10^4$–$5 \cdot 10^4$ (*p*-nitrophenol, picric acid) [14], the lowest possible sample concentration injected on the column is $1 \cdot 10^{-7}$ mol/l. For a 10-μl sample loop injection, such a concentration sensitivity corresponds to an MDQ of $1 \cdot 10^{-12}$ mol. The dipicrylamine MDQ, $1.8 \cdot 10^{-13}$ mol, is one order of magnitude lower than the best value assessed for spectrophotometry. For solutes having very low absorptivity, *e.g.*, 50 (aliphatic carboxylic acids at 200 nm) [14], the minimum sample concentration for spectrophotometry is $1 \cdot 10^{-4}$ mol/l and the sample MDQ is $1 \cdot 10^{-9}$ mol for a 10-ml injection. In accordance with an MDQ of the order of 10^{-10}–10^{-11} mol typical of ionizing solutes, measured in reversed-phase systems with post-column detectors [1,2,7], MDQs of *ca.* $2 \cdot 10^{-10}$ mol were reached for caprylic, palmitic and stearic acids in a reversed-phase system with the column as a detector [8].

MDQs of the order of 10^{-13} mol were reported for a coulometric detector connected behind a 0.5 mm I.D. packed capillary column [15].

An increase in the detection sensitivity with the background current and a simple relationship between the detection sensitivity and the solute pK_a, reported for reversed-phase systems [1,7], were not verified by our experiments with normal-phase systems (Tables I, II and III). However, the dependence of Q on the solute retention was found, in agreement with the earlier observation [16]. Different effects of the solute retention and the background current on the detection sensitivity in normal- and reversed-phase systems can result from different effects of retained solutes on the solid surface charge.

The charge of the solid surface and the charge transported per unit time by the flowing liquid, equal to the streaming current, are directly proportional [4]. Acidic solutes in normal-phase systems can be considered to be retained on the polar silica gel surface at least partly in the form of anions [12]. In this instance the negative charge of silica gel will temporarily increase with increase in the surface solute concentration and hence also with the solute retention. As a result, the detection sensitivity will increase for a retained solute with increase in its retention. In a reversed-phase system the

solutes are retained in the form of molecules only [17]. Uncharged molecules retained on bonded chains have no effect on the solid-phase charge. A higher retention of the solute in a reversed-phase system therefore cannot increase the sensitivity of its detection. If the solid-phase charge increases permanently for a certain reason, both the detection sensitivity of any solute and the background current must increase simultaneously.

The explanation of the different influence of the solute pK_a on the detection sensitivity in normal- and reversed-phase systems requires the use of a theory of streaming current generation by a concentration gradient of the liquid. Such a theory has not yet been suggested.

REFERENCES

1 S. Terabe, K. Yamoto and T. Ando, *Can. J. Chem.*, 59 (1981) 1531.
2 W. Kemula, B. K. Glód and W. Kutner, *J. Liq. Chromatogr.*, 6 (1983) 1823.
3 M. Krejčí, K. Šlais and K. Tesařík, *J. Chromatogr.*, 149 (1978) 654.
4 R. J. Hunter, *Zeta Potential in Colloid Science*, Academic Press, London, 1981.
5 J. Neča and R. Vespalec, in preparation.
6 R. H. Hurd and N. Hackerman, *J. Electrochem. Soc.*, 102 (1955) 594.
7 B. K. Glód and W. Kemula, *J. Chromatogr.*, 366 (1986) 39.
8 J. Neča and R. Vespalec, *J. Chromatogr.*, 514 (1990) 161.
9 Landholt-Bornstein, *Zahlenwerte und Funktionen*, Bd. II, Teil 7, Springer, 6. Aufl., Berlin, 1960; Tokyo, 1966.
10 K. Pan and S.-F. Lin, *J. Chin. Chem. Soc., Ser. II*, (1955) 1.
11 S. G. Weber and W. G. Tramposch, *Anal. Chem.*, 55 (1983) 1771.
12 K. Šlais and M. Krejčí, *J. Chromatogr.*, 148 (1978) 99.
13 J. Gavis and I. Koszman, *J. Colloid Sci.*, 16 (1961) 375.
14 L. Lang (Editor), *Absorption Spectra in the Ultraviolet and Visible Region*, Akadémiai Kiadó, Budapest, 1959.
15 M. Vespalcová, K. Šlais, D. Kouřilová and M. Krejčí, *Cesk. Farm.*, 33 (1984) 278.
16 R. Vespalec and M. Cigánková, *J. Chromatogr.*, 364 (1986) 233.
17 B. K. Glód and W. Kemula, *J. Chromatogr.*, 321 (1985) 433.

Journal of Chromatography, 541 (1991) 265–272
Elsevier Science Publishers B.V., Amsterdam

CHROM. 22 989

Determination of glycerol in foods by high-performance liquid chromatography with fluorescence detection

TAKASHI HAMANO*, YUKIMASA MITSUHASHI, NOBUMI AOKI and SUSUMU YAMAMOTO
Public Health Research Institute of Kobe City, Minatozimanaka-machi, 4–6, Chuo-ku, Kobe 650 (Japan)
SUMIKO TSUJI and YOSHIO ITO
National Institute of Hygienic Science, Osaka Branch, Hoenzaka-cho 1–1, Chuo-ku 540 (Japan)
and
YOSHIKIYO OJI
Faculty of Agriculture, Kobe University, Rokkodai-cho 1–1, Nada-ku, Kobe 657 (Japan)
(First received August 23rd, 1990; revised manuscript received November 5th, 1990)

ABSTRACT

A high-performance liquid chromatographic method for the determination of glycerol in foods is described. The method involves the conversion of glycerol into formaldehyde by sequential enzymatic reactions (glycerokinase, glycerol-3-phosphate oxidase, catalase), followed by the derivatization of formaldehyde with 4-amino-3-penten-2-one. The calibration graph was linear in the range 0.1–4.0 μg/ml of glycerol. Many common ingredients of foods did not interfere. More than 90% of glycerol added at three levels was recovered from several foods. The method is simple and accurate. The detection limit was 1.0 μg/g when 5 g of sample were assayed.

INTRODUCTION

Glycerol (GL) is frequently added to various kinds of foods to increase the water-coating ability and it has also been used as a solvent for various food additives. Current regulations of the Ministry of Health and Welfare of Japan place no limit on the use of GL in foods. The use of the material and the absence of legal limits for its use initiated work on a quantitative method to meet demands, which are claimed by the consumer, to monitor excessive use.

Methods hitherto published for the determination of GL have involved gas chromatographic (GC) [1,2] high-performance liquid chromatographic (HPLC) [3–6] and enzymatic procedures [7]. The method of choice depends on the matrix in which GL is present, its relative concentration in the sample and the complexity of the latter.

Up to now, GL in foods has been determined chiefly by GC [2] or HPLC [5]. Both methods are very useful but require elaborate derivatization reactions and/or clean-up of the sample. In addition, the detection system in HPLC is not specific for GL, thus suffering interferences from other food ingredients when applied to some kinds of foods. Recently, an amperometric method has been applied successfully to the

0021-9673/91/$03.50

determination of GL in biological fluids [6], but the method has limitations and the instrument required is not commonly available in many laboratories.

GL can be converted by glycerokinase to glycerol-3-phosphate, which is then oxidized by second enzyme, glycerol-3-phosphate oxidase, to produce hydrogen peroxide. Preliminary experiments with use of existing techniques [8,9] resulted in the quantification of hydrogen peroxide with low presicion when working with certain kinds of foods, rich in reducing substances. Hydrogen peroxide can be determined as a suitable derivative by spectrophotometry and/or HPLC following the production of formaldehyde with a methanol–catalase system [10]. Formaldehyde is highly reactive toward reducing agents and/or proteins and cannot be detected directly when working with samples containing such substances. Therefore, the formation of suitable derivative is a prerequisite [11]. 4-Amino-3-penten-2-one (Fluoral-P) has been shown to be a specific derivatizing agent for formaldehyde in aqueous solution [12]. The purpose of this work was to develop a simple method for the determination of GL in foods with no special sample pretreatment or requirement for special instrumentation.

EXPERIMENTAL

Apparatus and conditions

The HPLC apparatus consisted of a Model 3A liquid chromatograph (Shimadzu, Kyoto, Japan) with a 20-μl loop injector (Rheodyne Model 7125), a fluorescence detector (Shimadzu Model RF-530) and a data processor (Shimadzu Model C-R3A). The chromatographic separation was carried out using a 25 cm × 4.6 mm I.D. reversed-phase column (Zorbax ODS, 5 μm) (Waters Assoc., Milford, MA, U.S.A.). The flow-rate of the mobile phase [acetonitrile–water (1:1)] was 1.0 ml/min. Separations were performed at ambient temperature (25°C).

Reagents

Fluoral-P was obtained from Wako (Osaka, Japan). Methanol and acetonitrile (both from Wako) were redistilled over dimedone prior to use. Adenosine 5′-triphosphate (ATP) was purchased from Wako and dissolved in cold distilled water to 1 mg/ml. A stock standard solution was prepared by diluting 1 g of guaranteed glycerol solution (Wako) with distilled water to 1 mg/ml. A working standard solution was prepared by diluting the stock solution with distilled water to 0.1–4.0 μg/ml.

Enzymes

Catalase (270 000 units/ml) was obtained from Boehringer (Mannheim, Germany). An enzyme solution was prepared by dilution with cold water to 1000 units/ml. This solution is stable for at least 3 weeks when kept refrigerated. Glycerokinase (500 units/ml) was also obtained from Boehringer and was diluted with cold distilled water to 10 units/ml. This solution can be used for more than 1 month without appreciable loss of activity. Glycerol-3-phosphate oxidase (from Boehringer) was dissolved in cold distilled water to give 100 units/ml. This enzyme solution should be prepared fresh daily.

Extraction

A 5-g sample of food was weighed accurately into a 50-ml test-tube and about 30

ml of distilled water were added, followed by 1 ml of 1% sodium hypochlorite solution. The sample was homogenized using a Polytron Model PT20 blender (Brinkmann, Westbury, NY, U.S.A.) for 1 min at maximum speed. After adjusting the pH to about 6 with 0.1 *M* HCl or 0.1 *M* NaOH, the contents were diluted to 50 ml with distilled water. Aliquots of 5 ml of the solution were filtered through a Millex-HA 0.45-μm filter (Millipore, Bedford, MA, U.S.A.). The filtrate is referred to as the sample solution.

Enzyme reaction

A 1-ml volume of sample solution was introduced into a 10-ml test-tube containing 3.35 ml of 0.4 *M* potassium phosphate buffer (pH 6.0; 0.1 m*M* $MgCl_2$), 0.1 ml of ATP solution and 0.25 ml of methanol. To this was added 0.1 ml of Fluoral-P (0.2 g/ml in acetonitrile), followed by 0.1 ml of catalase, 0.05 ml of glycerol-3-phosphate oxidase and 0.05 ml of glycerokinase. The reaction was carried out at ambient temperature for 20 min. Blank tests were performed by omitting glycerokinase. For clean-up of the reaction mixture, a Sep-Pak C_{18} cartridge column (Waters Assoc.) was used. The reaction mixture was charged on the cartridge column. After washing the column with a small volume of distilled water, the derivative of formaldehyde, formed by reaction with Fluoral-P, was eluted with 5 ml of acetonitrile–water (50:50). The eluate is referred to as the test solution.

HPLC analysis

A portion (20 μl) of the test solution was injected into the HPLC system. The eluent from the column was monitored with a fluorescence detector using emission and excitation wavelengths of 510 and 410 nm, respectively, because these conditions were optimum for detection of the formaldehyde derivative [12]. The peak height obtained was measured and the concentration of GL in the sample was calculated from a calibration graph prepared with working standards.

RESULTS AND DISCUSSION

Reaction conditions and clean-up

The reactions involved are illustrated in Fig. 1. In order to establish the optimum conditions for GL measurement, analyses were carried out at various pH values,

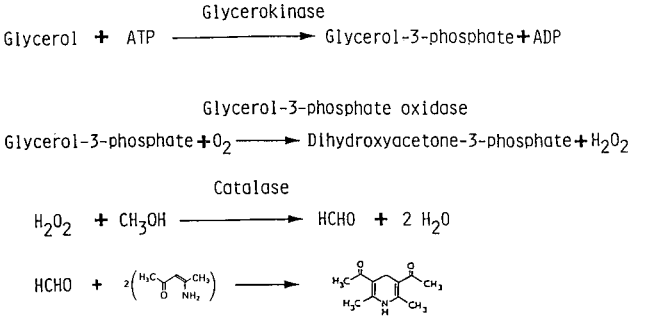

Fig. 1. Enzymatic and derivatization reactions by which glycerol was determined.

methanol concentrations, enzyme concentrations and reaction times. The effect of reaction pH was studied first. Given that the optimum pH of the three enzymes (glycerokinase, glycerol-3-phosphate oxidase and catalase) is around or above 7.0 [13–15] and that the maximum rate of reaction of formaldehyde with Fluoral-P is obtained around pH 2.4, a compromise pH range for the determination of GL would be expected to be 3.0–7.0. The peak height at various pH values was measured using 100 units of catalase, 5 units of glycerol-3-phosphate oxidase and 1 unit of glycerokinase. As shown in Fig. 2, the optimum pH for the determination of GL was 6.0. The reaction was also time dependent (Fig. 3). Considering the speed of analysis and optimum reaction rate, we selected 20 min for routine analysis.

The variables of glycerol-3-phosphate oxidase, glycerokinase and catalase were optimized individually. We first evaluated the amount of glycerol-3-phosphate oxidase, a crucial enzyme in this study, for optimization of the enzyme reaction. As shown in Fig. 4, the peak height increased significantly up to 3.0 units of glycerol-3-phosphate oxidase, after which it remained constant. Accordingly, 5 units of this enzyme were used routinely. The optimum amount of glycerokinase required was then determined and found to be >0.5 unit. Hence 1 unit of this enzyme was adopted in routine analysis. The optimum amount of catalase required was also determined and found to be > 50 units. Because the enzyme is inexpensive, an excess of catalase (100 units) was used in routine analysis.

The fluoral-P concentration is a critical factor in the determination of GL by the proposed method. The optimum concentration was found to be $>0.3\%$, as is clear from Fig. 5. Accordingly, 0.1 ml of a 20% solution was used in routine analysis (final concentration, 0.4%).

An additional variable that required optimization was the concentration of methanol, and the optimum was found to be 3–10%. Methanol concentrations $> 10\%$

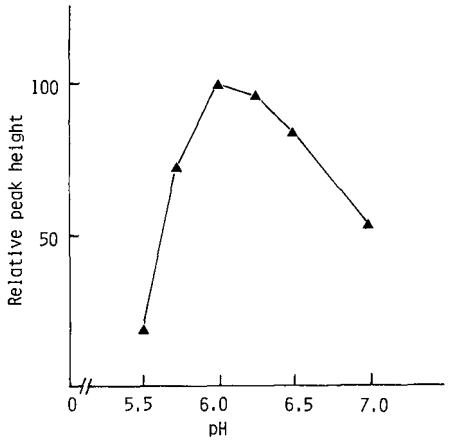

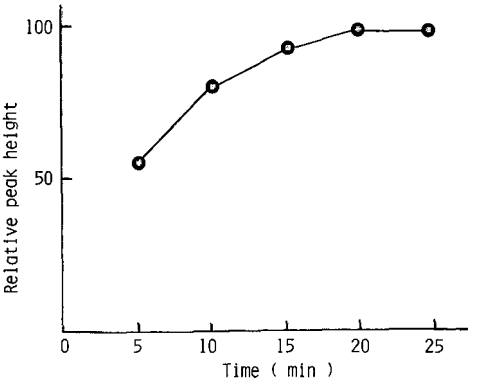

Fig. 2. Effect of pH on the determination of glycerol. A 2 μg/l standard glycerol solution was assayed at various pH values. Other conditions: glycerokinase, 5 units; glycerol-3-phosphate oxidase, 1 unit; catalase, 100 units; Fluoral-P, 0.4%; methanol, 5%; reaction time, 20 min; temperature, ambient.

Fig. 3. Effect of reaction time on the determination of glycerol. A 2 μg/ml standard glycerol solution was assayed with various reaction times. Other conditions as in Fig. 2.

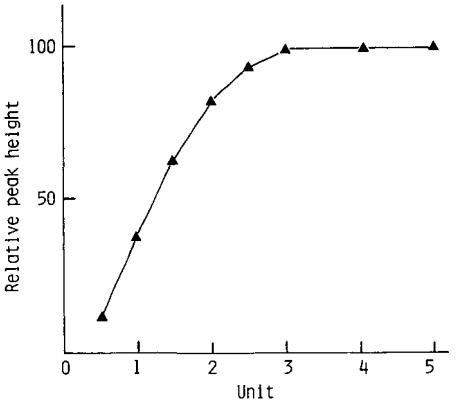

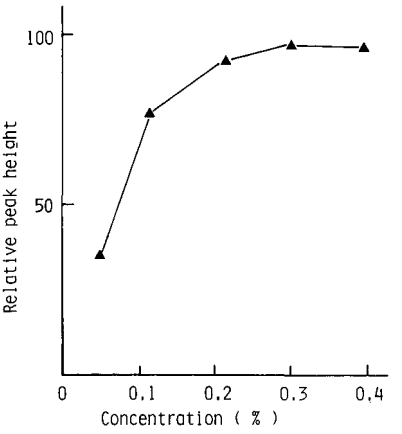

Fig. 4. Effect of amount of glycerol-3-phosphate oxidase on reaction rate. A 2 μg/ml standard glycerol solution was assayed with various amounts of glycerol-3-phosphate oxidase. Other conditions as in Fig. 2.

Fig. 5. Effect of Fluoral-P concentration on reaction rate. A 2 μg/ml standard glycerol solution was assayed with various concentrations of Fluoral-P. Other conditions as in Fig. 2.

decreased the peak height, probably owing to the retardation of the enzymes used and/or the derivatization reaction. Therefore, we used 0.25 ml of methanol, corresponding to 5% in the reaction mixture (5 ml).

Particles and/or proteins in the sample should be removed prior to HPLC, because they otherwise result in a deterioration of the column efficiency. We therefore used a Sep-Pak C_{18} cartridge column for clean-up of the reaction mixture, which effectively remove particles and proteins.

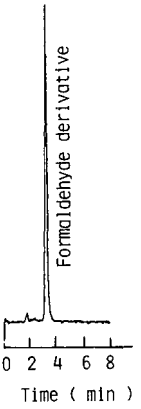

Fig. 6. Typical chromatograms of the formaldehyde derivative with Fluoral-P. Chromatographic conditions: column, Zorbax ODS C_{18} (250 mm × 4.6 mm I.D.); mobile phase, acetonitrile–water (1:1); flow-rate, 1 ml/min. A 2 μg/ml standard solution of glycerol was assayed according to the procedure described under Experimental.

Conditions for HPLC

Fig. 6 shows a typical HPLC trace obtained with the derivative of formaldehyde. The concentration of acetonitrile in the mobile phase was very important for a sharp resolution of the formaldehyde derivative on a reversed-phase column. At acetonitrile concentrations $<30\%$, the derivative was retained on the column, whereas it was eluted from the column without retention using $>70\%$ acetonitrile. The presence of an ionic strength modifier such as phosphate buffer had no effect on the retention time and peak shape of the derivative. Accordingly, acetonitrile–water (1:1) without any buffer was adopted in this study.

The relationship between the peak height and the amount of GL was evaluated over the range of 0.1–4 μg/ml in water. The relationship between peak height (y; μV s) and the amount of GL injected (x; ng) was obtained by the least-squares method: $y = 0.004x + 50$ ($n=3$, correlation coefficient $r=0.994$). The limit of detection for GL was 0.4 ng per 20-μl injection under the conditions adopted (signal-to-noise ratio = 3). This corresponds to a value of 1.0 μg/g in the sample when 5 g of sample were assayed. The reliability of the proposed method was evaluated by repeated analyses of standard GL solution (2 μg/ml in water). For five assays, the peak heights were found to be within 98% agreement.

Interference studies

The effect of possible interfering substances, particularly analogues of GL, was examined. The results are given in Table I. The relatively high specificity of two of the enzymes, glycerokinase and glycerol-3-phosphate oxidase, and the derivatization reaction make it unlikely that interferences will be encountered in most types of foods. Any interference resulting from reducing substances could be removed by using hypochlorite solution in the extraction step. Hypochlorite itself did not affect the proposed method. Fig. 7a shows the HPLC profile of fish sausage spiked with 20 μg/g of Gl. The peak detected was considered not to be derived from an interfering substance, as judged from Fig. 7b.

TABLE I

EFFECT OF POSSIBLE INTERFERING SUBSTANCES

A 50-μg amount of glycerol was assayed by the proposed method in the presence or absence of the substances indicated.

Substance	Amount (μg)	Relative peak height (%)
None		100
Propylene glycol	500	99.5
Ethylene glycol	500	101
Trimethylene glycol	500	100
Glucose	1000	100
Ethanol	100	99.7
Ascorbic acid	200	85.0 (99.8)[a]
Sulphur dioxide	50	43.6 (100)[a]

[a] The values in parentheses are results obtained by treatment with sodium hypochlorite prior to assay.

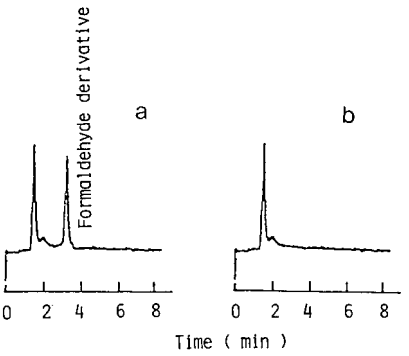

Fig. 7. HPLC elution profiles of fish sausage using the present method. Conditions as in Fig. 5. (a) Extract from fish sausage spiked with 20 μg/g of glycerol; (b) extract from fish sausage.

TABLE II

AMOUNTS OF GLYCEROL PRESENT IN SEVERAL FOODS AND RECOVERIES

Recoveries were determined in triplicate.

Sample	Amount present (μg/g)	Amount added (μg/g)	Amount recovered (μg/g)	Recovery (%)
White wine	1460	1000	2430	97.0
Red wine	1750	1000	2735	98.5
Fish sausage	N.D.[a]	20	19.4	97.0
Ice cream	140	100	95.7	95.7
Mayonnaise	N.D.	20	19.8	99.0
Salad dressing	N.D.	100	96.0	96.0

[a] N.D. = Not detected.

Recovery studies

Table II shows the recoveries obtained by spiking samples with GL at three levels prior to analysis. GL in water was added to the weighed samples in a test-tube and subjected to analysis as described under Experimental. Good recoveries were obtained in all instances, which demonstrated the accuracy (>95%) of the proposed method.

REFERENCES

1 G. E. Martin, R. H. Dyer and D. M. Figert, *J. Assoc. Off. Anal. Chem.*, 58 (1975) 1147.
2 M. Fujii (Editor), *Analytical Methods for Food Additives*, Kodansha, Tokyo, 1982, p. 584.
3 V. Kahle and K. Tesarik, *J. Chromatogr.*, 191 (1980) 121.
4 R. Pecina, G. Bonn, E. Burtscher and O. Bobleter, *J. Chromatogr.*, 287 (1984) 245.
5 G. Bonn, *J. Chromatogr.*, 350 (1985) 381.
6 S. V. Prabhu and R. P. Baldwin, *J. Chromatogr.*, 503 (1990) 227.
7 T. A. Kelly and G. D. Christian, *Analyst (London)*, 109 (1984) 453.
8 K. Kobayashi and S. Kawai, *J. Chromatogr.*, 245 (1982) 339.
9 M. Toyoda, Y. Ito, M. Iwaida and M. Fujii, *J. Agric. Food Chem.*, 30 (1982) 346.

10 H. U. Bergmeyer (Editor), *Methods of Enzymatic Analysis*, Vol. 2, Academic Press, New York, 1974, p. 438.
11 K. Kobayashi, M. Tanaka and S. Kawai, *J. Chromatogr.*, 187 (1980) 413.
12 J. C. Compton and W. C. Purdy, *Anal. Chim. Acta*, 119 (1980) 349.
13 K. Kobayashi and S. Kawai, *J. Chromatogr.*, 245 (1982) 339.
14 S. Hayashi and E. C. C. Lin, *J. Biol. Chem.*, 242 (1967) 1030.
15 T. W. Esders and C. A. Michrina, *J. Biol. Chem.*, 254 (1979) 2710.

Journal of Chromatography, 541 (1991) 273–284
Elsevier Science Publishers B.V., Amsterdam

CHROMSYMP. 2081

Improvements in automated analysis of catecholamine and related metabolites in biological samples by column-switching high-performance liquid chromatography[a]

G. GROSSI* and A. M. BARGOSSI
Laboratorio Centralizzato, Policlinico S. Orsola, Via Massarenti 9, I-40138 Bologna (Italy)
C. LUCARELLI
Istituto Superiore di Sanità, Rome (Italy)
R. PARADISI
Istituto di Fisiopatologia della Riproduzione, Università di Bologna, Bologna (Italy)
and
C. SPROVIERI and G. SPROVIERI
Laboratorio Centralizzato, Policlinico S. Orsola, Via Massarenti 9, I-40138 Bologna (Italy)
(First received August 14th, 1990; revised manuscript received November 13th, 1990)

ABSTRACT

Previously two fully automated methods based on column switching and high-performance liquid chromatography have been described, one for plasma and urinary catecholamines and the other for catecholamine urinary metabolites. Improvements in these methods, after 3 years of routine application, are now reported. The sample processing scheme was changed in order to eliminate memory effects and, in the procedure for plasma catecholamines, a pre-analytical deproteinization step was added which enhances the analytical column lifetime. The applied voltages for the electrochemical detector have been optimized, resulting in an automated method, suitable for the simultaneous determination of vanillylmandelic acid, 3,4-dihydroxyphenylacetic acid, homovanillic acid and 5-hydroxyindoleacetic acid. The sensitivity of the methods allows the detection of 2–3 ng/l of plasma catecholamines and 0.01–0.06 mg/l of urinary metabolites. Also, it is possible to switch from one method to the other in only 30 min. The normal values obtained from 200 healthy people are reported, together with a list of 57 potential interfering substances tested.

INTRODUCTION

High-performance liquid chromatography (HPLC) is usefully applied to determination of plasma and urinary catecholamines (C) and related metabolites by manual [1,2], and automated [3] methods. From the chromatographic point of view, all these analytes can be easily separated on a reversed-phase analytical column with

[a] Presented at the *14th International Symposium on Column Liquid Chromatography, Boston, MA, May 20–25, 1990*. The majority of the papers presented at this symposium have been published in *J. Chromatogr.*, Vols. 535 (1990) and 536 (1991).

0021-9673/91/$03.50

electrochemical detection [1,2], but the utilization of HPLC is adversely influenced by the fact that is very time consuming to change from a kind of analysis to another. Consequently, it was considered that it would be convenient, in the context of the routine activity of a clinical chemistry laboratory, not only to automate the determination of catecholamines, but also to effect a rationalization of the sequence of various applied methods.

We could optimize the analytical process by combining three steps, sample clean-up, chromatographic separation and detection, utilizing one only instrument, specially designed for this application. For this purpose we developed a fully automated analyser, that was first applied to the determination of C [4,5].

The apparatus was constructed by connecting in series a liquid handling station, a solid-phase autosampler operating with column switching, a highly reliable HPLC pump and an electrochemical detector. Being a versatile system, it could be used also for analysing C metabolites [6] and 5-hydroxytryptamine (5-HT) [7].

The experience gained in utilizing this system for over 3 years of routine analysis and research allowed us to implement some optimizations, which are reported in this paper.

EXPERIMENTAL

Chemicals and reagents

Venous blood was drawn in tubes containing 50 μl of 0.01 *M* tripotassium ethylenediaminetetraacetate. The protein precipitating solution was 0.8 *M* 5-sulphosalicylic acid dihydrate. The urine samples were preserved with 0.1 *M* hydrochloric acid. They can be kept for up to 1 week at 4°C and for 3 months at −30°C.

The extraction cartridges, containing octadecyl-bonded silica (AASP cassette C_{18}, for C extraction) or quaternary amine-bonded silica (AASP cassette SAX, for metabolite extraction), and the packing material for the 150 mm × 4.6 mm I.D. saturation column, (customer-packed), containing Sepralite reversed-phase C_{18} (40–60 μm), were obtained from Analytichem International (Harbor City, CA, U.S.A.) and the analytical column, octadecyl C_{18}, 3 μm (50 mm × 4.6 mm I.D.), from Baker (Deventer, The Netherlands).

Instrumentation

A Model 4233R refrigerated centrifuge was supplied by ALC (Milan, Italy) and a Microfuge 12 microcentrifuge by Beckman (Fullerton, CA, U.S.A.).

The HPLC instrumentation, employing a four-solvent HPLC pump, and the sample processor were the same as previously reported [6].

Preparation of standards

To obtain standard solutions, an acidified normal urine sample was fortified with norepinephrine (NE), epinephrine (E) and dopamine (D) to give concentrations of 0, 5, 25, 100 and 500 μg/l (NE and E) and 0, 25, 100, 400 and 2000 μg/l (D). Standard solutions of metabolites were as before [6]. The calibration standards obtained can be stored at −30°C for 3 months.

Stock solutions of the internal standard (I.S.) dihydroxybenzylamine (DHBA) (15 mg/l for urinary C; 100 μg/l for plasma C) and NE, E and D (100, 50 and 100 μg/l,

respectively, for plasma C) were prepared in 0.1 *M* perchloric acid and were kept at 4°C. A stock solution of the metabolites internal standard 3-hydroxy-4-methoxymandelic acid (iso-VMA, 500 mg/l) was prepared in 0.1 *M* hydrochloric acid and kept at 4°C.

To obtain plasma C standard solutions, a catecholamine-free plasma was fortified with NE, D and E to give concentrations of 0, 50, 200, 500 and 2500 ng/l (NE, D) and 0, 25, 100, 250 and 1250 ng/l (E). These standards were prepared fresh daily.

HPLC mobile phases

The four HPLC mobile phases, A (for plasma and urinary C determination), B and C (for urinary metabolites determination) and D (for washing the HPLC system when changing from C to C metabolites determination), were prepared as follows:

(A) methanol–acetonitrile–50 m*M* NaH_2PO_4 (pH 2.8, measured as the pH of the phosphate buffer) mixed in the ratio 15:8:77 and with 200 mg/l of sodium dodecyl sulphate (SDS) added;

(B) 50 m*M* NaH_2PO_4, (pH 2.8);

(C) acetonitrile–50 m*M* NaH_2PO_4 (pH 2.8, measured as the pH of the phosphate buffer) mixed in the ratio 1:3;

(D) methanol–water (3:2).

Buffers for sample processing

The compositions of the buffers and solvents employed in the sample processing were as follows:

(i) buffer containing the complexing agent for C analysis: 2.0 *M* NH_4Cl–NH_3 (pH 8.5) buffer containing 0.2% (w/v) of diphenylborate–ethanolamine (DPBEA) and 0.5% (w/v) of disodium ethylenediaminetetraacetate (EDTA);

(ii) buffer (pH 8.5): 0.2 *M* NH_4Cl–NH_3 buffer (pH 8.5) containing 0.05% EDTA;

(iii) plasma C diluting buffer: mix, on the day of utilization, 0.5 ml of I.S. (DHBA, 100 μg/l) + 18 ml of buffer containing the complexing agent + 36 ml of buffer (pH 8.5);

(iv) urinary C diluting buffer: mix, on the day of utilization, 0.5 ml of I.S. (DHBA, 15 mg/l) + 50 ml of buffer containing the complexing agent;

(v) urinary metabolite diluting buffer: mix, on the day of utilization, 0.25 ml of I.S. (iso-VMA, 500 mg/l) + 50 ml of buffer (pH 8.5).

Analyser connections

The AASP solid-phase autosampler was connected with the sample processor (Fig. 1). The fully automated analysis consisted of four steps:

(1) Dilution of plasma or urine sample with a buffer. For C determination, this buffer must contain a complexing agent for derivatization of C into less polar compound suitable for reversed-phase extraction. After sample dilution, the automatic processor mixed the tube by air insufflation.

(2) Filling the 5-ml loop with all the solvents necessary for the sample clean-up. To keep the solvents separated, 25 μl of air were included at the end of every suction.

(3) Flushing the AASP cartridge with these solvents (load line in Fig. 1).

(4) Switching the ten-port valve to inject the sample into the HPLC column (injection line in Fig. 1).

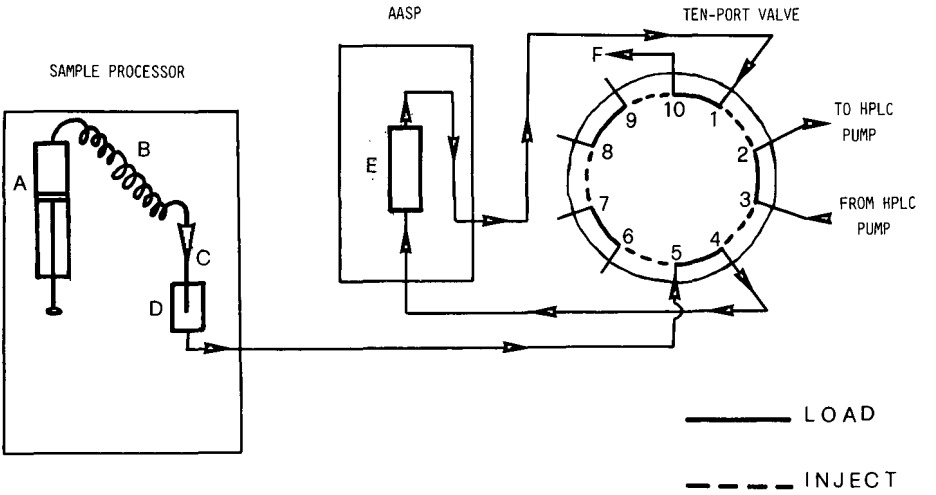

Fig. 1. Sample processing diagram. A = Syringe pump; B = 5-ml loop; C = needle of the autosampler; D = injection port; E = AASP extraction cartridge; F = purge solvent drain.

The first step can be applied to the whole batch of samples, before starting to apply steps 2, 3 and 4 to the first sample. Steps 2, 3 and 4 must be applied consecutively, completing the first sample clean-up and injection before starting with the next sample.

The diluter has a switching valve, positioned on the top of the syringe pump, which allows the syringe to suck the solution employed for washing the loop (Fig. 2,

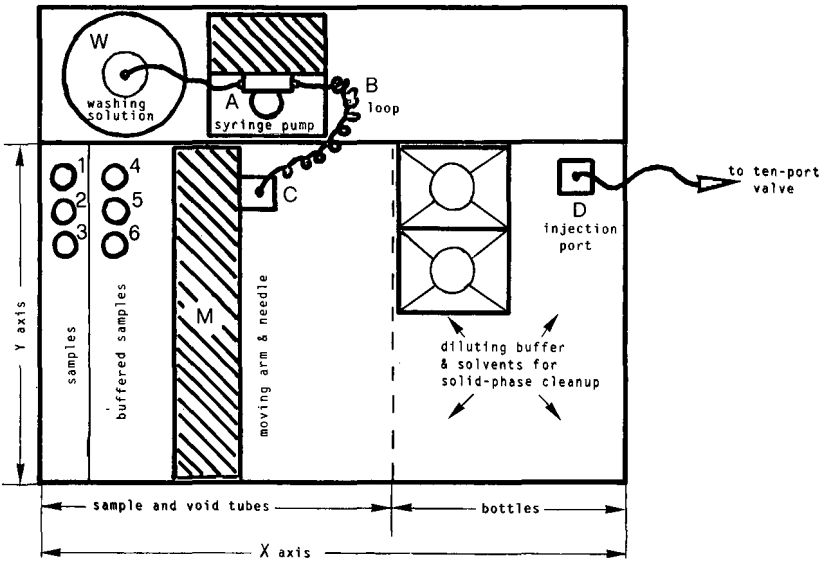

Fig. 2. Sample processor. The arm (M) moves the needle (C) along the axes *X* and *Y* on a tray containing the samples (up to 90), the buffers and the solvents (up to 8) necessary for the column switching clean-up (for details, see the text).

position W). In these applications, the loop washing step must occur just at the end of each analysis, five times, utilizing 5 ml of water.

Plasma C determination

For plasma C determination, 5 ml of venous blood were drawn and immediately centrifuged at 5500 *g* for 10 min at 4°C, then plasma samples were separated and kept at −30°C. On the day assigned for analysis, the samples were thawed at room temperature and deproteinized as follows: 0.5 ml of plasma were transferred to a centrifuge microtube and 50 µl of protein precipitating solution were added with gentle mixing. After refrigeration at 4°C for 15 min, the microtubes were centrifuged at 11 000 *g* for 10 min. The supernatant liquid was transferred to a plastic tube and positioned on the sample processor.

The details of the automated clean-up and HPLC analysis are as follows:

Step 1: sample, deproteinized plasma; dilution, 250 µl of sample + 750 µl of plasma C diluting buffer; apply step 1 to the whole batch of samples before starting to apply step 2;

Step 2: the syringe pump sucks, in sequence, 1.25 ml of water, 0.5 ml of methanol–buffer (pH 8.5) (1:4), 1 ml of buffer (pH 8.5), 0.8 ml of diluted sample, 0.5 ml of buffer (pH 8.5), 0.5 ml of methanol;

Step 3: the syringe pumps these solutions in reverse order through the cartridge (AASP cassette C_{18});

Step 4: valve reset, 0.1 min.

The HPLC mobile phase was A with isocratic elution at a flow-rate of 2 ml/min. The detector settings were as follows: conditioning cell, +0.45 V; high-sensitivity cell, detector 1 +0.10 V, detector 2 −0.35 V; gain, 100 × 10; response time, 4 s. The signal monitored (detector 2) was 10 mV; recorder, 10 mV; chart speed, 10 mm/min; and turnover time, 11 min.

Urinary C determination

Step 1: sample, acidified urine; dilution, 0.15 ml of sample +0.3 ml of urinary C diluting buffer;

Step 2: the syringe pump sucks, in sequence, 1.25 ml of water, 0.5 ml of methanol–buffer (pH 8.5) (1:4), 1 ml of buffer (pH 8.5), 0.15 ml of diluted sample, 0.5 ml of buffer (pH 8.5), 0.5 ml of methanol;

Step 3: the syringe pumps these solutions in reverse order through the cartridge (AASP cassette C_{18});

Step 4: valve reset, 0.1 min.

The HPLC mobile phase was A with isocratic elution at a flow-rate of 2 ml/min. The detector settings were as follows: conditioning cell, +0.45 V; high-sensitivity cell, detector 1 +0.10 V, detector 2 −0.35 V; gain, 10 × 5; response time, 4 s. The signal monitored (detector 2) was 10 mV; recorder, 10 mV; chart speed, 10 mm/min; and turnover, 11 min.

Urinary metabolite analysis

To switch the analyser from C to C metabolite analysis, it was necessary to wash the HPLC system with mobile phase D at a flow-rate of 1.5 ml/min for 15 min, to remove SDS from the saturation and analytical columns.

The details of the automated clean-up and HPLC analysis are as follows:

Step 1: sample, acidified urine; dilution, 50 μl of sample + 0.5 ml of urinary metabolite diluting buffer;

Step 2: the syringe pump sucks, in sequence, 0.8 ml of water, 25 μl of 0.3 *M* H_3PO_4, 0.5 ml of methanol–water (1:1), 1.0 ml of water, 50 μl of diluted sample, 0.5 ml of water, 0.5 ml of methanol;

Step 3: the syringe pumps these solutions in reverse order through the cartridge (AASP cassette SAX);

Step 4: valve reset, 0.1 min.

The HPLC mobile phase was a binary gradient between B and C with the following programme: from 2% to 10% C in 0.1 min; from 10% to 30% C in 0.9 min; from 30% to 60% C in 2.0 min; from 60% to 80% C in 2.0 min; from 80% to 100% C in 0.5 min; 100% C for 0.5 min; from 100% to 2% C in 1 min. The flow-rate was 2 ml/min. The detector settings were as follows: conditioning cell, −0.10 V; high-sensitivity cell, detector 1 +0.10 V, detector 2 +0.40 V; gain, 1 × 10; response time, 4 s. The signal monitored (detector 2) was 10 mV; recorder, 10 mV; chart speed, 10 mm/min; and turnover time, 11 min.

RESULTS AND DISCUSSION

Plasma and urinary C

For C detection the redox mode was adopted [5]. In Fig. 3, the chromatographic profile obtained by analysing urine from a healthy person is shown, and it can be seen that the analytical column, even if it is only 50 mm long, can separate the various analytes well.

In comparison with the previous model, we have changed the flow scheme. In the original set-up, the ten-port valve allowed the possibility of fitting a loop for manual injection. Problems occurred because if the treated sample contained substances eluted from the cartridge in a time range 0.1–0.2 min, the loop caused a memory effect by trapping a ghost peak, which was detected in the next sample profile, as the loop was not flushed during the sample loading step.

Fig. 4 shows a chromatographic profile obtained for plasma from a healthy person. In the procedure for the determination of plasma catecholamines, we have added a pre-analytical deproteinization step; in fact, if deproteinization is not effected one obtains an identical profile, but the analytical column lifetime is reduced and, after 190–200 analyses, the separation efficiency decreases and the back-pressure increases substantially.

On changing the column frits the back-pressure did not decrease, confirming that the problem was due to the deterioration of the stationary phase. Addition of EDTA to the mobile phase did not solve the problem, and the effect on the detector was a considerable increase in the background current and the displacement of C voltammograms, which obliged us to apply a higher voltage.

Considering that urinary C analysis did not experience such a problem, it appears clear that the effect on the analytical column was due to plasma proteins. We added 0.1% trifluoroacetic acid to the mobile phase, but the situation became worse.

We then tried to check the effect of metal parts of the apparatus: the AASP cassette cartridge frits are made of titanium, which is compatible with proteins; conse-

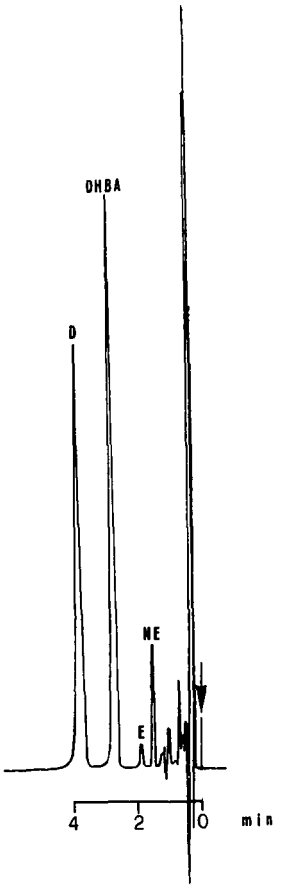

Fig. 3. Chromatogram of a urine containing NE 54 μg/l, E 10 μg/l and D 305 μg/l. Column, octadecyl C_{18}, 3 μm (50 × 4.6 mm I.D.); mobile phase, methanol–acetonitrile–50 m*M* sodium phosphate buffer (pH 2.8) (15:8:77), containing 200 mg/l of sodium dodecyl sulphate; flow-rate, 2 ml/min; detector conditioning cell, +0.45 V; detector 1, +0.10 V; detector 2, −0.35 V; gain, 10 × 5; response time, 4 s.

quently, we replaced all the tubes, including the internal ones to the AASP and those connecting with the ten-port valve. We utilized biocompatible materials, but the problem remained. Also, plasma centrifugation at 15 000 *g* did not have the desired effect.

Only after having introduced a plasma deproteinization step was the problem overcome; the average lifetime ($n = 6$) of the analytical column was optimized and no reduction in efficiency or pressure increases occurred after 800 analyses.

A further change to the original procedure was the dilution of plasma samples during step 1, the dilution rate being raised from 2:1 to 1:3. This dilution is very important, because it greatly improves the precision of the method with the most difficult samples, taken from patients affected by various and complicated pathologies.

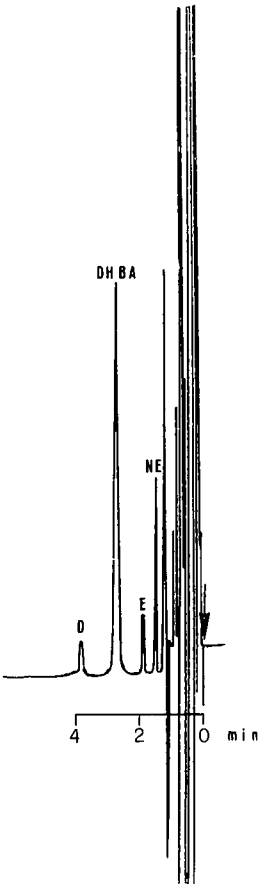

Fig. 4. Chromatogram of a plasma containing NE 82 ng/l, E 22 ng/l and D 21 ng/l. Conditions as in Fig. 3 except gain, 100 × 10.

The retention times for NE, E, DHBA and D were 1.50, 1.87, 2.70 and 3.77 min, respectively, and were not influenced either by column ageing or replacement.

The detector 2 background current (detection cell) is very low, -0.018 ± 0.002 μA, and gives a steady baseline, also at high sensitivity values. Hence it is possible to detect plasma concentrations of NE, E and D of 2, 3 and 3 ng/l, respectively. The recovery and precision of the method are unchanged in comparison with those obtained with the original method. With clinical specimens the intra- and inter-assay relative standard deviations (R.S.D.) for NE, E and D for urinary C were 2.4 and 2.8, 3.0 and 4.5 and 1.8 and 2.6% (n = 20), respectively, and for plasma C were 3.0 and 4.2, 3.4 and 5.1 and 3.5 and 5.2% (n = 10), respectively.

As previously reported, when mixed with the complexing agent, C are stable for more than 5 h at room temperature, giving the opportunity to analyse many samples in every batch [4].

In Table I are reported the up-dated normal ranges and Table II gives a list of

TABLE I

NORMAL RANGES OF CATECHOLAMINES

Catecholamines	Compound	Concentration[c]
Urinary[a]	NE	8.5 – 61.6
	$\bar{X}$ =	31.5 ± 15.30
	E	1.0 – 22.4
	$\bar{X}$ =	7.6 ± 12.53
	D	73 – 276
	$\bar{X}$ =	186 ± 63.4
Plasma[b]	NE	43 – 240
	$\bar{X}$ =	76 ± 61.4
	E	6 – 45
	$\bar{X}$ =	14 ± 22.4
	D	8 – 41
	$\bar{X}$ =	13 ± 31.7

[a] 24-h urine collection, n = 200 (100 males, 100 females); age 20–50 years.
[b] n = 100 (50 males, 50 females)
[c] Urine, μg/g urinary creatinine; plasma, ng/l.

TABLE II

HPLC RETENTION TIMES FOR CATECHOLAMINES AND POTENTIAL INTERFERING SUBSTANCES

Substance[a]	Relative retention time	Recovery (%)
Solvent peak	0.14	
HVA	0.18	<0.01
Artefact 1	0.23	
DL-β-3,4-Dihydroxyphenylalanine	0.27	<0.01
Artefact 2	0.36	
L-DOPA	0.36	3
NE	0.52	99
E	0.68	99
α-Methyldopa	0.82	3
DHBA	1.00	99
DL-Normetanephrine	1.02	0.1
α-Methylnoradrenaline	1.14	88
DL-Metanephrine	1.36	0.01
D	1.39	99
Deoxyepinephrine	1.59	76
α-Methyldopamine	1.73	4
Isoprenaline	1.82	41
Serotonine	2.77	3
3-Methoxytyramine	3.77	0.01

[a] The following substances gave no peak at all: VMA, iso-VMA, MHPG, DOPAC, 5-HIAA, β-phenylalanine, tryptophan, phenylethanolamine, octopamine, tyramine, tryptamine, tyrosine, uric acid, 3-methyluric acid, 1,3-dimethyluric acid, 1,3,7-trimethyluric acid, hypoxanthine, xanthine, creatine, creatinine, nicotine, nicotinamide, nicotinic acid, caffeine, theobromine, theophylline, promethazine, phenobarbital, salbutamol, amitriptyline, doxepin, imipramine, diazepam, nitrazepam, haloperidol, chlorpromazine, promazine, acetyl salicylate, ibuprofen, probenecid, furosemide.

potential interfering substances tested. All analytes at concentrations of at least 100 mg/l were determined with the fully automated method and those showing a peak were also injected manually to calculate the recovery. A difference in relative retention times of 0.10 is sufficient for complete (baseline) separation.

With clinical urine samples no problem due to overlapping of interfering substances was observed, as confirmed by the analysis of the voltammograms of the peaks. Ghost peaks were very unusual.

Urinary metabolites

Fig. 5 shows the voltammograms obtained for C metabolites. The voltammograms, even though maintaining the same shape, change in potential depending on the mobile phase composition, pH, cleanness and reliability of the HPLC pump. All the analytes are oxidized at an applied potential of +0.40 V, as occurs for many interfering substances. The addition of a counter ion, such as sodium heptane sulphonate or sodium dodecyl sulphate, influences the retention time of acidic metabolites, causing their reduction and decreasing the potential necessary for oxidation, so various interfering substances can be removed [6].

However, the difference among the optimized oxidization potentials is so high that it does not allow their simultaneous detection. For this reason, we removed the counter ion from the mobile phase, and to eliminate the interfering substances we operated on the potential of detector 1 (gate). Utilizing for detector 1 a potential of +0.10 V, many interfering substances are removed and the remainder can be separated with a suitable choice of HPLC elution gradient. Under these analytical condi-

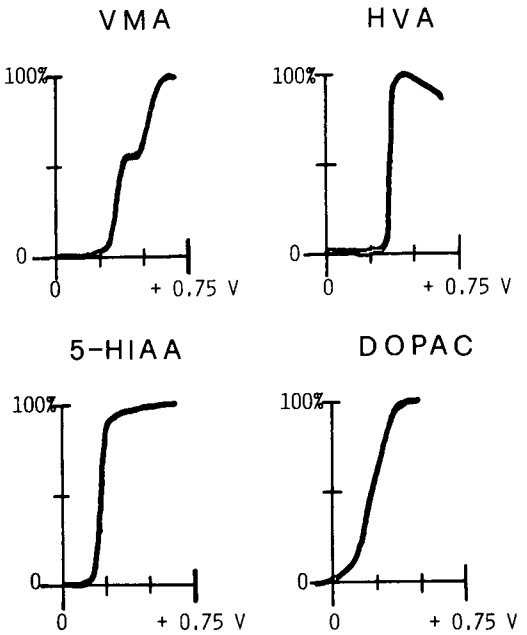

Fig. 5. Voltammograms obtained for catecholamine metabolites. Abscissa, applied voltage; ordinate, detector response, expressed as a percentage of maximum signals obtained.

tions, the conditioning cell is useless and is utilized at −0.10 V because with this potential it does not make any contribution. However, it cannot be omitted because it allows a quick transfer to the C determination stage and is useful for peak identification by recording redox-mode voltammograms.

In Fig. 6 a chromatographic profile obtained on analysing a urine sample from a healthy adult is shown. The retention times for vanillylmandelic acid (VMA), iso-VMA, 3,4-dihydroxyphenylacetic acid (DOPAC), 5-hydroxyindoleacetic acid (5-HIAA) and homovanillic acid (HVA) are 1.30, 2.40, 4.10, 5.90 and 6.30 min, respectively. The recovery and precision are unchanged compared with those in the original method. With clinical specimens, the intra- and inter-assay R.S.D.s for VMA, HVA, 5-HIAA and DOPAC were 2.0 and 3.6, 1.9 and 3.0, 2.1 and 3.4 and 2.3 and 3.8% (n = 20), respectively.

The sensitivity of the method allows urinary concentrations of VMA, DOPAC, 5-HIAA and HVA of 0.06, 0.04, 0.01 and 0.01 mg/l, respectively, to be detected. In Table III the normal ranges are listed. In clinical specimens, no overlapping of interfering peaks was observed.

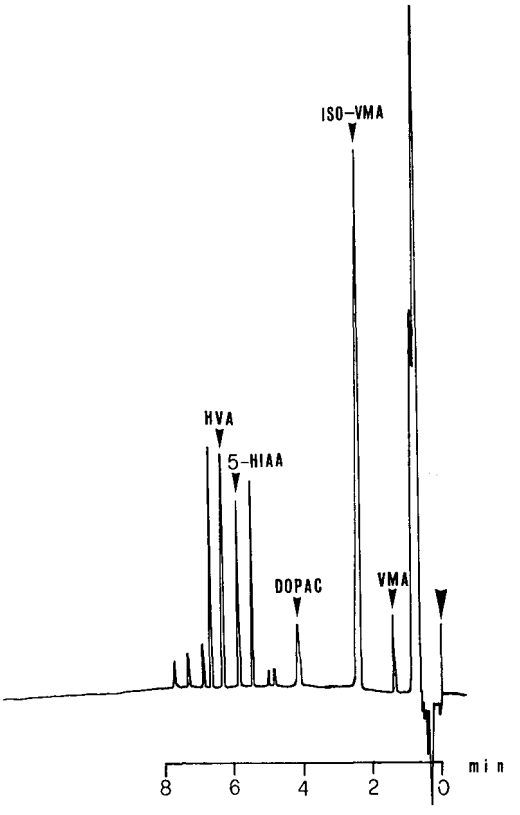

Fig. 6. Chromatogram of a urine containing VMA 2.8 mg/l, DOPAC 1.3 mg/l, 5-HIAA 2.2 mg/l and HVA 3.1 mg/l. Column, octadecyl C_{18}, 3 μm (50 × 4.6 mm I.D.); mobile phase, eluent B = 50 mM sodium phosphate buffer (pH 2.8), eluent C = acetonitrile–50 mM sodium phosphate buffer (pH 2.8) (1:3), binary gradient between B and C as described under *Urinary metabolite analysis*; flow-rate, 2 ml/min; detector conditioning cell, −0.10 V; detector 1, +0.10 V; detector 2, +0.40 V; gain, 1 × 10; response time, 4 s.

TABLE III

NORMAL RANGES OF URINARY METABOLITES

24-h urine collection; n = 200 (100 males, 100 females); age 20–50 years.

Compound		Concentration (mg/g urinary creatinine)
VMA		0.6 – 5.9
	$\bar{X}$ =	2.9 ± 2.31
DOPAC		0.2 – 3.5
	$\bar{X}$ =	1.0 ± 1.31
5-HIAA		0.5 – 6.1
	$\bar{X}$ =	2.6 ± 1.12
HVA		0.7 – 7.8
	$\bar{X}$ =	3.2 ± 2.42

CONCLUSIONS

The possibility of applying fully automated methods has many advantages. In addition to the fact that they require less manual intervention and consequently reduce random errors, only a minimum amount of sample is required for the analysis, which is of fundamental importance when the samples are drawn from very young patients (*e.g.*, aged 0–3 years). Moreover, the manual handling of unstable samples such as DOPAC (unstable at basic pH) or 5-HIAA (unstable at strongly acidic pH) can cause serious problems in their determination. The problems can be more easily overcome by applying fully automated methods, as the samples remain unaltered since they stay for less than 1 min under unstable conditions.

In the routine clinical chemistry laboratory fully automated methods can give rapid and simultaneous determinations of many substances, which allows time savings and the determination of substances present at very low concentrations and with optimum reliability of the analytical methods.

REFERENCES

1 A. M. Krstulovic, *J. Chromatogr.*, 229 (1982) 1.
2 F. Smedes, J. C. Kraak and H. Poppe, *J. Chromatogr.*, 231 (1982) 25.
3 K. S. Boos, B. Wilmers, R. Sauerbrey and E. Schlimme, *Chromatographia*, 24 (1987) 363.
4 G. Grossi, A. Bargossi, A. Lippi and R. Battistoni, *Chromatographia*, 24 (1987) 842.
5 G. Grossi, *Chromatographia*, 28 (1989) 417.
6 G. Grossi, A. Bargossi, R. Battistoni, A. Lippi and G. Sprovieri, *J. Chromatogr.*, 465 (1989) 113.
7 G. Grossi, A. Bargossi, G. Sprovieri, V. Bernagozzi and R. Pasquali, *Chromatographia*, 30 (1990) 61.

Journal of Chromatography, 541 (1991) 285–296
Elsevier Science Publishers B.V., Amsterdam

CHROMSYMP. 2075

High-performance liquid chromatographic determination of L-3-(3,4-dihydroxyphenyl)-2-methylalanine (α-methyldopa) in human urine and plasma[a]

C. LUCARELLI*, P. BETTO and G. RICCIARELLO
Istituto Superiore di Sanità, V. le Regina Elena 299, 00161 Rome (Italy)
and
G. GROSSI
Policlinico S. Orsola, Via Massarenti 9, Bologna (Italy)
(First received May 20th, 1990; revised manuscript received November 3rd, 1990)

ABSTRACT

A procedure is described for the determination of α-methyldopa (MD) [L-3-(3,4-dihydroxyphenyl)-2-methylalanine], its metabolite and catecholamines in the urine and plasma of patients undergoing MD therapy, by high-performance liquid chromatography with dual working electrode coulometric detection.

An efficient sample preparation procedure is presented for the isolation of endogenous MD, its metabolite and catecholamines from plasma or urine. After deproteinization of a plasma sample with methanol containing 2% of 0.5 *M* perchloric acid and dilution of a urine sample (1:200), MD, dihydroxyphenylacetic acid (DOPAC), 3-O-methylmethyldopa (3-OMMD) and homovanillic acid (HVA) were separated with a Supelcosil LC-18 column. Catecholamines were extracted from the supernatant of deproteinized plasma or from urine by ion exchange on a Sephadex CM-25 column and subsequent adsorption on alumina. The use of the same mobile phase for the concurrent assay of MD, its metabolite and catecholamines increased considerably the efficiency of sample separation. Recoveries were close to 100% for MD, DOPAC, 3-OMMD and HVA and 70% for catecholamines.

The effects of various experimental parameters related to mobile phase composition on chromatographic performance are reported. The purity of the eluted compounds was tested by recording both the first detector response (oxidation current) and the second detector response (reduction current). The ratio of the detector responses yielded a chemical reversibility ratio for the detected compound. A number of applications such as monitoring data from patients under MD therapy are presented.

INTRODUCTION

α-Methyldopa (MD), L-3-(3,4-dihydroxyphenyl)-2-methylalanine, is a well known hypotensive agent, structurally related to the catecholamines and their precursors [1–5]. Recently, MD has been used to treat hypertension during pregnancy and no serious adverse effects on the foetus have been reported [6].

[a] Presented at the *14th International Symposium on Column Liquid Chromatography, Boston, MA, May 20–25, 1990*. The majority of the papers presented at this symposium have been published in *J. Chromatogr.*, Vols. 535 (1990) and 536 (1991).

0021-9673/91/$03.50

MD has three major metabolic pathways [7]: sulphate conjugation catalysed by phenolsulphotransferase, O-methylation catalysed by catechol-O-methyltransferase and decarboxylation catalysed by aromatic L-amino acid decarboxylase. O-Methylation results in the formation of 3-O-methylmethyldopa (3-OMMD), while decarboxylation results in the formation of α-methyldopamine (α-MDA).

There is a wide range of individual variations in both MD metabolism and the dose of drug required to control blood pressure in hypertensive patients [8]. The individual differences in the activities of the above-mentioned enzymes might be one of the factors responsible for variations in MD metabolism [8]. Hence understanding the pharmacokinetics of MD is crucial to establishing the optimum therapeutic regimen for the drug. Also, the analysis of 24-h urine levels of MD and related compounds (3-OMMD, catecholamines and their metabolites) could be useful tools for studying how drug-metabolizing enzyme activities affect the wide range of individual variations in human MD metabolism [7]. Moreover, urine MD monitoring could be a sensitive and non-invasive means for clinical optimization of individual drug management.

Many methods have been developed for the determination of MD and its metabolites, such as fluorimetric [9], paper chromatographic [10], gas chromatographic [11,12] and high-performance liquid chromatographic (HPLC) methods with ultraviolet [13,14], fluorescence [15] and electrochemical detection [3,15–23]. Most of these methods have been applied to the evaluation of many interesting biogenic amines. There is general agreement that the complete profile is more informative in drug metabolism involving catecholamines. For this reason, we developed a procedure for detecting MD, 3-OMMD, norepinephrine (NE), epinephrine (E), dihydroxyphenylacetic acid (DOPAC) and homovanillic acid (HVA) in biological fluids. MDA was not determined because the authentic standard was not commercially available.

The two major problems that arise in determining MD, its metabolites and catecholamines are first the very low levels of free catecholamines with respect to the amounts of MD and second the half-wave potential of 3-OMMD and HVA, which is greater than those of catecholamines and MD.

The purpose of this study was to overcome these difficulties by using a coulometric detector to solve the problems of high electrode potentials and by employing a sample preparation method that separates catecholamines from other interfering endogenous compounds. The method includes deproteinization of serum with cold methanol solution containing 2% of 0.5 *M* perchloric acid followed by centrifugation. An aliquot of the supernatant was used to measure MD and its metabolite. For the determination of the catecholamines, an aliquot of the supernatant was purified using a Sephadex CM-25 column (where MD is not retained) and alumina. The use of the same mobile phase for the concurrent assay of MD, its metabolite and catecholamines increased considerably the efficiency of sample separation in the chromatographic system.

EXPERIMENTAL

Materials

NE, E, DA, DOPAC, HVA and N-methyldopamine (NMDA, internal standard) were purchased from Sigma (St. Louis, MO, U.S.A.) and MD and 3-OMMD

were gifts from Merck, Sharp & Dohme (Darmstadt, Germany). Sodium 1-octanesulphonate (OSA) and ethylene glycol-O,O′-bis-(2-aminoethyl-N,N,N′,N′-tetraacetic acid (EGTA) were purchased from Fluka (Buchs, Switzerland). Methanol (HPLC grade) and all other analytical-reagent grade chemicals were obtained from Carlo Erba (Milan, Italy). A Sephadex CM-25 column was obtained from Pharmacia (Uppsala, Sweden) and acid alumina AG-4 from Bio-Rad Labs. (Richmond, CA, U.S.A.). Water was treated with a Milli-Q system (Millipore, Milford, MA, U.S.A.).

HPLC apparatus

The HPLC system consisted of a Series 4 liquid chromatograph (Perkin-Elmer, Norwalk, CT, U.S.A.) and a Model 7125 injector (equipped with a 100-μl loop). The column used was a reversed-phase Supelcosil LC-18 (15 cm × 4.6 mm I.D.), particle size 5 μm (Supelco, Bellefonte, PA, U.S.A.). A Model 5100 A Coulochem detector (ESA, Bedford, MA, U.S.A.) was equipped with a Model 5011 A analytical cell. The potentials were set at +0.40 V for the first electrode and −0.30 V for the second electrode. The gain control used for signal amplification resulting in peak height and area changes was maintained at 2000 for the first electrode and 3500 for the second. Chromatograms were analysed with a Chromatopac C-R4A data processor (Shimadzu, Kyoto, Japan) monitoring both detector signals. The mobile phase was 13 m*M* sodium acetate containing 0.5 m*M* OSA (ion-pairing reagent), 0.5 m*M* disodium EDTA and 14% methanol (pH 3.10). The compounds were eluted isocratically at room temperature at a flow-rate of 1.0 ml/min.

Preparation of plasma sample

Blood samples from patients receiving MD were drawn by venipuncture and collected in tubes containing 50 μl of a solution of EGTA (60 mg/ml) and reduced glutathione (90 mg/ml) and immediately centrifuged at 4°C for 5 min at 2000 *g*. The supernatants were stored at −80°C for assay later. A sample was allowed to thaw at room temperature and an aliquot of plasma (1 ml) was deproteinized by the addition of three volumes of ice-cold methanol containing 2% of 0.5 *M* perchloric acid and centrifuged at 4°C for 3 min at 4000 *g*. The supernatant (0.2 ml) was collected, spiked with 0.1 ml of NMDA (80 ng/ml) and evaporated to dryness under vacuum. The residue was dissolved in 0.2 ml of mobile phase. The resulting solution (5–20 μl) was injected into the HPLC system for the determination of MD, DOPAC, 3-OMMD and HVA. The isolation of catecholamines was carried out in 1 ml of the supernatant spiked with 40 μl of NMDA (80 ng/ml) as an internal standard [24].

A 3-ml volume of 0.1 *M* phosphate buffer (pH 7) was added to the solution and the mixture was applied to a Sephadex CM-25 column (2 cm × 0.5 cm I.D.). The column was conditioned with 5 ml of 0.1 *M* hydrochloric acid and 10 ml of distilled water and buffered with 10 ml of 0.1 *M* phosphate (pH 7). The compounds retained in the column were washed with 5 ml of distilled water, then catecholamines were eluted with 5 ml of 1.5 *M* perchloric acid into conical tubes with caps. A 2-ml volume of 1.5 *M* Tris buffer (pH 9.3) containing 0.06 *M* EDTA and 20 mg of acid-washed alumina [25] were added to the solution. The tube was vortex mixed for 2 min, the supernatant was removed by vacuum aspiration and the alumina was washed three times with 1 ml of water. Each wash was followed by centrifugation. The catecholamines were extracted with 100 μl of 0.1 *M* acetic acid by vortex mixing for 2 min,

allowed to settle and then centrifuged at 4°C for 2 min at 3000 *g*. The resulting solution (20–50 μl) was injected into the HPLC system.

Preparation of urine samples

Urine samples (24 h) were collected (2 h after administration) in plastic containers containing 10 ml of 6 *M* hydrochloric acid as a preservative, and a 1-ml aliquot was frozen at −80°C for assay later. A 50-ml volume of water was added to the thawed urine sample (1 ml) and 10 μl of the solution were injected into the HPLC system for the determination of MD, 3-OMMD, DOPAC and HVA. The same procedure as described above for the determination of plasma catecholamines was followed for 0.2 ml of urine sample. The values obtained represented the amount of unconjugated compounds present. In order to determine total levels, the sample was adjusted to pH 1, flushed with nitrogen and kept in a boiling water-bath for 20 min [26]. The hydrolysed sample was then processed in the same manner as the non-hydrolysed sample.

RESULTS AND DISCUSSION

Separation

Several approaches can be used to improve the separation in the reversed-phase ion-pairing technique to obtain a balance between ion-pairing reagent, organic solvent and pH.

The pH of the mobile phase is perhaps the best means of separating the various substances as it can modify the charge of the functional groups. The finding that on increasing the pH the retention times of the carboxylic acids and amino acids decreased can be explained by the fact that ion-pair formation increases as the protonation of carboxylic groups increases [27]. The retention times of HVA, MD and 3-OMMD were the most affected by the modest pH range of 2.60–3.10, whereas the retention times of amines were not influenced.

Fig. 1A shows the effect of pH on the retention of the compounds in the acidic range. For MD, DOPAC, 3-OMMD and HVA (solid lines) good separation was obtained at the pH of the mobile phase (3.1), and these conditions also provide a good compromise between resolution and duration of chromatography. Throughout the test, the concentrations of sodium acetate and methanol were maintained at 13 m*M* and 14%, respectively.

An increase in the methanol content of the mobile phase caused a significant decrease in the k' values of all compounds in the standard mixture (Fig. 1B), the strongest effect being on HVA. The pH and sodium acetate concentration were 3.1 and 13 m*M*, respectively.

Finally, keeping a constant pH of 3.1 and a 14% methanol concentration, the effect of ionic strength on the retention was investigated. Fig. 1C shows that an increase in the molar concentration of sodium acetate caused a significant decrease in the capacity factors of all catecholamines and an increase in retention for DOPAC, MD, 3-OMMD and HVA. The increase in the capacity factors with increasing salt concentration implies that the retention is due to hydrophobic interaction [28].

A representative chromatogram illustrating the resolution of a standard mixture of MD, 3-OMMD, DOPAC and HVA, and also NE, E, DA and NMDA, is

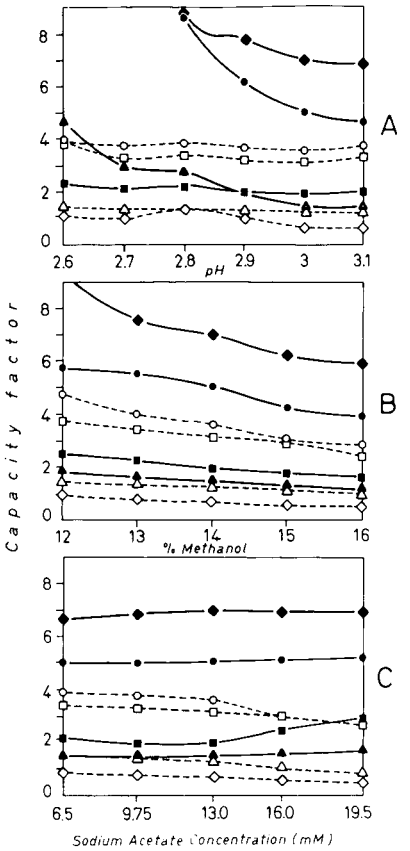

Fig. 1. Effect of (A) pH of mobile phase, (B) methanol content and (C) ionic strength on the capacity factors of (▲) MD, (●) 3-OMMD, (■) DOPAC, (◆) HVA, (△) E, (◇) NE, (□) DA and (○) NMDA. When analysing biological samples, the analytes are divided into two groups according to their different pretreatment procedures, *i.e.*, direct injection and treatment with Sephadex CM-25 and alumina (continuous and dotted lines, respectively). Column: Supelcosil LC-18, particle size 5 μm, 150 mm × 4.6 mm I.D. Mobile phase: the concentrations of OSA (0.5 m*M*) and disodium EDTA (0.5 m*M*) were always constant. The pH of the mobile phase (A) was varied by changing the ratio of sodium acetate to acetic acid, but maintaining the ionic strength (13 m*M*) and the methanol concentration (14%) constant. In (B), only the methanol concentration varied. The effect of ionic strength was investigated maintaining the pH at 3.1 and methanol concentration at 14% (C). The flow-rate was 1 ml/min.

shown in Fig. 2. When biological samples are processed, the eight compounds are divided into two groups according to their respective sample pretreatment (see Experimental) and analysed separately. This allows chromatograms to be obtained with more resolved peaks and the result could represent a substantial advantage as biological samples often include unknown substances (*i.e.*, endogenous compounds or drugs) which could give unexpected interfering peaks. Fig. 3 shows chromatograms from 24-h urine samples after administration of MD (Aldomet 250, MD 250 mg) (Merck Sharp & Dohme). Fig. 3A represents the detection of MD, DOPAC, 3-OMMD and HVA after direct injection of diluted urine. Aldomet is known to in-

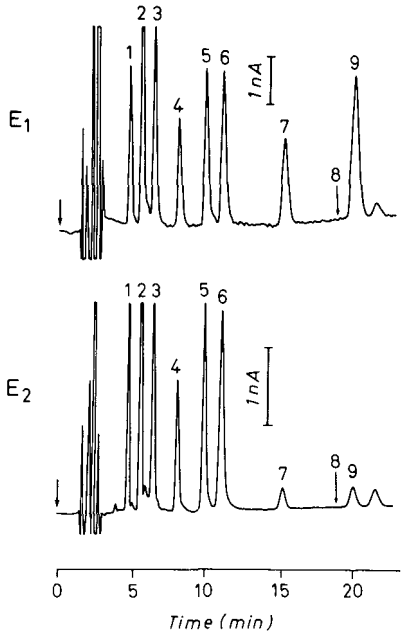

Fig. 2. Chromatograms of oxidation (E_1 level) and reduction (E_2 level) obtained from a mixture of standard NE (40 ng/ml), E (40 ng/ml), MD (80 ng/ml), DOPAC (40 ng/ml), DA (40 ng/ml), NMDA (80 ng/ml), 3-OMMD (80 ng/ml) and HVA (80 ng/ml). Peaks: 1 = NE; 2 = E; 3 = MD; 4 = DOPAC; 5 = DA; 6 = NMDA; 7 = 3-OMMD; 9 = HVA. The positions indicated by arrow No. 8 correspond to the retention time of the unknown peaks (No. 8) included in the urine chromatograms (Fig. 3), which perhaps could be ascribed to MDA. Conditions: column, Supelcosil LC-18, particle size 5 μm, 150 mm × 4.6 mm I.D.; flow-rate, 1 ml/min at ambient temperature; mobile phase, 13 m*M* sodium acetate containing 0.5 m*M* OSA, 0.5 m*M* disodium EDTA and 14% methanol (pH 3.1). Applied potential: E_1 = +0.40 V, E_2 = −0.35 V.

crease the level of MD in urine, *i.e.*, the size of MD peak is expected to be greater than those of other compounds. Therefore, the sample had to be further diluted 10-fold.

Fig. 3B shows catecholamines detected in the same urine sample as shown in Fig. 3A, which were obtained by analysing the extract from treatment with the Sephadex CM-25 column and alumina (see *Preparation of urine samples*). Interestingly, both (unknown) peaks No. 8 in Fig. 3A and B have the same retention time; the peak shown in Fig. 3B is out of the range and we confirmed its purity by the above reported "dilution and re-injection procedure". Further, we suspect that they could be due to MDA, one of the main MD metabolites in urine, but we have not been able to confirm this hypothesis as we were unable to obtain a pure standard. Our idea is based on the following: (a) the chemical structure of the unknown peak could be similar to that of other amines (NE, E, DA, NMDA), as it is also extracted by Sephadex CM-25 and alumina; (b) the k' value of the unknown peak could be compatible with MDA if it is compared with k' and the structures of DA and NMDA; (c) if we consider the different concentrations of the aliquots injected to determine catecholamines and MD, the area ratio of the unknown peak and the MD peak is not

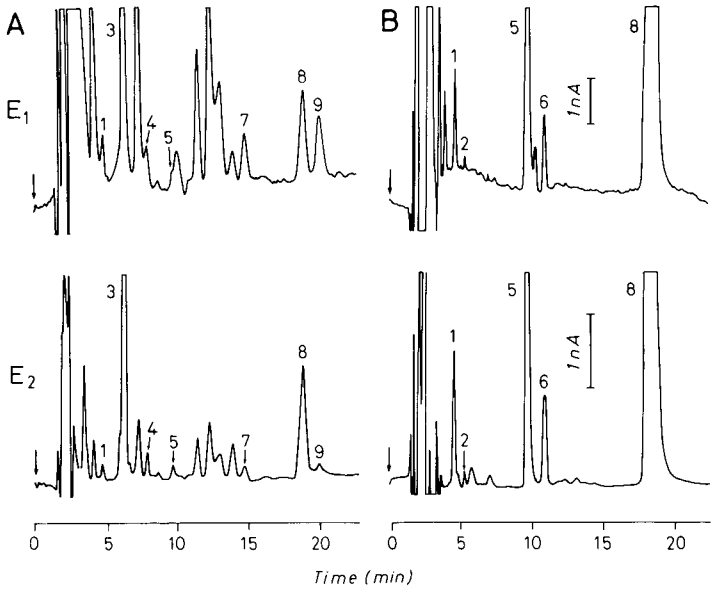

Fig. 3. Chromatograms of (A) 10 μl of 24-h urine (diluted to 1:200) from a hypertensive patient undergoing 250 mg per 24 h oral MD therapy and (B) 100 μl of acetic acid eluate from alumina using the same urine. Peaks: 1 = NE; 2 = E; 3 = MD; 4 = DOPAC; 5 = DA; 6 = NMDA; 7 = 3-OMMD; 8 = unknown; 9 = HVA. Peaks 1 and 4 reported in (A) cannot be ascribed to NE and DA because of their oxidation reduction peak-height ratios, which are different from those of standard compounds (some interfering substances are probably co-eluted). Peaks 8 are suspected to be due to MDA (see *Peak identification*). For chromatographic conditions, see Fig. 2.

very different from the concentration ratio between MDA and MD calculated from previous data [8].

Recovery and reproducibility

Deproteinization by adding trichloroacetic acid, perchloric acid, acetonitrile, methanol and methanol containing 2% of 0.5 or 1.0 *M* perchloric acid was examined. The use of methanol containing 2% of 0.5 *M* perchloric acid to prepare a protein-free sample from plasma gave highly reproducible recoveries of MD, its metabolite and HVA. The recovery was determined by comparing the peak heights of known amounts of standards added to pooled plasma from healthy subjects carried through the assay procedures with those resulting from the analysis of the same amount of a stock standard solution. Table I reports the data for plasma and urine recovery. Satisfactory recoveries were obtained with good relative standard deviations (R.S.D.). Table I also shows the linear regression analysis from calibration graphs for biological samples. The correlation coefficients for all these compounds were higher than 0.9909. Table II shows the between-assay and within-assay R.S.D.s for plasma and urine samples.

Peak identification

The peaks of MD, its metabolite and catecholamines were identified by a combination of methods. The peak identification was initially performed on the basis of

TABLE I

RECOVERY AND REGRESSION LINES OF MD, ITS METABOLITE AND CATECHOLAMINES IN NORMAL PLASMA AND URINE SAMPLES

The values were calculated by analysing plasma and urine samples spiked with standards at three different concentrations ($n = 5$). The recoveries of MD, DOPAC, 3-OMMD, HVA and NMDA(I) were obtained after the deproteinization and evaporation steps; the recoveries of NE, DA, E and NMDA(II) were obtained after the weak cation-exchange extraction procedure and subsequent adsorption on alumina. The internal standard NMDA was used in both experiments. x = added amount of MD, DOPAC, 3-OMMD, NMDA(I) (expressed as ng/ml) and NE, E, DA and NMDA(II) (expressed as pg/ml); y = amount found.

Compound	Plasma				Urine			
	Recovery (mean ± S.D.)	R.S.D. (%)	Concentration range	r	Recovery (mean ± S.D.)	R.S.D. (%)	Concentration range	r
MD	95.6 ± 5.0	5.2	0.8–3.2	0.9996	99 ± 4	4.3	0.4–4.0	0.9991
DOPAC	89.9 ± 4.3	4.8	0.4–1.6	0.9908	102 ± 3	4.9	0.2–3.2	0.9954
3-OMMD	91.8 ± 4.8	4.8	0.8–3.2	0.9999	104 ± 5	4.8	0.4–4.0	0.9996
HVA	102.3 ± 4.4	4.3	0.8–3.2	0.9997	98 ± 2	3.5	0.4–4.0	0.9972
NMDA(I)[a]	95.1 ± 3.4	4.1	0.8–3.2	0.9939	99 ± 4	3.2	0.4–4.0	0.9989
NE	74.5 ± 4.5	5.1	150 –1200	0.9919	73 ± 5	4.6	300 –3000	0.9939
E	68.9 ± 3.3	4.9	50 –800	0.9997	70 ± 4	4.8	50 –800	0.9992
DA	69.1 ± 4.2	6.1	50 –800	0.9968	68 ± 3	4.4	150 –2400	0.9967
NMDA(II)[b]	66.1 ± 5.2	5.7	400 –1600	0.9990	69 ± 5	4.3	400 –1600	0.9998

[a] NMDA internal standard used for determination of MD, DOPAC, 3-OMMD and HVA.
[b] NMDA internal standard used for determination of NE, E and DA.

TABLE II

REPRODUCIBILITY

Between-assay and within-assay R.S.D.s. Plasma and urine samples were spiked with known amounts of MD, its metabolite and catecholamines. MD, DOPAC, 3-OMMD, HVA and NMDA(I) are expressed as ng/ml and NE, E, DA and NMDA(II) as pg/ml.

Compound	Concentration	Plasma		Urine	
		Within-assay R.S.D. (%) ($n=6$)	Between-assay R.S.D. (%) ($n=20$)	Within-assay R.S.D. (%) ($n=5$)	Between-assay R.S.D. (%) ($n=10$)
MD	1.6	5.1	6.3	4.7	4.9
DOPAC	2.1	4.4	5.2	5.2	5.1
3-OMMD	1.6	3.2	4.1	4.3	4.5
HVA	3.8	5.4	5.7	3.9	4.2
NMDA(I)[a]	1.6	5.1	6.2	3.2	3.9
NE	300	4.5	5.3	4.1	4.2
E	50	4.8	5.5	4.4	4.6
DA	50	5.9	6.8	5.4	5.6
NMDA(II)[b]	400	5.2	6.3	3.9	4.1

[a] NMDA internal standard used for the determination of MD, DOPAC, 3-OMMD and HVA (deproteinization and evaporation steps).

[b] NMDA internal standard used for the determination of NE, E and DA (cation exchange and alumina extraction).

the chromatographic retention time and by simultaneous injection of a standard. Second, the ratios of the first detector response (E_1, oxidation current) *versus* the second (E_2, reduction current) were calculated and compared with those obtained with plasma or urine samples. The peak-height ratios of reference compounds and those obtained with plasma or urine samples are reported in Table III.

TABLE III

REVERSIBILITY RATIOS

The values represent the ratios of the detector responses (oxidation current/reduction current) of MD, 3-OMMD, DOPAC, HVA, NMDA and catecholamines. The results are the means ± S.D. of ten experiments. Under the conditions of detector sensitivity, the gain was set at 2000 for the first electrode and 3500 for the second. The plasma levels of E and DA were not determined.

Compound	Standard	Plasma	Urine
MD	1.05 ± 0.06	0.96 ± 0.08	0.98 ± 0.06
3-OMMD	3.37 ± 0.06	3.34 ± 0.03	3.40 ± 0.02
DOPAC	0.73 ± 0.01	0.69 ± 0.71	0.71 ± 0.03
HVA	8.24 ± 0.03	8.28 ± 0.06	8.23 ± 0.05
NE	0.74 ± 0.02	0.71 ± 0.05	0.72 ± 0.04
E	0.83 ± 0.04	–	0.80 ± 0.05
DA	0.73 ± 0.02	–	0.76 ± 0.03
NMDA	0.76 ± 0.01	0.78 ± 0.03	0.79 ± 0.04

The comparison of peak-height ratios allowed some false peak identifications to be avoided. As an example of this, the two chromatograms shown in Fig. 3A should be carefully observed. If peaks are simply identified by comparing their retention times with those of a standard mixture (Fig. 2), peaks 1 and 4 seem to be NE and DA, respectively. On closer examination of the two chromatograms, we observed that the ratios of peak heights (oxidation/reduction) for reference compounds was significantly different from those obtained with urine. As the chromatograms were obtained by direct injection of diluted urine, there are probably some interfering substances which are co-eluted with NE and DA. Our conclusion is that peaks 1 and 4 in Fig. 3A are not homogeneous and they cannot be ascribed to NE and DA. On the other hand, if samples are treated by the appropriate catecholamine extraction (Sephadex CM-25 and alumina) the peaks are clearly identified (Fig. 3B). The selection of the detector potentials is important in obtaining an effective resolution.

Fig. 4 shows the hydrodynamic voltammograms of the standard solution. The substances can be separated according to their half-wave potentials ($E_{1/2}$) into three classes: DA, NMDA, NE, E and DOPAC with the lowest $E_{1/2}$, MD with a higher $E_{1/2}$ value than catecholamines, and finally 3-OMMD and HVA with the highest $E_{1/2}$ values. An operating oxidation potential of +0.40 V was chosen for the determination detection of all the compounds tested, including MD and HVA. The reduction half-wave potential is less indicative and the value chosen of −0.30 V is sufficient for the complete reduction of all compounds.

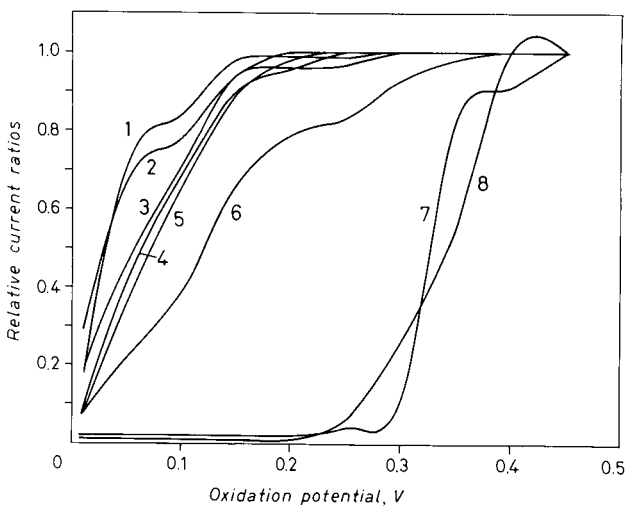

Fig. 4. Hydrodynamic voltammograms for standard substances obtained under the conditions described in Fig. 2. The response (current) at several potentials was recorded and the ratios of the current at any given potential to that of the average response at the plateau level were plotted as a function of oxidation potential. Each point represents the mean of two determinations. An oxidation potential of +0.40 V was chosen for the quantitative oxidation of all compounds. 1 = DA; 2 = NMDA; 3 = DOPAC; 4 = NE; 5 = E; 6 = MD; 7 = HVA; 8 = 3-OMMD.

TABLE IV

TIME COURSE OF CONCENTRATION OF MD PLASMA FOLLOWING AN ORAL DOSE OF 500 mg ALDOMET (MD 500 mg)

Each value represents the means ± standard errors of three determinations. The values are expressed as ng/ml.

Time after administration (h)	Subject No.				
	1	2	3	4	5
1	110 ± 13	642 ± 70	205 ± 20	104 ± 13	1027 ± 121
2	1820 ± 68	1072 ± 118	745 ± 121	580 ± 53	1842 ± 118
3	2576 ± 141	1480 ± 136	1152 ± 115	826 ± 46	2327 ± 265
4	1127 ± 103	1152 ± 116	908 ± 132	912 ± 68	1746 ± 70
5	942 ± 138	815 ± 75	648 ± 72	627 ± 51	1322 ± 145
6	525 ± 59	584 ± 64	552 ± 79	389 ± 53	827 ± 182
Mean	1183 ± 86	958 ± 52	702 ± 49	573 ± 53	1515 ± 149

Clinical applications and conclusion

The method described has been used extensively for the quantitative analysis of plasma and urine samples. Table IV gives the plasma MD concentrations for five patients with essential hypertension, dosed orally with 500 mg of MD. Maximum plasma concentrations occurred 2–3 h after administration.

Table V reports the 24-h urine excretion of MD, its metabolite and catecholamines (free and conjugate) from five hypertensive patients receiving 250 mg of MD orally. Urinary excretions of MD and 3-OMMD from twelve healthy subjects are shown in Table VI. None of the subjects were hypertensive and none of them was taking other medication. Each subject ingested 250 mg of MD and 24-h urine samples were collected.

TABLE V

URINARY CONCENTRATIONS OF FREE AND CONJUGATED MD, ITS METABOLITE AND CATECHOLAMINES IN FIVE PATIENTS RECEIVING MD ORALLY (250 mg)

24-h urine samples; urine collection began 2 h after drug administration. The results reported are the mean ± standard errors for five determinations (each value is the mean of three experiments). MD, 3-OMMD and HVA are expressed as μg/ml and NE, E and DA as ng/ml. The urine levels of HVA and E conjugated were not determined.

Compound	Free	Range	Conjugated	Range
MD	33.5 ± 6.9	25.5–40.6	19.5 ± 7.1	13.1–28.9
3-OMMD	4.9 ± 2.1	2.7–6.8	2.7 ± 0.8	1.7–3.7
DOPAC	0.9 ± 0.3	0.5–1.2	0.6 ± 0.2	0.4–0.8
HVA	3.8 ± 1.2	2.4–5.0	–	–
NE	37.2 ± 20.2	22–68	26 ± 6	19–34
E	13.8 ± 8.0	6–24	–	–
DA	376.1 ± 231.0	226–712	106 ± 24	81–136

TABLE VI

24-HOUR FREE MD AND 3-OMMD IN URINE FROM TWELVE HEALTHY PATIENTS RECEIVING 250 mg OF MD ORALLY

Urine collection began 2 h after drug administration. The results reported are the means of twelve values (each value is the mean of three experiments).

Compound	Mean ± S.E.M.[a] (μ/ml)	Range (μg/ml)
MD	17.70 ± 4.0	11.51–32.15
3-OMMD	3.80 ± 1.56	0.56–11.42

[a] Standard error of the mean.

The present procedure was found to be sufficiently reliable and simple to use for the clinical optimization of therapeutic regimes. Studies of the peak-height ratio reduced the risks of false identification of peaks. The method should be suitable for the study of how drug metabolic enzyme activities influence the wide individual variations in MD metabolism in man.

REFERENCES

1 *Drug Information 88*, American Hospital Formulary Service, American Society of Hospital Pharmacists, Bethesda, MD, 1988.
2 W. Kobinger, *Rev. Physiol. Biochem. Pharmacol.*, 81 (1978) 40.
3 C. R. Freed and P. A. Asmus, *J. Neurochem.*, 32 (1979) 163.
4 E. D. Frolich, *Arch. Int. Med.*, 140 (1980) 954.
5 F. R. J. Reid and W. F. Ganeng, *J. Pharmacol. Exp. Ther.*, 201 (1977) 400.
6 W. B. White, J. W. Andreoli and R. D. Cohn, *Clin. Pharmacol. Ther.*, 37 (1985) 387.
7 N. R. C. Campbell, J. H. Dunnette, G. Mwaluko, J. Van Loon and R. M. Weinshilboum, *Clin. Pharmacol. Ther.*, 35 (1984) 55.
8 N. R. C. Campbell, R. S. Sundaram, P. G. Werness, J. Van Loon and R. M. Weinshilboum, *Clin. Pharmacol. Ther.*, 37 (1985) 308.
9 B. K. Kim and R. T. Koda, *J. Pharm. Sci.*, 66 (1977) 1963.
10 W. Y. W. Au, L. G. Dring, D. G. Grahame-Smith and R. T. Williams, *Biochem. J.*, 129 (1972) 1.
11 J. R. Watson and R. C. Lawrence, *J. Chromatogr.*, 103 (1975) 63.
12 H. M. R. Jones and A. J. Cummings, *Br. J. Clin. Pharmacol.*, 6 (1978) 432.
13 L. D. Mell and A. B. Gustafson, *Clin. Chem.*, 24 (1978) 23.
14 P. D. Walson, K. S. Marshall, R. P. Forsyth, R. Rapoport, K. L. Melmon and N. Castagnoli, *J. Pharmacol. Exp. Ther.*, 195 (1975) 151.
15 J. A. Saavedra, J. L. Reid, W. Jordan, M. D. Rawlings and C. T. Dollery, *Eur. J. Pharmacol.*, 8 (1975) 381.
16 M. J. Cooper, R. F. O'Dea and B. L. Mirkin, *J. Chromatogr.*, 162 (1979) 601.
17 C. R. Freed and P. A. Asmus, *J. Neurochem.*, 32 (1979) 163.
18 G. M. Kochak and W. D. Mason, *J. Pharm. Sci.*, 69 (1980) 897.
19 D. A. Jenner, M. J. Brown and F. J. M. Lhoste, *J. Chromatogr.*, 224 (1981) 507.
20 J. A. Hoskings and S. B. Holliday, *J. Chromatogr.*, 230 (1982) 162.
21 H. Ong, S. Sved and N. Beaudoin, *J. Chromatogr.*, 229 (1982) 433.
22 G. P. Jackman, C. J. Oddie, H. Skews and A. Bobik, *J. Chromatogr.*, 308 (1984) 301.
23 C. Dilger, Z. Salama and H. Jaeger, *Arzneim.-Forsch.*, 37 (1987) 1399.
24 C. Lucarelli, P. Betto, G. Ricciarello, M. Giambenedetti, F. Sciarra, C. Tosti Croce and P. L. Mottironi, *Chromatographia*, 24 (1987) 423.
25 A. H. Anton and D. F. Sayre, *J. Pharmacol. Exp. Ther.*, 138 (1963) 360.
26 R. D. Hoeldtke and J. W. Sloan, *J. Lab. Clin. Med.*, 75 (1970) 159.
27 Cs. Horvath and W. Melander, *J. Chromatogr. Sci.*, 15 (1977) 393.
28 J. Wagner, M. Palfreyman and M. Zraika, *J. Chromatogr.*, 164 (1979) 41.

Journal of Chromatography, 541 (1991) 297–302
Elsevier Science Publishers B.V., Amsterdam

CHROM. 23 019

Resolution of 2,3,4,6-tetra-O-acetyl-β-D-glucopyranosylisothiocyanate derivatives of α-methyl amino acid enantiomers by high-performance liquid chromatography[a]

ZHENPING TIAN, TANYA HRINYO-PAVLINA and ROGER W. ROESKE*
Department of Biochemistry, Indiana University School of Medicine, 635 Barnhill Drive, Indianapolis, IN 46202-5122 (U.S.A.)
and
P. N. RAO
Department of Organic Chemistry, Southwest Foundation for Biomedical Research, San Antonio, TX 78228-0417 (U.S.A.)
(First received February 13th, 1990; revised manuscript received November 20th, 1990)

ABSTRACT

Diastereomers formed by precolumn derivatization of D,L-α-methyl amino acids with 2,3,4,6-tetra-O-acetyl-β-D-glucopyranosylisothiocyanate (GITC) were separated by high-performance liquid chromatography using a conventional C_{18} reversed-phase column. This method completely resolved all the α-methyl amino acids tested except D,L-4-chloro-α-methylphenylalanines which were less well separated. The D-enantiomer was eluted earlier than the L-enantiomer, which is opposite to the order of elution observed with GITC derivative of unmethylated amino acids.

INTRODUCTION

α-Methyl amino acids have been used extensively in biochemistry and drug development in recent years. They have been used as specific inhibitors of the enzymes which act on their α-amino acid counterparts [1–4]. α-Methyl amino acids have been incorporated into peptides for conformational studies because of the rigidity they provide to the peptide backbone and their tendency to promote α-helix or β-turn formation [5–10]. The use of α-methyl amino acids has been explored in peptide drugs, the so-called peptoid concept [11,12].

Even though several asymmetric synthetic methods have been elaborated for the synthesis of α-methyl amino acids [13-16], usually these do not provide an absolutely pure enantiomer but enantiomerically enriched mixtures [17–19]. Therefore it is necessary to know the enantiomeric excess (or the optical purity) of the mixture

[a] This paper is part of the Ph.D. dissertation of Z. Tian.

0021-9673/91/$03.50

obtained. Furthermore, it is always desirable to know the absolute configuration of the enatiomer even in an enantiomerically enriched mixture. Most of this information is now obtained by one of the following physical measurements. ^{1}H NMR has been used either in the presence of chiral ligands [20–22] or after derivatization with (*S*)-2-chloropropionyl chloride [23]. ^{19}F NMR has been also used after derivatization with Mosher's acid (see refs. 24 and 25). One disadvantage of the NMR method is that usually it requires large amounts of samples because of its low sensitivity. Column chromatography [26,27] and thin-layer chromatography [27] have been used to determine enantiomeric excess of the enriched mixtures using a chiral stationary phase. Diastereomeric isoindole derivatives of α-methyl glutamic acid, made from *o*-phthalaldehyde (OPA) and N-acetyl-L-cysteine (AcCys), have been separated by reversed-phase high-performance liquid chromatography (HPLC) [28].

2,3,4,6-Tetra-O-acetyl-β-D-glucopyranosylisothiocyanate (GITC) was introduced by Kinoshita and co-workers [29,30] as a chiral reagent for the derivatization of amino acid enantiomers followed by reversed-phase HPLC separation of the resulting diastereomers (Fig. 1). It has been shown to be very useful in the resolution and identification of a variety of both common and unusual amino acid enantiomers [31–34]. In conjunction with our work on synthetic peptides containing α-methyl amino acids, we explored its use in the resolution of α-methyl amino acid enantiomers. The results indicate that this method works well for the analytical resolution of all the α-methyl amino acid enantiomers tested. The elution order from the C_{18} column is exactly correlated with the absolute configuration of the α-methyl amino acids and is opposite to that of GITC derivatives of the common amino acids [30]. Using molecular modeling we suggest an explanation of this phenomenon.

EXPERIMENTAL

Materials

The optically pure D- and L-α-methyl amino acids were obtained as follows. α-Methyl-4-chlorophenylalanine was synthesized [35] and resolved [36] utilizing chy-

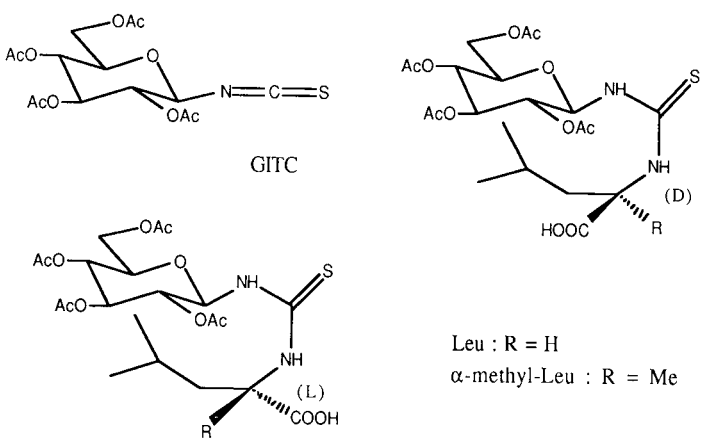

Fig. 1. Structure of GITC, diastereomeric GITC derivatives of D,L-leucine and D,L-α-methylleucine. Ac = Acetyl; Me = methyl.

motrypsin. α-Methylserine was not completely resolved but enriched by the action of chymotrypsin on O-benzyl-DL-α-methylserine [37]. α-Methyltryptophan, α-methyltyrosine, α-methyl-4-fluorophenylalanine were all obtained by the literature procedure [36]. α-Methylleucine was a gift from Dr. Jean Rivier of the Salk Institute. α-Methylornithine was synthesized and resolved by the procedure of *βey et al.* [38]. Optically pure α-methylarginine was prepared starting with optically pure α-methylornithine in our laboratory [37].

All the solvents used both for the derivatization and HPLC elution are HPLC grade. GITC was prepared according to the literature procedure [29] but is also available from Polysciences (Warrington, PA, U.S.A.). The 10 m*M* phosphate buffer was prepared from potassium phosphate (monobasic) and the pH was adjusted to 2.8 by addition of perchloric acid (70%).

Precolumn derivatization

Some modification of the original protocol was made in order to compensate for the low reactivity of the α-amino group of α-methyl amino acids [23,39]. A 5-mg amount of the α-methyl amino acid was dissolved in 5 ml of 50% (v/v) aqueous acetonitrile containing 0.4% (w/v) triethylamine. A 25-μl aliquot of this stock solution was mixed with 50 μl of a solution of 0.2% (w/v) GITC in acetonitrile. This reaction mixture was stirred at room temperature for 1 h and 4–6 μl was injected depending on the chemical purity of the synthesized α-methyl amino acids. For the resolution of α-methyl amino acids with an aromatic side chain, 10 μl of 0.25% (w/v) monoethanolamine in acetonitrile was added and the mixture was stirred for another 10 min after the 1 h reaction time.

Chromatographic conditions

Analytical HPLC analysis was performed using a Ranin Microsorb C_{18} reversed-phase column (5 μm, 250 × 4.6 mm I.D.), with a Varian-5000 liquid chromatography system, a Kipp & Zonen BD40 recorder, and a Hewlett-Packard integrator. The compounds, about 1 μg, were eluted with solvents: (A) 10 m*M* phosphate buffer (pH 2.8) and (B) methanol according to the gradient program shown and were detected by their absorbance at 250 nm, sensitivity set at 0.01 a.u.f.s.

RESULTS AND DISCUSSION

By using a longer derivatization time and higher reactant concentration than the original protocol, all the α-methyl amino acids tested react cleanly with GITC under alkaline conditions despite the steric hindrance around the α-amino group. Data obtained clearly indicate that GITC is a suitable chiral reagent for the derivatization of α-methyl amino acids. Analytical HPLC using a conventional C_{18} reversed-phase column can be used effectively to resolve the diastereomers formed from the derivatization and the elution order is well-correlated with the configuration of the α-methyl amino acids from which information on the enantiomeric excess and the configuration of the enantiomer can be extracted (Figs. 2 and 3). All the results obtained on the α-methyl amino acids tested are summarized in Table I: t_0 refers to the retention time of the unretained material, t_R, k', α, R_s refer to the retention time, capacity ratio, separation factor and resolution respectively for a pair of diastereomers.

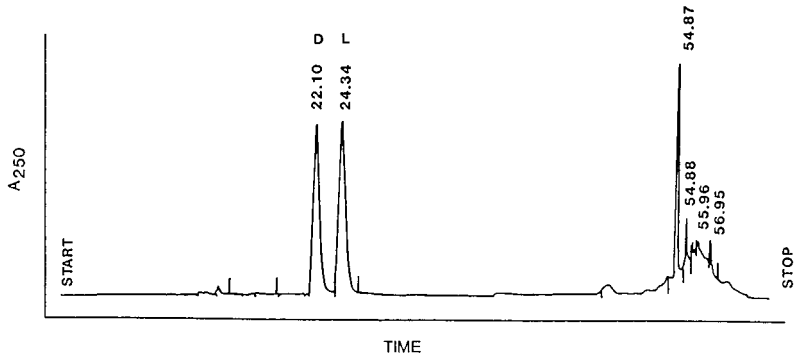

Fig. 2. Separation of diasteromeric GITC derivatives of DL-α-methyltryptophan. Gradient program: 0–10 min, 30–50%B; 10–40 min, 50%B constant; 40–50 min, 50–100%B; 50–55 min, 100–30%B. Time in min.

However, the elution order in all cases tested except for α-methylarginine is opposite that of GITC-derivatized α-amino acids. Thus GITC-L-amino acids except for histidine and arginine [40] are eluted before the D isomers, but GITC-α-methl-L-amino acids are eluted later than the D-isomers under the same conditions of chromatography. In order to understand the reversed order of elution between the common α-amino acids and α-methyl amino acids, a molecular modeling experiment was run on GITC leucine and α-methylleucine using a Silicon Graphics Workstation with QUANTA and energy minimization by CHARMm. It was shown that the GITC-amino acid derivatives have a turn at the thiourea region with the sulfur atom point-

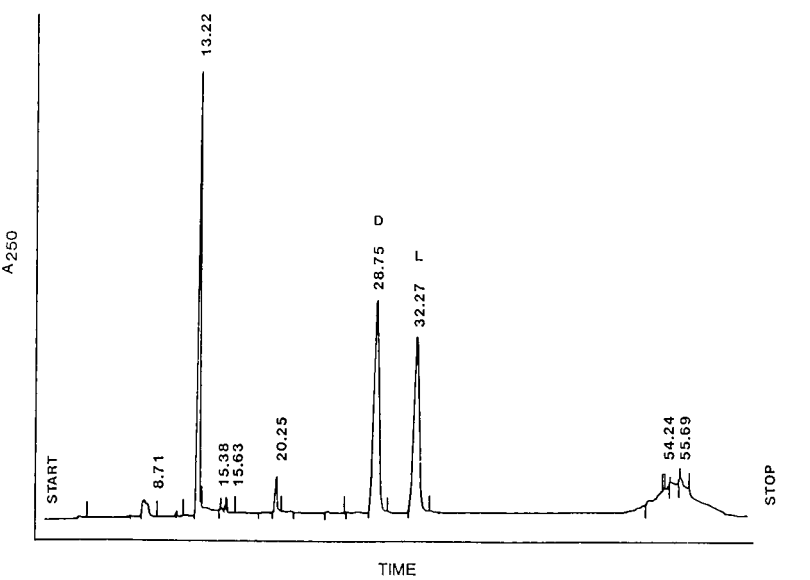

Fig. 3. Separation of diasteromeric GITC derivatives of DL-α-methylarginine. Gradient program: 0–10 min, 30–38%B; 10–45 min, 38%B constant; 45–50 min, 38–100%B; 50–55 min, 100–30%B.

TABLE I

SEPARATION OF GITC DERIVATIVES OF α-METHYL AMINO ACIDS

Gradient programs:
(A) 0–10 min, 30–53%B; 10–45 min, 53%B constant; 45–50 min, 53–100%B; 50–55 min, 100–30%B.
(B) 0–10 min, 30–57%B; 10–50 min, 57%B constant; 50–55 min, 57–100%B; 55–60 min, 100–30%B.
(C) 0–10 min, 30–40%B; 10–50 min, 40%B constant; 50–55 min, 40–100%B; 55–60 min, 100–30%B.
(D) See Fig. 2.
(E) 0–10 min, 20–30%B; 10–50 min, 30%B constant; 50–55 min, 30–100%B; 55–60 min, 100–20%B.
(F) 0–10 min, 30–46%B; 10–45 min, 46%B constant; 45–50 min, 46–100%B; 50–55 min, 100–30%B.
(G) See Fig. 3.
(H) 0–10 min, 30–48%B; 10–45 min, 48%B constant; 45–50 min, 48–100%B; 50–55 min, 100–30%B.

DL-α-Methyl amino acids	t_0 (min)	t_R(min)		k'		α	R_s	Elution gradient
		D	L	D	L			
α-Methyl--4-fluoro-Phe	2.98	33.26	35.16	10.16	10.80	1.06	1.24	A
α-Methyl-4-Cl-Phe	3.00	30.02	31.62	9.01	9.54	1.06	0.63	B
α-Methyl-Tyr	3.44	45.43	46.66	12.21	12.56	1.03	0.96	C
α-Methyl-Trp	3.03	28.75	32.27	8.49	9.65	1.14	3.49	D
α-Methyl-Ser	3.02	26.15	31.27	7.66	9.35	1.22	4.00	E
α-Methyl-Orn	3.29	33.90	44.52	9.30	12.53	1.35	3.82	F
α-Methyl-Arg	3.10	22.10	24.34	6.13	6.85	1.12	1.98	G
α-Methyl-Leu	3.00	29.35	35.94	8.78	10.98	1.25	5.81	H

ing outward. The model shows that the molecule is very rigid and crowded, which is consistent with the view of Kinoshita and co-workers [29,30] that conformational rigidity provides the basis of separation. The GITC-(L)-leucine and GITC-(D)-α-methylleucine are both crescent-shaped and present uneven surfaces whereas the later eluting diastereomers, GITC-(D)-leucine and GITC-(L)-α-methylleucine, are flat, presenting two smooth hydrophobic surfaces.

REFERENCES

1 G. C. Barret, in R. C. Sheppard (Senior Reporter), *Amino Acids, Peptides and Proteins, (Specialist Periodical Report,* Vol. 10), Chemical Society, London, 1979, p. 11.
2 U. Schöllkopf, *Tetrahedron,* 39 (1983) 2085.
3 D. F. Reinhold, R. A. Firestone, W. A. Gaines, J. M. Chemerda and M. Sletzinger, *J. Org. Chem.,* 33 (1968) 1209.
4 F. W. Bollinger, *J. Med. Chem.,* 99 (1971) 5203.
5 A. W. Burgess and S. L. Leach, *Biopolymers,* 12 (1973) 2691.
6 N. Shamala, R. Nagaraji and P. Balaram, *Biochem. Biophys. Res. Commun.,* 79 (1977) 292.
7 A. I. McMullen, D. J. Marlborough and P. M. Baylay, *FEBS Lett.,* 16 (1971) 278.
8 G. Jung, N. Dubischar and D. Leibfritz, *Eur. J. Biochem.,* 54 (1975) 395.
9 W. Mayr, R. Oekonomopulos and G. Jung, *Biopolymers,* 18 (1979) 425.
10 D. Leibfritz, R. M. Brunne, T. Weihrauch, J. Stelten, E. T. K. Haupt and W.-D. Stohrer, *Liebigs Ann. Chem.,* (1989) 1017.
11 M. Mutter, *Angew. Chem., Int. Ed. Engl.,* 24 (1985) 639.
12 J. L. Fauchere, *Adv. Drug. Res.,* 15 (1986) 29.
13 D. Seebach, M. Boes, R. Naef and W. B. Schweizer, *J. Am. Chem. Soc.,* 105 (1983) 5390.
14 D. Seebach, R. Imwinkelried, T. Weber, in R. Schefford (Editor), *Modern Synthetic Methods,* Vol. 4, Springer, Berlin, 1986, p. 125.

15 U. Schöllkopf, *Top. Curr. Chem.*, 109 (1983) 65.
16 U. Groth and U. Schöllkopf, *Synthesis*, (1983) 37.
17 U. Schöllkopf and H.-J. Neubauer, *Synthesis*, (1982) 861.
18 U. Schöllkopf, R. Lonsky and P. Lehr, *Liebigs Ann. Chem.*, (1985) 413.
19 M. Ihara, M. Takahashi, H. Niitsuma, N. Taniguchi, K. Yasui and K. Fukumoto, *J. Org. Chem.*, 54 (1989) 5413.
20 J. A. Bajgrowicz, B. Cossec, Ch. Pigière, R. Jacquier and Ph. Viallefont, *Tetrahedron Lett.*, 25 (1984) 1789.
21 F. Bjorkling, J. Boutelje, S. Gatenbeck, K. Hultand and T. Norin, *Tetrahedron Lett.*, 26 (1985) 4957.
22 K. Kabuto and Y. Sasaki, *Tetrahedron Lett.*, 31 (1990) 1031.
23 W. H. Kruizinga, J. Bolster, R. M. Kellog, J. Kamphuis, W. H. J. Boesten, E. M. Meijer and H. E. Schoemaker, *J. Org. Chem.*, 53 (1988) 1826.
24 D. Crich and J. W. Davies, *J. Chem. Soc., Chem. Commun.*, (1989) 1418.
25 J. A. Dale, D. L. Dull and H. S. Mosher, *J. Org. Chem.*, 34 (1969) 2543.
26 K. Nebel and M. Mutter, *Tetrahedron*, 44 (1988) 4793.
27 H. Brückner, I. Bosch, T. Graser and P. Fürst, *J. Chromatogr.*, 395 (1987) 569.
28 M. Maurs, F. Trigalo and R. Azerad, *J. Chromatogr.*, 440 (1988) 209.
29 N. Nimura, H. Ogura and T. Kinoshita, *J. Chromatogr.*, 202 (1980) 375.
30 T. Kinoshita, Y. Kasahara and N. Nimura, *J. Chromatogr.*, 210 (1981) 77.
31 H. Parnes and E. J. Shelton, *Int. J. Peptide Protein Res.*, 27 (1986) 239.
32 P. N. Rao, J. E. Burdett Jr., J. W. Cessac, C. M. Diinunno, D. M. Peterson and H. K. Kim, *Int. J. Peptide Protein Res.*, 29 (1987) 118.
33 J. Maribaum and D. H. Rich, *J. Org. Chem.*, 53 (1988) 869.
34 A. A. Tymiak, T. J. McCormick and S. E. Unger, *J. Org. Chem.*, 54 (1989) 1149.
35 L. Ghosez, J.-P. Antonie, E. Deffense, M. Navarro, V. Libert, M. J. O'Donnell, W. A. Bruder, K., Willey and K. Wojciechowski, *Tetrahedron Lett.*, 23 (1982) 4255.
36 G. M. Anantharamaiah and R. W. Roeske, *Tetrahedron Lett.*, 23 (1982) 3335.
37 Z. Tian, T. Hrinyo-Pavlina, R. W. Roeske and P. N. Rao, unpublished results.
38 P. Bey, C. Danzin, Dorsselaer, V. V. Mamont, P. M. Jung and C. Tardif, *J. Med. Chem.*, 21 (1978) 50.
39 P. Wipf and H. Heimgartner, *Helv. Chim. Acta*, 70 (1987) 354.
40 N. Nimura, A. Toyama and T. Kinoshita, *J. Chromatogr.*, 316 (9184) 547.

Journal of Chromatography, 541 (1991) 303–315
Elsevier Science Publishers B.V., Amsterdam

CHROM. 23 010

Comparison of polybutadiene-coated alumina and octadecyl-bonded silica for separations of proteins and peptides by reversed-phase high-performance liquid chromatography

JEROME E. HAKY* and ANIL RAGHANI
Department of Chemistry, Florida Atlantic University, Boca Raton, FL 33431 (U.S.A.)
and
BEN M. DUNN
Department of Biochemistry and Molecular Biology, University of Florida, Gainesville, FL 32610 (U.S.A.)
(First received August 16th, 1990; revised manuscript received November 22nd, 1990)

ABSTRACT

The chromatographic retention and separations of proteins and peptides on a novel polybutadiene-coated alumina (PBDA) high-performance liquid chromatographic stationary phase are compared to those obtained on a widely-used polymeric octadecylsilane (ODS) phase. Using acetonitrile–water mobile phase gradients containing 0.1% trifluoroacetic acid, the average peak capacities (which are inversely proportional to average peak widths) and peak resolutions obtained for chromatograms of mixtures of ribonuclease A, cytochrome *c*, lysozyme and carbonic anhydrase are five times lower on a column packed with PBDA than on one packed with ODS. Irreversible adsorption causes increases in column back-pressure during successive analyses of protein solutions on PBDA phases and 50% reductions in protein peak areas on the PBDA phase compared to ODS. In contrast to those results, peak capacities, resolutions and peak areas for synthetic octapeptides on the PBDA and ODS phases are more comparable to each other. Chromatographic capacity factors of 31 low-molecular-weight organic compounds on PBDA and ODS columns are shown to correlate well. The critical concentrations of organic modifier required to elute proteins and octapeptides from PBDA columns are lower than that required for ODS, but still correlate linearly with corresponding values from ODS columns. It is concluded from these results that the retentions of peptides, proteins and smaller molecules on both the PBDA and ODS phases are governed by similar hydrophobic interaction mechanisms, while peak broadening due to mass transfer resistance increases more rapidly with solute size on the PBDA stationary phase than it does on ODS. The increase in solute mass transfer resistance with solute size on the PBDA column is attributed to solute interactions with the uniquely-shaped PBDA particles.

INTRODUCTION

There has recently been much interest in the development of new stationary phases for high-performance liquid chromatography (HPLC) which have greater hydrolytic stability and fewer interfering surface acidic sites (*e.g.*, silanols) than for the commonly used alkyl-bonded silica phases. Much of this research has involved polymeric materials, or polymer-coated silica and alumina. Examples of such stationary phases include polystyrene–divinylbenzene (PRP) [1], polystyrene-coated silica [2,3], and polybutadiene-coated alumina [4].

0021-9673/91/$03.50

Although various applications of polymeric and polymer-coated stationary phases for the separations of low-molecular-weight compounds (*i.e.*, mol.wt. <300) have been reported [2,4,5], chromatographic peak symmetries and efficiencies for such separations are often lower than those obtained on alkyl-bonded silica phases. This has been attributed to the lower solute–solvent mass-transfer rates associated with polymeric phases. In spite of these limitations, many of these phases have been found to be useful in separating higher molecular weight compounds, such as proteins and peptides. Excellent separations of such compounds on wide-pore polymeric and polymer-coated phases, such as polystyrene–divinylbenzene [6], polystyrene [7], polystyrene-coated silica [3] and polymeric octadecylsilane [8] have been reported. Peak shapes and chromatographic efficiencies on these phases are often superior to those which can be obtained on monomeric alkyl-bonded silica.

A number of researchers have investigated the properties of polybutadiene-coated alumina as a stationary phase for reversed-phase HPLC [4,9–12]. Wieserman *et al.* [12] and Wilhelmy [13] developed such a phase (PBDA) which is unique in that it consists of polybutadiene-coated porous alumina particles which are not perfectly spherical, but rather are composed of microplatelets bound together in a highly symmetrical, spheroidal manner. Although this stationary phase has recently been employed for the estimation of octanol–water partition coefficients by reversed-phase HPLC [11], the potential of PBDA for separating high-molecular-weight compounds such as proteins and peptides has not been fully investigated. In this paper, we report on the application of this unique PBDA phase for the reversed-phase separation of proteins and peptides, and compare separations obtained on the PBDA phase with those obtained on a more commonly-used octadecylsilica (ODS) material.

EXPERIMENTAL

Materials

The protein standards ribonuclease A, lysozyme, carbonic anhydrase and cytochrome *c* were obtained from Sigma (St. Louis, MO, U.S.A.). The octapeptide standards listed in Table I were synthesized in the Protein Chemistry Core Facility of the University of Florida by the solid-phase technique, as reported elsewhere [14,15].

TABLE I

OCTAPEPTIDE STANDARDS

Nph = *p*-Nitrophenylalanine.

Octapeptide	Amino acid sequence
Ala-Pro-R	Ala-Pro-Ala-Lys-Phe-Nph-Arg-Leu
Leu-Pro-R	Leu-Pro-Ala-Lys-Phe-Nph-Arg-Leu
Ser-Pro-R	Ser-Pro-Ala-Lys-Phe-Nph-Arg-Leu
Lys-Ala-R	Lys-Ala-Ala-Lys-Phe-Nph-Arg-Leu
Lys-Arg-R	Lys-Arg-Ala-Lys-Phe-Nph-Arg-Leu
Lys-Asp-R	Lys-Asp-Ala-Lys-Phe-Nph-Arg-Leu
Lys-Leu-R	Lys-Leu-Ala-Lys-Phe-Nph-Arg-Leu
Lys-Ser-R	Lys-Ser-Ala-Lys-Phe-Nph-Arg-Leu

All solvents used were glass distilled, obtained from E. M. Science (Cherry Hill, NJ, U.S.A.). Trifluoroacetic acid (TFA) was obtained from Aldrich (Milwaukee, WI, U.S.A.).

Apparatus

The HPLC system consisted of a Perkin-Elmer Series 410 solvent-delivery system, a Rheodyne Model 7125 injector (20-μl loop) and a Perkin-Elmer Model LC-135 diode array UV–visible detector. Unless otherwise specified, the wavelength monitored was 280 nm, and the mobile phase flow-rate was set at 2 ml/min. Chromatographic data were recorded and processed on a Perkin-Elmer Omega data system.

The PBDA column used in this study was obtained from Biotage (Charlottesville, VA, U.S.A.). It was packed with an Alcoa Unisphere polybutadiene-coated alumina stationary phase. The Unisphere alumina particle consists of *ca.* 200 nm thick platelets bonded together to form spheroidal particles with open, readily accessible inner-platelet macroporosity and inter-platelet microporosity. These particles had a mean diameter of 8 μm and a medium pore size of 24 nm. The polybutadiene was coated and immobilized on the alumina surface using processes similar to those described by Bien-Vogelsang *et al.* [4]. The dimensions of the PBDA column were 250 mm × 4.6 mm I.D.

The Vydac ODS column packed with polymeric C_{18} bonded silica was obtained from the Separations Group (Hesperia, CA, U.S.A.). The packing had nominal particle diameter and pore size of 5 μm and 30 nm, respectively. The dimensions of the ODS column were 150 mm × 4.6 mm I.D.

Analytical conditions

Solutions of the protein and octapeptide standards were prepared at 1–4 mg/ml in 0.1% trifluoroacetic acid and stored at 0°C. HPLC analyses of the protein standards were performed on each column using a linear mobile phase gradient from 10 to 70% B over 20 min, where solvent A is 0.1% (v/v) TFA in water (pH 2.0) and B is 0.1% (v/v) TFA in acetonitrile. HPLC analyses of the octapeptide standards were performed on each column using the same solvents A and B and a linear gradient from 10–46% B over 24 min.

Six successive analyses of a solution of ribonuclease A (2 mg/ml in 0.1% TFA) on the PBDA column caused initial backpressures to rise *ca.* 80 p.s.i. (see Fig. 2). Backpressures could generally be restored to original levels (*ca.* 1200 p.s.i.) by backflushing the column with a solution of aqueous sodium hydroxide (0.1 *M*) for 10 min at a flow-rate of 2 ml/min. No increases in column backpressure were observed during successive injections of the ribonuclease A solution on the ODS column or successive injections of the octapeptide standards on either column.

Calculations

Peak capacity (*PC*) was calculated for each chromatographic peak in the chromatograms shown in Figs. 1 and 4 by the equation $PC = (t_1 - t_0)/4\sigma$, where t_1 = elution time in minutes of the last peak in the chromatogram, 4σ = width of the peak of interest at baseline, and t_0 = column dead time (ODS: 0.96 min; PBDA: 1.62 min). The value of t_0 was determined by injection of a sample of pure water. Since *PC* is

inversely proportional to stationary phase particle diameter [16], equivalent peak capacity, PC', for a phase with an 8-μm particle diameter was calculated by the equation $PC' = PC \cdot d/8$, where PC = the experimental peak capacity and d = the particle diameter of the phase (ODS: 5 μm; PBDA: 8 μm). Chromatographic resolutions were calculated by the method described by Snyder and Kirkland [17]. Corrected retention times, t', were calculated by the formula $t' = t - t_0$, where t = experimental retention time. Gradient dwell time, t_d, was determined to be 2.37 min using the procedure described by Snyder and Dolan [18]. Critical mobile phase concentrations (*i.e.*, the percentage of acetonitrile in the mobile phase at elution time of the solute) was calculated by eqn. 1:

$$CC = C_i + (C_f - C_i)\,[(t' - t_d/t_g] \quad (1)$$

where CC = the critical concentration, C_i = the initial percentage of acetonitrile in the mobile phase gradient, C_f = the final percentage of acetonitrile in the mobile phase gradient and t_g = gradient time [16].

RESULTS AND DISCUSSION

The structure and physical characteristics of the PBDA phase compares favorably with other polymeric and polymer-coated phases that have been successfully used for the HPLC analysis of proteins and peptides. Its pore size of 24 nm and particle size of 8 μm are similar to those of other phases used for peptide and protein separations [19,20]. Like most polymer-coated materials, PBDA is also stable in acidic mobile phases which are generally used in protein and peptide HPLC separations [4,12,13].

Separations on the PBDA column were compared with those obtained on a column packed with a polymeric octadecylsilane phase, Vydac ODS, that has been widely used for the HPLC analyses of peptides and proteins [8,19]. Two mixtures of protein and peptide standards were chosen for the comparisons. The first mixture consisted of four natural proteins in the molecular weight range of 12 000–30 000: ribonuclease A, lysozyme, carbonic anhydrase and cytochrome *c*. The second mixture consisted of the eight synthetic octapeptides listed in Table I which have molecular weights over an order of magnitude lower. These octapeptides were originally synthesized for studies of enzyme-substrate interactions [14,15,21], and were ideal for the present study, since they contained the amino acid residue *p*-nitrophenylalanine that strongly absorbs UV radiation, allowing for easy detection. Additionally, these octapeptides varied only in the identities of two amino acid residues, allowing for a controlled analysis of the factors affecting the retention of peptides of similar size and structure.

Comparisons of protein and peptide separations, peak capacities and general chromatographic properties

Chromatograms of the protein test mixture on the PBDA and Vydac ODS columns are shown in Fig. 1. Separations of these compounds on the PBDA column are inferior to that obtained on the ODS column. The smaller pore size (24 *vs.* 30 nm) and the larger particle size (8 *vs.* 5 μm) of the PBDA phase cannot entirely account for

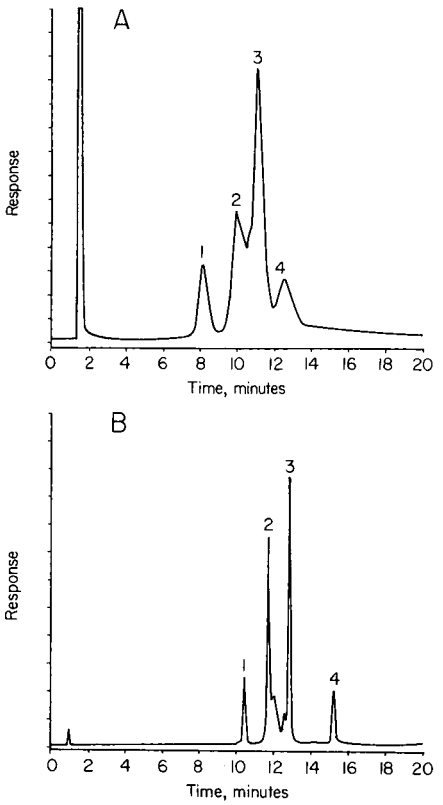

Fig. 1. Chromatograms of mixture of protein standards on PBDA (A) and ODS (B) columns. Peaks: 1 = ribonuclease A; 2 = cytochrome *c*; 3 = lysozyme; 4 = carbonic anhydrase. Other peaks correspond to impurities. Eluent described in Experimental.

the 5-fold differences in average peak capacity (a measure of column efficiency [22]) and chromatographic resolution (a measure of both efficiency and selectivity [17]) between the PBDA and Vydac ODS columns (Table II). Phases with particle dimensions similar to PBDA have produced *PC* and resolution data for similar proteins which are much more comparable to that obtained on the Vydac ODS phase [19,20]. Nor can the dimensional differences alone account for the increases in column backpressure observed during replicate injections of a protein sample on the PBDA column (see Fig. 2), or for the consistantly smaller cytochrome *c* peak areas obtained on the PBDA phase compared to those obtained on ODS (over 50% lower at all solute concentrations; see Fig. 3A). These observations suggest poor mass transfer and incomplete recovery of the proteins on the PBDA column, ultimately resulting in substantial irreversible protein adsorption on the stationary phase. Similar adsorption problems have also been observed for proteins on porous phases consisting of polystyrene–divinylbenzene (PRP) copolymers [6]; as in the present study, adsorbed protein material could be removed by backflushing the column with a protein-hydrolyzing solution [6].

TABLE II

RETENTION TIMES, PEAK CAPACITIES AND RESOLUTIONS FOR PROTEIN STANDARDS (FIG. 1)

t = Retention time in min; PC = peak capacity; PC' = equivalent peak capacity for a phase with 8-μm particle diameter; R_s = chromatographic resolution between the indicated protein and the protein eluting immediately before it.

Protein	Column	t	PC	PC'	R_s
Ribonuclease A	ODS	10.43	26.36	16.47	–
	PBDA	8.20	8.64	8.64	–
Cytochrome *c*	ODS	11.71	52.71	32.94	3.16
	PBDA	10.04	7.26	7.26	1.33
Lysozyme	ODS	12.84	75.70	47.31	5.35
	PBDA	11.14	10.89	10.89	0.88
Carbonic anhydrase	ODS	15.19	19.97	12.48	6.42
	PBDA	12.51	5.16	5.16	0.88
Mean	ODS	12.54	43.68	27.30	4.98
	PBDA	10.47	7.98	7.98	1.03

Separations of the lower-molecular-weight peptides on the PBDA phase are generally better than corresponding separations of proteins. Fig. 4 shows chromatograms of a mixture of three octapeptides on the PBDA and ODS columns. Table III displays peak capacity and resolution data calculated from these chromatograms. Although the average peak capacity (corrected for differences in particle size between the two phases [22]) obtained for the Vydac ODS column is higher than that obtained for the PBDA phase, the difference (less than a factor of 2) is not nearly as great as that observed with the higher-molecular-weight protein separations. In fact, the chromato-

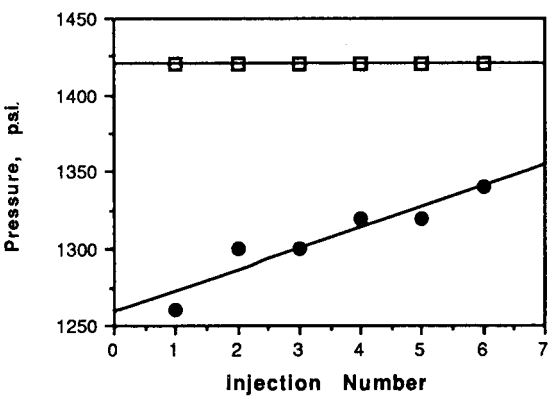

Fig. 2. Plot of column backpressure at the start of mobile phase gradient *vs.* injection number for successive analyses of ribonuclease A. □ = ODS column; ● = PBDA column.

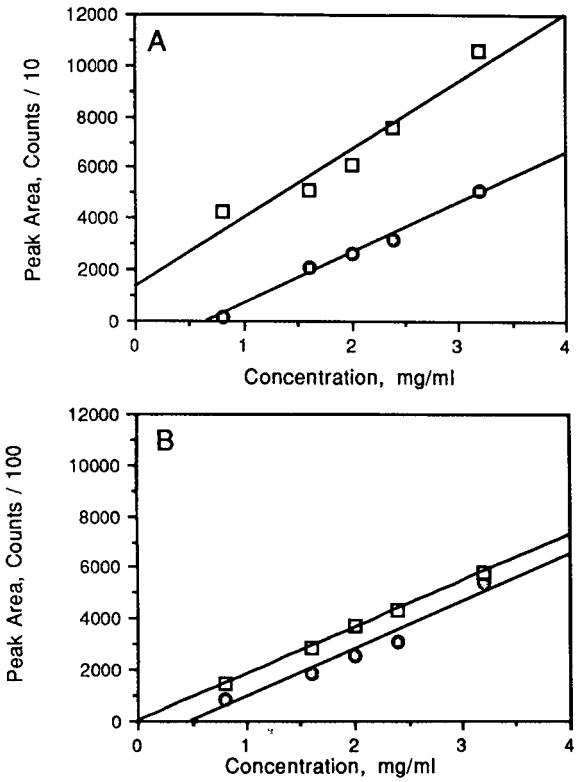

Fig. 3. Plots of chromatographic peak area *vs.* concentration of sample analyzed. (A) Plot for cytochrome *c*; (B) plot for Leu-Pro-R. □ = ODS column; ● = PBDA column.

graphic resolution between the first two peaks in the chromatogram of the octapeptide mixture is actually higher on the PBDA column than it is on the ODS column (Table III). In contrast to that observed with protein analyses on the PBDA column, backpressure did not increase with replicate octapeptide injections. Additionally, representative peptide peak areas obtained on the PBDA phase at various analyte concentrations are only about 15% lower than those obtained on the ODS phase (Fig. 3B), in contrast to the 50% reduction observed for cytochrome *c* peak areas on PBDA (Fig. 3A). Clearly, these data indicate that solute–stationary phase mass transfer resistance and irreversible solute adsorption on the PBDA phase are much higher for the proteins than for the octapeptides.

The higher solute adsorption and resistance to solute–stationary phase mass transfer observed for proteins than for the lower-molecular-weight octapeptides on the PBDA stationary phase indicates that the chromatographic efficiency of the PBDA phase is dependent upon solute size. Peak broadening and high solute mass transfer resistance has been observed previously during separations of small molecules on some polymer and alumina-based stationary phases, and was attributed to interactions of the π orbitals of solutes with those of the stationary phases [5], and acid–base

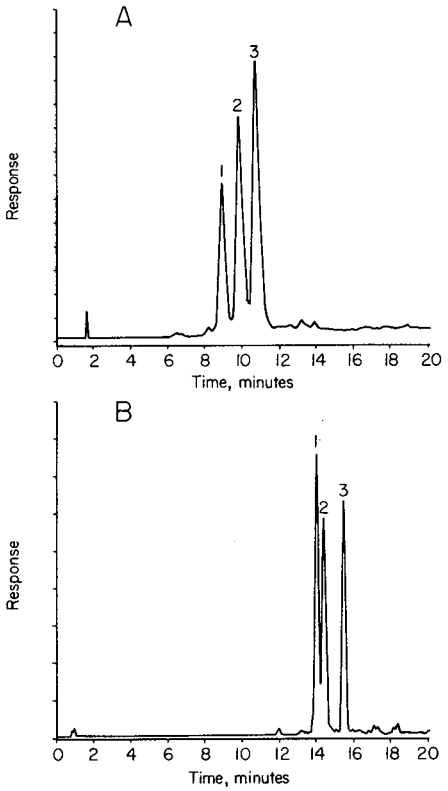

Fig. 4. Chromatograms of mixtures of octapeptide standards on PBDA (A) and ODS (B) columns. Peaks: 1 = Ala-Pro-R; 2 = Ser-Pro-R; 3 = Leu-Pro-R. Eluent described in Experimental.

TABLE III

RETENTION TIMES, PEAK CAPACITIES AND RESOLUTIONS FOR THREE OCTAPEPTIDE STANDARDS (FIG. 4)

Column heading abbreviations are the same as those used in Table II.

Peptide	Column	t	PC	PC'	R_s
Ala-Pro-R	ODS	13.98	39.01	24.38	–
	PBDA	8.79	18.31	18.31	–
Ser-Pro-R	ODS	14.34	38.89	24.30	0.98
	PBDA	9.71	9.75	9.75	1.32
Leu-Pro-R	ODS	15.39	21.95	13.72	2.18
	PBDA	10.59	11.08	11.08	1.02
Mean	ODS	14.57	33.28	20.80	1.58
	PBDA	9.70	11.08	11.08	1.17

interactions of solutes with the alumina support [10]. However, neither of these effects can be the controlling factor for solute–stationary phase mass transfer resistance on the PBDA phase for the separations discussed in the present study. π-Orbital interactions can be eliminated as a controlling factor because they would be expected to cause similar mass-transfer problems in the separations of proteins and peptides on other stationary phases containing unsaturated bonds, such as polystyrene-coated silica. These were not observed in a recently published study [3]. Interactions of solutes with exposed alumina sites can also be eliminated as a major factor controlling solute mass transfer. If present, such interactions would lead to greater peak broadening for the peptides than for the proteins, since, being smaller, the peptides could more readily access these sites than the proteins. The observed increases of chromatographic peak width and solute adsorption with increasing solute size on the PBDA phase can more reasonable be attributed to factors related to the interaction of solutes with the uniquely shaped PBDA particles. The larger protein molecules may become entrapped in the crevices between platelets of the PBDA particles more readily than the smaller peptide molecules, resulting in the observed greater mass transfer resistance for the proteins than for the peptides on PBDA.

It has been suggested that the unique shape of the PBDA particles allows for more efficient solvent flow through this material than that which can be obtained for standard spherical silica particles, which would result in lower column backpressures, especially at high mobile phase flow-rates [12,13,23]. The two upper curves in Fig. 5 are graphs of the normalized column backpressure (*i.e.*, pressure divided by column length) *vs.* mobile phase flow-rate for the ODS and PBDA columns under isocratic conditions. While column backpressures are indeed lower for the PBDA column, this comparison does not take into account the differences in the particle diameters of the two phases. Since column backpressure is inversely proportional to the square of particle diameter [16], a more accurate comparison can be made if the normalized backpressures for the ODS column are corrected to correspond to the same particle diameter as the PBDA phase by multiplying the experimentally-obtained pressure values by the factor 25/64, which is the ratio of the squares of the diameters of the ODS and PBDA phases. The lowest curve in Fig. 5 shows that these corrected backpressures

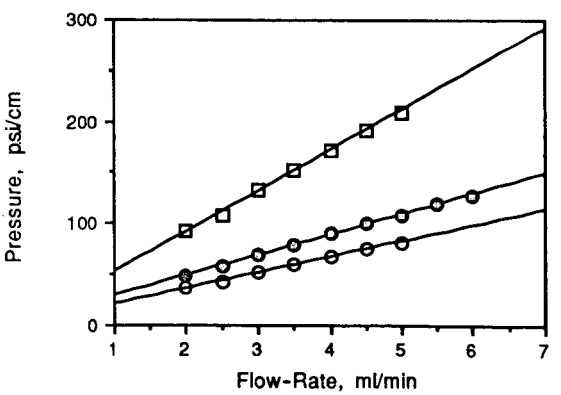

Fig. 5. Plot of the normalized column backpressure *vs.* the mobile phase flow-rate for the ODS and PBDA columns, using a mobile phase of 15% acetonitrile and 85% aqueous TFA (0.1%). □ = ODS column; ● = PBDA column; ○ = ODS column, corrected to correspond to an 8 μm particle size.

are in fact lower than those obtained on a PBDA column of equivalent length and particle diameter. Contrary to that which was previously speculated, column backpressure is not inherently lower for the PBDA phase particles, at least when compared with a phase consisting of highly porous silica-based spherical particles such as Vydac ODS.

Quantitative comparisons of retention mechanisms on ODS and PBDA

Although the incomplete resolutions, large peak widths and substantial peak area reductions for proteins on the PBDA phase clearly indicate a strong dependence of solute size on mass transfer resistance for the uniquely shaped PBDA particles, the retention of solutes on the PBDA phase can be governed by other factors. Comparison of the retention mechanisms of low-molecular-weight organic solutes on ODS and other phases has been accomplished by determining the degree of correlation of the isocratic capacity factors (k') of a large number of compounds on columns packed with ODS and other phases. For example, deviation of phenolic compounds from general correlations between capacity factors of other compounds on ODS and octadecyl-bonded alumina (ODA) has recently been interpreted as indicating the presence of solute-accessible basic alumina sites on the ODA phase [24]. Although a similar comparison has never been reported for such compounds on ODS and PBDA phases, appropriate retention data are available from an earlier study [11]. Fig. 6 shows a logarithmic graph of the capacity factors of 31 low-molecular-weight compounds on the PBDA column *vs.* their capacity factors on an ODS column. The degree of correlation between these retention parameters is high ($R = 0.961$), and there are no apparent deviations of the capacity factors of any specific class of compounds. Other studies have also shown high correlations between capacity factors of small solutes on PBDA and ODS phases and the octanol–water partition coefficients of these solutes [9–11]. The results from these two correlations indicate that retention of small solutes on the ODS and PBDA phases is governed by very similar hydrophobic interaction mechanisms.

Owing to their large size, higher-molecular-weight compounds such as peptides and proteins are retained on some reversed-phase columns by mechanisms other than

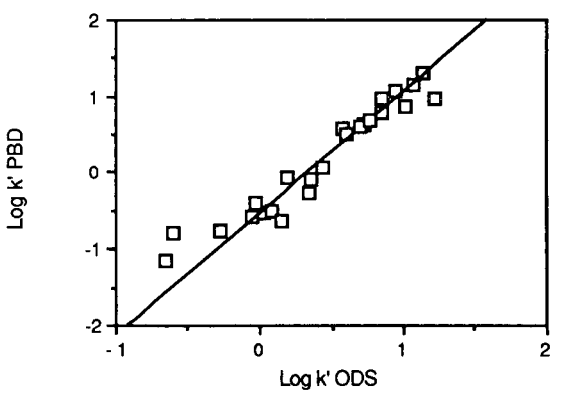

Fig. 6. Plot of the logarithm of the capacity factors of low-molecular-weight compounds on the PBDA column *vs.* the logarithm of their capacity factors on the ODS column. Linear correlation coefficient = 0.961. Data are from ref. 11.

hydrophobic interactions, such as solute size exclusion [22]. However, previous studies have indicated that size-exclusion effects are minimal on the Vydac ODS phase, even for the retention of proteins with molecular weights as high as 50 000 [19]. To determine the extent to which these size-exclusion effects are present on the PBDA phase, a quantitative comparison of the retention of peptides and proteins on the PBDA and Vydac ODS columns analogous to that described earlier for smaller solutes is desirable.

Since the elution of peptides and proteins on both the ODS and PBDA columns could not be performed in an isocratic mode without extensive peak tailing, correlation of their isocratic capacity factors in a manner similar to that discussed earlier for the low-molecular-weight solutes was not possible. Alternatively, the "critical concentrations" of acetonitrile, *CC* (eqn. 1), of the peptides and proteins on each column were correlated with each other. The critical concentration corresponds to the volume fraction of organic modifier at the time of solute elution, and has been shown to be

TABLE IV

CORRECTED RETENTION TIMES AND CRITICAL CONCENTRATIONS FOR PROTEIN AND OCTAPEPTIDE STANDARDS

t' = Corrected retention time (min); *CC* = critical mobile phase concentration, as defined in the text.

Peptide	Column	t'	*CC*
Ribonuclease A	ODS	9.47	31.30
	PBDA	6.58	22.62
Cytochrome *c*	ODS	10.75	35.14
	PBDA	8.42	28.14
Lysozyme	ODS	11.88	38.53
	PBDA	9.52	31.45
Carbonic anhydrase	ODS	14.23	45.59
	PBDA	10.89	35.55
Ala-Pro-R	ODS	13.02	25.97
	PBDA	6.02	15.48
Leu-Pro-R	ODS	14.43	28.09
	PBDA	8.44	19.10
Ser-Pro-R	ODS	13.38	26.51
	PBDA	7.13	17.14
Lys-Ala-R	ODS	11.92	24.33
	PBDA	5.01	13.96
Lys-Arg-R	ODS	11.92	24.33
	PBDA	5.67	14.95
Lys-Asp-R	ODS	11.58	23.81
	PBDA	3.63	11.89
Lys-Leu-R	ODS	13.90	27.30
	PBDA	8.48	19.16
Lys-Ser-R	ODS	11.58	23.81
	PBDA	7.79	15.70

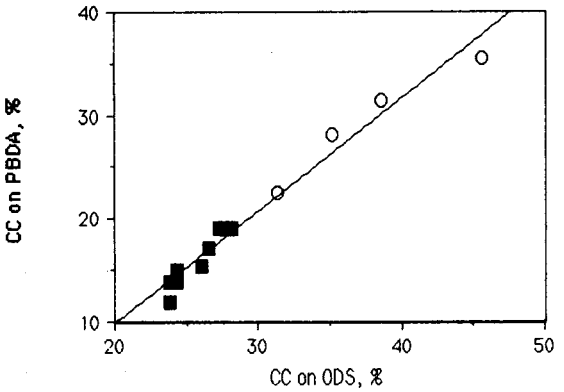

Fig. 7. Plot of critical acetonitrile concentrations of protein and octapeptide standards on PBDA column *vs.* their critical acetonitrile concentrations on the ODS column. ○ = Protein standards; ■ = octapeptide standards. Linear correlation coefficient for all data = 0.986.

roughly independent of column dimensions, gradient time, or stationary phase particle size for large molecules [19,22]. The critical concentration is thus a measure of the relative degree to which a protein or peptide is retained by the stationary phase; a lower critical concentration indicates a lower degree of protein retention.

CC values for the protein and peptide standards on the two columns are listed in Table IV. *CC* values for all solutes on the PBDA stationary phase are significantly lower than those on the ODS phase, indicating weaker protein and peptide hydrophobic interactions with PBDA. Nevertheless, the correlation between solute critical concentrations on the two columns, shown graphically in Fig. 7, is high ($R = 0.986$), indicating very similar retention mechanisms for peptides and proteins on both columns. Remarkably, the correlation between critical concentrations on the PBDA and ODS columns is identical for both peptides and proteins, as demonstrated by the excellent fit of the data for both sets of compounds on the same linear regression line (Fig. 7). Since solute size exclusion would be expected to have a greater effect on the proteins than the octapeptides, the absence of any significant difference in the CC correlations obtained for the proteins and octapeptides confirms the absence of size exclusion as a significant retention mechanism on either column.

CONCLUSIONS

In this study, the retention of peptides and proteins on the PBDA and ODS stationary phases is demonstrated to be predominantly controlled by the same hydrophobic interaction mechanisms which govern the retention of smaller molecules on these phases. Although the PBDA phase was shown to be somewhat less hydrophobic than ODS, the general selectivities of the two phases are quite similar toward compounds of all molecular weights. However, mass transfer resistance, peak broadening and irreversible solute adsorption is more dependent on solute size for the PBDA phase than it is for ODS, which results in low column efficiency for separations of proteins on PBDA columns. To at least some degree, this is attributable to

size-dependent interactions of solutes with the uniquely-shaped PBDA particles. On a practical basis, the results of this study indicate that the novel PBDA phase and other phases based upon similar fused microplatelet particles may be more effectively used for separations of lower-molecular-weight organic compounds and peptides than for separations of proteins and other large polymers.

ACKNOWLEDGEMENTS

This work was supported in part by grants from Biotage, Inc. (Charlottesville, VA, U.S.A.), the Florida Atlantic University Division of Sponsored Research, and the Florida High Technology and Industry Council. We thank Dr. Larry F. Wieserman (Alcoa Laboratories, Alcoa Center, PA, U.S.A.) for helpful discussions.

REFERENCES

1 D. P. Lee and J. H. Kindsvater, *Anal. Chem.*, 52 (1980) 2425.
2 A. Kurganov, O. Kuzmenko and V. Davankov, *J. Chromatogr.*, 261 (1983) 223.
3 V. V. Davankov, A. A. Kurganov and K. K. Unger, *J. Chromatogr.*, 500 (1990) 519.
4 U. Bien-Vogelsang, A. Deege, H. Figge, J. Kohler and G. Schomburg, *Chromatographia*, 19 (1984) 170.
5 J. R. Benson and D. J. Woo, *J. Chromatogr. Sci.*, 22 (1980) 386.
6 D. Lee, *J. Chromatogr.*, 443 (1988) 143.
7 W. G. Burton, K. D. Nugent, T. K. Slattery, B. R. Summers and L. R. Snyder, *J. Chromatogr.*, 443 (1988) 363.
8 M. W. Dong and D. Tran, *J. Chromatogr.*, 499 (1990) 125.
9 R. Kaliszan, R. W. Blain and R. A. Hartwick, *Chromatographia*, 25 (1988) 5.
10 R. Kaliszan, J. Petrusewicz, R. W. Blain and R. A. Hartwick, *J. Chromatogr.*, 458 (1988) 395.
11 J. E. Haky and S. Vemulapalli, *J. Liq. Chromatogr.*, 15 (1990) 3111.
12 L. F. Wieserman, R. R. Burr, K. Cross and F. J. Simpson, Jr., presented at the *39th Pittsburgh Conference on Analytical Chemistry and Applied Spectroscopy, New Orleans, LA, 1988*, paper 393.
13 R. B. Wilhelmy, presented at the *39th Pittsburgh Conference or Analytical Chemistry and Applied Spectroscopy, New Orleans, LA, 1988*, paper 390.
14 B. M. Dunn, B. Kammerman and K. R. McCurry, *Anal. Biochem.*, 138 (1984) 68.
15 B. M. Dunn, M. Jimenez, B. F. Parten, M. J. Valler, C. E. Rolph and J. Kay, *Biochem. J.*, 237 (1986) 899.
16 L. R. Snyder, J. L. Glajch and J. J. Kirkland, *Practical HPLC Method Development*, Wiley, New York, 1988, Ch. 2 and 3.
17 L. R. Snyder and J. J. Kirkland, *Introduction to Modern Liquid Chromatography*, Wiley, New York, 2nd ed., 1979, Ch. 2.
18 L. R. Snyder and J. W. Dolan, *LC·GC*, 8 (1990) 524.
19 J. D. Pearson, N. T. Lin and F. E. Regnier, *Anal. Biochem.*, 124 (1982) 217.
20 A. J. Banes, G. W. Link and L. R. Snyder, *J. Chromatogr.*, 326 (1985) 419.
21 J. Pohl and B. M. Dunn, *Biochemistry*, 27 (1988) 4827.
22 L. R. Snyder, M. A. Stadalius and M. A. Quarry, *Anal. Chem.*, 55 (1983) 1412A.
23 R. Stevenson, *Am. Biotech. Lab.*, Feb. (1990) 6.
24 J. E. Haky and S. Vemulapalli, *J. Chromatogr.*, 505 (1990) 307.

Journal of Chromatography, 541 (1991) 317–331
Elsevier Science Publishers B.V., Amsterdam

CHROM. 22 981

Comparison of the isolation of adducts of 2′-deoxycytidine and 2′-deoxyguanosine with phenylglycidyl ether by high-performance liquid chromatography on a reversed-phase column and a polystyrene–divinylbenzene column

E. VAN DEN EECKHOUT* and J. COENE
College of Pharmacy, University of Ghent, Harelbekestraat 72, B-9000 Ghent (Belgium)
J. CLAEREBOUDT
Department of Pharmacy, University of Antwerp (U.I.A.), Universiteitsplein 1, B-2610 Wilrijk (Belgium)
F. BORREMANS
Laboratory for Organic Chemistry, University of Ghent, Krijgslaan 281, B-9000 Ghent (Belgium)
M. CLAEYS
Department of Pharmacy, University of Antwerp (U.I.A.), Universiteitsplein 1, B-2610 Wilrijk (Belgium)
E. ESMANS
Laboratory for Organic Chemistry, University of Antwerp (R.U.C.A.), Groenenborgerlaan 171, B-2020 Antwerp (Belgium)
and
J. E. SINSHEIMER
College of Pharmacy, University of Michigan, Ann Arbor, MI 48109 (U.S.A.)
(First received May 14th, 1990; revised manuscript received October 23rd, 1990)

ABSTRACT

2′-Deoxycitidine (dCyd) and 2′-deoxyguanosine (dGuo) were subjected to reaction with phenylglycidyl ether (PGE) in methanol in order to study the formation of the corresponding 2′-deoxynucleoside adducts. Separation methods were developed on analytical and semi-preparative scales using high-performance liquid chromatography with photodiode-array detection on a reversed-phase column and on a polystyrene–divinylbenzene column. The use of the latter column was prompted by decomposition of the preparatively isolated dGuo–PGE adducts on the reversed-phase column. The use of a polystyrene–divinylbenzene column solved this problem and also revealed the presence of one more peak in both the dCyd– and dGuo–PGE reaction mixtures.

The adducts of dCyd and dGuo were isolated on preparative reversed-phase and polystyrene–divinylbenzene columns and characterized by UV, fast atom bombardment mass and 360 MHz ^{1}H NMR spectrometry. The adducts of dCyd were the diastereomers of N-3-(2-hydroxy-3-phenoxypropyl)-2′-deoxycytidine and N^4-(2-hydroxy-3-phenoxypropyl)-2′-deoxycytidine whereas those of dGuo were the two diastereomers of N-7-(2-hydroxy-3-phenoxypropyl)-2′-deoxyguanosine and a third peak which appeared to be mainly N^2-(2-hydroxy-3-phenoxypropyl)-2′-deoxyguanosine.

0021-9673/91/$03.50

INTRODUCTION

Aliphatic epoxides are important as commercial, industrial and laboratory chemicals; examples are styrene oxide, propylene oxide and gycidyl ethers. The U.S. National Institute of Occupational Safety and Health [1] surveyed the extent of occupational contact and potential damage from the glycidyl ether group of epoxides and established threshold limits for human exposure. Occupational and environmental vulnerability to aliphatic epoxides and *in vivo* production of epoxides and their toxicity have been reviewed by Manson [2] and Ehrenberg and Hussain [3].

It is generally believed that reactions of electrophilic reactants with sites in DNA or RNA are fundamental to the induction of mutations. Our continuing interest in the structure–mutagenicity relationship for aliphatic epoxides [4–10] and in the reactivity of these epoxides with 2′-deoxynucleosides and DNA [11–13] prompted us to extend the limited literature [14–16] on the reactivity and identification of adduct formation between phenyl glycidyl ether (PGE) and 2′-deoxynucleosides. In a recent paper, we reported on the separation and structure elucidation of the nucleoside adducts of 2′-deoxyadenosine and thymidine with PGE [17]. As an extension of that work, the adduct formation of 2′-deoxycytidine and 2′-deoxyguanosine with PGE was studied.

Chromatographic separations of purine and pyrimidine derivatives have been widely reported [18]. In general, the reversed-phase mode is used for the separation and analysis of nucleosides and bases. This mode was also used in our recent work [17] on 2-deoxyadenosine– and thymidine–PGE adducts with success. However, when a reversed-phase system was used for the preparative separation of the 2′-deoxyguanosine–PGE reaction mixtures, problems with decomposition of adducts were encountered. This phenomenon led to the use of a polystyrene–divinylbenzene column, as this type of column is well suited for the analysis of quaternary ammonium compounds [19], nucleic acids and their derivatives [20–27]. In this paper we report a comparison of the results obtained for the preparative isolation and identification of 2′-deoxycytidine–PGE and 2′-deoxyguanosine–PGE reaction mixtures on a reversed-phase column and a polystyrene–divinylbenzene column. The latter column proved to be superior for this analysis and led to the detection and identification of adducts not detected on the reversed-phase column. On-line identification during high-performance liquid chromatographic (HPLC) analysis was effected by means of a photodiode-array detector. The main adducts isolated were characterized by means of mass spectrometry and nuclear magnetic resonance (NMR) spectroscopy.

EXPERIMENTAL

Materials

All solvents were of analytical-reagent grade. 2,3-Epoxypropyl phenyl ether (phenyl glycidyl ether, PGE) was obtained from Janssen Chimica (Beerse, Belgium) and was distilled *in vacuo* before use. 2′-Deoxycytidine and 2′-deoxyguanosine were purchased from Sigma (St. Louis, MO, U.S.A.). Ammonium formate was obtained from BDH (Poole, U.K.).

Reaction of 2′-deoxynucleosides with phenyl glycidyl ether

2′-Deoxycytidine (10 mg) and 2′-deoxyguanosine (10 mg) were dissolved in 3 ml

of methanol, then 1 ml of 1 *M* PGE in methanol was added. The compounds were allowed to react for 24 h at 37°C in tightly sealed test-tubes equipped with a Teflon-lined screw-cap. For preparative purposes, 100 mg of 2′-deoxynucleoside in methanol were used.

Chromatography

The HPLC system was equipped with a Waters M-45 pump. Detection was effected with a Hewlett-Packard Model 1040A photodiode-array detector equipped with a Hewlett-Packard Model 8290M flexible disk drive and a Hewlett-Packard Model 85 computer. Analytical reversed-phase chromatography for the 2′-deoxycytidine–PGE and 2′-deoxyguanosine–PGE reaction mixtures was performed on a 10 RP-18 column (25 cm × 4.6 mm I.D.) (Alltech). The eluent composition for the 2′-deoxycytidine–PGE and 2′-deoxyguanosine–PGE mixtures was 0.01 *M* ammonium formate (pH 5.1)–methanol (80:20) at a flow-rate of 2.0 ml/min. Injection was with a six-way Valco valve with a 20-μl loop. The detection wavelength was 260 nm.

Preparative chromatography was carried out on a reversed-phase 10 RP-18 (Alltech) column (25 cm × 2.2 cm I.D.) and on a polystyrene–divinylbenzene PRP-1 (Hamilton) column (30.5 cm × 7.0 mm I.D.). Injection was with a six-way Valco valve with a 100-μl loop. The detection wavelength was 260 nm.

The solvent for reversed-phase chromatography for the 2′-deoxycytidine–PGE mixture was 0.01 *M* ammonium formate (pH 5.1)–methanol (80:20) at a flow-rate of 7.0 ml/min and that for the 2′-deoxyguanosine–PGE mixture was 0.01 *M* ammonium formate (pH 5.1)–methanol (70:30) at 7.0 ml/min. With the polystyrene–divinylbenzene column, two different solvent systems were used for each reaction mixture: for the 2′-deoxycytidine–PGE mixture, 0.01 *M* ammonium formate (pH 4.25)–methanol (60:40) and (50:50) at 1.6 ml/min and for the 2′-deoxyguanosine–PGE mixture 0.01 *M* ammonium formate (pH 4.25)–methanol (60:40) at 1.6 ml/min and (30:70) at 2.0 ml/min.

NMR spectroscopy

^{1}H NMR spectra were recorded at 500.13 MHz on a Bruker AM spectrometer using 0.01 *M* solutions in [$^2H_6$]dimethyl sulphoxide (DMSO-d_6) at room temperature. No precautions were taken to exclude moisture from the samples. Therefore, the readily exchangable NH and OH protons were not observed. Chemical shifts are quoted in ppm downfield relative to TMS internal standard – DMSO-d_5 signal at 2.500 ppm. Unequivocal assignments of the NMR resonances to the specific protons were obtained from standard two-dimensional proton–proton *J* correlation spectra.

Mass spectrometry

All analyses were performed on a VG 70-SEQ hybrid mass spectrometer (VG Analytical, Manchester, U.K.), equipped with an Ion Tech saddle field atom gun. The instrument consists of a high-resolution double-focusing mass spectrometer with EB configuration (MS-I), followed by an RF-only quadrupole collision gas cell and a high-performance quadrupole mass analyser (MS-II). Xenon atoms with energies of *ca.* 8 keV and a discharge current of 1 mA were used as the ionizing beam. Positive- and negative-ion fast atom bombardment (FAB) mass spectra were recorded under control of the VG 11-250 J data system by repetitive scanning of MS-I over the range 20–600 u,

using a scan time of 2 s per decade. Daughter ion (MS–MS) spectra were obtained by collisionally activated decomposition (CAD) in the RF-only quadrupole gas cell, using argon as collision gas, and by scanning MS-II.

Ultraviolet spectroscopy

UV spectra were recorded on-line during HPLC analysis in the HPLC solvent system used with the photodiode-array detector.

UV spectra from samples isolated preparatively were taken off-line on a Perkin-Elmer Lambda 15 UV–VIS spectrophotometer equipped with a Perkin-Elmer EX-800 printer.

Dried samples were diluted in water to obtain absorbance values between 0.5 and 1.0. UV spectra were recorded at acidic pH by mixing the aqueous samples with an equal volume of 0.1 *M* hydrochloric acid or at alkaline pH by mixing with an equal volume of 0.1 *M* sodium hydroxide solution.

RESULTS AND DISCUSSION

2′-Deoxycytidine and 2′-deoxyguanosine were subjected to reaction with PGE in methanol. After 24 h at 37°C, the resulting reaction mixtures were analysed using reversed-phase HPLC with photodiode-array detection. The analytical HPLC method was used to develop separations on a preparative scale. However, for the 2′-deoxyguanosine–PGE mixture, problems of decomposition with this system were encountered. Therefore, a second HPLC system on a polystyrene–divinylbenzene column was used for the preparative isolation of adducts of both the 2′-deoxyguanosine–PGE and 2′-deoxycytidine–PGE mixtures.

Analytical reversed-phase HPLC of 2′-deoxycytidine–PGE and 2′-deoxyguanosine–PGE with photodiode-array detection

In a recent paper [17], we described analytical HPLC with photodiode-array detection for thymidine– and 2′-deoxyadenosine–PGE mixtures as a powerful tool for the structure elucidation of alkylated nucleosides. As an extension of this work, similar eluents, namely 0.01 *M* ammonium formate (pH 5.1)–methanol mixtures on a reversed-phase 10 RP-18 column were used. For both the 2′-deoxycytidine–PGE and 2′-deoxyguanosine–PGE mixtures, two main adduct peaks (as characterized by their UV spectra) were observed at $k' = 18.4$ ($t_R = 19.4$ min) and 25.30 ($t_R = 26.6$ min) for deoxycytidine–PGE and at $k' = 16.1$ ($t_R = 17.1$ min) and 21.01 ($t_R = 22.1$ min) for deoxyguanosine–PGE (Fig. 1), and were labelled dGuo 1′, dGuo 2′, dCyd 1 and dCyd 2.

UV spectra taken on-line were identical for the peaks dGuo 1′ and dGuo 2′, and also for the peaks dCyd 1 and dCyd 2, suggesting that dGuo 1′ and dGuo 2′ and also dCyd 1 and dCyd 2 are both pairs of isomers. The analytical HPLC was then adapted to a preparative scale in order to obtain off-line UV data at different pH values and mass spectral and NMR data.

Preparative reversed-phase HPLC of 2′-deoxycytidine–PGE and 2′-deoxyguanosine–PGE reaction mixtures with photodiode-array detection

Preparative HPLC of 2′-deoxycytidine–PGE and 2′-deoxyguanosine–PGE on

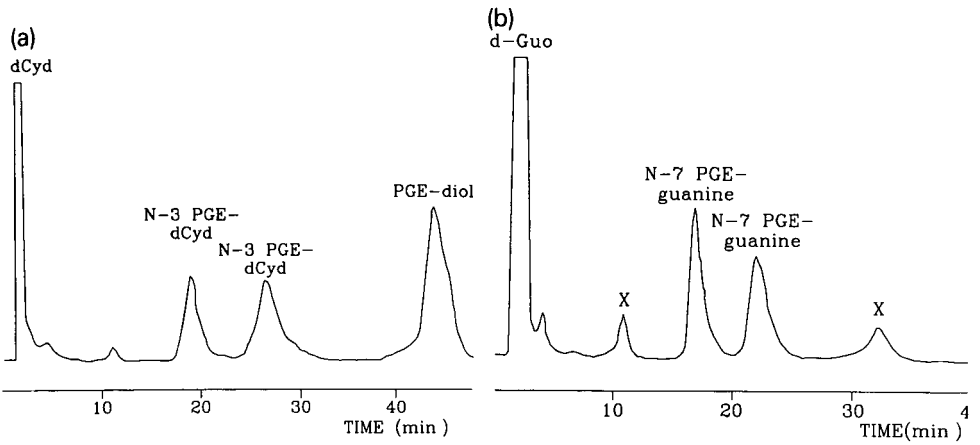

Fig. 1. Analytical reversed-phase HPLC of (a) dCyd–PGE and (b) dGuo–PGE reaction mixtures. Column, 10 RP-18 (25 cm × 4.6 mm I.D.); eluent, 0.01 *M* ammonium formate (pH 5.1)–methanol (80:20) at 2.0 ml/min. Concentration of sample: ±3 mg/ml; 0.1 a.u.f.s.

a reversed-phase RP-18 column gave similar results to the analytical HPLC. Two main adducts were isolated for both reaction mixtures at $k' = 2.7$ ($t_R = 29.0$ min) and 3.7 ($t_R = 35.5$ min) for 2′-deoxycytidine and at $k' = 2.7$ ($t_R = 29.0$ min) and 3.6 ($t_R = 36.5$ min) for 2′-deoxyguanosine.

After freeze-drying, all the adduct samples of 2′-deoxycytidine and 2′-deoxyguanosine were subjected to UV analysis off-line at different pH values in order to obtain an indication of the alkylation site. The UV data obtained off-line are given in Table I.

In previous UV studies [10–12,17] we have shown that UV spectra taken at different pH values give a strong indication of the site of alkylation of nucleosides by epoxides. The conclusions drawn from the UV studies are based on maximum wavelengths obtained for the different adduct fractions, on shifts in acidic or alkaline medium and on absorbance ratios obtained at 254 and 280 nm.

TABLE I

UV PEAK MAXIMA AND 254/280 nm ABSORBANCE RATIOS FOR PEAKS FROM DEOXYCYTIDINE–PGE AND DEOXYGUANOSINE–PGE REACTION MIXTURES

Peak	λ_{max} (nm) (ratio)		
	0.1 *M* HCl	H_2O	0.1 *M* NaOH
dCyd	279.0 (0.30)	270.4 (1.00)	270.8 (0.93)
dCyd 1	276.5 (0.40)	276.4 (0.40)	268.7 (1.05)
dCyd 2	276.5 (0.40)	276.4 (0.40)	268.7 (1.05)
dCyd 3	276.0 (0.45)	269.7 (0.93)	269.8 (0.93)
dGuo	254.5 (1.56)	252.4 (1.68)	265.6 (2.0)
dGuo 1′ (1)	257.1 (1.50)	259.0 (1.31)	266.6 (1.67)
dGuo 2′ (2)	257.1 (1.50)	259.0 (1.31)	266.6 (1.67)
dGuo 3	261.5 (1.30)	257.6 (1.55)	259.1 (1.67)

TABLE II

CAPACITY FACTORS (k'), UV PEAK MAXIMA AND 254/280 nm ABSORBANCE RATIOS AFTER PREPARATIVE HPLC OF 2'-DEOXYGUANOSINE- AND 2'-DEOXYCYTIDINE–PGE REACTION MIXTURES ON A POLYSTYRENE–DIVINYLBENZENE COLUMN

Peak	k'			λ_{max}[d]	Ratio (254/280 nm)
	A[a]	B[b]	C[c]		
dGuo	0.21			254	1.5
dGuo 1	1.04	2.37		260	1.4
dGuo 2	1.04	3.00		260	1.5
dGuo 3	8.23			258	1.6
dCyd	0.12		0.10	272	1.0
dCyd 1	1.05	2.87	0.65	278	0.4
dCyd 2	1.32	3.50	0.65	278	0.4
dCyd 3	2.87		1.35	272	0.9

[a] Solvent system: 0.01 *M* ammonium formate (pH 4.25)–methanol (50:50) at 1.6 ml/min.
[b] Solvent system: 0.01 *M* ammonium formate (pH 4.25)–methanol (60:40) at 1.8 ml/min.
[c] Solvent system: 0.01 *M* ammonium formate (pH 4.25)–methanol (40:60) at 1.6 ml/min.
[d] Wavelengths of maximum absorbances taken in the solvent system that separated the PGE adducts of 2'-deoxyguanosine and 2'-deoxycytidine.

For the two 2'-deoxycytidine adducts dCyd 1 and dCyd 2,N-3 alkylation was suggested. This hypothesis is based on Singer's research [28] in which 3-ethylcytidine displayed a λ_{max} in water of 279 and a 254/280 nm ratio of 0.40, compared with a similar λ_{max} and the same 254/280 nm ratios for both 2'-deoxycytidine adducts (Tables I and II). The lack of shift in 0.1 *M* hydrochloric acid for both dCyd 1 and dCyd 2 adducts is a further indication of N-3 alkylation. The UV spectra of dGuo 1' and dGuo 2' are very similar to that of 7-alkylated 2'-deoxyguanosine published by Singer [28]. Further, the shifts in acidic and alkaline media are very similar to those for the 7-alkyl products produced by propylene oxide, glycidol and epichlorohydrin with 2'-deoxyguanosine reported by Hemminki *et al.* [29]. An irreversible change in the spectra, whereby the maximum wavelength shifts from 259 to 266 nm, is also consistent with a 7-alkyl group. These UV assignments were then confirmed by FAB-MS and/or NMR.

Preparative HPLC of 2'-deoxycytidine–PGE and 2'-deoxyguanosine–PGE mixtures on a polystyrene–divinylbenzene column

Table II summarizes the results obtained for the preparative isolation of the deoxyguanosine- and deoxycytidine–PGE mixtures on a preparative PRP-1 column. For each reaction mixture, an additional adduct is detected, labelled dCyd 3 and dGuo 3, eluting much later than the adducts dCyd 1, dCyd 2, dGuo 1' and dGuo 2' previously detected on the reversed-phase column.

The deoxyguanosine adduct fractions on the reversed-phase column, dGuo 1' and dGuo 2', are labelled differently to those detected on the PRP-1 column, dGuo 1 and dGuo 2, as the mass spectral data which follow show that the former adducts have lost their sugar moiety, and are different from dGuo 1 and dGuo 2. For the preparative

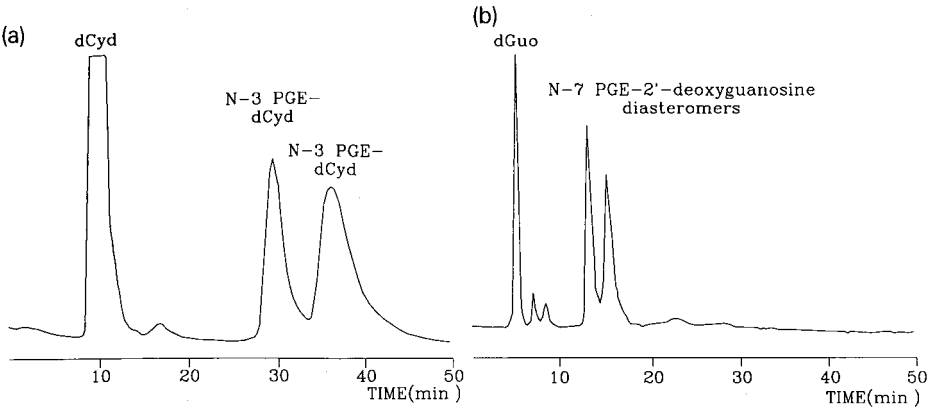

Fig. 2. Preparative HPLC on a polystyrene–divinylbenzene column of diastereomers of (a) N-3 alkylated 2′-deoxycytidine and (b) N-7 alkylated 2′-deoxyguanosine. Column, PRP-1 (30.5 cm × 7.0 mm I.D.); eluent, 0.01 *M* ammonium formate (pH 4.25)–methanol (60:40) at 1.6 ml/min. Concentration of sample: ±30 mg/ml; 0.1. a.u.f.s.

isolation of dGuo 3 and dCyd 3, a less polar solvent system in the range of 0.01 *M* ammonium formate (pH 4.25)–methanol (50:50) to (30:70) was used (Fig. 4). As expected, the diastereomers dCyd 1 and dCyd 2, dGuo 1 and dGuo 2 were not separated in this solvent system. A more polar solvent system had to be used, namely 0.01 *M* ammonium formate (pH 4.25)–methanol (60:40) (Fig. 2).

UV spectroscopy. All the adduct fractions were preparatively isolated, freeze-dried and UV spectra were taken off-line in water; 0.1 *M* hydrochloric acid and 0.1 *M*

TABLE III

MAJOR IONS OBSERVED IN THE POSITIVE- AND NEGATIVE-ION FAB MASS SPECTRA OF NUCLEOSIDE PGE ADDUCTS

Reaction mixture	HPLC column	Analysed fraction	Positive ions[a,b]		Negative ions[a,b]	
			$(M + H)^+$	Other	$(M - H)^-$	Other
PGE–2′-deoxycytidine	RP-18	dCyd 1	*m/z* 378		*m/z* 376	
		dCyd 2	*m/z* 378		*m/z* 376	
PGE–2′-deoxycytidine	PRP-1	dCyd 1	*m/z* 378		*m/z* 376	
		dCyd 2	*m/z* 378		*m/z* 376	
		dCyd 3	*m/z* 378		*m/z* 376	
PGE–2′-deoxyguanosine	RP-18	dGuo 1′	ND[c]	*m/z* 302	ND	*m/z* 300
		dGuo 2′	ND	*m/z* 302	ND	*m/z* 300
PGE–2′-deoxyguanosine	PRP-1	dGuo 1	*m/z* 418		*m/z* 416	
		dGuo 2	*m/z* 418		*m/z* 416	
		dGuo 3	*m/z* 418	*m/z* 568, *m/z* 586	*m/z* 416	*m/z* 566, *m/z* 584

[a] Fragment ions not listed because of possible interferences with matrix signals.
[b] The $(M + H)^+$ and $(M - H)^-$ ions are related to the monoalkylated nucleoside.
[c] ND = not detected, *i.e.*, negligible intensity (signal-to-noise ratio < 3).

TABLE IV

MASS NUMBERS AND RELATIVE INTENSITIES OF DAUGHTER IONS IN THE FAB-MS–CAD-MS OF THE NUCLEOSIDE–PGE ADDUCT $(M + H)^+$ IONS[a,b,c]

Compound	$(M + H)^+$	RBH_2^+	$(RBH_2 - C_6H_5OH)^+$	BH_2^+	R^+	S^+	Others
dCyd 1	378 (P)	262 (100)	168 (10)	112 (53)	151 (4)	117 (9)	244 (2); 150 (9); 133 (7); 125 (3); 107 (5); 105 (6); 99 (5); 95 (3); 73 (4); 71 (2)
dCyd 2	378 (P)	262 (100)	168 (11)	112 (51)	151 (3)	117 (9)	244 (3); 150 (8); 133 (8); 125 (4); 107 (5); 105 (7); 99 (6); 95 (2); 77 (2); 73 (4); 71 (2)
dCyd 3	378 (P)	262 (100)	168 (21)	112 (3)	151 (2)	117 (13)	244 (2); 152 (2); 150 (10); 133 (4); 125 (8); 124 (10); 107 (5); 105 (3); 99 (6); 73 (4); 71 (2)
dGuo 1	418 (P)	302 (100)	208 (19)	152 (64)	–	117 (48)	191 (3); 190 (6); 178 (2); 165 (7); 164 (4); 135 (13); 133 (15); 121 (2); 110 (3); 107 (8); 105 (13); 99 (21); 79 (2); 77 (2); 73 (11); 71 (6); 69 (4)
dGuo 2	418 (P)	302 (100)	208 (19)	152 (58)	–	117 (49)	191 (4); 190 (8); 178 (2); 165 (6); 164 (4); 135 (11); 133 (14); 110 (3); 107 (8); 105 (14); 99 (18); 95 (2); 81 (2); 79 (2); 77 (2); 73 (11); 71 (5); 69 (3)
dGuo 3	418 (P)	302 (100)	208 (28)	152 (57)	151 (1)	117 (54)	284 (2); 191 (4); 190 (11); 165 (5); 164 (5); 135 (17); 133 (17); 121 (2); 110 (3); 107 (9); 105 (16); 99 (18); 79 (2); 77 (2); 73 (13); 71 (6); 69 (2)

[a] The CAD mass spectra of the $(M + H)^+$ ions were recorded at a collision energy of 80 eV, using argon as the collision gas at a pressure of 2 mTorr (in the collision cell).

[b] The $(M + H)^+$ ions are related to the monoalkylated nucleoside.

[c] Nomenclature: M corresponds to RBS, where B = base moiety, S = sugar moiety and R = 2-hydroxy-3-phenoxypropyl substituent.

sodium hydroxide (Table I). The UV spectra for dCyd 1 and dCyd 2 were the same for the reversed-phase column and the polystyrene–divinylbenzene column, and have been discussed in the previous section. Also the UV spectra of the intact alkylated nucleosides dGuo 1 and dGuo 2 were the same as those for dGuo 1′ and dGuo 2′. It is known that the UV characteristics of deoxy bases are not influenced by the presence of their sugar moiety [30].

On the basis of the UV characteristics for dCyd 3, alkylation at O-2 could be excluded, since the peak maxima for O-2 alkylation are 262 or 263 nm for propylene oxide, trichloropropylene oxide, epichlorohydrin and glycidol-2′-deoxycytidine derivatives [11] and for ethylcytidine [28] and the 254/280 nm ratio for all the derivatives was 2.3. N^4-Ethylcytidine has λ_{max} of 272 nm (water) and 281 nm (pH 1) and a 254/280 nm ratio of 0.9. Our isolated material dCyd 3 has a λ_{max} of 272 nm (water) and a 254/280 nm ratio of 0.9. Further, the dCyd 3 adduct shows a shift towards longer wavelength in acidic medium, which is consistent with substitution on an amino group in a pyrimidine ring [30]. In contrast to dCyd 1 and dCyd 2, there is no shift in alkaline medium, which also points to alkylation on the exocyclic nitrogen. Thus, N-4 alkylation was suggested for dCyd 3.

On the basis of UV characteristics for dGuo 3, alkylation at O-6 could be ruled out, as neither the peak maxima in acidic medium nor the shape of the UV curve coincide with that of O^6-methyldeoxyguanosine [28]. Alkylation at N-2 is suggested by comparison of the UV spectra in acidic and alkaline media with N^2-methylguanosine [28]. Further, substitution of 2-aminopyridine by one or two methyl groups results in a small shift towards longer wavelengths [31], which is seen in the neutral and acidic UV spectra of dGuo 3 as compared with the unsubstituted dGuo. The HPLC behaviour of this compound is also consistent with N-2 alkylation as we also found an increase in apolarity for the N-4 alkylated material of 2′-deoxycytidine.

Mass spectra and NMR. A detailed discussion of the mass spectra will be published elsewhere [32]. The FAB mass spectra of dCyd 1 and dCyd 2 isolated on reversed-phase and polystyrene–divinylbenzene columns were identical. They yield intense peaks at *m/z* 378 in the positive-ion mode and at *m/z* 376 in the negative-ion mode (Table III). These ions can be assigned to the $(M + H)^+$ and $(M - H)^-$ ions of the monoalkylated adduct. Definite structural information as to the alkylation site is obtained by the FAB-MS–CAD-MS technique [33,34]. With this technique an ion of interest is selected by MS-I, induced to fragment by collisionally activated decomposition and a spectrum of the daughter ions is taken by MS-II. The FAB-MS–CAD-MS data for the $(M + H)^+$ and $(M - H)^-$ ions of the monoalkylated nucleosides are given in Tables IV and V. N-3 alkylation for dCyd 1 and dCyd 2 is confirmed by the daughter ion spectrum of the $(M - H)^-$ ion of the monoalkylated adducts (Fig. 3a and Table V).

Diagnostic fragment ions correspond to the RB^- ion (monoalkylated base) at *m/z* 260, $(RB - HNCO)^-$ at *m/z* 217, $(RB - phenol)^-$ at *m/z* 166 and phenolate anion at *m/z* 93. The fragment ion at *m/z* 183 originates from a retro-Diels–Alder rearrangement in the pyrimidine ring, with retention of the negative charge on the diene part of the molecule.

For dCyd 3, some differences are observed in the daughter ion spectra of the $(M - H)^-$ ions (*m/z* 376) in comparison with dCyd 1 (Fig. 3). The major fragment ion in the spectrum of dCyd 1 is detected at *m/z* 183, which is consistent with alkylation at

the N-3 position. The detection of the isocyanate anion at *m/z* 42 and the fragment ion at *m/z* 243 in the daughter ion spectrum of dCyd 3 indicates that the alkylation site for the adduct in dCyd 3 is not N-3, but N-4, as suggested by the UV data.

The positive-ion FAB mass spectra of the fractions dGuo 1′ and dGuo 2′, isolated from the 2′-deoxyguanosine–PGE reaction mixture on the reversed-phase column, were both characterized by an ion at *m/z* 302. This ion can be assigned either to the RBH_2 fragment ion or the $(M + H)^+$ ion of monoalkylated guanine. Constant neutral loss scanning of 116 u, which is a very useful method for the identification of the $(M + H)^+$ ions of modified deoxynucleosides, gives negative results for fractions dGuo 1′ and dGuo 2′. Therefore, the ions at *m/z* 302 must be attributed to the $(M + H)^+$ ions of monoalkylated guanine. This alkylated nucleobase is probably formed by depurination of the alkylated nucleoside on the RP-18 column. No differences are observed between the daughter ion spectra obtained for the ions at *m/z* 302 in the adduct samples dGuo 1′ and dGuo 2′. This indicates that the two isolated adducts are diastereomers; the alkylation site could not be determined from these MS data, but 7-alkylation was strongly suggested by the UV data.

The FAB MS data for the three adduct samples of 2′-deoxyguanosine (dGuo 1, dGuo 2 and dGuo 3), isolated on the polystyrene–divinylbenzene column (Table III), show high signal intensities for the $(M + H)^+$ ions at *m/z* 418 in the positive-ion mode and $(M - H)^-$ ions at *m/z* 416 in the negative-ion mode, indicating the presence of intact monoalkylated adducts in each of the fractions. The presence of ions at *m/z* 568 and 586 for dGuo 3 in the positive-ion FAB mass spectrum indicates the presence of two additional compounds in this fraction, namely the dialkylated adduct (MW 567) and its imidazole ring-opened derivative (MW 585). The alkylation site could not be assigned unequivocally from these MS data. The structures suggested by the UV spectra were confirmed by NMR.

TABLE V

MASS NUMBERS AND RELATIVE INTENSITIES OF DAUGHTER IONS IN THE FAB-MS–CAD-MS OF THE NUCLEOSIDE–PGE ADDUCT $(M - H)^-$ IONS[a,b,c]

Compound	$(M - H)^-$	$[(M - H) - C_3H_6O_3]^-$	$[(M - H) - C_6H_5OH]^-$	RB^-	$[(M - H) - C_6H_5OH - C_3H_6O_3]^-$
dCyd 1	376 (P)	–	–	260 (8)	192 (1)
dCyd 2	376 (P)	–	–	260 (9)	192 (1)
dCyd 3	376 (P)	286 (3)	282 (2)	260 (4)	192 (4)
dGuo 1	416 (P)	326 (12)	322 (42)	300 (9)	232 (18)
dGuo 2	416 (P)	326 (14)	322 (50)	300 (8)	232 (22)
dGuo 3	416 (P)	–	322 (62)	300 (4)	232 (14)

[a] The CAD mass spectra of the $(M - H)^-$ ions were recorded at a collision energy of 70 eV, using argon as the collision gas at a pessure of 2 mTorr (in the collision cell).

[b] The $(M - H)^-$ ions are related to the monoalkylated nucleoside.

[c] Nomenclature: M corresponds to RBS, where B = base moiety, S = sugar moiety and R = 2-hydroxy-3-phenoxypropyl substituent.

For the dCyd–PGE adducts isolated, namely dCyd 1, dCyd 2 and dCyd 3, the following NMR data were obtained [^{1}H NMR in DMSO-d_6; shifts in ppm (J in Hz)]:

dCyd 1: H-1′, 6.124 (6.8, 6.8); H-2′ and H-2″, isochronous, 2.003 (apparent couplings 4.6 and 8.0); H-3′, 4.202 (2.9, 4.5, 4.5); H-4′, 3.730 (2.8, 3.9, 3.9); H-5′, 3.532 and 3.510 (3.9, 3.9, −11.9); H-5, 5.854 (8.1); H-6, 7.340 (8.1), aromatic protons 7.263 (7.4, 8.6) *meta*, 6.910 (7.4) *para*, 6.861 (8.6) *ortho*; $CH_2(\alpha)$–$CH(\beta)$, 4.04–4.18 (ABC multiplet); $CH_2(\gamma)$ 3.88 (−10.5).

dCyd 2: H-1′, 6.116 (6.8, 6.8); H-2′ and H-2″, isochronous, 1.981 (apparent couplings 4.8, 6.7); H-3′, 4.198 (2.4, 4.7, 4.7); H-4′, 3.733 (2.4, 4.0, 4.0); H-5′, 3.532 and 3.510 (4.0, 4.0, −11.9); H-5, 5.880 (7.9); H-6, 7.376 (7.9), aromatic protons 7.26 (7.5, 8.4) *meta*, 6.906 (7.3) *para*, 6.854 *ortho*; $CH_2(\alpha)$–$CH(\beta)$, 4.031–4.180 (ABC multiplet); $CH_2(\gamma)$, 3.88 (−10.3).

dCyd 3: H-1′, 6.151 (6.0, 7.2); H-2′ and H-2″, 1.922 (6.2, 7.2, −13.1) and 2.090 (3.4, 5.9, −13.1); H-3′, 4.197 (6.0, 3.4, 3.0); H-4′, 3.750 (3.0, 4.0, 4.0); H-5′, 5.860 (7.5); H-6, 7.755 (7.5); NH-4, 7.972 (5.0, 5.0), aromatic protons, 7.278 *meta*, 6.92 *ortho* and *para*; $CH_2(\alpha)$, 3.316 and 3.480 (5, 6, −12.0); $CH(\beta)$, 3.974 (4 × 5.5); $CH_2(\gamma)$, 3.895 (6.6, −9.9) and 3.922 (4.3, −9.9).

The quasi-identical chemical shifts and couplings observed for dCyd 1 and dCyd 2 [especially the similarity in the $CH_2(\alpha)$–$CH(\beta)$–$CH_2(\gamma)$ alkyl fragment] strongly suggest their diastereomeric relationship. Monoalkylation could be deduced from these NMR data, but the alkylation site was proposed on the basis of UV and mass spectra data.

In dCyd 3, the presence of an NH proton and its J correlation to a CH_2 group is consistent with alkylation at N-4 and with the least substituted epoxide carbon atom of the PGE part of the molecule (Fig. 5).

For dGuo 3, the following NMR data were obtained: H-1′, 6.134 (7.7, 6.2); H-2′ under DMSO solvent peak 2, 5; H-2″, 2.198 (13.1, 5.8, 3.0); H-3′, 4.347 (5.6, 2.8, 2.8); H-4′, 3.814 (2.6, 4.8, 4.8); H-5′, 3.560 (11.6, 4.8); H-5″, 3.496 (11.6, 4.6); H-8, 7.94,

$(RB^- - C_6H_5OH)^-$	$C_6H_5O^-$	Others
166 (4)	93 (62)	217 (5); 183 (100); 135 (7); 123 (2)
166 (3)	93 (64)	217 (5); 183 (100); 135 (8); 123 (2)
166 (40)	93 (100)	285 (3); 243 (54); 42 (4)
206 (100)	93 (45)	265 (4); 188 (6); 176 (6); 173 (3); 164 (6); 162 (5); 150 (3); 133 (7); 89 (3)
206 (100)	93 (46)	304 (3); 265 (4); 188 (5); 176 (5); 174 (3); 164 (6); 150 (4); 133 (10); 89 (3)
206 (100)	93 (47)	188 (4); 176 (3); 164 (4); 150 (2); 133 (8); 89 (2)

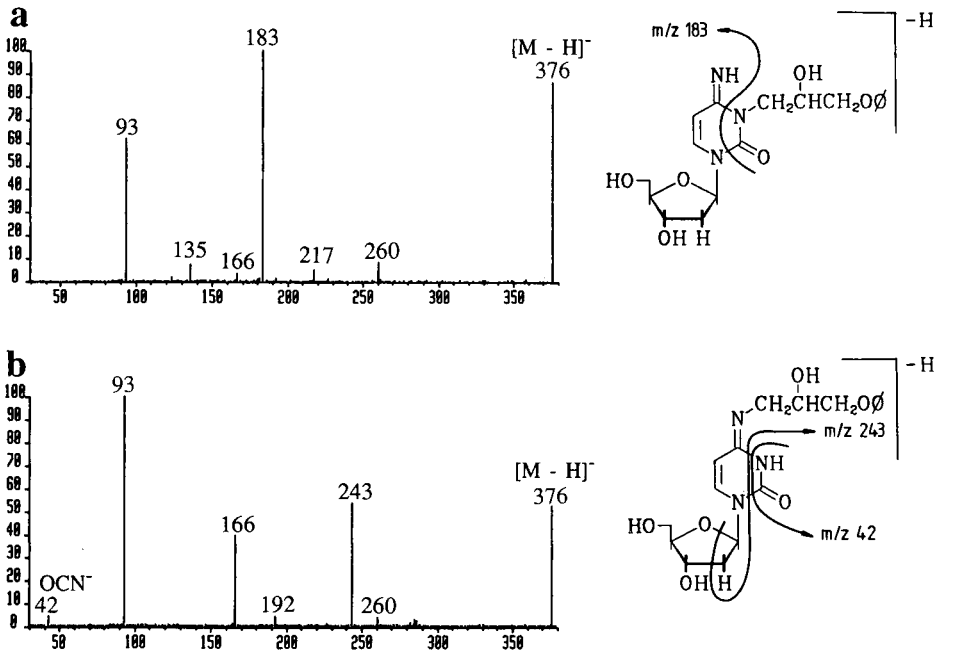

Fig. 3. Daughter ion spectra of the $(M - H)^-$ ions (*m/z* 376) of (a) N-3 alkylated 2′-deoxycytidine (dCyd 1 and dCyd 2) and (b) N-4 alkylated 2′-deoxycytidine (dCyd 3), obtained by CAD at E_{coll} = 70 eV and argon gas pressure = 2 mTorr.

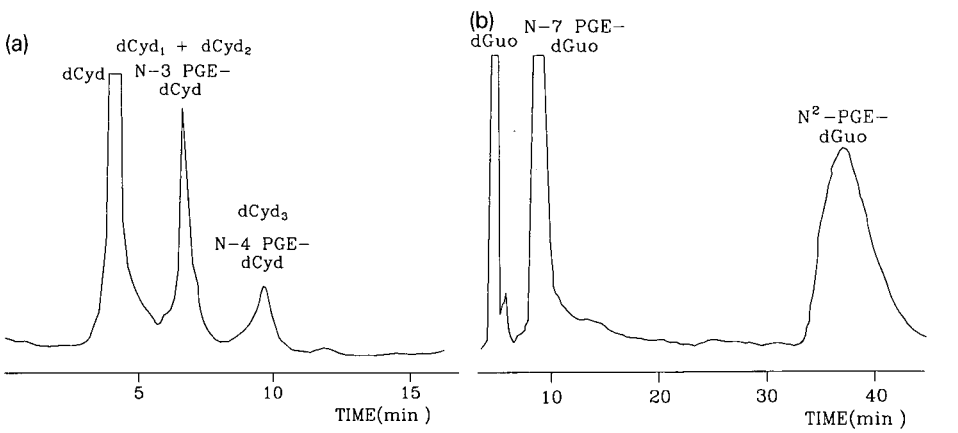

Fig. 4. Preparative HPLC on a polystyrene–divinylbenzene column of (a) dCyd–PGE and (b) dGuo–PGE reaction mixtures. Column, PRP-1 (30.5 cm × 7.0 mm I.D.); eluent for dCyd–PGE, 0.01 *M* ammonium formate (pH 4.25)–methanol (50:50) at 1.6 ml/min; eluent for dGuo–PGE, 0.01 *M* ammonium formate (pH 4.25)–methanol (30:70) at 2.0 ml/min. Concentration of sample: ±30 mg/ml; 0.1 a.u.f.s.

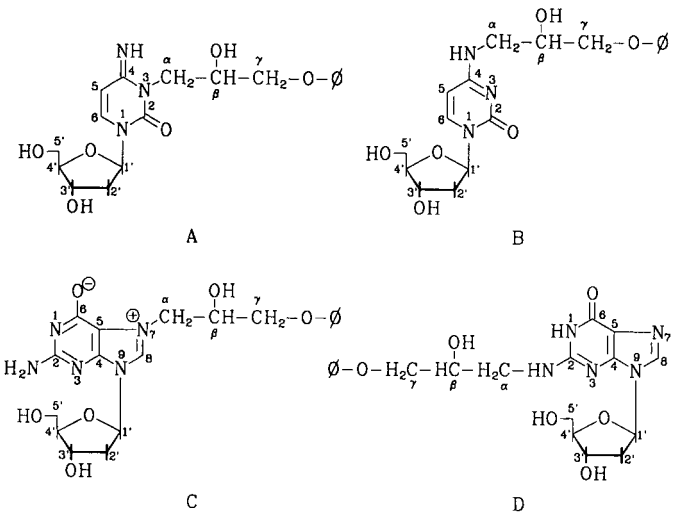

Fig. 5. Proposed structures for dCyd–PGE and dGuo–PGE adducts. (A) Diastereomers of N-3 alkylated dCyd (dCyd 1 and dCyd 2); (B) N^4 alkylated dCyd: (dCyd 3); (C) diastereomers of N-7 alkylated dGuo (dGuo 1 and dGuo 2); (D) N^2 alkylated dGuo: (dGuo 3). ϕ = Phenyl.

aromatic protons 7.282 (8.6), 6.90–6.93; CH(α), 4.243 (−14.6); CH(β), 4.163; $CH_2(\gamma)$–CH(α), 3.95 à 4.0.

The complexicity of the pattern of the proton in the region of 4.24 ppm suggest N^2 alkylation. N^2 alkylation is also consistent with the lower polarity found in the HPLC system and explains why this adduct was not detected on a reversed-phase column when a more polar solvent system than that on the PRP-1 column was used. The NMR spectrum of dGuo 3 reveals only one compound, and the minor amount of dialkylated material shown by FAB-MS is not detected. For dGuo 1 (1′) and dGuo 2 (2′), no NMR data were obtained because of the lack of sufficient material.

The instability of epoxide adducts of deoxyguanosine with trichloropropylene oxide has been observed previously [13]. Hemminki and Lax [31] noted that alkylation at N-7 of guanine in DNA, nucleosides and nucleotides greatly enhances the rate of two secondary reactions, imidazolẽ ring opening and depurination. These reactions are alkali- and acid-catalysed, respectively, but they are likely to proceed even under physiological conditions. The depurination reaction observed in our experiments could well be catalysed by traces of silica gel eluting from the reversed-phase column and catalysing the reaction during the preparative isolation of the 2′-deoxyguanosine adducts.

CONCLUSION

The proposed HPLC methods on reversed-phase and polystyrene–divinylbenzene columns proved to be efficient for the separation of the adducts formed between PGE and 2′-deoxycytidine and 2′-deoxyguanosine, respectively. These separations have the advantage of a shorter analysis time than existing methods for other adducts of aliphatic epoxides [11,13,31].

Further, the proposed methods separate diastereomers of N-7 alkylated 2′-deoxyguanosine and N-3 alkylated 2′-deoxycytidine. Hemminki and Lax [31] separated the diastereomers of trichloropropylene oxide–2′-deoxyguanosine products which were apolar, but not the polar glycidol–2′-deoxyguanosine adducts.

The use of a polystyrene–divinvylbenzene column showed several advantages. It solved the problem of decomposition of the two N-7 alkylated diastereomers. It also gave more symmetrical peaks than a reversed-phase column. The advantage of reduced tailing with polar samples, especially amines, was also pointed out by Smith [35] for polystyrene–divinylbenzene columns. Further, the use of a polystyrene–divinylbenzene column led to the isolation of one more adduct fraction for the 2′-deoxycytidine–PGE reaction mixture, characterized by MS and NMR as N^4 alkylated material. Also for the 2′-deoxyguanosine–PGE reaction mixture, an additional fraction was detected which appeared to be a mixture of mainly an N^2 alkylation adduct, as suggested by the NMR and UV data and a minor amount of dialkylated material and imidazole ring-opened dialkylated material as indicated by MS.

HPLC with photodiode-array detection combined with off-line UV studies at different pH values proved to be an excellent tool for preliminary identification of the adducts. The structures suggested by these UV data, *i.e.*, N-3-(2-hydroxy-3-phenoxypropyl)-2′-deoxycytidine (two diastereomers), N^4-(2-hydroxy-3-phenoxypropyl)-2′-deoxycytidine and N-7-(2-hydroxy-3-phenoxypropyl)-2′-deoxyguanosine (two diastereomers) and N^2-(2-hydroxy-3-phenoxypropyl)-2′-deoxyguanosine were confirmed by MS data and NMR for the 2′-deoxycytidine products and by MS or NMR for the 2′-deoxyguanosine products.

ACKNOWLEDGEMENT

J.E.S. acknowledges support by Grant ROI ES 03345 from the National Institute of Environmental Health Sciences DHHS. The excellent technical assistance of Hilde Cordemans is gratefully acknowledged. The typing of the manuscript was by C. Rawoens and the drawings by Jef Schrooten (R.U.C.A.), both of whom are gratefully thanked.

REFERENCES

1 NIOSH, *Criteria for a Recommended Standard, Occupational Exposure to Glycidyl Ethers*, U.S. Department of Education and Welfare, Public Health Service, Center for Disease Control, National Institute for Occupational Safety and Health, Cincinnati, OH, 1978, p. 197.
2 M. M. Manson, *Br. J. Ind. Med.*, 37 (1980) 317–336.
3 L. Ehrenberg and S. Hussain, *Mutat. Res.*, 86 (1981) 1–113.
4 D. R. Wade, S. A. Airy and J. E. Sinsheimer, *Mutat. Res.*, 58 (1978) 217–233.
5 S. W. Frantz and J. E. Sinsheimer, *Mutat. Res.*, 90 (1981) 67–78.
6 S. H. Neau, B. H. Hooberman, S. W. Frantz and J. E. Sinsheimer, *Mutat. Res.*, 93 (1982) 297–304.
7 S. W. Frantz, E. Van den Eeckhout, J. E. Sinsheimer, M. Yashihare and M. Koreeda, *Toxicol. Lett.*, 25 (1985) 265–271.
8 L. B. Rosman, V. G. Beylin, V. Gaddamidi, B. H. Hooberman and J. E. Sinsheimer, *Mutat. Res.*, 171 (1986) 63–70.
9 L. B. Rosman, V. Gaddamidi and J. E. Sinsheimer, *Mutat. Res.*, 189 (1987) 189–204.
10 L. B. Rosman, P. K. Chakraborty, E. A. Messerly and J. E. Sinsheimer, *Mutat. Res.*, 206 (1988) 115–126.

11 Z. Djuric and J. E. Sinsheimer, *Chem. Biol. Interact.*, 50 (1984) 219–231.
12 Z. Djuric and J. E. Sinsheimer, *Chem. Biol. Interact.*, 52 (1984) 243–253.
13 Z. Djuric, B. H. Hooberman, L. Rosman and J. E. Sinsheimer, *Environ. Mutat.*, 8 (1986) 369–383.
14 K. Sugiura and M. Goto, *Chem. Biol. Interact.*, 45 (1983) 153–169.
15 K. Hemminki and H. Vaino, in B. Holmstedt, R. Lauwereys, M. Mercier and M. Roberfroid (Editors), *Mechanism of Toxicity and Hazard Evaluation*, Elsevier/North Holland Biomedical Press, Amsterdam, 1980, pp. 241–243.
16 K. Hemminki, *Arch. Toxicol.*, 52 (1983) 249–285.
17 E. Van den Eeckhout, A. De Bruyn, H. Pepermans, E. Esmans, I. Vrijens, J. Claereboudt, M. Claeys and J. E. Sinsheimer, *J. Chromatogr.*, 504 (1990) 113–128.
18 P. R. Brown (Editor), *HPLC in Nucleic Acid Research*, Marcel Dekker, New York, 1984.
19 B. M. Van Liedekerke, H. J. Nelis, W. E. Lambert and A. P. De Leenheer, *Anal. Chem.*, 61 (1989) 728–732.
20 D. P. Lee and J. H. Kindsvater, *Anal. Chem.*, 52 (1980) 2425–2428.
21 S. Ikuta, R. Chattopadhyaya and R. E. Dickerson, *Anal. Chem.*, 56 (1984) 2253–2256.
22 M. W. Germann, R. T. Pon and J. H. Van de Sande, *Anal. Biochem.*, 165 (1987) 399–405.
23 Y. Kim and P. R. Brown, *J. Liq. Chromatogr.*, 10 (1987) 2411–2422.
24 E. Quintero, R. M. Sheeley, W. J. Hurst and R. A. Martin, *J. Liq. Chromatogr.*, 10 (1987) 2145–2150.
25 C. Lacrois, P. Levert, G. Laine, J. P. Goulle and A. Gringore, *J. Chromatogr.*, 345 (1985) 436–440.
26 A. M. Rustum and N. E. Hoffman, *J. Chromatogr.*, 421 (1987) 387–391.
27 A. M. Rustum and N. E. Hoffman, *J. Chromatogr.*, 426 (1988) 121–128.
28 B. Singer, in G. D. Fasman (Editor), *CRC Handbook of Biochemistry and Molecular Biology*, CRC Press, Cleveland, OH, 1975, pp. 409–447.
29 K. Hemminki, J. Paasvirta, T. Kurkirinne and L. Virkki, *Chem. Biol. Interact.*, 30 (1980) 259–270.
30 A. Albert, in W. W. Zorbach and R. S. Tipson (Editors), *Synthetic Procedures in Nucleic Acid Chemistry*, Vol. 2, Wiley-Interscience, New York, 1971, pp. 47–123.
31 K. Hemminki and M. Lax, *Acta Pharmacol. Toxicol.*, 59 (1986) 80–85.
32 J. Claereboudt, E. Van den Eeckhout, E. Esmans and M. Claeys, *Biomed. Environ. Mass Spectrom.*, in preparation.
33 J. Claereboudt, E. L. Esmans, E. G. Van den Eeckhout and M. Claeys, *Nucleosides Nucleotides*, 9 (1990) 333–344.
34 J. Claereboudt, E. L. Esmans, E. G. Van den Eeckhout, W. Baeten and M. Claeys, *37th Annual Conference on Mass Spectrometry and Allied Topics, Miami Beach, FL, 1989*, Abstracts, p. 923.
35 R. Smith, *J. Chromatogr.*, 291 (1984) 372–376.

Journal of Chromatography, 541 (1991) 333–339
Elsevier Science Publishers B.V., Amsterdam

CHROM. 22 990

Model studies on iron(III) ion affinity chromatography

Interaction of immobilized metal ions with nucleotides

GRAŻIYNA DOBROWOLSKA and GRAŻIYNA MUSZYŃSKA
Institute of Biochemistry and Biophysics, Polish Academy of Sciences, ul. Rakowiecka 36, 02-532 Warsaw (Poland)
and
JERKER PORATH*
Biochemical Separation Centre, Biomedical Centre, Uppsala University, Box 577, S-751 23 Uppsala (Sweden)

(First received August 29th, 1990; revised manuscript received November 7th, 1990)

ABSTRACT

Mononucleotides are able to bind with immobilized iron(III) ions at low pH in the presence of 1 *M* sodium chloride and can be desorbed by increasing the pH. All the mononucleotides studied, bound at pH 5.5 to gel-chelated iron(III) ions, were eluted from the adsorbent in the pH range 7.0–7.4. No significant difference was observed in the elution profiles of mono-, di-, tri- and tetraphosphate nucleotides or their deoxy forms. Nucleosides, cyclic mononucleotides and dinucleotides containing all phosphate groups in the internal position do not bind to the immobilized metal ion under these conditions. The results obtained indicate that for interaction of nucleotides with immobilized iron(III) ions, one free terminal phosphate group is responsible.

INTRODUCTION

Immobilized iron(III) ion chromatography has proved to be a promising technique for the selective separation of macromolecules [1–3]. There is evidence that immobilized iron(III) ions interact with phosphate-oxygen and to some extent with other negatively charged groups on peptides and proteins [4]. We have demonstrated that immobilized iron(III) ions can preferentially bind phosphoproteins [1,2] and can be used for the separation of phosphopeptides from a tryptic digest of proteins [5]. Moreover, some data suggest that the strength of binding is dependent on the phosphate content of proteins [2,6].

The aim of this work was to extend the previous studies and to look for a mode of interaction between the immobilized iron(III) and non-protein phosphocompounds. For this purpose nucleotides and their derivatives, differing in the number of phosphate and nucleotide groups, were chosen as models. The results could indicate whether the interaction might be exploited for the rapid and high-yield fractionation of

0021-9673/91/$03.50

nucleotides and nucleic acids by chromatography on iron(III) chelate adsorbent(s) on the basis of phosphate content.

EXPERIMENTAL

Materials

Nucleosides, mono- and dinucleotides, poly C (polycytidylic acid), DNA from calf thymus, morpholinoethanesulphonic acid (MES), Tris and iron(III) chloride were obtained from Sigma. All other chemicals were of analytical-reagent grade.

Buffers

Buffer 1 was 0.05 *M* MES + 1 *M* NaCl (pH 5.5), buffer 2 was 0.02 *M* MES + 1 *M* NaCl (pH 6.5) and buffer 3 was 0.10 *M* Tris + 1 *M* NaCl (pH 7.7).

Chromatography

Degassed chelating Sepharose Fast Flow (Pharmacia–LKB) was packed in columns (1.5 × 1 cm I.D.; $V_t \approx 1$ ml) in distilled water and charged with a few volumes of 20 m*M* iron(III) chloride. For removal of the excess of unbound and loosely bound metal ions the columns were washed with 10–15 volumes of water, buffer 3 and finally equilibration buffer 1. Before chromatography all solutions were degassed. Chromatography was conducted at room temperature with a flow-rate of 15 ml/h and 1.7-ml fractions were collected. In each run 1–2 μmol of an appropriate compound in 0.5 ml of buffer 1 was applied to the column. The column was subsequently washed with 8.5 ml of buffer 1, 8.5 ml of buffer 2 and finally by a continuous pH gradient formed by the gradual mixing of 17 ml of buffer 3 with 17 ml of buffer 2. The eluted compounds were detected by determination of the absorbance at 260 nm, and the pH of the eluate was measured using a pH meter. Other conditions used in some of the separation experiments are indicated in Table I.

Soon after each experiment, the columns were regenerated with 0.1 *M* EDTA–1 *M* sodium chloride and washed with redistilled water. The metal-free columns were stored at room temperature and charged with iron(III) ions directly before use. Each column was reused several times.

RESULTS

As can be seen from Table I, nucleosides (adenosine and guanosine) and cyclic mononucleotides (cAMP and cGMP) are not bound and are eluted from gel-immobilized iron(III) ions by the equilibration buffer at pH 5.5. Dinucleotides bearing one to five internal phosphate groups, polynucleotide (poly C) and DNA are not adsorbed on the metal chelate adsorbent in the presence of 1 *M* sodium chloride. Among the tested constituents of ribonucleic acids, adenine mononucleotides (AMP, ADP and ATP) and guanidine mononucleotides (GMP and Gpppp) bearing one to four phosphate groups are adsorbed on the iron(III)-chelated gel at pH 5.5 and can be eluted by a continuous pH gradient (pH 6.5–7.7) in the presence of 1 *M* sodium chloride (Figs. 1 and 2). A similar elution profile is obtained for deoxymonophosphate nucleotides (dAMP, dGMP, dCMP) (Fig. 3).

The elution patterns of all the mononucleotides studied are similar; purine

TABLE I

CHROMATOGRAPHIC BEHAVIOUR OF NUCLEOTIDES AND RELATED COMPOUNDS ON GEL-IMMOBILIZED IRON(III) CHELATE

Experimental conditions: *ca.* 2–3 optical units at 260 nm of tested compounds in 0.5 ml of buffer 1 were applied to an iron(III)-chelated column ($V_t \approx 0.5$ ml). The column was subsequently washed with 5 ml of buffer 1 and 5 ml of buffer 3 and 1-ml fractions were collected at a flow-rate of 10 ml/h. The compounds detected in the fractions eluted by buffers 1 and 3 were classified as "not bound" and "bound", respectively.

Compound[a]	Chromatographic behaviour	
	Not bound (−)	Bound (+)
Adenosine	−	
cAMP	−	
AMP		+
ADP		+
ATP		+
ApppA	−	
AppppA	−	
cGMP	−	
GMP		+
Gpppp		+
GpG	−	
GpppG	−	
GppppG	−	
poly C	−	
Deoxy-AMP		+
Deoxy-GMP		+
Deoxy-CMP		+
DNA from calf thymus	−	

[a] Abbreviations: ApppA = p^1,p^3-di(adenosine-5′)triphosphate; AppppA = p^1,p^4-di(adenosine-5′)tetraphosphate; cAMP = adenosine 3′5′-cyclic monophosphate, cGMP = guanosine 3′5′-cyclic monophosphate; Gpppp = guanosine 5′-tetraphosphate; GpG = guanylyl(3′–5′)guanosine; GpppG = p^1,p^3-di(guanosine-5′)triphosphate; GppppG = p^1,p^5-di(guanosine-5′)pentaphosphate; poly C = polycytidylic acid.

TABLE II

ELUTION OF NUCLEOTIDES FROM GEL-IMMOBILIZED IRON(III) CHELATE

The pH values are taken from Figs. 1–3.

Nucleotide[a]	pH of elution	Nucleotide[a]	pH of elution
AMP	7.30	Gpppp	7.25
ADP	7.40	Deoxy-AMP	7.25
ATP	7.40	Deoxy-GMP	7.25
GMP	7.20	Deoxy-CMP	7.00

[a] For abbreviations, see Table I.

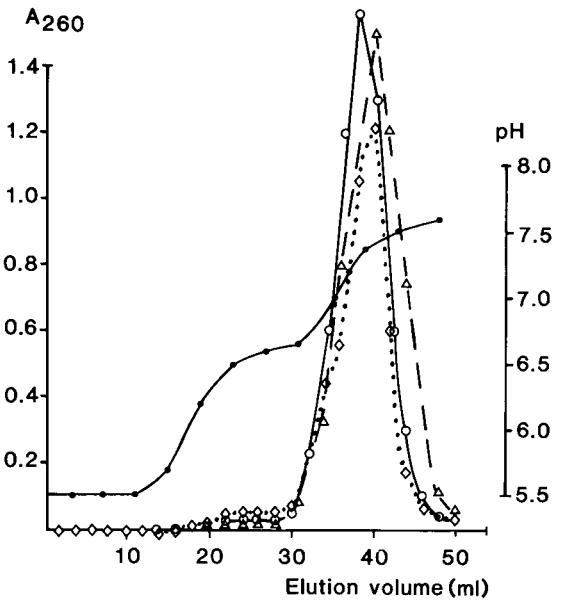

Fig. 1. Elution profiles of adenine nucleotides from Fe^{3+}-chelated gel. ○—○ = AMP; △- -△ = ADP; ◇ · · · ◇ = ATP; ●—● = pH.

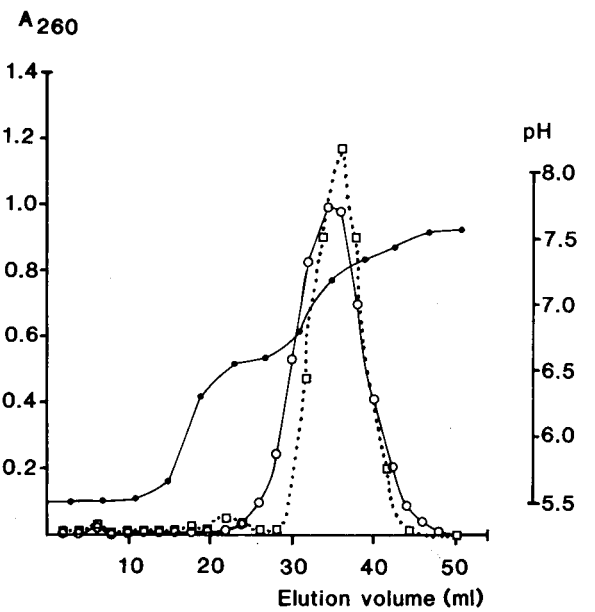

Fig. 2. Elution profiles of guanidine nucleotides from Fe^{3+}-chelated gel. ○—○ = GMP; □ · · · □ = Gpppp; ●—● = pH.

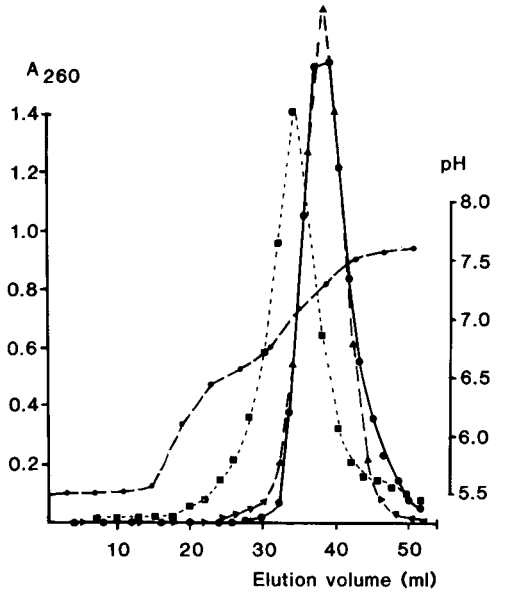

Fig 3. Elution profiles of deoxymonophosphate nucleotides from Fe^{3+}-chelated gel. O—O, Deoxy-AMP; ▲- -▲, deoxy-GMP; □- -□, deoxy-CMP; O- -O = pH.

mono-, di-, tri- and tetraphosphate derivatives in their ribo and deoxyriboforms are desorbed from gel-immobilized iron(III) ions in the pH range 7.2–7.4, whereas for elution of dCMP a lower pH (7.0) is sufficient (Table II).

DISCUSSION

Immobilized metal affinity chromatography (IMAC) has been extensively applied to the separation and fractionation of proteins. There is evidence that it can also be used for studying the behaviour of nucleic acid constituents. Hubert and Porath [7,8] indicated that pyrimidine nucleotides display weak interaction with immobilized divalent metal ions, such as copper and nickel. The stronger complexation of purine nucleotides on immobilized Cu^{2+} ions allowed their separation from pyrimidine mononucleotides and also provided sufficient selectivity to differentiate AMP from GMP [8]. The number of potential binding sites (particularly nitrogen atoms on the bases, and to a lesser extent the negatively charged oxygen atom in the phosphate residue and possibly the hydroxyl group on the ribose) might account for multiple site attachment with the Cu^{2+} in solution [9,10]. However, under the conditions described by Hubert and Porath [7,8], bases are more strongly adsorbed on immobilized copper ions than the corresponding nucleosides and nucleotides. This seems to exclude any contribution of either the phosphate or the ribose moieties to the binding with the immobilized metal ions.

The present results clearly indicate that for the interaction of nucleotides with gel-immobilized iron(III) ions only free phosphate groups are responsible, because only nucleotides with free terminal phosphate groups are able to bind to such gels. The

strength of binding is not influenced by an increase in the number (one to four) of phosphate groups of nucleotides. The same pH of elution of AMP or GMP and their deoxy homologues indicates the lack of a contribution of the 2′-OH group of ribose to the binding process. However, the slight difference in the chromatographic behaviour of deoxy-CMP compared with deoxypurine analogues suggests that the type of base may play a minor role in the interaction with immobilized trivalent iron.

Cyclic mononucleotides (cAMP and cGMP), where the phosphate group is bound in two positions to ribose (3′ and 5′), do not have any affinity to immobilized iron(III) ions. Also dinucleotides, bearing exclusively one to five internal phosphate groups, are not adsorbed on the column. Biopolymers such as poly C and DNA from calf thymus do not bind to the gel. The most probable explanation is that in large molecules, such as poly C or DNA, one terminal phosphate group is not sufficient for binding to the immobilized metal and/or this group is not very exposed because it is involved in the formation of a higher order structure. In simple molecules, such as cAMP and dinucleotides, even sufficiently exposed phosphate groups, but present as phosphodiesters, are not able to interact with immobilized iron(III) ions. The results suggest that for the formation of a binding site with the immobilized metal, oxygen atoms in the phosphate must be accessible and a phosphomonoester must be present.

The binding of macromolecules to immobilized metal ions involves different types of interactions. Adsorption of proteins to the immobilized metals is typically reinforced at an increased concentration of antichaotropic salts [11], which is probably an indication of metal coordination binding. This work demonstrates that the adsorption of free phosphate groups of nucleotides to immobilized iron(III) ions is not based on simple electrostatic interactions, as the chromatography was performed in the presence of 1 *M* sodium chloride. A similar observation was made with a phosphoprotein containing a phosphorylated residue [2]. Phosphorylation of a single serine residue on the histone molecule strengthens its binding to iron(III) chelated gel. Phosphorylated histone may be eluted by an increase in pH. As the chromatography was performed in the presence of 1–4 *M* sodium chloride, non-specific electrostatic interactions could not be the major factor responsible for the increase in pH required for the elution [2].

It should also be pointed out that groups other than phosphate might be able to interact with immobilized trivalent iron. Recent studies have shown that proteins lacking phosphate groups are adsorbed on the gel [3,12]. Our results [4] indicate that in addition to phosphate groups, clusters of carboxylic groups and hydroxy groups on the phenolic ring in tyrosine on proteins are important in the binding to immobilized iron(III) ions. However, among the predictable and documented interactions of immobilized iron(III) ions with proteins the ability to bind phosphate group(s) is most commonly encountered.

This work has demonstrated that for the interaction of nucleotides with immobilized iron(III) ions free, external phosphate groups are required. This observation might be utilized for the separation of mono- and oligonucleotides with exposed phosphate groups from the other constituents of nucleic acids. However, it is not yet clear whether large oligonucleotides can be separated by exploiting the properties of immobilized iron(III) ions. The size limit of nucleotides for effective binding is being investigated.

ACKNOWLEDGEMENTS

We are grateful to Professor Jyoti Chattopadyaya for discussions. This work was supported by the Nordic Industrial Fund, the Erna and Victor Hasselblad Foundation, the Swedish National Board for Technical Development (STUF) and the Swedish National Science Research Council.

REFERENCES

1 L. Andersson and J. Porath, *Anal. Biochem.*, 154 (1986) 250.
2 G. Muszyńska, L. Andersson and J. Porath, *Biochemistry*, 25 (1986) 6850.
3 G. Chaga, L. Andersson, B. Ersson and J. Porath, *Biotechnol. Appl. Biochem.*, 11 (1989) 424.
4 J. Porath, G. Dobrowolska, A. Medin, P. Ekman and G. Muszyńska, in preparation.
5 H. P. Michel and J. Bennett, *FEBS Lett.*, 212 (1987) 103.
6 G. Muszyńska, R. Sleigh, L. Andersson and J. Porath, *J. Chromatogr.*, submitted for publication.
7 P. Hubert and J. Porath, *J. Chromatogr.*, 198 (1980) 247.
8 P. Hubert and J. Porath, *J. Chromatogr.*, 206 (1981) 164.
9 G. L. Eichorn, P. Clark and E. D. Becker, *Biochemistry*, 5 (1966) 245.
10 N. A. Berger and G. L. Eichorn, *Biochemistry*, 10 (1971) 1847.
11 J. Porath and B. Olin, *Biochemistry*, 22 (1983) 1621.
12 E. Sulkowski, *Makromol. Chem., Macromol. Symp.*, 17 (1988) 335.

Journal of Chromatography, 541 (1991) 341–348
Elsevier Science Publishers B.V., Amsterdam

CHROMSYMP. 2078

Use of the 4-methoxy-4′-octyloxytrityl group as an affinity handle for the purification of synthetic oligonucleotides[a,b]

K. C. GUPTA*, R. K. GAUR and P. SHARMA

Nucleic Acids Research Laboratory, CSIR Centre for Biochemicals, V. P. Chest Institute Building, Delhi-110 007 (India)

(First received October 17th, 1989; revised manuscript received November 8th, 1990)

ABSTRACT

The use of triphenylmethyl protecting groups with long-chain alkyl substituents, *viz.*, (4-hexadecyloxyphenyl)diphenylmethyl (HTr) and (4-decyloxyphenyl)diphenylmethyl (DTr), as affinity handles in the purification of oligonucleotides results in significant depurination while removing these affinity groups from the high-performance liquid chromatographically purified oligonucleotides in 80% aqueous acetic acid. The separation and purification of solid-phase synthesized medium-to-large sized model oligonucleotides using the 4-methoxy-4′-octyloxytrityl (MOTr) group was investigated. Model studies demonstrated an excellent resolution of synthetic oligonucleotides and the MOTr group was removed under conditions identical with those used for the conventional 4,4′-dimethoxytrityl (DMTr) group, hence being less prone to depurination.

INTRODUCTION

High-performance liquid chromatography (HPLC) has become an important separation technique for the analytical and preparative separation of synthetic oligonucleotides. Different standard columns containing normal-phase silica gel [1], ion-exchange [2–6] and reversed-phase (RP) [7–15] materials have been used extensively for this purpose. During the solid-phase synthesis of oligonucleotides, a "capping" step involving acylation of the 5′-OH group is applied after each coupling then, on completion of the synthesis, if there are no other side-reactions, only the desired oligomer should carry a 5′-terminal 4,4′-dimethoxytrityl (DMTr) protecting group. The other DNA species, the "failure sequences", bear the base labile 5′-O-acetyl cap which is subsequently hydrolysed during work-up to leave a mixture of components that differ significantly in hydrophobicity from the desired product. The RP-HPLC separation takes advantages of this fact that rather than resolving oligomers differing

[a] Presented at the *International Symposium on Chromatography (CIS'89), Tokyo, October 17–20, 1989*. The majority of the papers presented at this symposium have been published in *J. Chromatogr.*, Vol. 515 (1990).

[b] Dedicated to Professor N. K. Mathur in honour of his 60th birthday.

0021-9673/91/$03.50

in chain length, the separation involves resolving a 5'-DMTr-DNA from 5'-hydroxy-DNA.

The DMTr group has been found to be suitable for the purification of DNA fragments up to 30 nucleotides in length [16], but oligomers larger than 30 nucleotides in length pose problems if the DMTr group is used as an affinity handle. In order to overcome this problem, the use of a triphenylmethyl protecting group with long-chain alkyl substituents, *e.g.*, the (4-hexadecyloxyphenyl)diphenylmethyl (HTr) group, for the affinity chromatographic purification of oligonucleotides of defined sequence and particularly of solid-phase synthesized products was recommended by Seliger and co-workers [17,18]. Recently, the same group [19] observed that the HTr group causes most oligonucleotides to be retained too strongly on a C_{18} stationary phase. The HTr-bearing oligonucleotides, particularly those of very low molecular weight, arising from incomplete capping will be eluted by nearly 100% acetonitrile, *i.e.*, their quantitative elution will be difficult or require a change of solvent. In fact, the monomeric (4-hexadecyloxyphenyl)diphenylmethyl deoxythymidine (HTrdT) was not eluted at all with acetonitrile, but required carbon tetrachloride as an eluent. These limitations of the HTr group prompted Seliger and Schmidt [20] to suggest an alternative group, (4-decyloxyphenyl)diphenylmethyl (DTr), for the purification of medium-to-large sized synthetic oligonucleotides.

It has been observed that the complete deprotection of HPLC-purified oligonucleotides containing either an HTr or DTr group required a considerably longer time in 80% acetic acid, resulting in significant depurination of the HPLC-purified oligonucleotides. The complete removal of the monomethoxytrityl group [20] takes 90 min at 27°C, which is almost 4.5 times longer than that of the dimethoxytrityl group [21] in 80% acetic acid at room temperature. The use of a triphenylmethyl protecting group with 4-methoxy-4'-alkoxy substituents was investigated in this study. 4-Methoxy-4'-octyloxytrityl, with a moderate-sized alkyl substituent on the trityl group, has been found to be a better choice for the purification of medium-to-large sized oligonucleotides useful for total gene synthesis and other applications in molecular biology.

EXPERIMENTAL

Chemicals and reagents

4-Hydroxybenzophenone, 1-bromopropane, 1-bromobutane, 1-bromopentane, 1-bromooctane, 1-bromododecane, 4-dimethylaminopyridine (DMAP) and diisopropylethylamine (DIPEA) were obtained from Fluka (Buchs, Switzerland), 2-cyanoethyl-N,N-diisopropylchlorophosphoramidite and N,N-diisopropylmethylphosphonamidic chloride were prepared using standard methods [22,23].

Pyridine was purified by distillation from ninhydrin and dried by refluxing over potassium hydroxide followed by distillation and stored over potassium hydroxide pellets under argon. Acetonitrile and dichloromethane were dried by refluxing with calcium hydride (5 g/l) for 16 h followed by distillation and stored over molecular sieves (4 Å). Tetrahydrofuran (THF) was purified by passing it through alumina and dried over lithium aluminium hydride.

Buffer for HPLC

The aqueous buffer for HPLC was 0.10 *M* triethylammonium acetate (TEAA) (pH 7.0). This was prepared by dilution from a 2 *M* stock solution which was ob-

tained in the following manner: 557 ml (4 mol) of triethylamine distilled from ninhydrin were slowly added with stirring to an aqueous solution containing 229 ml (4 mol) of glacial acetic acid at 4°C. When the addition was completed, the solution was diluted to 2 l and the pH adjusted to 7.0 by the addition of acetic acid or triethylamine as needed. The water used was obtained from a Milli-Q water purification system (Millipore). The organic component of the mobile phase was acetonitrile (Spectrochem, Bombay, India).

Apparatus

Thin-layer chromatography (TLC) was performed on silica gel 60 F_{254} plates (Merck, Darmstadt, Germany) with solvents as indicated and compounds were detected under short-wavelength UV light. Proton NMR spectra were recorded on a Perkin-Elmer R-32 spectrometer operating at 90 MHz and a Hitachi FT-60B spectrometer operating at 60 MHz. Melting points were recorded on a Tropical capillary melting-point apparatus and are uncorrected.

HPLC was performed on a Shimadzu LC-4A instrument equiped with a Shimadzu SPD-2AS variable-wavelength UV detector set 254 nm. Analytical HPLC was performed on a Zorbax ODS column (250 × 4.6 mm I.D.), particle size 10 μm (DuPont) and a μBondapack C_{18} column (300 × 3.9 mm I.D.), particle size 5 μm (Waters Assoc.).

Synthesis of 5′-O-(4-methoxy-4′-alkoxytrityl)deoxynucleosides ***3a–e***

4-Methoxy-4′-alkoxytrityl groups were introduced selectively into the 5′-position of base-protected nucleosides by a published procedure [18] with some modifications. The reaction schemes are depicted in Fig. 1. The purity of the intermediates were confirmed by TLC and NMR and IR spectroscopy. 4-Methoxy-4′-octyloxytrityldeoxythymidine was converted into the 4-methoxy-4′-octyloxytrityldeoxythymidine 3′-O-(2-cyanoethyl-N,N-diisopropylamino)phosphoramidites by the method described by Sinha *et al.* [23].

Oligodeoxynucleotide synthesis

Oligonucleotides were synthesized following the standard protocol using solid-phase phosphoramidite chemistry [24] on a Pharmacia–LKB Gene Assembler Plus using methyl or 2-cyanoethyl phosphoramidites. The synthesis was carried out on 1.3 μmol of support-bound first nucleoside. In the last coupling step, a 5′-DMTr or MOTr group containing nucleoside phosphoramidites was used and no change in the coupling time or the solvent was made. After the synthesis of the required sequence, the DMTr or MOTr group was kept intact. The internucleotide phosphate protecting groups were removed following the standard protocol [24]. Removal of the exocyclic base protecting groups and cleavage of the oligonucleotide from the support were achieved with 25% aqueous ammonia at 55°C for 16 h. The crude oligonucleotides with a DMTr or MOTr group at the 5′-terminus were then purified by RP-HPLC.

HPLC purification of oligonucleotides using the DMTr or MOTr group as an affinity handle

The crude oligonucleotide obtained as above was dissolved in 0.1 *M* TEAA buffer (pH 7.0) and desalted on a Bio-Gel P2 column using the same buffer as eluent.

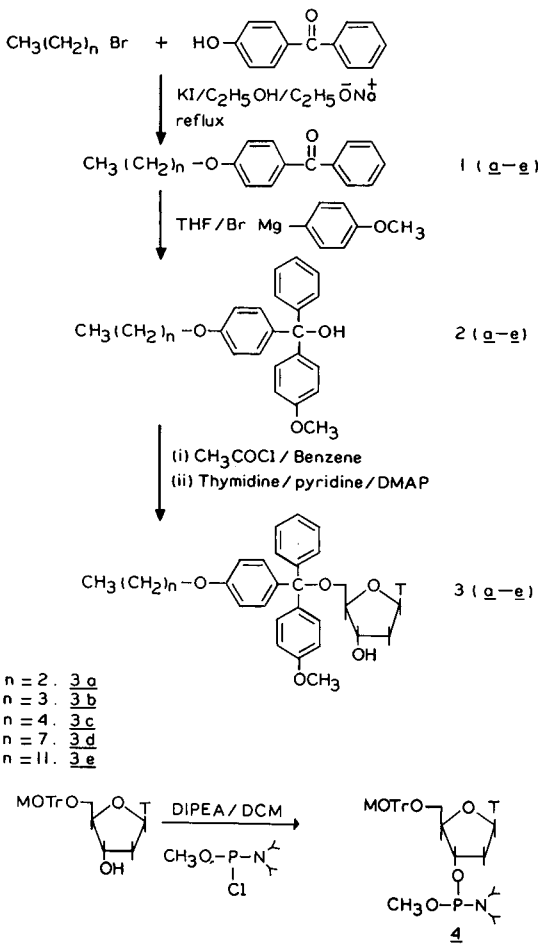

Fig. 1. Scheme for the synthesis of 5'-O-(4-methoxy-4'-alkoxytrityl)thymidine and 5'-O-(4-methoxy-4'-octyloxytrityl)thymidine 3'-O-(methyl N,N-diisopropylamino)phosphoramidite. DCM = dichloromethane.

The desalted product was collected and concentrated under vacuum and the residue was dissolved in 0.1 *M* TEAA buffer (pH 7.0) (500 μl) and then applied to a μBondapak C_{18} or Zorbax C_{18} column. The peak containing the desired material was collected.

Hydrolysis kinetics of 4-methoxy-4'-alkoxytrityl groups from nucleosides ***3a–f***

The kinetics of the hydrolysis of 4-methoxy-4'-alkoxytrityl group in compounds **3a–f** in 80% acetic acid was studied in the following manner: a solution of compounds **3a–f** in 1 ml of 80% acetic acid was kept at room temperature with occasional swirling. Aliquots were removed every 1 min and applied to a TLC plate. The TLC plate was developed in chloroform–methanol (9:1) and the compounds were revealed under UV light or by spraying with perchloric acid solution followed by heating at 100°C in an oven.

RESULTS AND DISCUSSION

We have attempted to investigate the use of the 4-methoxy-4′-alkoxytrityl group as an aid in the separation of solid-phase synthesized oligonucleotides. Two important considerations guided our approach: the first is that the group chosen can be introduced and removed from the 5′-position of nucleosides in a similar manner to the DMTr group, and the second is that the group selected should be moderately hydrophobic and allow the purification of medium-to-large sized oligonucleotides used for gene synthesis.

In order to satisfy these criteria, we selectively introduced 4-methoxy-4′-alkoxytrityl groups at the 5′-position of thymidine by known methods [18] with some modifications in 85–92% yields (Fig. 1).

In order to understand the effect of alkyl-chain substituents in the trityl function, compounds **3a–f** were simultaneously injected onto a C_{18} column. The elution profile is shown in Fig. 2. It is evident that the retention times of these thymidine derivatives increase with increase in the carbon chain length of the alkyl function. Hence the increase in carbon chain length of the alkyl substituents increases the overall hydrophobicity of the substituted trityl groups. On the basis of these results, it was concluded that the MOTr group could be a useful choice as an affinity handle for the purification of oligonucleotides. A very short alkyl substituent, *viz.*, butyl or hexyl, in the trityl function may not impart a sufficient hydrophobicity to this group to make it effective for the separation of medium-sized oligonucleotides and a very long-chain alkyl substituent in the trityl function would make it too hydrophobic and hence short nucleotides, *viz.*, the monomer or dimer resulting from the incomplete

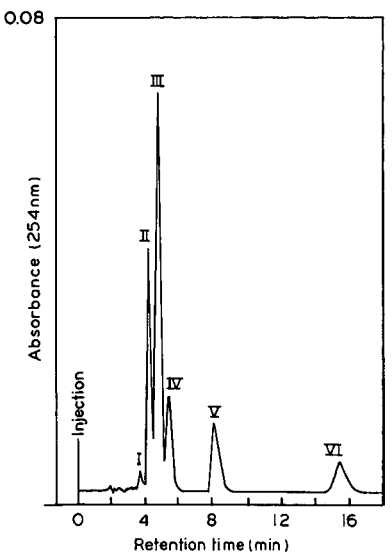

Fig. 2. HPLC profile of a mixture of compounds **3a–f** on a μBondapak C_{18} column. Eluent, THF–water–methanol (3:2:2); flow-rate, 1 ml/min; detection, 254 nm 0.08 a.u.f.s. Peaks: I = **3f**; II = **3a**; III = **3b**; IV = **3c**; V = **3d**; VI = **3e**.

capping, would be retained by the C_{18} column for a longer time or may not be eluted at all from the column completely. This has already been experienced with the HTr group [19].

The hydrolysis of 4-methoxy-4′-alkoxytrityl groups in 80% acetic acid acid was found to be complete in 15 min. Hence the MOTr group can be removed from the purified oligonucleotides under conditions identical with those used for the DMTr group. The reason for using a disubstituted trityl function (MOTr) was mainly its lability in 80% acetic acid. With a monosubstituted trityl function (DTr or HTr) the time required for the removal of these protecting groups from the HPLC-purified oligonucleotides was found to be considerable, which may cause significant depurination of the purified oligonucleotides. The MOTr group was therefore selected for further study as an affinity handle for the purification of solid-phase synthesized oligonucleotides.

Comparison of chromatographic behaviour of model DMTr-oligonucleotides of different chain length with model MOTr-oligonucleotides under identical conditions

We further extended our study to the comparison of model oligonucleotides differing not only in the nature of the 5′-protecting group, but also in the length of the nucleotide chain. Fig. 3 shows the elution profile after simultaneous injection of 5′-DMTr- and 5′-MOTr-oligonucleotides having chain lengths of 10, 20 and 30 bases. It can be seen that the gradient time, the concentration of the acetonitrile required to elute MOTr d(T_{29} C) is almost double that required for DMTr d(T_{29} C). It is clear that the difference in retention time of an oligomer bearing a 5′-MOTr is much larger than that of a similar oligomer bearing a 5′-DMTr group. This demonstrates that, although an increase in the length of the oligonucleotide reduces the retention time, the overall retention conferred by the longer alkyl substituent far exceeds the influence of the polyanionic chain.

Encouraged by the results shown in the Fig. 3, we synthesized a longer sequence, *viz.*, MOTr d$(T)_{60}$, to demonstrate the utility of the MOTr group for the purification of long-chain polynucleotides. Fig. 4 shows the HPLC purification profile of MOTr d$(T)_{60}$. Even at this chain length, the peak corresponding to the desired material is well resolved from the truncated sequences. The desired material at 10.2 min was collected, concentrated and re-injected under identical conditions. Again a single peak with the same retention time was obtained.

CONCLUSION

RP-HPLC has become an important technique for the purification of solid-phase synthesized oligonucleotides. In this work, a novel affinity handle, 4-methoxy-4′-octyloxytrityl (MOTr) was applied to the separation and purification of medium-to-large sized oligonucleotides useful for routine molecular biology and total gene synthesis. The main advantage of this group is that it can be removed from the HPLC-purified oligonucleotides under conditions identical with those used for the DMTr group, hence minimizing depurination. The utility of this group was demonstrated by purifying a reasonable-sized oligonucleotide, MOTr d$(T)_{60}$.

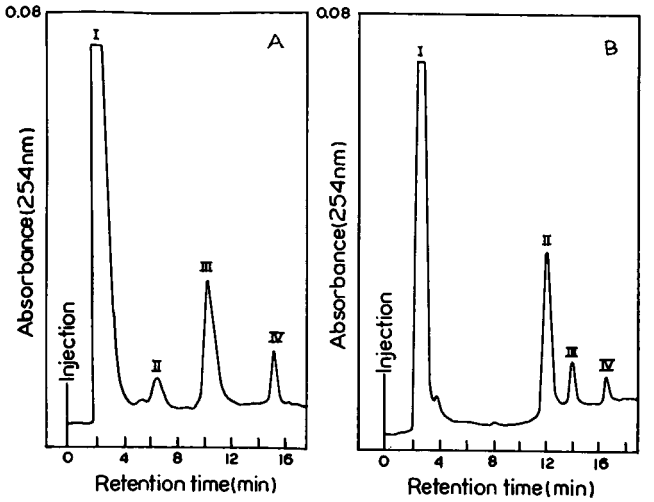

Fig. 3. (a) HPLC profile model DMTr-oligonucleotides with different chain lengths on a Zorbax ODS column (250 × 4.6 mm I.D.); Solvent A, 0.1 *M* TEAA buffer (pH 7.0); solvent B, 100% acetonitrile; gradient from 20 to 40% B in 20 min; flow-rate, 1 ml/min; detection, 254 nm (0.08 a.u.f.s.). Peaks: I = bulk of the non-tritylated truncated sequences; II = DMTr d(T_{29} C); III = DMTr d(T_{19} C); IV = DMTr d(T_9 C). (b) HPLC profile of model MOTr-oligonucleotides with different chain lengths on a Zorbax ODS column (250 × 4.6 mm I.D.). Conditions as in (a). Peaks: I = bulk of the non-tritylated truncated sequences; II = MOTr d(T_{29} C); III = MOTr d(T_{19} C); IV = MOTr d(T_9 C).

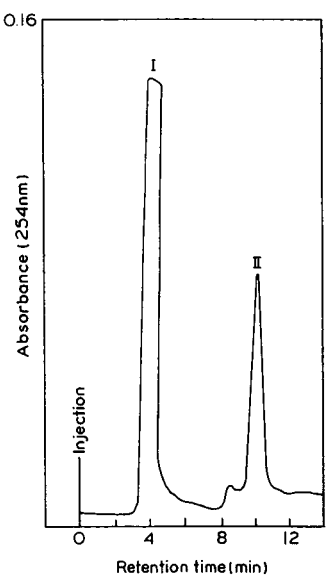

Fig. 4. HPLC purification of MOTr d($T)_{60}$ on a Zorbax ODS column (250 × 4.6 mm I.D.). Solvent A, 0.1 *M* TEAA buffer (pH 7.0); solvent B, 100% acetonitrile; gradient from 10 to 70% B in 40 min; flow-rate, 1 ml/min; detection, 254 nm 0.16 a.u.f.s. Peaks: I = bulk of the non-tritylated sequences; II = MOTr d($T)_{60}$.

ACKNOWLEDGEMENTS

Financial support from the Department of Biotechnology (India) through a grant to K.C.G. is gratefully acknowledged. The authors express their gratitude to Dr. A. P. Joshi, Scientist-in-charge, for laboratory facilities.

REFERENCES

1 K. K. Ogilvie and M. J. Nemmer, *Tetrahedron. Lett.*, 21 (1980) 4159.
2 T. F. Gabriel and J. E. Michalewsky, *J. Chromatogr.*, 80 (1973) 263.
3 M. J. Gait and R. C. Sheppard, *Nucleic Acids Res.*, 4 (1977) 1135.
4 T. G. Lawson, F. E. Regnier and H. L. Weith, *Anal. Biochem.*, 133 (1983) 85.
5 W. Haupt and A. Pingound, *J. Chromatogr.*, 260 (1983) 419.
6 M. V. Cubellis, G. Marino, L. Mayol, G. Piccialli and G. Sannia, *J. Chromatogr.*, 329 (1985) 406.
7 H. J. Fritz, R. Belagaje, E. L. Brown, R. H. Fritz, R. A. Jones, R. G. Lees and H. G. Khorana, *Biochemistry*, 17 (1978) 1257.
8 G. D. McFarland and P. N. Borer, *Nucleic Acids Res.*, 7 (1979) 1067.
9 A. F. Markham, M. D. Edge, T. C. Atkinson, A. R. Greene, G. R. Heathcliffe, C. R. Newton and D. Scanlon, *Nucleic Acids Res.*, 8 (1980) 5193.
10 K. Majumder, P. K. Latha and S. K. Brahmachari, *J. Chromatogr.*, 355 (1986) 328.
11 W. Jost, K. Unger and G. Schill, *Anal. Biochem.*, 119 (1982) 214.
12 J. B. Crowther, S. D. Fazio and R. A. Hartwick, *J. Chromatogr.*, 282 (1983) 619.
13 C. R. Becker, J. W. Efcavitch, C. R. Heiner and N. F. Kaiser, *J. Chromatogr.*, 326 (1984) 293.
14 S. Ikuta, R. Chattopadhyaya and R. E. Dickerson, *Anal. Chem.*, 56 (1984) 2253.
15 M. Kwiatkowski, A. Sandstrom, N. Balgobin and J. Chattopadhyaya, *Acta Chem. Scand., Ser. B*, 38 (1984) 721.
16 C. S. Craik, *Biotechniques*, 3 (1985) 12.
17 H. Seliger, M. Holupirek and H.-H. Gortz, *Tetrahedron Lett.*, (1978) 2115.
18 H.-H. Görtz and H. Seliger, *Angew. Chem., Int. Ed. Engl.*, 20 (1981) 681.
19 H. Seliger, A. Herold, U. Kotschi, J. Lyons and G. Schmidt, in K. S. Bruzik and W. J. Stec (Editors), *Biophosphates and Their Analogues, Synthesis, Structure, Metabolism and Activity*, Elsevier, Amsterdam, 1987, p. 43.
20 H. Seliger and G. Schmidt, *J. Chromatogr.*, 397 (1987) 141.
21 H. Schaller, G. Weimann, B. Lerch and H. G. Khorana, *J. Am. Chem. Soc.*, 85 (1963) 3821.
22 M. H. Caruthers, in H. G. Gassen and A. Lang (Editors), *Chemical and Enzymatic Synthesis of Gene Fragments*, Verlag Chemie, Weinheim, 1982, p. 71.
23 N. D. Sinha, J. Biernat, J. McManus and H. Köster, *Nucleic Acids Res.*, 12 (1984) 4539.
24 *Pharmacia–LKB Gene Assembler Plus Manual*, Pharmacia–LKB, Uppsala.

Journal of Chromatography, 541 (1991) 349–357
Elsevier Science Publishers B.V., Amsterdam

CHROM. 22 926

Enantiomeric separation of substituted 2-aryloxy propionic esters

Application to the determination of the enantiomeric excess in herbicide formulations

A. TAMBUTÉ*

Direction des Recherches et Études Techniques, Centre d'Études du Bouchet, B.P. No. 3, Le Bouchet, 91710 Vert-le-Petit (France)

and

L. SIRET, M. CAUDE and R. ROSSET

Laboratoire de Chimie Analytique de l'École Supérieure de Physique et Chimie Industrielles de Paris, 10 Rue Vauquelin, 75231 Paris Cedex 05 (France)

(First received July 13th, 1990; revised manuscript received September 12th, 1990)

ABSTRACT

The enantiomeric separation of twenty substituted 2-aryloxypropionic acid methyl esters was investigated using a π-acid chiral stationary phase derived from (*R,R*)-(N,N'-3,5-dinitrobenzoyl)-*trans*-1,2-diaminocyclohexane. Resolution factors in the range 2–4 were usually obtained. The parameters affecting the enantioselectivity (electronegativity and position of the aromatic substituents, nature and composition of the mobile phase) are discussed. Finally, the method was applied to the determination of the enantiomeric excess of an optically active herbicide formulation containing the *n*-butoxyethyl ester of 2-(4-chloro-2-methyl phenoxy)propionic acid.

INTRODUCTION

Substituted 2-aryloxypropionic acids (APAs) are the precursors of numerous herbicides produced in hundreds of thousands of tons annually [1,2]. Among them, methyl and 2-butoxyethyl (BOE) esters of 2-(4-chloro-2-methylphenoxy)propanoic acid (CMPP) and 2-(2,4-dichlorophenoxy)propanoic acid (2,4-DP) are the most important (Fig. 1).

The structure of these compounds contains an asymmetric centre, leading to two optical isomers. In the last few years, the different biological activities of each enantiomer have been evaluated, and it was found that the herbicidal activity is almost exclusively concentrated in the *R* form, the *S* form being herbicidally inactive [3].

Environmental considerations have recently led to the production and marketing of the single active *R* enantiomer. There is no doubt that this tendency will increase

0021-9673/91/$03.50

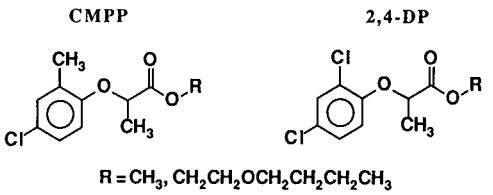

Fig. 1. Structures of CMPP and 2,4-DP esters.

in the next few years. Consequently, accurate analytical methods will be required in order to monitor the enantiomeric composition of herbicide formulations.

So far, the enantiomeric separation of numerous APA esters [methyl, ethyl, BOE, 2-ethylhexyl (EH)] has been investigated using three different chiral stationary phases (CSPs).

The resolution of a series of twenty APA methyl esters was carried out by Dernoncour and Azerad [4] using a covalently bound (*R*)-N-(3,5-dinitrobenzoyl)-phenylglycine (DNBPG) CSP. Selectivity values up to 1.26 were obtained, leading for some solutes (naphthyl derivatives) to baseline resolutions suitable for the determination of the enantiomeric excess. Similar results were also obtained by Müller and Bosshardt [3] with herbicides as methyl or BOE esters. A major contribution was made by Blessington and Crabb [1,2], who proposed a method for determining CMPP BOE and EH esters using an ionic DNBPG CSP.

Nevertheless, Müller and Bosshardt [3] claimed better results when using a Nucleosil Chiral-2 column [chiral selector based on tartaric acid and (dinitrobenzyl)-phenylethylamine]. Resolution factors in the range 2–4 were achieved for six herbicide APA esters.

Another approach was investigated by Gaffney *et al.* [5] using a Chiralcel OB CSP (cellulose tribenzoate coated on silica gel). The enantiomeric separation of 2-phenoxypropanoic acid methyl ester was carried out and was found to be closely related to the nature of the alcoholic polar modifier.

This work had a two-fold purpose: first, the ability of a CSP derived from (*R,R*)-(N,N′-3,5-dinitrobenzoyl)-*trans*-1,2-diaminocyclohexane (DACH-DNB) (Fig. 2), designed by Misiti and co-workers [6–8], to resolve a large series of 2-APA esters, and second, the determination of the enantiomeric composition of a CMPP BOE ester formulation.

EXPERIMENTAL

Apparatus

Liquid chromatography was performed using a modular liquid chromatograph (Gilson, Villiers-le-Bel, France) equipped with a Shimadzu C-R3A integrator (Touzart et Matignon, Vitry-sur-Seine, France). The standard operating conditions were flow-rate 2 ml/min UV detection at 230 nm (ethanol) or 254 nm (methylene chloride) and room temperature.

Chiral stationary phase

The structure of the DACH-DNB CSP is shown in Fig. 2. This CSP is obtained

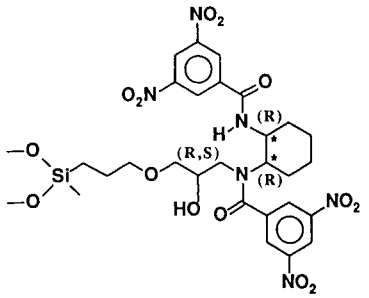

Fig. 2. Structure of the DACH-DNB CSP.

starting from 5-μm LiChrosorb Si-100 silica gel (Merck, Darmstadt, F.R.G.) modified with 3-glycidyloxypropyltrimethoxysilane [6–8]. For the present work, it was kindly provided by Professors D. Misiti and F. Gasparrini (University of Rome "La Sapienza") and packed into a 150 × 4.6 mm I.D. stainless-steel column by the classical slurry technique under 400 bar using ethanol as pumping solvent.

Mobile phase

Ethanol and hexane were of LiChrosolv grade (Merck) and methylene chloride [stabilized with 0.1% (w/w) of ethanol] of analytical-reagent grade was purchased from Prolabo (Paris, France).

Solutes

The methyl esters of APAs were kindly given by Dr. R. Azerad (Université René Descartes, Paris V, Paris, France) and the (±)- and (+)-BOE esters of CMPP and 2,4-DP by Mr. J. M. Pertuisot (Compagnie Française des Produits Industriels, Gennevilliers, France).

RESULTS AND DISCUSSION

Resolution of APA methyl esters

Chromatographic data for methyl esters are given in Table I. For each polar modifier, its content in the mobile phase (%), the capacity factor for the most retained enantiomer (k'_2), the selectivity value (α) and the resolution factor (R_s) are reported.

In all instances baseline resolution was achieved, except for nitro and carboxymethyl derivatives (solutes 16–18 and 14, respectively). The strong electron-withdrawing power of these substituents prevents the solutes from interacting with the CSP through a charge-transfer complex. It can therefore be assumed that the chiral recognition process of resolved compounds is partly governed by a π–π interaction, leading to high selctivity values for strong π-basic naphthyl derivatives.

This was evidenced for nine resolved solutes. The solutes listed in Table II differ only in the nature and/or the position of their aromatic ring substituent whose electronegativity can be quantified by a Hammet σ constant [9] (Table II). This constant was initially based on the ionization of substituted benzoic acids in water. The σ values defined by this reaction for *para* and *meta* substituents are constant characteristics of each substituent, independent of the nature of the reaction involved.

TABLE I

RESOLUTION OF APA METHYL ESTERS USING ETHANOL OR METHYLENE CHLORIDE AS POLAR MODIFIER

Column, 150 × 4.6 mm I.D.; mobile phase, *n*-hexane–ethanol or *n*-hexane–methylene chloride with ethanol and methylene chloride contents as indicated; flow-rate, 2 ml/min; UV detection at 230 nm with ethanol and 254 nm with methylene chloride; room temperature. Capacity factors k'_1 and k'_2 (for the first and the second eluted enantiomers, respectively) were calculated from the dead retention time t_0 (t_0 = 0.9 min, measured with heptane) using the equation $k' = (t_r - t_0)/t_0$. Selectivity: $\alpha = k'_2/k'_1$. Resolution: $R_s = 2(t_{r_2} - t_{r_1})/(\omega_1 + \omega_2)$ where ω is the baseline width.

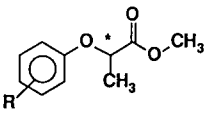

No.	R	Ethanol content (%)	k'_2	α	R_s	CH_2Cl_2 content (%)	k'_2	α	R_s
1	H	0.125	7.05	1.41	2.8	5	9.08	1.43	2.8
2	3-CH_3	0.125	9.13	1.53	4.5	5	11.69	1.55	3.8
3	4-CH_3	0.125	9.74	1.57	4.7	5	9.90	1.65	5.2
4	2-Cl	0.125	7.54	1.26	2.3	5	8.24	1.51	2.7
5	3-Cl	0.125	5.81	1.29	2.0	5	8.05	1.35	2.2
6	4-Cl	0.125	6.55	1.40	2.4	5	9.18	1.46	2.7
7	2,4-Cl	0.125	5.33	1.23	2.2	5	7.17	1.30	2.1
8	2-CH_3, 4-Cl	0.05	7.35[a]	1.32	2.6	3	5.32[a]	1.29	1.7
9	2,4,5-Cl	0.125	4.26	1.18	1.6	5	5.33	1.24	1.5
10	2-OCH_3	1.25	6.55	1.18	1.8	15	7.47	1.36	2.6
11	3-OCH_3	1.25	5.05	1.20	2.0	15	5.55	1.50	2.8
12	4-OCH_3	1.25	5.61	1.24	2.2	15	6.67	1.48	2.6
13	2-$COOCH_3$	1.25	11.60	1.11	1.3	15	14.53	1.19	1.3
14	3-$COOCH_3$	1.25	7.66	1.10	0.92[b]	15	8.74	1.20	1.5
15	4-$COOCH_3$	1.25	9.26	1.13	1.3	15	11.02	1.29	2.1
16	2-NO_2	1.25	10.70	1.04	0.36[b]	15	15.75	1.13	1.4
17	3-NO_2	1.25	5.77	1	0	15	7.50	1	0
18	4-NO_2	1.25	9.08	1	0	15	14.29	1.07	0.67[b]
19	1-Naphthyl	1.25	6.73	1.31	2.6	15	6.55	1.75	4.8
20	2-Naphthyl	1.25	10.03	1.81	6.8	15	11.00	2.71	6.3

[a] *R*(+) enantiomer eluted first.

[b] For a pair of partially resolved peaks the value was calculated as (mean of peak heights − trough to baseline height)/mean of peak heights.

For any process, σ provides a measure of the total electronic influence of the substituent (polarity, electronegativity) [9,10]. The more electron-withdrawing the substituent, the higher is the value assigned to it. Accordingly, the σ value is a convenient means for determining the π-basicity or the π-acidity of a given aromatic ring and hence the magnitude of a charge transfer complex.

In Fig. 3, the logarithms of the selectivity values of compounds 1, 2, 3, 5, 6, 11, 12, 14 and 15 are plotted *versus* the Hammet σ values of their substituents. A similar experiment was carried out for the enantiomeric separation of N-arylsulphinamoyl acetates on a CSP derived from tyrosine [11]. A good correlation between log α and σ was obtained when using hexane–ethanol (99:1, v/v) as the mobile phase. The π–π interaction may thus be considered as the driving force of the chiral recognition

TABLE II

HAMMET σ VALUES ACCORDING TO REF. 9

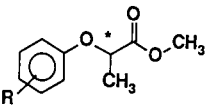

Solute	R	σ
1	H	0
2	3-CH_3	−0.069
3	4-CH_3	−0.17
11	3-OCH_3	0.115
12	4-OCH_3	−0.268
5	3-Cl	0.373
6	4-Cl	0.227
14	3-$COOCH_3$	0.32
15	4-$COOCH_3$	0.39

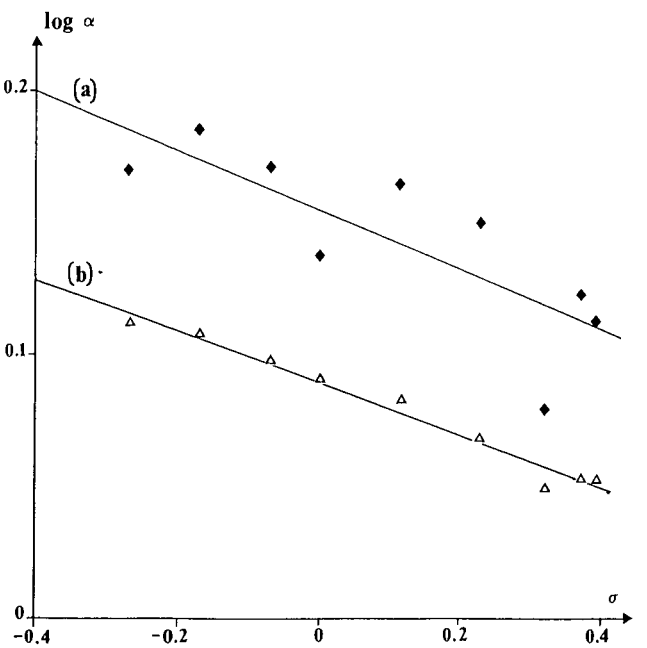

Fig. 3. Variation of log α with Hammet σ values (Table II) for compounds 1, 2, 3, 5, 6, 11, 12, 14 and 15 using (a) methylene chloride (15% in *n*-hexane) or (b) ethanol (1% in *n*-hexane) as polar modifier. Flow-rate, 2 ml/min; room temperature; UV detection at (a) 254 nm and (b) 230 nm.

mechanism. On the other hand, when using hexane–methylene chloride (85:15, v/v) as the mobile phase, this interaction seems to be of less importance (a poor correlation is obtained). The interactions between amide dipoles (hydrogen bonding or dipole stacking) prevail over the π–π interaction, probably because of their weaker solvation by methylene chloride than by ethanol. A similar conclusion was previously reached for N-arylsulphinamoyl acetates [11].

According to Table I, the retention of *ortho*-proton acceptor-substituted compounds (OCH_3, $COOCH_3$) is higher than that for the corresponding *para*- and *meta*-substituted compounds (solutes 10–15). Assuming that the polarities and the electronegativities of *ortho*- and *para*-substituted compounds are similar, it can be inferred that an additional hydrogen bonding takes place between the *ortho* substituent and a proton-donor site of the CSP. The only proton-donor site in the vicinity of the 3,5-DNB moiety of the CSP is the amidic proton. This is assumed to be involved in hydrogen bonding with the ethereal oxygen atom of the solute. This interaction is highly enantioselective as it hinders the free rotation around the C–O bond. The presence of a proton-acceptor substituent in the *ortho* position may compete with the formation of this interaction, leading to smaller selectivity values (Table I), especially with methylene chloride.

Selectivity was found to be dependent on the content of polar modifier in the mobile phase. In Fig. 4, the selectivity values obtained for solute 2 (R = 3-CH_3) are

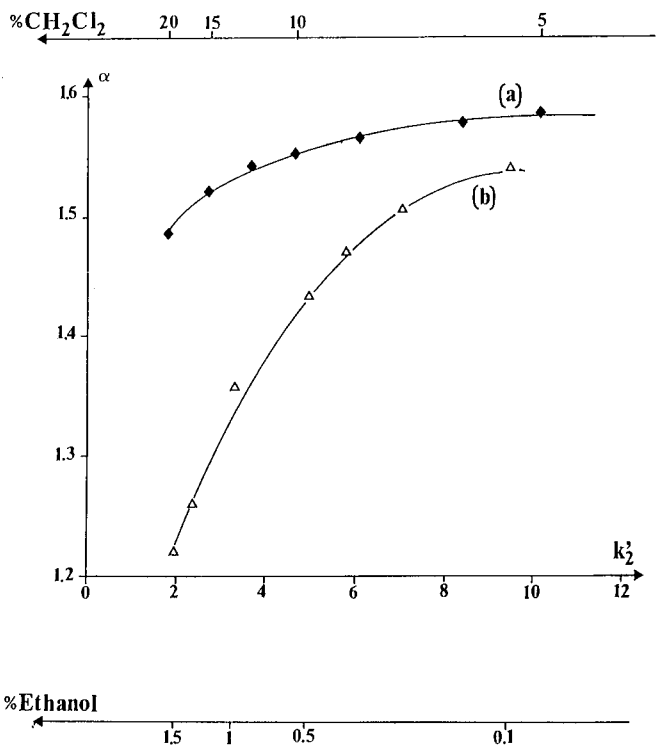

Fig. 4. Variation of α with k'_2 for solute 2 (R = 3-CH_3) using (a) methylene chloride (range 5–20%) or (b) ethanol (range 0.1–1.5%) as polar modifier in *n*-hexane. Other operating conditions as in Fig. 3.

plotted *versus* the capacity factor of the most retained enantiomer in the range 1–10. As reported previously for π-basic Pirkle-type CSPs [11,12], methylene chloride affords a greater enantioselectivity than ethanol. According to Pescher *et al.* [12], this phenomenon can be correlated with the fact that the amide dipoles of the CSP are more easily solvated by alcohols than by chlorinated solvents. Therefore, CSP–solute interactions are maximized when using the latter. According to Fig. 4, the enantioselectivity is much more affected by the ethanol content [$\Delta\alpha/\Delta k'_2 = 3.9\%$ and $\Delta\alpha/\Delta$(ethanol content) = 22.3%] than by methylene chloride [$\Delta\alpha/\Delta k'_2 = 1.2\%$ and $\Delta\alpha/\Delta$(methylene chloride content) = 0.7%]. Assuming that ethanol acts as a strong proton donor and/or acceptor and methylene chloride rather as a strong dipole, it can be inferred that the chiral recognition process involves hydrogen bonding rather than dipole stacking.

From the structure of APA methyl esters, three potential sites of interaction are evidenced (Fig. 5): the aromatic ring suitable for a π–π interaction, the ethereal oxygen atom (proton acceptor) and the ester function, which may be considered rather as a proton-acceptor site than as a dipole.

According to the above-mentioned statements, a π–π interaction and hydrogen bonding are involved in the chiral recognition. It can therefore be inferred that a 3,5-dinitrophenyl moiety and the proton-donor sites (amidic and hydroxyl proton) of the CSP are involved in the chiral recognition process.

Resolution of MCPP BOE ester

The second aspect of this work was the enantiomeric separation of MCPP BOE ester in order to determine its enantiomeric excess in a commercially available formulation. According to the above-mentioned chromatographic data, this separation should have been carried out using methylene chloride. Unfortunately, the formulation contains a second active constituent of high polarity, which is hardly eluted with methylene chloride. Consequently, the separation was better achieved using ethanol as polar modifier (0.125%, flow-rate 2 ml/min). The results obtained were $k'_2 = 6.87$, $\alpha = 1.34$ and $R_s = 3.1$. The complete separation is shown in the Fig. 6. The various additives (eluted within 4 min) and the second active constituent (eluted at 22 min) do not interfere with CMPP BOE ester enantiomers (eluted at 6 and 8 min).

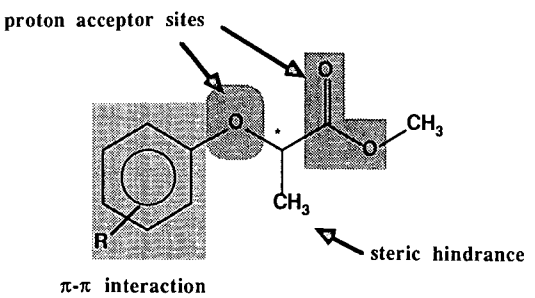

Fig. 5. Potential sites of interaction of APA methyl esters.

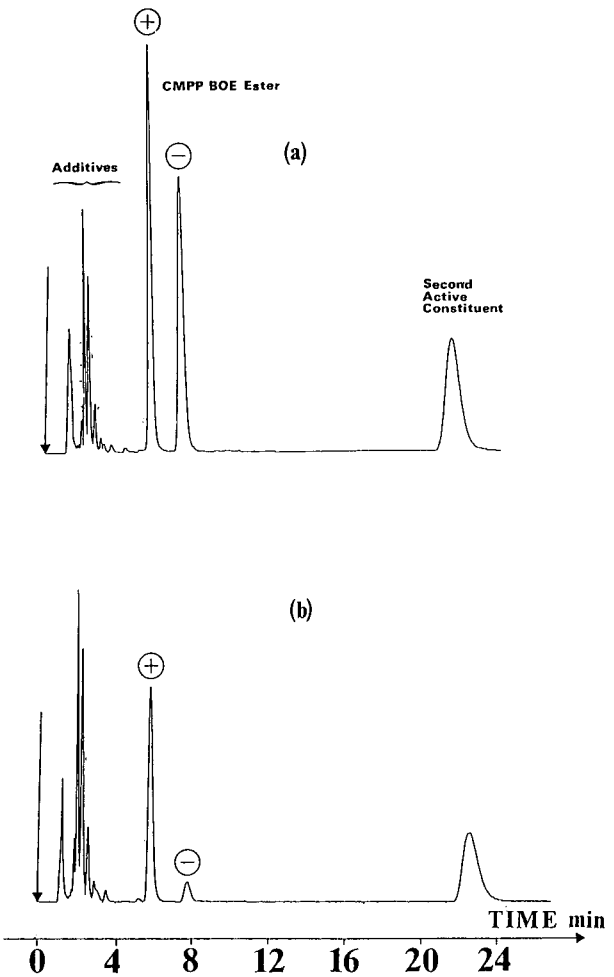

Fig. 6. Determination of the enantiomeric excess (e.e.) in a CMPP BOE ester formulation using a DACH-DNB CSP. Mobile phase, *n*-hexane–ethanol (99.875:0.125, v/v); flow-rate, 2 ml/min; room temperature; UV detection at 254 nm. (a) Racemic mixture; (b) e.e. = 75.4%.

CONCLUSION

The ability of the DACH-DNB CSP to resolve APA esters has been demonstrated. The selectivity values and resolution factors afforded by this CSP were higher than those reported previously for either ionic or covalent DNBPG [2,4]. We consider that the scope of application of this CSP is complementary to those of DNPG and CSPs derived from tyrosine. In fact, the DACH-DNB CSP affords a high enantioselectivity towards small molecules which are not or only poorly resolved on other Pirkle-type π-acid CSPs.

The chiral recognition mechanism involves a π–π interaction and hydrogen bondings. Enantioselectivity was found to be very sensitive to the electronegativity and

the position of the aromatic ring substituents when using ethanol and also to the polar modifier content in the mobile phase.

The enantiomeric separation of MCPP BOE ester was performed using a DACH-DNB CSP ($R_s = 3.1$). This method allows the determination of its enantiomeric excess in commercially available optically active formulations, such as those reported previously by Blessington and Crabb [2].

ACKNOWLEDGEMENTS

The authors express their grateful thanks to Dr. D. Misiti and F. Gasparrini (University of Rome "La Sapienza") for the gift of the chiral stationary phase, to Dr. R. Azerad (Université, René Descartes, Paris V) and to Mr. J. M. Pertuisot (C.F.P.I.) for gifts of solutes.

REFERENCES

1 B. Blessington and N. Crabb, *J. Chromatogr.*, 454 (1988) 450.
2 B. Blessington and N. Crabb, *J. Chromatogr.*, 483 (1989) 349.
3 M. D. Müller and H. P. Bosshardt, *J. Assoc. Off. Anal. Chem.*, 71 (1988) 614.
4 R. Dernoncour and R. Azerad, *J. Chromatogr.*, 410 (1987) 355.
5 M. H. Gaffney, R. M. Stiffin and I. W. Wainer, *Chromatographia*, 27 (1989) 15.
6 G. Gargaro, F. Gasparrini, D. Misiti and C. Villani, presented at the *10th International Symposium on Column Liquid Chromatography, San Francisco, CA, May 18–23, 1986.*
7 G. Gargaro, F. Gasparrini, D. Misiti, G. Palmieri, M. Pierini and C. Villani, *Chromatographia*, 24 (1987) 505.
8 F. Gasparrini, D. Misiti and C. Villani, *Ital. Pat.*, 21584A/89, 1989.
9 A. J. Gordon and R. A. Ford (Editors), *The Chemist's Companion: a Handbook of Practical Data, Techniques, and References*, Wiley, New York, 1972, pp. 145–147.
10 O. A. Reutov, in T. J. Katz (Editor), *Fundamentals of Theoretical Organic Chemistry*, Appleton Century Crofts, New York, 1967, pp. 364–365.
11 L. Siret, A. Tambuté, M. Caude and R. Rosset, *J. Chromatogr.*, 498 (1990) 67.
12 P. Pescher, M. Caude, R. Rosset and A. Tambuté, *J. Chromatogr.*, 371 (1986) 159.

Journal of Chromatography, 541 (1991) 359–364
Elsevier Science Publishers B.V., Amsterdam

CHROM. 22 956

Screening method for phenoxy acid herbicides in ground water by high-performance liquid chromatography of 9-anthryldiazomethane derivatives and fluorescence detection

TOSHINARI SUZUKI* and SATORU WATANABE

Tama Branch Laboratory, Tokyo Metropolitan Research Laboratory of Public Health, 3–16–25, Shibazaki-cho, Tachikawa, Tokyo 190 (Japan)

(First received April 3rd, 1990; revised manuscript received October 22nd, 1990)

ABSTRACT

A high-performance liquid chromatographic (HPLC) method for phenoxy acid herbicides using precolumn derivatization with 9-anthryldiazomethane (ADAM) is presented. The phenoxy acid herbicides investigated were (2,4-dichlorophenoxy)acetic acid, (4-chloro-2-methylphenoxy)acetic acid, 2-(4-chloro-2-methylphenoxy)propionic acid and (4-chloro-2-methylphenoxy)butyric acid. These herbicides reacted with ADAM under mild conditions and were converted into the corresponding fluorescent derivatives. The ADAM derivatives were separated by reversed-phase HPLC and determined using a fluorescence detector. The detection limits were about 500 pg per injection. For the application of ADAM to the determination of these herbicides in ground waters, the recoveries were more than 93% and the average relative standard deviation was 6.0% at 0.5 μg/l. The procedure is useful as a screening method for phenoxy acid herbicides in ground water samples.

INTRODUCTION

Phenoxy acid herbicides are used worldwide in agriculture and forestry for controlling the presence of broad-leaf weeds. In Japan, large amounts of the herbicides, especially (2,4-dichlorophenoxy)acetic acid (2,4-D), (4-chloro-2-methylphenoxy)acetic acid (MCPA), 2-(4-chloro-2-methylphenoxy)propionic acid (MCPP) and (4-chloro-2-methylphenoxy)butyric acid (MCPB), are scattered at golf courses, and it is suspected that these compounds may be leached from the soil into the local ground waters. Therefore, if such ground waters are to be supplied as drinking water, it is necessary to screen them for contamination by these herbicides.

Phenoxy acid herbicides in environmental water samples have been determined by gas chromatography (GC) [1–4] and high-performance liquid chromatography (HPLC) [5–13]. For GC analysis, the compounds must generally be derivatized because of their high polarity and low volatility. Many derivatization procedures, such as esterification [1,2] and silylation [3,4], have been reported.

On the other hand, for the determination of phenoxy acid herbicides by HPLC, no derivatization approach has been reported. Detection has been mainly based on the poor selectivity of UV detection at 230 or 280 nm [5–11], because many of the

0021-9673/91/$03.50

compounds absorb at these wavelengths. Therefore, in order to detect these herbicides in water samples at concentrations lower than 1.0 μg/l, sample enrichment and purification by means of a selective solid-phase extraction cartridge [6] or a complicated HPLC system with on-line column-switching valves [8,9] are needed. As the phenoxy acid herbicides contain carboxyl groups, we considered their precolumn fluorescence labelling for a sensitive and selective HPLC assay.

9-Anthryldiazomethane (ADAM) was developed by Nimura and Kinoshita [14] as a fluorescent reagent for fatty acids. This reagent reacts with carboxyl groups under mild conditions without a catalyst and permits the highly sensitive and selective detection of fatty acids by HPLC. ADAM has been applied to the determination of acidic biological compounds such as prostaglandins [15], carnitine [16] and fatty acids [17].

In this paper, we report the application of ADAM to the determination of 2,4-D, MCPA, MCPP and MCPB by reversed-phase HPLC and the evaluation of a screening method utilizing ADAM for these herbicides in ground water samples.

EXPERIMENTAL

Materials

2,4-D, MCPP were purchased from Gasukuro Kogyo, ADAM from Funakoshi Chemical and 9-hydroxymethylanthracene from Tokyo Kasei Kogyo (all Tokyo, Japan). Oxalyl chloride, silica gel, all organic solvents and other compounds were obtained from Wako (Osaka, Japan). (4-Chloro-2-methylphenoxy)butyric acid (MCPB) was supplied as the herbicide Tropotox (Nissan Kagaku Kogyo, Tokyo, Japan) and extracted and purified in our laboratory.

Instruments

Proton nuclear magnetic resonance (^{1}H NMR) spectra were obtained on a Model JNM-FX270 NMR spectrometer (JEOL, Tokyo, Japan) at 270 MHz. Mass spectra were measured with a Model JMS-D300 mass spectrometer (JEOL). The HPLC system consisted of a Model 880-PU pump (Jasco, Tokyo, Japan), a Model 7125 injector with a 20-μl loop (Rheodyne, Cotati, CA, U.S.A.) and a Model 820-FP spectrofluorimeter (Jasco), which was connected to a Model CR-6A chromatographic integrator (Shimadzu, Kyoto, Japan).

Preparation of ADAM derivatives of phenoxy acid herbicides

To 0.25 mmol of phenoxy acid herbicide were added 10 ml of a solution containing 0.25 mmol of ADAM in acetone. The mixture was allowed to stand in the dark for 4 h at 40°C, then evaporated to dryness with a rotary evaporator at 40°C. The residue was purified on a silica gel column with *n*-hexane–ethyl acetate (95:5) as eluent. The main fraction was evaporated to dryness and the residue was purified by recrystallization from *n*-hexane–ethyl acetate. The crystals obtained were used for ^{1}H NMR and mass spectrometric analysis. Chemical shift values (δ) in deuterochloroform were expressed in parts per million downfield from tetramethylsilane as internal standard.

Derivatization of phenoxy acid herbicides for HPLC

Phenoxy acid herbicides for working standards were prepared as solutions in acetone. An aliquot (1–500 ng) was dispensed into a 5-ml minivial and evaporated to dryness in a stream of nitrogen. To the residue were added 100 μl of a solution containing 0.025% ADAM in acetone. The reaction mixture was heated in the dark for 60 min at 40°C and then dried in a stream of nitrogen. The residue was dissolved in 75 μl of acetone and 15 μl of the solution were applied to the HPLC system.

Chromatographic conditions

The ADAM derivatives of the acid herbicides were separated by using a TSK-gel ODS120T reversed-phase column (25 cm × 4.6 mm I.D.) (Tosoh, Tokyo, Japan). The eluent was acetonitrile–water (75:25) containing 3% tetrahydrofuran, at a flow-rate of was 1.0 ml/min. The detection wavelengths were adjusted to 365 nm excitation and 412 nm emission.

Determination of phenoxy acid herbicides in ground water

A 20-ml volume of ground water was taken in a 25-ml glass-stoppered test-tube, 100 μl of concentrated hydrochloric acid (35%) were added and the phenoxy herbicides were extracted three times by vigorously shaking for 1 min with 2 ml of *n*-hexane–ethyl acetate (20:80). The extracts were collected and concentrated to *ca.* 0.5 ml with a rotary evaporator at 40°C. The resulting solution was transferred to a 5-ml minivial and evaporated to dryness in a stream of nitrogen. The derivatization with ADAM was performed as described above.

RESULTS AND DISCUSSION

Confirmation of ADAM derivatives of phenoxy acid herbicides

The structures of the ADAM derivatives of 2,4-D, MCPA, MCPP and MCPB shown in Fig. 1 were investigated. As an example, The ^{1}H NMR spectral data for the ADAM derivative of MCPP were as follows: δ 1.57 (3H,d,J = 6.60 Hz), 2.06 (3H,s), 4.69 (1H,q,J = 6.60 Hz), 6.18 (2H,s), 6.41 (1H,d,J = 8.57 Hz), 6.74 (1H,dd,J = 2.64, 8.57 Hz), 6.93 (1H,d,J = 2.64 Hz), 7.45–7.55 (4H,m), 8.02 (2H,m), 8.19 (2H,m), 8.50 ppm (1H,s). The methylene protons at the 9-position appeared at 6.18 ppm, which is in good agreement with the value of 6.19 ppm calculated by the method of Shoolery [18].

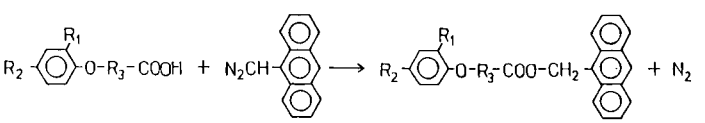

Phenoxy Acid Herbicides ADAM Esters

	R_1	R_2	R_3
2,4-D	Cl	Cl	CH_2
MCPA	CH_3	Cl	CH_2
MCPP	CH_3	Cl	$CH(CH_3)$
MCPB	CH_3	Cl	CH_2-CH_2-CH_2

Fig. 1. Reaction course of phenoxy acid herbicides with ADAM.

These results indicate a 9-anthrylmethyl ester bond in the derivative. The methylene protons at the 9-position of the ADAM derivatives of 2,4-D, MCPA and MCPB appeared at 6.28 (2H,s), 6.26 (2H,s) and 6.16 ppm (2H,s), respectively. No alteration of the signals other than that of the 9-position in the ^{1}H NMR spectrum was observed after derivatization with ADAM for all the ADAM derivatives of the herbicides.

The mass spectra of the ADAM derivatives of MCPP, 2,4-D, MCPA and MCPB showed the molecular ion (M^+) at *m/z* 404, 410, 390 and 418, respectively. For all ADAM derivatives of the herbicides, the base peak appeared at *m/z* 191; the peak is [9-anthryl–CH_2]$^+$ generated by fragmentation of the 9-anthrylmethyl group.

Further confirmation of the ADAM derivatives of the phenoxy acids was performed. The ^{1}H NMR and mass spectra of each 9-anthrylmethyl ester synthesized with 9-hydroxymethylanthracene and the acid chlorides of 2,4-D, MCPA, MCPP and MCPB, formed by treatment with oxalyl chloride were in good agreement with the spectra of the corresponding derivatives with ADAM (data not shown).

From these results, it is obvious that the phenoxy acid herbicides reacted with ADAM to form the corresponding 9-anthrylmethyl esters as shown in Fig. 1.

Derivatization of phenoxy acid herbicides for HPLC

The optimum conditions were examined for a reaction volume of 100 μl containing 100 ng of 2,4-D, MCPA, MCPP and MCPB. We first investigated the reaction solvents, using acetone, ethyl acetate and methanol. The fluorescence response of the ADAM ester of each of the four herbicides was the highest with acetone, and the average relative standard deviation (R.S.D.) was 2.4% ($n = 5$). The reaction of the herbicides with 0.025% ADAM at 40°C progressed more than 90% in 15 min and was completed within 60 min. Concentrations of the ADAM–acetone solution of 0.025, 0.05 and 0.1% were examined. The sensitivities of the four herbicides did not change with these concentrations. With 0.1% ADAM solution, the baseline rose owing to the impurities present in the ADAM reagent, hence it was unsuitable when determining a few nanograms of the phenoxy acid herbicides. From the above results, the optimum conditions were fixed as indicated under Experimental.

Chromatographic separation of the ADAM derivatives of phenoxy acid herbicides

A typical chromatogram of the ADAM derivatives of 2,4-D, MCPA, MCPP and MCPB is shown in Fig. 2. The four ADAM derivatives could be separated without clean-up after the derivatization with ADAM. The peaks in front of the peak of 2,4-D were always observed, regardless of the presence of the acid herbicides. The calibration graphs of each of the four herbicides, of amount of herbicide *versus* peak height of the fluorescent response, showed excellent linearity in the range 1.0–100 ng per injection and passed through the origin ($r = 0.998$–0.999). The detection limits of the herbicides under the optimum conditions were about 500 pg per injection (signal-to-noise ratio = 3).

Application to the determination of phenoxy acid herbicides in ground water

Ground water samples spiked with 2,4-D, MCPA, MCPP and MCPB at the 0.5 and 5.0 μg/l levels were extracted with *n*-hexane–ethyl acetate *ca.* pH 1.5. The recoveries of the four herbicides were more than 93% at both levels examined and the average R.S.D. was 6.0% ($n = 5$). These results indicated that the method gave high

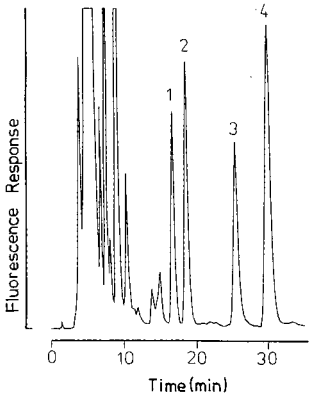

Fig. 2. HPLC separation of the ADAM derivatives of phenoxy acid herbicides. Peaks: 1 = 2,4-D (20 ng); 2 = MCPA (20 ng); 3 = MCPP (20 ng); 4 = MCPB (20 ng per injection). A mixture of the four herbicides (100 ng of each) was esterified with 100 μl of 0.025% ADAM and a 15-μl aliquot from 75 μl was injected.

recoveries and good reproducibility. Under the routine detection conditions used, moreover, the method could determine the phenoxy acid herbicides at concentrations down to 0.2 μg/l (signal-to-noise ratio = 5). These detection limits could be improved by sample pretreatment involving solid-phase extraction with an anion exchanger or a reversed-phase sorbent, and further study of this aspect is required. The chromatogram obtained on sampling 20 ml of a ground water spiked with 0.5 μg/l concentrations of each herbicide is shown in Fig. 3. Clean-up of the extracts from the water sample was unnecessary.

Under the extraction conditions, most acid compounds such as fatty acids and other analogues of phenoxy acid herbicides can be extracted and subjected to reaction with ADAM. For fatty acids, the ADAM derivatives of *n*-butyric, *n*-caproic and

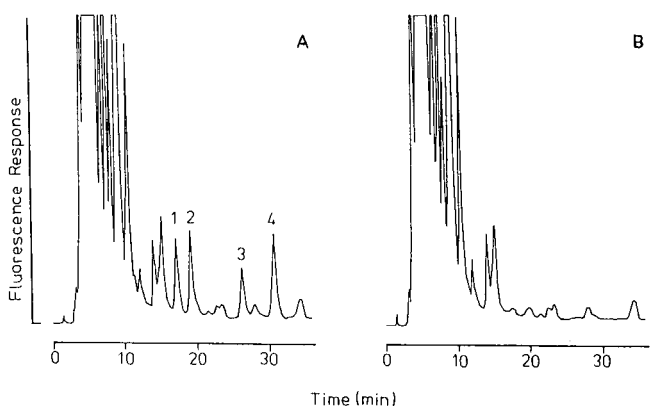

Fig. 3. Chromatograms of ground water extracts treated with ADAM. (A) Ground water sample spiked with 0.5 μg/l concentrations of phenoxy acid herbicides. Numbers on the peaks correspond to those in Fig. 2. (B) Blank ground water sample.

n-caprylic acid were detected at 14.2, 20.4, and 38.0 min, respectively, and under the chromatographic conditions used they were separated from the ADAM derivatives of the four herbicides. The investigation of other phenoxy herbicides is in progress.

In conclusion, the proposed procedure is useful as a rapid screening method for the presence of the herbicides in ground water. By sampling 20 ml of a ground water sample, the method can determine phenoxy acid herbicides at levels lower than 0.5 μg/l.

ACKNOWLEDGEMENT

Tropotox, a herbicide of MCPB, was a generous gift from Nissan Kagaku Kogyo.

REFERENCES

1 W. P. Cochrane, *J. Chromatogr. Sci.*, 13 (1975) 246.
2 W. P. Cochrane, *J. Chromatogr. Sci.*, 17 (1979) 124.
3 M. J. Bertrand, A. W. Ahmed, B. Sarrasin and V. N. Mallet, *Anal. Chem.*, 59 (1987) 1302.
4 A. W. Ahmed, V. N. Mallet and M. J. Bertrand, *J. Assoc. Off. Anal. Chem.*, 72 (1989) 365.
5 S. H. Hoke, E. E. Brueggmann, L. J. Baxter and T. Trybus, *J. Chromatogr.*, 357 (1986) 429.
6 A. Di Corcia, M. Marchetti and R. Samperi, *Anal. Chem.*, 61 (1989) 1363.
7 R. B. Grorud and J. E. Forrette, *J. Assoc. Off. Anal. Chem.*, 67 (1984) 837.
8 R. Hamann and A. Kettrup, *Chemosphere*, 16 (1987) 527.
9 R. B. Geerdink, C. A. A. Van Balkom and H.-J. Brouwer, *J. Chromatogr.*, 481 (1989) 275.
10 M. J. M. Wells and J. L. Michael, *Anal. Chem.*, 59 (1987) 1739.
11 M. Åkerblom, *J. Chromatogr.*, 319 (1985) 427.
12 R. L. Smith and D. J. Pietrzyk, *J. Chromatogr. Sci.*, 21 (1983) 282.
13 M. Fayyad, M. Alawi and T. El-Ahmad, *J. Chromatogr.*, 481 (1989) 439.
14 N. Nimura and T. Kinoshita, *Anal. Lett.*, 13 (1980) 191.
15 M. Hatsumi, S. Kimata and K. Hirosawa, *J. Chromatogr.*, 253 (1982) 271.
16 T. Yoshida, A. Aetake, H. Yamaguchi, N. Nimura and T. Kinoshita, *J. Chromatogr.*, 445 (1988) 175.
17 N. Ichinose, S. Abe, Y. Akishige, H. Yoshimura and K. Adachi, *Fresenius' Z. Anal. Chem.*, 329 (1987) 47.
18 J. N. Shoolery, *Technical Information Bulletin*, Vol. 2, No. 3, Varian Assoc., Palo Alto, CA.

Journal of Chromatography, 541 (1991) 365–373
Elsevier Science Publishers B.V., Amsterdam

CHROM. 22 976

Rapid and sensitive determination of phenylurea herbicides in water in the presence of their anilines by extraction with a Carbopack cartridge followed by liquid chromatography

ANTONIO DI CORCIA* and MARCELLO MARCHETTI
Dipartimento di Chimica, Università "La Sapienza" di Roma, Piazza Aldo Moro 5, 00185 Rome (Italy)
(First received May 22nd, 1990; revised manuscript received November 14th, 1990)

ABSTRACT

A rapid and sensitive method for determining phenylurea herbicides in environmental aqueous samples in the presence of their anilines is described. The water sample is preconcentrated by passage at a flow-rate of *ca.* 150 ml/min through a 250-mg graphitized carbon black (Carbopack B) cartridge. After washing with 0.6 ml of methanol, the Carbopack B trap is connected with a cartridge containing a strong cation exchanger. Organics trapped by the Carbopack cartridge are eluted by passage of 6 ml of methylene chloride–methanol (95:5, v/v). Anilines and other basic compounds are quantitatively substracted from the solvent system while flowing through the cation-exchange cartridge. After evaporation and redissolution, the sample is subjected to reversed-phase gradient elution high-performance liquid chromatography with UV detection at 250 nm. Recoveries of phenylureas added to water at levels between 30 and 3000 ng/l were higher than 92%. The limit of detection was about 1 ng/l, for a 2-l sample. With respect to an octadecyl (C_{18})-bonded silica cartridge, the Carbopack B cartridge had a far better extraction efficiency for polar phenylureas.

INTRODUCTION

Substituted phenylureas are selective herbicides used extensively in agriculture and are fairly persistent in the aquatic environment. This has led to the development of many analytical procedures for determining phenylurea residues in aqueous samples. Mostly gas chromatography [1–3] and liquid chromatography [4–8] have been used.

A particular problem which may be encountered in determining phenylureas is the simultaneous presence in water of their degradation products, *i.e.*, anilines, which can interfere with the determination of the parent pesticides. Goewie *et al.* [5] succeeded in eliminating anilines from the aqueous samples by adopting a special platinum phase packed in a short precolumn.

Carbopack B is a graphitized carbon black (GCB) which has proved to be a valuable material for the liquid–solid extraction (LSE) of organochlorine insecticides [9,10] and triazine [11,12] and phenoxy acid [13] herbicides from water. Carbopack B cartridges proved to be more efficient than commonly used octadecyl (C_{18})-bonded silica cartridges for the LSE of phenols [14] and chloroanilines [15].

0021-9673/91/$03.50

This paper describes a sensitive and rapid procedure for determining residues of phenylureas in drinking and surface waters in the presence of their anilines. The method first involves LSE of phenylureas by a Carbopack cartridge. The eluate is then passed through a strong cation exchanger to remove anilines and other bases prior to evaporation, redissolution and measurement by high-performance liquid chromatography (HPLC). Concentration factors of more than 6000 allowed the detection of phenylureas at concentrations of about 1 ng/l.

EXPERIMENTAL

Reagents and chemicals

Authentic phenylureas were purchased from both Riedel-de Haën (Seelze, Germany) and Eurobase (Milan, Italy): fenuron (N′-phenyl-N,N-dimethylurea); metoxuron (N′-3-chloro-4-methoxyphenyl-N,N-dimethylurea); monuron (N′-4-chlorophenyl-N,N-dimethylurea); monolinuron (N′-4-chlorophenyl-N-methoxy-N-methylurea); fluometuron (N′-3-fluoromethylphenyl-N,N-dimethylurea); chlortoluron (N′-3-chloro-4-methylphenyl-N,N-dimethylurea); metobromuron (N′-4-bromophenyl-N-methoxy-N-methylurea); difenoxuron (N′-4-methoxy-4-phenoxyphenyl-N,N-dimethylurea); isoproturon (N′-4-isopropylphenyl-N,N-dimethylurea); diuron (N′-3,4-dichlorophenyl-N,N-dimethylurea); linuron (N′-3,4-dichlorophenyl-N-methoxy-N-methylurea); chlorbromuron (N′-3-chloro-4-bromophenyl-N-methoxy-N-methylurea); chlorouxoron (N′-4-chloro-4-phenoxyphenyl-N,N-dimethylurea); and neburon (N-3,4-dichlorophenyl-N-butyl-N-methylurea). Individual standard solutions were prepared by dissolving 100 mg of each herbicide in 100 ml of methanol. A composite working standard solution was prepared by mixing 0.5 ml of each standard solution and diluting to 100 ml with methanol.

Except for 4-chloroaniline and 3,4-dichloroaniline, anilines of interest were prepared from the corresponding phenylureas by catalytic hydrolysis on silica [3].

For HPLC, distilled water was further purified by passing it through a Norganic cartridge (Millipore, Bedford, MA, U.S.A.). Acetonitrile and methanol of HPLC grade were obtained from Carlo Erba (Milan, Italy). All other solvents were of analytical-reagent grade (Carlo Erba) and were used as supplied.

Apparatus

A 250-mg amount of Carbopack B (120–400 mesh) (Supelco, Bellefonte, PA, U.S.A.) was packed in a polypropylene tube (6 cm × 1.4 cm I.D.) (Supelco). A 200-mg amount of Amberlite CG-120-I (100–200 mesh) (Fluka, Buchs, Switzerland) was packed in a plastic tube (6 cm × 0.5 cm I.D.) (Supelco). Polyethylene frits (20-μm pore size) (Supelco) were located above and below each sorbent bed. To avoid crushing of the Carbopack B particles, which results in a decrease in the permeability of the cartridge, the upper frit was gently rested above the sorbent bed. The connection between the two cartridges was made with a plastic adapter (Supelco). Before use, the Carbopack cartridge was washed sequentially with 4 ml of methylene chloride–methanol (95:5, v/v), 2 ml of methanol and 6 ml of water. The cation-exchange material was converted from the Na^+ to the H^+ form by washing it with 10 ml of 1 mol/l hydrochloric acid, 3 ml of water and 3 ml of acetonitrile. This cartridge was reused several times by restoring it with 2.5 ml of 1 mol/l methanolic potassium

hydroxide solution to elute trapped basic compounds, followed by 2 ml of water. From this point, the same sequence as reported above was followed to activate the cation exchanger cartridge. The Carbopack B cartridge was fitted into a side-arm filtering flask and liquids were forced to pass through the cartridge by vacuum (water pump).

Procedure

Aquous samples were fortified with known volumes of the composite working standard solution of phenylureas. When analysing hypochlorite-containing tap water samples, hypochlorite was reduced in advance by adding 0.4 g/l of sodium sulphite to avoid oxidation of the analytes. Water samples were then shaken for 1 min and, after 10 min, poured into a glass reservoir which was connected to the Carbopack cartridge. When necessary, after supplying surface water samples with the analytes, they were filtered through Whatman GF/C glass-fibre pads (pore size 10 μm) to remove algae and debris. Water was forced to pass through the cartridge at flow-rates of 130–150 ml/min. Just after the sample had passed through the column, the cartridge was filled with 6 ml of distilled water, which was allowed to pass through the cartridge at a flow-rate of 10–20 ml/min. This operation serves to eliminate drops of sample water adhering to the plastic walls of the cartridge, whose presence can decrease the efficiency of the organic solvent system used for desorbing the analytes.

Following the passage of large water volumes, some shrinkage of the sorbent bed may occur. In such an event, before washing with distilled water, the upper frit was pushed against the top of the sorbent bed. This expedient facilitates the subsequent removal of water from the sorbent bed and improves the effectiveness of the eluent system as it can permeate the sorbent bed more homogeneously.

After the distilled water had passed through the trap, most of it was removed by reducing to the minimum the pressure in the flask for 30 s. The water pump was then disconnected, 0.6 ml of methanol was poured into the cartridge, the pump was linked to the flask again and methanol was passed slowly through the sorbent bed to eliminate residual water. Thereafter, the Carbopack cartridge was connected to the cation exchanger, a conical glass vial was located below the two cartridges and the pesticides were eluted with 6 ml of methylene chloride–methanol (95:5, v/v) at a flow-rate of about 2 ml/min). The last drops of the eluent system were collected by using the vacuum. The extract was dried in a water-bath at 40°C under a stream of nitrogen and the residue was reconstituted with 0.3 ml of water–methanol (60:40, v/v). A 50-μl volume of this solution was injected into the HPLC apparatus.

HPLC apparatus

A Model 5000 liquid chromatograph (Varian, Walnut Creek, CA, U.S.A.) equipped with a Rheodyne Model 7125 injector having a 50-μl loop with a Model 2550 UV detector (Varian) was used, with a 25 cm × 4.6 mm I.D. column filled with 5-μm LC-18 reversed-phase packing (Supelco). The organic modifier was methanol–acetonitrile (85:15, v/v). Gradient elution of phenylureas was performed by increasing linearly the percentage of the organic modifier from 47% to 70% in 20 min. Phenylureas were detected with the UV detector set at 250 nm.

The concentrations of the herbicides in water samples were calculated by comparing the heights of the peaks obtained with the sample and with a standard solution. The latter was prepared by drying a known volume of the composite working standard solution and dissolving the residue in 0.3 ml of water–methanol (60:40, v/v).

RESULTS AND DISCUSSION

Chromatographic conditions

Reversed-phase HPLC fractionation of phenylureas was performed using a concave gradient with methanol as organic modifier [16]. Under the same chromatographic conditions as above, but using an HPLC column from a different manufacturer, we observed that chlortoluron and metobromuron were eluted as a single peak and isoproturon and diuron were poorly separated from each other.

In order to fractionate the fourteen phenylureas considered, the effect of various methanol–acetonitrile mixtures as organic modifiers on the relative retention of the analytes was studied. The results are reported in Fig. 1. The phenylureas having a methoxy substituent on the urea nitrogen, namely monolinuron, metobromuron, linuron and chlorobromuron, exhibited the lowest mobilities as the eluotropic strength of the mobile phase was increased by increasing the acetonitrile content in the organic modifier. It was found that 15% acetonitrile in methanol gave the best results in terms of fractionation of the phenylureas considered.

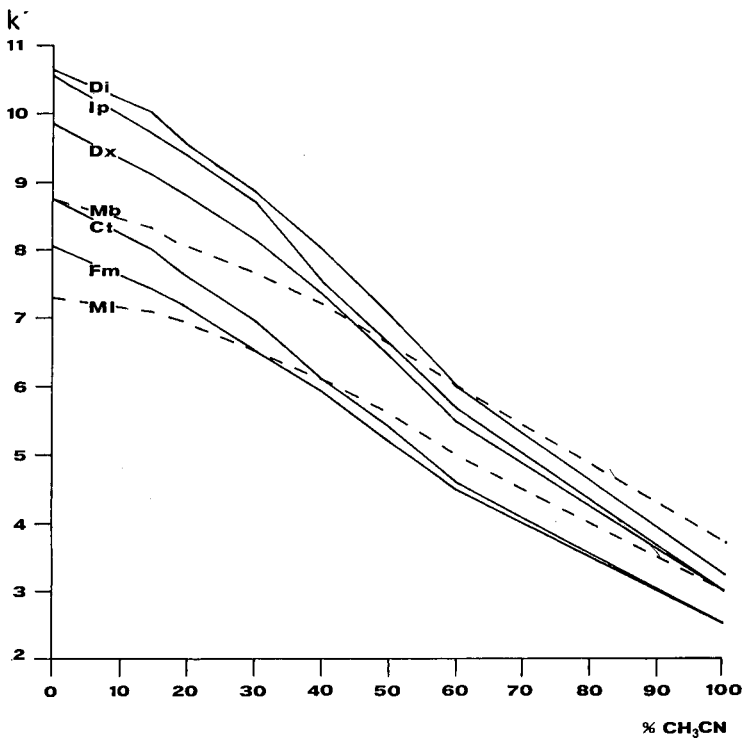

Fig. 1. Plots of retention (capacity factor, k') on a C_{18} silica column of some selected phenylureas *vs.* composition of the acetonitrile–methanol mixture used as organic modifier. Compounds: Ml = monolinuron; Fm = fluometuron; Ct = chlortoluron; Mb = metobromuron; Dx = difenoxuron; Ip = isoproturon; Di = diuron. The solvent programme was from 47 to 70% organic modifier in 20 min.

Recovery studies

In order to achieve sufficiently high enrichment factors, which enable pesticides to be monitored in drinking water samples in the ng/l range, extraction of large volumes of water is a prerequisite. In this respect, the ability of the Carbopack cartridge to retain quantitatively phenylureas on passing through it increasing volumes (1, 2 and 4 l) of a groundwater sample spiked with the herbicides at 150 ng/l was evaluated. The recovery data obtained from three determinations for each water volume considered showed that only when 4 l of groundwater were extracted was about 10% of fenuron, which is the most water-soluble phenylurea, lost in the water effluent.

The extraction efficiency of the Carbopack cartridge was compared with that of a 0.5-g C_{18} disposable extraction column (Supelco). The size of the plastic tube containing the siliceous material was the same as that containing Carbopack. Phenylureas were extracted in triplicate from 2 l of the same water sample used for experiments with the Carbopack cartridge and eluted with two 2-ml aliquots of methanol. Except for the most hydrophobic compounds, large losses of the other phenylureas were observed, the percentage recoveries ranging from 6.3% for fenuron to 69.6% for fluometuron. Hence, it appears that Carbopack is more suitable than the C_{18} material for extracting polar pesticides from aqueous samples. The extraction of large volumes of water by the C_{18} cartridge was also time consuming, as about 100 min were needed to pass 2 l of water through it, whereas the same operation with the Carbopack cartridge required only about 15 min.

Accuracy and precision

The recovery and the within-run precision of the proposed method with various concentrations of the fourteen herbicides considered were assessed. A sample of tap water made 0.4 g/l in sodium sulphite was divided into two portions, which were spiked with the analytes at levels of 30 and 3000 ng/l. Each portion was divided into six 2-l aliquots, each of which was analysed six times by the procedure. The quantitative results showed that the recovery of all phenylureas was independent of the herbicide concentration, demonstrating the absence of any adverse effect of irreversible adsorption by the materials composing the extraction apparatus. A slight loss of fenuron (recovery 83.2%) occurred at the highest phenylurea concentration considered. This can be accounted for by displacement chromatography of fenuron by the other more strongly retained phenylureas. The relative standard deviations (R.S.D.) at a concentration of 30 ng/l ranged from 3.76% for difenoxuron to 8.93% for fluometuron, and at 3000 ng/l the R.S.D. ranged from 0.69% for metoxuron to 2.64% for chlorouxoron. Quantitative results obtained by analysing water samples spiked with 30 ng/l of phenylureas showed that this method is well suited for monitoring compliance with the European Community standard for drinking water.

Matrix effect

Although LSE procedures with small cartridges have become popular during the last decade, this technique suffers mainly from the disadvantage that, when sampling large volumes of highly contaminated environmental aqueous samples, saturation effects due to organics present in the water may lead to abrupt and unpredictable decreases in the breakthrough volumes of the analytes of interest, as measured by

extracting them from pure water. The matrix effects on the recovery of phenylureas was evaluated by extracting in triplicate with the Carbopack cartridge 1- and 2-l aliquots of both river and sea water samples spiked with phenylureas at individual concentrations of 30 ng/l. As measured with a Beckman 915 A TOC Analyzer, the total organic carbon contents in the river and sea water samples were 6.5 and 1.7 mg/l, respectively. From these experiments, it was evident that only fenuron, among the phenylureas considered, was severely lost (recovery 53.5%) on extraction from 2 l of the river water sample.

Interferences

The analysis of phenylureas may be complicated by the presence in the water sample of their main degradation products, anilines. In addition, anilines may be

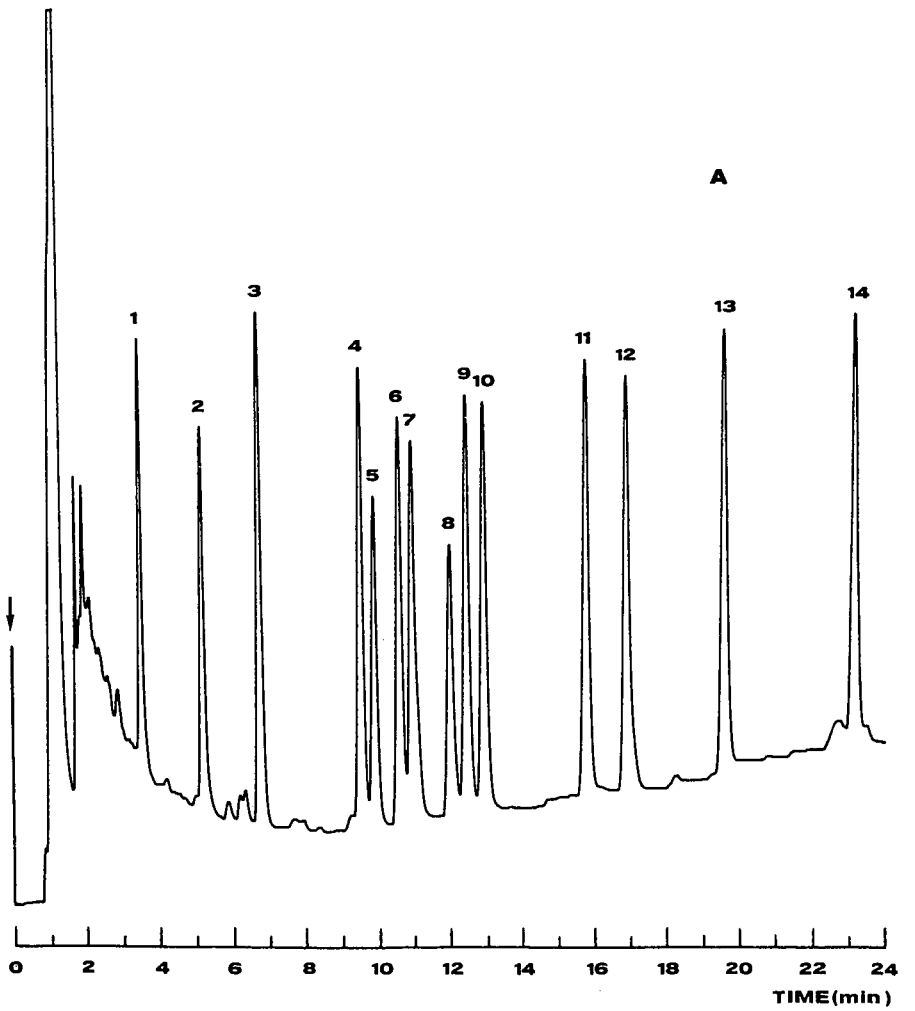

Fig. 2.

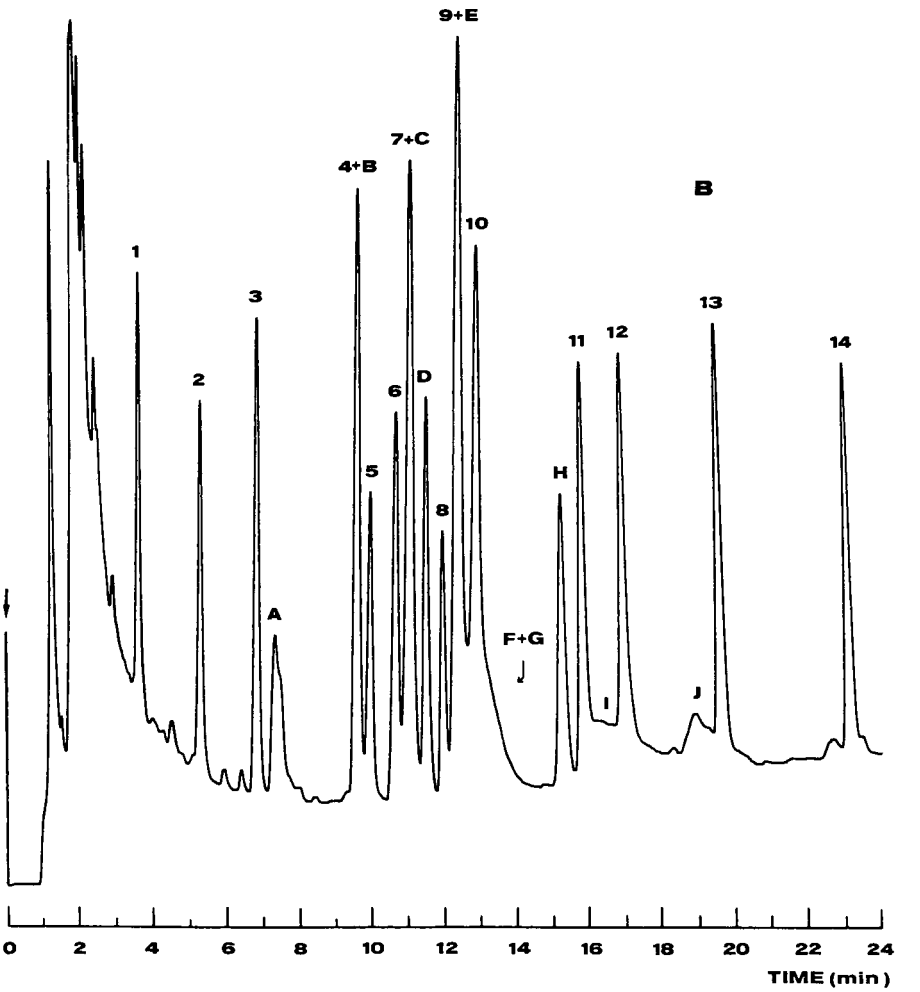

Fig. 2. Chromatograms obtained on analysing 1-l aliquots of river water (Tevere, February 1990) spiked with 300 ng/l of each phenylurea, 1000 ng/l of each corresponding aniline and 2000 ng/l of simazine, atrazine and propazine (A) by the proposed procedure and (B) with the Carbopack trap alone. Compounds: 1 = fenuron; 2 = methoxuron; 3 = monuron; 4 = monolinuron; 5 = fluometuron; 6 = chlortoluron; 7 = metobromuron; 8 = difenoxuron; 9 = isoproturon; 10 = diuron; 11 = linuron; 12 = chlorbromuron; 13 = chlorouxoron; 14 = neburon; A = simazine; B = 3-trifluoromethylaniline; C = atrazine; D = 3,4-dichloroaniline; E = 3-chloro-4-bromoaniline; F = 4-chloroaniline; G = 4-bromoaniline; H = propazine; I = 3-chloro-4-methoxyaniline; J = 3-chloro-4-methylaniline. The other anilines were eluted as very skewed peaks.

present in environmental aqueous samples as a result of industrial discharges from factories using anilines as synthetic intermediates. This problem was eliminated by incorporating a second cartridge containing a strong cation exchanger, having an exchange capacity of about 4 mequiv./g, which was connected in series with the Carbopack cartridge before desorbing the analytes. In such way, while phenylureas passed completely unretained through the second cartridge, any basic compound was

re-adsorbed on the exchanger from the methylene chloride–methanol mixture flowing through it. This double trap system has the advantage over that making use of a platinum phase [5] of being of more general use because, in addition to primary anilines, it also eliminates any other basic compound. As an example, Fig. 2 shows typical chromatograms obtained on analysing 1 l of a Tevere river water sample fortified with phenylureas, their corresponding anilines and simazine, atrazine and propazine, which are weakly basic herbicides, by the proposed procedure and with a single Carbopack cartridge.

Limit of detection

Under the chromatographic conditions selected and by extracting 2 l of drinking water samples, the limit of detection (signal-to-noise ratio = 3) for phenylureas was

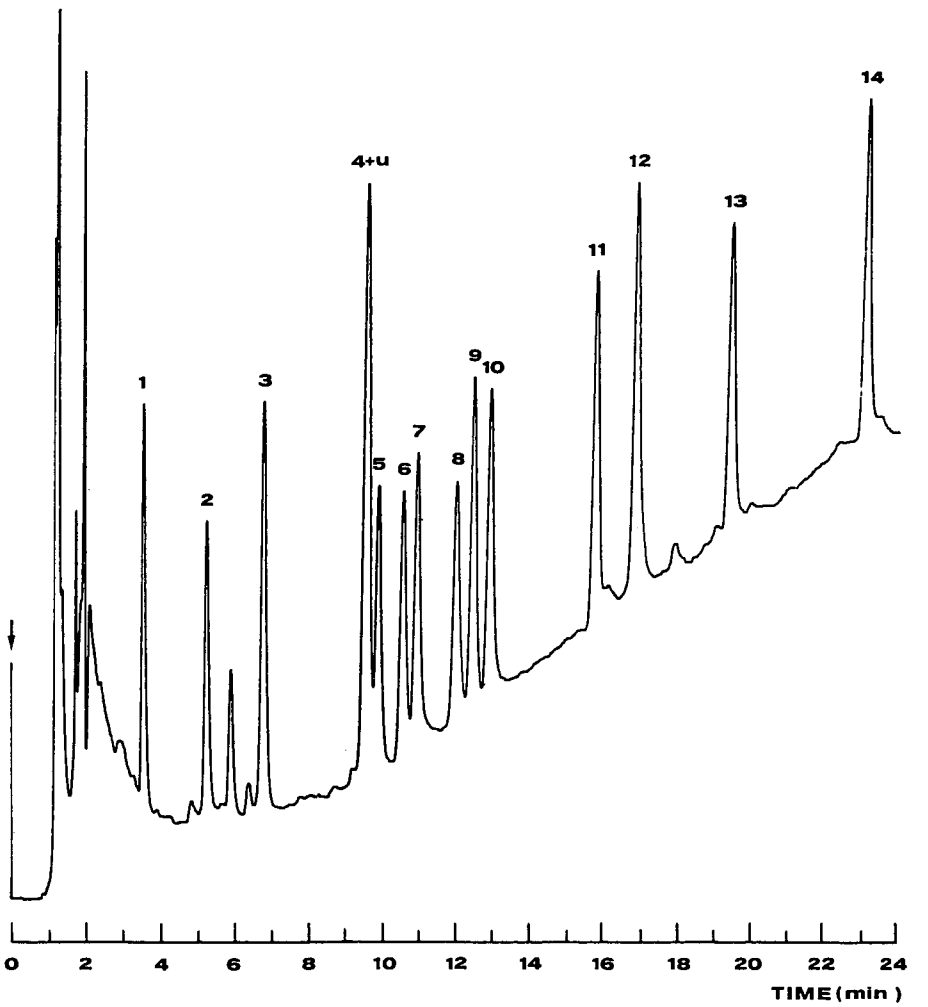

Fig. 3. Chromatogram obtained on analysing 2 l of a tap water specimen spiked with 30 ng/l of each phenylurea. Peaks as in Fig. 2; U, unknown compound eluted together with monolinuron.

estimated to be about 1.0 ng/l. Fig. 3 shows a typical chromatogram obtained on analysing 2 l of a drinking (tap) water sample spiked with 30 ng/l of phenylureas.

Sample storage

One of the advantages of liquid–solid extraction over liquid–liquid partitioning is that sampling and extraction of a water sample can be done simultaneously by passing the water through a sorbent trap as it is pumped at the sampling site. The small-volume cartridge could then be transported to the laboratory for desorption and chromatographic analysis. On the other hand, the original composition of extracts of heavily contaminated water samples might be altered after prolonged contact with the sorbent surface owing to some reactions catalysed by the adsorbing material itself. For phenylureas, the effect of storage was evaluated by extracting 1-l aliquots of a Tevere river sample spiked with 300 ng/l of each herbicide. After the water had been passed through them, the cartridges were stored at ambient temperature and analysed in duplicate after 5, 10 and 15 days of storage. In every case the recoveries of phenylureas were not significantly different from those obtained with unstored cartridges.

REFERENCES

1 C. E. McKone and R. J. Hance, *J. Chromatogr.*, 36 (1968) 234–237.
2 A. de Kok, I. M. Roorda, R. W. Frei and U. A. Th. Brinkman, *Chromatographia*, 14 (1981) 579.
3 A. de Kok, Y. J. Vos, C. Van Garderen, T. De Jong, M. Van Opstal, R. W. Frei, R. B. Geerdink and U. A. Th. Brinkman, *J. Chromatogr.*, 288 (1984) 71–89.
4 M. W. Nielen, G. Koomen, R. W. Frei and U. A. Th. Brinkman, *J. Liq. Chromatogr.*, 8 (1985) 315–332.
5 C. E. Goewie, P. Kwakman, R. W. Frei, U. A. Th. Brinkman, W. Maasfeld, T. Seshadri and A. Kettrup, *J. Chromatogr.*, 284 (1984) 73–86.
6 G. Chiavari and C. Bergamini, *J. Chromatogr.*, 346 (1985) 369–375.
7 M. W. F. Nielen, A. J. Walk, R. W. Frei, U. A. Th. Brinkman, P. Mussche, R. De Nijs, B. Ooms and W. J. Smink, *J. Chromatogr.*, 393 (1987) 69–83.
8 N. N. Senin, Yu. S. Filippov, N. F. Tolikina, G. A. Smolyaninov, S. Za. Volkov and V. S. Kukushkin, *J. Chromatogr.*, 364 (1986) 315–321.
9 A. Bacaloni, G. Goretti, A. Langanà, B. Petronio and M. Rotatori, *Anal. Chem.*, 52 (1980) 2033–2037.
10 F. Mangani, G. Crescentini and F. Bruner, *Anal. Chem.*, 53 (1981) 1627–1631.
11 A. Di Corcia, M. Marchetti and R. Samperi, *J. Chromatogr.*, 405 (1987) 357–363.
12 M. Battista, A. Di Corcia and M. Marchetti, *Anal. Chem.*, 61 (1989) 935–939.
13 A. Di Corcia, M. Marchetti and R. Samperi, *Anal. Chem.*, 61 (1989) 1363–1367.
14 A. Di Corcia, M. Marchetti and R. Samperi, *Anal. Chem.*, 58 (1986) 2048–2052.
15 A. Di Corcia and R. Samperi, *Anal. Chem.*, 62 (1990) 1490–1494.
16 S. M. Walters, B. C. Westerby and D. M. Gilvydis, *J. Chromatogr.*, 317 (1984) 533–544.

Journal of Chromatography, 541 (1991) 375–382
Elsevier Science Publishers B.V., Amsterdam

CHROM. 22 929

Separation and detection of styrene–alkyl methacrylate and ethyl methacrylate–butyl methacrylate copolymers by liquid adsorption chromatography using a dichloroethane mobile phase and a UV detector

SADAO MORI
Department of Industrial Chemistry, Faculty of Engineering, Mie University, Tsu, Mie 514 (Japan)
(First received June 7th, 1990; revised manuscript received October 17th, 1990)

ABSTRACT

Styrene (S)–methyl methacrylate (MMA), S–ethyl methacrylate (EMA) and EMA–*n*-butyl methacrylate (BMA) copolymers were separated according to chemical composition. Silica gel was used as the stationary phase and a mixture of 1,2-dichloroethane (DCE) and ethanol as the mobile phase. DCE was transparent at wavelengths over 230 nm and methacrylate homopolymers and copolymers could be monitored with a conventional UV detector at 233 nm. The molar absorption coefficients for both PS and PMMA at 233 nm were nearly equal and the chromatograms obtained at this wavelength reflected the relative amounts of the copolymers with different chemical compositions. A mixture of S–MMA copolymers having different compositions and PMMA was separated by a gradient elution method at constant column temperature. The initial mobile phase was a mixture of DCE and ethanol (99.0:1.0, v/v), and the ethanol content was increased to 5.0% in 20 min and then to 10.0% in another 5 min or to 10.0% in 20 min. The copolymers of S–MMA and S–EMA having higher styrene contents eluted earlier and the elution of the copolymers was in order of decreasing styrene content. Therefore, the chemical composition of the copolymers in a mixture can be determined directly from the chromatogram by knowing the retention volume of each copolymer. A mixture of PEMA, PBMA and their copolymers was also separated by a similar method. PBMA eluted earlier than PEMA. The affinity of the EMA component to the surface of silica gel was assumed to be stronger than that of the BMA component.

INTRODUCTION

Synthetic random copolymers usually have a molecular weight distribution (MWD) and a chemical composition distribution (CCD). The accurate determination of CCD is important for the characterization of copolymers and the determination of MWD. Although molecular weight averages and the MWD of a polymer can be measured by size exclusion chromatography (SEC), those of a copolymer cannot be obtained accurately without knowing the CCD of the copolymer [1]. The separation of styrene (S)–methyl methacrylate (MMA) random copolymers by high-performance liquid adsorption chromatography (LAC) has been reported in our previous papers [1–6] and the technique was applied to the separation of styrene–alkyl methacrylates and styrene–alkyl acrylate copolymers [7] and S–MMA block copolymers [8],

0021-9673/91/$03.50

respectively. High-conversion S–MMA random copolymers have been characterized by a combination of LAC and SEC [5]. Fractionation by LAC gave the CCD of the copolymers and the real MWD has been obtained by fractionation by SEC followed by LAC. A LAC separation mechanism has been proposed [9].

Several attempts have been reported by other workers for the separation of copolymers according to composition by high-performance liquid chromatography (HPLC), *e.g.*, S–MMA [10,11], S–methyl acrylate [12], S–acrylonitrile [13] and S–butadiene [14]. UV absorption detector had to be utilized to monitor the copolymers in the effluent from a column. Because mobile phase gradient elution is required to elute the copolymers according to composition, a differential refractive index detector cannot be employed. Solvents such as chloroform and tetrahydrofuran used as one component of mobile phases reported in the literature, are opaque at wavelengths below 245 nm, and a comonomer unit such as MMA and acrylonitrile is transparent above 250 nm. Therefore, only the styrene content in the effluent could be detected. Consequently, chromatograms recorded on a chart were not true concentration profiles for the copolymers in the effluent but profiles proportional to the styrene content in the copolymers.

1,2-Dichloroethane (DCE) is transparent at wavelengths above 230 nm, and polymethacrylates and polyacrylates have UV absorption near wavelengths of 230 nm at the foot of the absorption band. Therefore, a combination of DCE and a UV detector will make possible the measurement of chromatograms of methacrylate copolymers and homopolymers. In this work, copolymers of S–alkyl methacrylates (methyl, ethyl and *n*-butyl) were separated using a mixture of DCE and ethanol as the mobile phase and detected using a UV detector at 233 nm. Operating variables such as the gradient elution conditions and the selection of a wavelength which has equal molar absorption coefficients for both styrene and alkyl methacrylate units were investigated. The separation system was applied for the separation of ethyl methacrylate (EMA)–butyl methacrylate (BMA) copolymers, which have no UV absorption near 254 nm.

EXPERIMENTAL

Apparatus

LAC measurements were performed on a Jasco Trirotar-VI high-performance liquid chromatograph (Japan Spectroscopic, Tokyo, Japan) with a Uvidec-100VI variable-wavelength UV absorption detector. Silica gel with a pore size of 30 Å and a mean particle diameter of 5 μm was packed in a 50 mm × 4.6 mm I.D. stainless-steel tube. This column was thermostated at a specified temperature in a Model TU-300 column oven.

A Uvidec-610C UV–VIS spectrophotometer (Japan Spectroscopic) equipped with a microcomputer was used for the measurement of the UV absorption spectra of polystyrene (PS), poly(methyl methacrylate) (PMMA) and DCE, using a band width (resolution) of 2.00 nm, time constant 0.4 s, scan speed 10 nm/min and quartz cells of 1-cm path length.

Sample

Copolymers of S–MMA [2] and S–ethyl methacrylate (EMA) [7], having narrow

TABLE I

STYRENE CONTENT OF S–MMA AND S–EMA COPOLYMERS

Copolymer	Sample	Styrene content (mol-%)	Copolymer	Sample	Styrene content (mol-%)
S–MMA	I	85.5	S–MMA	VIII	26.5
	II	73.4		IX	15.2
	III	66.3	S–EMA	I	69.1
	IV	57.4		II	50.2
	V	48.7		III	30.4
	VI	42.1		IV	15.5

CCD, were the same as those prepared previously. These samples were prepared by solution polymerization in benzene at a low degree of conversion. PS, PMMA, PEMA and PBMA homopolymers and EMA–BMA copolymers were also prepared in the same manner [7].

The compositions of the styrene copolymers were measured by UV spectrophotometry and are shown as the styrene content in mole percent in Table I. The composition of EMA–BMA copolymers was not measured and only the mole percent of the feed of monomers is given, as follows: EMA–BMA I (25–75%), II (50–50%) and III (75–25%) (it was found by separate IR experiments that the copolymers had roughly the expected chemical compositions).

Elution

The solvents used in the mobile phases were DCE and ethanol. Elution was performed in the gradient elution mode. Three different mixtures of DCE and ethanol were prepared: (A) 99.0:1.0, (B) 95.0:5.0 and (C) 90.0:10.0 (v/v). The initial mobile phase was A and the composition of the mobile phase was changed linearly to 100% B in 15 min, or to 100% B in 20 min and to 100% C in a further 5 min or to 100% C in 20 min.

Samples were dissolved in mobile phase A and the injection volume of the sample solutions was 0.1 ml. At the beginning of the elution, the gradient programme of the mobile phase composition was started first, and the sample solutions were injected 1 min after the start of the gradient programme. The flow-rate of the mobile phase was 0.5 ml/min.

RESULTS AND DISCUSSION

UV spectra

Fig. 1 shows the UV spectra of PS, PMMA, chloroform and DCE. PS and PMMA were each dissolved in DCE at a concentration of 0.335 g/l and the UV spectra of the polymer solutions were measured with DCE as a reference solvent. Water was used as a reference for DCE and chloroform.

PMMA has UV absorption in the low-wavelength region and the foot of the PMMA absorption band can be observed near 230 nm. The UV absorbance at 250 nm for chloroform was 0.9 and that at 229 nm for DCE was 0.90. Therefore, the UV absorption spectra of PMMA in a DCE solution can be measured near 230 nm with

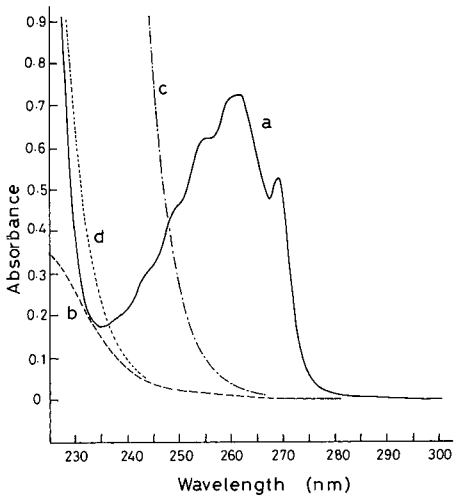

Fig. 1. UV absorption spectra of (a) PS and (b) PMMA homopolymers, (c) chloroform and (d) DCE. Solvent for PS and PMMA, DCE; reference for PS and PMMA, DCE; reference for chloroform and DEC, water; concentration for PS and PMMA, 0.335 g/ml.

a better signal-to-noise ratio. If the UV absorption of the copolymers in the effluent is monitored at a wavelength at which the absorption coefficient for PS is equal to that for PMMA, then the chromatograms of S–MMA copolymers express the concentrations of the copolymers in the effluent. To examine a wavelength at which PS and PMMA have the same absorption coefficient, PS and PMMA solutions at the same molar concentration were prepared and the UV absorption spectra of the solutions were measured as shown in Fig. 1.

Although a wavelength at which the absorption coefficient of PS was equal to that of PMMA could not be found, the wavelength of 233 nm was assumed to have nearly equal absorption coefficients. The absorbance at 233 nm for PS in Fig. 1 was 0.200 and that for PMMA was 0.195. Therefore, even if it was assumed that both homopolymers in Fig. 1 had the same absorbance at 233 nm, the relative error was within 3%. The only disadvantage of the use of a wavelength of 233 nm for monitoring the copolymer concentration in the effluent was that the UV absorption coefficient of PS at 233 nm was 28% of that at 254 nm. This drawback, however, can be partly overcome because the chromatograms obtained at 233 nm were the sum of the UV absorptions for PS and PMMA. Moreover, the attenuation for the UV detector could be increased to obtain reasonable peak heights for the copolymers.

Elution

When chloroform in the mobile phase was replaced with DCE, a large volume of ethanol was required to elute S–MMA copolymers from the column [3], although the elution behaviour of the copolymers in the DCE–ethanol system was similar to that with chloroform–ethanol as the mobile phase; an increase in the ethanol content in the mobile phase and/or a decrease in the column temperature was effective in eluting the copolymers which were retained in the column. At a column temperature of 10°C, for example, a PMMA homopolymer was eluted from the column completely using DCE–ethanol (95:5, v/v) as the mobile phase.

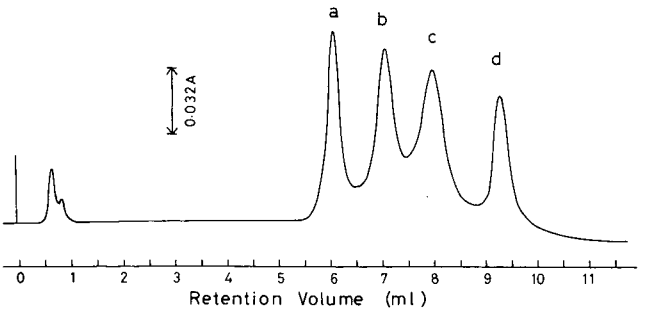

Fig. 2. LAC of S–MMA copolymers and PMMA. Column temperature, 10°C; sample, (a) S–MMA VI, (b) S–MMA VIII, (c) S–MMA IX, (d) PMMA; detection, 233 nm, 0.32 a.u.f.s.; sample concentration, *ca.* 0.01% each; gradient, 100% A to 100% B in 15 min.

A mixture of S–MMA VI, VIII and IX and PMMA was separated at a column temperature of 10°C and the result is shown in Fig. 2. The gradient elution conditions were as follows: the initial mobile phase was mixture A and the composition of the mobile phase was changed linearly from 100% A to 100% B in 15 min. The sample concentrations of the copolymers and PMMA were about 0.01% each. The peak height for each sample was nearly equal and a PMMA peak can also be seen in Fig. 2. Under these elution conditions, S–MMA copolymers I, II and III eluted at V_0 (the exclusion limit, *ca.* 0.6 ml), and copolymers IV and V eluted near copolymer VI.

To separate all the components of a mixture of S-MMA copolymers I–IX and PMMA simultaneously, the column temperature was increased to 50°C and the gradient elution conditions were improved as follows: the initial mobile phase was mixture A and the composition of the mobile phase was changed from 100% A to 100% B in 20 min and then to 100% C in a further 5 min. The results are shown in Fig. 3. The chromatograms obtained at 254 nm are also shown for comparison. S–MMA copolymer I appeared at the exclusion limit and is not shown in Fig. 3. The peak for

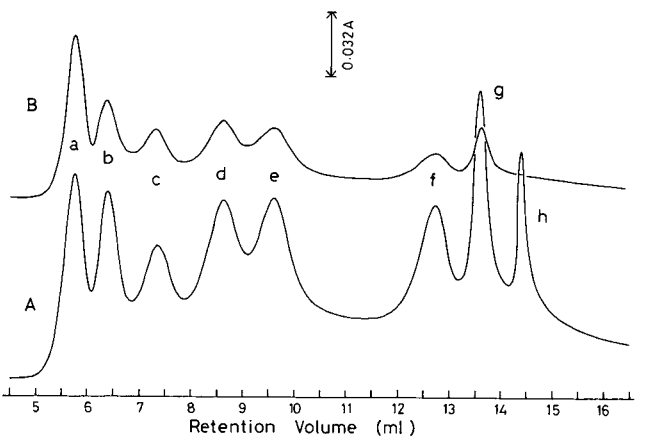

Fig. 3. LAC of S–MMA copolymers and PMMA. Column temperature, 50°C; sample, (a) S–MMA II, (b) S–MMA III, (c) S–MMA IV, (d) S–MMA V, (e) S–MMZ VI, (f) S–MMA VIII, (g) S–MMA IX, (h) PMMA; sample concentration, *ca.* 0.01% each; detection, (A) 233 nm, 0.16 a.u.f.s., (B) 254 nm, 0.32 a.u.f.s.; gradient, 100% A to 100% B in 20 min and to 100% C in a further 5 min.

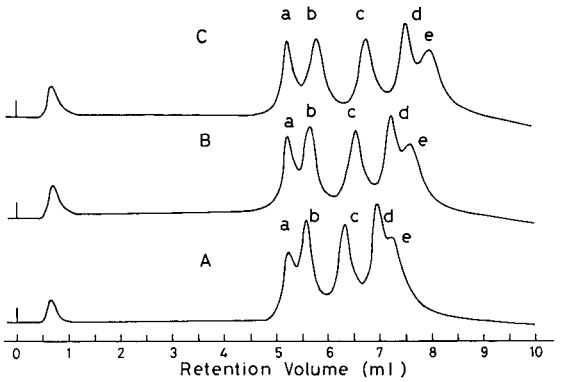

Fig. 4. Chromatograms of S–EMA copolymers and PEMA. Column temperature, (A) 50°C, (B) 60°C, (C) 70°C; sample, (a) S–EMA I, (b) S–EMA II, (c) S–EMA III, (d) S–EMA IV, (e) PEMA; sample concentration, *ca.* 0.01% each; detection, 233 nm, 0.32 a.u.f.s.; gradient, 100% A to 100% C in 20 min.

PMMA disappeared at 254 nm. The peak intensity of every component at 233 nm was higher than that at 254 nm, although the attenuation of the UV detector was not the same. This is because peaks obtained at 233 nm include both components S and MMA in the copolymers, although the UV absorption coefficient for the styrene component at 254 nm is higher than that at 233 nm.

Fig. 4 shows the chromatograms for a mixture of four S–EMA copolymers and PEMA at three different column temperatures. The retention volumes of the peaks increased with increasing column temperature, except for S–EMA copolymer I, and as a result the resolution between copolymers I and II and that between IV and PEMA was improved. The gradient elution conditions were as follows: the initial mobile phase was mixture A and the composition of the mobile phase was changed from 100% A to 100% C in 20 min.

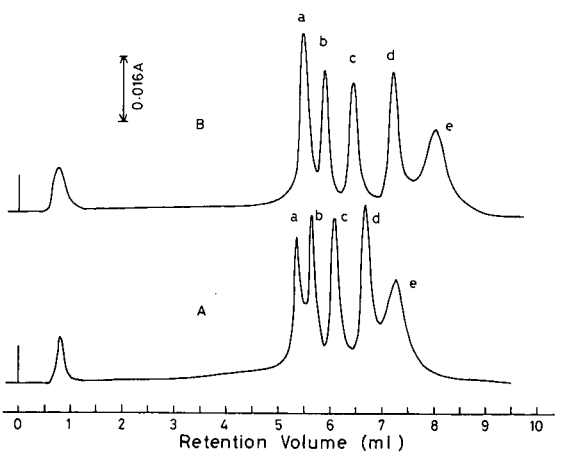

Fig. 5. Chromatograms of EMA–BMA copolymers, PEMA and PBMA. Column temperature, (A) 50°C, (B) 70°C; sample, (a) PBMA, (b) EMA–BMA I (25:75), (c) EMA–BMA (50:50), (d) EMA–BMA III (75:25), (e) PEMA; sample concentration, *ca.* 0.01% each; detection, 233 nm, 0.16 a.u.f.s.; gradient, 100% A to 100% C in 20 min.

TABLE II

REPRODUCIBILITY OF RETENTION VOLUME WITH GRADIENT ELUTION

Copolymer	Sample	Mean and S.D. of retention volume (ml)							
		First day		Second day		Third day		Overall	
		Mean	S.D.	Mean	S.D.	Mean	S.D.	Mean	S.D.
S–MMA	II	5.767	0.005	5.663	0.009	5.450	0.041	5.626	0.134
	III	6.420	0.008	6.435	0.026	6.230	0.024	6.367	0.099
	IV	7.370	0.0	7.480	0.056	7.297	0.004	7.382	0.082
	V	8.627	0.021	8.807	0.076	8.653	0.037	8.696	0.094
	VI	9.587	0.029	9.827	0.077	9.723	0.021	9.712	0.110
	VIII	12.667	0.047	12.937	0.062	12.887	0.012	12.830	0.126
	IX	13.600	0.0	13.730	0.043	13.680	0.008	13.670	0.059
PMMA	–	14.400	0.0	14.570	0.057	14.520	0.008	14.500	0.079

Fig. 5 shows the chromatograms of a mixture of PEMA, PBMA and their copolymers at different column temperatures. The gradient elution conditions were the same as in Fig. 4. As these polymers and copolymers do not have UV absorption at 254 nm, it is not possible to measure the chromatograms for these polymers and copolymers using a UV detector when tetrahydrofuran or chloroform is used as one component of the mobile phase. There has been only one report so far on the separation of mixtures of poly(alkyl methacrylates) or poly(alkyl acrylates) [15] in which a solvent-evaporative mass detector (an evaporative light-scattering detector) was used to detect the polymers in the effluent. In our system, a conventional UV detector can be employed and a special detector or detection system is not required.

The possibility of the separation of alkyl methacrylate and alkyl acrylate copolymers according to composition was pointed out in a previous paper [7], where a chloroform–ethanol mobile phase was used. On replacing chloroform in the mobile phase with DCE, a conventional UV detector could be used to monitor the concentrations of these copolymers in the effluent from a column and the possibility predicted in the previous paper [7] was proved in this work.

Reproducibility of gradient elution

Determination of the chromatograms shown in Fig. 3 was repeated three times a day for 3 days and the retention volumes of each component were measured. The results are given in Table II, with means and standard deviations for each day together with the mean and standard deviation for each set of nine measurements. The standard deviation of the retention volume for each component was between 0.06 and 0.14 ml. The range of data for each component obtained on the same day was between 0 and 0.18 ml and that obtained during the 3 days was between 0.23 and 0.39 ml.

ACKNOWLEDGEMENT

The author expresses his gratitude to Mr. M. Mouri for technical assistance.

REFERENCES

1 S. Mori, *J. Chromatogr.*, 411 (1987) 355.
2 S. Mori, Y. Uno and M. Suzuki, *Anal. Chem.*, 58 (1986) 303.
3 S. Mori and Y. Uno, *Anal. Chem.*, 59 (1987) 90.
4 S. Mori and Y. Uno, *J. Appl. Polym. Sci.*, 34 (1987) 2689.
5 S. Mori, *Anal. Chem.*, 60 (1988) 1125.
6 S. Mori, *Anal. Sci.*, 4 (1988) 365.
7 S. Mori and M. Mouri, *Anal. Chem.*, 61 (1989) 2171.
8 S. Mori, *J. Appl. Polym. Sci.*, 38 (1989) 95.
9 S. Mori, *J. Liq. Chromatogr.*, 12 (1989) 323.
10 M. Danielewicz and M. Kubín, *J. Appl. Polym. Sci.*, 26 (1981) 951.
11 G. Glöckner and J. H. M. van den Berg, *J. Chromatogr.*, 352 (1986) 511.
12 S. Teramchi, A. Hasegawa, Y. Shima, M. Akatsuka and M. Nakajima, *Macromolecules*, 12 (1979) 992.
13 G. Glöckner, J. H. M. van den Berg, N. L. J. Meijerink, T. G. Scholte and R. Koningsveld, *Macromolecules*, 17 (1984) 962.
14 H. Sato, H. Takeuchi, S. Suzuki and Y. Tanaka, *Makromol. Chem. Rapid Commun.*, 5 (1984) 719.
15 T. H. Mourey, *J. Chromatogr.*, 357 (1986) 101.

Journal of Chromatography, 541 (1991) 383–392
Elsevier Science Publishers B.V., Amsterdam

CHROM. 22 931

Determination of vitamin B_{12} in multivitamin–multimineral tablets by high-performance liquid chromatography after solid-phase extraction

JOHAN DALBACKE* and IRENE DAHLQUIST

Analytical and Quality Development Department, Gacell Laboratories AB, P.O. Box 839, S-201 80 Malmö (Sweden)

(First received May 2nd, 1990; revised manuscript received September 28th, 1990)

ABSTRACT

A method for the determination of vitamin B_{12} (cyanocobalamin) in multivitamin–multimineral tablets, containing 3 μg of vitamin B_{12} per tablet, is described. Powdered tablets are extracted with a mixture of ammonium pyrrolidinedithiocarbamate and citric acid in dimethyl sulphoxide and water. The extract is centrifuged and the supernatant is diluted with water before concentration and clean-up by solid-phase extraction using a quaternary amine and a phenyl column in series. The eluate from the solid-phase extraction is analysed by reversed-phase liquid chromatography using a methanol–water gradient with detection at 550 nm. A comparison with the frequently used microbiological method is presented. The validation of the procedure is described in terms of selectivity, linearity, accuracy and precision.

INTRODUCTION

Vitamin B_{12} is a water-soluble vitamin that belongs to the corrinoids. The core of vitamin B_{12} consists of a corrin ring with a central cobalt atom. The corrin ring has four pyrrole units. Vitamin B_{12} was isolated in crystalline form from liver in 1948 and its three-dimensional structure was elucidated by Hodgkin in 1956. The human need for vitamin B_{12} is about 1–2 μg per day. Vitamin B_{12} appears to be necessary for red cell formation because of its ability to make folic acid available to the bone marrow. A deficiency of vitamin B_{12} leads to a degeneration of both the sensory and motor columns in the spinal cord with loss of sensation and paralysis.

The determination of water-soluble vitamins has been a persistent problem largely because of the instability of these vitamins and the complexity of the matrices in which they are usually found. Vitamin B_{12} is usually determined by a time-consuming microbiological method using *Lactobacillus leichmannii* [1]. High-performance liquid chromatography (HPLC) has been used to determine vitamin B_{12} in pharmaceutical formulations [2–4]. Hudson *et al.* [5] described a method for the determination of vitamin B_{12} in multivitamin–multimineral tablets by HPLC. However, a combined preconcentration–sample clean-up step is required owing to the low level of vitamin B_{12} present in a large excess of potentially interfering compounds in multivitamin–

0021-9673/91/$03.50

multimineral tablets. A procedure for solid-phase extraction of vitamin B_{12} from multivitamin–multimineral tablets is described in a Baker publication [6].

This paper describes a method for the determination of vitamin B_{12} in multivitamin–multimineral tablets containing ten vitamins and eight minerals. Solid-phase extraction with a quaternary amine and a phenyl column in series is used to concentrate vitamin B_{12} and clean up the sample. Most compounds are retained on the quaternary amine column and vitamin B_{12} is retained on the phenyl column. The eluates are subjected to reversed-phase HPLC with binary gradient elution and detection at 550 nm.

EXPERIMENTAL

Chemicals and reagents

HPLC-grade methanol was obtained from Labscan (Dublin, Ireland). Ammonium pyrrolidinedithiocarbamate (APDC), citric acid and dimethyl sulphoxide of analytical-reagent grade were purchased from Merck (Darmstadt, Germany) and vitamin B_{12} from Sigma (St. Louis, MO, U.S.A.). Water purified with a Milli-Q water purification system (Millipore, Bedford, MA, U.S.A.) was used in all procedures. Multivitamin–multimineral tablets, Vitaplex mineral and placebo tablets (Vitaplex mineral without vitamin B_{12}) were kindly supplied by Ferrosan (Malmö, Sweden).

Extraction columns and vacuum apparatus

Bond-Elut quaternary amine (SAX 500 mg, 2.8 ml) and phenyl (PH 500 mg, 2.8 ml) columns were obtained from Analytichem International (Harbor City, CA, U.S.A.). The columns were used with a Vac-Elut 10 sample-processing station from Analytichem International.

Chromatographic equipment

The HPLC system consisted of a Model 600 multisolvent delivery system, a WISP Model 712 autosampler and a Model 490 programmable multiwavelength detector, all from Waters Assoc. (Milford, MA, U.S.A.). A Spectra-Physics (San Jose, CA, U.S.A.) Model SP4270 integrator was used to record chromatograms and calculate peak areas. A Spectra-Physics ChromStation-AT was used for data handling and storage. A Waters Assoc. Lambda-Max Model 481 LC spectrophotometer was also used during the method development. A Model HP 1040A diode-array detector was used together with an HP 79994A HPLC ChemStation from Hewlett-Packard (Waldbronn, Germany) when assessing the homogeneity of the vitamin B_{12} peak.

Extraction procedure

Approximately 25 mg of vitamin B_{12} was accurately weighed into a 50-ml volumetric flask and diluted to volume with water. This stock solution was diluted with water to a final concentration of 8 μg/ml. An extraction solution containing 0.25 g of APDC, 1.0 g of citric acid, 10.00 ml of dimethyl sulphoxide and 30.00 ml of water was added to 5.00 ml of the diluted stock solution. This mixture was shaken for 15 min at 40°C in a water-bath. The extract was centrifuged for 8 min at 2500 *g* and 15.00 ml of the supernatant were diluted with 100 ml of water.

Forty tablets were powdered in a mortar. An amount corresponding to ten

tablets was treated in the same way as the diluted stock solution, with the exception that 35.00 ml instead of 30.00 ml of water were added.

Solid-phase extraction

The solid-phase columns were conditioned immediately prior to use with one column volume of methanol followed by one column volume of water. The columns were held in a Vac-Elut 10 processing station operated at a pressure of 34 kPa. The columns were filled with water before the SAX columns were placed in adaptors on top of the phenyl columns, *i.e.*, the sample solution first passed through the SAX column and then through the phenyl column. Reservoirs with 20-μm frits were attached on top of the SAX columns.

The diluted extracts were aspirated through the columns by a vacuum of 85 kPa. After aspiration of the standard and sample solutions, the quaternary amine columns were removed and the phenyl columns were washed with one column volume of water followed by 1.0 ml of methanol–water (20:80). The columns were air-dried under vacuum (34 kPa) for 30 s. Vitamin B_{12} was eluted with two 0.50-ml aliquots of methanol–water (90:10) into 3-ml volumetric flasks. The eluates were diluted to volume with water.

Chromatography

The diluted eluates were analysed by reversed-phase HPLC on a 150 × 3.9 mm I.D. μBondapak C_{18} (10 μm) column (Waters Assoc.). A Waters Assoc. Guard-Pak precolumn module containing a Guard-Pak μBondapak C_{18} insert was used to protect the analytical column. Binary gradient elution was used (Table I). Reservoir A contained methanol–water (10:90) and reservoir B methanol–water (90:10). The reservoirs were continuously sparged with helium. Chromatography was carried out under ambient conditions at a flow-rate of 1.0 ml/min. The injection volume was 200 μl. Vitamin B_{12} was detected at 550 nm.

The HPLC system was considered to be acceptable when the relative standard deviation of the vitamin B_{12} peak area of six consecutive injections was less than 1.0%. A tailing factor (T) was calculated according to USP XXII [7] in order to check the asymmetry of the peak. The number of theoretical plates (n) was also calculated. Typical values of n were in the range 20 000–40 000 and of T in the range 1.1–1.2.

Quantification was achieved by comparing the vitamin B_{12} peak area of the sample preparation with that of the standard preparation.

TABLE I

GRADIENT USED

Time (min)	B (%)	Type of gradient
0	0	–
15	50	Linear
17	100	Linear
27	100	–
30	0	Linear
40	0	–

RESULTS AND DISCUSSION

Tablet extraction

It has been reported [8,9] that vitamin B_{12} is not stable in aqueous solutions containing vitamin C and copper(II) and/or iron(II) ions. Ascorbic acid (vitamin C) in aqueous solution is easily oxidized to dehydroascorbic acid. The oxidation is catalysed by copper(II) and iron(II) ions. The instability of vitamin B_{12} in aqueous solution is mainly due to the presence of dehydroascorbic acid [10]. As the multivitamin–multimineral tablets we were to analyse contained iron, copper and vitamin C, it was necessary to stabilize vitamin C in the tablet extracts so that vitamin B_{12} did not degrade. The active constituents of the tablets are given in Table II. Hudson *et al.* [5] have proposed an extraction solution containing APDC, citric acid and dimethyl sulphoxide when tablets containing iron and/or copper are to be analysed. These compounds have the ability to form stable coordination complexes with copper(II) and iron(II) ions. The extraction solution proposed by Hudson *et al.* was modified by decreasing the percentage of dimethyl sulphoxide. We investigated the stability of vitamin B_{12} in the extraction solution used in our method by analysing the supernatant 24 h after tablet extraction. A 10% degradation of vitamin B_{12} was observed in the tablet extract and no degradation was observed in the standard extract. It was not possible to increase the amount of tablets owing to greater problems with degradation of vitamin B_{12} in the extraction solution.

Solid-phase extraction

When tablets were extracted, readily oxidized and reduced constituents were dissolved and participated in several parallel reactions, which led to new potential interfering compounds. Hence a sample clean-up was needed. The mixture was too complex to be cleaned up by a single solid-phase extraction step.

The tablet extract was diluted prior to solid-phase extraction in order to decrease the solvent strength. Vitamin B_{12} was not retained on the phenyl column if this dilution step was excluded.

Most coloured substances in the extraction solution were retained on the SAX column and vitamin B_{12} was retained on the phenyl column. Vitamin B_{12} could be seen as a red band when it was eluted from the phenyl column. The stability of vitamin B_{12}

TABLE II

TABLET COMPOSITION

Active constituent	Amount per tablet	Active constituent	Amount per tablet
Vitamin A	0.9 mg	Nicotinamide	16 mg
Vitamin B_1	1.2 mg	Iron(II)	18 mg
Vitamin B_2	1.4 mg	Zinc(II)	15 mg
Vitamin B_6	2.1 mg	Copper(II)	2 mg
Vitamin B_{12}	3 μg	Iodine	0.15 mg
Folic acid	0.4 mg	Manganese	2.5 mg
Vitamin C	60 mg	Chromium	50 μg
Vitamin D_3	5 μg	Selenium(IV)	50 μg
Vitamin E	9 mg	Molybdenum	0.15 mg

in the eluates was investigated by analysing eluates 12 h after the elution. No degradation of vitamin B_{12} was observed.

Chromatography

The eluates were diluted three-fold with water in order to be able to inject as much as 200 μl without excessive peak broadening on the analytical column. The main reason for continuation of the gradient so long after vitamin B_{12} had been eluted was to ensure the elution of late-eluting compounds. If gradient elution was not used these compounds would be accumulated on the column and affect the stationary phase and thereby the chromatographic process. A chromatogram of the tablets registered at 360 nm (Fig. 1B) shows that there really were a large number of late-eluting compounds in spite of the clean-up procedure.

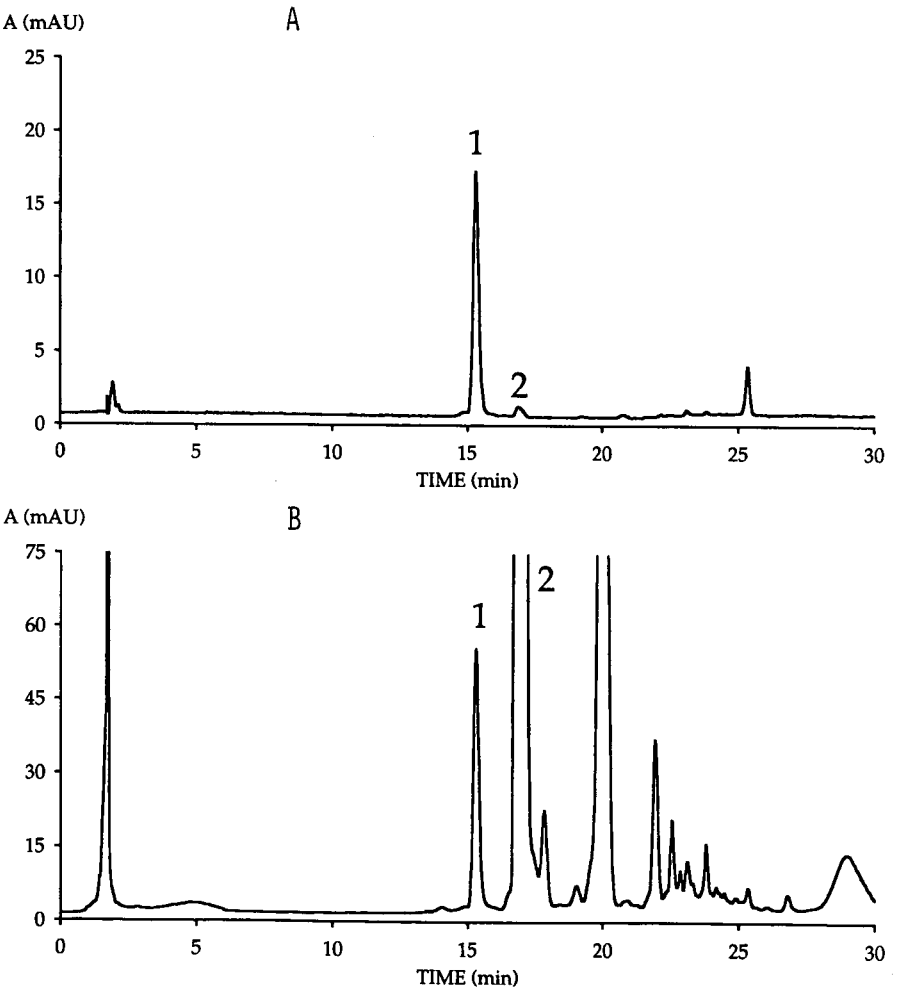

Fig. 1. Chromatogram of multivitamin–multimineral tablets at (A) 550 nm and (B) 360 nm after preconcentration and clean-up by solid-phase extraction. Peaks: 1 = vitamin B_{12}; 2 = vitamin B_2.

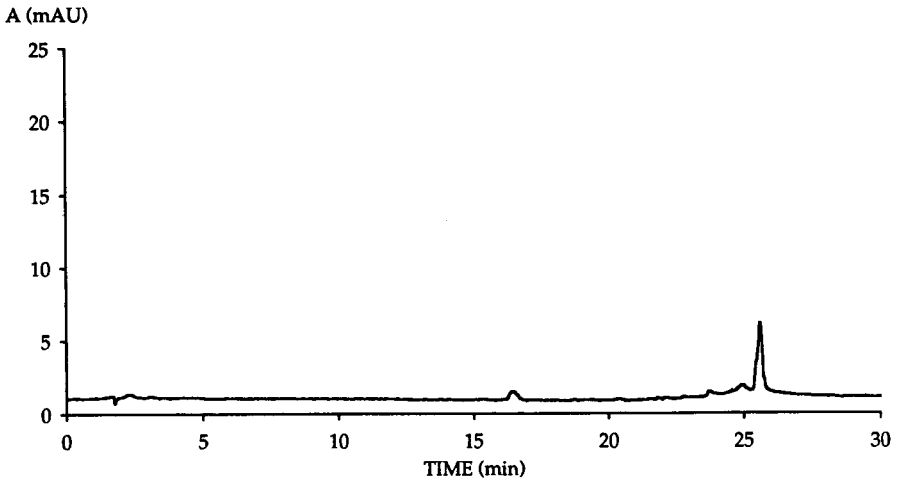

Fig. 2. Chromatogram at 550 nm of placebo tablets after solid-phase extraction.

Vitamin B_{12} was detected at 550 nm instead of 360 nm even though the response was three times higher at 360 nm. The reason for this was that the selectivity was much better at 550 nm than 360 nm. Typical chromatograms for multivitamin–multimineral tablets with detection at 550 and 360 nm are shown in Fig. 1. Vitamin B_{12} eluted as a symmetrical peak after about 15 min and vitamin B_2 2 min later.

Selectivity

A chromatogram at 550 nm of placebo tablets is shown in Fig. 2. No active or inactive ingredient interfered with the quantification of vitamin B_{12}, nor did hydroxycobalamin, which is a degradation product of vitamin B_{12}. The homogeneity of the vitamin B_{12} peak was assessed by analysing multivitamin–multimineral tablets and a standard solution according to the method and using a diode-array detector. Spectra acquired at the upslope, the apex and at the downslope of the vitamin B_{12} peak were normalized and overlayed (Fig. 3). The spectrum at the downslope differed in the

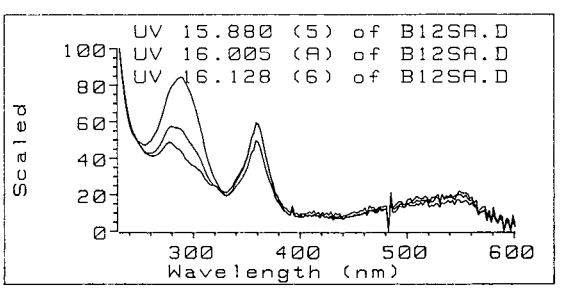

Fig. 3. Overlay of normalized spectra acquired at the upslope, apex and downslope of the vitamin B_{12} peak obtained after preconcentration and clean-up of multivitamin–multimineral tablets by solid-phase extraction.

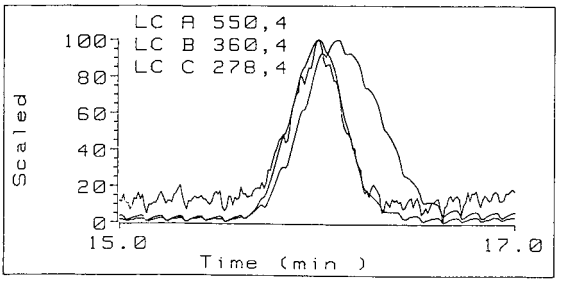

Fig. 4. Overlay of normalized signals of the vitamin B_{12} peak at 278, 360 and 550 nm obtained after preconcentration and clean-up of multivitamin–multimineral tablets by solid-phase extraction.

UV region from those at the apex and the upslope when multivitamin–multimineral tablets were analysed. This indicated that a UV-absorbing impurity eluted under the downslope of the peak. The spectra matched when a standard solution was analysed.

Signals acquired at 278, 360 and 550 nm were normalized and overlayed (Fig. 4). The retention time for the peak was not identical at these wavelengths when multivitamin–multimineral tablets were analysed. The peak at 278 nm had a longer retention time. The retention times were identical when a standard was analysed. A three-dimensional plot in which absorbance was plotted as a function of wavelength

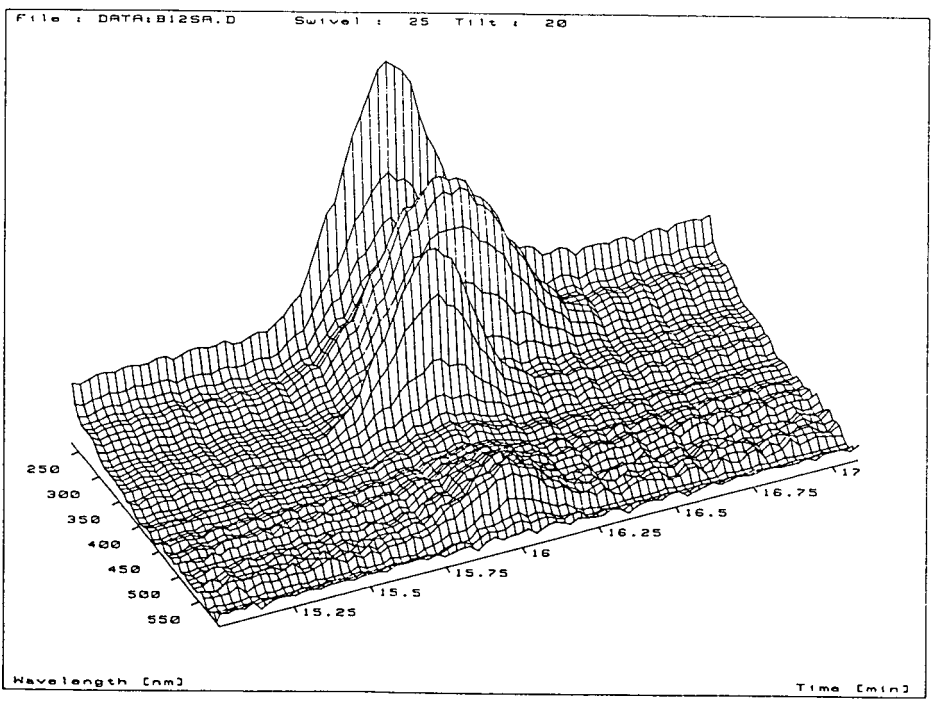

Fig. 5. Three-dimensional plot of the vitamin B_{12} peak obtained after preconcentration and clean-up of multivitamin–multimineral tablets by solid-phase extraction.

TABLE III

LINEAR REGRESSION ANALYSIS

Slope	144 773
Intercept	−2343
Correlation factor	0.9994

and time showed that the impurity did not interfere with the quantification of vitamin B_{12} at 550 nm (Fig. 5).

Two detectors from Waters Assoc., Models 481 and 490, were used during the method development. The chromatograms registered with the Model 490 at 550 nm did not have as many peaks as those registered with the Model 481 at the same wavelength, because the Model 490 automatically places an order filter which blocks all light below 300 nm when the operating wavelength is greater than 350 nm. When 550 nm is set as the detection wavelength the grating also gives a less intense band at 275 nm. As the sample contained many UV-absorbing compounds, the detector without the order filter (Model 481) gave chromatograms with a larger number of peaks.

Linearity

A series of six solutions of vitamin B_{12} in methanol–water (30:70) were prepared in the range 1.2–6.4 μg/ml, corresponding to 1.1–5.8 μg per tablet when tablets were analysed according to the method. Each solution was injected six times and the regression line was calculated by the method of least squares. The results from the linear regression analysis are given in Table III. The peak area was linear in the range 1.1–5.8 μg of vitamin B_{12} per tablet.

Accuracy

The accuracy of the described procedure was assessed by adding known amounts of vitamin B_{12} to powdered placebo tablets prior to analysis according to the method. The added amounts of vitamin B_{12} corresponded to 0.8, 3.3 and 5.4 μg of vitamin B_{12} per tablet. The recovery of vitamin B_{12} was determined by comparing the areas obtained with that obtained from a standard solution analysed according to the described method. The recovery of vitamin B_{12} ranged from 95 to 99% (Table IV). The areas obtained were also compared with those obtained from direct injections of

TABLE IV

ACCURACY

Added amount (μg per tablet)	Relative recovery (%)	Absolute recovery (%)
0.82	99	95
3.3	97	91
5.4	95	94

TABLE V

COMPARISON BETWEEN HPLC AND MICROBIOLOGICAL METHODS

Batch of tablets	Results (μg of vitamin B_{12} per tablet)	
	SPE + HPLC	Microbiological method
I	3.8	3.2
II	3.2	3.9
III	3.5	3.2

vitamin B_{12} in methanol–water (30:70). The absolute recovery of vitamin B_{12} ranged from 91 to 95% (Table IV).

Three batches of multivitamin–multimineral tablets were analysed according to the described method and by a microbiological method. The results obtained are given in Table V. The inter-method correspondence was satisfactory.

Precision

One batch of multivitamin–multimineral tablets was analysed on five occasions during 2 weeks. On each occasion 40 tablets were powdered and three determinations of vitamin B_{12} were made. One analyst performed the analyses using different batches of solid-phase columns and HPLC columns but the same pump, autosampler, detector and integrator. The results obtained are given in Table VI. A one-way analysis of variance (ANOVA) was used to evaluate the variance [11]. The results are given in Table VII. A one-tailed *F*-test was carried out to test whether the mean squares differed

TABLE VI

ASSAY OF TABLETS

Day	Individual results (μg of vitamin B_{12} per tablet)	Mean (μg of vitamin B_{12} per tablet)
1	3.8, 3.6, 3.9	3.8
2	3.4, 3.7, 3.6	3.6
3	3.2, 3.3, 3.3	3.3
4	3.4, 3.6, 3.5	3.5
5	3.5, 3.5, 3.5	3.5

TABLE VII

ANOVA TABLE

Source of variation	Degrees of freedom	Sum of squares	Mean squares	*F*-ratio
Between days	4	0.384	0.096	8.000
Within days	10	0.120	0.012	
Total	14	0.522		

TABLE VIII

PRECISION (RELATIVE STANDARD DEVIATION, R.S.D.)

Source of variation	R.S.D. (%)
Within days (repeatability)	3.1
Between days	4.8
Total (reproducibility)	5.7

significantly. The critical value of F for four and ten degrees of freedom was 3.48 ($P = 0.05$). As the calculated value of F exceeded the critical value, the variance between days, σ_1^2, differed significantly from zero. The within-day mean square gave an estimate of the variance within days, σ_0^2. Since the between-day sample mean square estimated $\sigma_0^2 + n\sigma_1^2$, where n is the number of replicate determinations on each day, the precision could be calculated. The results are given in Table VIII.

In conclusion, the method was found to be selective, linear, accurate and precise. The method is rapid compared with the frequently used microbiological method.

REFERENCES

1 *United States Pharmacopeia, XXII Revision*, U.S. Pharmacopeial Convention, Rockville, MD, 1989, pp. 1516–1518.
2 M. Amin and J. Reusch, *J. Chromatogr.*, 390 (1987) 448.
3 M. Amin and J. Reusch, *Analyst (London)*, 112 (1987) 989.
4 E. Wang and W. Hou, *J. Chromatogr.*, 447 (1988) 256.
5 T. S. Hudson, S. Subramanian and R. J. Allen, *J. Assoc. Off. Anal. Chem.*, 67 (1984) 994.
6 *Baker-10 SPE Applications Guide*, Vol. 1, J. T. Baker, Philipsburg, NJ, 1982, p. 40.
7 *United States Pharmacopeia, XXII Revision*, U.S. Pharmacopeial Convention, Rockville, MD, 1989, p. 1566.
8 H. Hulchin, P. Cravioto and T. Macek, *J. Am. Pharm. Assoc.*, 45 (1956) 806.
9 A. J. Rosenberg, *J. Biol. Chem.*, 219 (1956) 951.
10 A. J. Bartilucci, R. Di Giralamo and H. Eisen, *J. Am. Pharm. Assoc.*, 47 (1958) 42.
11 J. C. Miller and J. N. Miller, *Statistics for Analytical Chemistry*, Ellis Horwood, Chichester, 2nd ed., 1988, pp. 83–84.

Journal of Chromatography, 541 (1991) 393–400
Elsevier Science Publishers B.V., Amsterdam

CHROM. 22 925

Improvement of chemical analysis of antibiotics

XVII.[a] Application of an amino cartridge to the determination of residual sulphonamide antibacterials in meat, fish and egg

YOSHITOMO IKAI*, HISAO OKA, NORIHISA KAWAMURA, JUNKO HAYAKAWA and MASUO YAMADA
Aichi Prefectural Institute of Public Health, Nagare 7–6, Tsuji-machi, Kita-ku, Nagoya 462 (Japan)
KEN-ICHI HARADA and MAKOTO SUZUKI
Faculty of Pharmacy, Meijo University, Tempaku-ku, Nagoya 468 (Japan)
and
HIROYUKI NAKAZAWA
National Institute of Public Health, 4–6–1, Shirokanedai, Minato-ku, Tokyo 108 (Japan)
(First received May 2nd, 1990; revised manuscript received October 17th, 1990)

ABSTRACT

A simple, rapid and reliable method for the determination of residual sulphonamide antibacterials (SAs) (sulphathiazole, sulphisozole, sulphamethoxazole, sulphadiazine, sulphamerazine, sulphadimidine, sulphamonomethoxine, sulphadimethoxine, sulphamethoxypyridazine and sulphaquinoxaline) in meat, fish and egg was developed using a combination of high-performance liquid chromatography (HPLC) and clean-up with an amino-type prepacked cartridge. SAs were extracted with ethyl acetate and applied to a Baker 10 amino cartridge. After elution from the cartridge, SAs were determined by HPLC. The recoveries at the level of 0.5 ppm were 73.7–99.1% and the detection limits were 0.05 ppm. The analysis time per sample was about 45 min.

INTRODUCTION

Sulphonamide antibacterials (SAs) are widely used for the treatment and prevention of diseases of animal and fish, and more than ten kinds of SAs are applied to domestic animals and cultured fish in Japan. Several methods have been reported [1–20] for the determination of residual SAs in livestock products such as meat, fish and egg, but most of them are not suitable for routine analysis because of the long analysis time and complicated clean-up procedure. Thus, a simple, rapid and reliable method for the simultaneous determination of SAs is required.

[a] For Part XVI, see ref. 21.

0021-9673/91/$03.50

In order to simplify the clean-up procedure for SAs, prepacked cartridges [4–7,20] have been utilized, among which the reversed-phase type [4–6,20] are the most frequently used. However, we considered that normal-phase and ion-exchange types are more suitable than the reversed-phase type, because SAs have been successfully extracted from various samples with organic solvents [1–4,6–17]. For the clean-up of extracted SAs, reversed-phase cartridges need some time-consuming pretreatments such as evaporation of the organic solvents and elimination of fat from the extract, whereas normal-phase and ion-exchange cartridges do not require such pretreatments. For these reasons, normal-phase and ion-exchange cartridges may be more effective for carrying out the clean-up simply and rapidly.

On the basis of the above considerations, we tried to establish a simple, rapid and reliable clean-up system for the determination of residual SAs in livestock products using a normal-phase or an ion-exchange type of cartridge. This paper describes techniques for the clean-up of residual sulphathiazole (STZ), sulphisozole (SIZ), sulphamethoxazole (SMX), sulphadiazine SDZ), sulphamerazine (SMR), sulphadimidine (SDD), sulphamonomethoxine (SMMX), sulphadimethoxine (SDMX), sulphamethoxypyridazine (SMPD) and sulphaquinoxaline (SQ) in meat, fish and egg using an amino cartridge, and for the simultaneous determination of SAs using high-performance liquid chromatography (HPLC).

EXPERIMENTAL

Materials

Acetonitrile, anhydrous sodium sulphate, ethyl acetate, *n*-hexane, methanol, phosphoric acid and sodium hydroxide were of analytical reagent grade.

SMX, SDZ, SMR, SDD, SDMX and SMPD were obtained from Sigma (St. Louis, MO, U.S.A.), and STZ, SMMX, SQ and SIZ from Wako (Osaka, Japan), Daiichi Pharmaceutical (Tokyo, Japan), Dainippon Pharmaceutical (Osaka, Japan) and Takeda Chemical Industries (Osaka, Japan), respectively.

Baker 10 amino (catalogue No. 7088-3), Baker 10 cyano (7021-3), Baker 10 diol (7094-3), Baker 10 quaternary amine (7091-3), Baker 10 carboxylic acid (7211-3) and Baker 10 aromatic sulphonic acid (7090-3) cartridges were purchased from J. T. Baker (Phillipsburgh, NJ, U.S.A.).

Preparation of standard solution

Each standard (10 mg) was weighed accurately into a 100-ml volumetric flask and diluted with acetonitrile. Subsequent dilutions were made with the eluent.

Clean-up procedure

A 5-g amount of sample and 10 g of anhydrous sodium sulphate were weighed into a 50-ml centrifuge tube, blended with 20 ml of ethyl acetate for 30 s using a high-speed blender (Ultra-Turrax T25; IKA Werk, Staufen, Germany) and centrifuged (1500 rpm, 300 *g*) for 2 min and the supernatant was decanted. The above extraction procedure with ethyl acetate was repeated once more and the combined extracts were applied to a Baker 10 amino cartridge pre-washed with 10 ml of methanol. The cartridge was washed with 5 ml of *n*-hexane and air-dried by aspiration for 1 min. SAs were eluted from the cartridge with 5 ml of acetonitrile–0.02 *M* aqueous

phosphoric acid solution (24:76) and 20 μl of the eluate were injected into the HPLC system for the routine determination of SAs.

High-performance liquid chromatography

A high-performance liquid chromatograph equipped with a constant-flow pump (LC-6A; Shimadzu, Kyoto, Japan) was used with a UV detector (Shimadzu SPD-6AV) operated at 272 nm. The separation was performed on Wakosil $5C_{18}$ (5 μm, 250 × 4.6 mm I.D.) (Wako) with acetonitrile–0.02 *M* aqueous phosphoric acid solution (24:76) as mobile phase at a flow-rate of 1.0 ml/min at room temperature.

RESULTS AND DISCUSSION

Establishment of HPLC system

In order to determine SAs, thin-layer chromatography (TLC) [14–15,17], gas chromatography (GC) [1–2,16] and HPLC [3–13,18–20] have mainly been used. However, TLC is unsuitable for precise determinations and GC requires complicated treatment to derivatize SAs. On the other hand, HPLC enables SAs to be determined rapidly and with high sensitivity without any additional treatment such as GC, so we tried to separate ten kinds of SAs using a C_{18} HPLC column and a combination of acetonitrile and aqueous phosphoric acid solution as the mobile phase. After optimization of the mobile phase parameters, concentration of phosphoric acid, pH of the aqueous solution and ratio of the aqueous solution and the organic solvent, satisfactory separations of SAs could be obtained using acetonitrile–0.02 *M* aqueous phosphoric acid solution (pH unadjusted) (24:76). The flow-rate was 1.0 ml/min and the monitoring wavelength was adjusted to 272 nm, which is a common maximum absorption wavelength for all SAs. Under these conditions, the ten kinds of SAs were successfully separated in 26 min, as shown in Fig. 1, the calibration graphs were linear

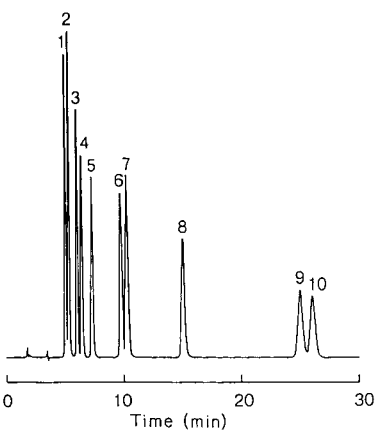

Fig. 1. Typical high-performance liquid chromatogram of SAs under the optimum conditions. Peaks: 1 = STZ; 2 = SDZ; 3 = SMR; 4 = SDD; 5 = SMPD; 6 = SMMX; 7 = SIZ; 8 = SMX; 9 = SDMX; 10 = SQ (50 ng each). Column, Wakosil $5C_{18}$ (5 μm) (250 × 4.6 mm I.D.); mobile phase, acetonitrile–0.02 *M* aqueous phosphoric acid solution (24:76); flow-rate, 1.0 ml/min; detection, 272 nm.

between 0.5 and 100 ng and the detection limits of SAs on the chromatograms were 0.5 ng (signal-to-noise ratio >5).

Establishment of clean-up system

In a previous study [21], the following clean-up procedure was successfully applied to the determination of residual pyridonecarboxylic acid antibacterials in fish. The analyte is extracted from the sample by blending with organic solvent, the resulting extract is centrifuged and the supernatant is decanted and applied to a prepacked cartridge. After elution from the cartridge with a suitable eluent, the analyte is determined by HPLC. Because this procedure is very simple and rapid, we wished to apply it to the determination of SAs. To apply this procedure effectively, various conditions were optimized as described below and a satisfactory clean-up system as given under Experimental was established.

Comparison of prepacked cartridges. The cartridge to be used in this method is required to possess both the ability to retain SAs with an organic solvent and then to release SAs with a suitable eluent. Several commercially available normal-phase and ion-exchange types (Baker 10 amino, cyano, diol, quaternary amine, carboxylic acid and aromatic sulphonic acid) prepacked cartridges were compared. SAs (5 μg each) were dissolved in 40 ml of ethyl acetate and applied to the cartridges. The ethyl acetate solution which passed through the cartridges was collected and evaporated to dryness. SAs in the residue were determined by HPLC and the amounts of SAs retained in the cartridge were calculated. Although SAs were perfectly retained on the amino and aromatic sulphonic acid cartridges, the proportions of SAs retained on the quaternary amino cartridge were 90–100% and those on the cyano, diol and carboxylic acid cartridges were less than 20%.

Because the amino and aromatic sulphonic acid cartridges gave satisfactory retention of SAs, they were successively compared with respect to the elution behaviour of SAs. After the application of SAs to the cartridges in the same manner as described above, SAs were eluted from the cartridges with the mobile phase, acetonitrile–0.02 *M* aqueous phosphoric acid solution (24:76), and then determined by HPLC. Whereas more than 95% of SAs could be recovered from the amino cartridge using 20 ml of the eluent, only SIZ and SMR were eluted from the aromatic sulphonic acid cartridge. We concluded that the amino cartridge is the most suitable for our objective.

Elution of SAs from the cartridge. In order to determine analytes in the eluent from the cartridge by HPLC, the eluent is usually evaporated and the residue is dissolved in a suitable solution before injection into the HPLC system. However, these treatments are not desirable for a simple and rapid determination, so we wished to elute the SAs with a small volume of the mobile phase, because the eluent can be injected into the HPLC system without any treatment. The elution patterns of SAs from the cartridge were investigated using the mobile phase as the eluent. Usually, the retention power of the cartridge is weakened by the influence of the sample matrix. SAs were applied to the cartridge with an extract of chicken meat. The sample (chicken meat, 5 g) was extracted by blending with 10 g of anhydrous sodium sulphate and 40 ml of ethyl acetate and the resulting extract was centrifuged. After addition of SAs (2.5 μg each) to the supernatant, the mixture was applied to the cartridge. The cartridge was washed with 5 ml of *n*-hexane and then aspirated to remove the *n*-hexane. The SAs

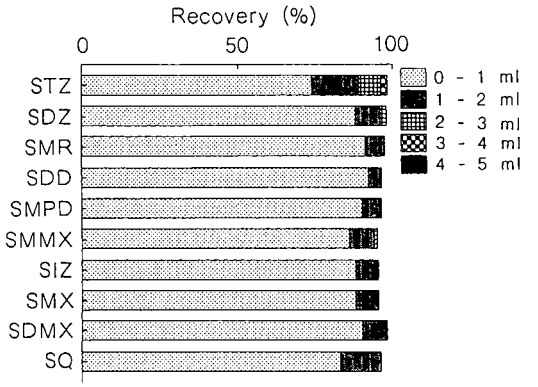

Fig. 2. Elution profiles of SAs from the amino cartridge. Integration of recoveries of SAs in each 1-ml fraction of eluent.

were then eluted from the cartridge with the eluent and the SAs in each collected fraction (1 ml) were determined. As SAs were sufficiently recovered in 4 ml of the eluate, as shown in Fig. 2, we used 5 ml of the mobile phase for elution of SAs from the cartridge.

Application of SAs to the cartridge. Because SAs must be applied to the cartridge together with a sample extract, the retention of SAs on the cartridge would be influenced by the volume of the extract. The influence on the recoveries of SAs was investigated. After the extraction of sample (chicken meat, 5 g) with 20, 40, 60, 80 or 100 ml of ethyl acetate, SAs (2.5 μg each) were added to each extract and the resulting solution was applied to the cartridge in the same manner as described above. SAs were eluted with 5 ml of the eluent and determined. As shown in Fig. 3, all the SAs were satisfactorily retained on the cartridge when 20 or 40 ml of ethyl acetate were used, whereas the retention of SDD became weak when over 60 ml was used, indicating that 40 ml of the extract is the volume limit.

In order to remove completely remaining matrix such as fat from the cartridge, the cartridge was washed with the extraction solvent used in a previous study [21].

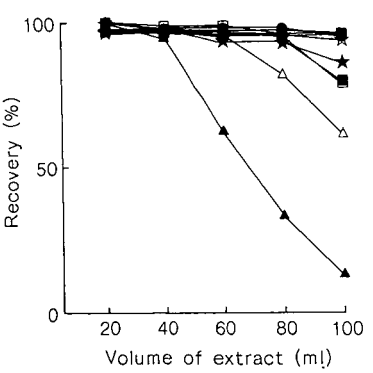

Fig. 3. Influence of volume of the extract on the retention of SAs on the amino cartridge. Recoveries of SAs which were applied to the cartridge with various volumes of extract. ○, STZ, ●, SDZ; △, SMR; ▲, SDD; □, SMPD; ◪, SMMX; ■, SIZ; ☆, SMX; ★, SDMX; ⁎, SQ.

However, the recoveries of SAs were decreased when ethyl acetate was used as a washing solvent. Various organic solvents were examined and *n*-hexane gave the most satisfactory result. We therefore used 5 ml of *n*-hexane as the washing solvent.

Extraction of SAs from the sample. Organic solvents such as methanol [5,9,20], acetone [3–4,8,16], acetonitrile [1,2,11], dichloromethane [12,15], chloroform [4,13–15] and ethyl acetate [14,15,17] have frequently been used for the extraction of SAs from various biological samples because of their excellent deproteinization effect. However, methanol, acetone and acetonitrile were unsuitable for the retention of SAs on the cartridge, and dichloromethane and chloroform also were not advantageous for decantation of the supernatant after centrifugation because of their gravity. Ethyl acetate was used as the solvent for the extraction of SAs from samples.

Because the use of less than 40 ml of ethyl acetate was favourable for the extraction, it was required to extract SAs from samples with at most 40 ml of ethyl acetate or to concentrate the extract to less than 40 ml. It was desirable to avoid the concentration of the extract, for the sake of simple and rapid clean-up. Therefore, extraction of SAs was carefully investigated. SAs (2.5 μg each) were added to the sample (chicken meat, 5 g) and were extracted five times using 20 ml of ethyl acetate. SAs in each extract were determined by HPLC after the treatment with the cartridge. It was found that 83–84% of SAs were recovered in the first extract, 12–13% in the second and 2–3% in the third. As satisfactory recoveries were given by the first and second extractions SAs were extracted twice using 20 ml of ethyl acetate.

We always used anhydrous sodium sulphate in extraction step throughout any optimization process. Probably it is effective in reducing the amount of water in the sample, so that a satisfactory extraction efficiency was obtained. In order to find a suitable amount of anhydrous sodium sulphate to be added, recoveries of SAs (2.5 μg each) from the sample (chicken meat, 5 g) were investigated using various amounts (0, 5, 10, 15 and 20 g). The recoveries increased with increasing amount of anhydrous sodium sulphate but remained almost constant with amounts above 10 g. Therefore, 10 g of anhydrous sodium sulphate were added to the sample before blending with ethyl acetate.

Application of various samples

Using the present method, the recoveries of SAs from chicken, beef, pork, eel, sweet fish, rainbow trout and egg were investigated at the addition level of 0.5 ppm. Although satisfactory recoveries (74.7–99.1%) and relative standard deviations (0.9–4.8%) were obtained, as shown in Table I, egg did not show satisfactory recoveries because of insufficient elution of SAs from the cartridge. However, adjustment of the pH of the aqueous solution to 2.5–5.0 gave satisfactory results. We therefore used acetonitrile–0.02 *M* aqueous phosphoric acid solution (pH adjusted to 3.0 with sodium hydroxide) (24:76) as the eluent for egg samples.

The detection limit for routine analysis was 0.05 ppm, which could be decreased to 0.01 ppm by injecting 100 μl of the eluent into the HPLC system. The time required for the analysis of one sample was about 45 min.

Typical chromatograms of fortified chicken and commercially available meats (chicken, pork and beef), fish (eel) and egg are shown in Fig. 4. Satisfactory clean-up could be achieved, because no interfering peaks appeared on the chromatograms and the peaks near the solvent front on the chromatograms were very small.

TABLE I

RECOVERIES OF SULPHONAMIDES FROM VARIOUS SAMPLES

Recoveries of SAs from 5 g of commercially available meats, fishes and egg at the level of 0.5 ppm according to the present method. Results are averages of six replicate determinations.

Sample	Recovery (%)[a]									
	STZ	SDZ	SMR	SDD	SMPD	SMMX	SIZ	SMX	SDMX	SQ
Chicken	92.0	97.6	95.7	90.0	96.7	95.7	95.7	94.9	94.1	94.8
	(3.4)	(1.2)	(3.3)	(4.8)	(1.4)	(2.3)	(1.6)	(1.9)	(4.5)	(3.0)
Pork	87.4	94.6	96.4	91.2	93.2	94.0	94.5	94.1	91.9	89.1
	(1.9)	(2.0)	(2.1)	(2.3)	(1.6)	(1.4)	(1.8)	(1.2)	(2.5)	(1.6)
Beef	86.3	93.4	95.6	87.7	92.8	93.0	93.8	94.6	91.0	85.2
	(2.9)	(2.5)	(1.6)	(4.0)	(1.7)	(3.4)	(3.0)	(1.5)	(2.1)	(4.4)
Eel	90.9	97.1	99.1	90.3	96.9	98.4	97.8	96.9	98.2	96.8
	(2.1)	(1.1)	(1.0)	(4.2)	(1.0)	(0.9)	(1.4)	(1.4)	(1.4)	(1.8)
Sweet fish	85.6	92.2	95.4	79.8	89.5	93.5	92.7	91.8	90.2	87.1
	(4.4)	(2.5)	(2.7)	(3.8)	(3.6)	(4.6)	(2.4)	(3.2)	(4.0)	(3.6)
Rainbow trout	89.2	95.6	97.6	74.7	91.5	93.7	95.1	95.0	92.8	91.1
	(0.9)	(0.9)	(1.1)	(4.5)	(1.5)	(4.5)	(1.6)	(0.9)	(0.9)	(1.6)
Egg[b]	73.7	86.2	93.0	81.6	91.7	88.9	83.2	88.2	92.2	89.2
	(3.9)	(3.9)	(1.7)	(5.6)	(1.7)	(1.6)	(2.8)	(2.0)	(0.9)	(2.2)

[a] Relative standard deviations (%) in parentheses.

[b] Acetonitrile–0.02 *M* aqueous phosphoric acid solution (pH 3.0) (24:76) was used as the eluent.

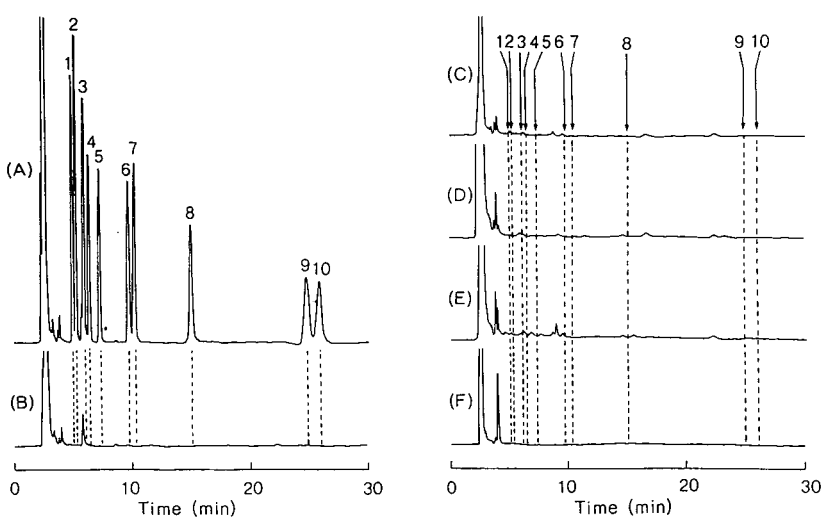

Fig. 4. Typical high-performance liquid chromatograms of commercially available meats, eel and egg. (A) Fortified chicken (0.5 ppm); (B) chicken; (C) pork; (D) beef; (E) eel; (F) egg. Peaks and HPLC conditions as in Fig. 1.

In conclusion, a method for the determination of residual SAs in meat, fish and egg was established using a combination of HPLC and clean-up with Baker 10 amino cartridge. The method is not only simple, rapid and reliable, but also permits the simultaneous determination of ten kinds of SAs with good accuracy, precision and reproducibility.

ACKNOWLEDGEMENTS

We greatly appreciate the encouragement given by Dr. S. Isomura, Director of the Aichi Prefectural Institute of Public Health. We also thank Takeda Chemical Industries for the kind gift of sulphisozole.

REFERENCES

1 *Official Analytical Methods for Residual Substances in Livestock Products, Veterinary Sanitation Division, Environmental Health Bureau,* Vol. 2, No. 3, Ministry of Health and Welfare, Tokyo, 1979, pp. 1–13.
2 *Official Analytical Methods for Residual Substances in Livestock Products, Veterinary Sanitation Division, Environmental Health Bureau,* Vol. 2, No. 4, Ministry of Health and Welfare, Tokyo, 1981, pp. 1–11.
3 *Official Analytical Methods for Residual Substances in Livestock Products, Veterinary Sanitation Division, Environmental Health Bureau,* Vol 2, No. 8, Ministry of Health and Welfare, Tokyo, 1988, pp. 1–6.
4 N. Haagsma and C. Van De Water, *J. Chromatogr.,* 333 (1985) 256.
5 M. Horie, Y. Hoshino, N. Nose, H. Iwasaki and H. Nakazawa, *Eisei Kagaku,* 91 (1985) 371.
6 H. Terada, M. Asanoma, H. Tubouchi, T. Ishihara and Y. Sakabe, *Eisei Kagaku,* 29 (1983) 226.
7 H. Nakazawa, K. Shinomiya, M. Fujita, Y. Kitada, M. Yamamoto, T. Nagata, S. Komiyama and E. Takabatake, *J. Food Hyg. Soc. Jpn.,* 26 (1985) 7.
8 H. Nakazawa, E. Takabatake, S. Hino and C. A. Mtema, *Bunseki Kagaku,* 32 (1983) 179.
9 T. Nagata and M. Saeki, *J. Food Hyg. Soc. Jpn.,* 29 (1988) 13.
10 Y. S. Endoh, R. Yamaoka and N. Sasaki, *J. Assoc. Off. Anal. Chem.,* 70 (1987) 1031.
11 Y. Hori, *J. Food Hyg. Soc. Jpn.,* 24 (1983) 447.
12 G. Weiss, P. D. Duke and L. Gonzales, *J. Agric. Food Chem.,* 35 (1987) 905.
13 J. D. Weber and M. D. Smedley, *J. Assoc. Off. Anal. Chem.,* 72 (1989) 445.
14 O. W. Parks, *J. Assoc. Off. Anal. Chem.,* 65 (1982) 632.
15 O. W. Parks, *J. Assoc. Off. Anal. Chem.,* 68 (1985) 20.
16 A. J. Manuel and W. A. Steller, *J. Assoc. Off. Anal. Chem.,* 64 (1981) 794.
17 M. H. Thomas, K. E. Soroka, R. M. Simpson and R. L. Epstein, *J. Agric. Food Chem.,* 29 (1981) 621.
18 A. R. Long, L. C. Hsieh, M. S. Malbrough, C. R. Short and S. A. Barker, *J. Agric. Food Chem.,* 38 (1990) 423.
19 A. R. Long, C. R. Short and S. A. Barker, *J. Chromatogr.,* 502 (1990) 87.
20 M. Horie, K. Saito, Y. Hoshino, N. Nose, N. Hamada and H. Nakazawa, *J. Chromatogr.,* 502 (1990) 371.
21 Y. Ikai, H. Oka, N. Kawamura, M. Yamada, K.-I. Harada, M. Suzuki and H. Nakazawa, *J. Chromatogr.,* 477 (1989) 397.

Journal of Chromatography, 541 (1991) 401–410
Elsevier Science Publishers B.V., Amsterdam

CHROM. 22 935

Optimization and ruggedness testing of the determination of residues of carbadox and metabolites in products of animal origin

Stability studies in animal tissues

G. M. BINNENDIJK, M. M. L. AERTS[a] and H. J. KEUKENS*
State Institute for Quality Control of Agricultural Products (RIKILT), P.O. Box 230, 6700 AE Wageningen (The Netherlands)
and
U. A. Th. BRINKMAN
Department of Analytical Chemistry, Free University of Amsterdam, De Boelelaan 1083, 1081 HV Amsterdam (The Netherlands)
(First received August 8th, 1990; revised manuscript received October 25th, 1990)

ABSTRACT

A method developed for the determination of residues of carbadox and its metabolites in swine tissues using high-performance liquid chromatography with on-line precolumn enrichment and postcolumn derivatization with UV–VIS detection was optimized and the applicability of the method was extended to plasma and eggs. With the optimized method, more than twenty samples per person per day can be analysed. In the matrices investigated, the observed limit of determination for carbadox is 0.5–1 μg/kg and for desoxy-carbadox 0.5–2 μg/kg. The mean recovery for desoxy-carbadox in kidney, muscle and liver as established by two laboratories over a 2-month period is 95% (relative standard deviation = 14%, $N = 37$, 10 μg/kg). In other matrices the recoveries are between 83 and 91%. The recovery for carbadox is 70–80% in muscle, plasma and eggs. The method has been used routinely in pharmacokinetic and surveillance studies.

Stability studies of kidney and liver samples spiked with carbadox showed that carbadox is rapidly decomposed (*in vitro* metabolism). After storage for about 1 h at 4°C, more than 50% of the added amount is converted by reduction to desoxy-carbadox. In contrast, carbadox is stable in eggs and muscle under spiking conditions and during storage at −20°C. Desoxy-carbadox is stable during spiking and storage at −20°C in eggs and muscle. In kidney and liver, its stability was good under spiking conditions but could not be proved unequivocally during storage.

INTRODUCTION

High-performance liquid chromatographic (HPLC) [1–4], polarographic [5–7], thin-layer chromatographic (TLC) [8] and gas chromatographic (GC) [9] methods

[a] Present address: AKZO-Intervet Int. B.V., P.O. Box 31, 5830 AA Boxmeer, The Netherlands.

0021-9673/91/$03.50

have been described for the determination of residues of the growth-promoting and chemotherapeutic agent carbadox (CBX) and its metabolites in various matrices. In a previous study, a method [10] was developed for the trace analysis of residues of carbadox in swine tissues. Therefore, the sample clean-up, chromatographic conditions and detection parameters were chosen according to the demands of this polar compound. After the method had been developed it was used in stability studies of reference materials and preliminary pharmacokinetic experiments with swine. The results of these studies showed that the toxic metabolite desoxycarbadox (desoxy-CBX) is the predominant residue in the target substrates liver and kidney. Further, it became evident that the spiking procedure for liver and kidney was very critical. These matrices markedly influenced the analytical recovery of CBX. Finally, the elution profiles of CBX and desoxy-CBX from the clean-up column were occasionally abnormal. Therefore, it was decided to optimize the method for the routine determination of desoxy-CBX, and further to investigate whether the scope of the method could be broadened to the analysis of other matrices, *i.e.*, egg and plasma.

EXPERIMENTAL

The experimental conditions were identical with those described earlier [10] with the exception that a Gilson 231-401 auto-injector (Gilson Medical Electronics, Villiers le Bel, France) was used instead of a Rheodyne Model 7125 injector. In Table I, a summary of the optimized analytical procedure is presented.

RESULTS AND DISCUSSION

Alumina/Florisil clean-up

In the original procedure [10], the first 10 ml of the total of 20 ml of column eluate were collected. This choice was mainly based on the speed of analysis. During routine analysis, however, it was observed that the desoxy-CBX concentrations found in

TABLE I

SUMMARY OF THE OPTIMIZED ANALYTICAL PROCEDURE

Parameter/step	Value/conditions	Parameter/step	Value/conditions
Sample size	10 g	Flushing time	20 min
Extraction	40 ml acetonitrile–methanol (1:1)	Back-flushing time	5 min
Alumina–Florisil clean-up	Take 10 ml of mixed total eluate	Eluent	Acetonitrile–0.01 *M* sodium acetate (pH 6) (14:86)
Evaporate to	0.9–1.1 ml	Eluent flow-rate	0.5 ml/min
Dilute to	4 ml with water	Analytical column	100 × 3 mm I.D., 5 μm Chromspher-C_{18}
Partition with	2 ml isooctane		
Inject	1 ml into the LC system	Derivatization	0.5 *M* NaOH
Enrichment-flush water flow	0.3 ml/min	reagent	(0.23 ml/min)
		Reaction coil	2 m × 0.5 mm I.D., knitted PTFE
Enrichment column	10 × 2.1 mm I.D., Sep-Pak C_{18}	Detection	390 nm, 0.001 a.u.f.s.

practice samples and the analytical recoveries for desoxy-CBX in spiked (10 μg/kg) liver, muscle and kidney samples were about 10% higher in the second 10-ml eluate fraction. Occasionally, even greater differences were observed for CBX in muscle samples (Table II). The latter result was at variance with the earlier observations [10] for CBX which indicated a slightly increased concentration in the first 10 ml. The irreproducible differences between the results obtained for the two eluate fractions are probably caused by adsorption of the analytes to the alumina. To circumvent this problem, the total eluate was collected and 10 ml were taken for further analysis. Table II gives some data on the recoveries obtained when 10 ml of the total eluate are used.

Enrichment column

In the original procedure [10], the LC enrichment column used was a 60 × 4.6 mm I.D. stainless-steel cartridge filled with 37–50-μm Bondapak C_{18}/Corasil material. These dimensions were necessary to retain CBX and its metabolites adequately. A drawback of this type of column was the occasional peak broadening resulting from the variation in homogeneity of the dry-packed column. Therefore, the possibility of using a small-sized enrichment column was investigated. On the basis of results obtained in other research programmes in our department, Sep-Pak C_{18} with a particle size of 55–105 μm [11], as present in commercially available off-line solid-phase extraction cartridges (Millipore), was tested. A 10 × 2.1 mm I.D. enrichment column, fitted with 20-μm screens, was slurry packed with this material. After successful preliminary experiments, the original and modified enrichment procedures were compared by carrying out routine analysis of 29 liver and kidney samples obtained from a pharmacokinetic study with CBX. For each sample the desoxy-CBX concentration was determined based on measurement of peak areas. The results were statistically evaluated by a Student *t*-test. The calculated *t*-value (1.68) was well below the critical value for a double-sided 95% confidence interval (2.05), showing that the

TABLE II

COMPARISON OF AVERAGE ANALYTICAL RECOVERIES (%) OBTAINED WITH SPIKED SAMPLES (10 μg/kg) USING DIFFERENT COLUMN ELUATE FRACTIONS[a] FROM THE ALUMINA/FLORISIL COLUMN ($n=4$)

Tissue	Eluate fraction[b]	Average recovery		R.S.D. %
		Analyte	%	
Muscle	A	CBX	59	7.9
		Desoxy-CBX	89	8.9
	B	CBX	86	0.6
		Desoxy-CBX	100	3.5
	T	CBX	70	3.2
		Desoxy-CBX	91	5.6
Kidney	A	Desoxy-CBX	88	18.0
	B	Desoxy-CBX	98	8.0
Liver	A	Desoxy-CBX	91	6.9
	B	Desoxy-CBX	99	17.0

[a] The final procedure in Table I was used.

[b] A = first 10 ml of eluate; B = second 10 ml of eluate; T = 10 ml of the combined total eluate.

results obtained with the two enrichment columns were not significantly different.

The average peak width at half-height obtained with the 10-mm Sep-Pak C_{18} column was slightly smaller and much more reproducible than that obtained with the 60-mm Bondapak C_{18}/Corasil column, *viz.*, 0.24 mm ± 9% *versus* 0.25 mm ± 23%. It can therefore be concluded that the Sep-Pak C_{18} material present in the 10-mm column, which is only 3% of the amount of Bondapak C_{18}/Corasil in the 60 × 4.6 mm I.D. column, retains CBX and its metabolites very efficiently in the presence of a biological matrix. To ensure that the low analytical recovery of CBX in muscle (see Table II) was not due to breakthrough on the 10-mm enrichment column, a number of 10 μg/kg spiked samples were also analysed using a 60 × 3 mm I.D. enrichment column filled with Sep-Pak material. The recovery results obtained were fully comparable.

The low cost of the packing material and the ease of packing the cartridge allow the daily replacement of the 10 × 2.1 mm I.D. Sep-Pak C_{18} column during routine analysis, *i.e.*, after about 20 samples.

Chromatography and detection

Chromatography. The chromatographic cycle as described earlier [10] takes about 55 min per sample. Owing to the technical features of the autosampler used, more than 10 min are required for a reliable injection of 2 ml of sample extract. Considering the large number of samples that have to be analysed in pharmacokinetic or monitoring studies, it is desirable to speed up the procedure. Chromatograms obtained with the original method [10] showed that the chromatographic separation between CBX and its metabolites, and also the separation from matrix components, are not very critical when a Chromspher C_{18} column (200 × 3 mm I.D.) (Chrompack) was used as the analytical column. Therefore, the length of the column was reduced to 100 mm. To maintain the separation of the N^1- and N^4-monooxy-CBX metabolites the eluent composition was modified slightly (*viz.*, the acetonitrile content was lowered from 15% to 14%). Fig. 1 shows chromatograms obtained for standard solutions with the two chromatographic systems.

The time required for the analytical separation after back-flushing from the enrichment column has now been reduced from 40 to 25 min. By applying a concurrent operation of the processes of enrichment and separation, as is shown in Fig. 2, the total analysis time per sample (except the first sample) was reduced to 31 min.

An alternative for speeding up the procedure is to connect the enrichment column directly with the valve of the auto-injector, omitting the sample loop. The special properties of the injector used and the small dimensions of the concentration column allow the sample injection to the enrichment column and its use to flush the enrichment column. Injection directly onto the enrichment column makes it possible to use a higher injection speed; as a result, the same volume can be injected in a shorter time with the same reliability. Further, only one solvent delivery system is necessary. With this procedure also a chromatographic cycle of about 31 min is possible.

Injection volume and detection. The injection volume was reduced from 2 to 1 ml, in order to be able to inject each extract in duplicate and to improve the performance of the enrichment column. To compensate for decreased sensitivity, the choice of detection wavelength was evaluated. The peak heights of standard solutions of CBX and its relevant metabolites were measured at four different wavelengths. Table III

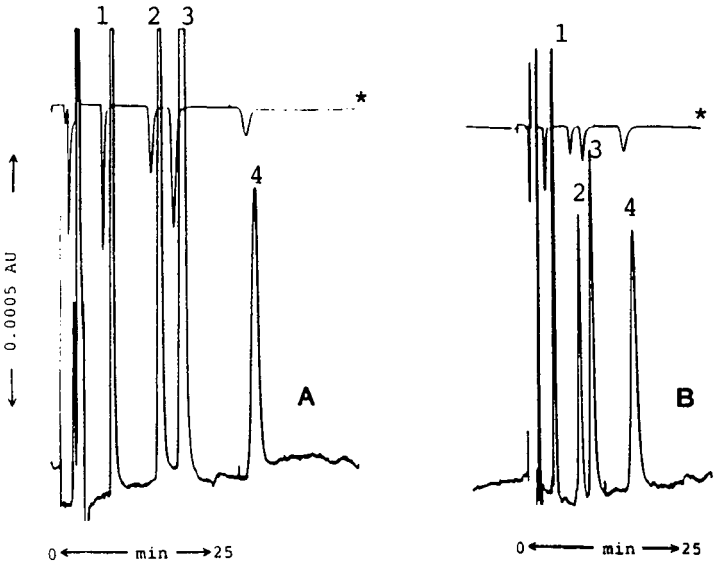

Fig. 1. LC separation of standard solutions of CBX and its metabolites under the conditions of (A) the original chromatographic system [10] and (B) the optimized conditions (Table I). Peaks: 1 = CBX; 2 = N^4-monoxy-CBX; 3 = N^1-monoxy-CBX; 4 = desoxy-CBX. The traces marked with asterisks were recorded at a 10-fold lower sensitivity.

shows the responses obtained. The system noise was found to be constant over the wavelength range investigated. From the data, it can be concluded that the 390-nm response for desoxy-CBX is more than double that at 420 nm. The responses of CBX and N^4-monoxy-CBX are also higher, although not so pronounced. The analysis of a number of blank muscle, liver and kidney samples, processed according to the modified procedure and detected at 390 nm, revealed no increase in matrix interferences in the chromatograms (see Fig. 3). Consequently, the decrease in sensitivity of desoxy-CBX resulting from the injection of only 1 ml was fully compensated by changing the detection wavelength. None of the compounds listed in Table IV interfered in the determination of CBX and desoxy-CBX.

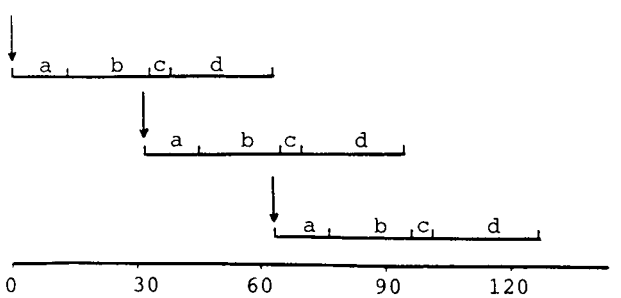

Fig. 2. Timetable showing the concurrent processes of (a) injection of sample, (b) enrichment and flushing of sample, (c) backflushing to the analytical column and (d) chromatographic separation; three sample cycles are shown.

TABLE III

UV–VIS RESPONSE (PEAK HEIGHT) AT FOUR WAVELENGTHS OF CBX AND ITS METABOLITES AFTER LC SEPARATION AND POSTCOLUMN REACTION

Wavelength (nm)	Peak height (cm)			
	CBX	N^4-Monoxy-CBX	N^1-Monoxy-CBX	Desoxy-CBX
380	26.0	10.2	12.6	10.5
390	25.0	11.9	14.1	10.7
400	23.5	11.8	16.1	8.4
420	21.5	10.2	17.9	4.2

Application in routine analysis

Swine tissues. The modified method was routinely used in a pharmacokinetic study with swine. More than 200 muscle, kidney and liver samples of carbadox-treated swine were analysed. The samples were processed at the Central Veterinary Institute (CDI) and the residue levels were determined at the RIKILT laboratories, using the column-switching LC procedure.

Results were calculated by use of a calibration graph. This graph proved to be linear over the range from 1 to at least 100 ng/ml of desoxy-CBX ($r^2 = 1.0000$) for peak area and peak height. Peak areas are routinely used for the calculations. The concentration of 100 ng/ml corresponds with a concentration of 190 μg/kg in tissues, which is more than the maximum level found for desoxy-CBX in liver and kidney from carbadox-treated animals after zero days withdrawal time. With each series of analysis, blank samples and samples spiked with desoxy-CBX (10 μg/kg) were analysed. The mean recovery for desoxy-CBX in the liver, kidney and muscle samples was 95% [relative standard deviation (R.S.D.) = 17%, $n = 17$, 10 μg/kg]. In the same period a number of spiked samples were analysed at the RIKILT laboratories by technicians having more experience with the method. The recovery found was also 95%, but the reproducibility was better, *viz.*, R.S.D. = 11%, $n = 20$. Recoveries found for tissue samples spiked at 10 and 100 μg/kg desoxy-CBX were comparable.

TABLE IV

VETERINARY DRUGS THAT DID NOT INTERFERE WITH THE DETERMINATION OF CBX AND DESOXY-CBX

Standard solutions corresponding to a tissue concentration of 100 μg/kg were injected into the HPLC system.

Chloramphenicol	Furaltadone	Nitrofurantoin	Sulphanilamide
Chlorotetracycline	Furazolidone	Nitrofurazone	Sulphadimethoxine
Clopidol	Fenbendazole	Nitrovin	Sulphadoxine
Dapsone	Furnicozone	Olaquindox	Sulphamerazine
Decoquinate	Halofuginone	Oxytetracycline	Sulphamethazine
Dimetridazole	Ipronidazole	Pyrantel tartrate	Sulphamethoxazole
Dinitolmide	Methylbenzoquate	Robenidine	Sulphaquinoxaline
Doxycycline	Nicarbazine	Ronidazole	Tetracycline
Ethopabate	Nifursol	Sulphadiazine	Thiophanate
			Trimethoprim

The limit of determination for desoxy-CBX in liver, kidney and muscle, calculated as the mean of the measured content of indepedent representative blank samples ($n=20$) plus six times the standard deviation of the mean [12], was 2 μg/kg.

Plasma. In the course of the pharmacokinetic study, a number of plasma samples were analysed. The procedure developed for swine tissue proved to be applicable unchanged to heparinized plasma. The recoveries for CBX and its reduced metabolites were high and reproducible. This is particularly important for CBX because it was found to be the major residue present in plasma. Table V shows the results of spiking experiments.

Eggs. The modified method was also applied to egg samples spiked with CBX and desoxy-CBX. When 10 g of homogenized whole egg, egg white or egg yolk were processed, very clean chromatograms and high, reproducible recoveries were obtained, as shown in Table V and Fig. 3. The limit of determination was about 0.5 μg/kg for both CBX and desoxy-CBX.

Stability of CBX and desoxy-CBX in animal products

During routine analysis, large series of liver and kidney samples had to be analysed and spiked samples were sometimes left to stand for a longer time before starting the extraction. These samples showed low CBX recoveries and interferences were observed in the chromatograms. A series of experiments were performed to investigate the stability of CBX after addition to liver and kidney (10–100 μg/kg). Homogenized bulk samples were spiked with CBX and stored at 4°C. Starting after 30 min, at regular intervals, 10-g aliquots were taken from the samples and extracted. The concentrations of CBX and desoxy-CBX were determined in each sub-sample while the concentrations of the monoxy metabolites could only be determined because only semi-quantitative standards were available.

Fig. 4 shows a typical example of the concentration profile that is obtained for kidney. On the basis of these experiments, it can be concluded that CBX is rapidly transformed *in vitro* to its reduced metabolites. First, the monoxy metabolites are formed, but after about 1 h most of the added amount of CBX is converted to desoxy-CBX. At these points in time less then 10% of the added amount was still present as CBX The results also lead to the conclusion that it is very unlikely that residues of CBX will be found in real liver and kidney samples and also that desoxy-CBX is the marker residue. The nature of the enzymes responsible for the *in vitro* metabolism of CBX in liver and kidney is not known yet.

TABLE V

AVERAGE RECOVERIES (%) OF CBX AND ITS METABOLITES IN BIOLOGICAL MATRICES

Matrix[a]	n	CBX	N^4-Monoxy-CBX	N^1-Monoxy-CBX	Desoxy-CBX
Plasma	5	81 ± 7	91 ± 5	93 ± 7	83 ± 7
Egg	8	81 ± 7	N.D.[b]	N.D.[b]	91 ± 5
Muscle	8	72 ± 3	80 ± 5	84 ± 7	91 ± 6
Liver/kidney/muscle	37				95 ± 14

[a] Spiking concentrations: 5–10 μg/kg (swine plasma), 5 μg/kg (eggs) and 10 μg/kg (muscle, liver and kidney).

[b] Not determined.

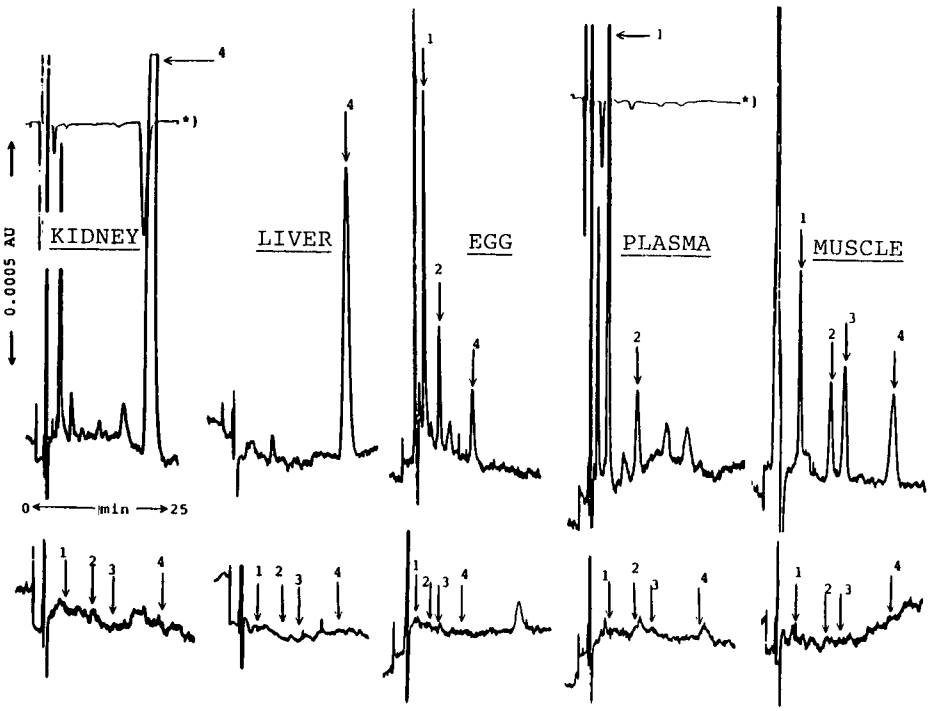

Fig. 3. Typical chromatograms obtained with the modified method under the conditions given in Table I. The lower chromatograms are blanks, the upper traces are for real or spiked samples of kidney (70 μg/kg desoxy-CBX), liver (14 μg/kg desoxy-CBX), egg (6 μg/kg CBX and 2 μg/kg desoxy-CBX), plasma (23 μg/kg CBX) and muscle (5 μg/kg spike of CBX and its metabolites). Peaks as in Fig. 1. The traces marked with asterisks, were recorded at a 10-fold lower sensitivity.

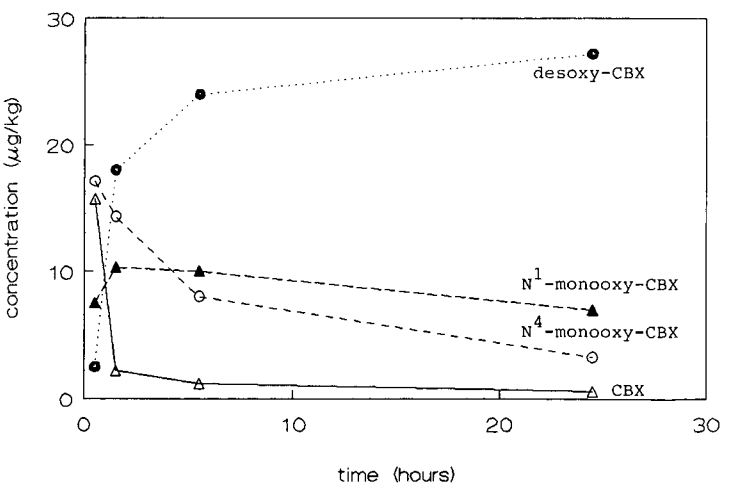

Fig. 4. *In vitro* transformation of carbadox after spiking into homogenized kidney tissue (50 μg/kg) and storage at 4°C. The concentrations of the monoxy metabolites are only estimates.

In contrast with the situation for liver and kidney, CBX proved to be stable under spiking conditions (< 10% decrease after storage of the spiked sample for 1 h at room temperature) in muscle and egg. In eggs that had been stored at −20°C for 6 months, no decrease in CBX concentration was observed ($n = 4$, 2–6 μg/kg). Similar results were found for muscle samples stored at −20°C for 2 months ($n = 4$, 10 μg/kg).

Desoxy-CBX was stable in eggs and swine muscle under the conditions mentioned for CBX and in liver and kidney under spiking conditions. In another experiment, kidney samples spiked with desoxy-CBX (5 μg/kg) were stable for 2 months at −20°C. In the future, additional storage stability studies will be of interest.

CONCLUSIONS

The procedure originally developed for the determination of residues of, mainly, CBX was modified to be routinely applicable to the determination of the major metabolite desoxy-CBX in swine liver, kidney, muscle and plasma and in eggs and to the determination of CBX in the latter three matrices. The concurrent operation of trace enrichment and separation in the column-switching LC procedure and the optimized LC parameters reduced the cycle time from 55 to 31 min. The ruggedness and reproducibility were improved by optimizing the dimensions of the enrichment column and its packing material, and also the off-line column purification. The overall recoveries for CBX in muscle, plasma and egg are 70–80%, with R.S.D. values of about 7%. For desoxy-CBX, the overall recoveries are 83–95% in all the matrices investigated. The corresponding R.S.D.s are between 5 and 17%, depending on the matrix and/or the conditions under which the data were obtained. The limit of determination for CBX is 1 μg/kg in muscle tissue and 0.5 μg/kg in plasma and egg. For desoxy-CBX the values are 2 μg/kg in muscle, kidney and liver and 0.5 μg/kg in eggs.

CBX rapidly decomposes (*in vitro* metabolism) to, mainly, its carcinogenic metabolite desoxy-CBX, when it is added to liver and kidney tissue. Therefore, desoxy-CBX can be considered as the marker residue in these matrices and it is very unlikely that CBX will be found in real samples. CBX has good stability in frozen muscle tissue and in eggs. In all the matrices investigated, desoxy-CBX was stable under the spiking conditions (1 h at room temperature).

ACKNOWLEDGEMENT

The contribution of Mr. G. J. de Graaf of the Central Veterinary Institute (Lelystad, The Netherlands) to the preparation of the swine samples is greatly appreciated.

REFERENCES

1 S. Hino, G. Imanaka, W. Matsunaga, T. Ishida, Y. Nakazawa and E. Takabata, *Okayama-Ken Kankyo Hoken Senta Nenpo*, 7 (1983) 150.
2 G. J. de Graaf and Th. J. Spierenburg, *J. Assoc. Off. Anal. Chem.*, 68 (1985) 658.
3 A. I. Macintosh and G. A. Neville, *J. Assoc. Off. Anal. Chem.*, 67 (1984) 958.
4 A. I. MacIntosh, G. Lauriault and G. A. Neville, *J. Assoc. Off. Anal. Chem.*, 68 (1985) 665.
5 V. Stara and M. Kopanica, *Anal. Chim. Acta*, 186 (1986) 21.

6 I. Sestakova, P. Skarda and D. Manousek, *Biol. Chem. Zivocisne Vyroby-Vet.*, 15 (1980) 29.
7 P. Skarda and I. Sestakova, *Arch. Toxicol.*, Suppl. 1 (1978) 207.
8 P. Skarda, I. Sestakova and K. Frgalova, *Biol. Chem. Vyz. Zvirat.*, 12 (1976) 209.
9 M. J. Lynch and S. R. Bartolucci, *J. Assoc. Anal. Chem.*, 65 (1982) 66.
10 M. M. L. Aerts, W. M. J. Beek, H. J. Keukens and U. A. Th. Brinkman, *J. Chromatogr.*, 456 (1988) 105.
11 W. Roth and K. Beschke, *J. Pharmacol. Biomed. Anal.*, 2 (1984) 289.
12 *EC Guideline*, No. 89/610, European Commission, Brussels, 14 November 1989.

Journal of Chromatography, 541 (1991) 411–418
Elsevier Science Publishers B.V., Amsterdam

CHROM. 22 972

On-line determination and resolution of verapamil enantiomers by high-performance liquid chromatography with column switching

YOSHIYA ODA*, NAOKI ASAKAWA, TAKASHI KAJIMA, YUTAKA YOSHIDA and TADASHI SATO

Department of Physical and Analytical Chemistry, Tsukuba Research Laboratories, Eisai Co., Ltd., 1–3 Tokodai 5-chome, Tsukuba-shi, Ibaraki 300-26 (Japan)

(First received July 4th, 1990; revised manuscript received October 12th, 1990)

ABSTRACT

High-performance liquid chromatography (HPLC) with column switching was applied to the on-line determination and resolution of the enantiomers of verapamil (VA). This system employs an achiral reversed-phase column coupled to a chiral ovomucoid column via a dilution tube and a trapping column. The reversed-phase column was used to separate VA from the plasma components and impurities, and to determine the total VA concentration using an internal standard method. The eluate containing VA was selectively transferred to the trapping column after suitable dilution with a new mobile phase and VA was concentrated on the trapping column, then passed to the ovomucoid column, where the resolution of enantiomers was performed. It was possible with this system to select independently the optimum mobile phases for both HPLC columns owing to the introduction of the dilution tube and trapping column between them. This method has advantages over the usual HPLC methods in that it is rapid, simple and highly sensitive.

INTRODUCTION

Verapamil (VA), an inhibitor of membrane transport of calcium, is used for the therapy of agina and arrhythmia [1]. VA has a chiral centre (Fig. 1), but is administered as a racemic mixture. However, the two enantiomers of VA differ in pharmacology and pharmacokinetics [2–5]. While methods for the optical resolution of VA are adequate for the analysis of VA standards, they cannot be directly used to determine VA in clinical samples, such as serum, owing to the presence of interfering substances. The conventional methods are also laborious and time consuming, requiring pretreatments

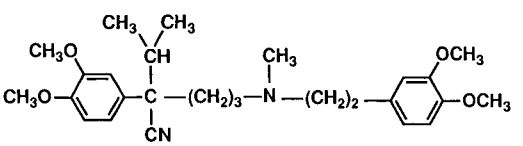

Fig. 1. Structure of verapamil.

0021-9673/91/$03.50

such as fractionation or desalting. Hence, a method is still required to measure the isomers in clinical samples accurately and rapidly.

Recently, Wainer and co-workers [6,7] reported a simple and rapid high-performance liquid chromatographic (HPLC) system for the direct resolution of the stereoisomers of several drugs. This system involved coupling an achiral column to a chiral column by using a column-switching technique. However, similar mobile phases had to be used for the two columns, so that each chromatographic step was not necessarily performed under the optimum conditions, and the peaks of enantiomers were broadened owing to diffusion of the sample during the column-switching procedures.

We have attempted to overcome these problems through the use of an improved column-switching HPLC system. The system was adapted for the determination of VA by coupling an achiral column to an ovomucoid column. The ovomucoid column contains ovomucoid protein as the stationary phase immobilized onto aminopropyl-silica gel [8,9]. The enantiomers of VA can be resolved by using this column with a reversed-phase solvent system. To prevent the mobile phase of the first column from flowing into the second column, we interposed a dilution tube and trapping column between the two columns, whereby the mobile phase of the first column was exchanged completely to the most favourable mobile phase for the second column. The potential usefulness of this technique is demonstrated and discussed.

EXPERIMENTAL

Reagents

Verapamil hydrochloride (VA · HCl) was supplied by Knoll Pharmaceuticals (Ludwigshafen, Germany), sodium 1-pentanesulphonate was purchased from Aldrich (Milwaukee, WI, U.S.A.), *n*-propyl *p*-aminobenzoate was purchased from Tokyo Kasei Kogyo (Tokyo, Japan) and dipotassium hydrogenphosphate, potassium dihydrogenphosphate and phosphoric acid of analytical-reagent grade were obtained from Wako (Osaka, Japan). HPLC-grade acetonitrile, ethanol and tetrahydrofuran were used. Distilled water was purified with a Milli-Q system (Millipore).

Apparatus

The HPLC system consisted of three high-pressure pumps (Model LC-9A; Shimadzu, Kyoto, Japan) (P1–P3), a system controller (Shimadzu SCL-6B), two variable-wavelength UV detectors (Shimadzu SPD-6A) (D1, D2) and three six-port switching valves (Rheodyne, Cotati, CA, U.S.A.). The switching diagram is given in Fig. 2 and is explained under *Procedure*. The HPLC columns were a 150 × 4.6 mm I.D. Inertsil ODS-2 column (C1) (Gasukuro Kogyo, Tokyo, Japan) to determine VA, a 10 × 4.0 mm I.D. Ultron ES-OVMG (C2) column as a trapping column and a 150 × 4.6 mm I.D. Ultron ES-OVM (C3) (Shinwa Kako, Kyoto, Japan) column to resolve the enantiomers. The three columns were connected through two Rheodyne switching valves (I and II). Valve I was equipped with a 2-ml sample loop.

Samples

n-Propyl *p*-aminobenzoate was used as an internal standard (I.S.). Sample solutions were prepared by dissolving known amounts of VA and I.S. in water or

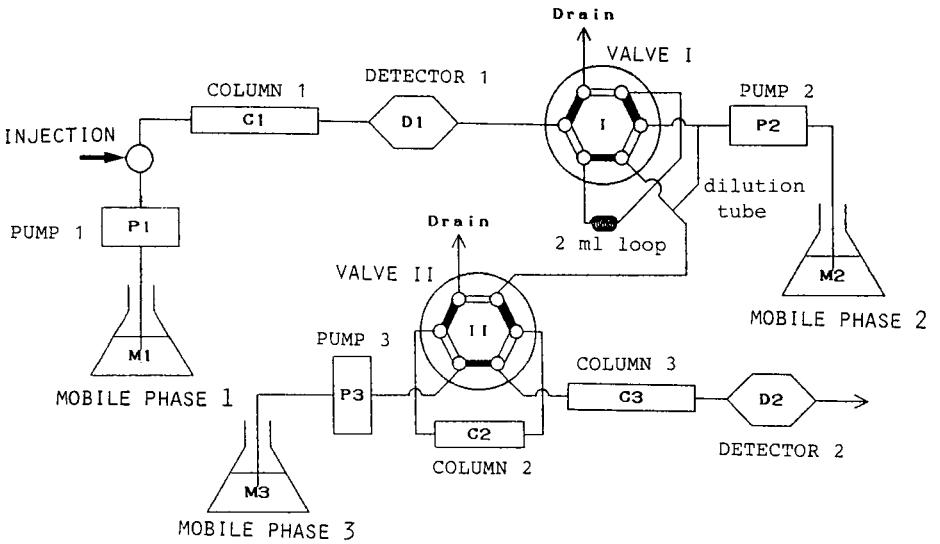

Fig. 2. Schematic diagram of the column-switching system finally developed and used.

human plasma. A 1-ml plasma sample was deproteinized by adding 1 ml of acetonitrile.

HPLC conditions

VA and I.S. were detected by measuring the absorption at 230 nm. Mobile phase 1 (M1) was prepared by mixing 5 m*M* sodium 1-pentanesulphonate with acetonitrile–water (3:7, v/v) and adjusting the pH to 3.0 by adding phosphoric acid. Mobile phase 2 (M2) was composed of dipotassium hydrogenphosphate and potassium dihydrogenphosphate. Mobile phase 3 (M3) consisted of tetrahydrofuran–ethanol–water (1:8:91, v/v/v) containing 20 m*M* potassium dihydrogenphosphate. M1, M2 and M3 were delivered by pump 1 at a flow-rate of 1.0 ml/min, pump 2 at a flow-rate of 4.0 ml/min and pump 3 at a flow-rate of 1.0 ml/min, respectively. All operations were carried out at ambient temperature.

Procedure

Samples were injected onto C1 and VA was determined with the aid of the I.S. The eluate containing VA was selectively switched for 2 min into the 2-ml loop via valve I. Then M2 was allowed to flow and wash the above eluate into C2 (trapping column). Finally, by switching valve II, VA was swept by flowing M3 from C2 to C3 (ovomucoid column), where enantiomeric separation was performed.

RESULTS AND DISCUSSION

An HPLC method for the simultaneous determination of VA and its metabolites in plasma has been reported by Kuwada *et al.* [10]. They used an ion-pair chromatographic procedure with a reversed-phase column. In this study, ion-pair

chromatography was performed with a mobile phase consisting of 5 m*M* pentanesulphonic acid in acetonitrile–water (3:7, v/v) as the first HPLC and an I.S. was used to determine the concentration of VA. Next, we examined the on-line resolution of VA enantiomers using a column-switching HPLC system.

First, the eluate containing VA in the 2-ml loop was passed to C3 directly via valve II without using C2 and M2. However, VA was not retained on C3 and was not resolved optically (data not shown), because the eluate contained a large amount of organic solvent (M1) and was too hydrophobic to allow the retention of VA on C3. We therefore developed a system to dilute the eluate in the 2-ml loop by using a dilution tube so that VA could be retained on C3. This attempt was not wholly successful, because diffusion occurred and the peak of VA was greatly broadened at D2 (data not shown). These results suggested that dilution of the eluate in the 2-ml loop followed by a concentration step would be needed in order to perform the on-line determination and resolution of VA. Therefore, the dilution tube was installed to dilute the eluate and C2 was introduced to concentrate the diluted VA.

Effect of dilution ratio

M2 was prepared from 5 m*M* potassium phosphate buffer (pH 7.5). The dilution ratio of the eluate could be varied by using the flow resistivity, which could be changed by altering the length of the diluting tube. Fig. 3 shows the chromatograms obtained with various dilution ratios. The peak of VA was almost undetectable at low dilution, as shown in Fig. 3C, probably because the high hydrophobicity of the eluate meant that VA was not trapped on C2 but passed through it. Moderate dilution allowed VA to be trapped on C2, as shown in Fig. 3B, but did not allow the enantiomeric composition of VA to be determined accurately. However, adequate dilution (1:9) allowed the determination of enantiomers, as shown in Fig. 3A.

Effects of pH and salt concentration of mobile phase 2

VA was not trapped on C2 when M2 was simply water. We therefore examined the conditions of M2. Fig. 4 shows the optical resolution of VA at D2 obtained with various pH values of M2. The peak area of the enantiomers decreased with decreasing pH. The enantiomeric ratios in Fig. 4B and C were different from that in Fig. 4A, and

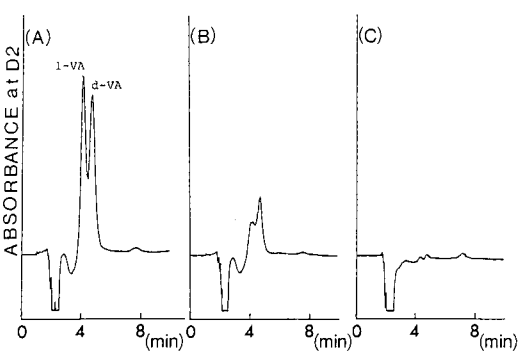

Fig. 3. Effect of dilution ratio. The eluate containing VA was diluted 1:x with M2: (A) $x = 9$; (B) $x = 3$; (C) $x = 0$.

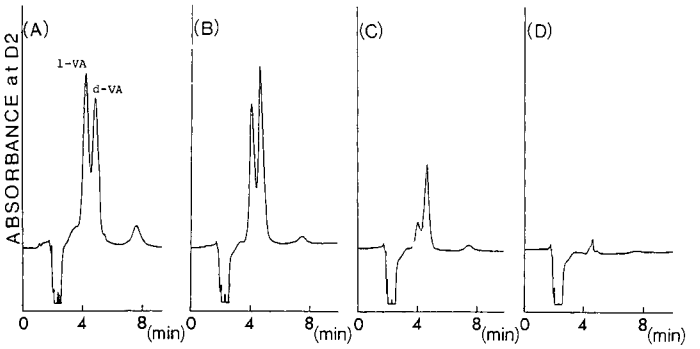

Fig. 4. Effect of pH of mobile phase 2. pH: (A) 7.5; (B) 7.2; (C) 6.9; (D) 6.5.

the peak of VA was almost unobservable in Fig. 4D. These results indicate that the affinity of VA for the ovomucoid column is not sufficiently strong at pH < 7.5, and VA is not completely trapped on C2. This may be the result of decreasing hydrophobicity of VA due to dissociation of the amino group [11]. The ovomucoid column exhibits strong hydrophobic interactions with basic solutes [9].

Fig. 5 shows chromatograms illustrating the effect of salt concentration in M2. The enantiomeric ratio could not be determined accurately with >20 mM salt and the elution of VA was retarded with increasing salt concentration in M2. Retention on the ovomucoid column is known to be affected by the addition of salt [8]. These results show that accurate determination of the enantiomeric ratio requires the use of the optimum pH and optimum salt concentration of M2.

Next, the flow-rate of M2 delivered by pump 2 was examined (data not shown). The retention and resolution of the enantiomers were little affected by changes in flow-rate in the range 1.0–6.0 ml/min.

Reproducibility

Fig. 6 shows chromatograms for the determination with C1 and the enantiomeric resolution with C3, where M2 consisted of 5 mM potassium phosphate buffer

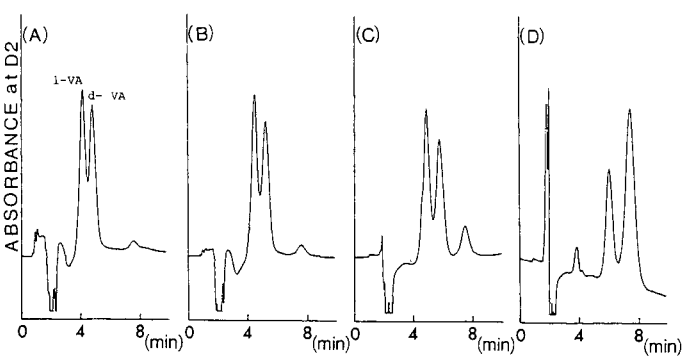

Fig. 5. Effect of salt concentration of mobile phase 2: (A) 5; (B) 10; (C) 20; (D) 50 mM.

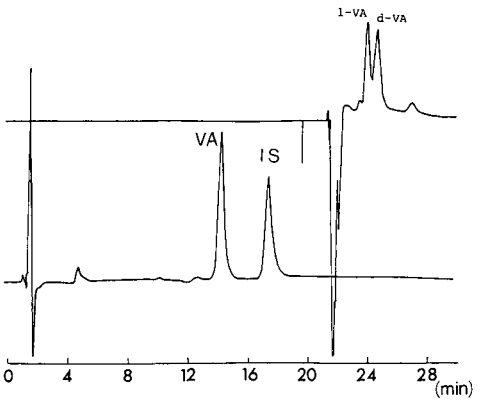

Fig. 6. Representative chromatograms obtained with the achiral reversed-phase column (lower chromatogram) and the ovomucoid column (upper chromatogram).

adjusted to pH 7.5 and the eluate containing VA was diluted 1:9 with M2. Table I indicates the reproducibility of the retention time on C3 and the enantiomeric ratio. The relative standard deviation (R.S.D.) for the retention time of *l*-VA was 1.8% (n = 8) and that of *d*-VA was 2.3% (n = 8). The R.S.D. for the enantiomeric ratio (*l*-VA/*d*-VA) was 2.1% (n = 8). These values are not necessarily satisfactory, but could be improved by further modification of the operating conditions with respect to trapping of sample materials on C2, and by rigorous control of temperature and the use of a reproducible column-switching procedure.

Detection limit

The limit of detection (at D2) for VA was 10 pg at a signal-to-noise ratio of 3. However, when a five-fold greater volume of the same sample concentration (1 ng/ml) was injected onto C1, five-fold larger peaks were observed at D2. The results indicate that this method effectively concentrates samples on C2 and enhances the sensitivity of enantiomer determination.

TABLE I

REPRODUCIBILITY DATA (n = 8)

See text for chromatographic conditions.

Value	Retention time (min)		*l*-VA/*d*-VA peak-area ratio
	l-VA	*d*-VA	
Mean	4.41	5.07	50.3:49.7
R.S.D.	1.78%	2.31%	2.06%

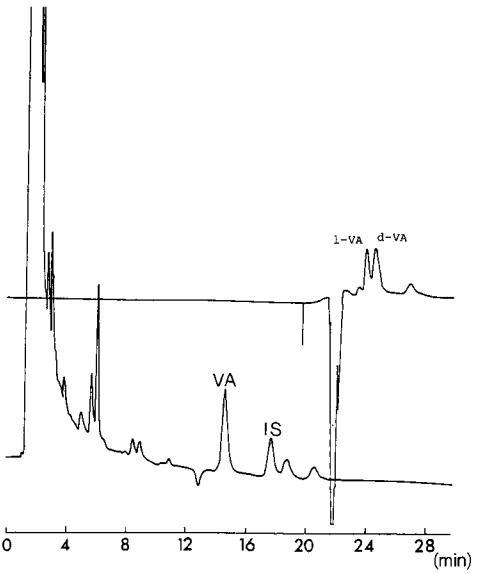

Fig. 7. Representative chromatograms obtained with the achiral reversed-phase column (lower chromatogram) and the ovomucoid column (upper chromatogram) for a plasma sample spiked with VA and internal standard.

CONCLUSION

A column-switching system employing a reversed-phase column coupled to an ovomucoid column via a dilution tube and a trapping column for concentration was developed for the on-line determination and enantiomeric resolution of VA. The use of a dilution tube in conjunction with the trapping column allowed both the achiral and chiral chromatographic steps to be performed under the respective optimum conditions, *i.e.*, each chromatographic step can employ the most favourable mobile phase independently.

This column-switching HPLC method has advantages over conventional HPLC in that it allows the on-line measurement of enantiomers after VA determination without pretreatments such as fractionation, desalting and evaporation, and high sensitivity can be achieved in a relatively short analytical time. Fig. 7 shows the chromatogram obtained by injection of a human plasma sample after deproteinization. VA was separated and determined on the achiral phase, and the enantiomeric measurement was performed on the ovomucoid column.

Applications of this system to pharmacokinetic studies of VA and for clinical purposes will be reported elsewhere.

ACKNOWLEDGEMENT

The authors are grateful to Mr. S. Ryo of Gasukuro Kogyo.

REFERENCES

1 B. N. Singh, G. Ellrodt and C. T. Peter, *Drugs*, 15 (1978) 169.
2 B. Vogelgesang, H. Echizen, E. Schmidt and M. Eichelbaum, *Br. J. Clin. Pharmacol.*, 18 (1984) 733.
3 M. Eichelbaum, G. Mikus and B. Vogelgesang, *Br. J. Clin. Pharmacol.*, 17 (1984) 453.
4 H. Echizen, T. Brecht, S. Niedergaesass, B. Vogelgesang and M. Eichelbaum, *Am. Heart J.*, 109 (1985) 210.
5 H. Echizen, B. Vogelgesang and M. Eichelbaum, *Clin. Pharmacol. Ther.*, 38 (1985) 71.
6 Y.-Q. Chu and I. W. Wainer, *Pharm. Res.*, 5 (1988) 680.
7 I. W. Wainer and R. M. Stiffin, *J. Chromatogr.*, 424 (1988) 158.
8 T. Miwa, M. Ichikawa, M. Tsuno, T. Hattori, T. Miyakawa, M. Kayano and Y. Miyake, *Chem. Pharm. Bull.*, 35 (1987) 682.
9 T. Miwa, T. Miyakawa, M. Kayano and Y. Miyake, *J. Chromatogr.*, 408 (1987) 316.
10 M. Kuwada, T. Tateyama and J. Tsutsumi, *J. Chromatogr.*, 222 (1981) 507.
11 J. Hasegawa, T. Fujita, Y. Hayashi, K. Iwamoto and J. Watanabe, *J. Pharm. Sci.*, 73 (1984) 442.

Journal of Chromatography, 541 (1991) 419–429
Elsevier Science Publishers B.V., Amsterdam

CHROM. 22 920

Determination of molecular size distributions of humic acids by high-performance size-exclusion chromatography

R. RAUSA*, E. MAZZOLARI and V. CALEMMA
ENIRICERCHE, Via Maritano 26, I-20097 S. Donato Milanese (Italy)
(First received May 15th, 1990; revised manuscript received October 4th, 1990)

ABSTRACT

High-performance size-exclusion chromatography (HPSEC) was applied to the study of humic acids and a method for the rapid determination of reliable molecular size distributions of these substances was developed. Using commercial HPSEC columns, in conjunction with a neutral saline solution as eluent, molecular size distributions of four samples of humic acids of various origin and nominal average molecular weights were obtained. Measurements were independent of the operating conditions and based on differences in the molecular sizes of the humic acids examined.

INTRODUCTION

Classical gel permeation chromatography (GPC) is widely used for the determination of molecular size distributions of natural humic substances [1]. However, although its use is now fairly well accepted, many problems remain to be solved. These problems concern adsorption phenomena, inter- and intramolecular solute interactions, etc., which hinder the acquisition of meaningful molecular size distributions [2]. Moreover, when GPC is performed in "classical" columns working at moderate pressures, the use of soft or semi-rigid gels hampers the production of well resolved chromatographic peaks in a reasonably short time. One of the commonest types of stationary phase utilized for GPC is Sephadex gel, which has usually been used in connection with alkaline inorganic [3,4] and organic [5] eluents or buffers (*e.g.*, Tris, pH 9) in order to avoid the occurrence of extra adsorptive phenomena [2,6,7]. Even though this gel is nowadays extensively used, some doubt have arisen regarding its general applicability [8] and the absence of adsorption of the sample on the gel stationary phase [6].

High-performance size-exclusion chromatography (HPSEC) is a relatively new technique, widely utilized for the characterization of synthetic organic polymers. Owing to the use of short, high-performance columns and sophisticated apparatus, very reproducible chromatograms can be rapidly obtained. HPSEC has not often been applied to the study of humic "polymer". The few examples in the literature are confined to the analysis of humic matter of particular origin (aquatic humic and fulvic acids), having peculiar solubility characteristics [9–11].

0021-9673/91/$03.50

In this work, HPSEC was applied to the study of humic acids of various origins. Using commercial high-performance size exclusion columns and a neutral salt solution as eluent, a reliable, fast and reproducible method was developed. Molecular size distributions of humic substances were obtained, avoiding the use of strongly alkaline buffers which could, in some instances, affect the characteristics of the substances being studied. Further, the method permits the calculation of nominal average molecular weights which can be utilized for relative comparisons among humic acid samples.

EXPERIMENTAL

The humic acids (HA), analysed as sodium humates, were samples of various origins, either produced by dry-phase coal oxidation ("regenerated" HA) or extracted from natural substrates. Regenerated HA were extracted from two coals of different rank, Sulcis sub-bituminous coal (HAS) and North Dakota lignite (HALG), oxidized under dry conditions in a pressurized fluidized bed as reported previously [12].

The "natural" HA samples were first a leonardite-derived humic acid (HAL) sample, kindly supplied by Professor Visser of Laval University (Quebec, Canada) and second HA extracted from a worm compost (HAW) (supplied by Quadriflor, Sassari, Italy) according to the International Humic Substances Society (IHSS) standard procedure. Their production and characteristics are described elsewhere [13].

Table I reports some analytical data for the samples analysed. The most important structural differences among the products consist in their aromaticity, which is related to their origin. Coal-derived humic acids (HAS and HALG), as described previously [12], are the most aromatic products because they are derived from the oxidation of the coal organic structure, which involves the consumption of most of the aliphatic part [14]. Leonardite-derived humic acids show a similar aromaticity and HAW are the most aliphatic products [13]. This is clearly shown by the values of the H/C atomic ratio, calculated from the compositional data, which are inversely related to sample's aromaticity and are reported in Table I.

The HPSEC apparatus consisted of a Perkin-Elmer (P.E.) Series 410 pump system, coupled with an autosampler (P.E. ISS-100) and equipped with a refractive index (RI Refractomonitor) and a variable-wavelength UV detector (P.E. LC-90, 262 nm) in series. The whole system was controlled by a P.E. 7700 computer. The evaluation of chromatograms was performed using the P.E. GPC-6 software.

TABLE I

ANALYTICAL CHARACTERISTICS OF THE HUMIC ACIDS STUDIED

Elemental composition is on a dried and ash-free (d.a.f.) basis.

Sample	Composition (wt.-%)					H/C
	C	H	N	S	O (by difference)	
HALG	62.9	3.2	1.3	0.4	28.5	0.61
HAS	64.0	3.0	2.1	5.2	25.8	0.56
HAL	64.2	3.5	1.5	0.7	30.0	0.65
HAW	54.7	4.3	4.5	1.1	35.4	0.94

Chromatographic runs were carried out on solutions of different concentration obtained by dissolving 10 mg of humic substance in 0.1 *M* sodium hydroxide solution and diluting to final values of 0.3–1.0% (w/v). Before injection, solutions were filtered through a Millipore filter (0.45 μm). As eluents, 0.03 and 0.05 *M* sodium nitrate solutions in triply distilled water (Millipore, Milli-Q water system) were used. The column system consisted of three Shodex columns, having different "nominal" molecular weight ranges, coupled in series, and thermostated at 30°C in a Waters (TCM) thermostating system.

The columns utilized were Shodex Ionpak S-802s (range 0–5000), Shodex Ionpak S-803s (range 5000–50 000) and Shodex Ionpak S-804s (range 50 000–500 000). The gel phase inside the columns consisted, according to manufacturers specifications, of cross-linked sulphonated polystyrene–divinylbenzene copolymer. The flow-rates were varied in the range 0.6–1.0 ml/min and sample concentrations in the range 0.3–1% (w/v).

The theoretical limits of the chromatographic system (total and the void volumes, V_t and V_0, respectively), and a linear calibration fit were established using polysaccharide (PL polymer) standards having different molecular weights. The total volume was determined with glucose. Polysaccharides were utilized because they were perfectly compatible with the column stationary phase and eluent system, giving very precise (average correlation coefficient 0.997) calibration graphs. The chromatographic characteristics of the experimental peaks were reported both in terms of retention volumes and K_{av}, according to Laurent and Killander [15]. The latter represents the fraction of the volume of the gel that is available for the substance. It represents a very useful and straightforward way of comparing results independently of flow or system geometry. K_{av} is defined as

$$K_{av} = (V_e - V_0)/(V_t - V_0)$$

where V_e is the elution volume, V_0 the void volume and V_t the total volume of the gel bed.

A semi-quantitative analysis of various molecular weight distributions was performed and average nominal molecular weights were calculated, referring raw chromatographic data to the polysaccharide linear calibration fit and using GPC software. In this way, indicative molecular weight values, useful for relative comparisons among samples analysed in the same experimental conditions, were obtained.

RESULTS AND DISCUSSION

Reliability of the chromatographic system

Owing to the peculiar structure of humic molecules, which are very prone to interact with each other and with most of the gel phases normally used in GPC, it is necessary to avoid, or minimize, coulombic effects and either reversible or irreversible adsorption phenomena. All of these extra-permeation factors, which depend on sample concentration and the nature and concentration of the eluent, produce distortions in the chromatogram and lead to the elution of sample peaks outside the theoretical range of permeation [2]. To overcome these problems, most reported

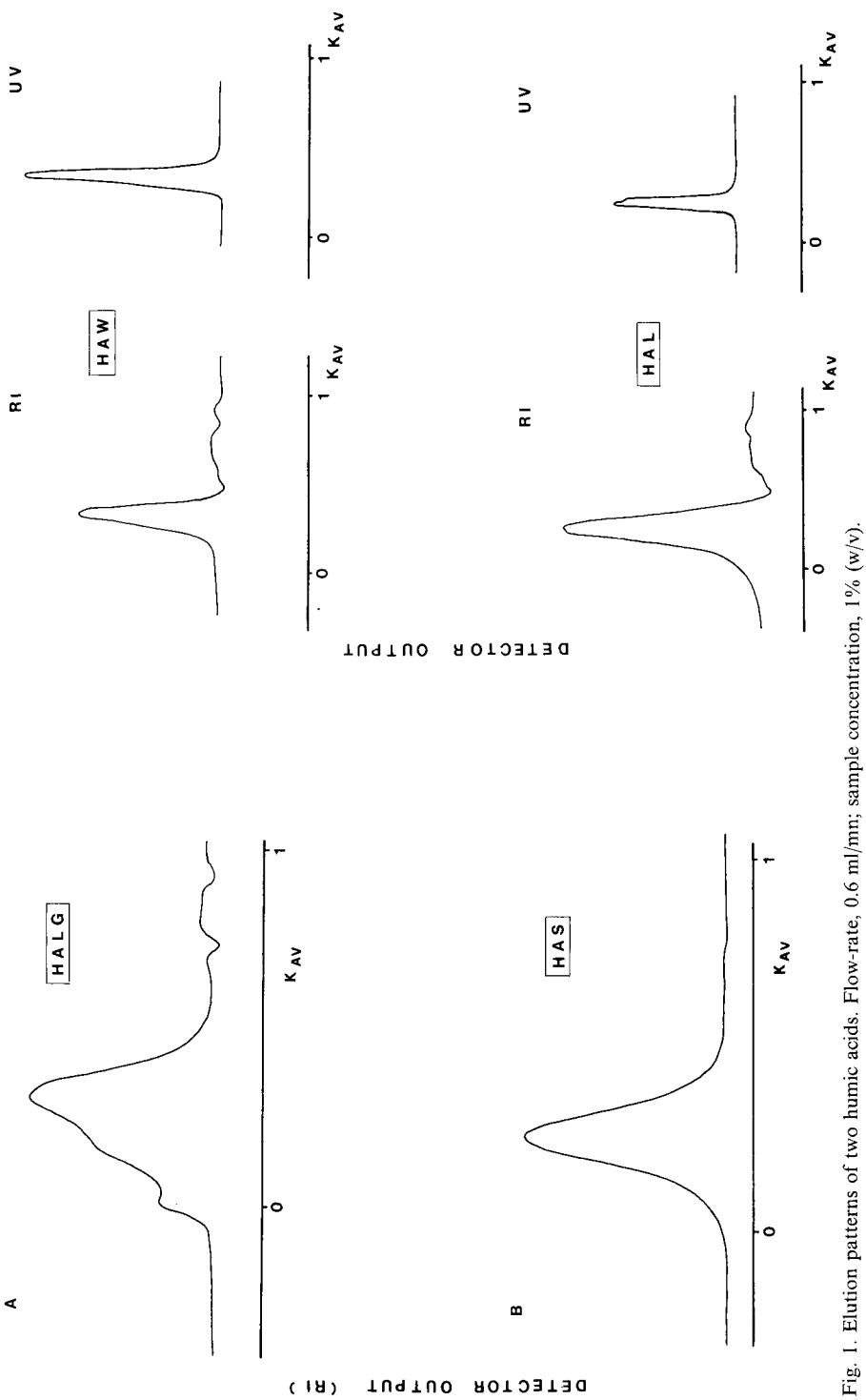

Fig. 1. Elution patterns of two humic acids. Flow-rate, 0.6 ml/mn; sample concentration, 1% (w/v).

Fig. 2. Comparison between the RI and UV elution patterns of worm compost and leonardite-derived humic acids.

classical GPC methods make use of alkaline buffers of high ionic strength and pH [6,7]. In this work, owing to the nature of the stationary phase utilized (sulphonated polystyrene), we found that the use of a strongly alkaline solution was not required and a neutral salt solution of suitable concentration allowed the determination of the chromatographic pattern of sodium humates, very rapidly and efficiently, without any detectable extra phenomena due to sample–sample or sample–gel interactions. The use of salt solutions of a certain ionic strength is necessary to avoid unwanted expansion of the charged acidic groups of the "humic molecule" and to produce a coiled form of the humic "polymer". Both phenomena increase the size of humic acids and produce a shift of the peaks obtained in the chromatograms towards lower elution volumes (or K_{av}) corresponding to larger nominal molecular weight values [16,17].

In this work sodium nitrate solutions of 0.03 and 0.05 *M* were tested as HPSEC mobile phases in order to minimize the above-mentioned effects. Some comparative preliminary tests performed with both solutions on regenerated humates (HALG) showed slight differences in K_{av}. However, using 0.05 *M* sodium nitrate solution, the K_{av} values obtained were slightly higher. Further, this higher concentration was found to be the best compromise between sample (sodium humate) solubility and the ability of humic molecules to form a fully coiled conformation in solution. In fact, as found by Ghosh and Schnitzer [16], such a concentration seems to be the threshold value at which natural humic molecules coil completely.

In an ideal gel permeation experiment, when the separation is based only on molecular size differences of the molecules constituting the sample, the chromatographic pattern must be independent of sample concentration and it must fall within the theoretical column range. Additionally, the elution volume should also be independent of flow-rates and the overall initial sample should be fully recovered at the end of the column. In this work, the absence of reversible and irreversible adsorption and the reliability of the conditions used for the determination of molecular size distribution (0.05 *M* sodium nitrate) of humic acids were tested for all the humic samples examined for the occurrence of the whole chromatogram within the theoretical limits calculated with the polysaccharide standards and by determining the effect on the chromatographic pattern of the operating parameters (sample concentration and flow-rate). The absence of irreversible adsorption was revealed indirectly by detecting variations among the peak areas of subsequent replicates, by evaluating the system efficiency (based on a standard with molecular weight of 48 000) after running the system for several months and by performing some overnight elutions of the system with 0.1 *M* sodium hydroxide solution.

Influence of the operational variables on chromatogram shape and precision of measurements

Fig. 1 shows typical chromatograms for two regenerate humate samples (HALG and HAS), obtained with 0.05 *M* sodium nitrate solution. The patterns were obtained by means of the refractive index detector. This detector is not based on molar absorptivities; its response depends on the sample concentration and it allows the detection of a larger number of chemical species than a UV detector. It should be used when molecular size distributions of polydisperse humic "polymers" have to be evaluated from the raw chromatogram.

Fig. 2 shows some comparative examples of chromatographic patterns obtained

TABLE II

ELUTION VOLUMES AND K_{av} VALUES OBTAINED FOR HALG UNDER DIFFERENT OPERATING CONDITIONS

HA (%, w/v)	Flow-rate (ml/min)			
	0.6		1.0	
	V (ml)[a]	K_{av}[a]	V (ml)[a]	K_{av}[a]
0.3	15.84 ± 0.04	0.210 ± 0.005	15.99 ± 0.03	0.224 ± 0.003
0.6	15.83 ± 0.02	0.209 ± 0.003	16.02 ± 0.02	0.227 ± 0.002
1.0	15.80 ± 0.01	0.206 ± 0.001	15.99 ± 0.03	0.224 ± 0.003

[a] Values are averages of at least three determinations, with standard deviations.

by the two detectors (RI and UV), and no large differences are present. However, some low-molecular-weight peaks (at high K_{av}) not detectable with the UV detector are evident when the RI detector is utilized. These non-UV-absorbing species, probably inorganic impurities in the samples, were not subsequently accounted for in the calculation of the average molecular weights. As shown in both Figs. 1 and 2, all the peaks fall within the void and total volume of the system, thus indicating that no evident adsorptive phenomena between the sample and the stationary phase are acting. The elution volumes and the respective K_{av} values of major peaks detected in all the chromatograms, obtained under various operating conditions, are reported in Tables II and III.

As further confirmation of the reliability of the chromatographic conditions utilized, all the measurements showed excellent repeatability and the elution patterns were almost always identical, as shown in Fig. 3, where the chromatograms of several replicates of HAS are shown. For HALG (Table II), within the same set of replicates, for the same flow-rate and concentration, the highest percentage standard deviation from the mean of the retention volumes is 0.3% at 0.6 ml/min and 0.2% at 1 ml/min. These values reach 2.4% and 1.3% when the standard deviations of K_{av} are considered. Almost the same values are obtained for HAL, HAS and HAW, as reported in Table III.

The effect of sample concentration was evaluated in the range 0.3–1% (w/v). Fig. 4 shows, as an example, the elution patterns obtained at 0.6 ml/min; the corresponding chromatograms at 1 ml/min were almost identical. In addition to the

TABLE III

ELUTION VOLUME AND K_{av} VALUES OBTAINED FOR HUMIC ACIDS EXTRACTED FROM SULCIS COAL, LEONARDITE AND WORM COMPOST

Flow-rate, 0.6 ml/min; concentration, 1% (w/v).

HA	V (ml)[a]	K_{av}[a]
HAS	20.11 ± 0.05	0.257 ± 0.007
HAL	20.40 ± 0.05	0.289 ± 0.004
HAW	20.68 ± 0.02	0.358 ± 0.002

[a] Values are averages of at least three determinations, with standard deviations.

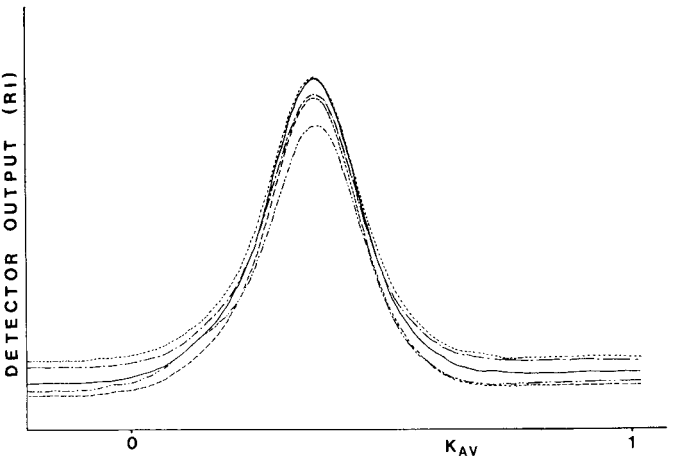

Fig. 3. Comparison among the elution patterns of five humic acid (HAS) replicates. Flow-rate, 0.6 ml/min; sample concentration, 0.6% (w/v).

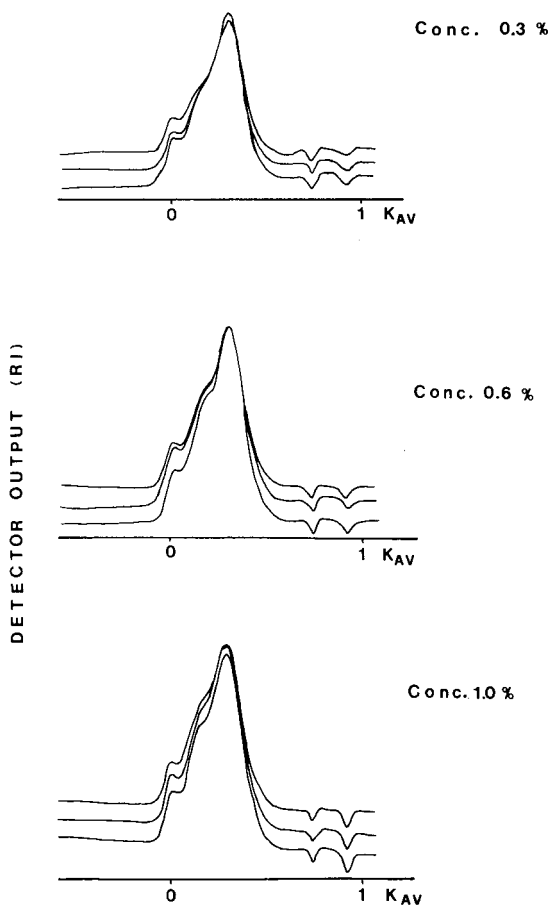

Fig. 4. Effect of sample concentration on the elution patterns of HALG. Flow-rate, 0.6 ml/min.

above-mentioned excellent repeatability, it is evident that the chromatograms are virtually independent of sample concentration. As Table II shows, the highest percentage differences between the mean values are 1.2% at 0.6 ml/min and 0.2% at 1.0 ml/min. The corresponding K_{av} differences are 1.9% and 1.3%, respectively. These results indicate that no macroscopic effects played by sample concentrations, which change the chromatographic patterns, as reported by Swift and Posner [2] using water as eluent in classical GPC, are present.

The effect of the flow-rate on the retention volume (or K_{av}) of HA was evaluated. Flow in HPSEC, as in chromatography in general, is one of the most important parameters, affecting the height equivalent to a theoretical plate (HETP) and peak resolution. In fact, owing to the intrinsic characteristics of the separation mechanism involved in this technique, which is entropy controlled, this parameter is a good indicator of the occurrence of undesirable phenomena within the column [2].

The flow dependence of the chromatograms was studied on HALG which were both chromatographed at 0.6 and 1 ml/min. Also in this instance, as demonstrated by Fig. 5 and Table II, the variations detected in the form of the chromatograms were

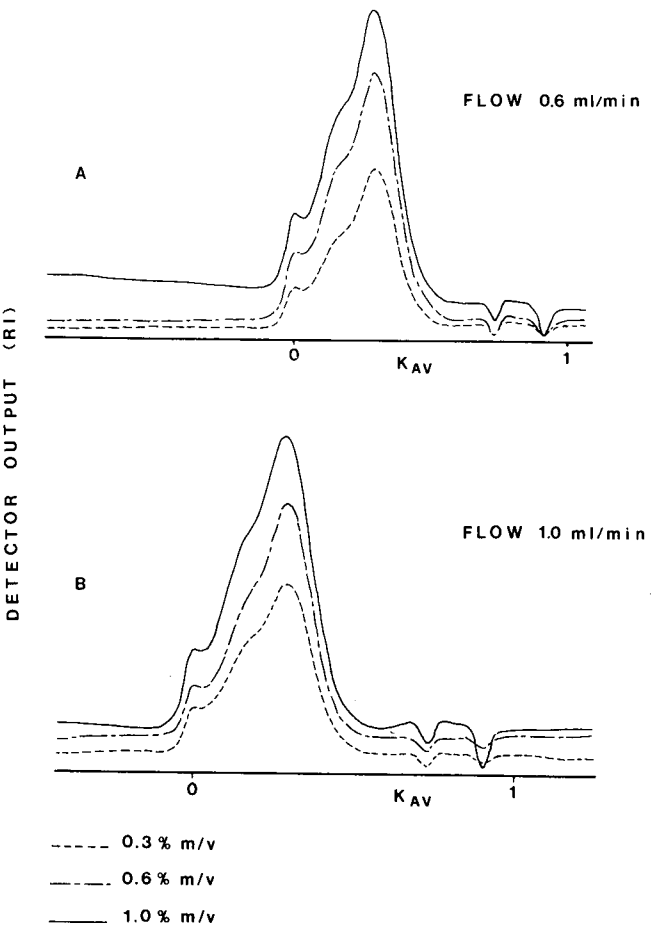

Fig. 5. Effect of flow-rate on the elution pattern of HALG.

small. The largest differences among the average retention volumes of the peaks of replicates, for the same concentrations at different flow-rates, were 1.2%, but for K_{av} they reached 9%. This variation can probably be ascribed mainly to differences in peak resolution due to band broadening related to the efficiency of the system [17], which was found to be significantly higher (18%) at the lowest flow-rate.

The absence of extra-permeation phenomena (irreversible adsorption on the column) was evaluated, as mentioned before, taking into account variations in peak areas, calculating the efficiency of the columns and "cleaning out" the overall system with an alkaline solution. Fig. 6 shows an example of the trend obtained by plotting the area counts (UV and RI) of five (HAS) replicates. The variations are very limited, and the largest differences detected between the most extreme values do not exceed 3%, suggesting that, at least under the conditions explored, there is no loss of the initial sample. The same conclusions can be drawn both from results obtained by calculating the efficiency of columns and from overnight sodium hydroxide elutions. In the first instance the efficiency of the column system, evaluated as plate number, calculated on a medium molecular weight standard (48 000) and checked at different times during several months, did not vary by more than 7%. In the second instance, no peaks were ever detected as a result of overnight alkaline elution.

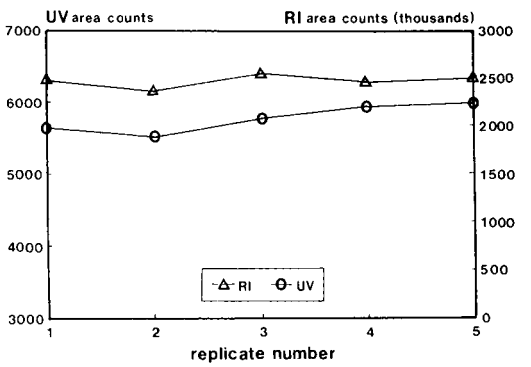

Fig. 6. Variations in area counts detected for five HAS replicates.

In conclusion, all the results indicate that the characteristics of the stationary phase utilized for the analysis are, under these conditions, virtually unaffected by the elution of humic molecules. Therefore, molecular size distributions so obtained can be considered to be related to the variations in the molecular size of the sample, thus confirming results obtained previously by comparative analyses of some ultrafiltered HA fractions [18].

Quantitative aspects

One of the most interesting possibilities offered by HPSEC, in analysing polydisperse systems, concerns the calculation of some average numerical values of molecular weights. This can be accomplished owing to the availability of extensive computerization and suitable software, which is not generally applicable with classical

GPC. Two of the most important average molecular weights that can be theoretically calculated are the number-average molecular weight (M_n) and the weight-average molecular weight (M_w), defined as

$$\bar{M}_n = \sum N_i M_i / \sum N_i \quad (1)$$

$$\bar{M}_w = \sum N_i M_i^2 / \sum N_i M_i \quad (2)$$

where N_i is the number of molecules of molecular weight M_i [17]. High-molecular-weight molecules strongly influence M_w whereas M_n is very sensitive to the low-molecular-weight components of the mixture. For polydisperse systems the value of M_w is always greater than M_n and the ratio M_w/M_n measures the breadth of the molecular weight distribution. Further details and references were reported by Yau *et al.* [17].

In Table IV, results obtained from calculations of the various average molecular weights are reported. It must be recalled that a true column calibration requires that the conformational and structural characteristics of the sample perfectly match those of the standards used, so that a unique relationship between molecular size and molecular weight can be established [17]. Unfortunately, as shown by Cameron *et al.* [19], humic substances do not behave precisely as either polysaccharides or proteins usually employed for column calibrations. Hence the absolute values obtained for these substances are necessarily nominal, and they must be used with care and only for relative comparisons.

TABLE IV

AVERAGE NOMINAL MOLECULAR WEIGHTS OBTAINED FOR THE VARIOUS HUMIC ACIDS

Flow-rate, 0.6 ml/min.

HA	Concentration (%, w/v)	$\bar{M}_n$[a]	$\bar{M}_w$[a]	$\bar{M}_w/\bar{M}_n$
HALG	1	72 273 ± 141	130 438 ± 336	1.8
HAS	1	53 585 ± 313	77 396 ± 277	1.4
HAL	1	49 622 ± 1761	79 042 ± 7312	1.6
HAW	1	42 845 ± 2701	49 345 ± 3461	1.1

[a] Values are averages of at least three determinations, with standard deviations.

Values obtained for the humic acids examined here, reported in Table IV, show differences both in the absolute values and in the ratio M_w/M_n, depending on their origin. In particular, products obtained by oxidation of lignite (HALG) have the higher average nominal absolute values. They contain very high-molecular-weight species, as indicated by their high average molecular weights (M_w). Conversely worm compost-derived HA show the lowest average values, while HA extracted from oxidized Sulcis coal and from leonardite are very similar and display, with respect to the other HA, intermediate average molecular weights.

Differences are also evident when the M_w/M_n ratio is considered. The latter, which is an indicator of the polydispersity of the macromolecular system, is high for HALG, HAS and HAW, as would be expected for products either generated by the random destruction of the parent matrix (coal) from which they are derived or extracted from a natural complex substrate (leonardite). Conversely, as shown in Table IV, humic acids extracted from worm compost denote a polyldispersity ratio close to unity. This could mean a close similarity of the molecules constituting HAW, owing to the different (biological) pathway which led to the formation of this humic acid sample.

CONCLUSIONS

Using commercial HPSEC columns with a neutral salt solution as eluent, precise molecular size distributions of different humic acids have been obtained rapidly. The conditions utilized give results that are independent of the operating parameters and thus related to differences in the molecular size of the sample. Further, using suitable software, average nominal molecular weights of humic acids useful for comparative purposes have been obtained.

REFERENCES

1 F. J. Stevenson, *Humus Chemistry: Genesis, Composition, Reactions*, Wiley, New York, 1982, Ch. 12, p. 285.
2 R. S. Swift and A. M. Posner, *J. Soil Sci.*, 22 (1971) 237–249.
3 N. N. Bambalov and T. P. Smychnik, *Vestsi Akad. Navuk BSSR, Ser. Khim. Navuk*, 2 (1983) 115–117.
4 T. P. Smychnik and N. N. Bambalov, *Vestsi Akad. Navuk BSSR, Ser. Khim. Navuk*, 2 (1980) 66–68.
5 V. N. Plechanov, *Org. Geochem.*, 5 (1983) 143–149.
6 R. Moliner, J. Osácar and J. M. Gavilán, *Fuel*, 61 (1982) 443–446.
7 E. Yu. Milanovskii, *Pochvovedenie*, 8 (1984) 42–46.
8 P. T. Hine and D. B. Bursill, *Water Res.*, 18 (1984) 1461–1465.
9 T. Vartiainen, A. Liimatainen and P. Kauranen, *Sci. Total Environ.*, 62 (1987) 75–84.
10 C. J. Miles and P. L. Brezonik, *J. Chromatogr.*, 259 (1983) 499–503.
11 Y. Saito and S. Hayano, *J. Chromatogr.*, 177 (1979) 390–392.
12 R. Rausa, V. Calemma and E. Girardi, *Proceedings of International Conference on Coal Science, Tokyo, October 23–27, 1989*, NEDO, Tokyo, Vol. 1, pp. 237–240.
13 S. Deiana, C. Gessa, B. Manunza, R. Rausa and R. Seeber, *Soil Sci.*, 150 (1991) 419–424.
14 R. Rausa, V. Calemma, S. Ghelli and E. Girardi, *Fuel*, 68 (1989) 1168–1172.
15 T. C. Laurent and J. Killander, *J. Chromatogr.*, 14 (1964) 317–330.
16 K. Ghosh and M. Schnitzer, *Soil Sci.*, 129 (1980) 266–276.
17 W. W. Yau, J. J. Kirkland and D. D. Bly, *Modern Size Exclusion Chromatography*, Wiley, New York, 1979.
18 A. Piccolo, R. Rausa and L. Camici, paper presented at the *198th ACS National Meeting Division of Geochemistry, Miami Beach, FL, September 10–15, 1989.*
19 R. S. Cameron, R. S. Swift, B. K. Thornton and M. A. Posner, *J. Soil Sci.*, 23 (1972) 342–349.

Journal of Chromatography, 541 (1991) 431–441
Elsevier Science Publishers B.V., Amsterdam

CHROM. 22 999

Determination of non-ionic surfactants with ester groups by high-performance liquid chromatography with post-column derivatization

YUKIHIRO KONDOH*, AKIO YAMADA and SATOSHI TAKANO
Tochigi Research Laboratories, Kao Corporation, 2606, Akabane, Ichikai-machi, Tochigi 321–34 (Japan)
(First received May 1st, 1990; revised manuscript received September 19th, 1990)

ABSTRACT

A high-performance liquid chromatographic (HPLC) method with a post-column reaction detector was developed for the determination of non-ionic surfactants with ester groups (NSEG) such as sorbitan fatty acid esters and sucrose fatty acid esters. NSEG from the mono- to pentaester are separated by reversed-phase HPLC with gradient elution. NSEG eluted from a chromatographic column are hydrolysed with potassium hydroxide, and the resulting fatty acids are reacted with 2-nitrophenylhydrazine in the presence of 1-ethyl-3-(3-dimethylaminopropyl)carbodiimide to form 2-nitrophenylhydrazides. The reaction mixture is then made strongly alkaline in order to reduce the blank absorbance and develop a violet colour of the hydrazide, which is detected at 550 nm. The post-column reaction detector, for example, can detect 1 μg of monomyristin. With the proposed method, NSEG are well separated and determined with high sensitivity and selectivity.

INTRODUCTION

Non-ionic surfactants with ester groups (NSEG) such as sorbitan fatty acid esters, sucrose fatty acid esters and polyoxyethylene sorbitan fatty acid esters are widely used as emulsifiers in the food and cosmetics industries. They are usually a complicated mixture, because they have distributions of the alkyl chain length of the fatty acids, the number of ester groups and the number of oxyethylene chain units. NSEG have been determined by means of thin-layer chromatography (TLC) [1–3], gas chromatography (GC) [4,5] and high-performance liquid chromatography (HPLC) [6–9]. However, TLC has poor separation and quantitativity and NSEG of high molecular weight cannot be measured by GC because they are non-volatile. On the other hand, many studies have been reported on the application of HPLC to NSEG, as HPLC is very suitable for the analysis of non-volatile compounds.

Reversed-phase and gel permeation chromatography are mainly used for the separation of NSEG. However, no satisfactory separation of NSEG from the mono- to pentaester has been achieved by either method. Refractive index (RI) and UV detection are frequently used, but both methods have poor sensitivity and selectivity. Hence there is no satisfactory method for the analysis of NSEG in terms of resolution, selectivity, sensitivity and quantitativity.

0021-9673/91/$03.50

We tried to separate NSEG from the mono- to pentaester by reversed-phase chromatography using an ODS column and a gradient elution method, and also tried to detect them by using a new post-column reaction detector with high sensitivity and selectivity. The basis of the post-column reaction was that NSEG are hydrolysed and the resulting fatty acids are derivatized and detected selectively and sensitively. For the colour development of fatty acids, the 2-nitrophenylhydrazine (ONPH) method [10], which has been used for the post-column reaction detector of water-soluble carboxylic acids [11], was chosen, because it was found that it is also applicable to fatty acids.

This paper describes the optimization of the chromatographic separation and the post-column reaction and also the determination of NSEG with high resolution and sensitivity.

EXPERIMENTAL

Apparatus

A schematic diagram of the liquid chromatograph equipped with a post-column reaction detector is shown in Fig. 1. The liquid chromatograph consisted of a reciprocating piston pump (Model 655; Hitachi, Tokyo, Japan), a gradient controller (Model L-5000; Hitachi), a variable-wavelength UV–VIS detector (Uvidec 100-VI; Japan Spectroscopic, Tokyo, Japan), an injector with a 100-μl loop (Model 7125; Rheodyne, Berkeley, CA, U.S.A.) and a circulator (Model FE; Haake, Karlsruhe, Germany) for column temperature control. The injector was heated at 60°C with a specially designed apparatus [12]. The post-column reaction detector consisted of an acid-resistant pump (NP-S-253; Nihon Seimitsu, Tokyo, Japan), a three-channel reaction pump (655A-13; Hitachi), a constant-temperature circulating bath (Model D1-L; Haake) for condensation reaction and two constant-temperature reaction baths (NRB-15; Nihon Seimitsu) for hydrolysis and the colour development reaction. The post-column reaction coil was made of Teflon tubing (0.5 mm I.D.). Chromatograms, peak areas and retention times were obtained by using a data processor (D-2000; Hitachi).

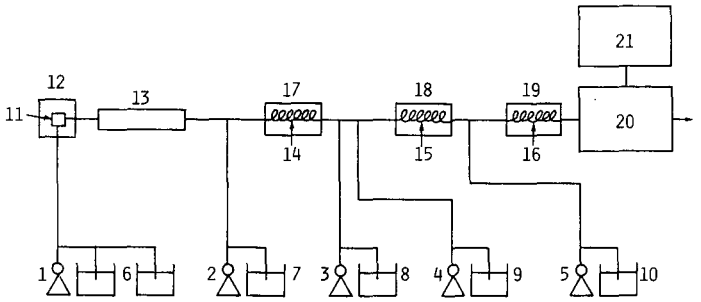

Fig. 1. Schematic diagram of the liquid chromatograph 1–5 = Pumps; 6 = eluent reservoirs; 7 = reservoir for potassium hydroxide reagent; 8 = reservoir for ONPH reagent; 9 = reservoir for EDC reagent; 10 = reservoir for sodium hydroxide reagent; 11 = sample injector; 12 = injector heater; 13 = analytical column; 14 = reaction coil (10 m × 0.5 mm I.D.); 15 = reaction coil (20 m × 0.5 mm I.D.); 16 = reaction coil (10 m × 0.5 mm I.D.); 17 = reaction bath (120°C); 18 = water-bath (70°C); 19 = reaction bath (100°C); 20 = UV–VIS detector; 21 = data processor.

Reagents.

Hitachi gel 3057, which is an ODS packing of average particle diameter 3 μm, was used as the stationary phase. Authentic fatty acids, monoacylglycerols and triacylglycerols were purchased from Sigma (St. Louis, MO, U.S.A.), methanol and ethanol of HPLC grade from Kanto Chemical (Tokyo, Japan), 2-nitrophenylhydrazine hydrochloride from Tokyo Chemical Industry (Tokyo, Japan), 1-ethyl-3-(3-dimethylaminopropyl)carbodiimide hydrochloride (EDC) from Wako (Osaka, Japan), sorbitan fatty acid esters (Wako practical grade) from Wako and sucrose fatty acid esters from Ryoto (Tokyo, Japan) and Dai-ichi Kogyo Seiyaku (Kyoto, Japan). Other reagents were of analytical-reagent grade.

In the post-column reactor, the following reagents were used: for the hydrolysis of NSEG, 0.45 *M* potassium hydroxide in ethanol–water (50:50); for the condensation of ONPH and fatty acids, 0.035 *M* ONPH in 0.25 *M* hydrochloric acid and 0.15 *M* EDC in 6% pyridine; and for the colour development reaction, 1.5 *M* sodium hydroxide. These reagents were renewed each day.

Procedure for the manual ONPH method

To 4 ml of 100 ppm myristic acid in methanol–water (85:15) containing 5.7 m*M* triethylamine (TEA) are added 1 ml of 0.45 *M* potassium hydroxide in ethanol–water (50:50) and 2 ml of ONPH and EDC solution and the mixture is heated at 60°C for 30 min. After cooling, 2 ml of sodium hydroxide solution are added and the mixture is heated at 80°C for 10 min. After cooling, the absorbance of the resulting solution is measured at 550 nm.

Post-column reactor

As shown in Fig. 1, potassium hydroxide solution (reservoir 7) is added at a flow-rate of 0.2 ml/min to the eluate from the chromatographic column and passed through PTFE tubing (reaction coil 14; 10 m × 0.5 mm I.D.) into a reaction bath (bath 17) kept at 120°C, where NSEG are hydrolysed to form fatty acids. Then ONPH and EDC solution (reservoirs 8 and 9) are added at a rate of 0.4 ml/min and passed through PTFE tubing (reaction coil 15; 20 m × 0.5 mm I.D.) in a circulating bath (bath 18) kept at 70°C, where fatty acids are condensed with ONPH. Sodium hydroxide solution (reservoir 10) is added to the flow at a rate of 0.4 ml/min, and the mixture is passed through PTFE tubing (reaction coil 16; 10 m × 0.5 mm I.D.) in a reaction bath (bath 19) kept at 100°C, where the blank absorbance is reduced and a violet colour of the hydrazide is developed. Finally, the flow is passed through the UV–VIS detector set at 550 nm.

Procedure for HPLC

A stainless-steel column (150 mm × 4.6 mm I.D.) packed with Hitachi gel 3057 was used and kept at 50°C. The mobile phases used were methanol–water (85:15) containing 5.7 m*M* TEA (solvent A) and ethanol–methanol (75:25) containing 5.7 m*M* TEA (solvent B) at a flow-rate of 0.8 ml/min. The analysis was done according to the gradient programme shown in Table I. A sample containing 10–500 μg of NSEG dissolved in 5–50 μl of ethanol or isopropanol was injected into the HPLC system.

TABLE I

GRADIENT ELUTION PROGRAMME

Time (min)	Solvent A (%)	Solvent B (%)
0	100	0
5	60	40
10	28	72
15	12	88
20	4	96
25	0	100
45	0	100
45.1	100	0
70	100	0

RESULTS AND DISCUSSION

Optimization of separation

The determination of NSEG by HPLC has been investigated in the reversed-phase mode using an ODS column and mixtures of isopropanol, methanol and water as the mobile phase [6,7]. In this study, Hitachi gel 3057 was chosen as the stationary phase because of the high resolution obtained. Mixtures of acetonitrile, methanol, ethaol, isopropanol and water were investigated as mobile phases. Among these solvents, acetonitrile was not suitable as it was hydrolysed to acetic acid, which gave a high blank absorbance. Poor resolutions were obtained by using isopropanol–water and ethanol–water mobile phases. Methanol–water could not elute esters higher than the triester. Finally, methanol–ethanol–water was adopted as the mobile phase because of the high resolution and good compatibility with the post-column reaction.

Gradient elution was necessary to separate NSEG from the mono- to pentaester simultaneously. The mobile phase composition and the gradient programme were determined as described under Experimental, taking the resolution and baseline drift into account. Under these conditions, sorbitan fatty acid esters from the mono- to tetraester and sucrose fatty acid esters from the mono- to pentaester could be simultaneously determined. A small amount of triethylamine was added to the mobile phase in order to eliminate the interferences from free fatty acids, as will be described later.

Optimization of post-column reaction

In order to investigate the post-column reaction, each reaction was optimized in the order of hydrolysis, condensation and colour development reaction.

The condensation and colour development reaction were investigated by the manual ONPH method with myristic acid instead of NSEG as a sample.

Optimization of hydrolysis reaction

Optimization of the hydrolysis reaction was investigated with triacylglyerol (tristearin) as a standard sample, which is difficult to hydrolyse [13] as a pure standard of the tetraester of sorbitan fatty acid esters and the pentaester of sucrose fatty acid

esters could not be obtained. If hydrolysis of tristearin is performed perfectly, one mole tristearin produces three moles of stearic acid. Therefore, the yield of hydrolysis was expressed as the relative peak area of tristearin to stearic acid of three times mole amount. With the tube length fixed at 10 m, the effects of the concentration of potassium hydroxide and reaction temperature on the relative peak area were investigated. The relative peak area increased with increase in concentration of potassium hydroxide and reached nearly 100% above 0.40 *M* potassium hydroxide. Therefore, 0.45 *M* potassium hydroxide was used for the hydrolysis reaction. As the relative peak area decreased at ethanol contents below 40% in the potassium hydoxide solution, the ethanol content was fixed at 50%. The temperature selected for the hydrolysis reaction was 120°C, as the relative peak area reached nearly 100% above 110°C.

Under these conditions, good linearities of concentration *versus* peak area were observed for NSEG, as will be described later. Further, the ester compositions of NSEG obtained by using these conditions were the same as those obtained by using a higher hydrolysis temperature and were in good agreement with the literature data and supplier's data, as will be described later. These results indicate that these conditions are suitable for NSEG, all of which are hydrolysed at the same rate. On the basis of these results, the conditions adopted for the hydrolysis reaction were those given under Experimental.

Optimization of condensation reaction

Fig. 2 shows the effect of the concentration of ONPH on the absorbance at 550 nm. The absorbance increased with increase in the concentration of ONPH and reached a nearly constant value above 0.02 *M*. Therefore, the concentration of ONPH was fixed at 0.035 *M*. The concentration of EDC adopted was 0.15 *M*, as the absorbance reached nearly constant value above 0.08 *M*.

Fig. 3 shows the effect of heating time and reaction temperature on the absorbance at 550 nm. As a high reaction rate is required in the post-column reaction, the reaction temperature was set at 70°C. The pH in the condensation reaction was

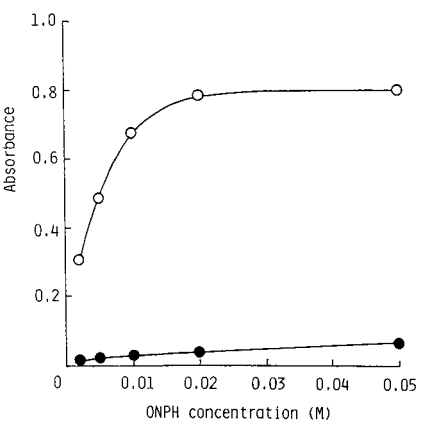

Fig. 2. Effect of concentration of 2-nitrophenylhydrazine on the absorbance at 550 nm. ○ = 100 ppm of myristic acid; ● = reagent blank.

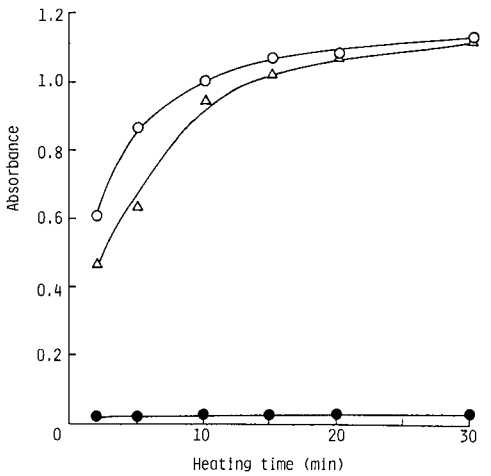

Fig. 3. Effect of heating time and reaction temperature on the absorbance at 550 nm. △ = 100 ppm of myristic acid, reaction temperature 40°C; ○ = 100 ppm of myristic acid, reaction temperature 60°C; ● = reagent blank, reaction temperature 60°C.

adjusted with pyridine–hydrochloric acid buffer, according to Horikawa and Tamimura [10]. It was found that the response of this post-column reaction detector varied under the gradient conditions because of the variation of the pH in the condensation reaction. Therefore, the concentrations of pyridine and hydrochloric acid were

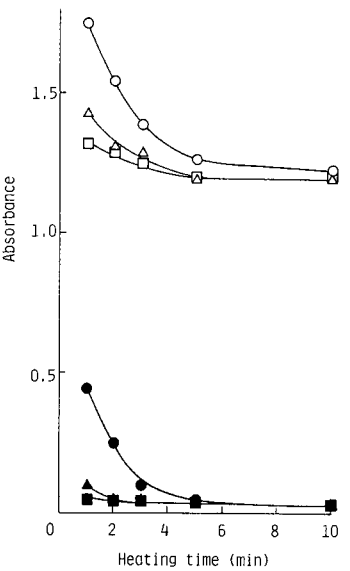

Fig. 4. Effect of concentration of sodium hydroxide and heating time on the absorbance at 550 nm (reaction bath temperature 80°C). ○ = 100 ppm of myristic acid, NaOH concentration 0.5 *M*; △ = 100 ppm of myristic acid, NaOH conentration 1.0 *M*; □ = 100 ppm of myristic acid, NaOH concentration 1.5 *M*; ● = reagent blank, NaOH concentration 0.5 *M*; ▲ = reagent blank, NaOH concentration 1.0 *M*; ■ = reagent blank, NaOH concentration 1.5 *M*.

investigated so as to minimize the variation of the response as will be described later. Finally, the effect of the length of Teflon tubing on the condensation reaction (peak area) was investigated and the optimum was determined to be 20 m. On the basis of these results, the conditions adopted for condensation reaction were those given under Experimental.

Optimization of colour development reaction

After the condensation reaction, the reaction mixture is made strongly alkaline and heated to develop a violet colour of the hydrazide and reduce the blank absorbance. Fig. 4 shows the effect of the concentration of sodium hydroxide and heating time on the absorbance at 550 nm. The blank absorbance decreased with increase in concentration of sodium hydroxide and reaction temperature. Therefore the concentration of sodium hydroxide adopted was determined 1.5 *M* and the reaction bath temperature was set at 100°C [11]. On the basis of these results, the conditions adopted for the colour development reaction were those given under Experimental.

Response and reproducibility of the detector

The ONPH method has been used for the analysis of water-soluble carboxylic acids, whereas fatty acids are not water soluble. Therefore, the linearity of concentration *versus* response for fatty acids was examined. Good linearities were observed from 0.5 to 250 μg for lauric, myristic, palmitic, stearic and oleic acid and the relative standard deviation of five measurements was found to be 0.80% for 20 μg of myristic acid. Moreover, the relative molar responses of lauric, palmitic stearic and oleic acid with respect to myristic acid were in the range 0.98–1.01, demonstrating equal molar responses.

It is most important to establish the molar response of the detector. Monomyristin was repeatedly injected at intervals of 5 min under the gradient conditions. Fig. 5 shows the relative peak area of monomyristin for each injection with respect to that of the first injection *versus* the analysis time. The response of the detector varies

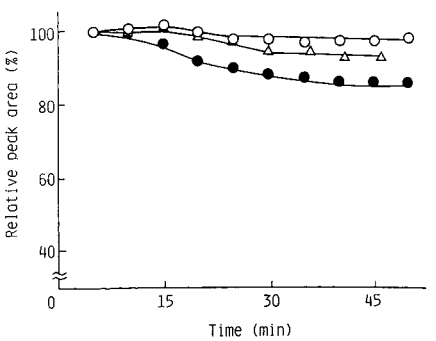

Fig. 5. Effect of concentration of hydrochloric acid in ONPH solution on the response of the detector to monomyristin for gradient analysis. Monomyristin (40 μg) was repeatedly injected at intervals of 5 min under the gradient conditions. Mobile phases: methanol–water (85:15) containing 5.7 m*M* TEA (solvent A) and ethanol–methanol (75:25) containing 5.7 m*M* TEA (solvent B). Pyridine concentration in EDC solution, 6%. HCl concentration in ONPH solution: (○) 0.25; (△) 0.30; (●) 0.40 *M*.

with the hydrochloric acid concentration in the ONPH solution and the degree of the variation is suppressed within 3% with 0.25 *M* hydrochloric acid. This result indicates that NSEG from the mono- to pentaester could be detected with a molar response regardless of the mobile phase composition. On the other hand, it is known that the low solubility of tri-, tetra- and pentaesters in the mobile phase decreases their molar response [12]. Therefore, the temperature of the injection port is maintained at 60°C with a specially designed apparatus [12]. The detection limit is 1 μg of monomyristin.

Application

NSEG usually contain small amount of free fatty acids, which overlap with the peaks of the monoesters and interfere in the analysis. This interference was eliminated by the addition of a small amount of triethylamine to the mobile phase and fatty acids were eluted at the void volume, as shown in Fig. 6. Fig. 7 shows chromatograms of commercial sorbitan fatty acid esters and sucrose fatty acid esters obtained by the proposed method. Each peak group was trapped immediately after the column and was identified by TLC [1,3]. The separated peaks in the peak groups for each ester will be due to the alkyl distribution of fatty acid moieties and positional isomers of NSEG [8]. However, their identification was difficult except for the monoester of sucrose fatty acid esters because no authentic standard sample was available. The identification of the monoester of sucrose fatty acid esters shown in Fig. 7 was done by comparing the chromatograms in Fig. 7C, D and E with their fatty acid compositions according to Jaspers *et al.* [8]. Good linearities of concentration *versus* peak area were observed from 10 to 500 μg for sorbitan fatty acid esters and sucrose fatty acid esters and the relative standard deviations for five measurements were in the range 1.1–2.0% for 200-μg amounts.

The results of ester distribution analyses of commercial sucrose fatty acid esters by the proposed method are summarized in Table II. This method affords a molar response to fatty acids produced by the hydrolysis of NSEG as described above. Therefore, it is necessary to correct the peak areas with the corresponding ester value to obtain the molar composition of NSEG from the mono- to pentaester. In Table II,

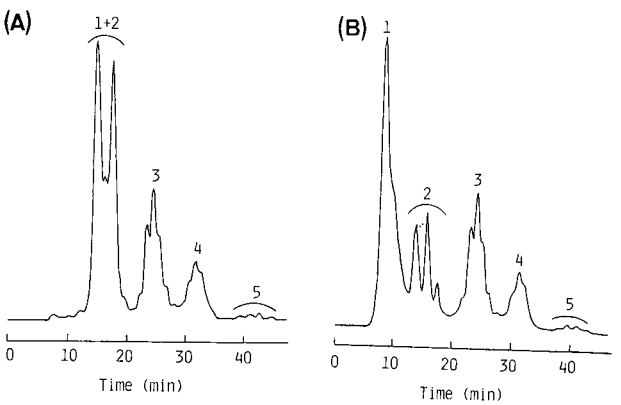

Fig. 6. Chromatogram of a mixture of sorbitan monostearate and fatty acids ($C_{16:0}$, $C_{18:0}$) using (A) eluents without triethylamine and (B) eluents with triethylamine. 1 = Fatty acid; 2 = monoester; 3 = diester; 4 = triester; 5 = tetraester.

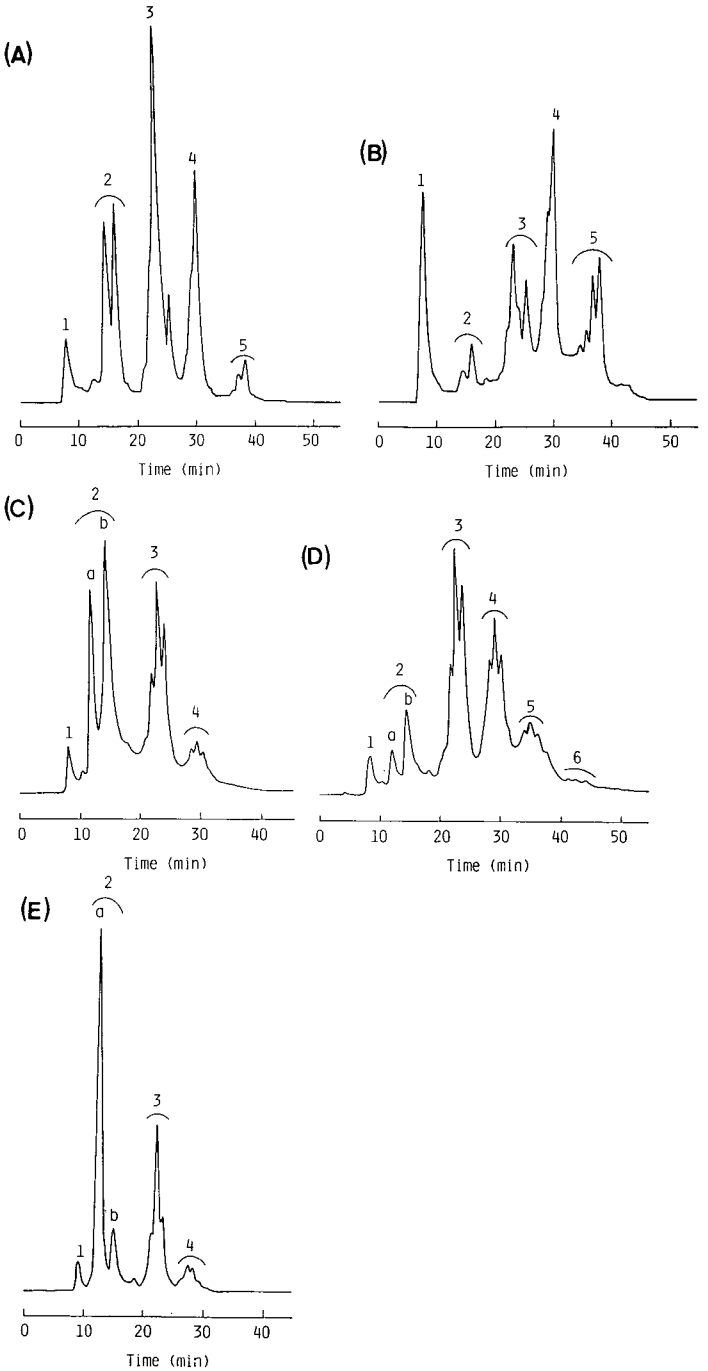

Fig. 7. Analysis of commercial sorbitan fatty acid esters and sucrose fatty acid esters. (A) Sorbitan monooleate; (B) sorbitan trioleate; (C) Ryoto sugar ester S-1570; (D) Ryoto sugar ester S-370; (E) Ryoto sugar ester P-1570. 1 = Fatty acid; 2 = monoester (a, $C_{16:0}$; b, $C_{18:0}$); 3 = diester; 4 = triester; 5 = tetraester; 6 = pentaester.

TABLE II

RESULTS OF ESTER DISTRIBUTION ANALYSES OF COMMERCIAL SUCROSE FATTY ACID ESTERS BY THE PROPOSED METHOD

Sucrose fatty acid ester	Concentration	Proposed method					Literature data[c]					Supplier's data[d]		
		Mono-	Di-	Tri-	Tetra-	Penta-	Mono-	Di-	Tri-	Tetra-	Penta-	Mono-	Di—penta-	Fatty acid composition
Ryoto sugar ester O-1570[a]	mol-%	77.3	19.8	2.9	—	—						70	30	Oleic acid (~70%)
	wt.-%	69.7	25.4	4.9	—	—								
Ryoto sugar ester P-1570[a]	mol-%	74.9	21.4	3.7	—	—								Palmitic acid/
	wt.-%	66.9	27.0	6.1	—	—						70	30	Stearic acid (~70:30)
Ryoto sugar ester S-1570[b]	mol-%	74.8	21.5	3.7	—	—								Hydrogenated
	wt.-%	66.5	27.4	6.1	—	—						70	30	tallow[f]
		(0.3)[e]	(0.8)[e]	(4.0)[e]	—	—								
Ryoto sugar ester S-370[b]	mol-%	30.0	36.6	23.3	8.7	1.4								Hydrogenated
	wt.-%	20.1	35.0	29.0	13.3	2.6						20	80	tallow[f]
		(2.8)[e]	(1.1)[e]	(1.5)[e]	(3.0)[e]	(9.9)[e]								
DK ester F-160[a]	mol-%	76.8	20.9	2.3	—									Hydrogenated
	wt.-%	69.2	26.9	3.9	—	—	71.0	24.0	5.0	—		70	30	tallow[f]
DK ester F-110[a]	mol-%	60.5	30.9	7.6	1.1	—								Hydrogenated
	wt.-%	50.4	36.4	11.6	2.0	—	50.0	36.0	12.0	2.0	—	50	50	tallow[f]
DK ester F-50[a]	mol-%	47.2	40.9	10.5	1.4	—								Hydrogenated
	wt.-%	36.8	45.5	15.2	2.5	—	33.0	49.0	16.0	2.0	—	30	70	tallow[f]

[a] Mean of two analyses.
[b] Mean of five analyses.
[c] Ref. 14.
[d] Catalogue data.
[e] Relative standard deviation (%).
[f] Stearic acid and palmitic acid.

ester compositions (mol-%) were calculated with the values obtained by division of the peak area by the corresponding ester value. Ester compositions (wt.-%) are also given in Table II; these were calculated with the values obtained by the product of ester composition (mol-%) and the corresponding avarage molecular weight, which was calculated with the fatty acid composition obtained by GC analysis of the methyl ester of fatty acids produced by alkaline hydrolysis of NSEG. The ester compositions (wt.-%) in Table II are in good agreement with the literature data [14] and supplier's data. The relative standard deviations for five measurements were within 4% for NSEG, except for the pentaester, which is a minor component.

By using the proposed method, NSEG can be determined with high sensitivity and high selectivity and the ester distributions of NSEG can also be determined.

REFERENCES

1 K. Yamanaka, *Yukagaku*, 18 (1969) 161.
2 H. Mima and N. Kitamori, *J. Am. Oil Chem. Soc.*, 41 (1964) 198.
3 S. Kinoshita, *Kogyo Kagaku Zassi*, 66 (1963) 450.
4 M. R. Sahasrabudhe and R. K. Chadha, *J. Am. Oil Chem. Soc.*, 46 (1969) 8.
5 C. Yomota, K. Nakamura and Y. Ito, *J. Soc. Cosmet. Chem. Jpn.*, 20 (1986) 5.
6 V. R. Kaufman and N. Garti, *J. Liq. Chromatogr.*, 4 (1981) 1195.
7 N. Garti, E. Wellner, A. Aserin and S. Sarig, *J. Am. Oil Chem. Soc.*, 60 (1983) 1151.
8 M. E. A. P. Jaspers, F. F. Leeuwen, H. J. W. Nieuwenhuis and G. M. Vianen, *J. Am. Oil Chem. Soc.*, 64 (1987) 1020.
9 C. G. Birch and F. E. Crowe, *J. Am. Oil Chem. Soc.*, 53 (1976) 581.
10 R. Horikawa and T. Tanimura, *Anal. Lett.*, 15 (1982) 1629.
11 Y. Shimazu and M. Watanabe, *J. Brew. Soc. Jpn.*, 76 (1981) 418.
12 Y. Kondoh and S. Takano, *J. Chromatogr.*, 393 (1987) 427.
13 Y. Kondoh and S. Takano, *Anal. Chem.*, 58 (1986) 286.
14 C. E. Walker, *Cereal Foods World*, 29 (1984) 286.

Journal of Chromatography, 541 (1991) 443–452
Elsevier Science Publishers B.V., Amsterdam

CHROM. 22 927

Preconcentration of divalent trace metals on chelating silicas followed by on-line ion chromatography

D. CHAMBAZ*, P. EDDER and W. HAERDI
Département de Chimie Analytique, Université de Genève, Quai Ernest Ansermet 30, 1211 Geneva 4 (Switzerland)

(First received July 3rd, 1990; revised manuscript received October 18th, 1990)

ABSTRACT

A novel method for the on-line preconcentration and chromatography of trace metals, *e.g.*, Mn, Co, Ni, Cu, Zn, Cd and Pb, on ethylenediamine triacetate-bonded silica is described. The preconcentrated metals were desorbed with 0.1 *M* nitric acid. Post-precolumn modification of the eluent was done by means of a tee mixer and a second high-performance liquid chromatographic pump. The modified eluent, consisting of tartaric acid and sodium nitrate, allows the separation of metals on a cation-exchange chromatographic column. The metals separated were detected by postcolumn reaction with 4-(2-pyridylazo)-resorcinol and measuring absorbances at 500 nm. Linear calibration graphs were obtained over the range $3 \cdot 10^{-9}$–$3 \cdot 10^{-6}$ *M*. The characteristics of this chelating silica are given and the on-line and off-line preconcentration methods were compared. Application of the method to the analysis of river water is described. The results show that the method is applicable to the determination of Co, Ni, Cu, Zn, Cd and Pb ions. It was also demonstrated that the method can be used for the determination of free metal ions and labile or moderately labile complexes.

INTRODUCTION

The determination of trace metal ions (concentrations less than 10^{-7} *M*) in natural waters by ion chromatography requires a preconcentration step. The large amounts of alkali and alkaline earth metals present in such samples have to be eliminated prior to metal separation to avoid interference effects. Elimination of these cations and concentration of trace metal ions may be achieved in a single step by using chelating silicas. On-line chromatography following preconcentration would be preferable as it would minimize contamination risks and at the same time allow the attainment of high concentration factors. In a previous paper [1], on-line preconcentration of trace metals on 8-quinolinol–silica followed by ion chromatographic separation was described. Potassium cyanide solution (0.1 *M*) was used to desorb metals and separation by ion pairing was achieved using tetrabutylammonium ions. The disadvantages of this method are that it is restricted to the determination of Cu(II) and Ni(II) ions and it necessitates the use of a diode-array detector because the cyano complexes of these two metals do not absorb at the same wavelength.

In this work, the use of ethylenediamine triacetate (ED3A) bonded chelating silica for the preconcentration of trace metal ions, *e.g.*, Mn(II), Co(II), Ni(II), Cu(II),

0021-9673/91/$03.50

Zn(II), Cd(II) and Pb(II), was evaluated. Ohshima *et al.* [2] prepared and characterized this type of silica for the preconcentration of trace elements in sea water. As desorption of metals in acidic media is not suitable for classical cation-exchange chromatography, a neutralization system incorporating a second high-performance liquid chromatographic (HPLC) pump and a tee mixer was developed. On-line and off-line preconcentration on a Vac-Elut system were compared. Finally, the applicability of ED3A-bonded silica to the preconcentration of trace metal ions in river water is discussed.

EXPERIMENTAL

Apparatus

On-line chromatography. The chromatographic equipment (Fig. 1) consisted of a Knauer metal-free electric valve, a Knauer 64 titanium pump for delivering 0.1 *M* nitric acid, a Knauer 64 pump with a stainless-steel microhead for neutralizing and delivering the eluent, a laboratory-made stainless-steel membrane pulse damper and a Dionex QIC preconcentration pump. Laboratory-made titanium precolumns (13 × 1.7 and 50 × 2 mm I.D.) were packed manually with ED3A–silica. The silica was placed in the precolumn with a microspatula and the precolumn was tapped to ensure that the solid was well packed. A Macherey, Nagel & Co. analytical column (30 cm × 4 mm I.D.) was packed with Nucleosil 10SA silica. Except for two Knauer tee pieces, plastic tubing was used. Postcolumn reagent was pumped under nitrogen pressure (4.5 atm) and to ensure 4-(2-pyridylazo)-resorcinol (PAR)–metal complexation a PTFE coil (3 m × 0.5 mm I.D.) was used. A Hewlett-Packard 1040 A diode-array UV–visible detector was used for detection of metal complexes.

Off-line chromatography. Preconcentration was achieved by using a modified metal-free Vac-Elut SPS 24 apparatus. Syringes (9 mm diameter) were packed manually with 0.5 g of ED3A–silica (height 2 cm). After eluting the metals, the sample was injected into an ion chromatographic system consisting of a Knauer 64 stainless-steel pump and a Knauer metal-free valve with a 20-μl sample loop.

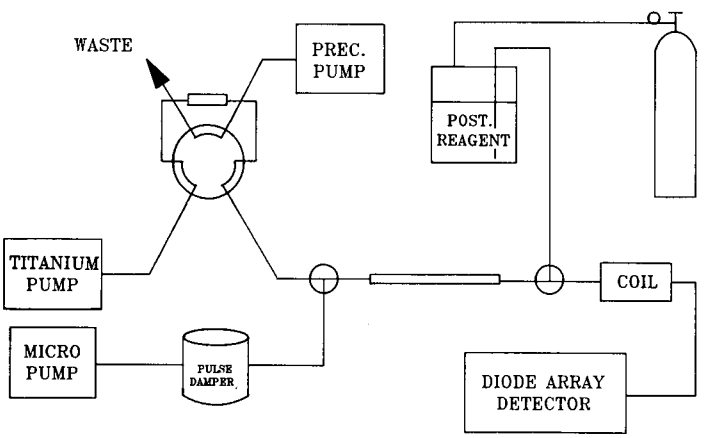

Fig. 1. Schematic representation of the chromatographic equipment.

A Stagroma analytical column (20 cm × 4 mm I.D.) was packed with Nucleosil 10SA silica. The postcolumn reactor and detector were the same as those described above.

Reagents

Preconcentration. Unless stated otherwise, all chemicals were analytical-reagent grade Merck or Fluka products. All solutions were made with freshly prepared doubly distilled water. Freshly prepared 0.1 *M* sodium acetate–acetic acid buffer (pH 5) was used for conditioning the precolumn. It was obtained by diluting a stock solution of 5 *M* acetate buffer (pH 5.4) prepared as follows: 26.7 g of sodium acetate (Suprapur, Merck) were dissolved in 90 ml of water, the pH was adjusted to 5.4 with concentrated acetic acid (Suprapur, Merck) and the solution was diluted to 100 ml with water. A 1-ml volume of this 5 *M* buffer solution was also added to 50-ml samples prior to preconcentration.

ED3A–silica was synthesized according to the procedure described by Ohshima *et al.* [2]. A 15-g amount of silica (Polygosil 100, 40–63 μm; Macherey, Nagel & Co.) was washed with 150 ml of concentrated H_2SO_4–HNO_3 (9:1) and rinsed with demineralized water until the washings were neutral. A 5% aqueous solution of sodium N-(trimethoxysilylpropyl)ethylenediamine triacetate (Petrarch Systems) was prepared and 60 ml of this solution were added to the silica, stirred for 3 h and filtered. The solid was washed with HCl (0.2 *M*), demineralized water, methanol and finally diethyl ether. The chelated silica thus prepared was dried under vacuum. The loading capacity (120 μmol/g) of the bonded silica was determined by measuring the difference in the copper(II) ion concentration before ($5 \cdot 10^{-3}$ *M* in acetate buffer, pH 5) and after contact with the bonded silica.

Eluent for on-line chromatography. Nitric acid (0.1 *M*) (Suprapur, Merck) was used for desorbing the metals from the precolumn (titanium pump). The eluent was modified before the inlet into the chromatographic column by pumping 0.5 *M* tartaric acid at pH 4.2 (Biochemica Microselect, Fluka), the pH being adjusted with NaOH. A few drops of pentachlorophenol solution (5 mg/l in 98% ethanol) were added to the tartrate solution to prevent bacterial growth.

Eluent for off-line chromatography. Nitric acid (1 *M*) (Suprapur, Merck) was used as eluent for desorbing metals. Tartaric acid (0.1 *M*) (Biochemica Microselect, Fluka) at pH 3 was used as the chromatographic eluent [3].

Postcolumn reagent. A solution containing $5 \cdot 10^{-4}$ *M* PAR and $5 \cdot 10^{-5}$ *M* Zn-EDTA in 2 *M* ammonia solution (pH 11) was used as the post-derivatizing reagent [3,4].

Procedures

On-line method. A 20-ml (or 50-ml) volume of sample solution containing the metal ions and acetate buffer was pumped into the chelating silica precolumn (flow-rate 5 ml/min), where the metals were preconcentrated. The precolumn was rinsed with 5 ml of water. The metals retained were desorbed with nitric acid by using the titanium pump (flow-rate 1.2 ml/min, pressure 100 atm). Then, before the analytical column, the acidic solution was neutralized with tartrate buffer delivered by the micro pump (flow-rate 0.24 ml/min). During the desorption process, the precolumn and the analytical column were linked. The metals, after separation on the analytical column, were derivatized with the PAR–Zn-EDTA solution (flow-rate

0.7 ml/min) and detected at 500 nm. The precolumn was disconnected from the analytical column 1.5 min after passing the eluent. While separation was proceeding, clean-up and conditioning of the precolumn were carried out by washing it with 5 ml of 1 *M* nitric acid followed by 10 ml of 0.1 *M* acetate buffer using the preconcentration pump. A new sample may be preconcentrated while the separation of the previous sample is under way.

Off-line method. The syringe containing the chelating silica was first cleaned and conditioned by passing 10 ml of 1 *M* nitric acid followed by 20 ml of water. A 200-ml volume of the solution containing the elements of interest and acetate buffer was preconcentrated. The metals were desorbed with 2 ml of 1 *M* nitric acid, collected in a plastic tube and injected directly into the ion chromatograph having a 20-μl sample loop.

RESULTS AND DISCUSSION

Characteristics of ED3A–silica

Maximum sample volumes that may be concentrated with the precolumns and syringes used in this work were determined under the experimental conditions described by Ohshima *et al.* [2], *i.e.*, using 0.1 *M* acetate buffer (pH 5), and the results are given in Table I. Acetate buffer is essential for the elimination of calcium ions present in excess in natural waters. In fact, in the absence of acetate ions, *ca.* 50% of the calcium present was retained by silica whereas in its presence, at pH 5, less than 1% was retained. Attempts were made to improve calcium elimination by varying the pH of the solution. As can be seen from Table II, the measured signals decrease with decreasing

TABLE I

BREAKTHROUGH VOLUMES

Metal	On-line method		Off-line method (ml)
	1.3-cm precolumn (ml)	5-cm precolumn (ml)	
Cu, Ni, Co, Zn, Cd	100	500	>1000
Pb	50	250	600
Mn	15	75	200

TABLE II

OFF-LINE METHOD: INFLUENCE OF pH ON METAL RETENTION ON ED3A–SILICA

Signals obtained (peak surface areas in absorbance units) by preconcentration of 200 ml of 0.1 *M* acetate buffer solutions containing 5×10^{-7} *M* of the various metal ions.

pH	Pb	Zn	Ni	Co	Cd	Mn	Ca	Ca preconcentrated (%)
5	1392	2054	2029	1317	1416	1227	5026	0.3
4.5	781	1916	1913	1088	1557	–	600	0.04
4	298	2158	1956	1208	1366	1179	–	0
3	167	2207	1879	1160	600	1023	–	0

pH and at pH < 4 calcium was not retained at all. However, under these conditions, the test metal ion signals also decrease, particularly that of Pb. Hence pH 5 seems to be the optimal.

The effect of major ions present in natural waters on the retention of trace metal ions was also studied. The results showed that metal retention is unaffected by the presence of up to 0.5 *M* Na^+ and 10^{-3} *M* Ca^{2+}, CO_3^{2-} and PO_4^{3-}.

Despite drastic treatment of ED3A–silica with acid (1 *M* HNO_3), it degrades very slowly. On-line experiments revealed that after nineteen preconcentration–elution cycles, a decrease of 6% in the capacity had occurred.

Off-line method

Limitations. This method is less attractive for several reasons. First, 2 ml of 1 *M* HNO_3 are required for the desorption of metals retained on the syringe. A preconcentration factor of 100 is only achieved with a 200-ml sample volume. In the ion chromatograph, injection of sample volumes greater than 20 μl was found to perturb the chromatographic separation markedly owing to the presence of a high concentration of HNO_3, hence limiting the maximum injection volume to 20 μl. Neutralizing the acid or substituting HCl for HNO_3 did not produce any improvement in the results.

Another drawback of the method is that the analytical column decomposes with increasing number of 1 *M* acid injections. The Cu(II) peak vanishes rapidly. Hence the determination of copper by this method is virtually impossible. Moreover, contrary to Yan and Schwedt's observations [3], complete chromatographic separation of Ca^{2+} and Mn^{2+} could not be achieved.

Reproducibility and sensitivity. The results of four replicate measurements made using 200-ml samples containing 10^{-6} *M* test metal ions are given in Table III. A comparison with the on-line method showed that the reproducibility is slightly poorer. The limit of detection was 10^{-8} *M* for a 200-ml sample volume. Linear calibration graphs were obtained over the range $3 \cdot 10^{-8}$–$3 \cdot 10^{-5}$ *M* for all metals except copper, for reasons mentioned earlier.

TABLE III

REPRODUCIBILITY

On-line method, 20 ml of 10^{-7} *M* metal solutions (five replicates); off-line method, 200 ml of 10^{-6} *M* metal solutions (four replicates).

Metal	Relative standard deviation (%)	
	On-line	Off-line
Cu	2.9	–
Pb	1.6	3.4
Zn	0.9	5.0
Ni	4.3	4.5
Co	0.6	5.9
Cd	1.0	4.5
Mn	2.2	3.2

On-line method

Desorption of metals. For Mn, Co, Zn, Cd and Pb, less than 0.5 ml of 0.1 *M* HNO_3 was required to desorb quantitatively 2-ml samples containing 10^{-5} *M* of the individual metal of interest. It should be pointed out that these determinations were made without the analytical column. HNO_3 (0.5 *M*) had to be used for the more strongly retained Cu and Ni ions. However, the signals obtained for these two metals by using 0.1 *M* HNO_3 were found to be proportional to the amount of metal preconcentrated.

Eluent modification. The conditions used for eluting the metals from the precolumn (0.1 *M* HNO_3) are not suitable for direct loading on an analytical column as the relatively high acid concentration does not allow metal separations. Therefore, the acid must be neutralized before performing the chromatographic separation. The high ionic strength of the neutralized eluent hampers the chromatographic separation of metal ions on low-capacity ion-exchangers such as that used by Sevenich and Fritz [5]. Consequently, a high-capacity cation-exchanger was used and metal separations were carried out using Yan and Schwedt's procedure [3]. (0.1 *M* tartrate, pH 3). By lowering the concentration of the tartrate and using a 30-cm column, it was found that well resolved peaks such as those reported by Yan and Schwedt were obtained for all the metals except Mn(II), which was co-eluted with calcium ions. Attempts to improve the resolution of these two metal ions using complexing agents such as citrate and phthalate did not alter the results. The final concentrations of the eluent components were 0.083 *M* $NaNO_3$ and 0.083 *M* tartrate (pH 3).

More concentrated nitric acid was tried in order to facilitate the desorption of copper and nickel, but the chromatographic separation under these conditions was poor.

Materials. The materials used in designing the apparatus play an important role. The preconcentration part of the system should be made of titanium or plastic. Titanium and plastic precolumns yielded similar results, but the former material was chosen because it is more practical to use at high pressures. The HPLC pump delivering HNO_3 must be made of titanium, as stainless-steel is oxidized too quickly by this eluent. A stainless-steel micro pump, pulse damper and analytical column may be used without any problems, however.

Eluent mixing. The mixing of eluents is a very critical parameter as inhomogeneous mixing will result in splitting of peaks during chromatographic separation. The following points are very important for obtaining sharp chromatographic peaks. The motors of the two pumps should turn at the same rate. Therefore, eluent flow-rates of 0.24 and 1.2 ml/min were chosen for the microhead and for the titanium pump, respectively. The pulse damper is an essential part of the system as it regulates the flow-rates of the two pumps, which is important for homogeneous mixing of eluents. Hence an efficient pulse damper must be used. Tests with an SSI pulse damper yielded unsatisfactory results. In this work, a diaphragm-type (4.5-cm diameter) pulse damper similar to that of Latex (Germany) was used. The tee piece should not have too small an inside diameter. Initial tests with a high-pressure Upchurch mixing tee did not give good results.

Comparison with direct injection. The results obtained by replacing the precolumn with an injection loop and injecting 20-μl samples containing 10^{-4} *M* of test metal ions were compared with on-line preconcentration–separation of 20-ml samples

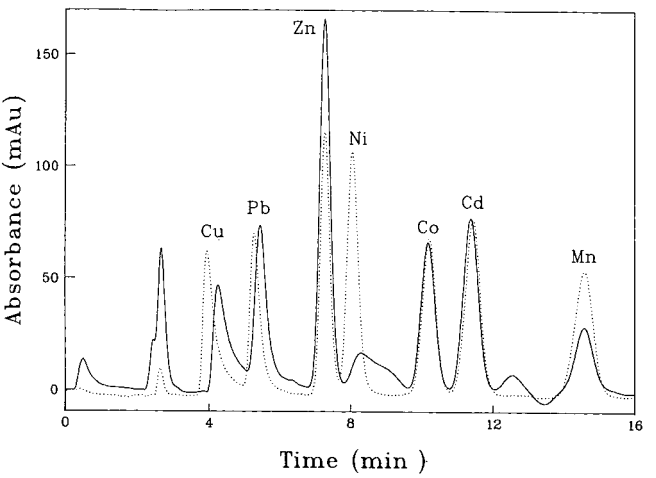

Fig 2. Comparison between on-line preconcentration and direct injection methods. Solid line: preconcentration of a 20-ml sample containing 10^{-7} *M* of each of the test metal ions. Dashed line: injection of a 20-μl sample containing 10^{-4} *M* of test metal ions. Elution conditions: titanium pump, 0.1 *M* HNO_3, flow-rate 1.2 ml/min; micropump, 0.5 *M* tartaric acid (pH 4.2), flow-rate 0.24 ml/min; postcolumn reagent, $5 \cdot 10^{-4}$ *M* PAR–$5 \cdot 10^{-5}$ *M* Zn-EDTA (pH 11), flow-rate 0.7 ml/min.

containing 10^{-7} *M* of test metal ions (Fig. 2). Analogous results were obtained for Pb, Co and Cd. The Zn peak is larger owing to the high blank signals. The Cu peak is smaller and slightly broader owing to the difficulties in eluting it. Ni yields a broad band which does not interfere with other metals and the integrated peak was found to be proportional to the amount of Ni preconcentrated. Hence the determination of Ni is possible despite the broad band. Finally, the Mn peak is smaller owing to the small breakthrough volume. In general, preconcentration with a precolumn yields well resolved peaks similar to direct injection and concentration factors of 1000 are achieved. The recoveries of various metals calculated using the surface area and subtracting from the blank were as follows: 100% for Cu, Pb, Zn, Co and Cd, 50% for Mn and 30% for Ni.

Reproducibility and sensitivity. The results obtained from five replicate measurements of 20-ml samples containing 10^{-7} *M* of various metal ions are shown in Table III. The detection limit for all the test metals was 10^{-9} *M* for 20 ml of sample solution. Linear calibration graphs were obtained over the range $3 \cdot 10^{-9}$–$3 \cdot 10^{-6}$ *M* for Cu, Co and Cd. Analogous results were obtained for Mn by using 5-cm precolumn. The Zn and Ni calibration graphs were linear over the range 10^{-8}–$3 \cdot 10^{-6}$ *M* owing to the high background levels. For Pb, linearity was observed over a narrow range, $3 \cdot 10^{-9}$–$3 \cdot 10^{-7}$ *M*, because of the low Zn-EDTA concentration employed in the postcolumn reagent. Zn-EDTA is usually added to the reagent to improve the detection of Pb by a substitution reaction [3,4]. However, the background absorption of the postcolumn reagent increases proportionally with the amount of Zn-EDTA added. Therefore, the minimum Zn-EDTA concentration required for detection of Pb was used to reduce the background signal. In any case, the Pb^{2+} concentration in natural water rarely exceeds $3 \cdot 10^{-7}$ *M*.

Stability of the analytical column. Slow decomposition of the analytical column is indicated by a decrease in retention times. However, retention times similar to those obtained with the freshly prepared column can be achieved by lowering the tartrate concentration. For instance, over a period of 2 weeks of continuous usage, the tartrate concentration was lowered from 0.5 to 0.48 *M*. All attempts to regenerate the column failed.

The copper peaks decreased slightly with increased number of runs and eventually disappeared. The column can be regenerated by the following procedure, however: every 3 days, the column should be flushed with 100 ml of 0.05 *M* tetramethylammonium hydroxide (pH 9) in 50% acetonitrile followed by 20 ml of acetonitrile and 20 ml of water.

Analytical application: determination of trace metals in river water. As natural aquatic systems are much more complex than the synthetic systems, it was ensured that on-line preconcentration and separation of metal ions was not affected by matrix effects. This was done by spiking a river Arve (Geneva, Switzerland) water sample, which had been filtered through a 0.2-μm filter, with 10^{-7} *M* metal ions. Samples of 50 ml were immediately preconcentrated and metal ions separated as described earlier (Fig. 3C). A comparison with a standard solution containing 10^{-7} *M* of test metal ions (Fig. 2) showed that no matrix effect is observed except that Mn is masked by calcium ions.

Experiments were done to establish whether this method gives the total metal concentration or allows speciation studies to be made. In this instance the spiked river water sample was left to stand for 90 min with stirring and then on-line preconcentration followed by chromatographic separation was carried out. The peak height of all the metals except Ni decreased, the decrease being marked for Pb (*ca.* 29%; see Table IV), indicating the formation of inert complexes which cannot be analysed by this method.

In order to obtain an idea of the proportion of metal ions transported by the suspended matter of river water, experiments were repeated with unfiltered river water

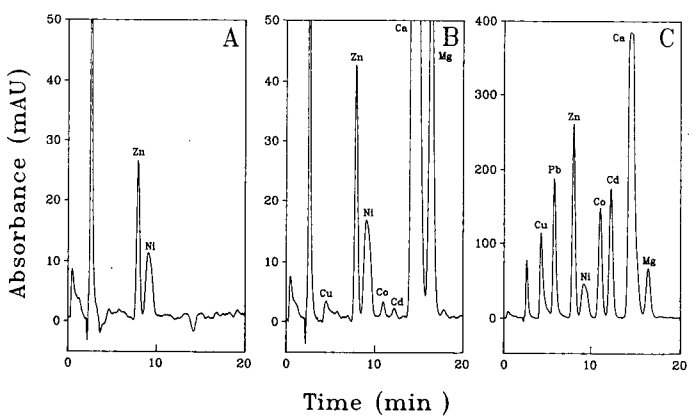

Fig. 3. Analysis of river Arve water by the on-line method. (A) Blank; (B) 50 ml of 0.2-μm filtered river water; (C) 50 ml of 0.2-μm filtered river water, spiked with 10^{-7} *M* of each of the test metal ions. Conditions as in Fig. 2.

TABLE IV

ANALYSIS OF RIVER ARVE WATER

Metal	Metal concentration found (M)[a]			
	Filtered	Filtered and 10^{-7} M spiked	Filtered, 10^{-7} M spiked and agitated	10^{-7} M spiked unfiltered
Cu	$2.4 \cdot 10^{-9}$	$9.0 \cdot 10^{-8}$ (−12)	$8.1 \cdot 10^{-8}$ (−21)	$4.1 \cdot 10^{-8}$ (−60)
Pb	–	$1.0 \cdot 10^{-7}$	$7.1 \cdot 10^{-8}$ (−29)	− (−100)
Zn	$7.8 \cdot 10^{-9}$	$1.2 \cdot 10^{-7}$ (+6.5)	$1.1 \cdot 10^{-7}$	$1.1 \cdot 10^{-8}$ (−89)
Ni	$2.2 \cdot 10^{-8}$	$1.2 \cdot 10^{-7}$	$1.3 \cdot 10^{-7}$	$1.0 \cdot 10^{-7}$ (−16)
Co	$1.7 \cdot 10^{-9}$	$1.0 \cdot 10^{-7}$	$9.8 \cdot 10^{-8}$ (−3.6)	$5.4 \cdot 10^{-8}$ (−37)
Cd	$1.2 \cdot 10^{-9}$	$1.0 \cdot 10^{-7}$	$9.6 \cdot 10^{-8}$ (−4.9)	$1,9 \cdot 10^{-8}$ (−81)

[a] Values in parentheses represent the percentage excess or loss in the measured metal ion concentration.

spiked with 10^{-7} M of each of the metal ions of interest. Solutions were stirred for 2 h, filtered through 0.2-μm filters, preconcentrated and metal ions separated chromatographically. A sharp decrease in the peak heights were observed (Table IV), indicating that most of the test ions present in water are adsorbed on the suspended particles of sediments.

Finally, the proposed method was tested to ascertain its applicability to the determination of trace metal ions in natural waters. River Arve water was filtered through a 0.2-μm filter and a 50-ml volume was preconcentrated and analysed by chromatography (Fig. 3b). The chromatogram of the blank is shown in Fig. 3a for comparison purposes. It can be seen that with the exception of Ni and Zn, all the other metal ions are present at close to the detection limits of the method. Trace amounts of Cu, Pb, Co and Cd could not be detected by the off-line method.

CONCLUSION

ED3A–silica can be used for the determination of trace amounts of free divalent metal ions and labile or moderately labile complexes. The on-line method allows the determination of Cu, Pb, Zn, Ni, Co and Cd at $3 \cdot 10^{-9}$ M concentration levels (20-ml sample volume) in natural water. The off-line method, on the other hand, can be used for the determination of Pb, Zn, Ni, Co and Cd at $3 \cdot 10^{-8}$ M levels (200-ml sample volumes). By using larger sample volumes, the sensitivity levels can be extended at the expense of the analysis time. These two methods are also applicable to other silicas such as 8-quinolinol–silica [6].

A search for chelating silica from which metal ions can be readily eluted is in progress. This will make possible the use of a single pump and consequently simplify the apparatus and manipulation. Finally, as trace metals in natural waters are present at levels close to the detection limits, there is a need for postcolumn reagents that are as universal as but more sensitive than PAR.

REFERENCES

1 D. Chambaz and W. Haerdi, *J. Chromatogr.*, 482 (1989) 335–342.
2 K. Ohshima, H. Watanabe and K. Haraguchi, *Anal. Sci.*, 2 (1986) 131–135.
3 D. Yan and G. Schwedt, *Fresenius' Z. Anal. Chem.*, 327 (1987) 503–508.
4 J. R. Jezorek and H. Freiser, *Anal. Chem.*, 51 (1979) 373–376.
5 G. J. Sevenich and J. S. Fritz, *Anal. Chem.*, 55 (1983) 12–16.
6 D. Chambaz, unpublished results.

Journal of Chromatography, 541 (1991) 453–458
Elsevier Science Publishers B.V., Amsterdam

CHROM. 22 963

Analysis of the soluble proteins in grape must by two-dimensional electrophoresis

RAMÓN GONZÁLEZ-LARA*
SUGELABOR S.A., Sicilia 36, 28038 Madrid (Spain)
and
LUIS MIGUEL GONZÁLEZ
Facultad de Ciencias Químicas, Universidad Complutense de Madrid, Madrid (Spain)
(First received November 20th, 1990; revised manuscript received October 22nd, 1990)

ABSTRACT

Soluble proteins were separated from grape musts by two-dimensional electrophoresis. Analysis of the electrophoretic patterns obtained yielded information about the structure and composition of these proteins. Structural and/or functional relationships between certain proteins, according to the fractions separated in the two dimensions, were also established.

INTRODUCTION

Previous interesting results from applying different one-dimensional electrophoretic techniques to the analysis of grape must proteins [1–3] encouraged us to study the possibility of applying a two-dimensional separation. Two-dimensional electrophoretic techniques have frequently been applied in the study of complex systems [4,5] and in the characterization of simple proteins [6]. The use of two concurrent separation criteria offers additional information, although the interpretation of the resulting electrophoretic patterns is often complex.

The protein compositions of many foods have been analysed using two-dimensional gel electrophoresis, including milk and dairy products [7,8], beer [9], cereals [10,11], grape must and wine [1,12].

The study of grape must and wine proteins is interesting from a genetic standpoint with a view to using the results in taxonomic classifications [2,13] and also as an indicator of viral infections, which cause changes in the patterns of the isozymes peroxidase and polyphenoloxidase [14].

In this work, two-dimensional gel electrophoresis was used to study the soluble protein fraction of different varieties of grape musts. The proteins were separated by native polyacrylamide gel electrophoresis (PAGE) in the first dimension, based on their relative electrophoretic mobilities (R_F). Sodium dodecyl sulphate (SDS)-PAGE in the second dimension was then used to achieve further separations according to the

0021-9673/91/$03.50

different molecular weights of the protein subunits originally constituting the proteins.

Separation based on the relative mobility (R_F) rather than on the isoelectric point (p*I*) conventionally employed in the first dimension was chosen because the former yields more interesting information for the genetic characterization of the variety of musts. A perfect classification of six different cultivars of Spanish origin was obtained by applying multivariate statistical methods (principal component and cluster analysis) to the R_F values for must proteins [2]. Information useful in genetic characterization according to variety has not been derived from isoelectric focusing (IEF), although the information so obtained has been useful in drawing other conclusions [3].

EXPERIMENTAL

Samples

Six samples of the following varieties were studied: Airen (2), Cabernet Sauvignon (2), Moscatel (1) and Monastrell (1). The corresponding musts were collected in various regions in Spain.

Materials

Analytical-reagent grade chemicals were used and deionized water was employed for all solutions. Polyethylene glycol (PEG) 20 000, glycerol, β-mercaptoethanol, SDS, silver nitrate and N,N,N′,N′-tetramethylenediamine (TEMED) were supplied by Merck (Darmstadt, Germany), acrylamide, N,N′-methylenebisacrylamide and tris(hydroxymethyl)aminomethane (Tris) from Sigma (St. Louis, MO, U.S.A.), Coomassie Brilliant Blue G-250 dye (Serva Blau) from Serva (Heidelberg, Germany) and absolute ethanol and acetic acid from Panreac (Barcelona, Spain).

Sample preparation

The musts were obtained by light pressing. They were centrifuged at 4000 *g* for 15 min and the proteins were separated by dialysis of 100 ml of must against tap water for 18 h using a Spectra POR3 membrane, which retains molecules with molecular weights greater than 3500 dalton. The samples so obtained were concentrated 40-fold by introducing the dialysis bags into 20% (w/v) PEG 20 000 solution.

Two-dimensional gel electrophoresis

Native PAGE was applied in the first dimension to separate the proteins according to their relative electrophoretic mobilities. The first dimension electrophoresis was performed according to the method of Hillier [15] employing polyacrylamide gels (70 × 80 × 0.75 mm) at 9.4% T and C = 4.25[a]. The buffer used in the gels was 0.0625 *M* Tris–HCl buffer (pH 8.8).

Vertical electrophoresis of the samples (10 μl of protein solution concentrated 40-fold, 10 μl of glycerol and 2 μl of bromophenol blue) was performed at I = 2.5 mA per plate for 2 h. The gels were stained with Coomassie Brilliant Blue G-250 as described by Blakesley and Boezi [16].

---

[a] C = g N,N′-methylenebisacrylamide (Bis)/%T; T = g acrylamide + g Bis per 100 ml of solution.

SDS-PAGE was applied in the second dimension to determine the molecular weight of the subunits of the proteins separated in the first dimension. Strips of the first-dimension gels were cut and equilibrated for 5 min in a 0.0625 *M* Tris–HCl buffer solution (pH 8.8) containing 10% (w/v) glycerol, 5% (v/v) β-mercaptoethanol and 2.5% (w/v) SDS.

It was determined experimentally that equilibration for 5 min sufficed for the denaturation reaction and formation of the SDS–protein complex.

The gel strips were placed on glass plates, following which the second-dimension gel slabs were prepared (Fig. 1). The plate size was 70 × 80 × 0.75 mm. The composition of the gels per 15 ml of solution was as follows: acrylamide–N,N′-methylenebisacrylamide solution (80:0.8), 7.5 ml; 3 *M* Tris–HCl buffer (pH 8.8), 1.9 ml; distilled water, 5.0 ml; ammonium peroxodisulphate, 0.15 ml; SDS, 0.15 ml; and N,N,N′,N′-tetramethylenediamine, 15.0 μl.

The polymerization of the gels provided perfect fusion between the gels, minimizing the possible distortion when the bands enter the new gel. Vertical electrophoresis in the second dimension was run at a constant current of 5 mA per plate for 3 h. The gels were stained with silver nitrate following a modified procedure of

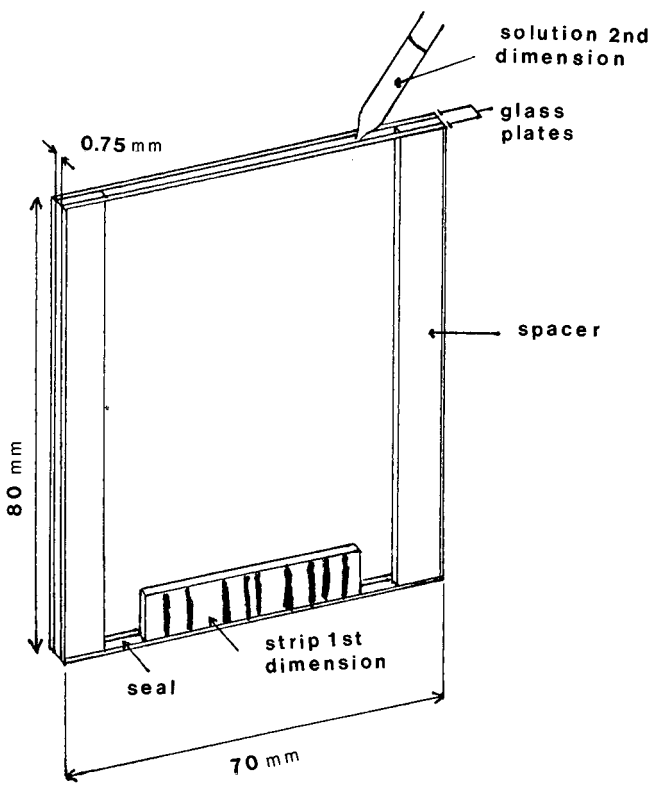

Fig. 1. Preparation of slab gels for the second dimension: the strips of the first-dimension gels are placed in the bottom of the glass plate sandwiches and the second dimension solution is poured from the top in order to avoid the formation of air bubbles; polymerization results in a perfect fusion between the two gels, facilitating migration of the bands.

Blum *et al.* [17], placing the gels in a fixer solution (30% ethanol–10% acetic acid) for 3 h in order to eliminate the excess of SDS, and thereby prevent the gels from blackening too rapidly under the effect of the silver nitrate.

RESULTS AND DISCUSSION

The gel formation technique employed enabled flat gels to be used in the first dimension, as opposed to the traditional use of tubes [4,8,19]. In addition, the two-dimensional electrophoresis with double separation on flat gels permitted the use of techniques other than IEF with high-resolution in the first dimension.

The use of flat gels yielded improved resolution and shortened separation, equilibration, and staining times. Further, polymerization of the second gel on top of a previously equilibrated strip allowed the proteins to pass from one gel to the other without distortion.

Table I gives the R_F data (calculated with respect to bromophenol blue) obtained for the different samples in the first dimension. Twelve bands were obtained.

Complex patterns resulted from the application of the second dimension (Fig. 2). Several of the formerly single bands split into various spots. In order to simplify the study, a general pattern of the separations obtained for the different samples was constructed with all the bands (Fig. 3); to interpret this pattern, the bands of the first dimension for each sample (Table I) are considered and the bands for the other samples disregarded, yielding the pattern for the variety concerned.

The analysis of this pattern showed that the most important fraction of protein subunits was that with a molecular weight of *ca.* 30 000 dalton [1,3,8].

Application of the two-dimensional technique showed that bands V, VI, VII, X and XI were those which contained the subunits with these molecular weights whereas bands III, IV and XII yielded fractions with lower molecular weights.

Some bands (I, II, III, IV and XII) did not split; hence these bands contained proteins with a simple structure, made up of one or more identical subunits.

Bands VIII and IX split into two spots, which may be different subunits of a single protein or of different proteins with the same mobilities that were not separated in the first dimension.

TABLE I

DISTRIBUTION OF THE BANDS SEPARATED IN THE FIRST DIMENSION BY APPLYING NATIVE PAGE TO THE SOLUBLE PROTEINS FROM GRAPE MUST OF DIFFERENT VARIETIES

+ Means present and − means absent in the sample.

Grape	Relative mobility (R_F)											
	0.09 I	0.13 II	0.30 III	0.35 IV	0.39 V	0.43 VI	0.46 VII	0.51 VIII	0.55 IX	0.63 X	0.70 XI	0.85 XII
Airen (2)	−	−	−	+	+	−	+	+	+	−	+	−
Cabernet Sauvignon (2)	+	+	+	+	+	+	+	+	−	−	−	−
Moscatel (1)	+	+	−	+	−	+	+	+	−	+	+	+
Monastrell (1)	+	+	+	+	+	−	+	+	+	+	−	+

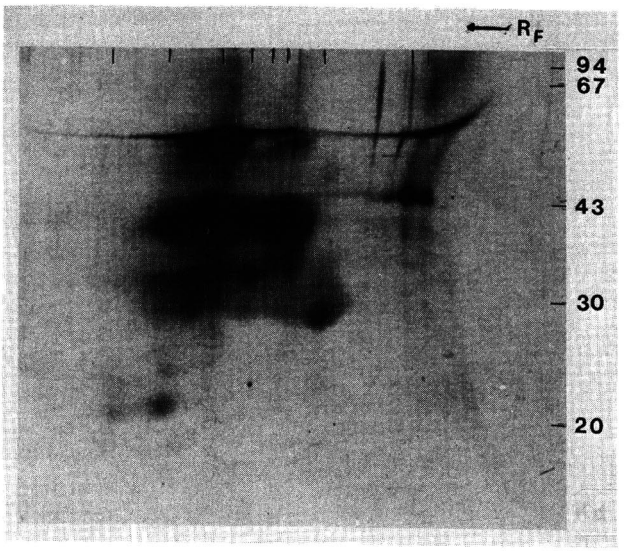

Fig. 2. Must proteins (Moscatel variety) separated by two-dimensional PAGE and stained with silver nitrate. Numbers on the ordinate represent molecular weight in kilodalton.

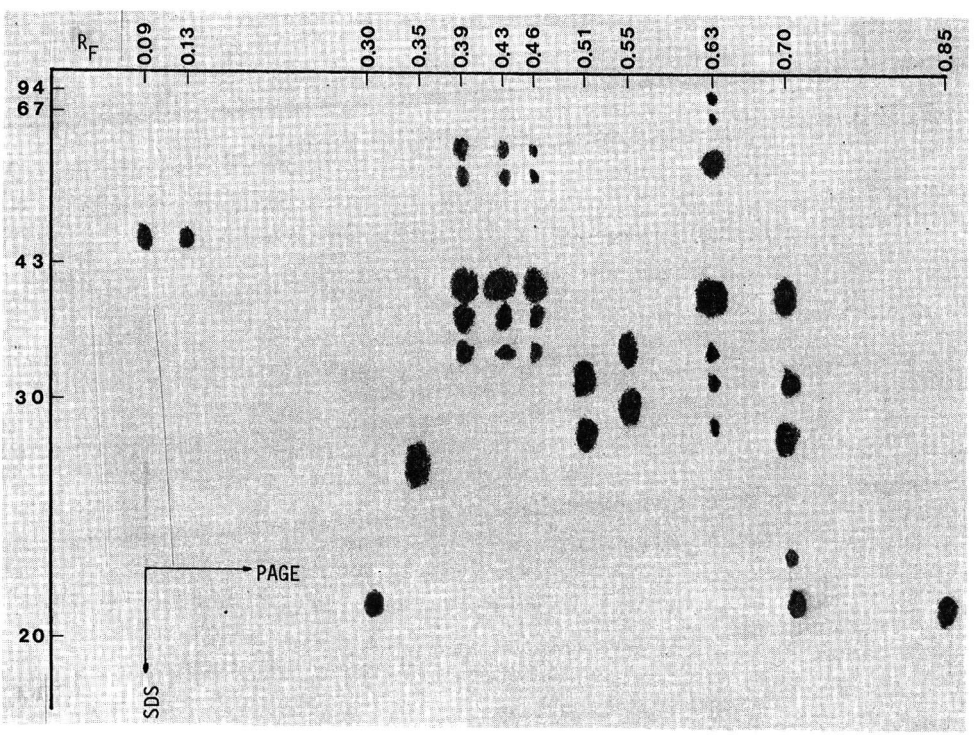

Fig. 3. A general banding pattern obtained by two-dimensional electrophoresis of must proteins of different varieties (see text for interpretation). Numbers on the ordinate represent molecular weight in kilodalton.

Bands V, VI, VII, X and XI split into several spots, indicative of a group of proteins that were incompletely resolved or a complex protein group of enzymic nature formed by unlike subunits with different molecular weights. Enzymic systems such as this have been described by Wolfe [20], Sciancalepore *et al.* [21] and others.

It is interesting that bands V, VI and VII split into the same subunits. This suggests proteins of a similar nature, which is very useful when trying to determine their characteristics and also results in time saving when planning future experiments (on enzymic activity, sequentially, etc.).

CONCLUSIONS

Two-dimensional electrophoresis with double separation on flat gels permits the use of techniques other than IEF in the first dimension without loss of resolution.

Application of native PAGE plus SDS-PAGE to soluble grape must proteins yielded important information about the characteristics of the composition of the subunits and protein structure, and also gave some indication of protein similarity as reflected by their electrophoretic behaviour. This information was in part speculative but nonetheless valuable.

In view of the difficulties attached to the study of proteins, especially because of their molecular complexity, the use of two-dimensional electrophoresis in the study of must proteins can be extremely useful in simplifying analyses and confirming results.

ACKNOWLEDGEMENT

The authors thank Miss M[a]. Carmen Sanchez for her help with the English translation.

REFERENCES

1 J. C. Hsu and D. A. Heatherbell, *Am. J. Enol. Vitic.*, 38 No. 1 (1987) 6.
2 R. González-Lara, I. Correa, C. Polo, P. J. Martin-Alvarez and M. Ramos, *Food Chem.*, 34 (1989) 103.
3 R. González-Lara, C. Polo, I. Correa and M. Ramos, *Rev. Agroquim. Tecnol. Aliment.*, 29 (1989) 332.
4 P. J. O'Farrell, *J. Biol. Chem.*, 250 (1975) 4007.
5 I. Russ, S. Günther and F. Pirchner, *Electrophoresis*, 10 (1989) 273.
6 C. Eckerskorn, P. Jungblut, W. Mewes, J. Klose and F. Lottspeich, *Electrophoresis*, 9 (1988) 830.
7 T. Marshall and K. Williams, *Electrophoresis*, 9 (1988) 143.
8 F. Goldfarb, M. S. Savadove and J. A. Inman, *Electrophoresis*, 10 (1989) 67.
9 J. C. Dale and T. C. Young, *J. Inst. Brew.*, 94 (1988) 28.
10 A. Görg, W. Postel, A. Domscheit and S. Günther, *Electrophoresis*, 9 (1988) 681.
11 P. R. Shewry, S. Parman and J. M. Field, *Electrophoresis*, 9 (1988) 727.
12 O. J. Lamikanra, *J. Food Sci.*, 52 (1987) 483.
13 F. Drawert and A. Görg, *Z. Lebensm.-Unters.-Forsch.*, 154 (1974) 328.
14 G. P. Martelli, A. Graniti and G. L. Ercolani, *Experientia*, 42 (1986) 933.
15 R. M. Hillier, *J. Dairy Res.*, 43 (1976) 259.
16 R. W. Blakesley and J. A. Boezi, *Anal. Biochem.*, 82 (1977) 580.
17 H. Blum, H. Beier and H. J. Gross, *Electrophoresis*, 8 (1987) 93.
18 N. L. Anderson and N. G. Anderson, *Anal. Biochem.*, 85 (1978) 341.
19 T. Marshall, *Electrophoresis*, 5 (1984) 245.
20 W. H. Wolfe, *Am. J. Enol. Vitic.*, 27 No. 2 (1976) 68.
21 V. Sciancalepore, V. Londone and F. S. Alviti, *Am. J. Enol. Vitic.*, 36, No. 2 (1985) 105.

Journal of Chromatography, 541 (1991) 459–463
Elsevier Science Publishers B.V., Amsterdam

CHROM. 23 030

Short Communication

Determination of dimethyl sulphate in air by gas chromatography with flame photometric detection

SHOZO FUKUI*, MAYUMI MORISHIMA, SHUNJIRO OGAWA and YUKIKO HANAZAKI
Kyoto Pharmaceutical University, Yamashina-ku, Kyoto 607 (Japan)
(First received September 10th, 1990; revised manuscript received December 12th, 1990)

ABSTRACT

A rapid and precise analytical method for the determination of dimethyl sulphate in air, involving sampling with a Florisil adsorption tube and determining of the amount of desorbed dimethyl sulphate by gas chromatography using a flame photometric detector for the detection of sulphur, is described. The application of a flame photometric detector for sulphur detection serves as a simple gas chromatographic procedure which does not require the derivatization of dimethyl sulphate and solvent flashing techniques. The coefficients of variation including the desorption of dimethyl sulphate from the Florisil tube are 2.70–3.65%. The detection limit for a sample size of 10 l and an injection volume of 1.0 μl is 0.03 ppm of dimethyl sulphate in air.

INTRODUCTION

Dimethyl sulphate is commonly used as a methylating agent for amines and phenols in industry and laboratories. It is an extremely hazardous compound but it has no warning characteristics; it can be absorbed through the skin and can give serious poisoning without immediately noticeable signs [1,2]. Evidence regarding mutagenic and possible carcinogenic effects of dimethyl sulphate has been presented [3]. The American Conference of Governmental Industrial Hygienists recommended a tentative change in the threshold limit value (TLV) of dimethyl sulphate from 1.0 to 0.01 ppm in 1973. Currently, a limit of 0.1 ppm has been adopted [4].

The determination of dimethyl sulphate in air requires a sensitive and simple method for the routine determination of ppb levels of dimethyl sulphate. An obstacle to the application of gas chromatography (GC) for this purpose is the difficulty of the complete separation of the peak of dimethyl sulphate from those of solvents. Gilland and Bright [5] described a procedure which involves desorption of dimethyl sulphate adsorbed on silica gel with acetone followed by analysis using a gas chromatograph equipped with a solvent venting valve to allow the escape of acetone. Sidhu [6] report-

0021-9673/91/$03.50

ed a similar method using distilled water as a solvent instead of acetone and a solvent flushing technique in GC.

Williams [7] reported a high-performance liquid chromatographic (HPLC) procedure involving sampling with a silica gel adsorption tube, reaction of the trapped dimethyl sulphate with sodium *p*-nitrophenoxide in acetone solution and determination of the resulting *p*-nitroanisole by HPLC.

In this paper we describe a procedure for the determination of dimethyl sulphate involving sampling with a Florisil adsorption tube and determination of the desorbed dimethyl sulphate by GC with flame photometric detection of sulphur, which is highly sensitive to dimethyl sulphate and poorly sensitive to non-sulphur-containing solvents. Hence no derivatization of dimethyl sulphate or venting of solvent is required.

EXPERIMENTAL

Materials

Analytical-reagent grade dimethyl sulphate was purchased from Nacalai Tesque Co. Florisil (60–80 mesh) for GC was purchased from Nacalai Tesque and was washed with 10% hydrochloric acid until the washings become colourless, washed with distilled water, then heated at 450°C for 5 h. Silica gel (60–80 mesh) for chromatography was purchased from Nacalai Tesque. Methyl isobutyl ketone (MIBK), methanol, butyl acetate and toluene were of analytical-reagent grade.

Instrumentation

GC was carried out with a Shimadzu Model GC-4CM gas chromatograph equipped with a Shimadzu Model FPD-1A flame photometric detector for sulphur and a flame ionization detector. The transmission of the optical filter attached to the flame photometric detector was maximum at 384 nm. The separation was performed on a 2 × 3 mm I.D. glass column packed with 3% silicone OV-330 on 80–100-mesh Chromosorb W AW DMSC.

Preparation of dimethyl sulphate standards

Dimethyl sulphate standards ranging in concentration from 1.0 to 20.0 μg/ml in MIBK were prepared.

Preparation of adsorption tube

A 50 mm × 3 mm I.D. glass tube was packed with 100 mg of Florisil or silica gel and both ends were stopped with glass-wool.

Sampling and analysis of dimethyl sulphate

A metered flow of air (0.5–1.0 l/min) was drawn over the adsorption tube. The adsorbent in the tube was placed in a glass vial containing 1.0 ml of solvent and the mixture was sonicated for 10 min. An aliquot of the solution was injected into the gas chromatograph. The concentration of dimethyl sulphate was determined with the aid of a calibration graph obtained as a log–log plot of peak height *versus* concentration of dimethyl sulphate. The analytical conditions were column temperature 100°C isothermal, inlet temperature 220°C, detector temperature 220°C, nitrogen carrier gas

flow-rate 60 ml/min, hydrogen pressure 0.5 kg/cm^2 and air pressure 0.6 kg/cm^2. The sensitivity and range were set at 100 MΩ and 8 × 0.01 V, respectively.

Adsorption efficiency study

Two adsorption tubes packed with Florisil or silica gel were connected in series and held horizontally. Volumes of 100 and 200 μl of 20.0 μg/ml dimethyl sulphate standard solution were dripped onto the inner wall of the front tube by using a microsyringe. Air was drawn over the tubes for 90 min at a flow-rate of 1.0 l/min at room temperature. Dimethyl sulphate in the standard solution was vaporized and carried into the adsorbent during the air drawing. The amounts of dimethyl sulphate adsorbed in the front and back tubes were determined as described above.

Studies on recovery efficiency and stability of desorbed dimethyl sulphate

The adsorption tubes were loaded with dimethyl sulphate as described above and the tubes were allowed to equilibrate for 1 h. The analyte was desorbed with solvents (MIBK, methanol, butyl acetate or toluene). Analysis of the desorbed sample was carried out in the usual manner immediately and after storage for 48 h at room temperature.

RESULTS AND DISCUSSION

The results obtained for dimethyl sulphate standards revealed that dimethyl sulphate can be determined by GC on silicone OV-330 using a flame photometric detector for sulphur. The calibration graph is linear with a slope of 1.72 on a log–log plot as shown in Fig. 1. The precision [relative standard deviation (R.S.D.)] with 4.0 ng of dimethyl sulphate was 2.04% ($n=10$). The R.S.D.s for five determinations at the 2.0 and 4.0 μg per tube levels were 3.65 and 2.70%, respectively.

A gas chromatogram obtained by the proposed procedure is shown in Fig. 2. A sharp peak with a retention time of 4.8 min which was completely separated from the solvent peak was obtained, whereas the peaks overlapped with flame ionization detection.

The recovery efficiencies of dimethyl sulphate from Florisil by desorption with solvents and after subsequent storage of the solution for 48 h in the dark are shown in Table I.

Polar solvents except methanol gave good desorption efficiencies of dimethyl sulphate from Florisil; the recovery of dimethyl sulphate dissolved in methanol decreased after storage for 48 h. MIBk gave the highest recovery and was chosen as the optimum solvent. The adsorption efficiencies of dimethyl sulphate on Florisil and silica gel are given in Table II.

Dimethyl sulphate in air was trapped quantitatively in the front tube packed with either silica gel or Florisil. Florisil gave a slightly better reproducibility. No adsorption of dimethyl sulphate on glass-wool used as the stopper in the adsorbent tube was observed.

The sample capacity for an adsorption tube was found to be at least 90 l of air. With a volume of 10 l (1 l/min flow-rate and 10-min sampling time), the detection limit of *ca.* 1.5 ng with an injection volume of 1.0 μl corresponds to 0.03 ppm. If neccesary, the detection limit could be improved by use of a larger injection volume or a larger sample size.

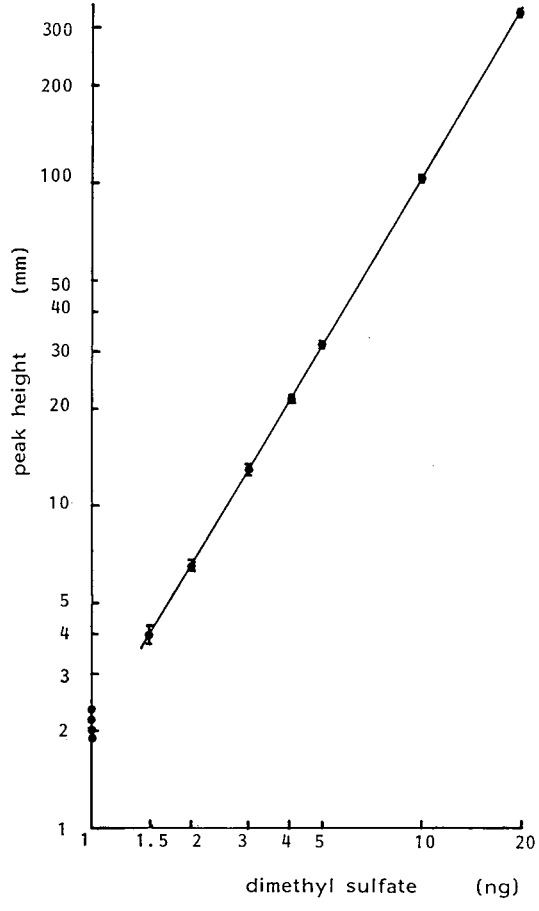

Fig. 1. Calibration graph. Analytical conditions: column temperature, 100°C isothermal: inlet and detector temperature, 220°C; carrier gas (nitrogen) flow-rate 60 ml/min; sensitivity, 100 MΩ; range, 8 × 0.01 V.

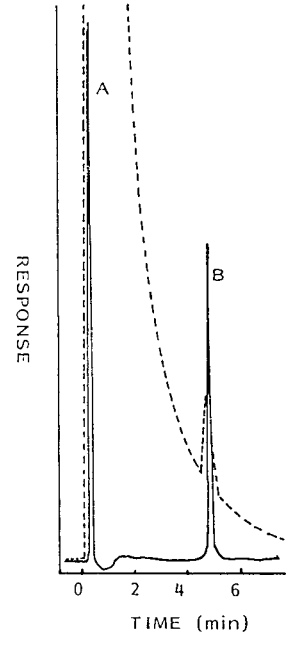

Fig. 2. Typical gas chromatogram of dimethyl sulphate. Solid line: flame photometric detection; 4 μl of a 2 μg/ml dimethyl sulphate standard solution were injected. Flame ionization detection; 10 μl of a 20 μg/ml dimethyl sulphate standard solution were injected. Analytical conditions as shown in Fig. 1. A = MIBK; B = dimethyl sulphate.

TABLE I

RESULTS OF RECOVERY EFFICIENCY STUDY

Dimethyl sulphate loaded: 2 μg.

Solvent	Storage time (h)	Recovery (%) ($n=3$)
Methanol	0	94.2–98.4
	48	30.2–36.5
Butyl	0	92.0–96.2
acetate	48	91.2–92.5
MIBK	0	95.0–101.2
	48	95.0–98.7
Toluene	0	60.8–75.3
	48	60.8–75.5

TABLE II

ADSORPTION EFFICIENCY OF DIMETHYL SULPHATE ON FLORISIL AND SILICA GEL

Dimethyl sulphate loaded (μg)	Adsorbent	Dimethyl sulphate recovered (μg)		
		Front tube[a]	Back tube	Glass-wool
2.0	Silica gel	1.86 ± 0.06	0	0
	Florisil	1.96 ± 0.04	0	0
4.0	Silica gel	3.91 ± 0.12	0	0
	FLorisil	3.94 ± 0.08	0	0

[a] Mean ± S.D. for five runs.

CONCLUSION

A simple, rapid and accurate method for the determination of dimethyl sulphate in air at levels well below the current TLV has been developed. The method involves adsorption of dimethyl sulphate on Florisil, desorption with MIBK and subsequent GC identification on silicone OV-330 with flame photometric detection of sulphur.

REFERENCES

1 A. Hammilton and H. L. Hardy, *Industrial Toxicology*, Publishing Sciences Group, Acton, MA, 3rd ed., 1974, p. 314.
2 N. I. Sax, *Dangerous Properties of Industrial Materials*, Reinhold, New York, 4th ed., 1975, p. 684.
3 D. B. Couch, N. L. Forbes and A. W. Hsie, *Mutat. Res.*, 57 (1978) 217.
4 American Conference of Governmental Industrial Hygienists, *TLVs for Chemical Substances in the Work Environment Adopted with Intended Change for 1986–1987*, ACGIH, Cincinnati, OH, 1986.
5 J. C. Gilland, Jr. and A. P. Bright, *Am. Ind. Hyg. Assoc. J.*, 41 (1980) 459.
6 K. S. Sidhu, *J. Chromatogr.*, 206 (1981) 381.
7 R. G. Williams, *J. Chromatogr.*, 245 (1982) 381.

Journal of Chromatography, 541 (1991) 464–468
Elsevier Science Publishers B.V., Amsterdam

CHROM. 23 001

Short Communication

Enantiomeric separation of racemic thiosulphinate esters by high-performance liquid chromatography

RUDOLF BAUER, WALTER BREU and HILDEBERT WAGNER*
Institute of Pharmaceutical Biology, Ludwig-Maximilians University, Karlstrasse 29, D-8000 Munich 2 (Germany)
and
WOLFGANG WEIGAND
Institute of Inorganic Chemistry, Ludwig-Maximilians University, Meiserstrasse 1, D-8000 Munich 2 (Germany)
(Received October 12th, 1990)

ABSTRACT

High-performance liquid chromatographic methods using chiral stationary phases were developed for the separation of racemic mixtures of biologically active alk(en)ylsulphinothioic acid alk(en)yl esters (syn. thiosulphinate esters, ts) from natural (*Allium cepa* L.) or synthetic origin. Aromatic substituted thiosulfinate esters could be baseline resolved using helical (+)-poly(triphenylmethyl methacrylate)-coated silica gel [Chiralpak OT (+)] as chiral stationary phase and methanol as eluent. A correlation between chromatographic resolution and the structures of the thiosulphinate esters could be established. A preparative separation of diphenyl-ts was achieved with cellulose triacetate (CTA) as the stationary phase. The elution sequence of diphenyl-ts enantiomers on the CTA column is reversed when compared to that on the Chiralpak OT (+).

INTRODUCTION

The use of high-performance liquid chromatography (HPLC) for the separation of racemates is increasing rapidly [1–4], especially owing to the often observed different biological activities of the enantiomers [5].

Chiral alk(en)ylsulphinothioic acid alk(en)yl esters (syn. thiosulphinate esters, ts) have recently been described as anti-asthmatic active constituents of onion juice [6] and as potent dual *in vitro* inhibitors of 5-lipoxygenase and cyclooxygenase [7]. They have also shown an inhibitory effect on platelet aggregation [8].

Thiosulphinate esters in Allium extracts (*Allium cepa* L. or *Allium sativum* L.) occur as racemic mixtures; stereoselective synthesis of enantiomerically pure thiosulphinate esters has succeeded in only a few cases [9]. Therefore, a suitable method for

0021-9673/91/$03.50

the separation of thiosulphinate ester racemates is needed in order to study the biological effects of pure enantiomers.

In this paper we describe HPLC methods for the separation of racemic thiosulphinate esters using helical (+)-poly(triphenylmethyl methacrylate)-coated silica gel and microcrystalline cellulose triacetate (CTA) as chiral stationary phases.

EXPERIMENTAL

Synthesis of thiosulphinate esters

Methyl phenyl disulphide and allyl phenyl disulphide were prepared by disproportionation of a symmetrical disulphide, dimethyl disulphide and diallyl disulphide, respectively, and thiophenol in alkaline solution [10]. These non-symmetrical disulphides and dimethyl, diallyl, diphenyl and ditolyl disulphide (obtained from Merck, Darmstadt, Germany) were oxidized by 3-chloroperbenzoic acid according to the method of Small *et al.* [11]. The corresponding thiosulphinate esters were purified by flash chromatography or medium-pressure LC [12].

HPLC procedure

The HPLC system consisted of a Hewlett-Packard (HP) 1090A liquid chromatograph, an HP 1040A photodiode-array detector, an HP 3392A integrator and an HP 7470 plotter. Aliphatic thiosulphinate esters were detected at 210 nm and aromatic esters at 280 nm. Polarimetric detection was performed using an ACS ChiraMonitor (Applied Chromatography Systems, Cheshire, U.K.) with a 20-μl flow cell of path length 20 mm using a 2-mW collimated near-IR laser diode (830 nm) as light source.

The HPLC separation of racemic thiosulphinate esters was performed with a (+)-poly(triphenylmethyl methacrylate)-coated silica gel column [Chiralpak OT (+), 250 mm × 4.6 mm I.D.; Daicel] with methanol as eluent at a flow-rate of 0.5 ml/min. For preparative enantiomeric separations we used a Hibar cellulose triacetate (10 μm) column (250 mm × 10 mm I.D.) (Merck) eluted with ethanol. All solvents were of HPLC grade (Promochem, Wesel, Germany). The separations were performed at 20 ± 1°C. The injection volume was 3 μl of a 0.1% solution of thiosulphinate esters in ethanol; when using the ACS ChiraMonitor the injection volume was 10–30 μl.

RESULTS AND DISCUSSION

Enantiomeric separation of racemic thiosulphinate derivatives **1**–**11** (Fig. 1) was performed by HPLC using helical (+)-poly(triphenylmethyl methacrylate)-coated silica gel as chiral stationary phase and methanol as eluent. Five racemic thiosulphinate esters, **1**–**3**, **5** and **6**, were baseline resolved ($R_s > 1$). Their chromatographic data are shown in Table I and Fig. 2.

Polarimetric detection showed that all dextrorotary enantiomers were eluted first from the column (Fig. 3). This type of detection was *ca.* 100 times less sensitive than UV detection.

The highest chromatographic resolution ($R_s = 3.75$) and separation factor ($\alpha = 1.31$) were found for the enantiomers of phenylsulphinothioic acid S-phenyl ester (diphenyl-ts) **1**. Introduction of a methoxy group in the 4-position (**4**) decreased the resolution drastically ($R_s = 1.01$). This negative effect could be compensated for by

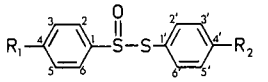

	R_1	R_2
1	H	H
2	CH_3	CH_3
3	H	OCH_3
4	OCH_3	H
5	OCH_3	OCH_3
6	Cl	H

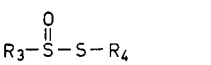

	R_3	R_4
7	C_6H_5	CH_3
8	CH_3	C_6H_5
9	C_3H_5	C_6H_5
10	C_3H_5	C_3H_5
11	CH_3	CH_3

Fig. 1. Structures of compounds.

a further *p*-methoxy substituent in the second aromatic ring, as in **5** (R_s = 1.52), while the chromatographic resolution of the enantiomers of phenylsulphinothioic acid S-*p*-methoxyphenyl ester **3** (R_s = 3.22, α = 1.27) was similar to that of diphenyl-ts **1**. Good resolutions were also observed for ditolyl-ts **2** (R_s = 1.52) and *p*-chlorophenylsulphinothioic acid S-phenyl ester **6** (R_s = 2.05). Therefore, the resolution of diphenyl-ts enantiomers seems to be negatively influenced especially by substituents in the *para* position to the sulphoxide, whereas substituents in the 4'-position have less effect.

The enantiomers of dimethyl-ts **11** and dially-ts **10**, which also occur in extracts of onion (*Allium cepa* L.) and garlic (*Allium sativum* L.), respectively, could not be resolved by the described separation system. Also, synthetic enantiomers of non-symmetrically substituted thiosulphinate esters, such as methylsulphinothioic acid S-phenyl ester (methyl phenyl-ts) **8** and allylsulphinothioic acid S-phenyl ester (allyl phenyl-ts) **9**, both containing an aliphatic sulphinothioic acid moiety, but an aromatic ester moiety, were not resolved. However, optical resolution was achieved for the enantiomers of phenylsulphinothioic acid S-methyl ester (phenyl methyl-ts) **7**. These results clearly showed that an aromatic sulphinothioic acid moiety is necessary for the

TABLE I

CHROMATOGRAPHIC DATA FOR RACEMIC THIOSULPHINATES

Stationary phase: (+)-poly(triphenylmethyl methacrylate)-coated silica gel. Mobile phase: methanol (0.5 ml/min). t_R = Retention time; R_s = resolution factor = 1.18 × (distance between the peaks of the enantiomers)/(sum of band widths of the two peaks at the peak half-height); k' = capacity factor = (retained volume of enantiomer − void volume of column)/void volume of column; α = separation factor = $k'(-)/k'(+)$.

ts	$t_R(+)$ (min)	$k'(+)$	$t_R(-)$ (min)	$k'(-)$	α	R_s
1	13.19	2.56	16.11	3.35	1.31	3.75
2	11.06	1.99	12.22	2.30	1.16	1.52
3	12.32	2.33	14.66	2.96	1.27	3.22
4	12.56	2.39	13.51	2.65	1.11	1.01
5	11.97	2.24	13.16	2.56	1.14	1.52
6	12.26	2.31	14.84	3.01	1.30	2.05

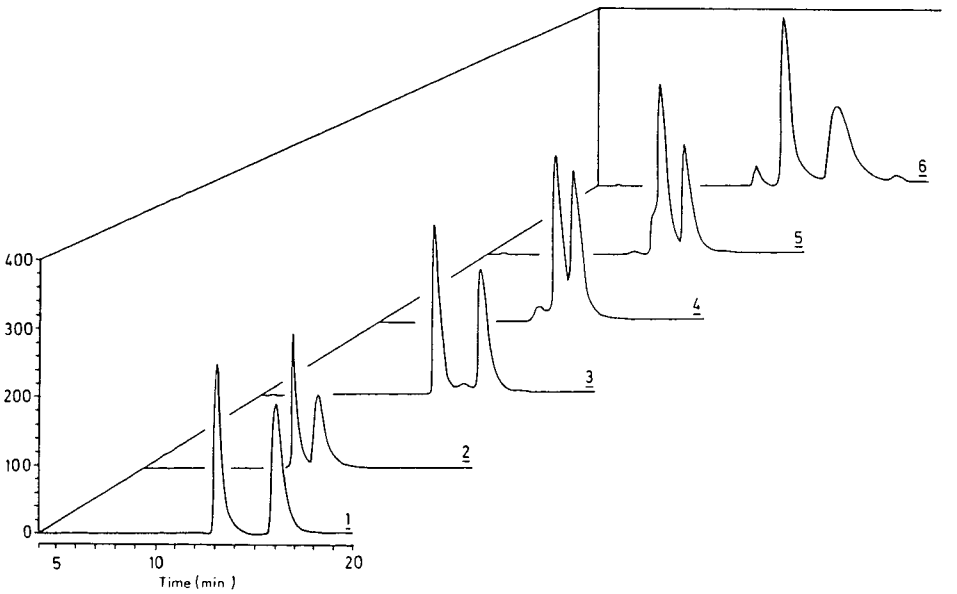

Fig. 2. HPLC separations of ts **1–6** on (+)-poly(triphenylmethyl methacrylate)-coated silica gel. Mobile phase: methanol at a flow-rate of 0.5 ml/min. Photometric detection at 280 nm.

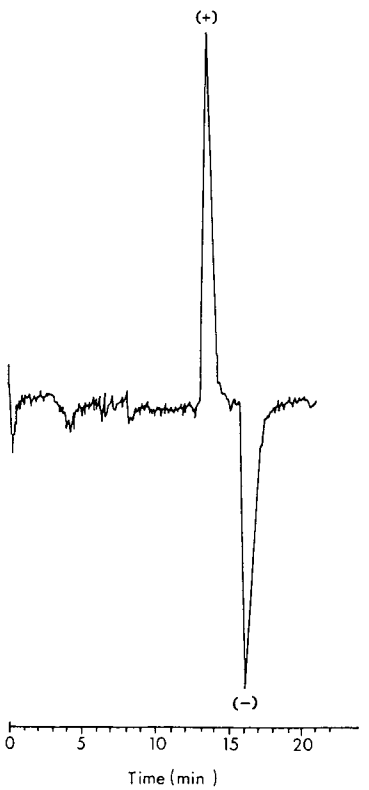

Fig. 3. HPLC separation of diphenyl-ts on (+)-poly(triphenylmethyl methacrylate)-coated silica gel. Mobile phase: methanol at a flow-rate of 0.5 ml/min; ACS ChiraMonitor.

separability of thiosulphinate esters by helical (+)-poly(triphenylmethyl methacrylate)-coated silica gel. This again supports the assumption that an interaction between the aromatic part of the molecules and the pendant trityl groups of the polymeric chain is an important factor for enantiomeric separations on this type of stationary phase [13].

For the preparative separation of diphenyl-ts **1** we used cellulose triacetate (CTA) as stationary phase. Of various alcohols, *e.g.*, methanol (R_s = 0.64) and isopropanol (R_s = 0.59), ethanol (R_s = 1.11) was found to be the best mobile phase. By using this method we could isolate the enantiomers of diphenylthiosulphinate ester for the first time.

Testing the purity of the isolates by HPLC using helical (+)-poly(triphenylmethyl methacrylate)-coated silica gel we observed that the isolated peaks were enantiomerically pure. It also became obvious that the elution sequence of diphenyl-ts enantiomers from the CTA column was reversed compared with the separation using helical (+)-poly(triphenylmethyl methacrylate)-coated silica gel.

Before starting investigations on the biological activities, the stability of isolated diphenyl-ts enantiomers must be examined. A possible racemization of the enantiomers during biological assay methods can now be monitored by the established HPLC method using helical poly(triphenylmethyl methacrylate)-coated silica gel as chiral stationary phase and methanol as eluent.

ACKNOWLEDGEMENTS

We are indebted to Zinsser Analytic (Frankfurt/M.) for the opportunity of testing the ACS ChiraMonitor, Boehringer (Mannheim) for the synthesis of diphenylthiosulphinate derivatives and Miss Birgit Hauser for excellent technical assistance.

REFERENCES

1 V. R. Meyer, *Pharm. Unserer Zeit*, 18 (1989) 140.
2 C. Pettersson, *Eur. Chromatogr. News*, 2 (1988) 16.
3 G. Blaschke, *J. Liq. Chromatogr.*, 9 (1986) 341.
4 Y. Okamoto, M. Kawashima and K. Hatada, *J. Chromatogr.*, 363 (1986) 173.
5 I. W. Wainer and D. Drayer, *Drug Stereochemistry*, Marcel Dekker, New York and Basle, 1988.
6 W. Dorsch, H. Wagner, Th. Bayer, B. Fessler, G. Hein, J. Ring, P. Scheftner, W. Sieber, Th. Strasser and E. Weiss, *Biochem. Pharmacol.*, 37 (1988) 4479.
7 H. Wagner, W. Dorsch, Th. Bayer, W. Breu and F. Willer, *Prostaglandins Leukotrienes Essential Fatty Acids*, 39 (1990) 59.
8 K. J. Baghurst, M. J. Raj and A. S. Truswell, *Lancet*, i (1977) 101.
9 J. Drabowicz and M. Mikolajczyk, *Tetrahedron Lett.*, 26 (1985) 5703.
10 D. T. McAllan, T. V. Cullum, R. A. Dean and F. A. Fidler, *J. Am. Chem. Soc.*, 73 (1951) 3627.
11 V. D. Small, J. H. Bailey and C. J. Cavallito, *J. Am. Chem. Soc.*, 69 (1947) 1710.
12 Th. Bayer, *Ph.D. Thesis*, University of Munich, Munich, 1988.
13 S. Antus, R. Bauer, A. Gottsegen and H. Wagner, *J. Chromatogr.*, 508 (1990) 212.

Journal of Chromatography, 541 (1991) 469–473
Elsevier Science Publishers B.V., Amsterdam

CHROM. 23 049

Short Communication

Reversed-phase high-performance liquid chromatography of ketoxime analogues of β-adrenergic blockers

LASZLO PROKAI, ANTAL SIMAY[a] and NICHOLAS BODOR*

Center for Drug Discovery, College of Pharmacy, University of Florida, Box J-497, J. H. Miller Health Center, Gainesville, FL 32610 (U.S.A.)

(First received March 1st, 1990; revised manuscript received December 12th, 1990)

ABSTRACT

Reversed-phase high-performance liquid chromatography of aryloxyalkylaminoketone-oximes is optimized by implementing bonded-phase (C_8 and C_{18}) column packings deactivated for basic compounds, and competing base as mobile phase additive. The retention of *Z* isomers is prolonged because of intramolecular hydrogen bonding. The selectivity coefficient for the separation of *E* and *Z* compounds is influenced by internal constraints and intramolecular interaction of polar functional groups.

INTRODUCTION

Several compounds with hydroxyimino functional group show biological activity. A number of ketoximes (Fig. 1) to be used as potential antiglaucoma agents have recently been synthesized [1,2] based on the structure of some known β-adrenergic blockers. Most oximes are, however, known to exist in alternative *Z* (*syn*) or *E* (*anti*) configuration, and there may be differences in the activity of the stereoisomers [3]. The two isomers may even tend to form a equilibrium mixture, either by metabolism or by acid-catalyzed isomerization, in biological media [4]. A proper analytical method should, therefore, be able to distinguish the oxime isomers, and also to determine the composition of isomeric mixtures.

Based on retention data of selected model compounds [5], which have revealed the dependence of capacity factors (k') on the orientation of the oxime hydroxyl group, reversed-phase high-performance liquid chromatography (RP-HPLC) appears to be a suitable technique. However, predictions on compounds which have not been

[a] Present address: Institute for Drug Research, Szabadságharcosok útja 47-49, H-1045 Budapest, Hungary.

0021-9673/91/$03.50

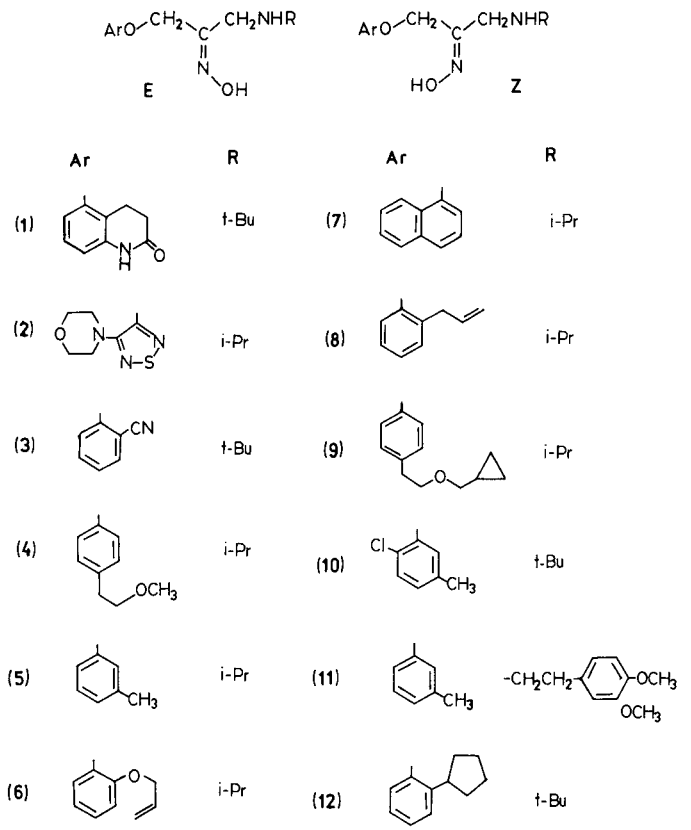

Fig. 1. Structure of the oximes. t-Bu = *tert.*-Butyl; i-Pr = isopropyl.

analyzed are rather difficult due to the existence of enumerable structural parameters that may affect the retention times. The elution order of *Z* and *E* isomers of oximes has not shown uniformity either [5], and there is no apparent explanation to this phenomenon. The evaluation of the retention behavior of aryloxyalkylamino-ketoximes involved in this study may also reveal the interaction of selected functional groups that can influence the separation of oximes in RP-HPLC.

EXPERIMENTAL

Chemicals and solvents

The preparation of oximes has been described previously [1,2]. HPLC-grade monobasic potassium phosphate, phosphoric acid (85%, w/w, aqueous solution), triethylamine and acetonitrile were supplied by Fisher Scientific (Fair Lawn, NJ, U.S.A.). Water was purified by reverse osmosis and ion exchange. Additional chemicals used throughout the studies were commercially available, analytical reagent-grade products.

High-performance liquid chromatography

The HPLC system consisted of Spectra-Physics (San Jose, CA, U.S.A.) SP 8810 precision isocratic pump, SP 8450 variable-wavelength UV–VIS detector and SP4290 computing integrator. Injections were made by a Rheodyne 7125 valve (Cotati, CA, U.S.A.) equipped with a 10-μl sample loop. A Spectroflow 430 (Kratos Analytical, Manchester, U.K.) low-pressure solvent mixer and gradient former was used to generate mobile phase compositions with variable organic modifier content.

We compared 5 cm × 4.6 mm I.D. Supelcosil LC-8-DB (octyldimethylsilyl bonded phase) and LC-18-DB (octadecyldimethylsilyl bonded phase) analytical columns with 5 μm particle-size packings in this study. The guard columns were 2-cm cartridges filled with 5 μm packing that contained the bonded phase identical to that of the analytical column. All columns and accessories were supplied by Supelco (Bellofonte, PA, U.S.A.).

The mobile phases applied for the separations were mixed from two components: 0.02 *M* monobasic phosphate buffer solution (pH was set to 3.0 with phoshoric acid) which also contained 100 μl/l triethylamine (final pH 3.15), and acetonitrile as organic modifier. The flow-rate was 1.0 or 1.5 ml/min.

RESULTS AND DISCUSSION

For selection of the analytical HPLC columns and appropriate separation conditions, one should consider certain inherent properties of the aryloxyalkylaminoketone-oximes (**1–12**) and their implications to reversed-phase chromatography. Upon attempting analyses on conventional bonded-phase (C_8 and C_{18}) columns, poor peak shapes (tailing) resulting in mostly inadequate, if any, separation of the oxime isomers were obtained [1]. This was due to the presence of the basic alkylamino functional groups, thus specifically deactivated (end-capped) column packings were applied. Additionally, a competing base (triethylamine) as mobile phase constituent was found to improve the peak shapes, although to a much lesser extent than the column deactivation. By taking these measures, even short (5 cm long, 5 μm packing) columns have provided efficient chromatographic performance. A value of 93000 theoretical plates/m has been obtained for the earlier eluting peak ($k' = 3.30$) of **7** under optimal conditions [6] (30% acetonitrile in the mobile phase), with resolution (R_s) reaching 2.33 and providing baseline separation of the oxime isomers.

Configurational analysis of isomeric aryloxyalkylaminoketone-oximes by ^1H and ^{13}C NMR spectrometry has been reported recently [2]. By using samples representing stereoisomerically pure samples (or significantly enriched in one of the oxime stereoisomers) characterized by the above techniques, the present studies have shown that the *E* isomers elute first in reversed-phase liquid chromatography. Intramolecular hydrogen-bonding between hydroximino group and the ethereal oxygen appears to provide an explanation to the prolonged retention of the *Z* isomer. This interaction probably represents a stronger bonding than the possible oxime-amine intramolecular association in the *E* isomer. The *Z* form also represents the thermodynamically more stable configuration of the compound [2].

Table I lists retention data and selectivity coefficients for C_8 and C_{18} bonded phases under identical chromatographic conditions. (Compound **12** represents an exception, since the elution of the isomers was not possible within reasonable time.)

TABLE I

CAPACITY FACTOR (k') AND SELECTIVITY COEFFICIENT (α) OF ARYLOXYALKYLAMINO-KETONE-OXIME ISOMERS

$k' = (t_R - t_0)/t_0$, where t_R = retention time and t_0 (determined by injection of sodium nitrate solution [7]) = dead time; $\alpha = k'(Z)/k'(E)$. Mobile phase: acetonitrile–aqueous buffer (20:80, v/v). See Experimental section for details.

Oxime	Octyldimethylsilyl (C_8) bonded phase			Octadecyldimethylsilyl (C_{18}) bonded phase		
	$k'(E)$	$k'(Z)$	α	$k'(E)$	$k'(Z)$	α
1	0.68	0.83	1.21	0.68	0.82	1.21
2	1.96	2.70	1.38	2.07	3.01	1.45
3	2.62	3.94	1.50	2.80	4.18	1.49
4	3.42	4.70	1.37	3.67	5.20	1.42
5	7.27	10.52	1.45	7.53	11.55	1.53
6	9.58	15.09	1.58	10.52	16.46	1.56
7	21.20	27.64	1.30	26.14	34.77	1.33
8	22.90	31.28	1.37	26.64	37.34	1.35
9	21.54	31.58	1.47	25.88	40.08	1.55
10	25.12	33.80	1.35	32.46	45.12	1.39
11	33.24	41.40	1.24	43.50	53.72	1.24
12[a]	(4.23)	(5.06)	(1.20)	(6.14)	(7.47)	(1.22)

[a] Eluted with acetonitrile–aqueous buffer (40:60, v/v).

This approach has allowed more relevant comparison of the retention characteristics than the one that applies different amounts of organic modifier to reach conditions preferred for real analyses [2]. Nevertheless, the order of lipophilicity from chromatographic data conforms to that predicted for the parent β-blockers [8] (aryloxyalkylaminoalcohols). The selectivity coefficient (α) varies only slightly, if at all, with the stationary phase for a given compound, but it is probably influenced by many structural features. Although one may observe a tendency that less polar aryloxyalkylaminoketone-oximes show less isomer separation, internal constraints [5] (steric factors) and intramolecular interaction (possible hydrogen bonding, dipole–dipole interactions, etc.) of polar functional groups with the oxime hydroxyl group should be responsible to the magnitude of α. Although the number of compounds involved in the study is limited, certain conclusions may be made. Bulky, non-polar substituents at *ortho* position of the aromatic moiety (**1**, **7**, **12**) will possibly decrease α. On the other hand, the separation of the oxime isomers is increased by the presence of polar functional groups (**3**, **6**) able to attract the oxime hydroxyl.

In conclusion, the retention behavior of aryloxyalkylaminoketone-oximes can be interpreted in terms of several intramolecular interactions, most notably hydrogen bonding between the functional groups, and steric effects. These interactions may affect the elution order of the E and Z isomers, and the selectivity coefficient. Continuing studies on a variety of other oximes are to reveal further structure–chromatographic retention relationships.

ACKNOWLEDGEMENTS

Partial financial support from Xenon Vision (Alachua, FL, U.S.A.) is gratefully acknowledged.

REFERENCES

1 N. Bodor, A. Elkoussi, M. Kano and T. Nakamura, *J. Med. Chem.*, 31 (1988) 100.
2 A. Simay, L. Prokai and N. Bodor, *Tetrahedron*, 45 (1989) 4102.
3 R. Pearlman and N. Bodor, in E. C. Olson and R. E. Christoffersen (Editors), *Computer-Assisted Drug Design* (*ACS Symposium Series*, No. 112), American Chemical Society, Washington, DC, 1979, p. 489.
4 R. J. Bopp and D. J. Miner, *J. Pharm. Sci.*, 71 (1982) 1402.
5 J. W. Bovenkamp, B. V. Lacroix and P. F. Henshaw, *J. Chromatogr.*, 301 (1984) 492.
6 L. R. Snyder, *J. Chromatogr. Sci.*, 7 (1969) 352.
7 M. J. M. Wells and C. R. Clark, *Anal. Chem.*, 53 (1981) 1341.
8 N. Bodor, unpublished results.

Journal of Chromatography, 541 (1991) 474–479
Elsevier Science Publishers B.V., Amsterdam

CHROM. 23 050

Short Communication

Reversed-phase high-performance liquid chromatography–thermospray mass spectrometry of alprenolol and its ketoxime analogues

LASZLO PROKAI and NICHOLAS BODOR*

Center for Drug Discovery, College of Pharmacy, University of Florida, Box J-497, J. H. Miller Health Center, Gainesville, FL 32610 (U.S.A.)

(First received March 1st, 1990; revised manuscript received December 12th, 1990)

ABSTRACT

Thermospray mass spectrometric detection is applied for alprenolol and its isomeric (*E* and *Z*) ketoxime analogues separated by reversed-phase high-performance liquid chromatography. The thermospray process results in high-intensity $[M+H]^+$ ion formation. This method of detection provides high level of molecular specificity, and offers advantages for the identification of the stereoisomeric oximes due to the unique fragmentation pattern of the spectra.

INTRODUCTION

The general analytical aspects of drug delivery have been discussed recently [1]. There seems to be an increased demand to the sensitive and selective determination of low levels of compounds in the related studies. The ketoxime analogue (a mixture of *E* and *Z* isomers) of alprenolol, a potent β-adrenergic antagonist, has been designed to deliver the drug into the site of the action (*i.e.*, to the eye) via sequential bioactivation [2]. This new concept holds the promise for an improved glaucoma treatment. Monitoring the expected biotransformation in selected compartments of the eye usually requires the determination of very small amounts of compounds with high selectivity. Gas and liquid chromatography have been successfully applied to the analysis of β-blockers [3], although their routine detection methods often lack selectivity.

Retaining the apparent advantages of a chromatographic technique, a combination with mass spectrometry (MS) has been emerged as a promising way of providing additional selectivity to the detection of the separated compounds, and the sensitivity may als be increased. Gas chromatography–MS has been applied for selected β-blockers [4–7], and for some ketoxime analogues [8]. Derivatization is, however,

0021-9673/91/$03.50

necessary to permit gas chromatographic analysis by increasing the volatility and thermal stability of the compounds. This may be accompanied by unwanted side reactions for β-blockers [7], or preclude the separation of oxime isomers [8]. Labetalol has been analysed by coupling high-performance liquid chromatography (HPLC) with thermospray (TSP) MS [9], which eliminates the need for derivatization. In addition, the isomeric ketoxime analogues of several β-blockers have shown excellent separation using reversed-phase HPLC [10]. In the present paper, the development of an on-line reversed-phase HPLC–TSP-MS method will be reported and evaluated for alprenolol and its ketoxime analogues.

EXPERIMENTAL

Chemicals and solvents

The preparation of oximes has been described previously [11,12]. Alprenolol tartarate was obtained from Aldrich (Milwaukee, WI, U.S.A.). HPLC-grade ammonium acetate, triethylamine and acetonitrile were supplied by Fisher Scientific (Fair Lawn, NJ, U.S.A.). Water was purified by reverse osmosis and ion exchange.

High-performance liquid chromatography and mass spectrometry

The mass spectrometer was an MS80RFA (Kratos Analytical, Manchester, U.K.) double focusing instrument, operated at 4 kV accelerating voltage and at a nominal resolution of 1000. The experiments were performed with the manufacturer's thermospray option. The HPLC apparatus consisted of a Spectroflow 400 solvent delivery system, a Spectroflow 430 gradient former and a Spectroflow 480 injector module equipped with a Rheodyne 7125 valve and a 20-μl sample loop. A 5 cm × 4.6 mm I.D. Supelcosil LC-8-DB column with a Supelguard cartridge (Supelco, Bellefonte, PA, U.S.A.) was used for separation. The aqueous buffer solution applied as mobile phase component contained 0.1 *M* ammonium acetate and 0.02 *M* acetic acid, as well as 0.02% (v/v) triethyamine (pH 4.54). At 1.0 ml/min flow-rate and with 25% acetonitrile in the mobile phase, optimal thermospray conditions were achieved by setting the probe, vaporizer, source and jet temperatures to 135, 165, 175 and 220°C, respectively. These parameters were readjusted upon changing mobile phase compositions; higher percentages of organic modifier required proportionally lower temperature settings, and *vice versa* [13].

The mass spectrometer was scanned repetitively (at 4.0 kV accelerating voltage) from *m/z* 800 to 100 using a scan speed of 3 s/mass decade, under the control of the DS90 data system. The nominal mass resolution was set to 1000. Mass scale calibration was established using the positive ions of polyethylene oxide oligomers (PEG 600) produced under TSP conditions; the calibrated mass range extended from *m/z* 167 to 653.

Desorption chemical ionization (CI) mass spectra were obtained with the same instrument. The samples (*ca.* 0.1 μg) were supplied onto the platinum-iridium coil of the probe using the thermospray solvent (25% acetonitrile in ammonium acetate buffer, as described above) which was then gently evaporated with a heat-gun. The probe was inserted into the electron impact (EI)/CI source of the mass spectrometer. The following conditions were applied: reagent gas, ammonia; electron energy, 40 eV; emission current, 500 μA; source temperature 220°C; source pressure, *ca.* 10^{-5} Torr

(measured with the source vacuum gauge). Mass spectra were recorded at 4.0 kV accelerating potential by scanning the mass range of *m/z* 700 to 100 (calibrated with the positive ions of perfluorokerosene obtained under EI conditions). The instrument was operated at a scan rate of 1 s/decade, while the direct exposure probe was inserted into the heated ion source. The CI spectrum recorded at the apex of the total ion current (TIC) chromatogram was evaluated.

RESULTS AND DISCUSSION

Adapting an existing HPLC method [10] to TSP-MS detection requires the substitution of the phosphate buffer in the mobile phase with a suitable one containing volatile salts. Ammonium acetate is preferred for its high ionization efficiency [13]. We have applied its plain 0.1 *M* solution, but it has been realized that the mobile phase tolerates additive used for setting the pH (acetic acid) and that for improving the chromatographic separation (triethylamine) without noticeably influencing the process of TSP ionization. This is not surprising, since it is generally thought that ions

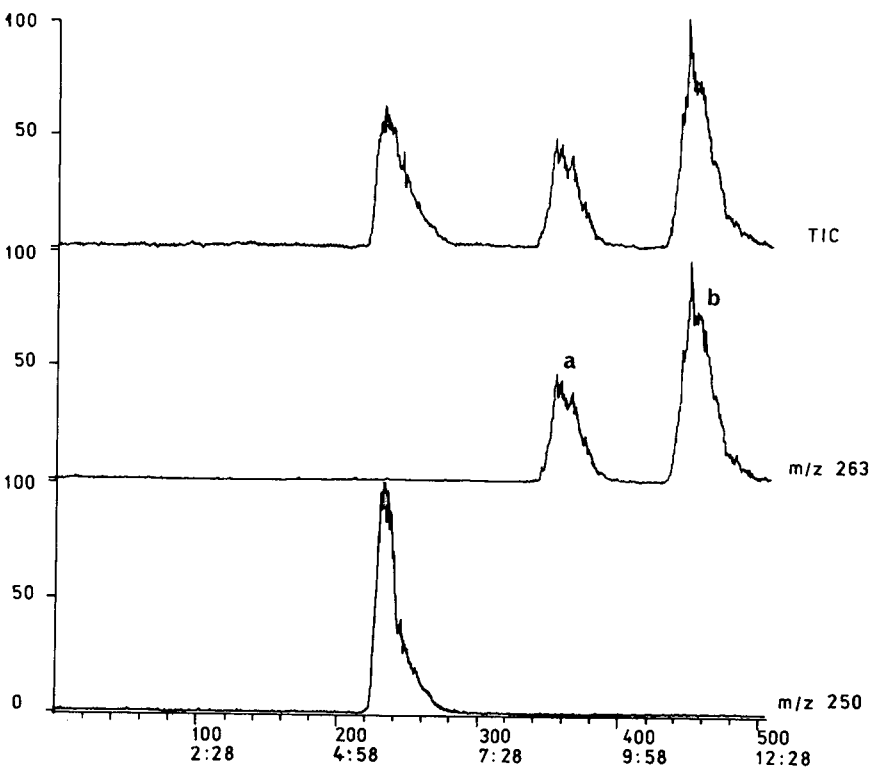

Fig. 1. Reconstructed total-ion current (TIC) and selected-ion chromatograms of 1-(isopropylamino)-3-(2-allylphenoxy)-2-propanol (alprenolol, $[M + H]^+$ at *m/z* 250) and 1-(isopropylamino)-3-(2-allylphenoxy)-2-propanone oxime (alprenolone oxime, $[M + H]^+$ at *m/z* 263) obtained by HPLC–TSP-MS. Column: Supelcosil LC-8-DB (5 cm × 4.6 mm I.D.), mobile phase: acetonitrile–0.1 *M* ammonium acetate buffer (25:75, v/v) (see Experimental), 1.0 ml/min flow-rate. Ordinate: intensity (%); abscissa: top scale, scan No., bottom scale, time in min:s.

leaving the TSP source obey the rules of gas-phase thermochemistry [14]. Triethylamine, a strong base, has been ineffective for thermospray ionization [13] (lack of protonated molecular ion formation), while acetic acid (applied in molar ratio representing only one fifth of the amount of ammonium acetate) merely affects dissociation equilibria in the solution. Thus, both are compatible with the TSP solvent.

The TSP ionization of the title compounds results in high-intensity $[M + H]^+$ ion formation. In fact, this is the only ion detectable for alprenolol. Loss of water from the aryloxyalkylaminoalcohol due to thermolysis in the ion source, as described for labetalol [9], is absent. Fig. 1 shows selected-ion chromatograms for alprenolone oxime isomers ($[M + H]^+$ at m/z 263) and alprenolol ($[M + H]^+$ at m/z 250), together with the reconstructed TIC chromatogram. In addition, the TSP mass spectra of the oxime isomers feature fragmentation related to the steric position of the oxime hydroxyl, as exemplified in Fig. 2. The loss of the alkyl group from the nitrogen (m/z 221) is noteworthy. This process is very pronounced when the oxime hydroxyl is oriented toward the aryloxy group (Z isomer). On the other hand, the cleavage of the

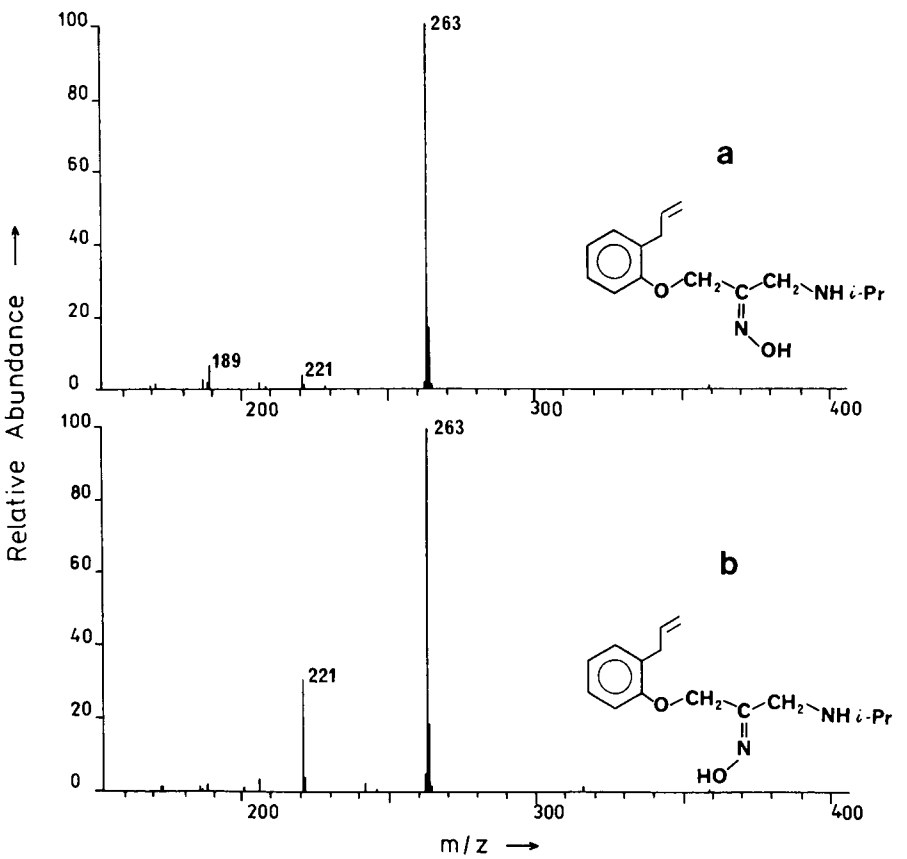

Fig. 2. Thermospray mass spectra of alprenolone oxime isomers. (a) E isomer, (b) Z isomer. i-Pr = Isopropyl.

carbon–carbon bond at the alkylamino side of the ketoxime resulting in *m/z* 189 appears to be characteristic exclusively to the *E* isomer.

The possible reasons for fragmentation in TSP is usually thermolysis and collision-induced dissociation. It is difficult to speculate on the origin of the above process, since experiments involving variation of the thermospray conditions (temperature settings, buffer concentrations, etc.) were inconclusive. The ionization processes operating under thermospray conditions are believed to be very similar to those prevailing during chemical ionization [15]. Gas-phase ionization, by NH_4^+ from the ammonium acetate buffer, appears to be predominant in TSP. We have, therefore, compared desorption CI mass spectra (with ammonia reagent gas) to those obtained by TSP ionization. We attempted to imitate TSP conditions by depositing the sample onto the direct exposure probe by dissolving it in the mobile phase used for HPLC–TSP-MS. The probe was then introduced into the heated ion source and exposed to the CI plasma. The spectrum obtained from the pure *Z* oxime isomer is shown in Fig. 3. Surprisingly, no common fragment ions with the corresponding TSP spectrum (Fig. 2b) was found. From the $[M + H]^+$ ion, loss of water (*m/z* 245) results in the most prominent fragment in the CI spectrum. Preliminary experiments on the collision-induced dissociation of the protonated alprenolone oxime isomers (*m/z* 263) have given neither *m/z* 221 nor *m/z* 189 as daughter ions. There has to be a process of yet unknown origin, perhaps specific thermolytic reaction, peculiar to thermospray ionization that results in the appearance of those ions. Nevertheless, the latter characteristically reflect the steric position of the oxime hydroxyl.

In quantitative terms, HPLC–TSP-MS is able to detect 10–50 ng of alprenolol or alprenolone oxime in full-scan mode, while the limit may reach several hundred pg by selected-ion monitoring. However, HPLC with UV spectrophotometric detection [10] gives better sensitivities (3 ng for alprenolol, with 3:1 signal-to-noise ratio at 272 nm) than full-scan TSP-MS. The inherent instability of the thermospray jet, which is observed as "spiking" on the peak profile in the reconstructed TIC chromatogram [16], dictates that deuterated or ^{13}C internal standards be employed for accurate determination of these compounds.

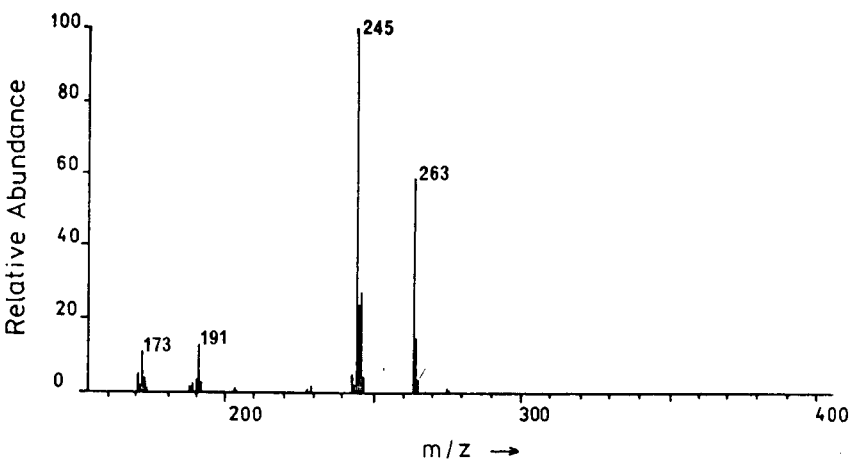

Fig. 3. Desorption chemical ionization mass spectrum alprenolone (*Z*-) oxime.

In conclusion, on-line HPLC–TSP-MS provides a high level of molecular specificity and increased detection sensitivity for the β-adrenergic antagonist alprenolol, and for its ketoxime analogues. The method also offers advantages with respect of the identification of stereoisomeric oximes due to the unique fragmentation pattern of the TSP spectra obtained from the chromatographically separated compounds.

ACKNOWLEDGEMENT

Partial support of the work by Xenon Vision (Alachua, FL, U.S.A.) is gratefully acknowledged.

REFERENCES

1 L. A. Sternson and T. Malefyt, in R. T. Borchardt, A. J. Repta and V. J. Stella (Editors), *Directed Drug Delivery —A Multidisciplinary Approach*, Humana Press, Clifton, NJ, 1984, p. 291.
2 N. Bodor and L. Prokai, *Pharm. Res.*, 7 (1990) 723.
3 C. L. Davies, *J. Chromatogr.*, 531 (1990) 131.
4 P. Hermann, J. Fraisse, J. Allen, P. L. Morselli and J. P. Tenot, *Biomed. Mass Spectrom.*, 11 (1984) 29.
5 C. Y. Sum and A. Yacobi, *J. Pharm. Sci.*, 73 (1984) 1177.
6 C. R. Lee, A. C. Coste and J. Allen, *Biomed. Environ. Mass Spectrom.*, 16 (1988) 387.
7 M. S. Leloux, E. D. DeJong and R. A. A. Maes, *J. Chromatogr.*, 488 (1989) 357.
8 L. Prokai and N. Bodor, in *Proceedings of the 37th ASMS Conference on Mass Spectrometry and Allied Topics, May 21–26, 1989, Miami Beach, FL*, American Society for Mass Spectrometry, East Lansing, MI, p. 1354.
9 M. S. Lant, J. Oxford and L. E. Martin, *J. Chromatogr.*, 394 (1987) 223.
10 L. Prokai, A. Simay and N. Bodor, *J. Chromatogr.*, 541 (1991) 469.
11 N. Bodor, A. Elkoussi, M. Kano and T. Nakamura, *J. Med. Chem.*, 31 (1988) 100.
12 A. Simay, L. Prokai and N. Bodor, *Tetrahedron*, 45 (1989) 4102.
13 R. D. Voyksner and C. A. Haney, *Anal. Chem.*, 57 (1985) 991.
14 K. B. Tomer and C. E. Parker, *J. Chromatogr.*, 492 (1989) 189.
15 R. W. Smith, C. E. Parker, D. M. Johnson and M. M. Bursey, *J. Chromatogr.*, 394 (1987) 261.
16 G. Schmelzeisen-Redeker, M. A. McDowall, U. Giessmann, K. Levsen and F. W. Röllgen, *J. Chromatogr.*, 323 (1985) 127.

Journal of Chromatography, 541 (1991) 480–482
Elsevier Science Publishers B.V., Amsterdam

CHROM. 23 023

Short Communication

2-Trichloromethylbenzimidazole, a selective chromogenic reagent for the detection of *o*-phenylenediamine on thin-layer plates

LESZEK KONOPSKI
Institute of Industrial Organic Chemistry, Annopol 6, 03-236 Warsaw (Poland)
(First received September 17th, 1990; revised manuscript received December 5th, 1990)

ABSTRACT

A new, selective method for the detection of *o*-phenylenediamine and some of its derivatives on thin-layer plates is described. *o*-Phenylenediamine is treated with methyl trichloromethylacetimidate and exposed to pyridine vapours. The derivatization is performed before the chromatography or *in situ* on the thin-layer chromatographic plate. The detection limit is between 80–2000 ng, depending on the procedure and the compound detected.

INTRODUCTION

In previous papers [1,2], the application of 2-trichloromethylbenzimidazole (TCMB) for the detection of the azines on thin-layer chromatographic (TLC) plates was described. TCMB was synthesized from *o*-phenylenediamine (**1**) and methyl trichloroacetimidate [3] and was then used as a spray reagent for the detection of the azines on TLC plates due to the formation of a highly coloured product (**4**):

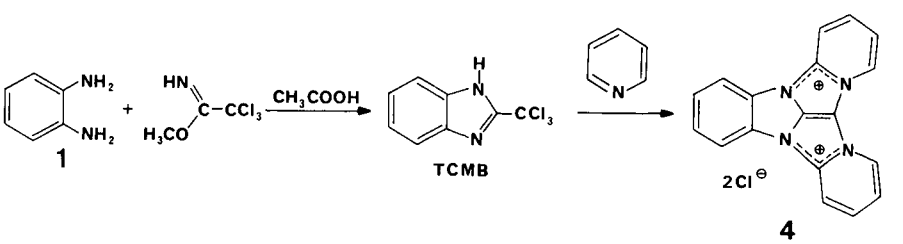

1 4

The most probably structure of the major component of **4** seems to be 4*a*,4*c*,8*b*,12*b*-tetraazadibenzo[*a*,*f*]lindano[1,2,3-*cd*]pentalene-4*a*,4*c*-diinium dichloride dihydrate [2].

0021-9673/91/$03.50

The analogous spray reagent *o*-phenylenediamine (**1**)–trichloroacetic acid is also known [4–6], but this mixture is not a source of TCMB [3]. It appears that the reaction of **1** with methyl trichloroacetimidate is the only way to synthesize TCMB [3].

In this work, the reaction pathway shown above was applied to the selective detection of **1** and some its derivatives on TLC plates.

EXPERIMENTAL

Materials

Methyl trichloroacetimidate [7] was purified by distillation over anhydrous potassium carbonate (b.p. 150–152°C). Pre-coated silica gel 60 F_{254} plastic sheets, 0.2 mm thick (Merck, Darmstadt, Germany) were used for TLC. All tested amines were of analytical-reagent grade.

Detection of o-phenylenediamine

Procedure A. Methyl trichloroacetimidate (150 μl) was added to 1 ml of a solution of **1** (100–1000 μg) in acetic acid and the mixture was shaken once and left for 15 min. A 1-μl volume of the solution obtained was spotted directly on the TLC plates. Chromatograms were developed in acetone as eluent; the migration distance was 8 cm. The dried chromatograms were placed in pyridine vapour at room temperature. The colour appeared after 10–20 min.

Procedure B. A solution of **1** (50–1000 ng) in acetone was spotted on the TLC plate and developed with acetone. The dried chromatograms were sprayed with 10% methyl trichloroacetimidate in glacial acetic acid, allowed to stand for 15 min and placed in pyridine vapour.

Procedure C. A solution of **1** (1–10 μg) in acetone, methyl trichloromethylacetimidate (1 μl) and acetic acid (10 μl) were succesively spotted on the TLC plate. After 15 min the plates were dried, developed and detected in pyridine vapour.

RESULTS AND DISCUSSION

The results are presented in Table I. No difference was observed between procedures A and B, but procedure C seems to be less sensitive. The detection limit was less than 100 ng and depends on the procedure.

TABLE I

DETECTION LIMITS, R_F VALUES AND COLOURS OF THE AROMATIC DIAMINES EXAMINED ON TLC PLATES

1,2-Diamine	Procedure	R_F	Colour (for 1000 ng in spot)	Detection limit (ng)
o-Phenylenediamine (**1**)	A,B	0.67	Amaranth-brown	100
	C		Amaranth-brown	2000
3,4-Diaminotoluene (**2**)	A,B	0.58	Brown	100
4-Nitro-*o*-phenylenediamine (**3**)	A	0.66	Brown	80

Of the other compounds tested, 3,4-diaminotoluene (**2**) and 4-nitro-*o*-phenylenediamine (**3**) gave similar results to **1**. The following compounds gave no colour using any of the procedures: 1,2- and 2,3-naphthylenediamine and 2,3-diaminophenazine (all *ortho*-substituted) and 1,8-naphthylenediamine (*peri*-), probably for steric reasons; 1,2-ethylenediamine, 2,3-dimethyl-2,3-butylenediamine and *m*- and *p*-phenylenediamine, because the aromatic benzimidazole ring cannot be formed; *o*-aminophenol and N-methyl-*o*-phenylenediamine, which probably form a suitable benzoxazole or benzimidazole ring in the reaction with methyl trichloroacetimidate, but the heterocyclic obtained do not react subsequently with pyridine and the formation of another highly coloured product such as **4** does not occurs; and 2-amino-3-hydroxyphenazine for the same reason and also for steric reasons.

The R_F values, spot colours and detection limits of the aromatic 1,2-diamines **1–3** are presented in Table I.

This highly selective method for the detection of *o*-phenylenediamine and some aromatic diamines may be applied to the determination of residues, *e.g.*, *o*-phenylenediamine in the presence of *o*-nitroaniline and *m*- and *p*-phenylenediamine or in some pesticides such as carbendazim and benomyl. This will be the object of further investigations.

ACKNOWLEDGEMENTS

The author expresses his gratitude to Mr. Jerzy Zakrzewski for valuable assistance.

REFERENCES

1 L. Konopski and B. Jerzak, *J. Chromatogr.*, 363 (1986) 394.
2 L. Konopski and B. Jerzak, *J. Chromatogr.*, 481 (1989) 477.
3 G. Holan, E. L. Samuel B. C. Ennis and R. W. Hinde, *J. Chem. Soc. C.*, (1967) 20.
4 T. Wieland and E. Fisher, *Naturwissenschaften*, 36 (1949) 219.
5 *Dyeing Reagents for Thin Layer Chromatography*, E. Merck, Darmstadt, 1980, procedure 226, p. 67.
6 H. Jork, W. Funk, W. Fisher and H. Winner, *Thin-Layer Chromatography, Reagents and Detection Methods*, Vol. 1a, VCH, Weinheim, 1990, p. 372.
7 F. Kramer, K. Pawelzik and H. J. Badlauf, *Chem. Ber.*, 91 (1958) 1049.

Journal of Chromatography, 541 (1991) 483–488
Elsevier Science Publishers B.V., Amsterdam

CHROM. 23 025

Short Communication

Simultaneous pH and ionic strength effects and buffer selection in capillary electrophoretic techniques

JOHAN VINDEVOGEL and PAT SANDRA*
Laboratory of Organic Chemistry, State University of Ghent, Krijgslaan 281 S4, B-9000 Ghent (Belgium)
(First received October 24th, 1990; revised manuscript received December 10th, 1990)

ABSTRACT

Under certain conditions, a decrease in electroosmotic flow can be observed when the pH is increased at constant buffer concentration. This unusual behaviour is related to changes in the ionic strength caused by the titrant.

INTRODUCTION

During optimization of the resolution in the analysis of steroid esters by micellar electrokinetic chromatography [1], it was observed that an increase in pH caused a decrease in the electroosmotic mobility. The result, obtained by using a statistical design technique in which several parameters were varied at the same time, has been confirmed experimentally. This contradicts the general ideas about the dependence of mobility on pH [2–7]. This phenomenon has practical consequences as resolution in both capillary zone electrophoresis [8] and micellar electrokinetic chromatography [9] is influenced by the electroosmotic mobility.

THEORY

A potential difference orginates from the charge separation between a capillary wall and a solution. In fused-silica capillaries, this can be ascribed to the dissociation of surface silanol groups, leaving an excess of negative charges on the wall. Owing to the presence of ions in the solution, the potential difference decays rapidly. At a small distance from the wall, at the shear plane, beyond tightly absorbed ions and solute molecules, the potential difference attains its electrokinetically relevant value, the ζ-potential. The electroosmotic mobility μ_{eo} is proportional to this ζ-potential [10]:

$$\mu_{eo} = \varepsilon_0 \varepsilon_r \zeta / \eta$$

0021-9673/91/$03.50

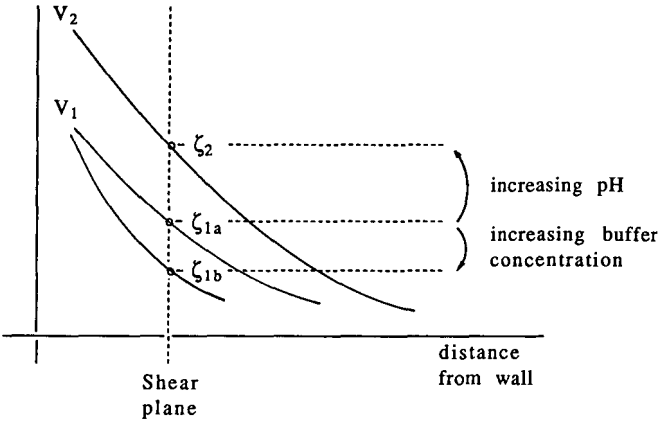

Fig. 1. Influence of buffer pH and concentration on the ζ-potential. See Theory for details.

where μ_{eo} = electroosmotic mobility ($m^2/s \cdot V$), ζ = zeta-potential (V), ε_0 = permittivity of vacuum (8.85 $C^2/N \cdot m^2$), ε_r = dielectric constant and η = viscosity (kg/m · s).

Using a simple model, and ignoring the subtle differences between the Debye–Hückel, Goüy–Chapman or Stern treatments [11,12], the effect of buffer composition on the ζ-potential is shown in Fig. 1. Let the surface potential V_1 and the ζ-potential ζ_{1a} represent a reference situation. By increasing the pH of the buffer, the charge on the wall is increased, increasing the surface potential from V_1 to V_2, and resulting in a higher potential ζ_2, as observed at the shear plane. When the buffer concentration, or more precisely the ionic strength, is increased, a given potential V_1 will decay faster, resulting in a decreased potential ζ_{1b}. As represented here, it is assumed that changing the buffer concentration does not affect the surface charge density on the wall. Depending on the case, this may not be a realistic assumption.

Of the two factors, pH and buffer concentration, the latter has been less intensively studied, at least within the context of capillary electrophoretic techniques. Electroosmotic mobilities, or equivalent linear velocities and migration times have been related to buffer concentration [13–17] and ionic strength [17,18]. The studies confirm that, at a fixed pH, mobility decreases with increasing concentration, but confusion exists regarding the mathematical model that should be used to describe this behaviour. VanOrman *et al.* [17] have shown that ionic strength is a more meaningful quantity than concentration.

Many workers have studied the pH dependence of the electroosmotic mobility in fused-silica capillaries [2–6]. The effect has also been studied with micellar solutions [7]. Many more data can be found, hidden in graphs and tables relating analyte mobilities (or equivalent migration times) to pH, as often methanol or another neutral marker is included. It is now generally accepted that the electroosmotic mobility increases strongly up to pH 7–8. At higher pH, the mobility still increases, but more slowly. This continued increase at higher pH does not seem to be universally valid. Apart from our own results (Fig. 2), five other examples were found in the literature where the reverse occurred. Fujiwara and Honda [13,19] reported a decrease in mobility between pH 6 and 10, using a phosphate buffer [13,19]. They ascribed this

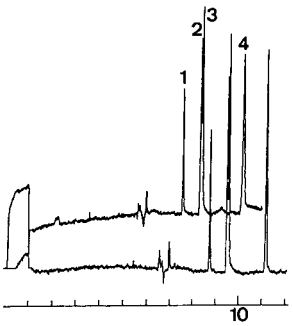

Fig. 2. Effect of buffer pH on electroosmotic flow; micellar electrokinetic chromatographic analysis of testosterone esters: 1 = propionate; 2 = phenylpropionate; 3 = isocaproate; 4 = decanoate. Conditions: 440 V/cm, 35°C, 40 mM SDS, 40% acetonitrile 20 m*M* boric acid–borax buffer; pH 8 (top) and 9 (bottom). Time scale in min.

phenomenon to a "decrease in the ζ-potential with pH" [19], which is just a restatement of the same as no important changes in dielectric constant or viscosity are to be expected. Data by Cohen *et al.* [20] showed a decreased mobility when increasing the pH from 7 to 9, using a sodium dodecyl sulphate (SDS) solution with a phosphate–borax buffer, but they did not comment on this fact. Nishi *et al.* [21] showed the same effect in the range 7–9, again with a phosphate-borax buffer, but in a bile salt solution. The phenomenon was not discussed although the data differed from an earlier report [22], where the electroosmotic mobility remained nearly constant. Using the same buffer, a higher electroosmotic mobility at pH 7 was demonstrated with four different bile salts [23].

EXPERIMENTAL

Electroosmotic mobilities in fused-silica capillaries were measured with an integrated and automated capillary zone electrophoresis instrument, the P/ACE System 2000 (Beckman, Palo Alto, CA, U.S.A.). Standard P/ACE capillaries (57 cm × 75 μm I.D.) were used with detection at 50 cm. Before each run they were rinsed with 0.1 *M* NaOH, water, 0.1 *M* HCl, water and running buffer.

Mesityl oxide was used as the marker, injected by pressure (1 s) and detected at 214 nm. Electroosmotic mobilities were measured with an applied voltage of 10 kV (157 V/cm) at 25 ± 0.1°C. Three measurements were made. The relative standard deviations were better than 0.5%.

Buffers were prepared in deionized water (Milli-Q system; Millipore, Bedford, MA, U.S.A.). Borax concentrations are expressed as equivalent borate, for reasons which are explained in the text.

RESULTS AND DISCUSSION

The electroosmotic mobility was measured in four buffer systems (Fig. 3): Tris–HCl, H_3BO_3–NaOH, $Na_2B_4O_7$–NaOH and $Na_2B_4O_7$–HCl. The results confirm that boric acid and borax are funtionally similar when titrated with a base [24]:

$$Na_2B_4O_7 + 7\,H_2O = 2\,Na^+\,B(OH)_4^- + 2\,H_3BO_3 = 2\,NaOH + 4\,H_3BO_3$$

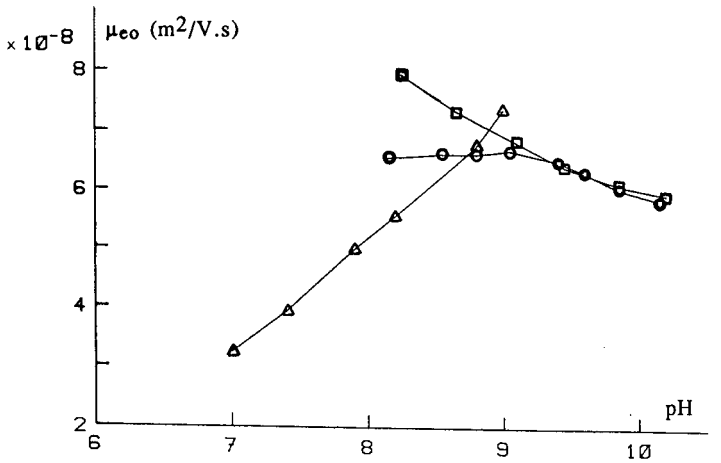

Fig. 3. Influence of buffer pH on electroosmotic mobility. △ = Tris–HCl; □ = boric acid–NaOH ○ = borax–HCl; ● = borax–NaOH. Buffer concentration: 50 m*M*.

For this reason, we express borax concentrations as their boric acid equivalent (*e.g.*, 25 m*M* borax buffer is equivalent to 100 m*M* boric acid buffer).

Three different cases remain to relate pH and ionic strength during titration, assuming that for these weak electrolytes the ion concentrations are equal to the analytical concentrations of the titrant:

(a) $Tris + HCl = TrisH^+ + Cl^-$
(b) $H_3BO_3 + NaOH = Na^+ + B(OH)_4^-$
(c) $2\ Na^+ + 2B(OH)_4^- + HCl = 2\ Na^+ + B(OH)_4^- + Cl^- + H_3BO_3$

In case (a) a decrease in pH is accompanied by an increase in the number of ions, and thus of the ionic strength. Both effects are cooperative in producing a relatively strong dependence of the electroosmotic mobility on the pH. In case (b), however, increasing the pH will result in an increase in the ionic strength. Apparently, the ionic strength effect is stronger than the "pure" pH effect, resulting in an inverted dependence of the electroosmotic flow on the pH. The borax–NaOH case is similar as it can be considered as a boric acid–NaOH system that has already been partially neutralized. All the cited examples, showing lower electroosmotic mobility at higher pH, belong to this category. Case (c) is interesting, as the amount of ions remains constant during neutralization. Provided that wall interactions do not differ too much from the boric acid–NaOH system, the data confirm that, indeed, the mobility increases slightly with pH, as expected. In this pH range however, the effect is so moderate that it is easily overcompensated by ionic strength effects.

When differences in the amount of titrant are compensated for by adding a calculated amount of salt, the anomalous decrease in mobility with pH disappears and a fairly flat profile is obtained (Fig. 4). The confusion between constant concentration and constant ionic strength explains the anomaly. In published studies, the use of a pH scale with fixed ionic strength [3] is exceptional. In most of the op-

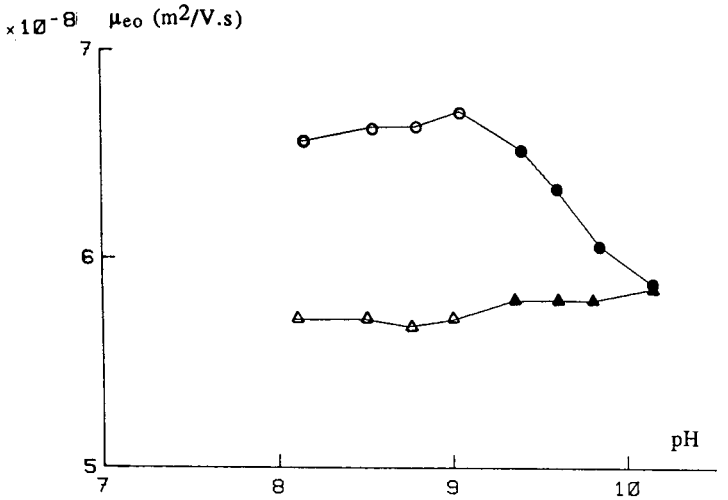

Fig. 4. Influence of added salt on electroosmotic mobility: (●) borax–NaOH and (○) borax–HCl at constant concentration (50 m*M*); (▲) borax–NaOH and (△) borax–HCl at constant ionic strength (50 m*M*).

timization reports, where the pH change was limited to only a few units, constant-concentration buffers [1,2,4,6,13,19–23] were used, often by mixing two constituents, *e.g.*, primary and secondary phosphate, in varying ratios. There may be valid practical reasons for doing so, but a numerical example demonstrates the possible pitfall of such a procedure. A 100 m*M* borate buffer, 5% neutralized with NaOH (considering the first neutralization step only), has a pH of 8.1 and an ionic strength of 5 m*M*. Doubling the concentration will double the ionic strength. However, increasing the pH of the 100 m*M* solution by 1 unit will require a degree of neutralization of *ca.* 24%, resulting in an ionic strength of 24 m*M*, nearly a five-fold increase. This explains why ionic strength effects are more prominent through pH than through buffer concentration, as we aboserved in our own optimization set-up [1].

CONCLUSIONS

When using constant-concentration buffers, decreased electroosmotic mobility can be observed at higher pH values. This effect is attributable to the ionic strength and will be observed with buffers obtaind by titrating a weak acid with a strong base. To obtain an increased electroosmotic flow, weak base–strong acid-type buffers are to be preferred. If, on the other hand, pure pH effects are desired, buffers at constant ionic strength, rather than at constant concentration, should be used.

ACKNOWLEDGEMENT

We thank Analis (Belgium) for the loan of the Beckman instrument.

REFERENCES

1 J. Vindevogel and P. Sandra, *Anal. Chem.*, submitted for publication.
2 T. Tsuda, K. Nomura and G. Nakagawa, *J. Chromatogr.*, 264 (1983) 385.
3 K. D. Lukacs and J. W. Jorgenson, *J. High. Resolut. Chromatogr. Chromatogr. Commun.*, 8 (1985) 407.
4 K. D. Altria and C. F. Simpson, *Chromatographia*, 24 (1987) 527.
5 R. M. McCormick, *Anal. Chem.*, 60 (1988) 2322.
6 R. D. Smith, H. R. Udseth, J. A. Loo, B. W. Wright and G. A. Ross, *Talanta*, 36 (1989) 161.
7 K. Otsuka and S. Terabe, *J. Microcolumn Sep.*, 1 (1989) 150.
8 J. W. Jorgenson and K. D. Lukacs, *Anal. Chem.*, 53 (1981) 1298.
9 S. Terabe, K. Otsuka and T. Ando, *Anal. Chem.*, 57 (1985) 834.
10 J. H. Knox, *Chromatographia*, 26 (1988) 329.
11 S. Hjertén, *Top. Bioelectrochem. Bioenerg.*, 2 (1978) 89.
12 D. C. Grahame, *Chem. Rev.*, 41 (1947) 441.
13 S. Fujiwara and S. Honda, *Anal. Chem.*, 58 (1986) 1811.
14 G. J. M. Bruin, J. P. Chang, R. H. Kuhlman, K. Zegers, J. C. Kraak and H. Poppe, *J. Chromatogr.*, 471 (1989) 429.
15 K. Salomon, D. S. Burgi and J. S. Helmer, presented as a poster at the *2nd International Symposium on High Performance Capillary Electrophoresis, San Francisco, CA, January 29–31, 1990*, P306.
16 D. S. Burgi, K. Salomon and R.-L. Chien, presented as a poster at the *2nd International Symposium on High Performance Capillary Electrophoresis, San Francisco, CA, January 29–31, 1990*, P112.
17 B. B. VanOrman, G. G. Liversidge, G. L. McIntire, T. M. Olefirowicz and A. G. Ewing, *J. Microcolumn Sep.*, 2 (1990) 176.
18 V. Dolnik, J. Liu, F. Banks, M. V. Novotny and P. Bocek, *J. Chromatogr.*, 480 (1989) 321.
19 S. Fujiwara and S. Honda, *Anal. Chem.*, 59 (1987) 2773.
20 A. S. Cohen, S. Terabe, J. A. Smith and B. L. Karger, *Anal. Chem.*, 59 (1987) 1021.
21 H. Nishi, T. Fukuyama, M. Matsuo and S. Terabe, *J. Chromatogr.*, 513 (1990) 279.
22 H. Nishi, T. Fukuyama, M. Matsuo and S. Terabe, *J. Chromatogr.*, 498 (1990) 313.
23 H. Nishi, T. Fukuyama, M. Matsuo and S. Terabe, *J. Microcolumn Sep.*, 1 (1989) 234.
24 R. K. Momii and N. H. Nachtreib, *Inorg. Chem.*, 6 (1967) 1189.

Journal of Chromatography, 541 (1991) 489–495
Elsevier Science Publishers B.V., Amsterdam

CHROM. 23 061

Short Communication

Capillary electrophoresis in [^{2}H]water solution

PATRICK CAMILLERI* and GEORGE OKAFO
SmithKline Beecham Pharmaceuticals, The Frythe, Welwyn, Herts, AL6 9AR (U.K.)
(First received September 18th, 1990; revised manuscript received November 14th, 1990)

ABSTRACT

Capillary electrophoresis in [^{2}H]water-based buffer solution has been shown to give enhanced resolution of a number of nucleosides and dansyl amino acids, compared to electrophoresis carried out in water solution of the same acidity. These effects are thought to result from a lowering of electroosmotic flow due to the higher viscosity of [^{2}H]water and to a reduction of the zeta potential.

INTRODUCTION

Capillary electrophoresis (CE) has become a popular separation technique as it is complementary to high-performance liquid chromatography (HPLC). The mechanism of separation by these two techniques depends on different physico-chemical properties of solutes. Unlike HPLC, where separation of molecules occurs due to differences in partitioning between the mobile and stationary phases, in CE resolution occurs due to differences in the mobilities of ions in an electric field [1]. CE can be applied for the resolution of a variety of molecules of different sizes: organic [2] and inorganic [3] species, peptides [4], DNA fragments [5] and proteins [6].

A number of experimental parameters can influence retention and resolution in CE. These include applied voltage, length of capillary, pH of buffer and the use of organic modifiers. CE studies reported to date have been largely carried out in water-based buffer solution. In this paper we have explored the effect on some separations by CE after replacement of water (H_2O) by deuterium oxide (^2H_2O). The latter solvent has properties such as viscosity and ionisation which are significantly different to those of water and which can play an important role in CZE separations. Viscosity of ^2H_2O at 25°C is 1.23 times greater than that of H_2O at the same temperature whereas the ionisation constants of H_2O and ^2H_2O are $1.00 \cdot 10^{-14}$ and $1.95 \cdot 10^{-15}$, respectively.

Our preliminary studies have revealed that the analytical quality of CE separations can be improved considerably when carried out in ^2H_2O rather than in water, although the time of analysis is always longer in the former solvent. We describe

0021-9673/91/$03.50

two examples of CE separations where the use of ^2H_2O in place of water has been shown to give a better resolution (R_s) of components in a mixture, due primarily to lowering of electroosmotic flow in agreement with the relationship [7]:

$$R_s = \frac{1}{4}\left(\frac{V}{2D}\right)^{\frac{1}{2}}\left(\frac{l}{L}\right)^{\frac{1}{2}}\frac{\Delta\mu_{ep}}{(\bar{\mu}_{ep} + \mu_{eo})^{\frac{1}{2}}} \quad (1)$$

where V is the applied voltage, D is the diffusion coefficient of the solute, l is the effective length of the capillary from the injection end to the detection portion, L is the total length of the capillary, $\Delta\mu_{ep}$ is the difference in electrophosphoretic mobility of two solutes, $\bar{\mu}_{ep}$ is the average electrophoretic mobility and μ_{eo} is the electroosmotic mobility.

EXPERIMENTAL

Reagents and chemicals

Adenosine-5′-O-thiomonophosphate (AMP-S) and adenosine-5′-O-(2-thiophosphate) (ADP-β-S) were obtained from Calbiochem, adenosine-5′-monophosphate (AMP), adenosine-5′-diphosphate (ADP), adenosine-3′,5′-cyclic monophosphate (cAMP) and cytidine-5′-monophosphate (CMP) were purchased from Sigma, and adenosine-3′,5′-cyclic-O-thiomonophosphate (Rp-cAMP-S) was synthesized at SmithKline Beecham Pharmaceuticals. The dansyl amino acid derivatives of ε-amino-*n*-caproic acid, leucine, glycine, γ-aminobutyric acid (GABA), β-alanine, valine and phenylalanine and reagent-grade tricine were purchased from Sigma. ^2H_2O and 40% (w/w) solution of NaO^2H in ^2H_2O were from Aldrich. AnalaR-grade sodium dihydrogenphosphate and sodium monohydrogenphosphate were supplied by BDH. Water was of distilled-deionised quality (Milli-Q) and all solutions were filtered through 0.2-μm Millipore filters before use for CE.

Apparatus and procedure

The apparatus for CE consisted of a Glassman high-voltage d.c. supply (Whitehouse Station, U.S.A.) and a CE absorbance detector (CV^4, ISCO). CE measurements were carried out within a protective Perspex enclosure with interlock switches. Electrophorerograms were recorded on a Kipp and Zonen chart recorder and data were also acquired on a Perkin-Elmer LIMS/CLAS system. Fused-silica capillaries (Applied Biosystems) of 50 μm internal diameter and of 122 cm total length (L) were used. The separation distance (l) from the anode to the detector was 95 cm. Capillaries were cleaned and filled with solution using a high-pressure syringe pump (Harvard Model 440). Platinum electrodes were used for the connection of the voltage supply to the buffer reservoirs at each end of the capillary. pH and p^2H measurements were recorded on a Radiometer PHM82 pH meter calibrated with standard pH buffers. p^2H was measured by adding 0.4 units to the reading of the meter [8].

Before use for CE, capillaries were cleaned with 0.5 *M* NaOH or 0.5 *M* NaO^2H for 10 to 20 min and then flushed with the appropriate buffer for about 15 min. All samples analysed were dissolved in the separation buffer containing a trace of methanol and were loaded electrokinetically by applying 5 kV for 1–5 s.

For the CE separation of nucleosides in H_2O or ^2H_2O, tricine (40 m*M*) buffer was used as the electrolyte and the pH or p^{2}H was adjusted in the range 8.60 to 9.45 with 0.1 *M* NaOH or 0.1 *M* NaO^{2}H, as apropriate. The voltage across the ends of the capillary was set at 40 kV and detection of nucleosides was by UV absorption at 254 nm.

The separation of dansyl amino acids was carried out in phosphate buffer made up to 10 m*M* NaH_2PO_4 with 10 m*M* Na_2HPO_4, adjusted to a pH of 7.83 with 0.1 *M* NaOH. In ^2H_2O-based solutions the buffer constituents were as in water and the p^{2}H was adjusted to 7.85 with 0.1 *M* NaO^{2}H. The separation voltage and the wavelength of detection were the same as for the CE of nucleosides.

RESULTS AND DISCUSSION

The first set of closely related compounds studied were six nucleosides namely cAMP, Rp-cAMP-S, AMP, AMP-S, ADP, ADP-β-S. The CE separation of these molecules together with that of cytindine-5′-monophosphate (CMP) is shown in Fig. 1 where experiments A and B refer to separations carried out in H_2O (pH 9.02) and ^2H_2O (p^{2}H 9.03) solutions. Under both conditions the adenosine-thiophosphate analogue has been found to be less mobile than the corresponding phosphate derivative. Although the migration time in water is shorter than in ^2H_2O at pH = p^{2}H = 9.0, the resolution of the seven nucleosides is markedly better in the latter solvent. Fig. 2 shows the variation of migration time of the adenosine nucleosides with pH or p^{2}H. At pH or p^{2}H values close to 8.5 migration times in H_2O and ^2H_2O are very close. At values above 9 migration times are much lower in water than in ^2H_2O. As the pK_a values of the nucleosides under study is between 5.0 and 6.5 (the thiophosphates have the lower pK_a values) these molecules are expected to be fully ionised at pH values above 8.5 used in this study. For ionised species migration times result from the influence of both electroosmotic flow and electrophoretic flow. In general, higher pH

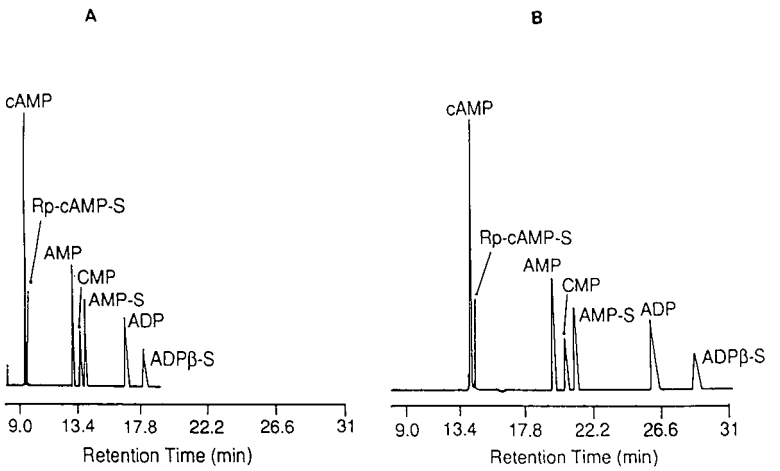

Fig. 1. CE separaton of nucleosides in (A) H_2O- and (B) ^2H_2O-based buffer solutions. Buffer, 40 m*M* tricine in H_2O (pH 9.02) or ^2H_2O (p^{2}H 9.03); L = 122 cm; l = 95 cm; separation voltage, 40 kV; current, 50 μA; injection voltage, 5 kV for 2 s; detection, UV at 254 nm; temperature, ambient.

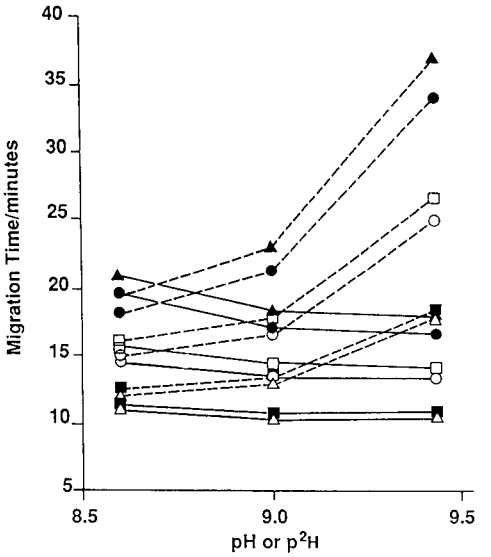

Fig. 2. Variation of the migration time of nucleosides with pH or p^{2}H in H_2O- and ^2H_2O-based buffer solution. ▲ = ADP-β-s; ● = ADP; □ = AMP-s; ○ = AMP; ■ = Rp-cAMP-s; △ = cAMP; solid lines: H_2O; dashed lines: ^2H_2O.

or p^{2}H values give higher electroosmotic flow due to the higher concentration of dissociated Si–OH groups on the inner surface of the capillary increasing the amount of negative surface charge.

The electroosmotic velocity (v_{osm}) at a pH of 9.4 is found to be about 45% higher than that at a p^{2}H of the same value using tricine as a buffer, v_{osm} is usually expressed by the relationship [9]:

$$v_{osm} = \frac{V}{L}\frac{\varepsilon\zeta}{4\pi\eta} \tag{2}$$

where V is the applied voltage across the ends of a capillary tube of length L, D is the dielectric constant, ζ is the zeta potential and η is the viscosity coefficient.

All experiments in this study have been carried out at the same applied voltage (V) using the same length of capillary (L). Moreover, the dielectric constant (D) of water (78.30) at 25°C is almost equal to that of ^2H_2O (78.25) at the same temperature. Thus any differences in electroosmotic flow in water and ^2H_2O can only be accounted for in terms of viscosity and zeta potential. In fact, the viscosity of water (η = 0.890 Nsm^{-2}) is markedly lower (about 23%) than that of ^2H_2O (η = 1.098 Nsm^{-2}) at 25°C and must therefore be a major contributory factor in slowing down the migration of the nucleosides in ^2H_2O compared to water (Figs. 1 and 2).

The zeta potential (ζ) is directly related to the amount of charge per unit surface area on the inner wall of the capillary. The magnitude of ζ will depend both on the concentration of dissociated ions in the buffer solution and the dissociation of the Si–OH groups on the inner surface of the capillary. The pK_a values of both the tricine

buffer and that of the Si–OH groups are expected [10] to be about 0.6 units higher in ^2H_2O than in water. Thus the pK_a of tricine will increase from 8.2 in water to about 8.8 in ^2H_2O, and that of the silyl groups will increase from 9.8 (based on the pK_a of silicic acid) [10] to about 10.4. At a pH or p^2H of 9.4 a higher degree of ionisation of the Si–OH groups is expected to occur in H_2O compared to ^2H_2O leading to a correspondingly higher ζ potential. Moreover, a lower amount of negatively charged free base of the tricine buffer will exist in ^2H_2O compared to H_2O when the p^2H or pH is set at 9.4, again contributing to a decrease in the ζ potential and hence a decrease in the mobility of the nucleosides in ^2H_2O. The concentration of tricine free base is calculated to be 94 and 80% in water and ^2H_2O, respectively. Finally, the magnitude of the zeta potential may also be affected by the degree of negative charge on the substrates. In fact, slow down in mobility is greatest for the multi charged nucleosides at the pH or p^2H under study.

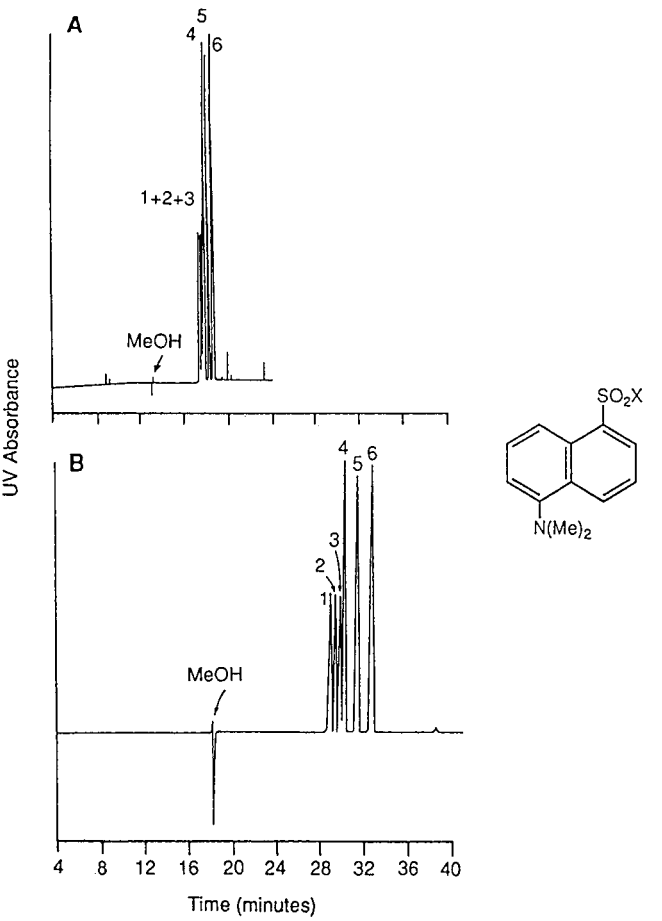

Fig. 3. CE separation of dansyl amino acids in (A) H_2O (pH 7.83) and (B) ^2H_2O (p^2H 7.85). L = 122 cm; l = 95 cm; buffer, 20 mM NaH_2PO_4–Na_2HPO_4, p^2H or pH $\approx$ 7.8; separation voltage, 40 kV; current, 50 μA; injection voltage, 5 kV for 1 s; detection, UV at 254 nm; temperature, ambient. Peaks (see structure): X = (1) ε-amino-n-caproic acid; (2) Leu; (3) Gly; (4) GABA; (5) β-Ala; (6) Val. Me = Methyl.

The second set of model solutes that were initially investigated for separation in H_2O and ^2H_2O were the dansyl derivatives of the following six amino acids: ε-aminocaproic acid, glycine, valine, leucine, β-alanine and GABA. The separation of these solutes in phosphate buffer at pH 7.83 is poor as shown in Fig. 3a. In comparison, almost baseline resolution is obtained for all the six compounds at a p^2H of 7.85 using the same concentration of phosphate buffer in ^2H_2O. Having obtained such excellent analytical improvement dansyl phenylalanine was added to the original solute mixture. Partial separation of this dansyl derivative from the remaining compounds was only obtained in ^2H_2O (Fig. 4). No attempt was made to improve this separation further.

The electroosmotic velocity in phosphate buffer was found to be about 35% lower at p^2H 7.85 compared to pH 7.83. As in the case of the CE separation of the nucleosides in these two solvent media, the increase in viscosity in ^2H_2O has to be a major cause for the longer migration time. The pK_a of phosphoric acid and deutrophosphoric acid have been reported [11] as 7.2 and 7.8 respectively. Thus, at a pH or p^2H around 7.8 the percentage of phosphate free base is 80% in H_2O compared to 50% in ^2H_2O, again indicating that differences in the concentration of the ratio of free acid to free base plays some part in affecting the mobility of the dansyl substrates in H_2O and ^2H_2O solution.

In both the case of the CE separation of the nucleosides and dansyl amino acids the enhanced resolution observed can be ascribed to a reduction in electrophoretic mobilities according to eqn. 1. However, an increase in viscosity would also mean

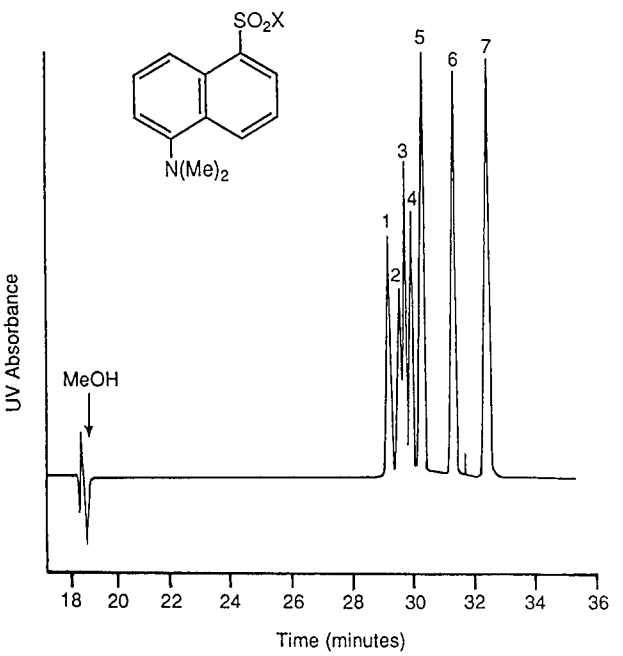

Fig. 4. CE separation of dansyl phenylalanine from the other dansyl derivatives shown in Fig. 3. Peaks (see structure): X = (1) ε-amino-*n*-caproic acid; (2) Leu; (3) Phe; (4) Gly; (5) GABA; (6) β-Ala; (7) Val.

a reduction in electrophoretic mobility because the average electrophoretic velocity v is related [12] to μ_{ep} and μ_{eo} by eqn. 3:

$$v = (\mu_{ep} + \mu_{eo})/(V/L) \quad (3)$$

Thus, the enhanced resolution in ^2H_2O rather than H_2O-based buffer solutions must be certainly ascribed to a reduction in electroosmotic flow primarily due to a reduction in zeta potential.

In conclusion, we have shown that CE separation in ^2H_2O-based buffer solutions can considerably improve electrophoretic resolution compared to H_2O solution. Carrying out CE separations both in H_2O and ^2H_2O can also provide insight on the influence of electroosmotic flow on the electrophoretic mobility of the compounds under study. Moreover, the use of ^2H_2O may have the advantage in that it can be used to control electroosmotic flow without the aid of the addition of other components to the buffer system, in particular ionic surfactants [13] or organic modifiers [14].

REFERENCES

1 D. J. Rose and J. W. Jorganson, *Anal. Chem.*, 60 (1988) 642.
2 T. Tsuda, K. Nomura and G. K. Nakagawa, *J. Chromatogr.*, 248 (1982) 241.
3 T. Tsuda, K. Nomura and G. K. Nakagawa, *J. Chromatogr.*, 264 (1983) 385.
4 J. W. Jorgenson and K. D. Lukas, *J. Chromatogr.*, 218 (1981) 209.
5 H. Drossman, J. A. Lucking, A. J. Kostichka, J. D'Cunbra and L. M. Smith, *Anal. Chem.*, 62 (1990) 800.
6 G. J. M. Bruin, J. P. Chang, R. H. Kuhlman, K. Zegers, J. C. Kraak and H. J. Poppe, *J. Chromatogr.*, 471 (1989) 429.
7 S. Terabe, T. Yoshima, N. Tanaka and M. Araki, *Anal. Chem.*, 60 (1988) 1673.
8 P. K. Glasoe and F. A. Long, *J. Phys. Chem.*, 64 (1960) 188.
9 A. W. Adamson, *Physical Chemistry of Surfaces*, Intersciences, New York, 2nd ed., 1967, Ch. 4.
10 W. P. Jencks, *Catalysis in Chemistry and Enzymology*, McGraw-Hill, New York, 1969, Ch. 4.
11 *Large's Handbook of Chemistry*, McGraw-Hill, New York, 12th ed., 1979, Section 5.
12 J. W. Jorgenson and K. D. Lukas, *Anal. Chem.*, 53 (1981) 1298.
13 H. H. Lawer and D. McManigill, *Anal. Chem.*, 58 (1986) 166.
14 T. Tsuda, C. Nakagawa, M. Sato and K. Yagi, *J. Appl. Biochem.*, 5 (1983) 330.

Author Index

Errata

J. Chromatogr., 520 (1990) 21–31.
Pages 29 and 30, in Tables III and IV, the t_R values should not be in minutes; they are relative values.

J. Chromatogr., 520 (1990) 47–54.
Page 52 in Table III, second row, last column, the value for $\bar{b}$ should read "4.19"

J. Chromatogr., 520 (1990) 157–162.
Page 160, Figures 3 and 4 should be interchanged (the legends are correct).

J. Chromatogr., 520 (1990) 307–313.
Page 308, 8th line from the bottom, "particle diameters of 3.5 and 10 μm", should read "particle diameters of 3, 5 and 10 μm".
Page 308, 4th line from the bottom, "The plate number, N", should read "The minimum reduced plate height, h_{min}".
Page 312, Table II, the concentration value for dopamine "3.3", should read "8.3".

J. Chromatogr., 520 (1990) 403–410.
Page 403, 3rd line of abstract; page 403, 6th line of text and page 404, 2nd line from the bottom, "N-phenylamides of benzoylacetic acid" should read "N-phenylamides of phenoxyacetic acid".

J. Chromatogr., 520 (1990) 425–431.
Page 427, 3rd paragraph, 4th line, "100 × 2.6 mm I.D.", should read "100 × 2.6 cm I.D.".

J. Chromatogr., 521 (1990) 251–265.
Page 261, Table IV, column headings, "2β-" should read "Unidentified metabolite" and "11β-" should read "2β-".

J. Chromatogr., 535 (1990) 317–323.
Page 317, 4th line of abstract; page 318, 6th line from the bottom and page 319, 13th line from the bottom "0.025 M" should read "0.0025 M".

PUBLICATION SCHEDULE FOR 1991

Journal of Chromatography and Journal of Chromatography, Biomedical Applications

MONTH	D 1990	J	F	M	A	M	
Journal of Chromatography	535/1 + 2	536/1 + 2 537/1 + 2 538/1	538/2 539/1 539/2	540/1 + 2 541/1 + 2 542/1	542/2 543/1	543/2 544/1 + 2 545/1	the publication schedule for further issues will be published later
Cumulative Indexes, Vols. 501–550							
Bibliography Section				560/1			
Biomedical Applications		562/1 + 2 563/1	563/2	564/1	564/2 565/1 + 2	566/1 566/2	

INFORMATION FOR AUTHORS

(Detailed *Instructions to Authors* were published in Vol. 522, pp. 351–354. A free reprint can be obtained by application to the publisher, Elsevier Science Publishers B.V., P.O. Box 330, 1000 AH Amsterdam, The Netherlands.)

Types of Contributions. The following types of papers are published in the *Journal of Chromatography* and the section on *Biomedical Applications:* Regular research papers (Full-length papers), Review articles and Short Communications. Short Communmications are usually descriptions of short investigations, or they can report minor technical improvements of previously published procedures; they reflect the same quality of research as Full-length papers, but should preferably not exceed six printed pages. For Review articles, see inside front cover under Submission of Papers.

Submission. Every paper must be accompanied by a letter from the senior author, stating that he/she is submitting the paper for publication in the *Journal of Chromatography*.

Manuscripts. Manuscripts should be typed in double spacing on consecutively numbered pages of uniform size. The manuscript should be preceded by a sheet of manuscript paper carrying the title of the paper and the name and full postal address of the person to whom the proofs are to be sent. As a rule, papers should be divided into sections, headed by a caption (*e.g.*, Abstract, Introduction, Experimental, Results, Discussion, etc.). All illustrations, photographs, tables, etc., should be on separate sheets.

Introduction. Every paper must have a concise introduction mentioning what has been done before on the topic described, and stating clearly what is new in the paper now submitted.

Abstract. All articles should have an abstract of 50–100 words which clearly and briefly indicates what is new, different and significant.

Illustrations. The figures should be submitted in a form suitable for reproduction, drawn in Indian ink on drawing or tracing paper. Each illustration should have a legend, all the *legends* being typed (with double spacing) together on a *separate sheet.* If structures are given in the text, the original drawings should be supplied. Coloured illustrations are reproduced at the author's expense, the cost being determined by the number of pages and by the number of colours needed. The written permission of the author and publisher must be obtained for the use of any figure already published. Its source must be indicated in the legend.

References. References should be numbered in the order in which they are cited in the text, and listed in numerical sequence on a separate sheet at the end of the article. Please check a recent issue for the layout of the reference list. Abbreviations for the titles of journals should follow the system used by *Chemical Abstracts.* Articles not yet published should be given as "in press" (journal should be specified), "submitted for publication" (journal should be specified), "in preparation" or "personal communication".

Dispatch. Before sending the manuscript to the Editor please check that the envelope contains four copies of the paper complete with references, legends and figures. One of the sets of figures must be the originals suitable for direct reproduction. Please also ensure that permission to publish has been obtained from your institute.

Proofs. One set of proofs will be sent to the author to be carefully checked for printer's errors. Corrections must be restricted to instances in which the proof is at variance with the manuscript. "Extra corrections" will be inserted at the author's expense.

Reprints. Fifty reprints of Full-length papers and Short Communications will be supplied free of charge. Additional reprints can be ordered by the authors. An order form containing price quotations will be sent to the authors together with the proofs of their article.

Advertisements. Advertisement rates are available from the publisher on request. The Editors of the journal accept no responsibility for the contents of the advertisements.

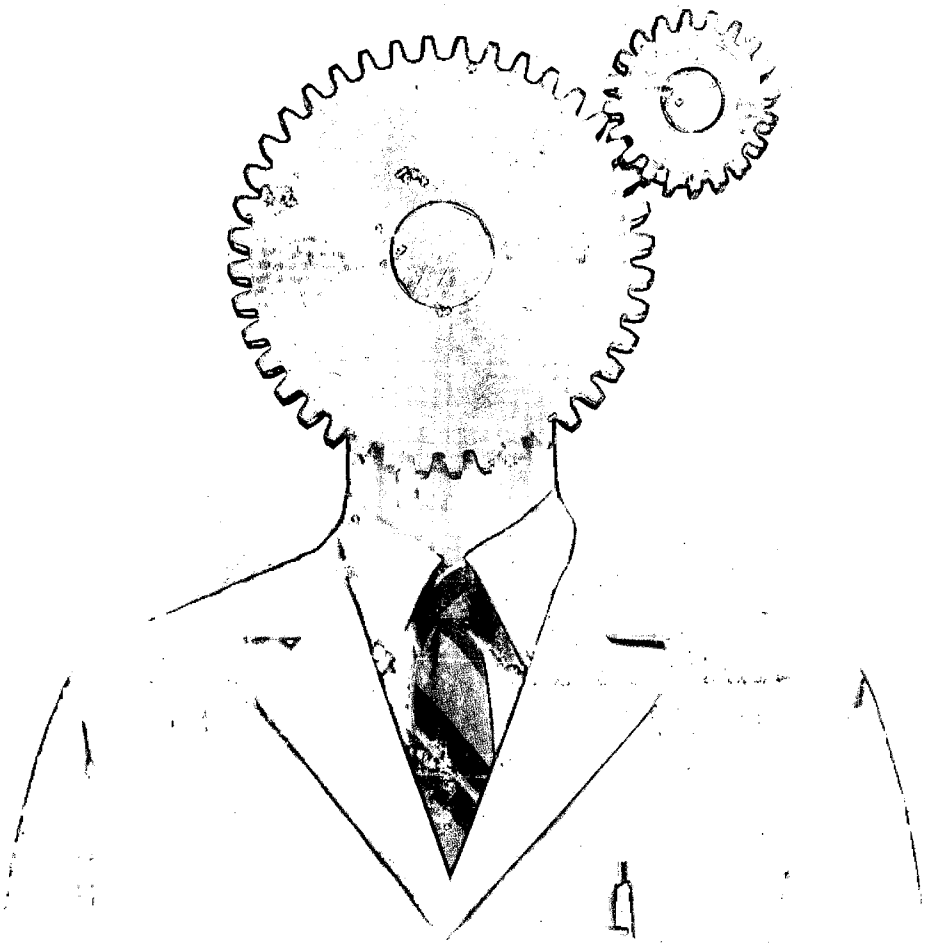

There's more to our CE autosampler than automation.

On the new Model 270A-HT High Throughput Capillary Electrophoresis System, a unique sample cooling system minimizes sample degradation. Our special design eliminates evaporation. Ion replenishment can be fully automated with the multiple buffer system. The software makes it easy to custom-tailor analysis parameters to each sample...Whether you need unattended overnight operation on 50 samples or just a few, optimal performance is ensured. The Model 270A-HT High Throughput Capillary Electrophoresis System. Higher sensitivity, greater reliability and more performance than ever. Contact Applied Biosystems today.

Applied Biosystems

Foster City, U.S.A. Tel: (415) 570-6667. Telex: 470052 APBIO UI. Fax: (415) 572-2743.
Mississauga, Canada. Tel: (416) 821-8183. Fax: (416) 821-8246.
Warrington, U.K. Tel: 0925-825650. Telex: 629611 APBIO G. Fax: 0925-828196.
Weiterstadt, Germany. Tel: 06151-87940. Telex: 4197318 Z ABI D. Fax: 06151-84899.
Paris, France. Tel: (1) 48 63 24 44. Telex: 230458 ABIF. Fax: (1) 48 63 22 82.
Milan, Italy. Tel: (02) 8940561. Fax: (02) 8321655.
Maarssen, The Netherlands. Tel: (0) 3465-74868. Telex: 70896. Fax: (0) 3465-74904.
Burwood, Australia. Tel: (03) 808-7777. Fax: (03) 887-1469.
Tokyo, Japan. Tel: (03) 699-0700. Fax: (03) 699-0733.